PROBIOTIC TRIGGER MOLECULES IN ACTION

EDITED BY: Jasna Novak (maiden Beganovic), Emmanuelle Maguin, Afef Najjari and Konstantinos Papadimitriou
PUBLISHED IN: Frontiers in Microbiology and Frontiers in Cellular and Infection Microbiology

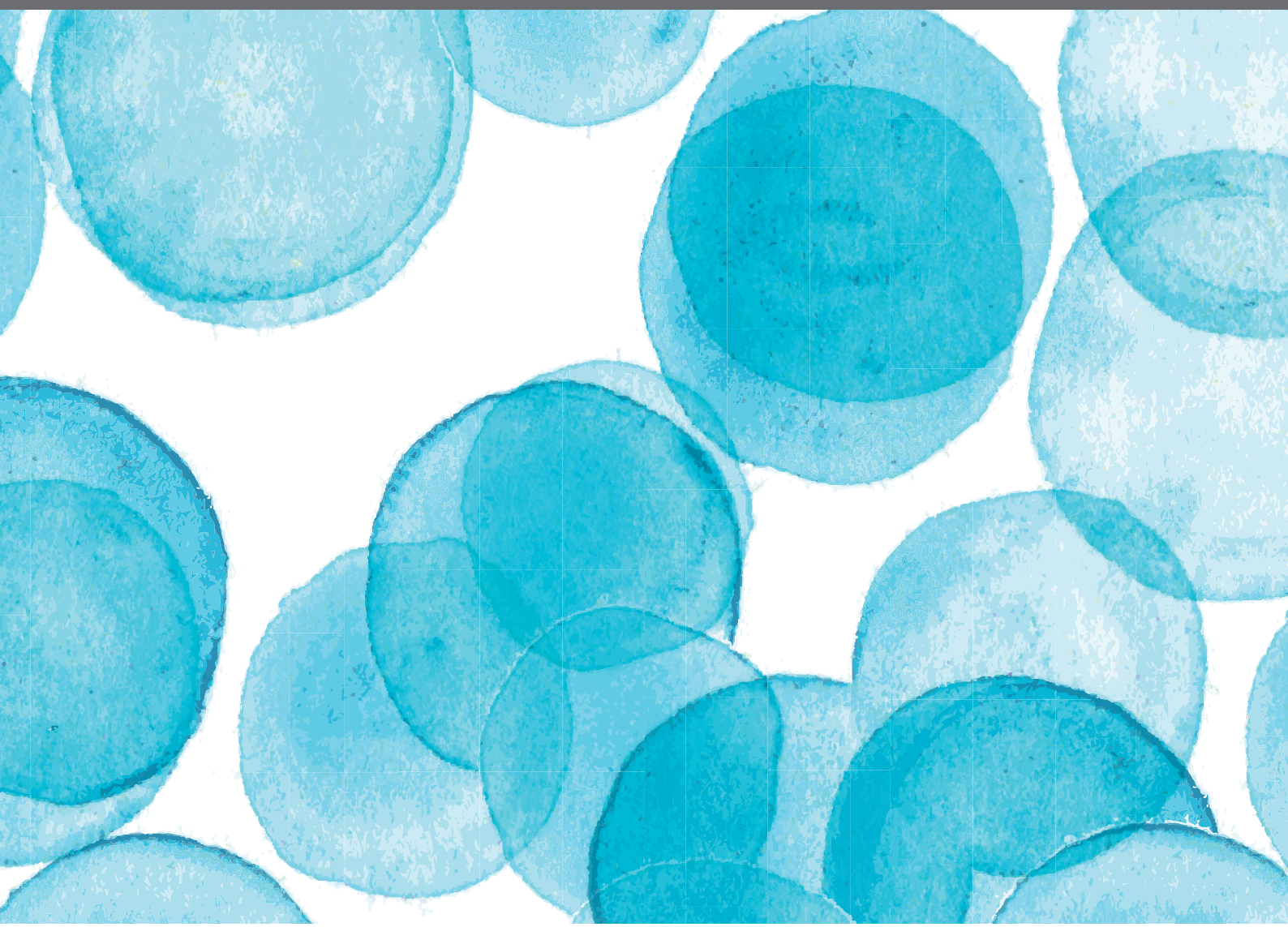

frontiers Research Topics

ISSN 1664-8714
ISBN 978-2-88971-346-2
DOI 10.3389/978-2-88971-346-2

About Frontiers

Frontiers is more than just an open-access publisher of scholarly articles: it is a pioneering approach to the world of academia, radically improving the way scholarly research is managed. The grand vision of Frontiers is a world where all people have an equal opportunity to seek, share and generate knowledge. Frontiers provides immediate and permanent online open access to all its publications, but this alone is not enough to realize our grand goals.

Frontiers Journal Series

The Frontiers Journal Series is a multi-tier and interdisciplinary set of open-access, online journals, promising a paradigm shift from the current review, selection and dissemination processes in academic publishing. All Frontiers journals are driven by researchers for researchers; therefore, they constitute a service to the scholarly community. At the same time, the Frontiers Journal Series operates on a revolutionary invention, the tiered publishing system, initially addressing specific communities of scholars, and gradually climbing up to broader public understanding, thus serving the interests of the lay society, too.

Dedication to Quality

Each Frontiers article is a landmark of the highest quality, thanks to genuinely collaborative interactions between authors and review editors, who include some of the world's best academicians. Research must be certified by peers before entering a stream of knowledge that may eventually reach the public - and shape society; therefore, Frontiers only applies the most rigorous and unbiased reviews.
Frontiers revolutionizes research publishing by freely delivering the most outstanding research, evaluated with no bias from both the academic and social point of view. By applying the most advanced information technologies, Frontiers is catapulting scholarly publishing into a new generation.

What are Frontiers Research Topics?

Frontiers Research Topics are very popular trademarks of the Frontiers Journals Series: they are collections of at least ten articles, all centered on a particular subject. With their unique mix of varied contributions from Original Research to Review Articles, Frontiers Research Topics unify the most influential researchers, the latest key findings and historical advances in a hot research area! Find out more on how to host your own Frontiers Research Topic or contribute to one as an author by contacting the Frontiers Editorial Office: frontiersin.org/about/contact

PROBIOTIC TRIGGER MOLECULES IN ACTION

Topic Editors:
Jasna Novak (maiden Beganovic), University of Zagreb, Croatia
Emmanuelle Maguin, Institut National de recherche pour l'agriculture, l'alimentation et l'environnement (INRAE), France
Afef Najjari, Tunis El Manar University, Tunisia
Konstantinos Papadimitriou, University of Peloponnese, Greece

Citation: Novak, J., Maguin, E., Najjari, A., Papadimitriou, K., eds. (2021). Probiotic Trigger Molecules in Action. Lausanne: Frontiers Media SA.
doi: 10.3389/978-2-88971-346-2

Table of Contents

05 ***Diverse Expression of Antimicrobial Activities Against Bacterial Vaginosis and Urinary Tract Infection Pathogens by Cervicovaginal Microbiota Strains of* Lactobacillus gasseri *and* Lactobacillus crispatus**
Fabrice Atassi, Diane L. Pho Viet Ahn and Vanessa Lievin-Le Moal

18 ***Exopolysaccharides From* Streptococcus thermophilus *ST538 Modulate the Antiviral Innate Immune Response in Porcine Intestinal Epitheliocytes***
Hiroya Mizuno, Kae Tomotsune, Md. Aminul Islam, Ryutaro Funabashi, Leonardo Albarracin, Wakako Ikeda-Ohtsubo, Hisashi Aso, Hideki Takahashi, Katsunori Kimura, Julio Villena, Yasuko Sasaki and Haruki Kitazawa

32 ***Extracellular Vesicles Produced by the Probiotic* Propionibacterium freudenreichii *CIRM-BIA 129 Mitigate Inflammation by Modulating the NF-κB Pathway***
Vinícius de Rezende Rodovalho, Brenda Silva Rosa da Luz, Houem Rabah, Fillipe Luiz Rosa do Carmo, Edson Luiz Folador, Aurélie Nicolas, Julien Jardin, Valérie Briard-Bion, Hervé Blottière, Nicolas Lapaque, Gwenaël Jan, Yves Le Loir, Vasco Ariston de Carvalho Azevedo and Eric Guédon

46 ***First Evidence of Acyl-Hydrolase/Lipase Activity From Human Probiotic Bacteria:* Lactobacillus rhamnosus *GG and* Bifidobacterium longum *NCC 2705***
Panagiotis Manasian, Atma-Sol Bustos, Björn Pålsson, Andreas Håkansson, J. Mauricio Peñarrieta, Lars Nilsson and Javier A. Linares-Pastén

57 ***Lipoproteins Contribute to the Anti-inflammatory Capacity of* Lactobacillus plantarum *WCFS1***
I-Chiao Lee, Iris I. van Swam, Sjef Boeren, Jacques Vervoort, Marjolein Meijerink, Nico Taverne, Marjo Starrenburg, Peter A. Bron and Michiel Kleerebezem

68 ***Topic Application of the Probiotic* Streptococcus dentisani *Improves Clinical and Microbiological Parameters Associated With Oral Health***
María D. Ferrer, Aranzazu López-López, Teodora Nicolescu, Salvadora Perez-Vilaplana, Alba Boix-Amorós, Majda Dzidic, Sandra Garcia, Alejandro Artacho, Carmen Llena and Alex Mira

82 ***Isolation and Characterization of Nitrate-Reducing Bacteria as Potential Probiotics for Oral and Systemic Health***
Bob T. Rosier, Eva M. Moya-Gonzalvez, Paula Corell-Escuin and Alex Mira

101 ***Probiotics, Prebiotics, Synbiotics, and Paraprobiotics as a Therapeutic Alternative for Intestinal Mucositis***
Viviane Lima Batista, Tales Fernando da Silva, Luís Cláudio Lima de Jesus, Nina Dias Coelho-Rocha, Fernanda Alvarenga Lima Barroso, Laisa Macedo Tavares, Vasco Azevedo, Pamela Mancha-Agresti and Mariana Martins Drumond

118 ***Single-Cell Transcriptomics Reveals That Metabolites Produced by* Paenibacillus bovis *sp. nov. BD3526 Ameliorate Type 2 Diabetes in GK Rats by Downregulating the Inflammatory Response***
Zhenyi Qiao, Xiaohua Wang, Huanchang Zhang, Jin Han, Huafeng Feng and Zhengjun Wu

131 ***Evaluation of an O2-Substituted (1–3)-β-D-Glucan, Produced by* Pediococcus parvulus *2.6, in* ex vivo *Models of Crohn's Disease***
Sara Notararigo, Encarnación Varela, Anna Otal, Iván Cristobo, María Antolín, Francisco Guarner, Alicia Prieto and Paloma López

144 ***Probiotic Effector Compounds: Current Knowledge and Future Perspectives***
Eric Banan-Mwine Daliri, Fred Kwame Ofosu, Chen Xiuqin, Ramachandran Chelliah and Deog-Hwan Oh

frontiers in Microbiology

ORIGINAL RESEARCH
published: 20 December 2019
doi: 10.3389/fmicb.2019.02900

Diverse Expression of Antimicrobial Activities Against Bacterial Vaginosis and Urinary Tract Infection Pathogens by Cervicovaginal Microbiota Strains of *Lactobacillus gasseri* and *Lactobacillus crispatus*

Fabrice Atassi[1,2], *Diane L. Pho Viet Ahn*[3,4,5] *and Vanessa Lievin-Le Moal*[3,4,5]*

[1] ISNERM UMR-S 1166, Sorbonne University, Paris, France, [2] INSERM, UMR-S 1166, CHU Pitié-Salpêtrière, Faculty of Medicine, Paris, France, [3] INSERM UMR-S 996, University of Paris-Sud, Orsay, France, [4] INSERM UMR-S 996, Paris-Saclay University, Saint-Aubin, France, [5] INSERM, UMR-S 996, Clamart, France

OPEN ACCESS

Edited by:
Jasna Novak,
University of Zagreb, Croatia

Reviewed by:
Jürgen Schrezenmeir,
Johannes Gutenberg University Mainz, Germany
Young Min Kwon,
University of Arkansas, United States

***Correspondence:**
Vanessa Lievin-Le Moal
vanessa.lievin-le-moal@u-psud.fr

Specialty section:
This article was submitted to Food Microbiology, a section of the journal Frontiers in Microbiology

Received: 12 October 2019
Accepted: 02 December 2019
Published: 20 December 2019

Citation:
Atassi F, Pho Viet Ahn DL and Lievin-Le Moal V (2019) Diverse Expression of Antimicrobial Activities Against Bacterial Vaginosis and Urinary Tract Infection Pathogens by Cervicovaginal Microbiota Strains of Lactobacillus gasseri and Lactobacillus crispatus. Front. Microbiol. 10:2900. doi: 10.3389/fmicb.2019.02900

We aimed to analyze the strain-by-strain expression of a large panel of antimicrobial activities counteracting the virulence mechanisms of bacterial vaginosis-associated *Prevotella bivia* CI-1 and *Gardnerella vaginalis* 594, pyelonephritis-associated *Escherichia coli* CFT073, and recurrent cystitis- and preterm labor-associated IH11128 *E. coli* by *Lactobacillus gasseri* and *Lactobacillus crispatus* clinical strains, and *L. gasseri* ATCC 9857 and KS 120.1, and *L. crispatus* CTV-05 strains isolated from the cervicovaginal microbiota of healthy women. All *L. gasseri* and *L. crispatus* strains exerted antimicrobial activity by secreted lactic acid, which killed the microbial pathogens by direct contact. Potent bactericidal activity was exerted by a very limited number of resident *L. gasseri* and *L. crispatus* strains showing the specific ability to a strain to produce and release antibiotic-like compounds. These compounds eradicated the microbial pathogens pre-associated with the surface of cervix epithelial cells, providing efficient protection of the cells against the deleterious effects triggered by toxin-producing *G. vaginalis* and uropathogenic *E. coli*. Furthermore, these compounds crossed the cell membrane to kill the pre-internalized microbial pathogens. In addition, all *L. gasseri* and *L. crispatus* cells exhibited another non-strain specific activity which inhibited the association of microbial pathogens with cervix epithelial cells with varying efficiency, partially protecting the cells against lysis and detachment triggered by toxin-producing *G. vaginalis* and uropathogenic *E. coli*. Our results provide evidence of strain-level specificity for certain antimicrobial properties among cervicovaginal *L. gasseri* and *L. crispatus* strains, indicating that the presence of a particular species in the vaginal microbiota is not sufficient to determine its benefit to the host. A full repertory of antimicrobial properties should be evaluated in choosing vaginal microbiota-associated *Lactobacillus* isolates for the development of live biotherapeutic strategies.

Keywords: cervicovaginal microbiota, *Lactobacillus gasseri*, *Lactobacillus crispatus*, bacterial vaginosis, urinary tract infections, antimicrobial

INTRODUCTION

Vaginal dysbiosis (De Seta et al., 2019), bacterial vaginosis (BV) (Onderdonk et al., 2016) and urinary-tract infections (UTIs) (Foxman, 2014) are major health problems that are difficult to treat and highly recurrent. BV is the most common cervicovaginal condition among women of childbearing age and is associated with adverse reproductive health outcomes, including preterm birth and low birth weight, as well as an increased risk of acquiring or transmitting sexually transmitted infections, including HIV-1 (Onderdonk et al., 2016). Clinically, UTIs are differentiated into lower (cystitis) and upper UTIs (pyelonephritis). Nearly half of all women will experience a UTI in their lifetime and 20–30% of those with acute cystitis will have a recurrence within 3 to 4 months (Foxman, 2014). A recent study showed that bladder exposure to BV-associated *Gardnerella vaginalis* can activate uropathogenic *Escherichia coli* (UPEC) from latent bladder epithelial reservoirs, thus triggering the recurrence of cystitis (Gilbert et al., 2017).

The human urogenital tract is colonized by a large diversity of microorganisms, representing a complex microbial ecosystem in which host and microbes exist in homeostasis (Whiteside et al., 2015; Smith and Ravel, 2017). The resilience of this ecosystem greatly depends on environmental exposure and behavioral factors, as well as a range of host factors, which vary between individuals, during life and geographically. Genomic and functional comparison of vagina- or bladder-associated bacterial strains are suggesting that these two body sites are microbiologically linked (Thomas-White et al., 2018). Cervicovaginal microbiota can affect women's health since microbiota dominated by *Lactobacillus* spp. (Ravel et al., 2011; Romero et al., 2014) has been shown to be associated with a reduced risk of microbial infections (Amabebe and Anumba, 2018). *Lactobacillus crispatus*, *Lactobacillus gasseri*, *Lactobacillus jensenii*, and *Lactobacillus iners* are commonly found in the cervicovaginal microbiota of apparently healthy women (Antonio et al., 1999). Molecular analyses have identified at least five major types of cervicovaginal microbiota, called community state types (CSTs), which differ in bacterial composition and relative abundance. Four are dominated by either *L. crispatus* (CST I), *L. gasseri* (CST II), *L. iners* (CST III), or *L. jensenii* (CST V) (Ravel et al., 2011; Romero et al., 2014). The fifth CST (CST IV) comprised facultative anaerobic bacteria, including *G. vaginalis, Atopobium vaginae,* and *Megasphaera* spp., among others, and resembles the composition of the vaginal microbiota associated with BV (Ravel et al., 2011; Romero et al., 2014). A meta-analysis of clinical studies has demonstrated that women with low-*Lactobacillus* CST IV cervicovaginal microbiota are at increased risk of *Prevotella bivia*, *G. vaginalis*, *Chlamydia trachomatis* and human papillomavirus infections, whereas women with *Lactobacillus*-dominated cervicovaginal microbiota are at lower risk (Tamarelle et al., 2019). However, the association between the risk of UTIs and the composition of the vaginal microbiota is still unclear (Whiteside et al., 2015).

Probiotic *Lactobacillus*-based therapeutics to treat BV and UTIs are available (Foxman and Buxton, 2013; Geerlings et al., 2014; Reid, 2017). Moreover, "live biotherapeutic" drugs are being developed under the FDA regulatory framework (FDA, 2016). The *in vitro* probiotic antimicrobial properties (FAO/WHO, 2002; Hill et al., 2014) associated with whole bacterial cells, secreted metabolites or released compounds of *L. gasseri* and *L. crispatus*. urogenital isolates have been well documented (Servin, 2004; Spurbeck and Arvidson, 2011; Petrova et al., 2013; Smith and Ravel, 2017). Clinical trials have confirmed the therapeutic interest of some of these strains to treat dysbiosis, BV and UTIs (MacPhee et al., 2010; Hanson et al., 2016; De Vrese et al., 2019; van de Wijgert and Verwijs, 2019). Here, we aimed to evaluate the distribution of a range of *in vitro* antimicrobial activities against BV-associated *P. bivia* and *G. vaginalis*, UPEC, and recurrent cystitis and infection-related preterm labor-associated *E. coli* in cervicovaginal strains of *L. gasseri* and *L. crispatus*. Vaginal (Onderdonk et al., 2016) and urinary tract (Hannan et al., 2012; Servin, 2014; Flores-Mireles et al., 2015; Mobley, 2016; Tamadonfar et al., 2019) bacterial pathogens have evolved sophisticated virulence mechanisms, including, among others, flagella, adhesins, toxins, and siderophores associated with biofilm formation, epithelial cell colonization and invasion, and cytotoxic activities. Thus, our analysis of the repertory of probiotic antimicrobial activities of urogenital strains *L. gasseri and L. crispatus* included bactericidal and bacteriostatic effects on free, adhering, or internalized pathogens and biofilm disrupting activity; inhibition of pathogen association with cervix epithelial cells by competition, exclusion, or displacement; and protective properties against the deleterious cellular effects of specific pathogen toxins.

MATERIALS AND METHODS

Lactobacillus Strains

The collection of twenty two *Lactobacillus* strains isolated from cervicovaginal samples of healthy women were from strains collection of UMR-S 510 Inserm (Faculty of Pharmacy, University of Paris-Sud, Châtenay-Malabry. 92296. France) (Atassi et al., 2006a,b). Bacteria are identified by biochemical test (Kandler and Weiss, 1986) and analysis of *tuf* sequences (Chavagnat et al., 2002). The human cervicovaginal *L. gasseri* strain ATCC 9857 was obtained from American Type Culture Collection (Manassas, VA, United States). The human cervicovaginal *L. gasseri* strain KS 120.1 was provided by ProbioSwiss SA (Zurich, Switzerland). The human cervicovaginal *L. crispatus* strain CTV-05 was kindly provided by Pr. P. B. Heczko (Department of Microbiology, Jagiellonian University Medical College, Krakow, Poland).

All *Lactobacillus* strains were grown in De Man, Rogosa, Sharpe (MRS) broth (Gibco, Thermo Fisher Scientific, Paris, France) for 18 h at 37°C with 5% CO_2 (Atassi et al., 2006a). For assays, 18-h cultures adjusted to 10^9 CFU/ml were used. Bacterial cells and cell-free culture supernatants (CFCSs) were obtained by centrifuging the *Lactobacillus* cultures at 10,000 × *g* for 30 min at 4°C. Separated bacterial cells were washed three times with sterile MRS and resuspended in fresh MRS. CFCSs were passed through a sterile 0.22-mm Millex GS filter unit (Millipore, Molsheim,

France). The absence of cells from CFCSs was verified using a colony-count assay.

Bacterial Pathogens

Human *G. vaginalis* strain 594 of Gardner and Dukes (DSM 4944, ATCC 14018) was obtained from Deutsche Sammlung von Mikroorganismen und Zellkulturen (Braunschweig, Germany). Human clinical isolate *P. bivia* strain CI-1 was provided by the Department of Obstetrics and Gynecology, Zurich University Hospital (Switzerland). Strains were grown on *Gardnerella* agar plates purchased from BioMerieux (Marcy-l'Etoile, France, France). The agar plates were incubated under anaerobic conditions, using a sealed anaerobic jar (Becton Dickinson, United States), at 37°C for a maximum of 36 h. Before use, *G. vaginalis* and *P. bivia* strains were sub-cultured in Brain-Heart-Infusion (BHI) medium (Gibco, Thermo Fisher Scientific) supplemented with yeast extract, maltose, and horse serum, under anaerobic conditions, using a sealed anaerobic jar, at 37°C (Atassi et al., 2006a).

The human prototypic wildtype pyelonephritis-associated *E. coli* strain CFT073 (UPEC CFT073) (Mobley et al., 1990) was provided by Pr. Harry Mobley (Department of Microbiology and Immunology, University of Michigan Medical School, Ann Arbor, MI, United States). The human prototypic wildtype *E. coli* strain IH11128 (Nowicki et al., 1987), a member of the diffusely adhering *E. coli* family that expresses Afa/Dr. adhesins and associated with recurrent cystitis and infection-related preterm labor, was provided by Dr. Bogdan J. Nowicki (Department of Obstetrics and Gynecology, Meharry Medical College, Nashville, TN, United States). The strains were maintained on Luria-Bertani (LB) plates. Before infection, bacteria were grown in LB broth Miller (Gibco, Thermo Fisher Scientific) at 37°C (Atassi et al., 2006b).

Killing Assay

A colony count assay was performed to measure the effect on viability of the test bacterial pathogens (10^8 CFU/ml) incubated in the appropriate culture medium described above, with or without an 18-h *Lactobacillus* culture (adjusted to 10^9 CFU/ml) or CFCS at 37°C. Incubations were conducted in BHI or Dulbecco's modified Eagle's minimum essential medium (DMEM) (Gibco), as indicated. Aliquots were removed initially and at predetermined intervals, serially diluted, and plated on appropriate bacterial media, described above, to determine the bacterial colony counts of the pathogens. According to the guidelines of the Clinical and Laboratory Standards Institute (Standards, 1999), the minimum bactericidal effect is conventionally defined as a 3 $\log_{10}$ CFU/ml ($MBE_{99.9\%}$) decrease in the number of viable bacteria. Here, we used a more restrictive criterion, using an $MBE_{99.99\%}$ value, defined as a reduction of the viable bacterial count of 4 $\log_{10}$ CFU/ml.

Treatment With Catalase

The *Lactobacillus* CFCSs were treated prior to the assay at 37°C for 1 h, with or without catalase (5 μg/ml) (Sigma-Aldrich, L'Isle d'Abeau Chesnes, France), to determine the part of the killing effect dependent on hydrogen peroxide.

Growth Inhibition Assay

The effect on growth of the bacterial pathogens was measured by incubating a test bacterial pathogen (10^6 CFU/ml) in its appropriate culture medium with an aliquot of CFCS of an 18-h *Lactobacillus* culture (adjusted to 10^9 CFU/ml). Under all experimental conditions, bacterial growth was quantified by optical density at 620 nm on a Tecan GENios Microplate Reader (Tecan, Trappes, France).

Biofilm Assay

Uropathogenic *Escherichia coli* CFT073 forming biofilm (Luterbach et al., 2018) was used as a pathogen test strain. Bacteria were grown (10^8 CFU/ml) in LB in wells of a 96-well plate for 72 h at 37°C. The biofilms were gently washed twice with sterile phosphate-buffered saline (PBS) to remove non-adherent cells. For determination of activity of *Lactobacillus* CFCSs on pre-formed biofilms, CFCS (250 μl) of 18 h culture adjusted to 10^9 CFU/ml) was added in the presence of DMEM. Quantification of the biofilms was determined by Crystal Violet staining (addition of 0.5% Crystal Violet per well, incubation for 5 min, and then discarded) and measuring optical density at 600 nm. The remaining numbers of viable biofilm-associated bacteria after treatment were determined by scraping the biofilms, dispersing the cells in PBS, and plating dilutions for bacterial colony counts.

Cell Culture

Human cervical epithelial HeLa cells were seeded (5×10^5 cells per well) in culture plates (TPP, Dominique Dutscher SAS, Brumath, France) and were cultured at 37°C in 5% CO2/95% air in RPMI 1640 with L-glutamine (21875-034 – Gibco, Thermo Fisher Scientific), supplemented with 10% heat-inactivated (30 min, 56°C) fetal calf serum (FCS; Gibco, Thermo Fisher Scientific) (Atassi et al., 2006a,b; Lievin-Le Moal et al., 2011). Cells were used for infection assays at post-confluence (7 days in culture).

Killing Assay in Infected Cells

Bacterial pathogens associated with HeLa cells were quantified by infecting the confluent cell monolayers for 60 min with a test bacterial pathogen (10^8 CFU/ml). The plates were then washed five times with sterile PBS to remove non-adhering bacteria and then incubated for 3 h with *Lactobacillus* CFCSs in DMEM.

Bacterial internalized into untreated and *Lactobacillus*-treated cells were quantified using the gentamicin assay. Confluent cell monolayers were infected for 120 min with a test bacterial pathogen (10^8 CFU/ml). Infected cells were washed with sterile PBS and incubated for 60 min with cell culture medium containing 100 g/ml gentamicin (Invitrogen, Thermo Fisher Scientific), an antibiotic that does not cross the cell membrane and which rapidly kills the cell membrane-associated bacteria but not those located inside the cells. After washing four times with sterile PBS, the cell monolayers were then incubated with a CFCS for 3 h in the presence of DMEM.

All cell infections were conducted at 37°C in 10% CO_2/90% air. At the end of each assay, the cells were washed three times with sterile PBS and lysed with sterile H_2O. Dilutions were plated on the appropriate culture medium to determine the number of viable cell-associated or internalized bacteria by colony counts.

Competition, Exclusion, and Displacement Assays

For the competition assay, confluent HeLa cell monolayers were incubated for 3 h with a test bacteria pathogen (10^8 CFU/ml), with or without *Lactobacillus* cells (10^8 CFU/ml), in DMEM. For the exclusion assay, confluent cell monolayers were incubated for 3 h with or without *Lactobacillus* cells (10^8 CFU/ml) in DMEM, washed three times with sterile PBS, and then infected for 3 h with a test bacterial pathogen (10^8 CFU/ml). For the displacement assay, confluent cell monolayers were incubated for 3 h with a test bacterial pathogen, washed three times with sterile PBS, and then sub-cultured with or without *Lactobacillus* cells (10^8 CFU/ml) for 3 h in DMEM. All incubations were conducted at 37°C in 10% CO_2/90% air. The numbers of viable cell-associated pathogenic bacteria were determined by lysing the cells in sterile H_2O and plating dilutions on the appropriate medium for bacterial colony counting. Each assay was conducted in triplicate, with three successive cell passages. Results are expressed as the percent of adhering bacteria.

Cytoprotection Assays

The cytoprotective effect of pre-adhering *Lactobacillus* cells was assessed by pre-colonization of the confluent HeLa cell monolayers by *Lactobacillus* cells (10^8 CFU/ml, 3 h of incubation), washing away the non-adherent bacteria, and infection with a test bacterial pathogen (10^8 CFU/ml). The cytoprotective effect of CFCSs of 18-h *Lactobacillus* cultures (adjusted to 10^9 CFU/ml) was tested by incubating confluent cell monolayers with a test bacterial pathogen (10^8 CFU/ml), with or without CFCSs in DMEM. The attached HeLa cells were counted by phase-contrast light microscopy. Cells were examined using an Aristoplan microscope (Leitz, Germany) with epifluorescence (Plan Aprochromat 100X/1.32–0.6 oil-immersion objective). For each sample more than 15 random microscopic fields were examined. The source of the images was hidden from the people counting the number of attached cells in order to eliminate any possible bias. Photographic images were resized, organized and labeled using Adobe Photoshop software (San Jose, CA, United States).

Analysis

Results are expressed as the means ±standard error of the mean. Student's *t*-test was performed for statistical comparisons.

RESULTS

Killing Activity by Direct Contact

We assessed the antibiotic-like killing activities of isolates dependent or not of secreted lactic acid using a previously described method that allows discrimination of the lactic acid-dependent and -independent activities of *Lactobacillus* against *Salmonella enterica* typhimurium (Fayol-Messaoudi et al., 2005). DL-lactic acid at pH 4.5 in the presence of BHI decreased the viability of BV-associated *P. bivia* CI-1 and *G. vaginalis* 594, pyelonephritis-associated CFT073 (UPEC CFT073), and recurrent cystitis and preterm labor-associated IH11128 (UPEC IH11128) in a concentration-dependent manner (**Figure 1A**). Adding DMEM to the medium abolished the antimicrobial activity of DL lactic acid against urogenital microbial pathogens without modifying the pH (pH 4.5 ± 0.4). In addition, the concentration-dependent killing activity of hydrogen peroxide was not affected by adding DMEM (**Figure 1B**).

Lactobacillus gasseri ATCC 9857 CFCS exerted killing activity against *P. bivia* CI-1 and *G. vaginalis* 594 (2.43 ± 0.72 $\log_{10}$ and 2.65 ± 0.83 $\log_{10}$ CFU/ml decrease in viability, respectively) and UPEC CFT073 and IH11128 (1.76 ± 0.56 and 1.84 ± 0.44 $\log_{10}$

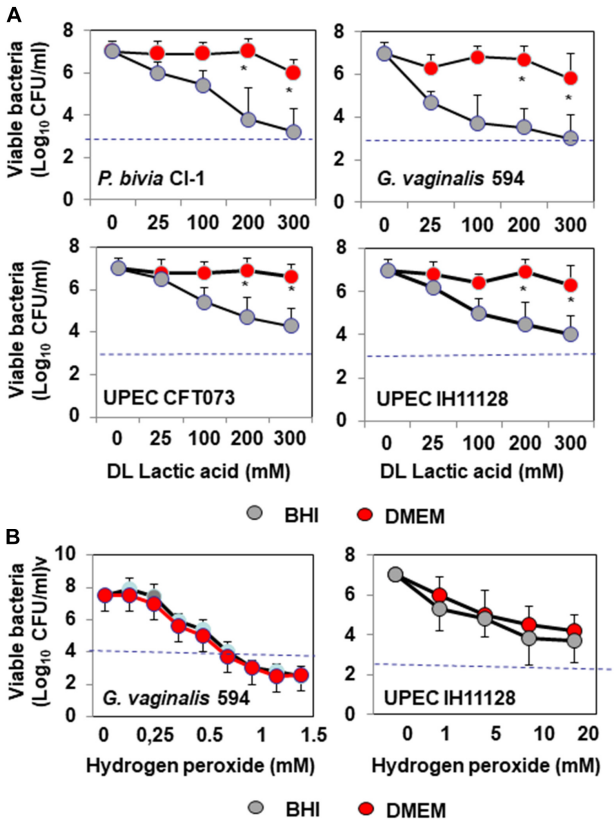

FIGURE 1 | *In vitro* lactic acid-dependent and -independent killing activity by direct contact against BV-associated *P. bivia* CI-1 and *Gardnerella. vaginalis* 594 strains, pyelonephritis-associated *E. coli* strain CFT073, and recurrent cystitis- and preterm labor-associated *E. coli* strain IH11128.
(A) Concentration-dependent killing activity of DL-lactic acid in BHI or DMEM.
(B) Concentration-dependent killing activity of hydrogen peroxide in the presence of BHI or DMEM. Each value shown is the mean ±SD from three experiments. Student *t*-test, $^*p < 0.01$ compared to BHI. The dotted line shows the $MBE_{99.99\%}$ value, defined as a reduction in the viable cell count of 4 $\log_{10}$.

CFU/ml decrease in viability, respectively), which was dependent on lactic acid, as it was completely abolished by the addition of DMEM (**Figure 2A**). *L. gasseri* KS 120.1 CFCS also exerted killing activity against *P. bivia* CI-1 and *G. vaginalis* 594 (6.43 ± 0.61 $\log_{10}$ and 6.35 ± 0.58 $\log_{10}$ CFU/ml decrease in viability, respectively), and UPEC CFT073 and IH11128 (5.33 ± 0.56 and 5.04 ± 0.48 $\log_{10}$ CFU/ml decrease in viability, respectively), which largely persisted in the presence of DMEM (*P. bivia* CI-1: 4.20 ± 0.6, *G. vaginalis* 594: 4.30 ± 0.41, UPEC CFT073: 3.21 ± 0.67, and UPEC IH11128: 3.00 ± 0.47 $\log_{10}$ CFU/ml decrease in viability) (**Figure 2A**). Similarly, *L. crispatus* CTV-05 CFCS also exerted killing activity, but to a lesser extent (*P. bivia* CI-1: 4.61 ± 0.53, *G. vaginalis* 594: 5.05 ± 0.42, UPEC CFT073: 3.51 ± 0.49, and UPEC IH11128: 4.23 ± 0.67 $\log_{10}$ CFU/ml decrease in viability), which was diminished by approximately one half in the presence of DMEM (*P. bivia* CI-1: 2.80 ± 0.68, *G. vaginalis* 594: 2.60 ± 0.41, UPEC CFT073: 1.72 ± 0.67, and UPEC IH11128: 2.31 ± 0.47 $\log_{10}$ CFU/ml decrease in viability). We next measured lactic acid-independent killing activity in the presence of DMEM over 4 h. *L. gasseri* KS 120.1 CFCS achieved maximum efficacy against *P. bivia* CI-1 and *G. vaginalis* 594 after 2 h, whereas the activity against UPEC CFT073 and UPEC IH11128 developed more slowly (**Figure 2B**). In contrast, the lactic acid-independent killing activity of *L. crispatus* CTV-05 CFCS against the four bacterial pathogens developed slowly (**Figure 2B**).

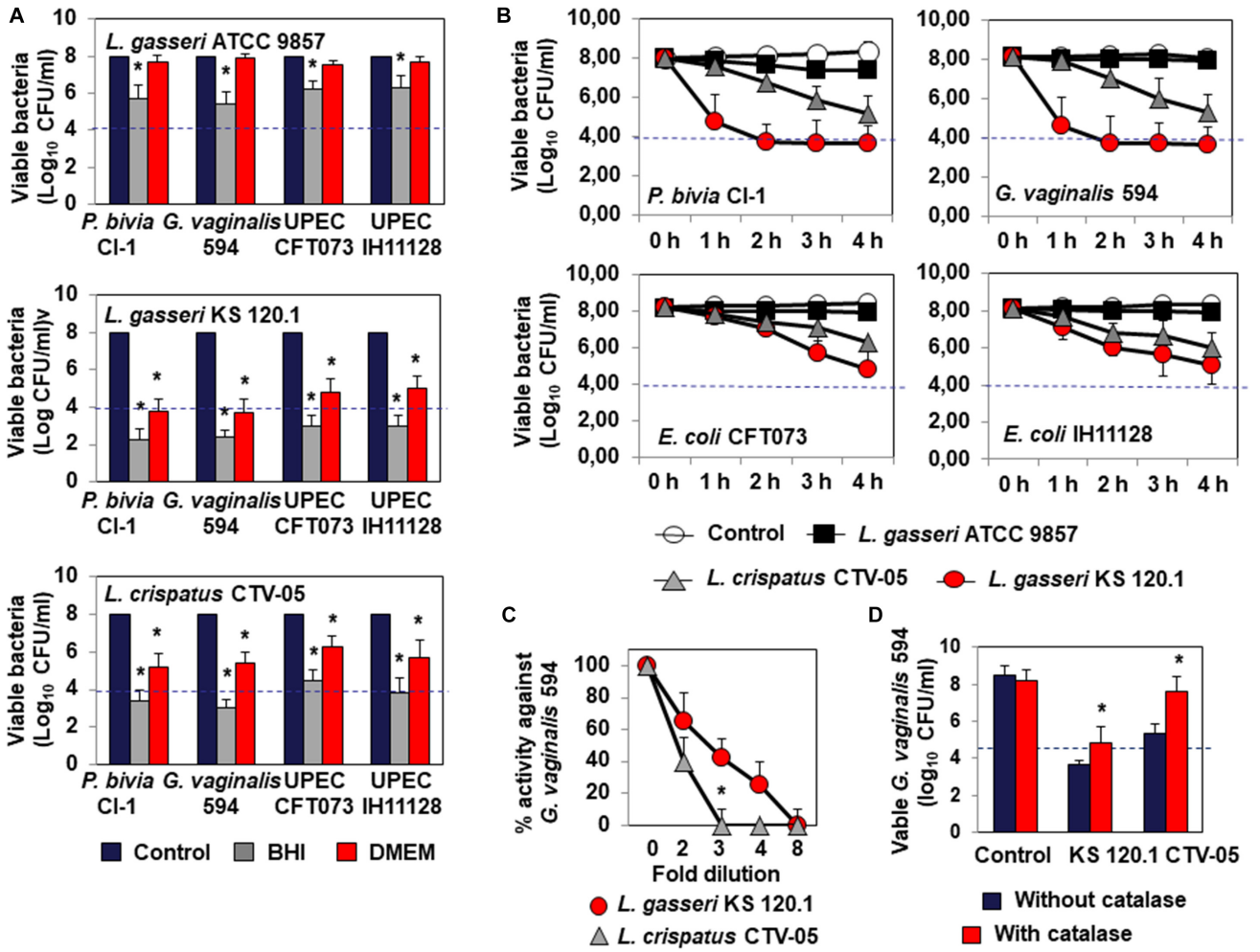

FIGURE 2 | Characteristics of the killing activity by direct contact of *L. gasseri* ATCC 9857, *L. gasseri* KS 120.1, and *L. crispatus* CTV-05 strains against BV-associated *P. bivia* CI-1 and *G. vaginalis* 594 strains, pyelonephritis-associated *E. coli* strain CFT073, and recurrent cystitis- and preterm labor- associated *E. coli* strain IH11128. **(A)** Lactic acid-dependent (BHI) and -independent (DMEM) killing activities exerted by each *Lactobacillus* strain in co-culture conditions. **(B)** Time-course of lactic acid-independent killing activity of *L. gasseri* ATCC 9857, *L. gasseri* KS 120.1, and *L. crispatus* CTV-05 CFCSs. **(C)** Concentration-dependent killing activity of *L. gasseri* KS 120.1 and *L. crispatus* CTV-05 CFCSs. **(D)** Effect of catalase treatment on the killing activity of *L. crispatus* CTV-05 CFCS. In **(A)**, killing activity was determined after 4 h of direct contact with *Lactobacillus* cultures (18 h of culture adjusted to 10^8 CFU/ml *Lactobacillus* bacteria). In **(A)**, the dotted line shows the $MBE_{99.99\%}$ value, defined as a reduction in the viable cell count of 4 $\log_{10}$ CFU/ml. In **(C,D)**, killing activity was determined in the presence of DMEM after 4 h of direct contact. Each value shown is the mean ±SD from three experiments. In **(A)**, Student *t*-test, $^*p < 0.01$ compared to control. In **(B)**, Student *t*-test, $^*p < 0.01$ at 3 and 4 h. In **(C,D)**, Student *t*-test, $^*p < 0.01$ compared to control.

The lactic acid-independent killing activities of *L. gasseri* KS 120.1 and *L. crispatus* CTV-05 CFCSs displayed the concentration-dependent pharmacodynamics characteristic of antimicrobial agents (Levison and Levison, 2009). The lactic acid-independent killing activities of *L. gasseri* KS 120.1 and *L. crispatus* CTV-05 CFCSs were concentration-dependent, with the CFSC of *L. gasseri* KS 120.1 maintaining potency at higher dilutions than that of *L. crispatus* CTV-05 (**Figure 2C**). In addition, the lactic acid-dependent and -independent killing activity of *L. crispatus* CTV-05 CFCS was abolished after catalase treatment (**Figure 2D**). The lactic acid-independent killing activity of *L. gasseri* KS 120.1 CFCS was only diminished by 1.2 ± 0.4 $\log_{10}$ after catalase treatment (**Figure 2D**), in agreement with a previous report (Atassi et al., 2006b).

Bacteriostatic Activity

Testing bacteriostatic activity against *G. vaginalis* 594 and UPEC HI11128 as the pathogen test strains showed the following results After 24 h of contact, *L. gasseri* ATCC 9857 CFCS inhibited the growth of *G. vaginalis* DSM 594 and UPEC HI11128, whereas *L. gasseri* KS 120.1 and *L. crispatus* CTV-05 CFCSs completely abolished the growth of the two pathogens (**Figure 3A**). The bacteriostatic activity of *L. gasseri* ATCC 9857 CFCS against *G. vaginalis* DSM 594 and UPEC HI11128 was time-dependent (**Figure 3B**). The abolition of growth by *L. gasseri* KS 120.1 and *L. crispatus* CTV-05 CFCSs after 24 h of contact (**Figure 3A**) could potentially be the result of their killing activity (**Figure 2**). However, we observed significant inhibition of UPEC IH11128 growth (**Figure 3C**) using an eight-fold dilution of *L. gasseri* KS 120.1 and *L. crispatus* CTV-05 CFCSs, which no longer had killing activity (**Figure 2C**).

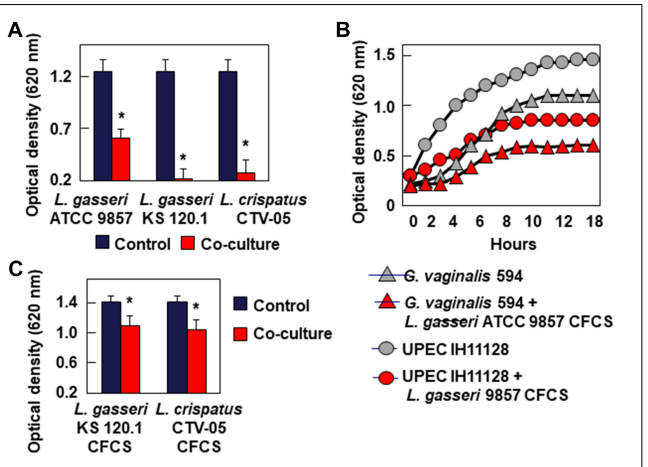

FIGURE 3 | Inhibition of growth of BV-associated *G. vaginalis* 594, and recurrent cystitis- and preterm labor-associated *E. coli* strain IH11128. **(A)** Inhibition of *G. vaginalis* 594 growth after 24 h of co-culture with *L. gasseri* ATCC 9857, *L. gasseri* KS 120.1, or *L. crispatus* CTV-05 strains. **(B)** Inhibition of *G. vaginalis* 594 and UPEC IH11128 growth during a time-course of co-culture with *L. gasseri* ATCC 9857 CFCS. **(C)** Inhibition of UPEC IH11128 growth after 24 h of co-culture in the presence of 8-fold diluted *L. gasseri* KS 120.1, and *L. crispatus* CTV-05 CFCSs. Each value shown is the mean ±SD from three experiments. Student *t*-test, $^*p < 0.01$ compared to control.

Activity Against Biofilms

Bacterial pathogens associated with urogenital infections often form biofilms at the epithelial cell surface (Hannan et al., 2012; Tamadonfar et al., 2019; Verstraelen and Swidsinski, 2019). Crystal Violet uptake, as measured by the OD_{600}, showed that the size of pre-formed UPEC CFT073 biofilms (Untreated: 0.65 ± 0.05 $OD_{600\ nm}$) was not modified after 48 h of treatment with *L. gasseri* ATCC 9857, *L. gasseri* KS 120.1, or *L. crispatus* CTV-05 CFCSs (0.62 ± 0.05, 0.61 ± 0.12, and 0.71 ± 0.09 $OD_{600\ nm}$, respectively). Moreover, the number of viable UPEC CFT073 bacteria present within the pre-formed biofilms (Untreated: 8.59 ± 0.25 $\log_{10}$ CFU/ml) were not significantly decreased, only by approximately 1 $\log_{10}$ CFU/ml by *L. gasseri* ATCC 9857, *L. gasseri* KS 120.1, and *L. crispatus* CTV-05 CFCSs (7.69 ± 0.45, 7.48 ± 0.92, and 7.68 ± 0.98 $\log_{10}$ CFU/ml, respectively).

Competition, Exclusion, and Displacement Activities Against Epithelial Cell Colonization

Bacterial pathogens associated with BV or UTIs can often colonize cervicovaginal and urinary tract epithelia (Hannan et al., 2012; Servin, 2014; Flores-Mireles et al., 2015; Mobley, 2016; Onderdonk et al., 2016). We thus evaluated whether *L. gasseri* ATCC 9857, *L. gasseri* KS 120.1 and *L. crispatus* CTV-05 cells can inhibit HeLa cell colonization by *G. vaginalis* 594 and UPEC IH11128 (**Figure 4**). Under conditions of competition, in which the pathogens and *Lactobacillus* cells were co-incubated with the HeLa cells, there was a significant decrease of adhesion of *G. vaginalis* 594 and UPEC IH11128 in the presence of *L. gasseri* ATCC 9857 (50.2 ± 7.2 and 45.5 ± 5.4% decrease, respectively), *L. gasseri* KS 120.1 (40.5 ± 4.2 and 35.8 ± 8.2% decrease, respectively), or *L. crispatus* CTV-05 cells (38.6 ± 5.5 and 35.1 ± 7.4% decrease, respectively) (**Figure 4A**). Under conditions of exclusion, the adhesion of *G. vaginalis* 594 and UPEC IH11128 to HeLa cells was decreased in the presence of pre-adhering *L. gasseri* ATCC 9857 (78.1 ± 9.3 and 72.8 ± 8.6% decrease, respectively), *L. gasseri* KS 120.1 (68.0 ± 7.7 and 65.8 ± 12.1% decrease, respectively), or *L. crispatus* CTV-05 cells (65.5 ± 9.8 and 62.4 ± 12.1% decrease, respectively) (**Figure 4B**). Under conditions of displacement, the level of pre-adhering pathogens was not affected by the addition of *L. gasseri* ATCC 9857, *L. gasseri* KS 120.1, or *L. crispatus* CTV-05 cells (**Figure 4C**).

Evaluating the ability of *L. gasseri* KS 120.1 and *L. crispatus* CTV-05 CFCSs to kill pathogens pre-associated with Hela cells, we found: The level of viable *G. vaginalis* 594 and UPEC IH11128 pre-adhering onto HeLa cells was reduced after treatment of pre-infected cells with *L. gasseri* KS 120.1 CFCS (3.0 ± 0.61 and 4.02 ± 0.22 $\log_{10}$ CFU/ml decrease of viable pre-adhering bacteria, respectively) and *L. crispatus* CTV-05 CFCS (1.49 ± 0.45 and 3.05 ± 0.29 $\log_{10}$ CFU/ml decrease of viable pre-adhering bacteria, respectively) (**Figure 4D**). Consistent with the absence of lactic acid-independent killing activity of *L. gasseri* ATCC 9857 CFCS (**Figure 2**), *L. gasseri* ATCC 9857 CFCS treatment in the presence of DMEM failed to affect the level of viable, pre-adhering *G. vaginalis* 594 or UPEC IH11128 (**Figure 4D**).

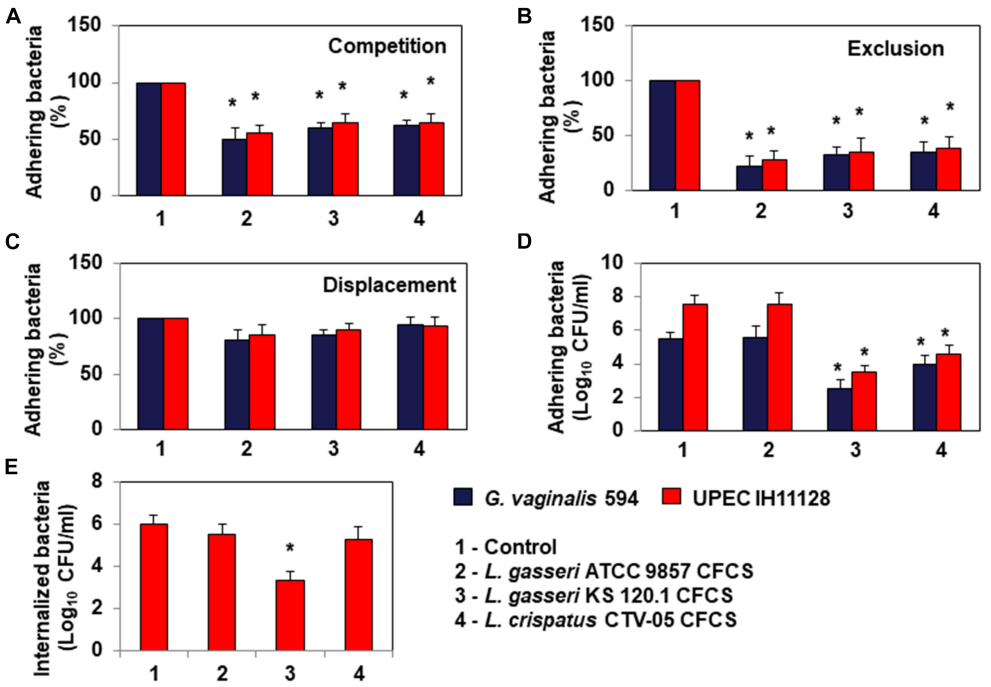

FIGURE 4 | Antagonistic activities of *Lactobacillus* cells and CFCSs against BV-associated *G. vaginalis* 594 and recurrent cystitis- and preterm labor-associated *E. coli* IH11128 adhering to HeLa cells. **(A)** Inhibition under competition conditions. **(B)** Inhibition under exclusion conditions. **(C)** Lack of inhibition under displacement conditions. **(D)** Killing of pre-adhering UPEC IH11128. **(E)** Killing of pre-internalized UPEC IH11128. In **(A–C)**, 100% adhesion corresponds to 5.1 ± 0.5 CFU/ml for *G. vaginalis* 594 and 7.6 ± 0.4 CFU/ml for *E. coli* IH11128. Competition, exclusion and displacement experimental condition are described in section "Materials and Methods". Each value shown is the mean ±SD from three experiments. Student *t*-test, $^*p < 0.01$ compared to control.

Uropathogenic *Escherichia coli* internalization into cells lining the urothelium is an important step of pathogenesis because it creates a reservoir of dormant bacteria (Hannan et al., 2012; Servin, 2014; Flores-Mireles et al., 2015; Mobley, 2016). Thus, we evaluated the ability of *L. gasseri* KS 120.1 and *L. crispatus* CTV-05 CFCSs to kill UPEC IH11128 pre-internalized within Hela cells. *L. gasseri* KS 120.1 CFCS, in the presence of DMEM, decreased the viability of pre-internalized UPEC IH11128 cells (2.65 ± 0.461 $\log_{10}$ CFU/ml decrease of viable pre-internalized bacteria) (**Figure 4E**). In contrast, given that *L. crispatus* CTV-05 CFCSs exerts lactic acid-independent killing activity against free and adhering UPEC IH11128 (**Figures 2**, **4D**, respectively), it failed to decrease the level of pre-internalized UPEC IH11128 in the presence of DMEM (**Figure 4E**). Consistent with *L. gasseri* ATCC 9857 CFCS lacking lactic acid-independent killing activity against free and adhering UPEC IH11128 (**Figures 2**, **4D**, respectively), it also did not decrease the level of pre-internalized UPEC IH11128 in the presence of DMEM.

Cytoprotective Effect Against Bacterial Toxins Produced Cell-Detachment

Epithelial exfoliation is a hallmark of both BV (Amegashie et al., 2017) and UTIs (Mulvey et al., 2000). *G. vaginalis* 594, producing the cytotoxin, vaginolysin (Yeoman et al., 2010), and UPEC IH11128, producing the Sat toxin (Lievin-Le Moal et al., 2011), are often used as pathogen test strains. *G. vaginalis* 594-infected HeLa cell monolayers on glass slides showed time-dependent disappearance of the cells, with only a small number of cells still attached 8 h post-infection (PI) (2.4 ± 1.7% of the cells remained attached) (**Figure 5A**). When the confluent HeLa cell monolayers were pre-colonized by *Lactobacillus* cells, there was a partial but significant decrease in *G. vaginalis* 594-induced cell-detachment (*L. gasseri* ATCC 9857 cells: 38.1 ± 15.2%, *L. gasseri* KS 120.1 cells: 48.4 ± 7.9%, and *L. crispatus* CTV-05 CFCS: 42.5 ± 6.1% of the cells were still attached 8 h post-infection) (**Figure 5A**).

For UPEC IH11128, 20.6 ± 5.2% of the HeLa cells were still attached to the glass slide after 18 h of infection (**Figure 5B**). There was partial protection against UPEC IH11128-induced cell-detachment when HeLa cells were pre-colonized with *Lactobacillus* cells (*L. gasseri* ATCC 9857 cells: 45.1 ± 9.2%, *L. gasseri* KS 120.1 cells: 60.4 ± 7.9%, and *L. crispatus* CTV-05 CFCS: 48.5 ± 6.1% of the cells were still attached at 18 h post-infection) (**Figures 5B,C**). We then examined whether the above observed killing of cell-associated UPEC IH11128 by *L. gasseri* KS 120.1 and *L. crispatus* CTV-05 CFCSs in the presence of DMEM improves cell protection. When confluent HeLa cell monolayers were infected by UPEC IH11128 in the presence of *L. gasseri* KS 120.1 or *L. crispatus* CTV-05 CFCSs and DMEM, only a small number of cells had detached by 18 h PI (98 ± 3.1% and 88 ± 6.8% of cells remained attached, respectively) (**Figure 5D**). As expected, the *L. gasseri* ATCC 9857 CFCS, which lacks lactic acid-independent killing activity (**Figure 2**), showed no

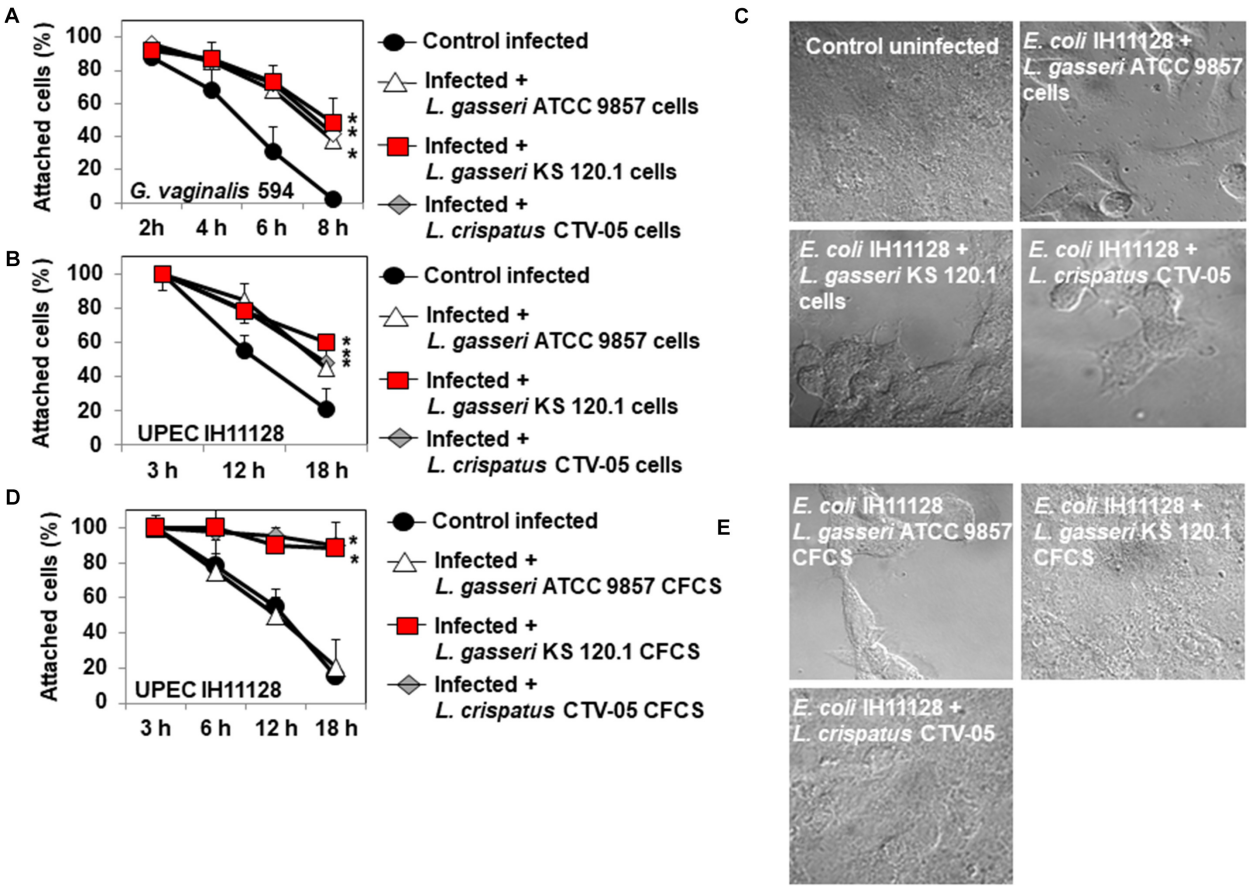

FIGURE 5 | Protective effect of cells and CFCSs of *L. gasseri* ATCC 9857, *L. gasseri* KS 120.1, or *L. crispatus* CTV-05 strains against the cytotoxic activities of BV-associated *G. vaginalis* 594 and preterm labor and recurrent cystitis-associated *E. coli* IH11128. **(A)** Quantification of time-dependent *G. vaginalis* 594-induced cell-detachment in the presence, or not, of pre-colonizing *Lactobacillus* cells. **(B)** Quantification of time-dependent UPEC IH11128-induced cell detachment, in the presence, or not, of pre-colonizing *Lactobacillus* cells. **(C)** Micrographs illustrating the partial inhibition of UPEC IH11128-induced cell detachment in the presence of pre-colonizing *Lactobacillus* cells. **(D)** Quantification of cell detachment in cell monolayers infected with UPEC IH11128, showing the total inhibition of cell detachment in the presence *L. gasseri* KS 120.1 or *L. crispatus* CTV-05 CFCSs and the lack of inhibition in the presence of *L. gasseri* ATCC 9857 CFCS. **(E)** Micrographs illustrating the entire inhibition of UPEC IH11128-induced cell detachment in the presence *L. gasseri* KS 120.1 or *L. crispatus* CTV-05 CFCSs. Phase-contrast micrographs are representative of two separate experiments. The number of attached cells was monitored by phase-contrast light microscopy. Each value shown is the mean ±SD from three experiments. Student *t*-test, $^{*}p < 0.01$ compared to *G. vaginalis* 594 or UPEC IH11128.

protective effect against UPEC IH11128-induced cell-detachment in the presence of DMEM (20.2 ± 6.6% of cells remained attached) (**Figures 5D,E**).

Expression of Killing Activity and Inhibition of Pathogen Adhesion in Human Cervocovaginal Microbiota-Associated *L. gasseri* and *L. crispatus* Isolates

The lactic acid-dependent and -independent killing activity of a set of fourteen *L. gasseri* and eight *L. crispatus* isolates is depicted in **Figures 6A,B**, respectively, highlighting the large variation in the potency of the isolates against *G. vaginalis* 594 and UPEC IH11128. Evaluation of the ability of the isolates to inhibit the adhesion of UPEC IH11128 onto human cervicovaginal epithelial HeLa cells by competition showed that cells of almost all isolates were able to prevent adhesion by UPEC IH11128 but with variable efficacy (**Figure 6C**). Plotting the killing activity in the presence of BHI versus the inhibition of adhesion by competition shows the lactic acid-dependent killing activity and competitive inhibition by *Lactobacillus* cells against UPEC IH11128 adhesion to be two properties that are widely distributed among *L. gasseri* and *L. crispatus* vaginal isolates (**Figure 6D**). Furthermore, plotting the killing activity measured in the presence of DMEM versus competitive inhibition by *Lactobacillus* cells against UPEC IH11128 adhesion shows that only a small number of *L. gasseri* vaginal isolates expressed lactic acid-independent killing activity dependent on released compound(s) (4 of the 14 isolates: isolates 1, 7, 10 and 14) (**Figure 6E**). In contrast, the lactic acid-independent killing activity dependent on released compound(s) appeared to be more widely expressed in *L. crispatus* vaginal isolates (5 of the 8 isolates: isolates 17, 18, 20, 21, and 22) (**Figure 6E**).

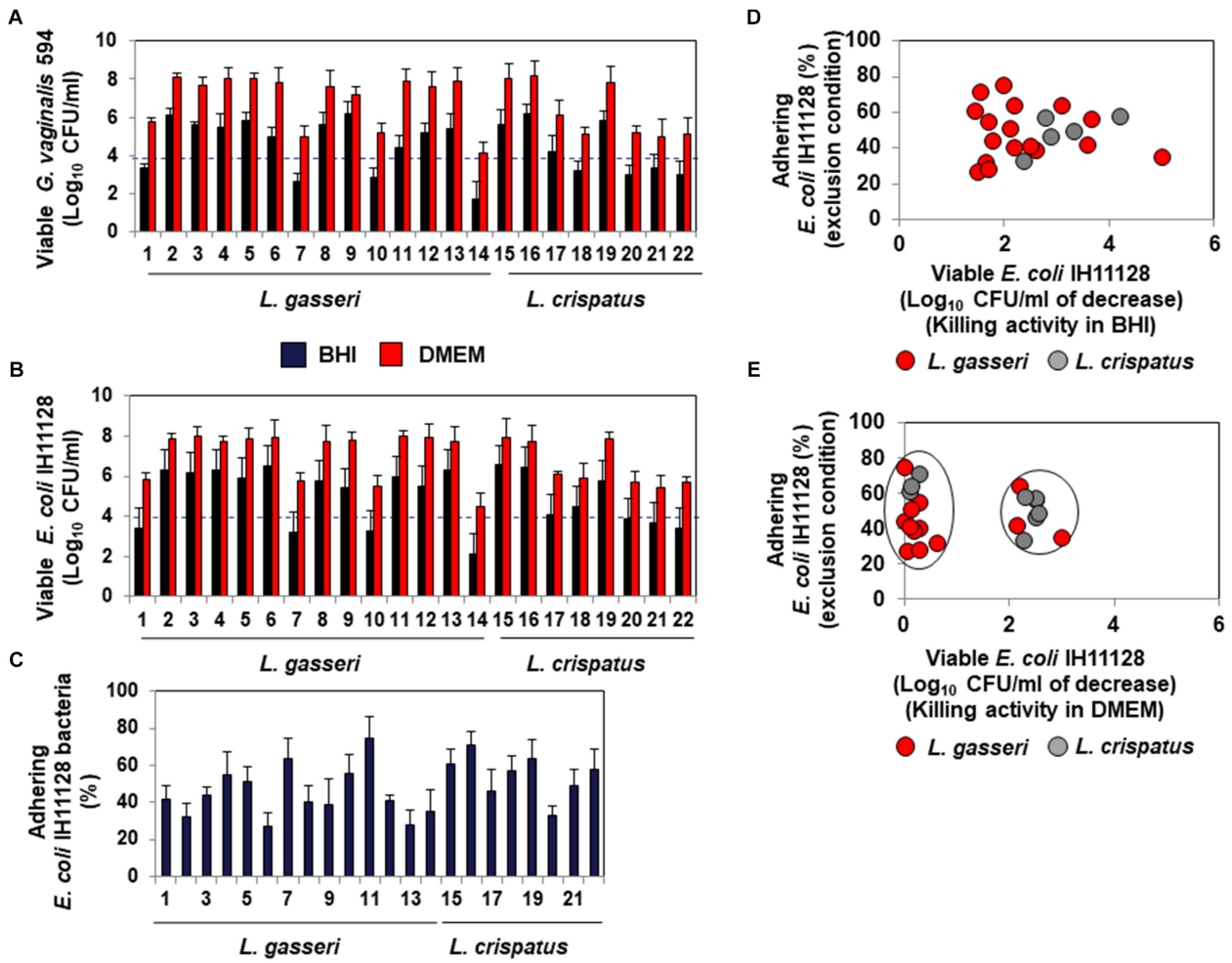

FIGURE 6 | Distribution of the killing activities and adhesion inhibition activity among *L. gasseri* and *L. crispatus* strains isolated from cervicovaginal samples of healthy women. **(A)** Killing activity against BV-associated *G. vaginalis* 594 was determined in the presence of BHI or DMEM. **(B)** Killing activity against recurrent cystitis- and preterm labor- associated UPEC IH11128 was determined in the presence of BHI or DMEM. **(C)** Competitive inhibition activity exerted by *L. gasseri* and *L. crispatus* strains against adhesion of UPEC IH11128 onto cervicovaginal epithelial HeLa cells. **(D)** Strain-by-strain expression of total killing activity (in the presence of BHI) versus inhibition of pathogen adhesion by *Lactobacillus* cells. **(E)** Strain-by-strain expression of killing activity independent of secreted lactic acid (in the presence of DMEM) versus inhibition of pathogen adhesion by *Lactobacillus* cells. In **(A,B)**, the killing activity was measured after 4 h of direct contact with the pathogens (Control: 5×10^8 CFU/ml). The dotted line shows the $MBE_{99.99\%}$ value, defined as a reduction in the viable cell count of 4 $\log_{10}$ CFU/ml. In C, the inhibition of adhesion was measured after 3 h of incubation. 100% UPEC IH11128 adhesion corresponds to 7.1 ± 0.7 CFU/ml. Each value shown is the mean ±SD from three experiments. Graphs in **(D,E)** were constructed by plotting the killing activities (measured in the presence of BHI or DMEM) shown in **Figure 1B** versus the exclusion inhibition activities shown in **Figure 1C**.

DISCUSSION

This study contributes to our understanding of the protective mechanisms provided by key members of the cervicovaginal microbiota against major microbial pathogens involved in BV and UTIs. We demonstrate that all cervicovaginal microbiota-associated *L. gasseri* and *L. crispatus* strains examined possess non-strain-specific physical and chemical defensive properties and that very few strains express strain-specifically properties. In the urogenital tract, *Lactobacillus* species largely contribute to the defense against microbial pathogens by secreting antimicrobial metabolites, mainly lactic acid, hydrogen peroxide, or proteinaceous or non-proteinaceous compounds (Servin, 2004; Spurbeck and Arvidson, 2011; Smith and Ravel, 2017). *In vivo*, vaginal microbiota-associated *Lactobacillus* species are the main source of the organic acid metabolite, lactic acid (Boskey et al., 2001), which is responsible for acidifying the cervicovaginal tract to a pH of ∼3.8–4.2 (Boskey et al., 1999; O'Hanlon et al., 2013). Moreover, lactic acid in its protonated form exerts broad antimicrobial activity against urogenital microbial pathogens *in vitro* and *in vivo* (Atassi and Servin, 2010; O'Hanlon et al., 2011, 2013; Breshears et al., 2015). Lactic acid has also been shown to permeabilize the bacterial outer membrane (Alakomi et al., 2000) and improve the bactericidal activity of hydrogen peroxide against Gram-negative pathogens *in vitro* (Atassi and Servin, 2010). Here, we show

that all strains of *L. gasseri* and *L. crispatus* tested had similar lactic acid-dependent killing activity against the four BV- and UTI-associated bacterial pathogens tested, consistent with the constitutive metabolic nature of lactic acid (Tachedjian et al., 2017). Hydrogen peroxide is secreted mostly by the resident *L. crispatus* strains of the cervicovaginal microbiota of healthy women (Eschenbach et al., 1989; Hillier et al., 1992, 1993). It is an antimicrobial molecule that exerts strong *in vitro* bactericidal activity against urogenital BV-associated *P. bivia*, *G. vaginalis*, and *E. coli* (Klebanoff et al., 1991; Strus et al., 2002, 2006; Atassi and Servin, 2010). Consistent with these findings, we found that 75% of the cervicovaginal *L. crispatus* isolates tested display hydrogen peroxide-dependent killing activity by direct contact, as well as against pre-adhering pathogens. The observed absence of killing of intracellular pathogens by the CFCS of the hydrogen peroxide-producing *L. crispatus* CTV-05 is certainly due to the previously demonstrated very poor transmembrane passage of hydrogen peroxide in cultured cells, including HeLa cells, due to a low membrane permeability close to that of water (Bienert et al., 2006; Lim et al., 2016). Importantly, the effectiveness of the antimicrobial effect of hydrogen peroxide in the vagina has been recently called into question (Tachedjian et al., 2018). First, hydrogen peroxide at the physiological concentrations present in the vagina has no antimicrobial effect against BV-associated microbial pathogens *in vitro* (O'Hanlon et al., 2010). Second, cervicovaginal fluid and semen have the capacity to neutralize its bactericidal activity *in vitro* (O'Hanlon et al., 2010), whereas, they do not affect lactic acid-dependent microbicidal activity (O'Hanlon et al., 2011).

We show that approximately 30% of *L. gasseri* vaginal isolates and *L. gasseri* KS 120.1, but not *L. gasseri* ATCC 9857, have a high level of non-lactic acid-dependent, non-hydrogen peroxide-dependent bactericidal activity against BV-associated bacteria and UPEC due to released compound(s). The observed absence of bactericidal activity of *L. gasseri* ATCC 9857 when tested in the presence of DMEM is in accordance with its previously reported absence of killing activity against UPEC isolates (Charteris et al., 2001) and gonococci (Spurbeck and Arvidson, 2008). We show that the released molecule(s) display the capacity to kill pre-adhering and pre-internalized bacterial pathogens. This is important, as it is well-known that internalized bacterial pathogens in the bladder can constitute an intracellular reservoir of dormant bacteria that can lead to the recurrence of infection following the exfoliation of infected cells from the urothelium (Hannan et al., 2012). Moreover, intracellular UPEC are difficult to eradicate by antibiotics (Blango and Mulvey, 2010) and subinhibitory concentrations of antibiotics enhance the formation of intracellular bacterial communities (Goneau et al., 2015). Thus, our data suggest that only certain strains of microbiota-associated *Lactobacillus* could provide strong protection against UTI recurrence by eliminating internalized UPEC.

A large variety of bacteriocins are encoded in the genomes of lactobacilli in a strain-specific manner (Acedo et al., 2018). *L. gasseri* ATCC 9857 has been shown to inhibit the growth of *E. coli* by compounds resembling gassericin C and D (Charteris et al., 2001). In accordance with this finding, we observed the inhibition of UPEC IH11128 growth by *L. gasseri* ATCC 9857. *L. crispatus* CTV-05 possesses seven class-II and class-III bacteriocin-related proteins (Ojala et al., 2014) and inhibits the growth of pyelonephritis-associated J96 and cystitis-associated R45 *E. coli* strains (Butler et al., 2016). Not surprisingly, we observed that its CFCS decreases the growth of UPEC IH11128. Our observation that KS 120.1 CFCS inhibits the growth of IH11128 confirms and supplements those of previous data study (Atassi et al., 2006b) and indicates the production of bacteriocins or bacteriocin-like molecules by this strain.

Bacterial biofilms are difficult to eradicate by antibiotic treatment (Blango and Mulvey, 2010) and subinhibitory concentrations of antibiotics increase UPEC biofilm formation (Goneau et al., 2015). The observed absence of activity is likely related to the fact that bacterial biofilms are formed by tight bacterial cell-to-cell contacts, making the biofilm matrix an impermeable barrier (Flemming et al., 2016). CFCSs of *L. gasseri* KS 120.1 and *L. crispatus* CTV-05 were unable to kill UPEC CFT073 bacteria within its pre-formed biofilm, despite exerting a killing activity against the free pathogen after direct contact. A limited capacity of *L. crispatus* ATCC 33820 to decrease the area, depth, and density of *G. vaginalis* biofilms has been reported (Saunders et al., 2007). In contrast, *L. crispatus* EX533959VC06 (Machado et al., 2013) and 24-9-7 (Breshears et al., 2015) and *L. gasseri* SF1109 (Zanfardino et al., 2017) are able to inhibit the growth of *G. vaginalis*, *Neisseria gonorrhoeae*, and UPEC within their biofilms. These results show that the capacity to counteract the biofilms of urogenital pathogenic bacteria is variably expressed among urogenital *L. gasseri* and *L. crispatus* strains.

Many strains of *Lactobacillus* spp. have been shown to interfere with bacterial pathogen colonization of urogenital epithelium through the adhesive properties of their bacterial cells (Spurbeck and Arvidson, 2011; Smith and Ravel, 2017). Cells of *L. gasseri* ATCC 9857 (Spurbeck and Arvidson, 2008) and KS 120.1 (Atassi et al., 2006a,b) and *L. crispatus* CTV-05 (Kwok et al., 2006; Antonio et al., 2009; Hemmerling et al., 2010; Butler et al., 2016) display adhesiveness or the capacity to colonize. We found that the cells of the *Lactobacillus* strains examined in this study are able to reduce the colonization of HeLa epithelial cells by *G. vaginalis* and UPEC under competition or exclusion conditions, with varying efficacy. Our observation that *L. gasseri* ATCC 9857 cells can inhibit the adhesion of UPEC IH11128 onto cervicovaginal epithelial cells is in accordance with a report by Spurbeck et al. (Spurbeck and Arvidson, 2008), showing that *L. gasseri* ATCC 9857 cells inhibited the association of *N. gonorrhoeae* with cells of the endometrial epithelial cell line Hec-1-B. *L. crispatus* CTV-05 cells have been shown to decrease the adhesion of pyelonephritis-associated J96 and cystitis-associated R45 *E. coli* onto vaginal epithelial cells (Butler et al., 2016). We similarly found that they are able to inhibit the association of *G. vaginalis* and UPEC with cervicovaginal epithelial cells. Our results showing that *L. gasseri* KS 120.1 cells inhibit the association of *G. vaginalis* and UPEC with epithelial cells under competition and exclusion conditions confirm and complement those of previous studies

(Atassi et al., 2006a,b). In contrast, we found that *L. gasseri* ATCC 9857, *L. gasseri* KS 120.1, and *L. crispatus* CTV-05 cells were unable to displace pathogens already adhering to the epithelial cells. This is not surprising, because bacterial pathogens often intimately or irreversibly associate with host target cells using adhesive factors that recognize membrane-associated molecules, acting as specific receptors (Berne et al., 2018).

We observed that pre-adhering *L. gasseri* ATCC 9857 and KS 120.1, and *L. crispatus* CTV-05 cells provide partial protection to the epithelial cells against the cytotoxic effects of the toxins vaginolysin and Sat produced by *G. vaginalis* and UPEC, respectively. Our result with pre-adhering *L. crispatus* CTV-05 cells are in accordance with a recent report showing that they have the capacity to attenuate the cytotoxic activity of pyelonephritis-associated J96 and cystitis-associated R45 *E. coli* expressing α-hemolysin (Butler et al., 2016). The observed partial protection by pre-adhering *Lactobacillus* cells is likely because vaginolysin (Gelber et al., 2008) and Sat (Guignot et al., 2007; Lievin-Le Moal et al., 2011) are secreted by the pathogens and therefore highly accessible to the epithelial cells, such that access cannot be prevented by the pre-adhering bacterial cells. In contrast, our results demonstrate that epithelial cells are fully protected against the deleterious effects of pathogen-secreted toxins if the toxin-producing bacterial pathogens are killed at the luminal domain of epithelial cells by a potent bactericidal activity strain-specifically produced by a *Lactobacillus* strain.

The increasing emergence of multi-drug resistant pathogenic bacteria requires the development of innovative therapeutic strategies (O'Brien et al., 2016; Tamadonfar et al., 2019). Importantly, our results provide evidence of high strain-level specificity of antimicrobial properties among cervicovaginal *L. gasseri* and *L. crispatus* strains, suggesting that the presence of one species in the vaginal microbiota is not sufficient to determine its benefits to the host. The development of biotherapeutic strategies based on *L. gasseri* and *L. crispatus* strains isolated from human vaginal microbiota of healthy women will require that the candidate strains be phenotypically well characterized. In particular, antimicrobial properties should be evaluated to determine whether the candidate strains possess a full repertory of potent antimicrobial properties to counteract the diverse deleterious effects of the targeted microbial pathogens. There is great interest in compounds with strong antibiotic-like activities that are released by *L. gasseri* of the urogenital microbiota for their development and application to women's health. However, the isolation and identification of such compounds has encountered several technical difficulties due to their small molecular mass and relative instability. New technologies, such as imaging mass spectrometry, hold promise for the future objective of identifying and designing more stable effective molecules.

DATA AVAILABILITY STATEMENT

The datasets generated for this study are available on request to the corresponding author.

AUTHOR CONTRIBUTIONS

VL-L led the project, guided the experiments, procured funding, and drafted the manuscript. FA, DP, and VL-L were involved in the experimental design, conducting the experiments, and collecting the data. All authors reviewed the manuscript.

FUNDING

This work has been funded in part by a Research service contract (N° 8521 0 – Principal investigator: VL-L) between University of Paris-Sud (CNRS URM 8076) and ProbioSwiss (CH-8005 Zürich, Switzerland). The funder has no role in the study design, data collection and analysis, decision to publish, or preparation of the manuscript. CNRS UMR 8076 BIOCIS and UMR-S 911 are members of LabEx LERMIT (Laboratoire d'Excellence en Recherche sur le Médicament et l'Innovation Thérapeutique), supported by a grant from the ANR (ANR-10-LABX-33).

ACKNOWLEDGMENTS

Because of the vast literature in this domain, we only selected specific citations and apologize to the authors whose work is not mentioned. We thank Jacques Ravel (Department of Microbiology and Immunology, University of Maryland School of Medicine, Baltimore, MD, United States) for his critical review of the manuscript.

REFERENCES

Acedo, J. Z., Chiorean, S., Vederas, J. C., and Van Belkum, M. J. (2018). The expanding structural variety among bacteriocins from Gram-positive bacteria. *FEMS Microbiol. Rev.* 42, 805–828. doi: 10.1093/femsre/fuy033

Alakomi, H. L., Skytta, E., Saarela, M., Mattila-Sandholm, T., Latva-Kala, K., and Helander, I. M. (2000). Lactic acid permeabilizes gram-negative bacteria by disrupting the outer membrane. *Appl. Environ. Microbiol.* 66, 2001–2005. doi: 10.1128/aem.66.5.2001-2005.2000

Amabebe, E., and Anumba, D. O. C. (2018). The Vaginal microenvironment: the physiologic role of Lactobacilli. *Front. Med.* 5:181. doi: 10.3389/fmed.2018.00181

Amegashie, C. P., Gilbert, N. M., Peipert, J. F., Allsworth, J. E., Lewis, W. G., and Lewis, A. L. (2017). Relationship between nugent score and vaginal epithelial exfoliation. *PLoS One* 12:e0177797. doi: 10.1371/journal.pone.0177797

Antonio, M. A., Hawes, S. E., and Hillier, S. L. (1999). The identification of vaginal Lactobacillus species and the demographic and microbiologic characteristics of women colonized by these species. *J. Infect. Dis.* 180, 1950–1956. doi: 10.1086/315109

Antonio, M. A., Meyn, L. A., Murray, P. J., Busse, B., and Hillier, S. L. (2009). Vaginal colonization by probiotic Lactobacillus crispatus CTV-05 is decreased by sexual activity and endogenous lactobacilli. *J. Infect. Dis.* 199, 1506–1513. doi: 10.1086/598686

Atassi, F., Brassart, D., Grob, P., Graf, F., and Servin, A. L. (2006a). *Lactobacillus* strains isolated from the vaginal microbiota of healthy women inhibit *Prevotella*

bivia and *Gardnerella vaginalis* in coculture and cell culture. *FEMS Immunol. Med. Microbiol.* 48, 424–432.

Atassi, F., Brassart, D., Grob, P., Graf, F., and Servin, A. L. (2006b). Vaginal Lactobacillus isolates inhibit uropathogenic *Escherichia coli*. *FEMS Microbiol. Lett.* 257, 132–138.

Atassi, F., and Servin, A. L. (2010). Individual and co-operative roles of lactic acid and hydrogen peroxide in the killing activity of enteric strain *Lactobacillus johnsonii* NCC933 and vaginal strain *Lactobacillus gasseri* KS120.1 against enteric, uropathogenic and vaginosis-associated pathogens. *FEMS Microbiol. Lett.* 304, 29–38. doi: 10.1111/j.1574-6968.2009.01887.x

Berne, C., Ellison, C. K., Ducret, A., and Brun, Y. V. (2018). Bacterial adhesion at the single-cell level. *Nat. Rev. Microbiol.* 16, 616–627. doi: 10.1038/s41579-018-0057-5

Bienert, G. P., Schjoerring, J. K., and Jahn, T. P. (2006). Membrane transport of hydrogen peroxide. *Biochim. Biophys. Acta* 1758, 994–1003. doi: 10.1016/j.bbamem.2006.02.015

Blango, M. G., and Mulvey, M. A. (2010). Persistence of uropathogenic *Escherichia coli* in the face of multiple antibiotics. *Antimicrob. Agents Chemother.* 54, 1855–1863. doi: 10.1128/AAC.00014-10

Boskey, E. R., Cone, R. A., Whaley, K. J., and Moench, T. R. (2001). Origins of vaginal acidity: high D/L lactate ratio is consistent with bacteria being the primary source. *Hum. Reprod.* 16, 1809–1813. doi: 10.1093/humrep/16.9.1809

Boskey, E. R., Telsch, K. M., Whaley, K. J., Moench, T. R., and Cone, R. A. (1999). Acid production by vaginal flora in vitro is consistent with the rate and extent of vaginal acidification. *Infect. Immun.* 67, 5170–5175.

Breshears, L. M., Edwards, V. L., Ravel, J., and Peterson, M. L. (2015). Lactobacillus crispatus inhibits growth of *Gardnerella vaginalis* and *Neisseria gonorrhoeae* on a porcine vaginal mucosa model. *BMC Microbiol.* 15:276. doi: 10.1186/s12866-015-0608-0

Butler, D. S. C., Silvestroni, A., and Stapleton, A. E. (2016). Cytoprotective effect of *Lactobacillus crispatus* CTV-05 against uropathogenic *E. coli*. *Pathogens* 5, 27–38.

Charteris, W. P., Kelly, P. M., Morelli, L., and Collins, J. K. (2001). Antibacterial activity associated with *Lactobacillus gasseri* ATCC 9857 from the human female genitourinary tract. *World J. Microbiol. Biotechnol.* 17, 615–625.

Chavagnat, F., Haueter, M., Jimeno, J., and Casey, M. G. (2002). Comparison of partial tuf gene sequences for the identification of lactobacilli. *FEMS Microbiol. Lett.* 217, 177–183. doi: 10.1016/s0378-1097(02)01072-8

De Seta, F., Campisciano, G., Zanotta, N., Ricci, G., and Comar, M. (2019). The vaginal community state types microbiome-immune network as key factor for bacterial vaginosis and aerobic vaginitis. *Front. Microbiol.* 10:2451. doi: 10.3389/fmicb.2019.02451

De Vrese, M., Laue, C., Papazova, E., Petricevic, L., and Schrezenmeir, J. (2019). Impact of oral administration of four *Lactobacillus* strains on Nugent score - systematic review and meta-analysis. *Benef. Microbes* 10, 483–496. doi: 10.3920/BM2018.0129

Eschenbach, D. A., Davick, P. R., Williams, B. L., Klebanoff, S. J., Young-Smith, K., Critchlow, C. M., et al. (1989). Prevalence of hydrogen peroxide-producing *Lactobacillus* species in normal women and women with bacterial vaginosis. *J. Clin. Microbiol.* 27, 251–256.

FAO/WHO (2002). Joint FAO/WHO Expert Consultation on Evaluation of Health and Nutritional Properties of Probiotics in Food including Powder Milk with Live Lactic Acid Bacteria. Available at: www.fao.org/documents/pub_dett.asp?lang=en&pub_id=61756

Fayol-Messaoudi, D., Berger, C. N., Coconnier-Polter, M. H., Lievin-Le Moal, V., and Servin, A. L. (2005). pH-, Lactic acid-, and non-lactic acid-dependent activities of probiotic lactobacilli against *Salmonella enterica* Serovar Typhimurium. *Appl. Environ. Microbiol.* 71, 6008–6013. doi: 10.1128/aem.71.10.6008-6013.2005

FDA (2016). *Guidance for Industry Early Clinical Trials With Live Biotherapeutic Products: Chemistry, Manufacturing, and Control Information*. Available at: www.fda.gov/downloads/BiologicsBloodVaccines/GuidanceComplianceRegulatoryInformation/Guidances/General/UCM292704.pdf

Flemming, H. C., Wingender, J., Szewzyk, U., Steinberg, P., Rice, S. A., and Kjelleberg, S. (2016). Biofilms: an emergent form of bacterial life. *Nat. Rev. Microbiol.* 14, 563–575. doi: 10.1038/nrmicro.2016.94

Flores-Mireles, A. L., Walker, J. N., Caparon, M., and Hultgren, S. J. (2015). Urinary tract infections: epidemiology, mechanisms of infection and treatment options. *Nat. Rev. Microbiol.* 13, 269–284. doi: 10.1038/nrmicro3432

Foxman, B. (2014). Urinary tract infection syndromes: occurrence, recurrence, bacteriology, risk factors, and disease burden. *Infect. Dis. Clin. North Am.* 28, 1–13. doi: 10.1016/j.idc.2013.09.003

Foxman, B., and Buxton, M. (2013). Alternative approaches to conventional treatment of acute uncomplicated urinary tract infection in women. *Curr. Infect. Dis. Rep.* 15, 124–129. doi: 10.1007/s11908-013-0317-5

Geerlings, S. E., Beerepoot, M. A., and Prins, J. M. (2014). Prevention of recurrent urinary tract infections in women: antimicrobial and nonantimicrobial strategies. *Infect. Dis. Clin. North Am.* 28, 135–147. doi: 10.1016/j.idc.2013.10.001

Gelber, S. E., Aguilar, J. L., Lewis, K. L., and Ratner, A. J. (2008). Functional and phylogenetic characterization of vaginolysin, the human-specific cytolysin from *Gardnerella vaginalis*. *J. Bacteriol.* 190, 3896–3903. doi: 10.1128/JB.01965-07

Gilbert, N. M., O'brien, V. P., and Lewis, A. L. (2017). Transient microbiota exposures activate dormant *Escherichia coli* infection in the bladder and drive severe outcomes of recurrent disease. *PLoS Pathog.* 13:e1006238. doi: 10.1371/journal.ppat.1006238

Goneau, L. W., Hannan, T. J., Macphee, R. A., Schwartz, D. J., Macklaim, J. M., Gloor, G. B., et al. (2015). Subinhibitory antibiotic therapy alters recurrent urinary tract infection pathogenesis through modulation of bacterial virulence and host immunity. *mBio* 6:e00356-e1. doi: 10.1128/mBio.00356-15

Guignot, J., Chaplais, C., Coconnier-Polter, M. H., and Servin, A. L. (2007). The secreted autotransporter toxin, Sat, functions as a virulence factor in Afa/Dr diffusely adhering *Escherichia coli* by promoting lesions in tight junction of polarized epithelial cells. *Cell Microbiol.* 9, 204–221. doi: 10.1111/j.1462-5822.2006.00782.x

Hannan, T. J., Totsika, M., Mansfield, K. J., Moore, K. H., Schembri, M. A., and Hultgren, S. J. (2012). Host-pathogen checkpoints and population bottlenecks in persistent and intracellular uropathogenic *Escherichia coli* bladder infection. *FEMS Microbiol. Rev.* 36, 616–648. doi: 10.1111/j.1574-6976.2012.00339.x

Hanson, L., Vandevusse, L., Jerme, M., Abad, C. L., and Safdar, N. (2016). Probiotics for treatment and prevention of urogenital infections in women: a systematic review. *J. Midwifery Womens Health* 61, 339–355. doi: 10.1111/jmwh.12472

Hemmerling, A., Harrison, W., Schroeder, A., Park, J., Korn, A., Shiboski, S., et al. (2010). Phase 2a study assessing colonization efficiency, safety, and acceptability of *Lactobacillus crispatus* CTV-05 in women with bacterial vaginosis. *Sex. Transm. Dis.* 37, 745–750. doi: 10.1097/OLQ.0b013e3181e50026

Hill, C., Guarner, F., Reid, G., Gibson, G. R., Merenstein, D. J., Pot, B., et al. (2014). Expert consensus document. The international scientific association for probiotics and prebiotics consensus statement on the scope and appropriate use of the term probiotic. *Nat. Rev. Gastroenterol. Hepatol.* 11, 506–514. doi: 10.1038/nrgastro.2014.66

Hillier, S. L., Krohn, M. A., Klebanoff, S. J., and Eschenbach, D. A. (1992). The relationship of hydrogen peroxide-producing lactobacilli to bacterial vaginosis and genital microflora in pregnant women. *Obstet. Gynecol.* 79, 369–373. doi: 10.1097/00006250-199203000-00008

Hillier, S. L., Krohn, M. A., Rabe, L. K., Klebanoff, S. J., and Eschenbach, D. A. (1993). The normal vaginal flora, H2O2-producing lactobacilli, and bacterial vaginosis in pregnant women. *Clin. Infect. Dis.* 16(Suppl. 4), S273–S281. doi: 10.1097/00006250-199203000-00008

Kandler, O., and Weiss, N. (1986). "Lactobacillus," in *Bergey's Manual of Systematic Bacteriology*, eds P. H. A. Sneath, N. S. Mair, M. E. Sharpe, and J. G. Holt, (Baltimore, MD: Williams and Wilkins), 1209–1234.

Klebanoff, S. J., Hillier, S. L., Eschenbach, D. A., and Waltersdorph, A. M. (1991). Control of the microbial flora of the vagina by H2O2-generating lactobacilli. *J. Infect. Dis.* 164, 94–100. doi: 10.1093/infdis/164.1.94

Kwok, L., Stapleton, A. E., Stamm, W. E., Hillier, S. L., Wobbe, C. L., and Gupta, K. (2006). Adherence of *Lactobacillus crispatus* to vaginal epithelial cells from women with or without a history of recurrent urinary tract infection. *J. Urol.* 176, 2050–2054. doi: 10.1016/j.juro.2006.07.014

Levison, M. E., and Levison, J. H. (2009). Pharmacokinetics and pharmacodynamics of antibacterial agents. *Infect. Dis. Clin. North Am.* 23, 791–815. doi: 10.1016/j.idc.2009.06.008

Lievin-Le Moal, V., Comenge, Y., Ruby, V., Amsellem, R., Nicolas, V., and Servin, A. L. (2011). Secreted autotransporter toxin (Sat) triggers autophagy in epithelial cells that relies on cell detachment. *Cell Microbiol.* 13, 992–1013. doi: 10.1111/j.1462-5822.2011.01595.x

Lim, J. B., Langford, T. F., Huang, B. K., Deen, W. M., and Sikes, H. D. (2016). A reaction-diffusion model of cytosolic hydrogen peroxide. *Free Radic. Biol. Med.* 90, 85–90. doi: 10.1016/j.freeradbiomed.2015.11.005

Luterbach, C. L., Forsyth, V. S., Engstrom, M. D., and Mobley, H. L. T. (2018). TosR-mediated regulation of adhesins and biofilm formation in uropathogenic *Escherichia coli*. *mSphere* 3:e00222-18. doi: 10.1128/mSphere.00222-18

Machado, A., Jefferson, K. K., and Cerca, N. (2013). Interactions between *Lactobacillus crispatus* and bacterial vaginosis (BV)-associated bacterial species in initial attachment and biofilm formation. *Int. J. Mol. Sci.* 14, 12004–12012. doi: 10.3390/ijms140612004

MacPhee, R. A., Hummelen, R., Bisanz, J. E., Miller, W. L., and Reid, G. (2010). Probiotic strategies for the treatment and prevention of bacterial vaginosis. *Expert Opin. Pharmacother.* 11, 2985–2995. doi: 10.1517/14656566.2010.512004

Mobley, H. L., Green, D. M., Trifillis, A. L., Johnson, D. E., Chippendale, G. R., Lockatell, C. V., et al. (1990). Pyelonephritogenic *Escherichia coli* and killing of cultured human renal proximal tubular epithelial cells: role of hemolysin in some strains. *Infect. Immun.* 58, 1281–1289.

Mobley, H. L. T. (2016). Measuring *Escherichia coli* gene expression during human urinary tract infections. *Pathogens* 5:E7. doi: 10.3390/pathogens5010007

Mulvey, M. A., Schilling, J. D., Martinez, J. J., and Hultgren, S. J. (2000). Bad bugs and beleaguered bladders: interplay between uropathogenic *Escherichia coli* and innate host defenses. *Proc. Natl. Acad. Sci. U.S.A.* 97, 8829–8835. doi: 10.1073/pnas.97.16.8829

Nowicki, B., Barrish, J. P., Korhonen, T., Hull, R. A., and Hull, S. I. (1987). Molecular cloning of the *Escherichia coli* O75X adhesin. *Infect. Immun.* 55, 3168–3173.

O'Brien, V. P., Hannan, T. J., Nielsen, H. V., and Hultgren, S. J. (2016). Drug and vaccine development for the treatment and prevention of urinary tract infections. *Microbiol. Spectr.* 4, doi: 10.1128/microbiolspec.UTI-0013-2012

O'Hanlon, D. E., Lanier, B. R., Moench, T. R., and Cone, R. A. (2010). Cervicovaginal fluid and semen block the microbicidal activity of hydrogen peroxide produced by vaginal lactobacilli. *BMC Infect. Dis.* 10:120. doi: 10.1186/1471-2334-10-120

O'Hanlon, D. E., Moench, T. R., and Cone, R. A. (2011). In vaginal fluid, bacteria associated with bacterial vaginosis can be suppressed with lactic acid but not hydrogen peroxide. *BMC Infect. Dis.* 11:200. doi: 10.1186/1471-2334-11-200

O'Hanlon, D. E., Moench, T. R., and Cone, R. A. (2013). Vaginal pH and microbicidal lactic acid when lactobacilli dominate the microbiota. *PLoS One* 8:e80074. doi: 10.1371/journal.pone.0080074

Ojala, T., Kankainen, M., Castro, J., Cerca, N., Edelman, S., Westerlund-Wikstrom, B., et al. (2014). Comparative genomics of *Lactobacillus crispatus* suggests novel mechanisms for the competitive exclusion of *Gardnerella vaginalis*. *BMC Genomics* 15:1070. doi: 10.1186/1471-2164-15-1070

Onderdonk, A. B., Delaney, M. L., and Fichorova, R. N. (2016). The human microbiome during bacterial vaginosis. *Clin. Microbiol. Rev.* 29, 223–238. doi: 10.1128/CMR.00075-15

Petrova, M. I., Van Den Broek, M., Balzarini, J., Vanderleyden, J., and Lebeer, S. (2013). Vaginal microbiota and its role in HIV transmission and infection. *FEMS Microbiol. Rev.* 37, 762–792. doi: 10.1111/1574-6976.12029

Ravel, J., Gajer, P., Abdo, Z., Schneider, G. M., Koenig, S. S., Mcculle, S. L., et al. (2011). Vaginal microbiome of reproductive - age women. *Proc. Natl. Acad. Sci. U.S.A.* 108, 4680–4687. doi: 10.1073/pnas.1002611107

Reid, G. (2017). The development of probiotics for women's health. *Can. J. Microbiol.* 63, 269–277. doi: 10.1139/cjm-2016-0733

Romero, R., Hassan, S. S., Gajer, P., Tarca, A. L., Fadrosh, D. W., Nikita, L., et al. (2014). The composition and stability of the vaginal microbiota of normal pregnant women is different from that of non-pregnant women. *Microbiome* 2:4. doi: 10.1186/2049-2618-2-4

Saunders, S., Bocking, A., Challis, J., and Reid, G. (2007). Effect of Lactobacillus challenge on *Gardnerella vaginalis* biofilms. *Coll. Surf. B Biointerf.* 55, 138–142. doi: 10.1016/j.colsurfb.2006.11.040

Servin, A. L. (2004). Antagonistic activities of lactobacilli and bifidobacteria against microbial pathogens. *FEMS Microbiol. Rev.* 28, 405–440. doi: 10.1016/j.femsre.2004.01.003

Servin, A. L. (2014). Pathogenesis of human diffusely adhering *Escherichia coli* expressing Afa/Dr adhesins (Afa/Dr DAEC): current insights and future challenges. *Clin. Microbiol. Rev.* 27, 823–869. doi: 10.1128/CMR.00036-14

Smith, S. B., and Ravel, J. (2017). The vaginal microbiota, host defence and reproductive physiology. *J. Physiol.* 595, 451–463. doi: 10.1113/JP271694

Spurbeck, R. R., and Arvidson, C. G. (2008). Inhibition of *Neisseria gonorrhoeae* epithelial cell interactions by vaginal *Lactobacillus* species. *Infect. Immun.* 76, 3124–3130. doi: 10.1128/IAI.00101-08

Spurbeck, R. R., and Arvidson, C. G. (2011). Lactobacilli at the front line of defense against vaginally acquired infections. *Fut. Microbiol.* 6, 567–582. doi: 10.2217/fmb.11.36

Standards, N. C. F. C. L. (1999). *Methods for Determining Bactericidal Activity of Antimicrobial Agents. Approved Guideline*. Wyane, PA: Clinical and Laboratory Standards Institute.

Strus, M., Brzychczy-Wloch, M., Gosiewski, T., Kochan, P., and Heczko, P. B. (2006). The in vitro effect of hydrogen peroxide on vaginal microbial communities. *FEMS Immunol. Med. Microbiol.* 48, 56–63. doi: 10.1111/j.1574-695x.2006.00120.x

Strus, M., Malinowska, M., and Heczko, P. B. (2002). In vitro antagonistic effect of *Lactobacillus* on organisms associated with bacterial vaginosis. *J. Reprod. Med.* 47, 41–46.

Tachedjian, G., Aldunate, M., Bradshaw, C. S., and Cone, R. A. (2017). The role of lactic acid production by probiotic Lactobacillus species in vaginal health. *Res. Microbiol.* 168, 782–792. doi: 10.1016/j.resmic.2017.04.001

Tachedjian, G., O'hanlon, D. E., and Ravel, J. (2018). The implausible "in vivo" role of hydrogen peroxide as an antimicrobial factor produced by vaginal microbiota. *Microbiome* 6:29. doi: 10.1186/s40168-018-0418-3

Tamadonfar, K. O., Omattage, N. S., Spaulding, C. N., and Hultgren, S. J. (2019). Reaching the end of the line: urinary tract infections. *Microbiol. Spectr.* 7, doi: 10.1128/microbiolspec.BAI-0014-2019

Tamarelle, J., Thiebaut, A. C. M., De Barbeyrac, B., Bebear, C., Ravel, J., and Delarocque-Astagneau, E. (2019). The vaginal microbiota and its association with human papillomavirus, *Chlamydia trachomatis*, *Neisseria gonorrhoeae* and *Mycoplasma genitalium* infections: a systematic review and meta-analysis. *Clin. Microbiol. Infect.* 25, 35–47. doi: 10.1016/j.cmi.2018.04.019

Thomas-White, K., Forster, S. C., Kumar, N., Van Kuiken, M., Putonti, C., Stares, M. D., et al. (2018). Culturing of female bladder bacteria reveals an interconnected urogenital microbiota. *Nat. Commun.* 9:1557. doi: 10.1038/s41467-018-03968-5

van de Wijgert, J., and Verwijs, M. C. (2019). Lactobacilli-containing vaginal probiotics to cure or prevent bacterial or fungal vaginal dysbiosis: a systematic review and recommendations for future trial designs. *BJOG* doi: 10.1111/1471-0528.15870 [Epub ahead of print].

Verstraelen, H., and Swidsinski, A. (2019). The biofilm in bacterial vaginosis: implications for epidemiology, diagnosis and treatment: 2018 update. *Curr. Opin. Infect. Dis.* 32, 38–42. doi: 10.1097/QCO.0000000000000516

Whiteside, S. A., Razvi, H., Dave, S., Reid, G., and Burton, J. P. (2015). The microbiome of the urinary tract - a role beyond infection. *Nat. Rev. Urol.* 12, 81–90. doi: 10.1038/nrurol.2014.361

Yeoman, C. J., Yildirim, S., Thomas, S. M., Durkin, A. S., Torralba, M., Sutton, G., et al. (2010). Comparative genomics of *Gardnerella vaginalis* strains reveals substantial differences in metabolic and virulence potential. *PLoS One* 5:e12411. doi: 10.1371/journal.pone.0012411

Zanfardino, A., Criscuolo, G., Di Luccia, B., Pizzo, E., Ciavatta, M. L., Notomista, E., et al. (2017). Identification of a new small bioactive peptide from *Lactobacillus gasseri* supernatant. *Benef. Microbes* 8, 133–141. doi: 10.3920/BM2016.0098

Conflict of Interest: VL-L is principal investigator of Contract N° 852 1 between University Paris-Sud and ProbioSwiss.

The remaining authors declare that the research was conducted in the absence of any commercial or financial relationships that could be construed as a potential conflict of interest.

frontiers in Microbiology

ORIGINAL RESEARCH
published: 19 May 2020
doi: 10.3389/fmicb.2020.00894

Exopolysaccharides From *Streptococcus thermophilus* ST538 Modulate the Antiviral Innate Immune Response in Porcine Intestinal Epitheliocytes

Hiroya Mizuno[1,2†], Kae Tomotsune[1,2†], Md. Aminul Islam[1,2,3‡], Ryutaro Funabashi[1,2], Leonardo Albarracin[1,4,5], Wakako Ikeda-Ohtsubo[1,2], Hisashi Aso[2,6], Hideki Takahashi[7,8], Katsunori Kimura[9], Julio Villena[1,4], Yasuko Sasaki[10] and Haruki Kitazawa[1,2]**

[1] Food and Feed Immunology Group, Laboratory of Animal Products Chemistry, Graduate School of Agricultural Science, Tohoku University, Sendai, Japan, [2] Livestock Immunology Unit, International Education and Research Center for Food and Agricultural Immunology (CFAI), Graduate School of Agricultural Science, Tohoku University, Sendai, Japan, [3] Department of Medicine, Faculty of Veterinary Science, Bangladesh Agricultural University, Mymensingh, Bangladesh, [4] Laboratory of Immunobiotechnology, Reference Centre for Lactobacilli (CERELA-CONICET), San Miguel de Tucumán, Argentina, [5] Scientific Computing Laboratory, Computer Science Department, Faculty of Exact Sciences and Technology, National University of Tucuman, San Miguel de Tucumán, Argentina, [6] Laboratory of Animal Health Science, Graduate School of Agricultural Science, Tohoku University, Sendai, Japan, [7] Laboratory of Plant Pathology, Graduate School of Agricultural Science, Tohoku University, Sendai, Japan, [8] Plant Immunology Unit, International Education and Research Center for Food and Agricultural Immunology (CFAI), Graduate School of Agricultural Science, Tohoku University, Sendai, Japan, [9] Food Microbiology and Function Research Laboratories, Meiji Co., Ltd., Kanagawa, Japan, [10] Laboratory of Fermented Foods, Graduate School of Agriculture, Meiji University, Kanagawa, Japan

It was reported that exopolysaccharides (EPSs) from lactobacilli are able to differentially modulate mucosal antiviral immunity. Although research has described the ability of EPSs derived from *Streptococcus thermophilus* to modulate the mucosal immune system, their impact on antiviral immunity was less explored. In this work, we investigated the capacity of the EPS-producing *S. thermophilus* ST538 to modulate the innate antiviral immune response triggered by the activation of the Toll-like receptor 3 (TLR3) in porcine intestinal epitheliocytes (PIE cells). Moreover, in order to study the immunomodulatory potential of *S. thermophilus* ST538 EPS, we successfully developed two mutant strains through the knockout of the *epsB* or *epsC* genes. High-performance liquid chromatography and scanning electron microscopy studies demonstrated that the wild type (WT) strain produced as high as 595 μg/ml of EPS in the skim milk medium, while none of the mutant strains (*S. thermophilus* Δ*epsB* and Δ*epsC*) were able to produce EPS. Studies in PIE cells demonstrated that the EPS of *S. thermophilus* ST538 is able to significantly improve the expression of interferon β (*IFN*-β), interleukin 6 (*IL-6*), and C-X-C motif chemokine 10 (*CXCL10*) in response to TLR3 stimulation. The role of EPS in the modulation of antiviral immune response in PIE cells was confirmed by comparative studies of cell free culture supernatants and fermented skim

OPEN ACCESS

Edited by:
Konstantinos Papadimitriou, Agricultural University of Athens, Greece

Reviewed by:
Diego Mora, University of Milan, Italy
Franca Rossi, Istituto Zooprofilattico Sperimentale dell'Abruzzo e del Molise "Giuseppe Caporale", Italy

***Correspondence:**
Yasuko Sasaki
y_sasaki@meiji.ac.jp
Haruki Kitazawa
haruki.kitazawa.c7@tohoku.ac.jp

[†]*These authors have contributed equally to this work*

[‡]*JSPS Postdoctoral Fellow*

Specialty section:
This article was submitted to Food Microbiology, a section of the journal Frontiers in Microbiology

Received: *21 January 2020*
Accepted: *16 April 2020*
Published: *19 May 2020*

Citation:
Mizuno H, Tomotsune K, Islam MA, Funabashi R, Albarracin L, Ikeda-Ohtsubo W, Aso H, Takahashi H, Kimura K, Villena J, Sasaki Y and Kitazawa H (2020) Exopolysaccharides From Streptococcus thermophilus ST538 Modulate the Antiviral Innate Immune Response in Porcine Intestinal Epitheliocytes. Front. Microbiol. 11:894. doi: 10.3389/fmicb.2020.00894

milks obtained from *S. thermophilus* Δ*epsB* and Δ*epsC*. These results suggest that *S. thermophilus* ST538 could be used as an immunobiotic strain for the development of new immunologically functional foods, which might contribute to improve resistance against viral infections.

Keywords: *Streptococcus thermophilus* ST538, exopolysaccharides, *epsB*, *epsC*, gene-knockout, PIE cells, antiviral immunity

INTRODUCTION

Streptococcus thermophilus is a Gram-positive, non-pathogenic lactic acid bacterium, commonly used as starter culture for yogurt manufacturing. Several strains of *S. thermophilus* have been shown to produce exopolysaccharides (EPS). Since it is naturally produced by a microorganism with the "generally regarded as safe" status, EPS produced by *S. thermophilus* is considered to be safe and therefore, it has been widely used to improve rheological and sensory attributes of fermented food products (Petersen et al., 2000; Fialho et al., 2008; Iyer et al., 2010; Caggianiello et al., 2016). The EPS production among the majority of *S. thermophilus* strains varies from 20 to 600 μg/ml in milk-based medium under optimum conditions (Petersen et al., 2000; Vaningelgem et al., 2004). Therefore, the dairy industry has been interested in the search and study of strains capable of the greatest production of EPS.

Structurally, the EPS produced by *S. thermophilus* are heteropolysaccharides made up of oligosaccharide repeating unit synthetized in the cytoplasm by the action of a number of glycosyltransferases and branched chains containing glucose and galactose, rhamnose and sometimes N-acetyl-glucosamine and fucose (Doco et al., 1990; Petit et al., 1991; Dan et al., 2009). Genome-scale studies revealed that the EPS biosynthetic pathway in *S. thermophilus* involves the sugar uptake system, nucleotide sugar synthesis, polysaccharide synthesis, and export of EPS, which are controlled by several housekeeping genes and a cluster of EPS-related genes (Laws et al., 2001; Wu et al., 2014; Cui et al., 2017; Alexandraki et al., 2019; Xiong et al., 2019). In lactic acid bacteria (LAB), the typical EPS gene cluster was described to contain five highly conserved genes *epsA*, *epsB*, *epsC*, *epsD*, and *epsE*, and a variable region, which includes the genes for polymerases, flippases, and a variable number of glycosyltransferases and other modifying enzymes [reviewed in Zeidan et al. (2017)]. It has been shown that the phosphoregulatory system, constituted by *epsB*, *epsC*, and *epsD*, is responsible for the control of the polysaccharide assembly machinery (Yother, 2011; Grangeasse, 2016). Recent genomic studies have demonstrated a similar organization in the EPS clusters of *S. thermophilus* (Alexandraki et al., 2019). Although the genome analysis of several *S. thermophilus* strains revealed variable sizes in the EPS gene clusters, the 5′ and the 3′ ends were highly conserved and their differences are located mainly in the middle of the clusters. Moreover, the *epsA*, *epsB*, *epsC*, and *epsD* genes were found at the 5′ end in all the EPS gene clusters studied (Alexandraki et al., 2019).

In the last decades, EPS produced by beneficial bacteria have received attention because of their contribution to health maintenance (Laiño et al., 2016). Some recent studies demonstrated that EPS produced by probiotic bacteria are able to modulate the systemic and mucosal immune responses, and in turn to provide direct health-promoting benefits. In this regard, EPS-producing strains such as *S. thermophilus* ST1342, ST1275, and ST285 have shown to exert immunomodulatory effects on acute ulcerative colitis and to have the ability to improve the intestinal barrier function restricting adhesion and invasion of pathogens (Purwandari and Vasiljevic, 2009; Kebouchi et al., 2016). It was demonstrated that the purified EPS produced by *S. thermophilus* MN-BM-A01 protected the intestinal barrier integrity after the challenge with LPS and significantly reduced the expression of pro-inflammatory cytokines in a murine model of colitis induced by dextran sulfate sodium (DSS) (Chen et al., 2019). Marcial et al. (2017) reported that *S. thermophilus* CRL1190 and its EPS are able to adhere to the stomach gastric mucosa, reduce the adhesion of the pathogen *Helicobacter pylori* and significantly diminish the expression of pro-inflammatory factors. Although research has described the ability of EPSs derived from *S. thermophilus* to modulate the mucosal immune system in the contexts of inflammation and bacterial infections, their impact on antiviral immunity was less explored.

Taking into consideration that the EPS produced by lactobacilli have been shown to beneficially modulate the systemic and mucosal antiviral responses and to reduce the severity of viral infections (Kitazawa et al., 1998; Makino et al., 2006, 2010, 2016; Nagai et al., 2011; Kanmani et al., 2018a,b), the aim of this work was to evaluate whether the EPS-producing *S. thermophilus* ST538 or its EPS were able to modulate the innate antiviral immune response triggered by the activation of the Toll-like receptor 3 (TLR3) in porcine intestinal epitheliocytes (PIE cells). Moreover, in order to conclusively demonstrate the role of the EPS in the immunomodulatory effect of the ST538 EPS strain, two mutant strains for the *epsB* or *epsC* genes were successfully developed.

MATERIALS AND METHODS

Bacteria Strain and Growth Conditions

Streptococcus thermophilus ST538 was obtained from the Food Research and Development Center, Meiji Dairies Corporation (Tokyo, Japan). This strain has been used for the commercial production of yogurt because of its great capacity of acidification when compared to other strains of the same species. *S. thermophilus* ST538 was cultured at 37°C for 16 h in M17 broth medium (Becton, Dickinson and Co., Franklin Lakes, New Zealand) supplemented with 1% of lactose (LM17 medium) or skim milk medium.

The LM17 broth medium was used for genetic manipulation and bacterial stimulation experiments. The stock bacteria cultures were inoculated at 1% (vol/vol) in fresh LM17 medium at 37°C for 16 h. These cultures were also used for inoculation of LM17 medium.

The skim milk medium was used for EPS extraction and quantification. *S. thermophilus* was cultured in skim milk medium supplemented with 2% (vol/vol) casamino acid (Nippon Shinyaku Ltd., Kyoto, Japan) or 0.1% peptide from casein hydrolysates (CE90GMM, Nippon Shinyaku Ltd., Kyoto, Japan). In the case of skim milk medium with casamino acid, the stock bacteria cultures were inoculated at 1% (vol/vol) into skim milk medium that was prepared with 10% (vol/vol) of skim milk powder and 0.05% (vol/vol) yeast extract (Oxoid Limited, United Kingdom) in water and sterilized at 121°C for 7 min. The cultures were maintained at 37°C for 16 h. These cultures were used for inoculation of the skim milk medium supplemented with 2% (vol/vol) casamino acid at 43°C. The preparation and sterilization of skim milk medium was performed according to the method described by Kitazawa et al. (1998). *S. thermophilus* was also cultured in the skim milk medium with 0.1% peptide from casein hydrolysates that was sterilized at 95°C for 2 min for EPS quantification. The preparation and sterilization of skim milk medium was performed according to the method described by Yamauchi et al. (2019).

Sequence Analysis of epsAD Fragment of *S. thermophilus* ST538

According to Kyoto Encyclopedia of Genes and Genomes (KEGG), the sequences of the *epsA-B-C-D* genes of the EPS locus are highly conserved among *S. thermophilus* strains. The DNA fragment corresponding to this region, called *epsAD* fragment, was amplified and sequenced with primers LAB276 and LAB277 (**Table 1** and **Figure 1**). The DNA sequences were analyzed by Genetic Analyzer (3130, Applied Biosystems). The sequences were submitted to GeneBank under the accession numbers LC529489, LC529490, LC529491, and LC529492.

Development of *S. thermophilus* ST538 epsB and epsC Knockout Mutants

The construction of the *epsB*- and *epsC*-knockout mutants (*S. thermophilus*Δ*epsB* and *S. thermophilus*Δ*epsC*, respectively) from wild type *S. thermophilus* ST538 (*S. thermophilus* WT) was performed according to the method described by Yamauchi et al. (2019). Briefly, the 351-bp in-frame deletion of *epsB* was obtained by PCR using primers LAB363 and LAB364, and then the primers LAB365 and LAB366 (**Table 1** and **Figure 1**). Those fragments were combined by overlap extension PCR using primers LAB363 and LAB366 (**Table 1** and **Figure 1**). This combined fragment was digested by *Bam*HI and *Xho*I, and inserted to a thermo-sensitive replicon containing plasmid pG$^+$host6 (Appligene, Pleasanton, CA, United States) (**Table 2**) using the DNA Ligation Kit Ver1 (Takara Bio Inc., Tokyo, Japan) to generate the pG$^+$epsB plasmid. This vector construction was performed in *Escherichia coli* TG1. The pG$^+$epsB plasmid was first electroporated into *Lactococcus lactis* IL1403 followed by electroporation into *S. thermophilus* ST538. Similarly, the 351-bp in-frame deletion of *epsC* was obtained using primers LAB367, LAB368, LAB369, and LAB370 (**Table 1** and **Figure 1**), and pG$^+$epsC was electroporated into *S. thermophilus* ST538 following same protocol described for pG$^+$epsB. Finally, the double crossover event was performed according to the method described by Biswas et al. (1993). The deletion 351-bp from the genome of *S. thermophilus*Δ*epsB* and Δ*epsC* knockout mutants were confirmed by sequence analysis.

TABLE 1 | The list of the primers used for mutants development.

Primer	Sequence
LAB276	GAAATGAGCATCGTGGTTCC
LAB277	CGATGTGCTCTTGAATGACC
LAB278	CTACTGGGTTTGCAGAGTTG
LAB279	GCACGAATTAACTTCACATC
LAB280	CAACAGAGCTAATCGCAATC
LAB281	GTCCTATTCCACCTAATCCAAC
LAB284	GGAAAGTGCCTCTCAAGCTATC
LAB285	CGTTGTGACATCTTCAACTTTTGTCACCTTC
LAB286	CGCGTATCCGCATCAATCAGAAG
LAB293	GCGTATGCACAACACTCAATTTGCTTTG
LAB294	CCTAAGAAACTGAAAGCAGCGAAA
LAB295	GGTTCATATGGTTGCAAGCGA
LAB296	CCAAAGAGCTTTGGTTTGAGGACA
LAB298	GGGCGTAACTTTCACCAATGAGG
LAB318	GCCAGAGCATTAATGGTATCTAGAGACA
LAB321	GTGTTGAAATCGACATACTAGCATTGCTAC
LAB322	CCCTTGTGTGAAAGCTTGATCATTATGGACT
LAB323	CGCTCGAAGAAGCTAAATTACCAGAGTCA
LAB324	GCTAGCATAAGAGCCACTCAAGACCATAG
LAB334	GCTCGTGAAGGAAAATCAACGACA

Scanning Electron Microscope (SEM)

Scanning Electron Microscope (SEM) was used to analyze the bacterial surfaces of wild type *S. thermophilus* ST538 (WT) and *S. thermophilus*Δ*epsB* and Δ*epsC* knockout mutants. For this purpose, the bacteria were cultured for 16 h at 37°C in LM17 broth, then centrifuged (6,000 × *g*, for 5 min at 5°C), and the pellets were diluted 10-fold with PBS. Samples were dropped into Membrane Filter polycarbonate of 0.2 μm × 13 mm (ADVANTEC®), and the bacterial cells were placed on the filter using suction filtration. These filters were allowed to stand in 2% (vol/vol) glutaraldehyde for 1 h at room temperature to fix the cells. The membrane was immersed in sterile water to remove excess glutaraldehyde. Thereafter, the membrane was soaked serially in 50, 60, 70, 80, 85, 90, 99, and 100% (anhydrous) ethanol for 20 min for each case. Finally, the membrane was immersed in T-butanol followed by lyophilization, platinum-palladium vapor deposition, and image capturing with a SEM (Hitachi SU8000, Tokyo, Japan) at 3 kV.

Exopolysaccharide Concentration

The quantification of EPS production was performed according to the method described by Makino et al. (2006). *S. thermophilus*

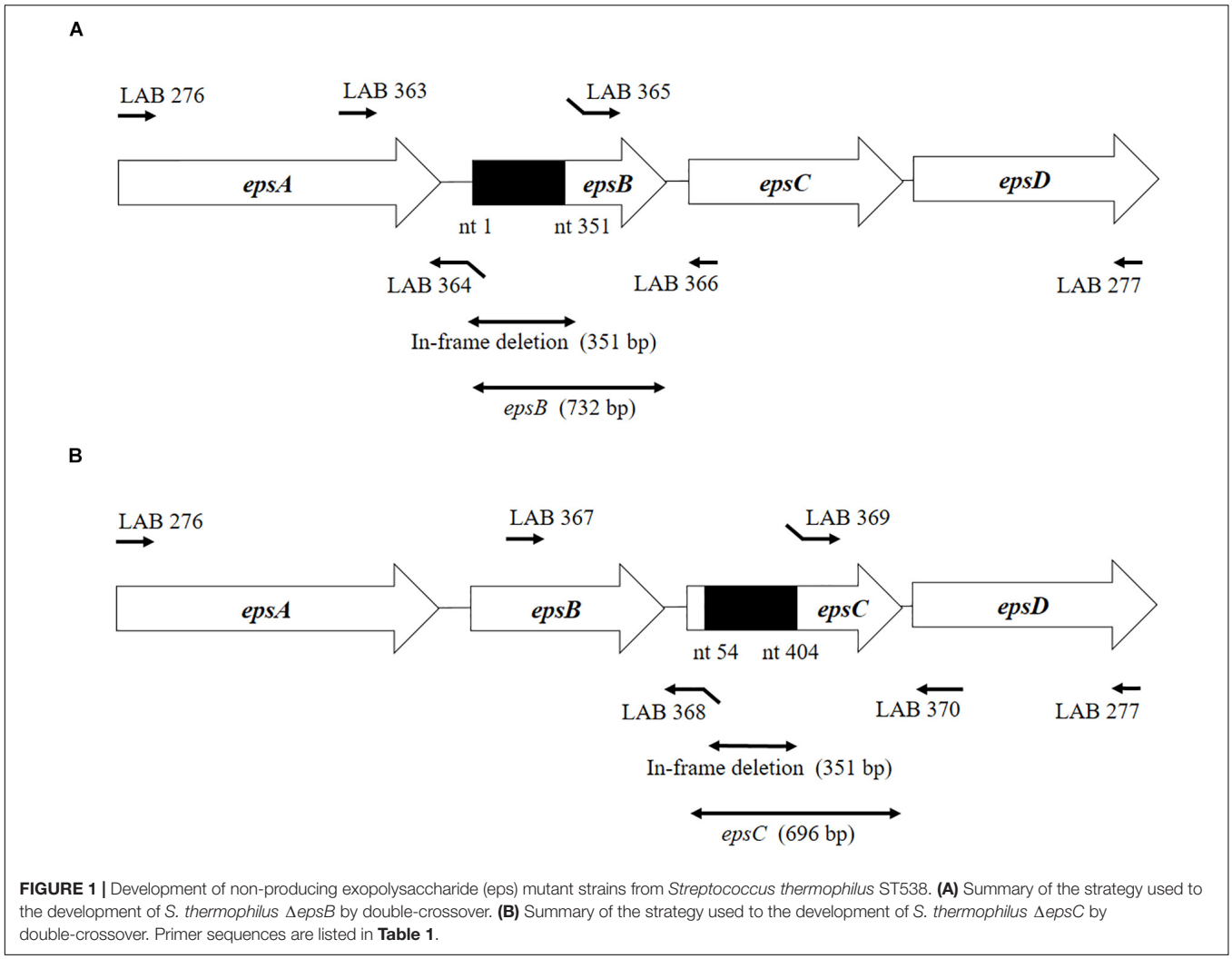

FIGURE 1 | Development of non-producing exopolysaccharide (eps) mutant strains from *Streptococcus thermophilus* ST538. **(A)** Summary of the strategy used to the development of *S. thermophilus* Δ*epsB* by double-crossover. **(B)** Summary of the strategy used to the development of *S. thermophilus* Δ*epsC* by double-crossover. Primer sequences are listed in **Table 1**.

WT, Δ*epsB* and Δ*epsC* strains cultures were inoculated (2%) into the skim milk medium supplemented with 0.1% peptide from casein hydrolysates and maintained at 43°C for 24 h. The samples of skim milk medium were collected at every 2 h. The acidity of culture medium was measured according to the method described by Yamauchi et al. (2019). For EPS determination, 10 g skim milk medium were mixed with trichloroacetic acid (10% vol/vol) (FUJIFILM Wako Pure Chemical Co., Japan), left for 10 min at 4°C and then centrifuged (16,000 × *g*, 20 min, 4°C). Supernatants were collected into 2 ml eppendorf tube, mixed with 1.5 times volume of cold Ethanol (99.5%, FUJIFILM Wako Pure Chemical Co., Japan), left for 2 h at 4°C and then centrifuged (16,000 × *g*, 20 min, 4°C). The pellets were resuspended with MilliQ water and purified using a Millex-HV PVDF 0.45 mm filter (Merck Co., Tokyo, Japan). These suspensions were used to measure EPS amount using standard curve by high performance liquid chromatography (HPLC) on OHpak SB-806HQ (Showa Denko K.K., Japan) and SB-G (Showa Denko K. K., Japan). The HPLC system used Aquity H-class (Waters Co., Milford, MA, United States) and the detector RI 2414 (Waters Co., Milford, MA, United States). The elution was performed with distilled water containing 0.2 M of NaCl at 40°C at a flow rate of 0.5 ml/min.

Extraction of Crude EPS From *S. thermophilus* ST538

The extraction of crude EPS from *S. thermophilus* ST538 was performed using the LM17 medium and the skim milk medium supplemented with 2% casamino acid. For LM17 medium, the cultures of WT and Δ*epsB* and Δ*epsC* strains were inoculated at 2% (vol/vol) to fresh medium and maintained at 37°C for 16 h. These cultures were centrifuged (6,000 × *g*, 5 min, room temperature) and the supernatants were collected, then stored at −20°C for immunoassay. Then, the supernatants were mixed with equal volume of 99.5% ethanol, and the pellets were picked up and diluted to 1/10 volume of the samples. The quantification sugars in samples were performed by Phenol sulfate method described by Kitazawa et al. (1998). For skim milk medium supplemented with 2% casamino acid, the cultures of *S. thermophilus* WT, Δ*epsB* and Δ*epsC* were inoculated at 2% (vol/vol) to the fresh medium and maintained at 43°C for 24 h.

TABLE 2 | Bacterial strains and plasmids used.

		Phenotypic characters	References
Strain	*Streptococcus thermophilus* ST538	EPS producing strain	This study
Plasmids	pG$^+$host6	Thermos-sensitive replicon[1]	Maguin et al., 1996
	pG$^+$epsB	*epsB* deleted fragment of pG$^+$host6	This study
	pG$^+$epsC	*epsC* deleted fragment of pG$^+$host6	This study

[1] *Erthromycin-resistant.*

The extraction of crude EPS was performed according to the method described by Kitazawa et al. (1998). Briefly, the cultures were adjusted at pH = 4.6 and centrifuged (13,000 × *g*, 20 min, 4°C). The supernatant was neutralized and heated at 105°C, 10 min and centrifuged (13,000 × *g*, 20 min, 4°C). Cold ethanol was added to the supernatant and kept at 4°C. The samples were centrifuged (13,000 × *g*, 20 min, 4°C) and the pellets were collected, and treated with DNase and RNase (each 7 μg/ml concentration, SIGMA, St. Louis, United States) for 6 h at 37°C. Samples were treated with proteinase K (Boehringer Mannheim, Germany) with a dose of 200 μg/ml for 16 h at 37°C. The samples were heated for 10 min at 105°C, mixed with ethanol and kept at 4°C for 24 h. Finally, samples were centrifuged (13,000 × *g*, 20 min, 4°C), dialyzed against water for 48 h and subjected to lyophilization.

PIE Cells

The PIE cell line was originally derived from intestinal epithelia isolated from an unsuckled neonatal swine (Moue et al., 2008). PIE cells are intestinal non-transformed cultured cells that assume a monolayer with a cobblestone and epithelial-like morphology and with close contact between cells during culture (Moue et al., 2008). PIE cells were maintained in Dulbecco's modified Eagle's medium (DMEM) (Invitrogen Corporation, Carlsbad, CA, United States) supplemented with 10% fetal calf serum (FCS), 100 U/ml streptomycin, and 100 mg/ml penicillin at 37°C in an atmosphere of 5% CO_2 (Moue et al., 2008; Albarracin et al., 2017).

Immunomodulatory Effect of Streptococci in PIE Cells

The study of the immunomodulatory capacity of *S. thermophilus* WT, Δ*epsB* and Δ*epsC* strains, their cell-free culture supernatants or the EPS from *S. thermophilus* ST538 was performed in PIE cells as described previously (Albarracin et al., 2017; Kanmani et al., 2018a,b). PIE cells were seeded at 3 × 10^4 cells per well in 12-well type I collagen-coated plates (Sumitomo Bakelite Co., Tokyo, Japan) and cultured for 3 days. After changing medium, streptococci (5 × 10^8 cells/ml) were added and 48 h later, each well was washed vigorously with medium at least three times to eliminate all stimulants. Then cells were stimulated with poly(I:C) (60 ug/ml) for 12 h for RT-PCR studies. Similarly, PIE cells were stimulated with cell-free culture supernatants or 20, 50, or 100 μg/ml of purified EPS and then challenged with poly(I:C) (60 ug/ml) for 12 h for RT-PCR studies.

Quantitative Expression Analysis by Two-Step Real-Time Quantitative PCR

Two-step real-time quantitative PCR (qPCR) was performed to characterize the expression of selected genes in PIE cells as described previously (Albarracin et al., 2017; Kanmani et al., 2018a,b). TRIzol reagent (Invitrogen) was used for total RNA isolation from each PIE cell sample and, Quantitect reverse transcription (RT) kit (Qiagen, Tokyo, Japan) was used for the synthesis of all cDNAs according to the manufacturer's recommendations. Real-time quantitative PCR was carried out using a 7300 real-time PCR system (Applied Biosystems, Warrington, United Kingdom) and the Platinum SYBR green qPCR SuperMix uracil-DNA glycosylase (UDG) with 6-carboxyl-X-rhodamine (ROX) (Invitrogen). The primers used in this study were described before (Albarracin et al., 2017; Kanmani et al., 2018a,b). The PCR cycling conditions were 2 min at 50°C, followed by 2 min at 95°C, and then 40 cycles of 15 s at 95°C, 30 s at 60°C, and 30 s at 72°C. The reaction mixtures contained 5 μl of sample cDNA and 15 μl of master mix, which included the sense and antisense primers. According to the minimum information for publication of quantitative real-time PCR experiments guidelines, β-actin was used as a housekeeping gene because of its high stability across porcine various tissues (Nygard et al., 2007; Bustin et al., 2009). Expression of β-actin was used to normalize cDNA levels for differences in total cDNA levels in the samples.

Statistical Analysis

The qRT-PCR raw data were log-transformed followed by normality check by Kolmogorov-Smirnov test and convergence by clubs rejection test. One-way ANOVA was performed in GraphPad prism v5.1 followed by calculating the Fisher's least significant difference for multiple mean comparisons were defined as significant at $p < 0.05$.

RESULTS

Development of Δ*epsB* and Δ*epsC* Mutants From *S. thermophilus* ST538

We analyzed the sequence *epsA-D* in *S. thermophilus* ST538 by using the Applied Biosystems 3130 Genetic Analyzer and the result showed that there was high base sequence homology with *epsA*, *epsB*, *epsC*, and *epsD* from *S. thermophilus* CNRZ1066; being 98, 96, 92, 97% respectively (data not shown). Then, it was postulated that EpsB, EpsC, and EpsD constituted a phosphorylation-dependent regulatory system of EPS production in the ST538 strain. *S. thermophilus*Δ*epsB* (**Figure 1A**) and Δ*epsC* (**Figure 1B**) were produced by double-crossover and the deletion of 351-bp in the *epsB* and *epsC* genes, respectively. In order to confirm the targeted deletion of nucleotides in *S. thermophilus*Δ*epsB* and Δ*epsC* strains, we performed PCR analysis (**Figure 2**) and sequencing

(**Supplementary Figure S1**). As expected, the amplicon length of *epsB* in *S. thermophilus*Δ*epsB* was decreased when compared to *S. thermophilus* WT (**Figure 2A**). Similarly, the amplicon length of *epsC* in *S. thermophilus*Δ*epsC* was decreased when compared to the wild type strain (**Figure 2B**). The reduction of DNA length in approximately 400-bp for both mutant strains indicated the successful deletion of *epsB* and *epsC* genes. The DNA sequencing of both *S. thermophilus*Δ*epsB* and Δ*epsC* strains also confirmed the deletion of 351-bp in the *epsB* and *epsC* genes, respectively (**Supplementary Figure S1**).

We next evaluated the potential changes in the phenotype of *S. thermophilus* WT induced by the deletion of 351-bp in the *epsB* and *epsC* genes. We studied growth curves in LM17 medium to check the effect of the *eps* genes deletion. The **Figure 3A** shows the growth curves of WT, Δ*epsB* and Δ*epsC*. A delay of growth in the early logarithmic growth phase and a recover at the late logarithmic phase was observed for the both mutants strains when compared to the WT. In addition, we comparatively evaluated the production of EPS in *S. thermophilus* WT, Δ*epsB* and Δ*epsC* strains (**Figure 3B**). For the analysis of EPS production by *S. thermophilus* WT and the mutant strains, bacteria were cultured in skim milk medium (**Supplementary Figure S2**) and the EPS was measured at every 2 h by HPLC. As shown in **Figure 3B**, the wild type *S. thermophilus* ST538 was able to produce EPS from hour 2 and reaching a maximum production at hour 6. The EPS production by *S. thermophilus* WT was noticed as high as 595 μg/ml. On the contrary, neither *S. thermophilus* Δ*epsB* nor Δ*epsC* were able to produce detectable levels of EPS during all the studied period (**Figure 3B**). We also performed electron microscopic analysis in order to further evaluate the production of EPS (**Figure 3C**). The electron microscopic analysis demonstrated that *S. thermophilus* WT contains EPS molecules associated to its surface while both Δ*epsB* and Δ*epsC* mutant strains had no such fibrous structures on their surfaces (**Figure 3C**). Then, the inability of mutants Δ*epsB* and Δ*epsC* to synthetize EPS indicated the successful development of non-EPS producing *S. thermophilus* ST538 strains.

Effect of *S. thermophilus* ST538 and Δ*epsB* and Δ*epsC* Mutants on the Innate Antiviral Immune Response in PIE Cells

In order to evaluate the immunomodulatory properties of *S. thermophilus* WT and the mutant strains, we performed *in vitro* experiments in PIE cells stimulated with *S. thermophilus* WT, Δ*epsB* or Δ*epsC* strains and then challenged with the TLR3 agonist and viral molecular associated pattern poly(I:C) (Albarracin et al., 2017; Kanmani et al., 2018a,b). The challenge of PIE cells with poly(I:C) significantly increased the expression of *IFN*-β, *IL-6*, *CXCL10*, and *CCL2* (**Figure 4**) when compared to basal levels (data not shown) as we have reported previously (Albarracin et al., 2017; Kanmani et al., 2018b). The expression of *IFN*-β in poly(I.C)-challenged PIE cells was not changed by the prestimulation with *S. thermophilus* WT or the mutants Δ*epsB* or Δ*epsC*. On the contrary, the expression levels of *IL-6* and *CCL2* were significantly increased in PIE cells treated with *S. thermophilus* WT when compared to control cells (**Figure 4**). The same effect was observed for *S. thermophilus*Δ*epsC* and with no significant differences when compared to the WT strain. Although *S. thermophilus*Δ*epsB*-treated PIE cells had an increased the expression of *IL-6* and *CCL2* than control cells, the values of both inflammatory factors were significantly lower than the observed for the WT strain (**Figure 4**). In addition, *S. thermophilus* WT was able to significantly reduce the expression of *CXCL10* in poly(I:C)-challenged PIE cells. Similarly, *S. thermophilus*Δ*epsB* reduced the expression of the pro-inflammatory chemokine while no differences were detected when *S. thermophilus*Δ*epsC*-treated and control PIE cells were compared (**Figure 4**).

Effect of *S. thermophilus* ST538 EPS on the Innate Antiviral Immune Response in PIE Cells

We next aimed to evaluate whether the EPS produced by *S. thermophilus* ST538 was able to modulate the innate antiviral immune response in PIE cells. For these experiments, *S. thermophilus* WT, Δ*epsB* or Δ*epsC* strains were grown in LM17 broth medium. No differences in pH values were observed when the medium inoculated with WT, Δ*epsB* or Δ*epsC* were compared (data not shown). The cell-free supernatants (CS) were used for PIE cells stimulation followed by the challenge with poly(I:C). As shown in **Figure 5**, the CS from *S. thermophilus* WT was able to significantly improve the expression of *IFN*-β, *IL-6*, *CXCL10*, and *CCL2* in PIE cells after the activation of TLR3. Interestingly, PIE cells treated with the CS from *S. thermophilus*Δ*epsB* had significantly lower expression levels of *IFN*-β, *IL-6*, *CXCL10*, and *CCL2* when compared to the cells stimulated with the CS from the WT strain. Moreover, *CXCL10* and *CCL2* expressions levels in the CS Δ*epsB* group were not different from control cells (**Figure 5**). Similarly, PIE cells treated with the CS from *S. thermophilus*Δ*epsC* had significantly lower expression levels of *IFN*-β, *IL-6*, and *CXCL10* when compared to the cells stimulated with the CS WT (**Figure 5**). However, no differences were found when the expression of *CCL2* was compared between CS WT and CS Δ*epsC* groups. These results indicate that the products contained in the culture supernatant of *S. thermophilus* ST538, mainly the EPS, are capable of modulating the antiviral immunity in PIE cells. Then, in order to demonstrate conclusively the immunomodulatory potential of the EPS of *S. thermophilus* ST538, we performed a second set of experiments in PIE cells by using different concentrations of purified EPS. For this purpose, PIE cells were stimulated with different concentrations of crude EPS extracted from ST538 strain grown in LM17 medium and then challenged with poly(I:C) (**Figure 6**). The EPS of *S. thermophilus* ST538 in concentrations superior to 50 μg/ml was able to significantly increase the expression of *IFN*-β, *IL-6*, and *CXCL10* when compared to control cells. In addition, in our experiments only the concentration of 50 μg/ml of the EPS of *S. thermophilus* ST538 enhanced the expression of *CCL2* when compared to control cells (**Figure 6**).

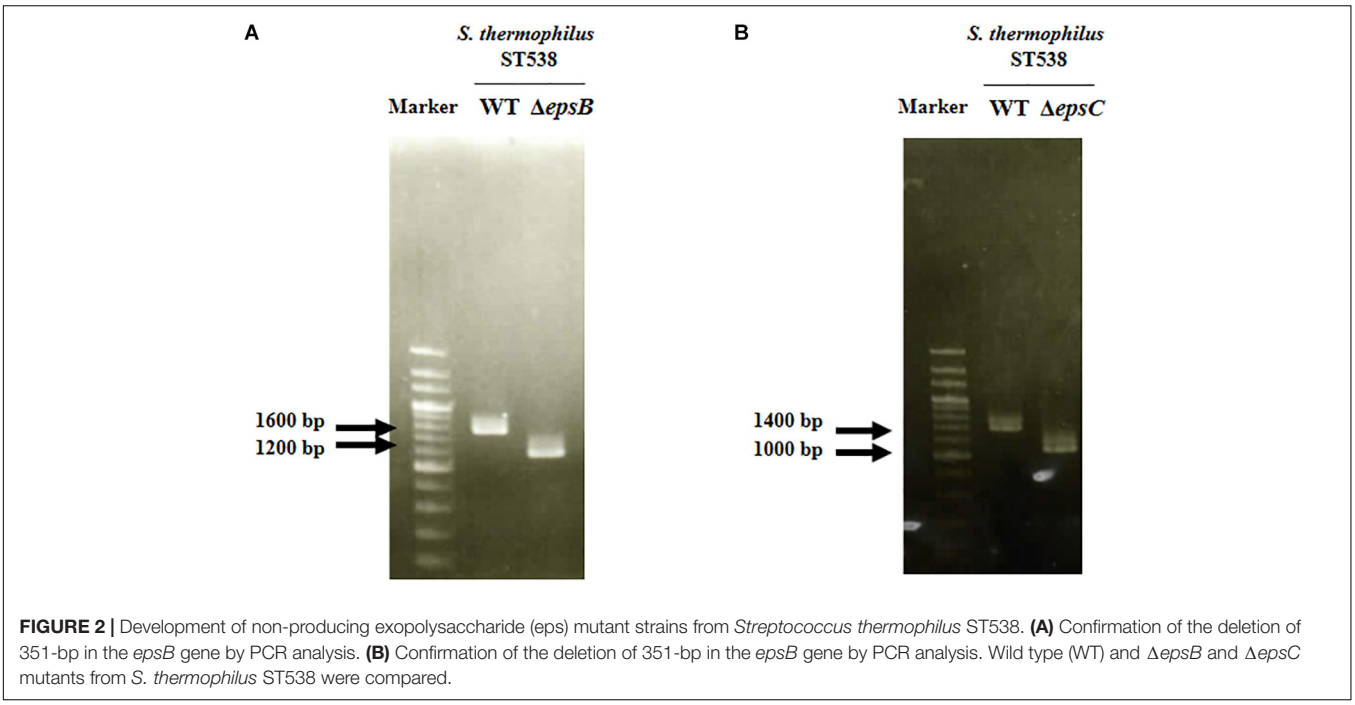

FIGURE 2 | Development of non-producing exopolysaccharide (eps) mutant strains from *Streptococcus thermophilus* ST538. **(A)** Confirmation of the deletion of 351-bp in the *epsB* gene by PCR analysis. **(B)** Confirmation of the deletion of 351-bp in the *epsB* gene by PCR analysis. Wild type (WT) and Δ*epsB* and Δ*epsC* mutants from *S. thermophilus* ST538 were compared.

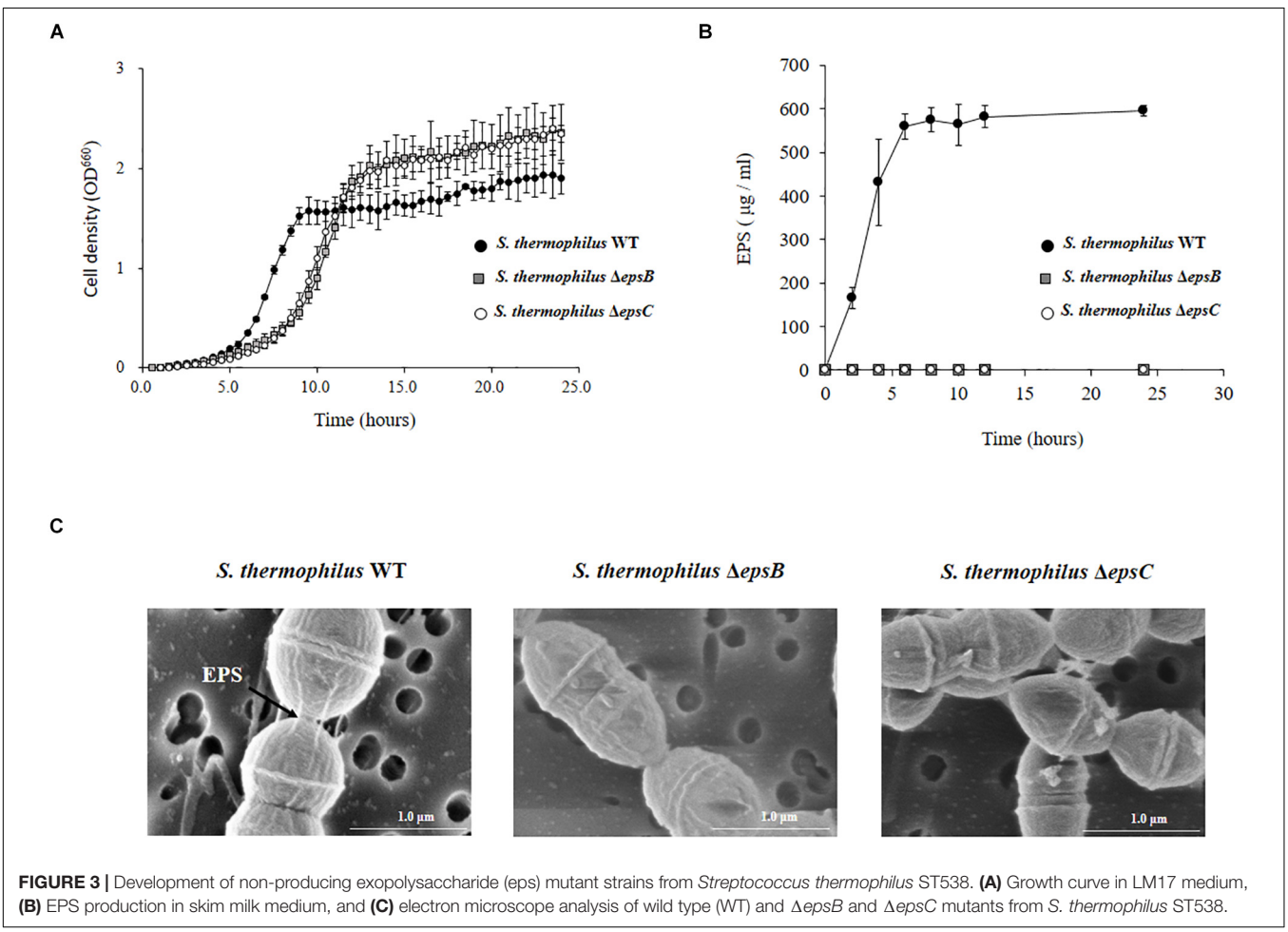

FIGURE 3 | Development of non-producing exopolysaccharide (eps) mutant strains from *Streptococcus thermophilus* ST538. **(A)** Growth curve in LM17 medium, **(B)** EPS production in skim milk medium, and **(C)** electron microscope analysis of wild type (WT) and Δ*epsB* and Δ*epsC* mutants from *S. thermophilus* ST538.

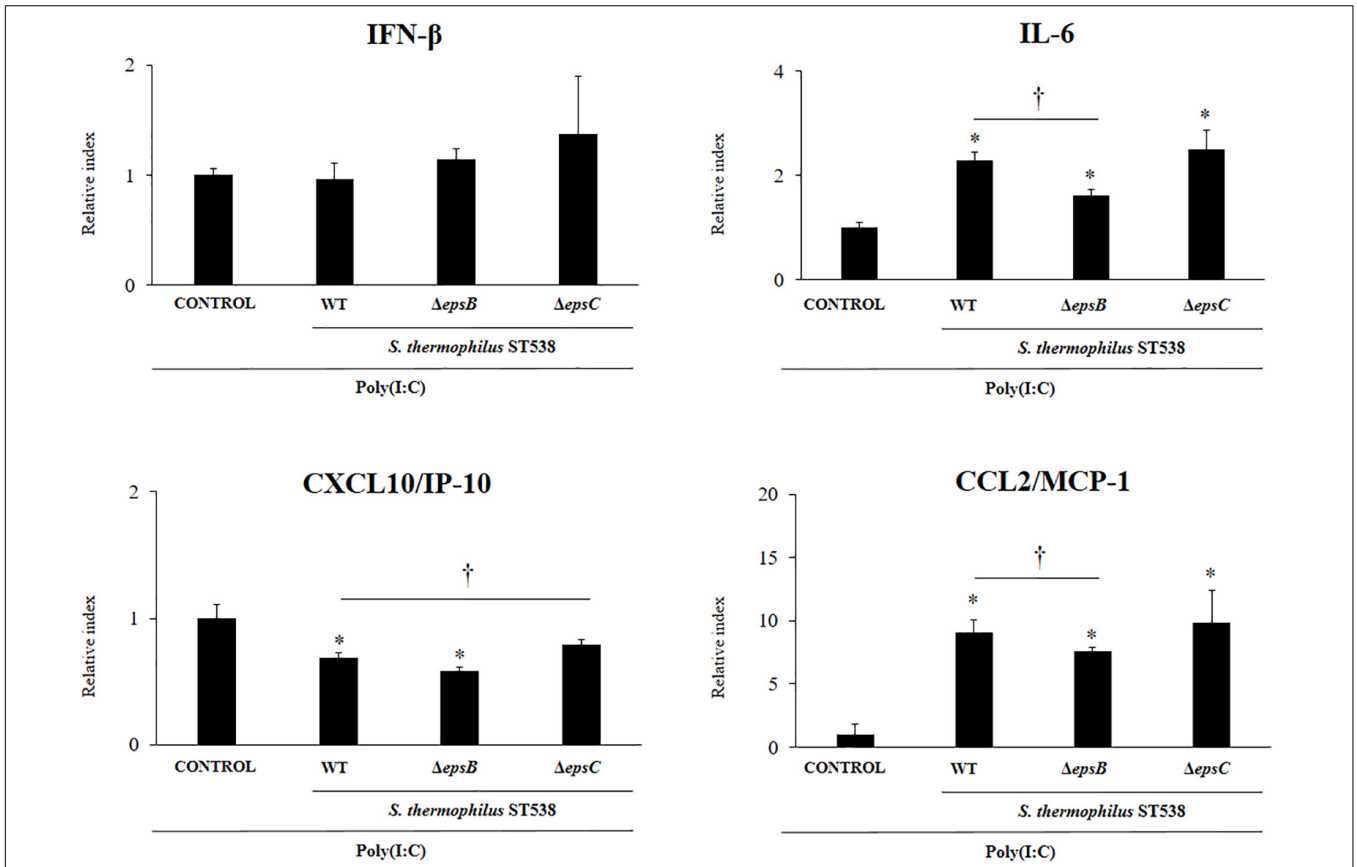

FIGURE 4 | Effect of *Streptococcus thermophilus* ST538 and its exopolysaccharide (eps) mutant strains on the innate antiviral immune response triggered by Toll-like receptor 3 (TLR3) activation in porcine intestinal epithelial cells (PIE cells). Expression of *IFN*-β, *IL-6*, *CXCL-10/IP-10*, and *MCP-1/CCL2* genes in PIE cells treated with wild type (WT) *S. thermophilus* ST538 or its Δ*epsB* or Δ*epsC* mutants and challenged with the viral molecular associated pattern poly(I:C). PIE cells with no bacterial treatment and stimulated with poly(I:C) were used as controls. The results represent data from three independent experiments. Significant differences when compared to the control group $^{*}P < 0.05$. Significant differences when compared to the indicated group $^{\dagger}P < 0.05$.

Effect of *S. thermophilus* ST538 Fermented Skim Milk on the Innate Antiviral Immune Response in PIE Cells

Finally, we evaluated the effect of the EPS derived from a skim milk fermented by *S. thermophilus* ST538 on the antiviral immune response of PIE cells. The EPS fraction of *S. thermophilus* WT or the same fractions (EPS negative) in the cultures of the mutants *S. thermophilus*Δ*epsB* or Δ*epsC* in skim milk supplemented with 2% (vol/vol) casamino acid were used for comparisons (**Figure 7**). PIE cells treated with the WT EPS and then challenged with poly(I:C) had significantly higher levels of *IFN*-β, *IL-6*, and *CXCL10* when compared to control cells. No differences were found between those groups when the expression of *CCL2* was evaluated. Of note, PIE cells treated with the EPS negative fractions from Δ*epsB* or the Δ*epsC* had significantly lower expression levels of *IFN*-β, *IL-6*, and *CXCL10* when compared to the WT group (**Figure 7**). The most notable effect was observed for the Δ*epsB* group. No differences were found between WT EPS and EPS negative fractions from Δ*epsB* when the expression of *CCL2* was evaluated. On the contrary, EPS negative fractions from Δ*epsC* significantly increased *CCL2* expression when compared to the WT group (**Figure 7**).

DISCUSSION

Studies have demonstrated that the EPSs produced by some immunobiotic lactobacilli are able to enhance antiviral immunity (Kitazawa et al., 1998; Makino et al., 2006, 2010, 2016; Nagai et al., 2011). Moreover, those studies have reported the impact of EPSs on immune cells and had described their ability to activate macrophages, induce lymphocytes proliferation, stimulate IFN-γ production or enhance NK cell activity (Nishimura-Uemura et al., 2003; Makino et al., 2006, 2010, 2016; Nagai et al., 2011). However, the ability of EPSs derived from LAB to differentially modulate the innate antiviral immune response in IECs was not addressed in details before. In this regard, we have previously investigated the capacity of EPSs produced by the immunobiotic strains *Lactobacillus delbrueckii* OLL1073R-1 (Kanmani et al., 2018a) and *Lactobacillus delbrueckii* TUA4408L (Kanmani et al., 2018b) to beneficially modulate the innate immune response in PIE cells. This *in vitro* system has been particularly useful for the

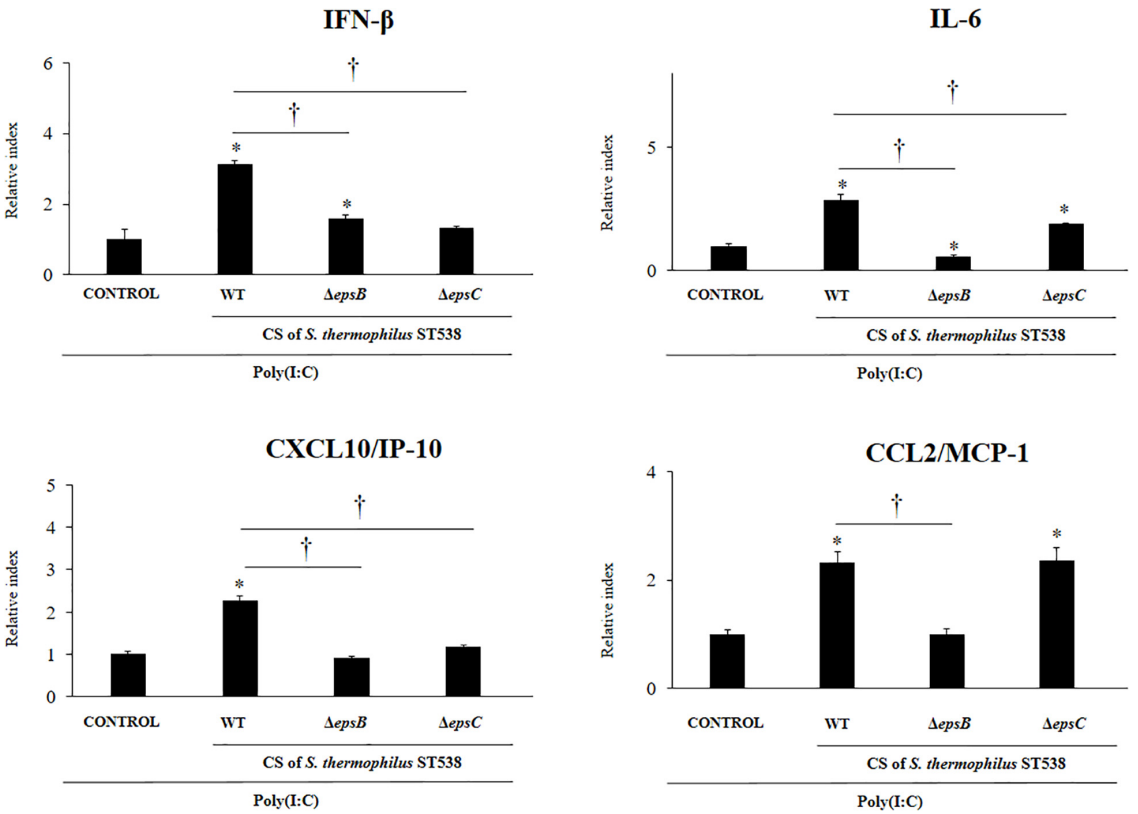

FIGURE 5 | Effect of cell-free supernatants (CS) from *Streptococcus thermophilus* ST538 and its exopolysaccharide (eps) mutant strains on the innate antiviral immune response triggered by Toll-like receptor 3 (TLR3) activation in porcine intestinal epithelial cells (PIE cells). Expression of *IFN-β*, *IL-6, CXCL-10/IP-10*, and *MCP-1/CCL2* genes in PIE cells treated with CS from wild type (WT) *S. thermophilus* ST538 or its Δ*epsB* or Δ*epsC* mutants grown in LM17 medium, and challenged with the viral molecular associated pattern poly(I:C). PIE cells with no treatment and stimulated with poly(I:C) were used as controls. The results represent data from three independent experiments. Significant differences when compared to the control group $^{*}P < 0.05$. Significant differences when compared to the indicated group: $^{\dagger}P < 0.05$.

study of innate immunity in IECs, since the PIE cell line highly expresses the antiviral PRRs TLR3 and responds to poly(I:C) stimulation by producing antiviral factors and inflammatory cytokines and chemokines resembling the response to rotavirus infection (Hosoya et al., 2011; Ishizuka et al., 2016; Kanmani et al., 2018a,b). In this work, we reported and analyzed, for the first time, the capacity of the EPS-producing *S. thermophilus* ST538 strain to improve the innate antiviral immune response in IECs. Moreover, by the purification of the EPS and the successful development of Δ*epsB* and Δ*epsC* mutants derived from the ST538, we clearly demonstrated the involvement of the EPS in the immunomodulatory ability of this *S. thermophilus* strain.

Despite the vast structural diversity, bacteria produce EPS by using four different pathways [reviewed in Zeidan et al. (2017)]. One of them, the Wzy-dependent pathway, allows bacteria to produce polysaccharides by using an *en bloc* mechanism. In LAB, this is the pathway of choice for the synthesis of heteropolymeric EPS (Ryan et al., 2015; Torino et al., 2015). Genes encoding Wzy-dependent EPSs biosynthesis proteins in *S. thermophilus* are typically organized in a cluster with an operon structure and are generally chromosomal (Zeidan et al., 2017; Nourikyan et al., 2015). In the EPS cluster, the genes in the 5′ end are involved in the modulation and assembly machinery of polysaccharide biosynthesis. Those genes consist of five genes: *epsA*, *epsB*, *epsC*, *epsD*, and *epsE*, which display the highest level of overall conservation among different *Streptococcus* strains (Zeidan et al., 2017; Jolly and Stingele, 2012; Goh et al., 2011; Alexandraki et al., 2019). The *epsC* gene encodes a membrane-bound protein with a cytoplasmic C-terminal domain required for kinase activation. The *epsC* product triggers *epsD* kinase activity leading to the autophosphorylation of the tyrosine cluster and therefore, acting as a modulator component. On the other hand, the *epsB* gene encodes a phosphotyrosine protein phosphatase in *S. thermophilus*, with the ability to dephosphorylate the tyrosine cluster, acting also as a modulatory protein (Jolly and Stingele, 2012; Goh et al., 2011). Then, the current model of EPS synthesis proposes that cycling between phosphorylated and non-phosphorylated forms of the tyrosine cluster is required for proper synthesis and export of the EPS (Yother, 2011; Grangeasse, 2016; Zeidan et al., 2017). Therefore, in this work we hypothesized that the mutation of the *epsB* or *epsC* genes, would allow us to obtain two strains derived from *S. thermophilus* ST538 with the inability to produce EPS. Indeed, we successfully developed *S. thermophilus* Δ*epsB* and

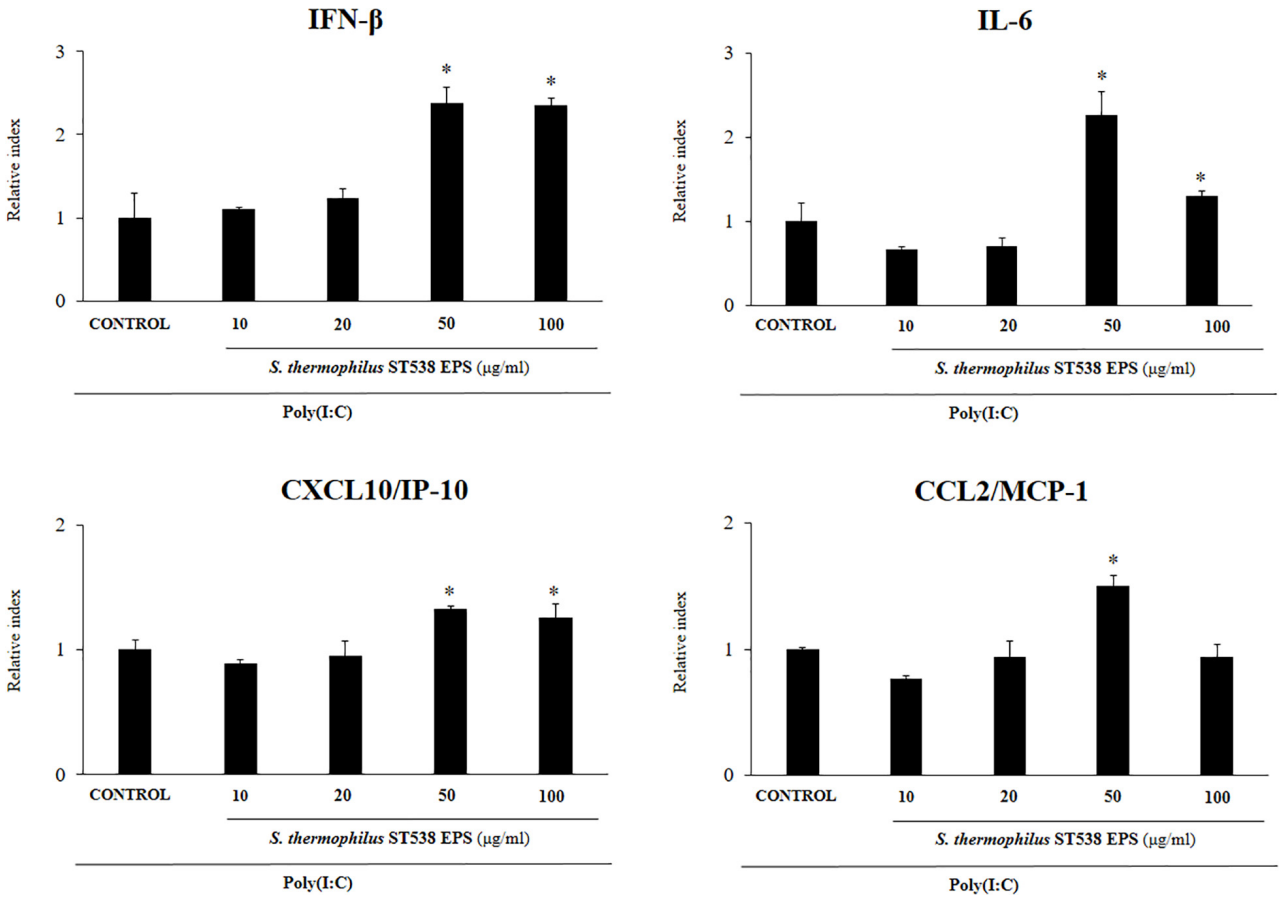

FIGURE 6 | Effect of the purified exopolysaccharide (eps) from *Streptococcus thermophilus* ST538 on the innate antiviral immune response triggered by Toll-like receptor 3 (TLR3) activation in porcine intestinal epithelial cells (PIE cells). Expression of *IFN-β*, *IL-6, CXCL-10/IP-10*, and *MCP-1/CCL2* genes in PIE cells treated with different concentrations of EPS from *S. thermophilus* ST538 in LM17 medium and challenged with the viral molecular associated pattern poly(I:C). PIE cells with no EPS treatment and stimulated with poly(I:C) were used as controls. The results represent data from three independent experiments. Significant differences when compared to the control group $^*P < 0.05$.

Δ*epsC* carrying 351-bp deletion in the *epsB* and *epsC* genes, respectively. Moreover, we demonstrated that neither of the two mutants was able to produce detectable amounts of EPS in our experimental conditions.

The lack of the ability of *S. thermophilus* Δ*epsC* to produce EPS shown here is in line with several reports studying the role of this gene in the biosynthesis of EPS in this species of bacterium. Studies evaluating the protein–protein interactions between the genetic products of *epsC-epsD* derived from *S. thermophilus* MR-1C demonstrated the ability of EpsD to interact with the protein tyrosine kinase EpsC (Cefalo et al., 2011a,b). In addition, the requirement of *epsC* for the phosphorylation of *epsD* was verified *S. thermophilus* CNRZ1066 (Minic et al., 2007). The work demonstrated that EPS is not synthesized in *epsC* or *epsD* mutants, indicating that both proteins are essential for EPS synthesis. Moreover, studies by Li et al. (2016), clearly demonstrated the role of the *epsC* gene on the quantity and quality of EPS production by *S. thermophilus* 05–24. The work examined the levels of *epsC* expression under different fermentation conditions and found that in the optimal fermentation condition the *epsC* gene is up-regulated in almost 3-folds.

On the other hand, the phosphotyrosine phosphatase function of purified EpsB was demonstrated in *S. thermophilus* MR-1C (Cefalo et al., 2013; Cefalo et al., 2013) and the *epsB-epsD* interaction was verified (Cefalo et al., 2011a,b). Recent studies evaluated the impact of fermentation conditions in the production of EPS by *S. thermophilus* ASCC1275 using transcriptomic (Wu and Shah, 2018) and proteomics (Wu et al., 2019) approaches. Those works reported that the production of EPS by the ASCC1275 strain could be improved by reducing the pH from 6.5 to 5.5. Interestingly, authors also demonstrated that there was a significant down-regulation of *epsB* at both mRNA and protein level in pH 5.5 compared to the pH 6.5 conditions. Of note, Minic et al. (2007) were able to obtain a *S. thermophilus* Δ*epsB* derived from the CNRZ1066 strain and found no differences between wild type and the Δ*epsB* mutant when the production of the EPS was compared. Moreover, the work reported an increase in the EpsE enzymatic activity in the *S. thermophilus* strain lacking the *epsB* gene. Those works

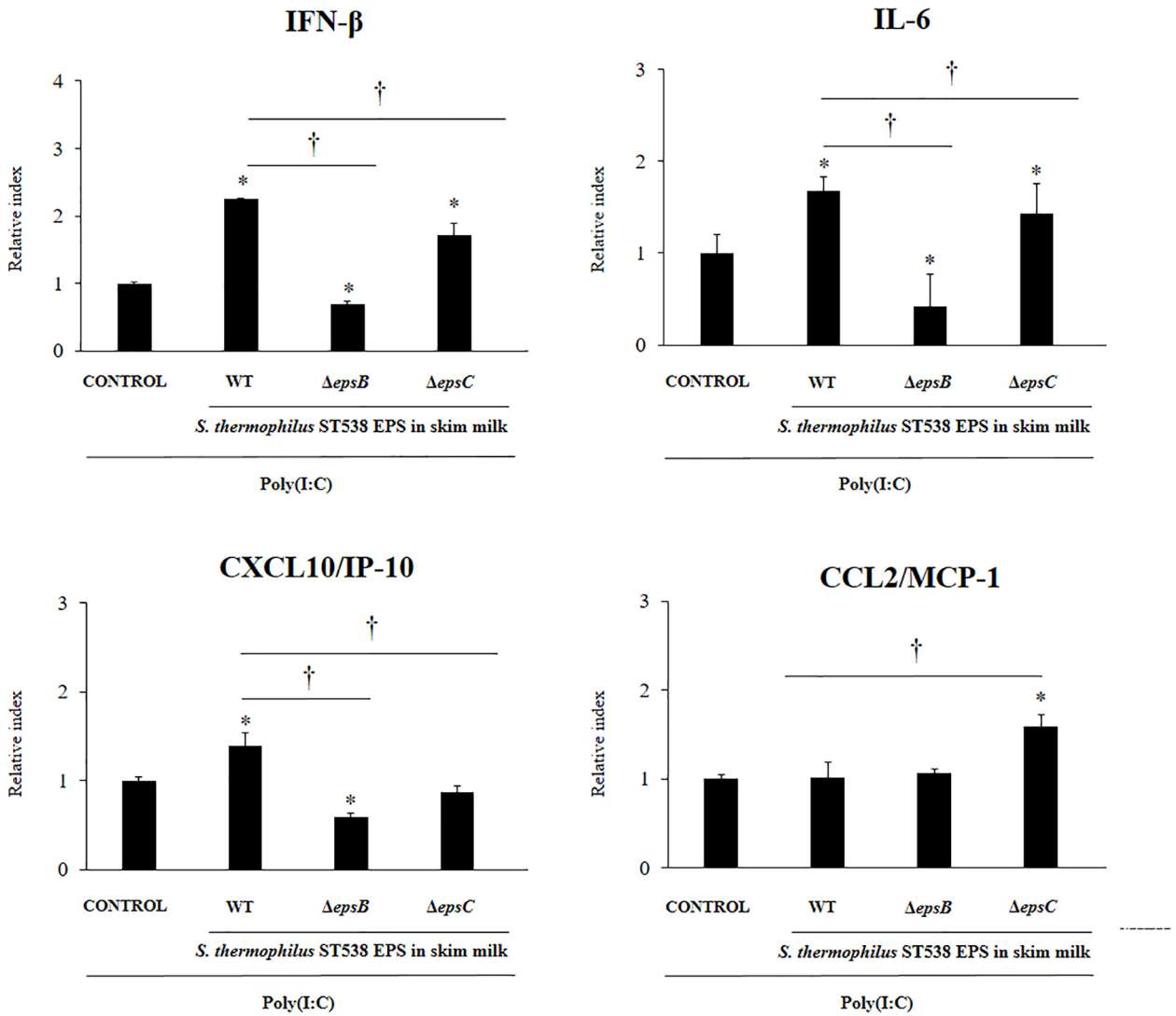

FIGURE 7 | Effect of the EPS derived from skim milk fermented by *Streptococcus thermophilus* ST538 and its exopolysaccharide (eps) mutant strains on the innate antiviral immune response triggered by Toll-like receptor 3 (TLR3) activation in porcine intestinal epithelial cells (PIE cells). Expression of *IFN-β*, *IL-6*, *CXCL-10/IP-10*, and *MCP-1/CCL2* genes in PIE cells treated with the EPS from skim milk fermented by wild type (WT) *S. thermophilus* ST538 or the same fractions (EPS negative) in the cultures of Δ*epsB* or Δ*epsC* mutants, and challenged with the viral molecular associated pattern poly(I:C). PIE cells with no treatment and stimulated with poly(I:C) were used as controls. The results represent data from three independent experiments. Significant differences when compared to the control group $^{*}P < 0.05$. Significant differences when compared to the indicated group $^{\dagger}P < 0.05$.

indicate that the down-regulation or the elimination of the *epsB* gene in *S. thermophilus* do not modify EPS biosynthesis or can even increase it. In contrast with those results, we observed here that the *S. thermophilus* Δ*epsB* derived from the ST538 was not able to produce detectable amounts of EPS. Moreover, we recently developed another Δ*epsB* mutant strain derived from *S. thermophilus* ST499 that was not able to produce detectable amounts of EPS (unpublished results). The difference between Δ*epsB* mutants derived from CNRZ1066, ST538, and ST499 strains in their ability to produce EPS may indicate that the control mechanism of EPS production by phosphorylation/dephosphorylation may differ between strains. More detailed biochemical and genetic comparative studies using different *S. thermophilus* strains are necessary in order to conclusively clarify the molecular mechanisms involved in EPS production.

Interestingly, we also observed in this work that there was a delay of growth in the early logarithmic phase when Δ*epsB* and Δ*epsC* strains were compared to the WT *S. thermophilus*. Nourikyan et al. (2015) showed that the phosphoregulatory system CpsBCD involved in the capsule production in *S. pneumoniae* is also closely related with the cell division. Although there are marked differences between capsular and EPS production, it can be speculated that the deletion of *epsB* and *epsC* in ST538 may have affected the cell division even if, preliminary electron microscope analysis did not show significant

differences in cell morphology or chain length, between wild type bacteria and mutants. Further studies are necessary to determine the exact roles of *epsB* or *epsC* genes in the cell division of *S. thermophilus* ST538.

The EPS of *S. thermophilus* ST538 was able to significantly improve the expression of *IFN*-β, *IL-6*, and *CXCL10* in PIE cells in response to TLR3 activation. On the contrary, the EPS negative fractions from skim milk or culture supernatants from the mutants *S. thermophilus* Δ*epsB* and Δ*epsC* had significantly lower levels of expression of *IFN*-β, *IL-6*, and *CXCL10* in PIE cells when compared to cells treated with the wild type EPS or supernatant. Those experiments conclusively demonstrated the role of the EPS in the modulation of TLR3-mediated immune response by the ST538 strain.

The three immune factors modulated by the EPS of *S. thermophilus* ST538, *IFN*-β, *IL-6*, and *CXCL10*, have been associated to the protection against viral infections. The activation of TLR3 in IECs triggers the IRF3 signaling conducting to the production of type I IFNs and activates NF-κB signaling that leads to up-regulation of pro-inflammatory factors. Cytokines and chemokines production induced by the TLR3-NF-κB signaling pathway in IECs include IL-6 and CXCL10, which alerts host to induce the recruitment and activation of immune cells to combat the invading pathogen (Kondo et al., 2012; Villena et al., 2016). In addition, it was reported that infection with rotavirus induces a significant up-regulation of type I IFNs by DCs and IECs (Sen et al., 2012). The binding of these IFNs to their cognate cell surface receptors activate positive feedback loops that amplifies the expression of IFNs as well as more than 300 different IFN-stimulated genes (Hoffmann et al., 2015). This IFNs release then efficiently amplifies the expression of antiviral proteins targeting a variety of viral replication steps in uninfected bystander cells. Then, considering those protective effects induced by IFNs, it can be speculated that EPS of *S. thermophilus* ST538 could have the ability to improve the resistance against enteric viruses. In support of this hypothesis, we previously demonstrated that the immunobiotic strains *Bifidobacterium infantis* MCC12 (Ishizuka et al., 2016) and *L. rhamnosus* CRL1505 (Albarracin et al., 2017) were able to significantly increase IFN-β in response to poly(I:C) challenge in PIE cells. The enhanced IFN-β induced a concomitant up-regulation of the antiviral factors NPLR3, OAS1, OASL, MX2, RNASEL, and RNASE4 in PIE cells. Moreover, the CRL1505 strain has been shown to beneficially modulate the antiviral innate immune response triggered by TLR3 activation in mice (Tada et al., 2016) and reducing the severity of viral infections in children (Villena et al., 2012). Whether *S. thermophilus* ST538 or its EPS are able to reduce the replication of enteric virus *in vitro* and *in vivo* thought the induction of IL-6, CXCL10, and type I IFNs is an open question, which we propose to address in the near future.

The global market is so far dominated by polysaccharides produced by plants and algae, however, bacteria in general and LAB in particular represent an interesting source of a polysaccharide repertoire that can be exploited for improving human and animal health. Our results suggest that EPS from ST538 strain have potential to be used for improving intestinal innate antiviral response and protecting against intestinal viruses such as rotavirus. Then, *S. thermophilus* ST538 could be used as an immunobiotic strain for the development of new immunologically functional foods, which might contribute to improve resistance against viral infections.

DATA AVAILABILITY STATEMENT

The datasets generated for this study are available on request to the corresponding authors.

AUTHOR CONTRIBUTIONS

YS, JV, and HK designed the study. HM, KT, RF, and MI performed the experiments. HM and LA performed the bioinformatic studies. JV, KK, HT, YS, and HK provided the financial support. JV, WI-O, HT, KK, YS, and HK contributed to data analysis and results interpretation. MI and JV wrote the manuscript. WI-O, HT, HA, KK, YS, and HK reviewed the manuscript. YS and HK approved the final version of the manuscript.

FUNDING

This study was supported by a Grant-in-Aid for Scientific Research (A) (19H00965) and Open Partnership Joint Projects of JSPS Bilateral Joint Research Projects from the Japan Society for the Promotion of Science (JSPS) to HK. This research was supported by grants from the project of NARO Bio-oriented Technology Research Advancement Institution (research program on the development of innovative technology, No. 01002A) to HK, and the grants for "Scientific Research on Innovative Areas" from the Ministry of Education, Culture, Sports, Science and Technology (MEXT) of Japan (Grant numbers: 16H06429, 16K21723, and 16H06435) to HT. This study was also supported by ANPCyT–FONCyT Grant PICT-2016-0410 to JV and by JSPS Core-to-Core Program, A. Advanced Research Networks entitled Establishment of international agricultural immunology research-core for a quantum improvement in food safety.

SUPPLEMENTARY MATERIAL

The Supplementary Material for this article can be found online at: https://www.frontiersin.org/articles/10.3389/fmicb.2020.00894/full#supplementary-material

FIGURE S1 | Development of non-producing exopolysaccharide (eps) mutant strains from *Streptococcus thermophilus* ST538. **(A)** Comparison of the *epsB* sequence in wild type (WT) and Δ*epsB* strains of *S. thermophilus*. **(B)** Comparison of the *epsC* sequence in wild type (WT) and Δ*epsC* strains of *S. thermophilus*.

FIGURE S2 | Development of non-producing exopolysaccharide (eps) mutant strains from *Streptococcus thermophilus* ST538. Growth curve in skim milk medium of wild type (WT) and Δ*epsB* and Δ*epsC* mutants from *S. thermophilus* ST538.

REFERENCES

Albarracin, L., Kobayashi, H., Iida, H., Sato, N., Nochi, T., Aso, H., et al. (2017). Transcriptomic analysis of the innate antiviral immune response in porcine intestinal epithelial cells: influence of immunobiotic lactobacilli. *Front. Immunol.* 8:57. doi: 10.3389/fimmu.2017.00057

Alexandraki, V., Kazou, M., Blom, J., Pot, B., Papadimitriou, K., and Tsakalidou, E. (2019). Comparative genomics of *Streptococcus thermophilus* support important traits concerning the evolution, biology and technological properties of the species. *Front. Microbiol.* 10:2916. doi: 10.3389/fmicb.2019.02916

Biswas, I., Gruss, A., Ehtlich, S. D., and Maguin, E. (1993). High-efficiency gene inactivation and replacement system. *J. Bacteriol.* 175, 3628–3635. doi: 10.1128/jb.175.11.3628-3635.1993

Bustin, S. A., Benes, V., Garson, J. A., Hellemans, J., Huggett, J., Kubista, M., et al. (2009). The MIQE guidelines: minimum information for publication of quantitative real-time PCR experiments. *Clin. Chem.* 55, 611–622. doi: 10.1373/clinchem.2008.112797

Caggianiello, G., Kleerebezem, M., and Spano, G. (2016). Exopolysaccharides produced by lactic acid bacteria: from health-promoting benefits to stress tolerance mechanisms. *Appl. Microbiol. Biotechnol.* 100, 3877–3886. doi: 10.1007/s00253-016-7471-2

Cefalo, A. D., Broadbent, J. R., and Welker, D. L. (2011a). Intraspecific and interspecific interactions among proteins regulating exopolysaccharide synthesis in *Streptococcus thermophilus*, *Streptococcus iniae*, and *Lactococcus lactis* subsp. *cremoris* and the assessment of potential lateral gene transfer. *Can. J. Microbiol.* 57, 1002–1015. doi: 10.1139/w11-090

Cefalo, A. D., Broadbent, J. R., and Welker, D. L. (2011b). Protein-protein interactions among the components of the biosynthetic machinery responsible for exopolysaccharide production in *Streptococcus thermophilus* MR-1C. *J. Appl. Microbiol.* 110, 801–812. doi: 10.1111/j.1365-2672.2010.04935.x

Cefalo, A. D., Broadbent, J. R., and Welker, D. L. (2013). The *Streptococcus thermophilus* protein Wzh functions as a phosphotyrosine phosphatase. *Can. J. Microbiol.* 59, 391–398. doi: 10.1139/cjm-2013-0094

Chen, Y., Zhang, M., and Ren, F. (2019). A role of exopolysaccharide produced by *Streptococcus thermophilus* in the intestinal inflammation and mucosal barrier in Caco-2 monolayer and dextran sulphate sodium-induced experimental murine colitis. *Molecules* 24:E513. doi: 10.3390/molecules24030513

Cui, Y., Jiang, X., Hao, M., Qu, X., and Hu, T. (2017). New advances in exopolysaccharides production of *Streptococcus thermophilus*. *Arch. Microbiol.* 199, 799–809. doi: 10.1007/s00203-017-1366-1

Dan, T., Fukuda, K., Sugai-Bannai, M., Takakuwa, N., Motoshima, H., and Urashima, T. (2009). Characterization and expression analysis of the exopolysaccharide gene cluster in *Lactobacillus fermentum* TDS030603. *Biosci. Biotechnol. Biochem.* 73, 2656–2664. doi: 10.1271/bbb.90502

Doco, T., Wieruszeski, J. −M., Fournet, B., Carcano, D., Ramos, P., and Loones, A. (1990). Structure of an exocellular polysaccharide produced by *Streptococcus thermophilus*. *Carbohydrate Res.* 198, 313–321. doi: 10.1016/0008-6215(90)84301-a

Fialho, A. M., Moreira, L. M., Granja, A. T., Popescu, A. O., Hoffmann, K., and Sa-Correia, I. (2008). Occurrence, production, and applications of gellan: current state and perspectives. *Appl. Microbiol. Biotechnol.* 79, 889–900. doi: 10.1007/s00253-008-1496-0

Goh, Y. J., Goin, C., O'Flaherty, S., Altermann, E., and Hutkins, R. (2011). Specialized adaptation of a lactic acid bacterium to the milk environment: the comparative genomics of *Streptococcus thermophilus* LMD-9. *Microb. Cell Fact.* 10:S22. doi: 10.1186/1475-2859-10-S1-S22

Grangeasse, C. (2016). Rewiring the pneumococcal cell cycle with serine/threonine- and tyrosine-kinases. *Trends Microbiol.* 24, 713–724. doi: 10.1016/j.tim.2016.04.004

Hoffmann, H. H., Schneider, W. M., and Rice, C. M. (2015). Interferons and viruses: an evolutionary arms race of molecular interactions. *Trends Immunol.* 36, 124–138. doi: 10.1016/j.it.2015.01.004

Hosoya, S., Villena, J., Shimazu, T., Tohno, M., Fujie, H., Chiba, E., et al. (2011). Immunobiotic lactic acid bacteria beneficially regulate immune response triggered by poly (I:C) in porcine intestinal epithelial cells. *Vet. Res.* 42:1. doi: 10.1186/1297-9716-42-111

Ishizuka, T., Kanmani, P., Kobayashi, H., Miyazaki, A., Soma, J., Suda, Y., et al. (2016). Immunobiotic bifidobacteria strains modulate rotavirus immune response in porcine intestinal epitheliocytes via pattern recognition receptor signaling. *PLoS One* 11:e0152416. doi: 10.1371/journal.pone.0152416

Iyer, R., Tomar, S., Maheswari, T. U., and Singh, R. (2010). *Streptococcus thermophilus* strains: multifunctional lactic acid bacteria. *Int. Dairy J.* 20, 133–141.

Jolly, L., and Stingele, F. (2012). Molecular organization and functionality of exopolysaccharide gene clusters in lactic acid bacteria. *Int. Dairy J.* 11, 733–745.

Kanmani, P., Albarracin, L., Kobayashi, H., Hebert, E. M., Saavedra, L., Komatsu, R., et al. (2018a). Genomic characterization of *Lactobacillus delbrueckii* TUA4408L and evaluation of the antiviral activities of its extracellular polysaccharides in porcine intestinal epithelial cells. *Front. Immunol.* 9:2178. doi: 10.3389/fimmu.2018.02178

Kanmani, P., Albarracin, L., Kobayashi, H., Iida, H., Komatsu, R., Humayun Kober, A. K. M., et al. (2018b). Exopolysaccharides from *Lactobacillus delbrueckii* OLL1073R-1 modulate innate antiviral immune response in porcine intestinal epithelial cells. *Mol. Immunol.* 93, 253–265. doi: 10.1016/j.molimm.2017.07.009

Kebouchi, M., Galia, W., Genay, M., Soligot, C., Lecomte, X., Awussi, A. A., et al. (2016). Implication of sortase-dependent proteins of *Streptococcus thermophilus* in adhesion to human intestinal epithelial cell lines and bile salt tolerance. *Appl. Microbiol. Biotechnol.* 100, 3667–3679. doi: 10.1007/s00253-016-7322-1

Kitazawa, H., Harata, T., Uemura, J., Siato, T., Kaneko, T., and Itoh, T. (1998). Phosphate group requirement of mitogenic activation of lymphocytes by an extracellular phosphopolysaccharide from *Lactobacillus delbruecki* ssp. *bulgaricus*. *Int. J. Food Microbiol.* 40, 169–175. doi: 10.1016/s0168-1605(98)00030-0

Kondo, T., Kawai, T., and Akira, S. (2012). Dissecting negative regulation of toll-like receptor signaling. *Trend. Immunol.* 33, 449–458. doi: 10.1016/j.it.2012.05.002

Laiño, J., Villena, J., Kanmani, P., and Kitazawa, H. (2016). Immunoregulatory effects triggered by lactic acid bacteria exopolysaccharides: new insights into molecular interactions with host cells. *Microorganisms* 4:27. doi: 10.3390/microorganisms4030027

Laws, A., Gu, Y., and Marshall, V. (2001). Biosynthesis, characterisation, and design of bacterial exopolysaccharides from lactic acid bacteria. *Biotechnolo. Adv.* 19, 597–625. doi: 10.1016/s0734-9750(01)00084-2

Li, D., Li, J., Zhao, F., Wang, G., Qin, Q., and Hao, Y. (2016). The influence of fermentation condition on production and molecular mass of EPS produced by *Streptococcus thermophilus* 05-34 in milk-based medium. *Food Chem.* 197, 367–372. doi: 10.1016/j.foodchem.2015.10.129

Maguin, E., Prevost, H., Ehrlich, S. D., and Gruss, A. (1996). Efficient insertional mutagenesis in lactococci and other gram-positive bacteria. *J. Bacteriol.* 178, 931–935. doi: 10.1128/jb.178.3.931-935.1996

Makino, S., Ikegami, S., Kano, H., Sashihara, T., Sugano, H., Horiuchi, H., et al. (2006). Immunomodulatory effects of polysaccharides produced by *Lactobacillus delbrueckii* ssp. *bulgaricus* OLL1073R-1. *J. Dairy Sci.* 89, 2873–2881. doi: 10.3168/jds.S0022-0302(06)72560-7

Makino, S., Ikegami, S., Kume, A., Horiuchi, H., Sasaki, H., and Orii, N. (2010). Reducing the risk of infection in the elderly by dietary intake of yoghurt fermented with *Lactobacillus delbrueckii* ssp. *bulgaricus* OLL1073R-1. *Br. J. Nutr.* 104, 998–1006. doi: 10.1017/S000711451000173X

Makino, S., Sato, A., Goto, A., Nakamura, M., Ogawa, M., Chiba, Y., et al. (2016). Enhanced natural killer cell activation by exopolysaccharides derived from yogurt fermented with *Lactobacillus delbrueckii* ssp. *bulgaricus* OLL1073R-1. *J. Dairy Sci.* 99, 915–923. doi: 10.3168/jds.2015-10376

Marcial, G., Villena, J., Faller, G., Hensel, A., Font, and de Valdéz, G. (2017). Exopolysaccharide-producing *Streptococcus thermophilus* CRL1190 reduces the inflammatory response caused by *Helicobacter pylori*. *Benef. Microbes* 8, 451–461. doi: 10.3920/BM2016.0186

Minic, Z., Marie, C., Delorme, C., Faurie, J. M., Mercier, G., Ehrlich, D., et al. (2007). Control of EpsE, the phosphoglycosyltransferase initiating exopolysaccharide synthesis in *Streptococcus thermophilus*, by EpsD tyrosine kinase. *J. Bacteriol.* 189, 1351–1357. doi: 10.1128/JB.01122-06

Moue, M., Tohno, M., Shimazu, T., Kido, T., Aso, H., Saito, T., et al. (2008). Toll-like receptor 4 and cytokine expression involved in functional immune response in an originally established porcine intestinal epitheliocyte cell line. *Biochim. Biophys. Acta* 1780, 134–144. doi: 10.1016/j.bbagen.2007.11.006

Nagai, T., Makino, S., Ikegami, S., Itoh, H., and Yamada, H. (2011). Effects of oral administration of yogurt fermented with *Lactobacillus delbrueckii* ssp. *bulgaricus* OLL1073R-1 and its exopolysaccharides against influenza virus infection in mice. *Int. Immunopharmacol.* 11, 2246–2250. doi: 10.1016/j.intimp.2011.09.012

Nishimura-Uemura, J., Kitazawa, H., Kawai, Y., Itoh, T., Oda, M., and Saito, T. (2003). Functional alteration of murine macrophages stimulated with extracellular polysaccharides from *Lactobacillus delbrueckii* ssp. *bulgaricus* OLL1073R-1. *Food Microbiol.* 20, 267–273.

Nourikyan, J., Kjos, M., Mercy, C., Cluzel, C., Morlot, Cecile, M., et al. (2015). Autophosphorylation of the bacterial tyrosine-kinase CpsD connects capsule cynthesis with the cell cycle in *Streptococcus pneumoniae*. *PLoS Genetics* 11:e1005518. doi: 10.1371/journal.pgen.1005518

Nygard, A. B., Jorgensen, C. B., Cirera, S., and Fredholm, M. (2007). Selection of reference genes for gene expression studies in pig tissues using SYBR green qPCR. *BMC Mol. Biol.* 8:67. doi: 10.1186/1471-2199-8-67

Petersen, B. L., Dave, R. I., McMahon, D. J., Oberg, C. J., and Broadbent, J. R. (2000). Influence of capsular and ropy exopolysaccharide-producing *Streptococcus thermophilus* on Mozzarella cheese and cheese whey. *J. Dairy Sci.* 83, 1952–1956. doi: 10.3168/jds.S0022-0302(00)75071-5

Petit, C., Grill, J. P., Maazouzo, N., and Marczak, R. (1991). Regulation of polysaccharide formation by *Streptococcus thermophilus* in batch and in fed−batch cultures. *Appl. Microbiol. Biotechnol.* 36, 216–221.

Purwandari, U., and Vasiljevic, T. (2009). Rheological properties of fermented milk produced by a single exopolysaccharide producing *Streptococcus thermophilus* strain in the presence of added calcium and sucrose. *Int. J. Dairy Technol.* 62, 411–421.

Ryan, P. M., Ross, R. P., Fitzgerald, G. F., Caplice, N. M., and Stanton, C. (2015). Sugar-coated: exopolysaccharide producing lactic acid bacteria for food and human health applications. *Food Funct.* 6, 679–693. doi: 10.1039/c4fo00529e

Sen, A., Rothenberg, M. E., Mukherjee, G., Feng, N., Kalisky, T., Nair, N., et al. (2012). Innate immune response to homologous rotavirus infection in the small intestinal villous epithelium at single-cell resolution. *Proc. Nat. Acad. Sci. USA.* 109l, 20667–20672. doi: 10.1073/pnas.1212188109

Tada, A., Zelaya, H., Clua, P., Salva, S., Alvarez, S., Kitazawa, H., et al. (2016). Immunobiotic Lactobacillus strains reduce small intestinal injury induced by intraepithelial lymphocytes after Toll-like receptor 3 activation. *Inflamm. Res.* 65, 771–783. doi: 10.1007/s00011-016-0957-7

Torino, M. I., Font, de Valdez, G., and Mozzi, F. (2015). Biopolymers from lactic acid bacteria. Novel applications in foods and beverages. *Front. Microbiol.* 6:834. doi: 10.3389/fmicb.2015.00834

Vaningelgem, F., Zamfir, M., Mozzi, F., Adriany, T., Vancanneyt, M., Swings, J., et al. (2004). Biodiversity of exopolysaccharides produced by *Streptococcus thermophilus* strains is reflected in their production and their molecular and functional characteristics. *Appl. Environ. Microbiol.* 70, 900–912. doi: 10.1128/aem.70.2.900-912.2004

Villena, J., Salva, S., Nuñez, M., Corzo, J., Tolaba, R., Faedda, J., et al. (2012). Probiotics for everyone! The novel immunobiotic *Lactobacillus rhamnosus* CRL1505 and the beginning of Social Probiotic Programs in Argentina. *Int. J. Biotechnol. Wellness Industries* 1, 189–198.

Villena, J., Vizoso-Pinto, M. G., and Kitazawa, H. (2016). Intestinal innate antiviral immunity and immunobiotics: beneficial effects against rotavirus infection. *Front. Immunol.* 7:563. doi: 10.3389/fimmu.2016.00563

Wu, Q., Chu, H., Padmanabhan, A., and Shah, N. P. (2019). Functional genomic analyses of exopolysaccharide-producing *Streptococcus thermophilus* ASCC 1275 in response to milk fermentation conditions. *Front. Microbiol.* 10:1975. doi: 10.3389/fmicb.2019.01975

Wu, Q., and Shah, N. P. (2018). Comparative mRNA-seq analysis reveals the improved EPS production machinery in *Streptococcus thermophilus* ASCC 1275 during optimized milk fermentation. *Front. Microbiol.* 9:445. doi: 10.3389/fmicb.2018.00445

Wu, Q., Tun, H. M., Leung, F. C. C., and Shah, N. P. (2014). Genomic insights into high exopolysaccharide-producing dairy starter bacterium *Streptococcus thermophilus* ASCC1275. *Sci. Rep.* 4:4974. doi: 10.1038/srep04974

Xiong, Z. Q., Kong, L. H., Lai, P. F. H., Xia, Y. J., Liu, J. C., Li, Q. Y., et al. (2019). Genomic and phenotypic analysis of exopolysaccharide biosynthesis in *Streptococcus thermophilus* S-3. *J. Dairy Sci.* 102, 4925–4934. doi: 10.3168/jds.2018-15572

Yamauchi, R., Maguin, E., Horiuchi, H., Hosokawa, M., and Sasaki, Y. (2019). The critical role of urease in yogurt fermentation with various combinations of *Streptococcus thermophilus* and *Lactobacillus delbruecki* spp. *bulgaricus*. *J. Dairy Sci.* 102, 1033–1043. doi: 10.3168/jds.2018-15192

Yother, J. (2011). Capsules of *Streptococcus pneumoniae* and other bacteria: paradigms for polysaccharide biosynthesis and regulation. *Annu. Rev. Microbiol.* 65, 563–581. doi: 10.1146/annurev.micro.62.081307.162944

Zeidan, A. A., Poulsen, V. K., Janzen, T., Buldo, P., Derkx, P. M. F., Øregaard, G., et al. (2017). Polysaccharide production by lactic acid bacteria: from genes to industrial applications. *FEMS Microbiol. Rev.* 41, S168–S200.

Conflict of Interest: KK was employed by the company Meiji Co., Ltd.

The remaining authors declare that the research was conducted in the absence of any commercial or financial relationships that could be construed as a potential conflict of interest.

frontiers in Microbiology

ORIGINAL RESEARCH
published: 07 July 2020
doi: 10.3389/fmicb.2020.01544

Extracellular Vesicles Produced by the Probiotic *Propionibacterium freudenreichii* CIRM-BIA 129 Mitigate Inflammation by Modulating the NF-κB Pathway

*Vinícius de Rezende Rodovalho[1,2], Brenda Silva Rosa da Luz[1,2], Houem Rabah[1], Fillipe Luiz Rosa do Carmo[2], Edson Luiz Folador[3], Aurélie Nicolas[1], Julien Jardin[1], Valérie Briard-Bion[1], Hervé Blottière[4], Nicolas Lapaque[4], Gwenaël Jan[1], Yves Le Loir[1], Vasco Ariston de Carvalho Azevedo[2] and Eric Guédon[1]**

[1] *INRAE, Institut Agro, STLO, Rennes, France,* [2] *Laboratory of Cellular and Molecular Genetics, Institute of Biological Sciences, Federal University of Minas Gerais, Belo Horizonte, Brazil,* [3] *Biotechnology Center, Federal University of Paraíba, João Pessoa, Brazil,* [4] *INRAE, AgroParisTech, Paris-Saclay University, Micalis Institute, Jouy-en-Josas, France*

OPEN ACCESS

Edited by:
Jasna Novak, University of Zagreb, Croatia

Reviewed by:
Haruki Kitazawa, Tohoku University, Japan
Julio Villena, CONICET Centro de Referencia para Lactobacilos (CERELA), Argentina
Veera Kainulainen, University of Helsinki, Finland

***Correspondence:**
Eric Guédon
eric.guedon@inrae.fr

Specialty section:
This article was submitted to Food Microbiology, a section of the journal Frontiers in Microbiology

Received: *09 March 2020*
Accepted: *15 June 2020*
Published: *07 July 2020*

Citation:
Rodovalho VR, Luz BSR, Rabah H, do Carmo FLR, Folador EL, Nicolas A, Jardin J, Briard-Bion V, Blottière H, Lapaque N, Jan G, Le Loir Y, de Carvalho Azevedo VA and Guédon E (2020) Extracellular Vesicles Produced by the Probiotic Propionibacterium freudenreichii CIRM-BIA 129 Mitigate Inflammation by Modulating the NF-κB Pathway. Front. Microbiol. 11:1544. doi: 10.3389/fmicb.2020.01544

Extracellular vesicles (EVs) are nanometric spherical structures involved in intercellular communication, whose production is considered to be a widespread phenomenon in living organisms. Bacterial EVs are associated with several processes that include survival, competition, pathogenesis, and immunomodulation. Among probiotic Gram-positive bacteria, some *Propionibacterium freudenreichii* strains exhibit anti-inflammatory activity, notably via surface proteins such as the surface-layer protein B (SlpB). We have hypothesized that, in addition to surface exposure and secretion of proteins, *P. freudenreichii* may produce EVs and thus export immunomodulatory proteins to interact with the host. In order to demonstrate their production in this species, EVs were purified from cell-free culture supernatants of the probiotic strain *P. freudenreichii* CIRM-BIA 129, and their physicochemical characterization, using transmission electron microscopy and nanoparticle tracking analysis (NTA), revealed shapes and sizes typical of EVs. Proteomic characterization showed that EVs contain a broad range of proteins, including immunomodulatory proteins such as SlpB. *In silico* protein-protein interaction predictions indicated that EV proteins could interact with host proteins, including the immunomodulatory transcription factor NF-κB. This potential interaction has a functional significance because EVs modulate inflammatory responses, as shown by IL-8 release and NF-κB activity, in HT-29 human intestinal epithelial cells. Indeed, EVs displayed an anti-inflammatory effect by modulating the NF-κB pathway; this was dependent on their concentration and on the proinflammatory inducer (LPS-specific). Moreover, while this anti-inflammatory effect partly depended on SlpB, it was not abolished by EV surface proteolysis, suggesting possible intracellular sites of action for EVs. This is the first report on identification of *P. freudenreichii*-derived

EVs, alongside their physicochemical, biochemical and functional characterization. This study has enhanced our understanding of the mechanisms associated with the probiotic activity of *P. freudenreichii* and identified opportunities to employ bacterial-derived EVs for the development of bioactive products with therapeutic effects.

Keywords: extracellular vesicles, membrane vesicles, probiotic, propionibacteria, immunomodulation, anti-inflammatory, IL-8, NF-κB

INTRODUCTION

Intercellular communication is an essential biological process that involves several soluble biomolecules that may be secreted, surface-exposed or packed inside extracellular vesicles (EVs) (Gho and Lee, 2017; Toyofuku, 2019). EVs are lipid bilayer nanoparticles which range in size from 20 to 300 nm and are released by cells from all living kingdoms (Brown et al., 2015; Kim et al., 2015a; Liu et al., 2018a). They play a pivotal role in cell-to-cell communication through their ability to transport bioactive molecules (proteins, nucleic acids, lipids, metabolites) from donor to recipient cells. Bacterial EVs are implicated in virulence factor delivery, antibiotic resistance, competition, survival, and host cell modulation (Kim et al., 2015b; Toyofuku et al., 2019).

The participation of EVs in the beneficial roles of probiotic bacteria has been increasingly reported (Molina-Tijeras et al., 2019). The release of EVs by *Lactobacillus* species is well documented; *Lactobacillus reuteri* DSM 17938-derived EVs are associated with extracellular DNA-dependent biofilm formation (Grande et al., 2017) and EVs secreted by *Lactobacillus casei* BL23 have also been reported and shown to contain diverse biomolecules which include nucleic acids and proteins previously associated with its probiotic effects, such as p40 and p75 (Rubio et al., 2017). *Lactobacillus rhamnosus* GG-derived EVs have been associated with the apoptosis of hepG2 cancer cells (Behzadi et al., 2017), and *Lactobacillus plantarum* WCFS1-derived EVs modulated the response of human cells to vancomycin-resistant enterococci (Li et al., 2017). Moreover, EVs derived from other probiotic species, such as *Bifidobacterium longum* KACC 91563, impact host cell responses by inducing mast cell apoptosis, which has implications for the treatment of food allergies (Kim et al., 2016). Furthermore, probiotic strains of *Escherichia coli* release outer membrane vesicles (OMVs) that are involved in reinforcement of the gastrointestinal epithelial barrier (Alvarez et al., 2016), the regulation of inflammatory responses and intestinal homeostasis, via the NOD1-signaling pathway (Cañas et al., 2018).

Propionibacterium freudenreichii has also been regarded consistently as a probiotic species, mainly because of its immunomodulatory properties and protective effects against experimentally induced inflammation *in vivo* (Lan et al., 2007a, 2008; Foligne et al., 2010; Cousin et al., 2012; Rabah et al., 2018a; Do Carmo et al., 2019). *P. freudenreichii* is a Gram-positive, pleiomorphic, microaerophilic dairy bacterium that is generally recognized as safe (GRAS) and has a qualified presumption of safety (QPS) status (Loux et al., 2015; Deutsch et al., 2017; Rabah et al., 2017). This species is also known for its involvement in the ripening, texture, and flavor of cheese (Ojala et al., 2017) and in vitamin B12 synthesis (Deptula et al., 2017). A *P. freudenreichii* strain was recently isolated from the gut microbiota of a human breast milk-fed preterm infant, suggesting that this species could also be considered as a commensal inhabitant of the human digestive tract (Colliou et al., 2017).

As for the molecular mechanisms underlying its probiotic effects, some studies have focused on identifying the surface proteins of *P. freudenreichii* and their role in cytokine induction (Le Maréchal et al., 2015; Deutsch et al., 2017; Do Carmo et al., 2019). Notably, cell wall-related proteins, S-layer type proteins, moonlighting proteins and proteins related to interactions with the host have been identified as important actors in immunomodulation of *P. freudenreichii* strain CIRM-BIA 129 (Le Maréchal et al., 2015). Specifically, recent studies reported the role of surface-layer protein B (SlpB) from this strain in bacterial adhesion to intestinal HT-29 cells and immunomodulation (Do Carmo et al., 2017, 2019; Rabah et al., 2018b), as well as that of large surface layer protein A (LspA) from strain P. UF1 in the regulation of colonic dendritic cells during inflammation via SIGNR1 binding (Ge et al., 2020). As well as surface proteins, additional metabolites may contribute to the probiotic effect, such as 1,4-Dihydroxy-2-naphthoic acid (DHNA) from *P. freudenreichii* ET3, which is linked to AhR pathway activation (Fukumoto et al., 2014). DHNA has also been implicated in colitis regression (Okada et al., 2013). Moreover, short-chain fatty acids (SCFAs) from strains TL133 and TL142 have been demonstrated to play a role in inducing apoptosis of tumor cell lines (Lan et al., 2007b, 2008; Cousin et al., 2016).

In view of the fact that EVs are emerging as important carriers of biologically active cargos and that vesiculogenesis is a generally occurring phenomenon, we hypothesized that they might explain some of the probiotic properties of *P. freudenreichii.* For the first time, our findings have shown that this species produces EVs, and we have characterized their physiochemical, biochemical and functional features. We report that *P. freudenreichii* CIRM-BIA 129-derived EVs are implicated in its anti-inflammatory properties, via modulation of the NF-κB pathway, thus building on knowledge regarding this important probiotic bacterium.

MATERIALS AND METHODS

Bacterial Strain and Growth Conditions

Propionibacterium freudenreichii CIRM-BIA 129 (equivalent to the ITG P20 strain) was supplied, stored and maintained by the CIRM-BIA Biological Resource Center (Centre International de Ressources Microbiennes-Bactéries d'Intérêt Alimentaire,

INRAE, Rennes, France). *P. freudenreichii* CIRM-BIA 129 and its isogenic *P. freudenreichii* CIRM-BIA 129 Δ*slpB* mutant strain (Do Carmo et al., 2017) were cultured in cow milk ultrafiltrate (UF) supplemented with 100 mM sodium lactate and 5 g L^{-1} casein hydrolysate at 30°C and without agitation, until stationary phase (72 h of incubation, 2×10^9 CFU mL^{-1}), as reported previously (Cousin et al., 2012).

Purification of EVs

Cells were pelleted by the centrifugation (6000 *g*, 15 min, room temperature) of cultures in UF (500 mL) and the supernatant fraction was filtered using 0.22 μm Nalgene top filters (Thermo Scientific) to remove any remaining bacterial cells. The supernatant was then concentrated 1000 times using Amicon ultrafiltration units with a 100 kDa cut-off point in successive centrifugations at 2500 *g*. The concentrated suspension of EVs was recovered in TBS buffer (Tris-Buffered Saline, 150 mM NaCl; 50 mM Tris–HCl, pH 7.5) and further purified by size exclusion chromatography (qEV original 70 nm; iZON), as recommended by the manufacturer (Böing et al., 2014). Briefly, 0.5 mL of EV samples was applied to the top of the chromatographic column, followed by TBS buffer for elution. Then, fractions of 0.5 mL were recovered in separate tubes. Fractions 1–6 were discarded as void, EVs-containing fractions (fractions 7–9) were pooled together and the remaining fractions were discarded due to protein contamination or low EV content.

Negative Staining for Transmission Electron Microscopy

To characterize the shape of purified EVs, negative staining electron microscopy was conducted as previously described (Tartaglia et al., 2018). Briefly, a drop of EV solution was applied on a glow-discharged formvar-coated copper EM grid and blotted with a filter paper to remove excess solution. A drop of 2% uranyl acetate was applied to the EM grid, blotted again and finally dried before imaging under a Jeol 1400 transmission electron microscope (JEOL Ltd.) operating at 120 Kv.

Nanoparticle Tracking Analysis for EV Size and Concentration Assessment

To measure the size and concentration of EVs, nanoparticle tracking analysis (NTA) was performed at 25.0°C using a NanoSight NS300 instrument (Malvern Panalytical) with a sCMOS camera and a Blue488 laser (Mehdiani et al., 2015). Samples were applied in constant flux with a syringe pump speed of 50. For each measurement, 5×60-s videos were recorded with camera level 15. Other parameters were adjusted accordingly to achieve image optimization.

Proteomic Analysis

Three independent biological replicates of purified EVs from *P. freudenreichii* CIRM-BIA 129 (approximately 1 μg per sample) and the whole cell proteome were separated and visualized using 12% SDS-PAGE (Laemmli, 1970) and silver staining (Switzer et al., 1979). Next, EV proteins were hydrolyzed with trypsin for NanoLC-ESI-MS/MS analysis, as previously described (Gagnaire et al., 2015; Huang et al., 2016). Briefly, gel pieces were washed with acetonitrile and ammonium bicarbonate solution and dried under a vacuum. Next, in-gel trypsin digestion was performed overnight at 37°C and stopped with trifluoroacetic acid (Sigma-Aldrich). After digestion, the peptides were identified from the MS/MS spectra using X!TandemPipeline software (Langella et al., 2017) and searches were performed against the genome sequence of *P. freudenreichii* CIRM-BIA 129. The database search parameters were specified as follows: trypsin cleavage was used and the peptide mass tolerance was set at 10 ppm for MS and 0.05 Da for MS/MS. Methionine oxidation was selected as a variable modification. For each peptide identified, a maximum *e*-value of 0.05 was considered to be a prerequisite for validation. A minimum of two peptides per protein was imposed, resulting in a false discovery rate (FDR) of 0.15% for protein identification.

Proteomic data were further analyzed and visualized using Python libraries Pandas, NumPy, Matplotlib, and Seaborn. Functional annotations and Clusters of Orthologous Groups (COGs) were obtained using the eggNOG-mapper v2 web tool (Huerta-Cepas et al., 2017, 2019), while proteins and gene data were retrieved from NCBI and Uniprot (Bateman, 2019). Subcellular location prediction was performed with CELLO2GO (Yu et al., 2014) and the prediction of lipoproteins was conducted using PRED_LIPO (Bagos et al., 2008).

Prediction of Protein-Protein Interactions

In order to screen for potential biological functions of EVs, the prediction of interactions between EV proteins and human proteins was carried out. The reference human proteome was retrieved from Uniprot (UP000005640) and contained 74,788 protein sequences. For the first method of prediction, EVs and human proteins were submitted to the InterSPPI web server (Lian et al., 2019), a machine-learning-based predictor. For the second method of prediction, a interolog-based approach was used (Folador et al., 2014), establishing homology relationships with the interactions described in the String and Intact databases (Kerrien et al., 2012; Szklarczyk et al., 2017). The resulting interactions were filtered according to the prediction scores (intersppi: minimum score of 0.9765, for a specificity 0.99; interolog: minimum score of 500 out of 1000). Next, the dataset was reduced to a canonical representation, only retaining the human protein isoform appearing in highest-scoring interactions and removing non-reviewed human proteins. For the predicted interactions, the human counterpart was programmatically mapped to KEGG pathways in order to identify the associated functional modules. Data analysis and graphic representations were obtained using Python libraries Pandas, Seaborn, Matplotlib, Matplotlib_venn, and Cytoscape software (Shannon, 2003).

Culture of Eukaryotic Cells

HT-29 human epithelial cells were used for immunomodulation assays; either the parental lineage (HT-29, colon adenocarcinoma; ATCC HTB-38) or a lineage transfected with the secreted alkaline phosphatase (SEAP) reporter

gene for NF-kB activation monitoring (HT-29/kb-seap-25) (Lakhdari et al., 2010). The reporter HT-29/kb-seap-25 cells were cultured in RPMI-Glutamine medium (Sigma-Aldrich), supplemented with 10% fetal bovine serum (Corning), 1% non-essential amino acids, 1% sodium pyruvate, 1% HEPES buffer (Thermofisher Scientific), and 1% penicillin-streptomycin (Lonza) according to Lakhdari et al. (2010). The parental HT-29 cells were cultured in high-glucose DMEM medium (Dominique Dutscher) supplemented with 10% fetal bovine serum and 1% penicillin-streptomycin (Do Carmo et al., 2017). For subcultures, cells were rinsed with DPBS (Thermofisher Scientific) and detached with a trypsin (0.05%) – EDTA (0.02%) solution (Sigma). Periodically, 100 μg/mL Zeocin (Invivogen) was applied to the HT-29/kb-seap-25 cell culture in order to maintain selective pressure on the cells containing the transfected plasmid.

NF-κB Modulation Assays

HT-29/kb-seap-25 cells were seeded on 96-well plates at 3×10^4 cells/well and incubated for 24 h at 37°C under 5% CO_2 prior to stimulation (Lakhdari et al., 2010). Monolayer confluence was checked under the microscope before and after every stimulation. TNFα (1 ng mL^{-1}; PeproTech), IL-1β (1 ng mL^{-1}; Invivogen), and LPS from *E. coli* O111:B4 (1 ng mL^{-1}; L3024-5MG, Sigma-Aldrich) were used to induce inflammation. The cells were stimulated with the samples (controls and EV preparations) and inflammation inducers for 24 h. The supernatants from all the wells were then revealed with Quanti-Blue™ reagent (Invivogen) to assess SEAP activity. Cell proliferation was evaluated under all conditions using the CellTiter 96® AQueous One Solution Cell Proliferation Assay (MTS, Promega), according to the manufacturer's instructions. Absorbance was read at 655 nm for the SEAP activity assay and at 490 nm for the MTS assay using a Xenius (SAFAS Monaco) microplate reader. For surface protein assays, 10^9 EV ml^{-1} were applied directly or after incubation at 37°C for 1 h in the presence or absence of proteinase K (20 μg mL^{-1}; Qiagen), in order to evaluate a possible role for EV surface proteins in immunomodulation.

ELISA Cytokine Assay

Enzyme-linked immunosorbent assay (ELISA) tests tests were performed under the same conditions as the NF-κB modulation assays using HT-29 parental cells. The human IL-8/CXCL8 DuoSet (R&D Systems) kit was used to evaluate cell culture supernatants after stimulation, according to the manufacturer's instructions. Absorbance was read at 450 nm using a Xenius (SAFAS Monaco) microplate reader.

Statistical Analysis

All experiments were conducted independently and in triplicate at least, and the results are expressed as means ± standard deviations of biological replicates. For absorbance measurements, the values were normalized by the control condition. The differences between groups were verified using one-way ANOVA followed by Tukey's multiple comparisons test with GraphPad Prism (GraphPad Software, San Diego, CA, United States).

RESULTS

Propionibacterium freudenreichii Produces Extracellular Vesicles

In order to determine whether *P. freudenreichii* produced EVs, strain CIRM-BIA 129 was cultured in cow milk UF medium and EVs were purified from the cell-free supernatants of stationary phase cultures. As a control, we checked that EVs were absent from the UF medium before being used for bacterial culture. Visualization by electron microscopy revealed that *P. freudenreichii* strain CIRM-BIA 129 produced EVs of a typical shape, i.e., spherical cup-shaped structures (**Figure 1A**). Size characterization by NTA showed that the EVs presented a monodisperse profile with modal diameter of 84.80 ± 2.34 nm (**Figure 1B**).

P. freudenreichii-Secreted EVs Contain a Functionally Diverse Set of Proteins, Including Immunomodulatory Proteins

Cargo proteins associated with *P. freudenreichii*-secreted EVs were determined by Nano LC-ESI-MS/MS analysis from three biological replicates of EVs. A total of 319 proteins was identified consistently in EVs derived from UF medium cultures (**Supplementary Table S1**), which corresponds to 11% of the whole theoretical proteome of *P. freudenreichii* CIRM-BIA 129. **Figure 2A** confirmed a much more complex proteome in the whole cell *P. freudenreichii* extract than in the EV extract.

The proteins associated with these EVs were distributed between most of the COG categories (**Figure 2B**). The majority of proteins could be assigned to COGs related to the general category of "metabolism," e.g., energy production and conversion (C, 14.8%), amino acid transport and metabolism (E, 10.4%), and carbohydrate transport and metabolism (G, 8%). The most common COGs in the general category of "information, storage and processing" were translation, ribosomal structure and biogenesis (J, 7.1%) and transcription (K, 4.2%). Finally, cell wall/membrane/envelope biogenesis (M, 5.3%) and post-translational modifications, protein turnover and chaperones (O, 5%), were the most frequently counted COGs in the general category of "cellular processes and signaling." Interestingly, several proteins previously identified as important actors in immunomodulation were packed within EVs: enolase (Eno1, PFCIRM129_06070), aconitase (Acn, PFCIRM129_04640), glutamine synthetase (GlnA1, PFCIRM129_11730), glucose-6-phosphate isomerase (Gpi, PFCIRM129_10645), triosephosphate isomerase (Tpi1, PFCIRM129_11290), the surface-layer proteins SlpB (PFCIRM129_00700) and SlpE (PFCIRM129_05460), the BopA solute binding protein (PFCIRM129_08120), internaline A (InlA, PFCIRM129_12235), the hypothetical protein PFCIRM129_10785 and the GroL2 chaperonin (PFCIRM129_10100) (Le Maréchal et al., 2015; Deutsch et al., 2017; Do Carmo et al., 2017).

Regarding predictions of the subcellular localization of the proteins, they were mainly predicted to be cytoplasmic (n = 239), but some membrane (n = 51), and extracellular (n = 29) proteins were also identified (**Figure 2C**). Lipoprotein

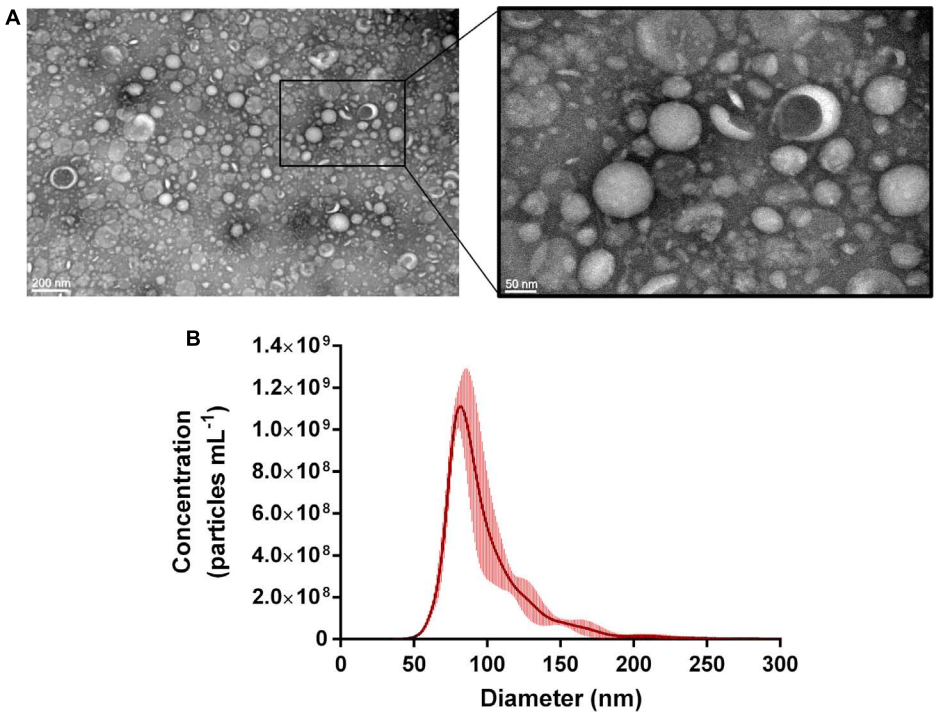

FIGURE 1 | *P. freudenreichii* CIRM-BIA 129 secretes extracellular vesicles. **(A)** Transmission electron microscopy image after the negative staining of *P. freudenreichii*-secreted EVs purified from UF culture supernatants. **(B)** Size distribution (diameter) of purified EVs as measured by nanoparticle tracking analysis (NTA). Concentration data are expressed as mean ± standard deviation from three independent biological replicates.

signal peptides were also predicted in a small fraction of the proteins (n = 22). Other proteins were predicted to contain a secretory signal peptide I (n = 22) and transmembrane motifs (n = 34) (**Figure 2D**). Regarding the protein abundance index (Ishihama et al., 2005), it displayed a non-normal distribution with a tail of highly expressed proteins, including immunomodulatory SlpB, 60 kDa chaperonin 2 (GroL2) and enolase 1 (Eno1), as well as cold shock-like protein CspA, iron/manganese superoxide dismutase (SodA), cysteine synthase 2 (Cys2), alkyl hydroperoxide reductase subunit C (AhpC), and malate dehydrogenase (Mdh) (**Figure 2E**).

The Proteins From *P. freudenreichii*-Secreted EVs Potentially Interact With Human Immunomodulatory Proteins

The proteins found in *P. freudenreichii*-derived EVs were tested against the human proteome *in silico* in order to predict their interactions. Machine learning-based (intersppi) and homology-based (interolog) methods were employed for this task. There was a considerable difference regarding the number of predicted interactions which depended on the method used. Intersppi predicted 117,513 interactions, while the interolog method predicted 2,890 interactions; there were 143 common interactions between the two methods (**Figure 3A** and **Supplementary Tables S2–S4**). Regarding interacting bacterial proteins, 115 proteins appeared exclusively in intersppi interactions, 51 proteins appeared exclusively in interolog interactions and 90 proteins appeared in interactions predicted by both methods (**Figure 3B** and **Supplementary Table S5**). As for interacting human proteins, the majority was predicted by the intersppi method only (6,883 proteins), whereas 747 proteins appeared exclusively in interolog interactions and 611 proteins appeared in interactions shared by both methods of prediction (**Figure 3C** and **Supplementary Table S6**).

The predicted interactions mapped to diverse KEGG terms, including metabolism, signal transduction, infectious diseases and the immune system (**Supplementary Figure S1**). Interestingly, the nuclear factor NF-κB p105 subunit (NFKB1, P19838) was the most frequent interacting human protein considering common and intersppi-exclusive interactions. The subnetwork of interactions mapping to the KEGG NF-κB signaling pathway (**Figure 3D**) included both interactions with adapter molecules (e.g., TICAM1, TICAM2, TRAF6) and Toll-like receptors (e.g., TLR1, TLR4, TLR5, TL6), as well as NFKB1 itself (**Supplementary Figures S2, S3**). These results therefore indicated some interesting potential roles for EV proteins in immunomodulation that need to be verified experimentally.

P. freudenreichii-Secreted EVs Modulate the NF-κB Pathway in a Dose and Inducer-Dependent Manner

In view of the finding that *in silico* predictions showed interactions between EV proteins and human

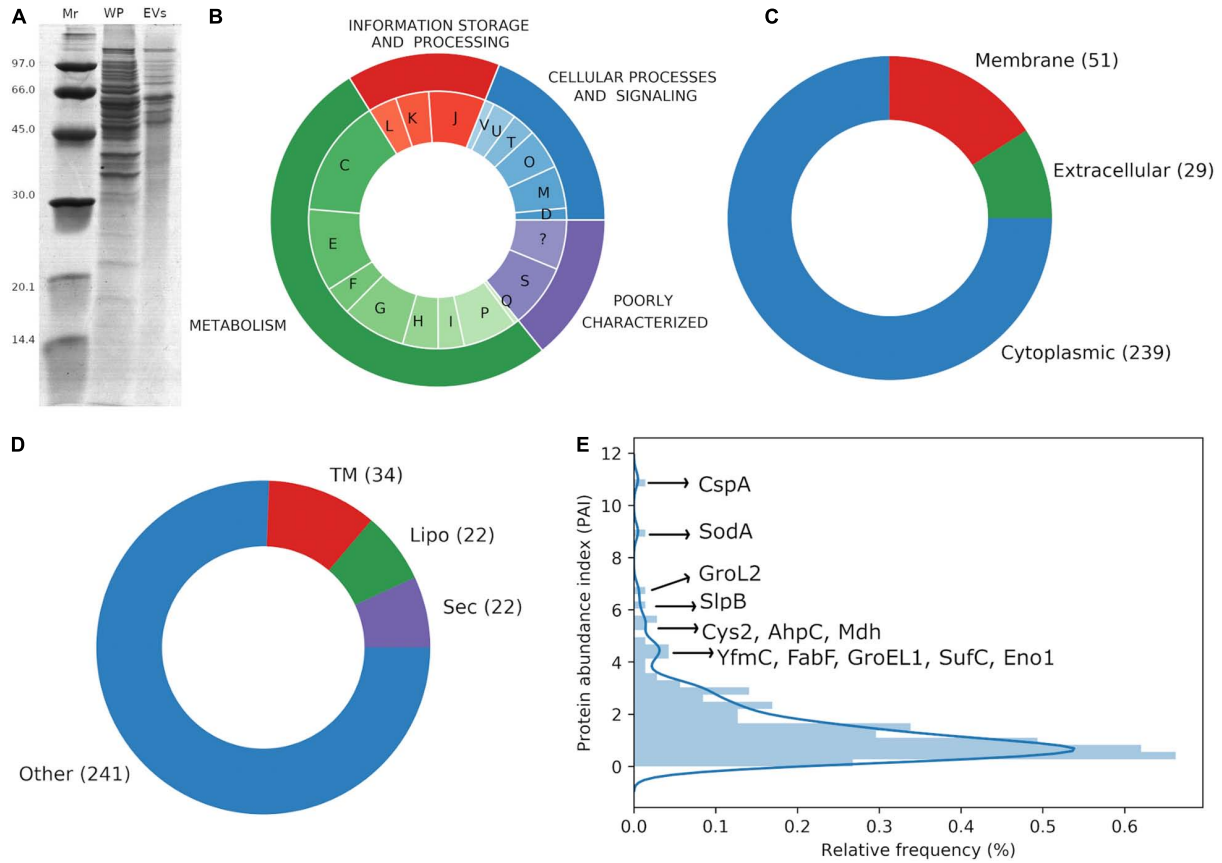

FIGURE 2 | *P. freudenreichii*-secreted EVs contain proteins involved in interactions with the host. **(A)** SDS-PAGE showing the protein profile of the whole proteome (WP) and vesicular proteome (EVs). Molecular weight standards are indicated on the left (Mr, kDa). **(B)** Functional annotation of EV proteins by the prediction of COG categories: D – Cell cycle control, cell division, chromosome partitioning, M – Cell wall/membrane/envelope biogenesis, O – Post-translational modification, protein turnover, and chaperones, T – Signal transduction mechanisms, U – Intracellular trafficking, secretion, and vesicular transport, V – Defense mechanisms, J – Translation, ribosomal structure and biogenesis, K – Transcription, L – Replication, recombination and repair, C – Energy production and conversion, E – Amino acid transport and metabolism, F – Nucleotide transport and metabolism, G – Carbohydrate transport and metabolism, H – Coenzyme transport and metabolism, I – Lipid transport and metabolism, P – Inorganic ion transport and metabolism, Q – Secondary metabolites biosynthesis, transport, and catabolism, S – Function unknown, ? – Not predicted. **(C)** Subcellular localization of EV proteins as predicted by Cello2GO. **(D)** Prediction of lipoproteins by PRED-LIPO: Sec: secretion signal peptide, Lipo: lipoprotein signal peptide, TM: transmembrane, Other: no signals found. **(E)** Protein abundance index (PAI) frequency distribution for EV proteins, highlighting the most frequently expressed proteins.

immunomodulatory proteins (and particularly NFKB1), together with previous evidence of immunomodulatory roles for *P. freudenreichii*, we investigated this potential *in vitro*. A cellular reporter system regarding modulation of the regulatory activity of the NF-κB transcription factor (HT-29/kb-seap-25) was therefore employed (Lakhdari et al., 2010). Cells were kept in contact with proinflammatory inducers (LPS, TNF-α or IL-1β) and EV preparations, in order to test the ability of EVs to attenuate the induced inflammatory response.

Among cells that were not treated with proinflammatory inducers, their exposure to EVs did not affect the activity of the reporter, keeping a basal level of NF-κB activity (**Figure 4A**). When HT-29/kb-seap-25 cells were treated with LPS in the absence of EVs, NF-κB activation increased, thus showing LPS-dependent induction of the NF-κB pathway. With the addition of EVs at increasing concentrations, a dose-dependent reduction of NF-κB activation was observed. With the highest EV concentration tested (1.0×10^9 EVs ml^{-1}), NF-κB activation was comparable to that of untreated control cells. Furthermore, when the EV concentration was kept at a constant level, NF-κB modulation was also dependent on the pathway inducer. In the presence of EVs, there was a significant reduction in NF-κB activation in LPS-treated cells, but not in cells treated with other inducers (TNF-α and IL-1β) (**Figure 4B**).

P. freudenreichii-Secreted EVs Also Modulate IL-8 Release in a Dose and Inducer-Dependent Manner

To further investigate the anti-inflammatory role suggested by the reduction in NF-κB activity, release of the proinflammatory chemokine IL-8 by HT-29 cells was determined in the presence of various EV concentrations and proinflammatory inducers.

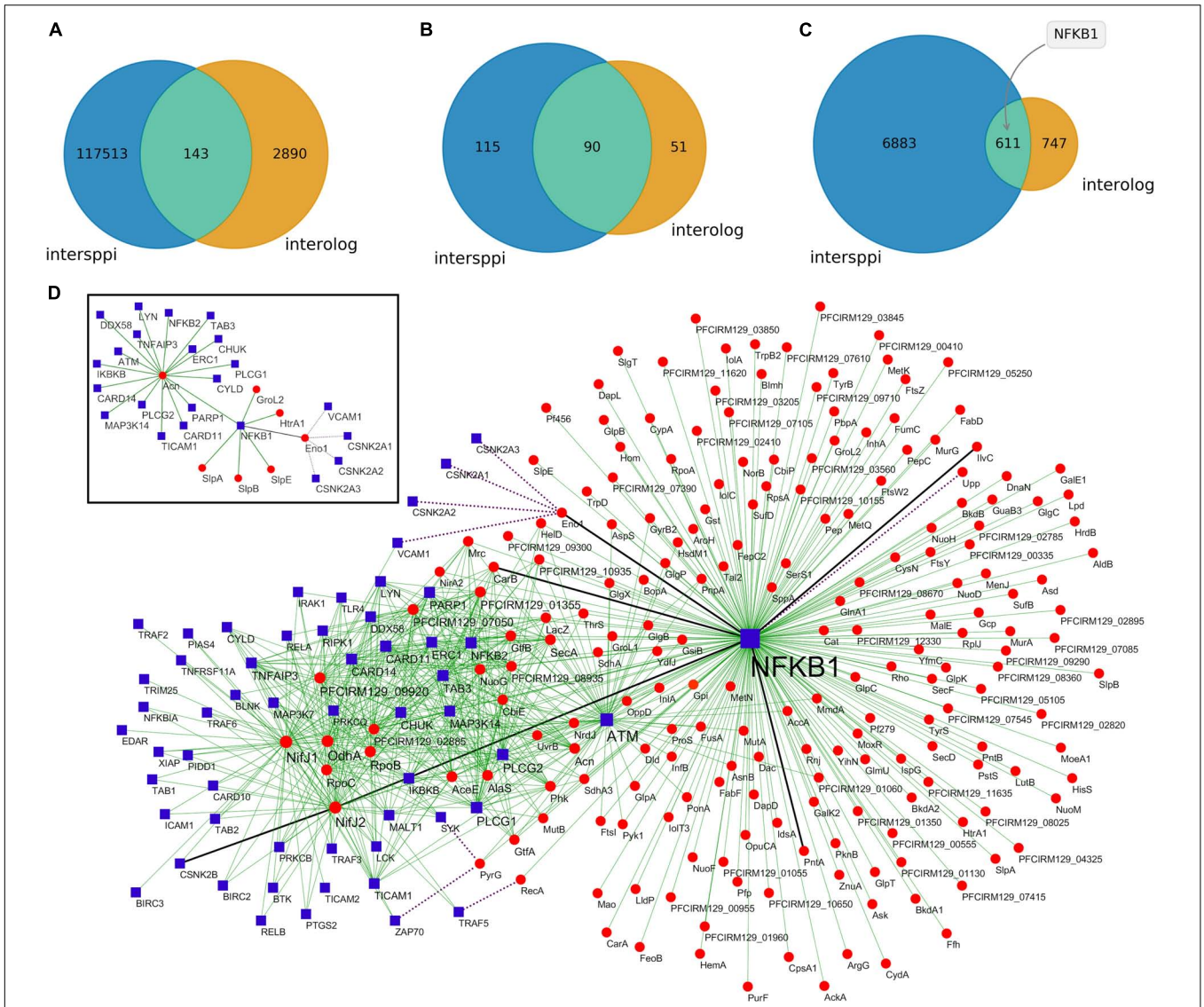

FIGURE 3 | Predictions of protein-protein interactions suggest a modulation of the NF-κB signaling pathway by *P. freudenreichii*-secreted EVs. **(A)** Number of interactions predicted by each methodology. **(B)** Number of bacterial proteins predicted to interact as a function of the prediction method. **(C)** Number of human proteins predicted to interact as a function of the prediction method, highlighting the top-interacting NFKB1 protein. **(D)** Subnetwork of predicted interactions mapping to the KEGG NF-κB pathway. Blue square nodes represent human proteins, red round nodes represent bacterial proteins, full thin green lines represent intersppi-predicted interactions, dotted purple lines represent interolog-predicted interactions and full thick black lines represent interactions shared by both methods. Inset: selected interactions involving bacterial proteins previously associated with immunomodulatory roles.

In the absence of proinflammatory inducers, EVs had no effect on IL-8 release from HT-29 cells (**Figure 5A**). In the TBS buffer control group, LPS-treated HT-29 cells displayed an increase in IL-8 release when compared to untreated cells, reflecting the LPS-induced proinflammatory effect. In the presence of EVs, a significant and dose-dependent decrease of IL-8 release by LPS-stimulated cells was observed. At the highest concentration (1.0×10^9 EVs ml^{-1}), IL-8 release was reduced down to a level comparable to that seen in untreated control cells.

Moreover, as in the case of NF-κB activity, the EV-mediated reduction in IL-8 release was specific to treatment with the LPS proinflammatory inducer (**Figure 5B**). When cells were treated with TNF-α or IL-1β, no effect of EVs could be detected on IL-8 release by HT-29 cells. Taken together, these results showed that *P. freudenreichii*-derived EVs were endowed with anti-inflammatory properties that depended on the concentration and inflammatory stimulus.

P. freudenreichii-Secreted EVs Are Not Cytotoxic Against Intestinal Epithelial Cells

In order to ensure that reductions in NF-κB activation and IL-8 release were associated with regulatory

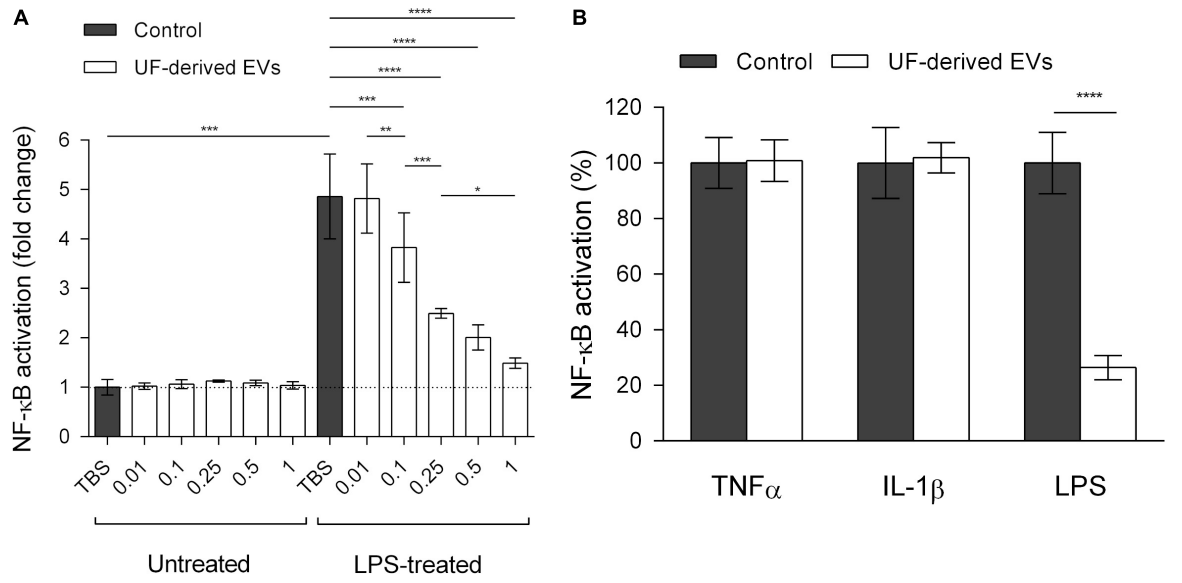

FIGURE 4 | *P. freudenreichii*-secreted EVs specifically mitigate LPS-induced NF-κB activation in intestinal epithelial cells. **(A)** Measure of regulatory activity of the NF-κB transcription factor in HT-29 intestinal epithelial cells untreated or treated with LPS (1 ng mL^{-1}) in the presence of TBS buffer control or different concentrations of EVs purified from the supernatants of *P. freudenreichii* CIRM-BIA 129 culture in UF medium. EV concentrations: 0.01 = 1.0 × 10^7 EVs ml^{-1}, 0.1 = 1.0 × 10^8 EVs ml^{-1}, 0.25 = 2.5 × 10^8 EVs ml^{-1}, 0.5 = 5.0 × 10^8 EVs ml^{-1}, 1 = 1.0 × 10^9 EVs ml^{-1}. **(B)** Percentage NF-κB activation in HT-29 intestinal epithelial cells after stimulation by LPS (1 ng mL^{-1}), TNF-α (1 ng mL^{-1}) or IL-1β (1 ng mL^{-1}) inducers, in the presence or absence of UF-derived EVs (1.0 × 10^9 EVs ml^{-1}). The values are normalized by the control conditions (stimulation by the inducer in the absence of EVs). ANOVA with the Tukey's multiple comparison test: $^*P < 0.05$, $^{**}P < 0.01$, $^{***}P < 0.001$, $^{****}P < 0.0001$.

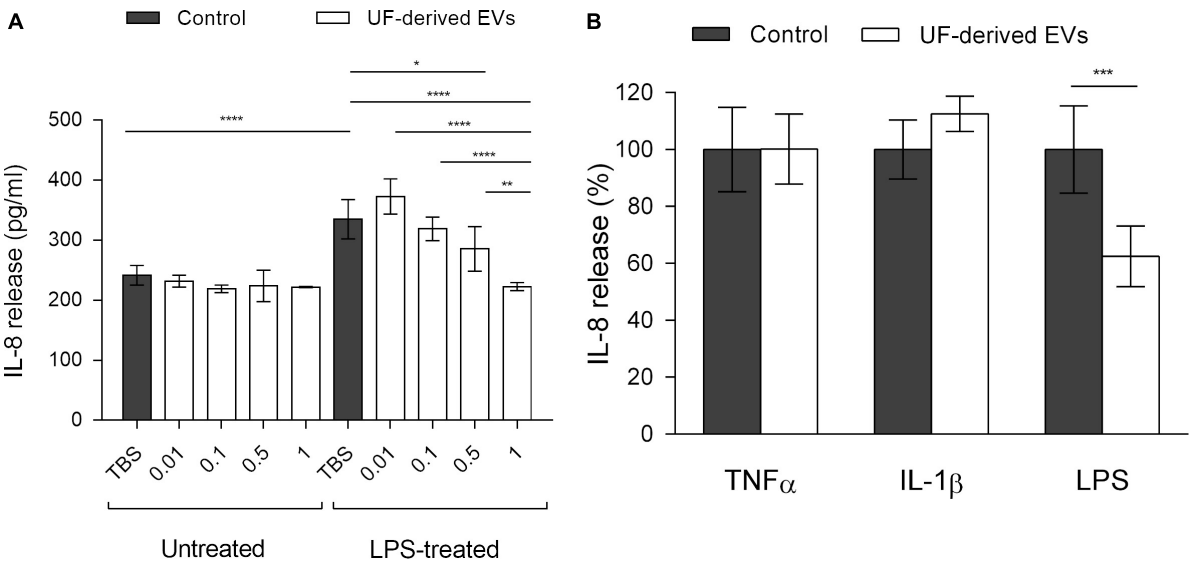

FIGURE 5 | *P. freudenreichii*-secreted EVs mitigate the release of IL-8 induced by LPS. **(A)** Concentration of IL-8 (pg ml^{-1}) released by HT-29 intestinal epithelial cells untreated or treated with LPS (1 ng mL^{-1}) in the presence of different concentrations of EVs purified from the supernatants of *P. freudenreichii* CIRM-BIA 129 culture in UF medium. EV concentrations: 0.01 = 1.0 × 10^7 EVs ml^{-1}, 0.1 = 1.0 × 10^8 EVs ml^{-1}, 0.5 = 5.0 × 10^8 EVs ml^{-1}, 1 = 1.0 × 10^9 EVs ml^{-1}. **(B)** Percentage of IL-8 released by HT-29 intestinal epithelial cells after stimulation by LPS (1 ng mL^{-1}), TNF-α (1 ng mL^{-1}) or IL-1β (1 ng mL^{-1}) inducers, in the presence or absence of UF-derived EVs (1.0 × 10^9 EVs ml^{-1}). The values are normalized by the control conditions (stimulation by inducer in the absence of EVs). One-way ANOVA followed by Tukey's (left panel) or Dunnett's (right panel) multiple comparisons test: $^*P < 0.05$, $^{**}P < 0.01$, $^{***}P < 0.001$, $^{****}P < 0.0001$.

activity and not simply with cell death, an MTS cell proliferation assay was also performed (**Figure 6**). This assay showed that there was no significant difference in cell viability between the control and test groups in terms of both parental HT-29 and HT-29/kb-seap-25 reporter cells.

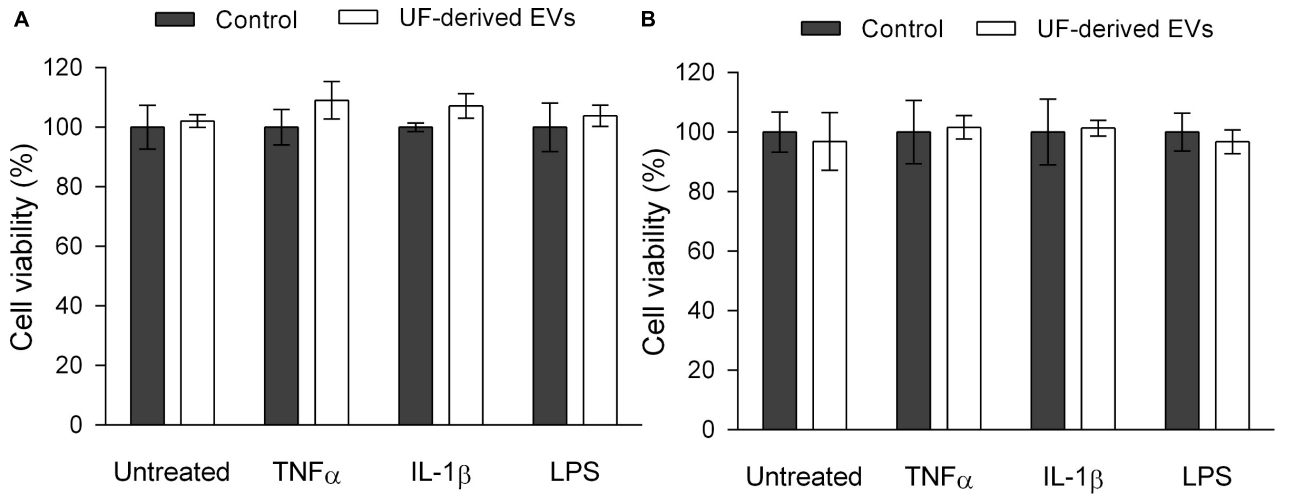

FIGURE 6 | *P. freudenreichii*-secreted EVs are not cytotoxic against intestinal epithelial cells. Viability percentage of HT-29 intestinal epithelial cells **(A)** and HT-29/kb-seap-25 cellular reporter cell line **(B)** before or after stimulation by LPS (1 ng mL^{-1}), TNF-α (1 ng mL^{-1}) or IL-1β (1 ng mL^{-1}) inducers, in the presence or absence of UF-derived EVs (1.0×10^9 EVs ml^{-1}). The values are normalized by the control conditions (control buffer or stimulation by an inducer in the absence of EVs). There are no statistically significant differences between group means as determined by one-way ANOVA followed by Tukey's multiple comparisons test.

Influence of Surface Proteins on NF-κB Modulation

Further tests were performed to determine whether the modulation of NF-κB by *P. freudenreichii* EVs was influenced by a surface-layer protein (SlpB), recognized as being immunomodulatory in the studied strain (Deutsch et al., 2017; Do Carmo et al., 2017; **Figure 7**). EVs derived from an isogenic mutant *P. freudenreichii* CIRM-BIA 129 Δ*slpB* and proven not to produce this specific protein, displayed a partial reduction of NF-κB activation, when compared to wild type-derived EVs. This suggested that SlpB plays a fundamental role in EV modulation of the NF-κB pathway, but it is likely that other important effectors also need to be considered.

Furthermore, in order to determine whether NF-κB pathway modulation by EVs is dependent on proteins that might be exposed on the EV surface, they were treated with proteinase K prior to the cellular assays (**Figure 7**). The incubation of EVs at 37°C for 1 h, in the presence or absence of proteinase K, did not result in significant differences in NF-κB activation, when compared to the wild-type untreated control. This suggested that these immunomodulatory effectors may be inside EVs and not at their surface.

DISCUSSION

Although research on bacterial EVs focused initially on Gram-negative and pathogenic bacteria, a major increase in the number of studies involving Gram-positive and probiotic bacteria has been seen during the past decade (Liu et al., 2018b; Molina-Tijeras et al., 2019). That is in line with the growing recognition of the widespread occurrence and diverse functions of EVs (Brown et al., 2015; Liu et al., 2018a,b). In the case of *P. freudenreichii*, a Gram-positive dairy probiotic bacterium, a recent study indicated the presence of an extracellular structure resembling a potential EV, which bulged out from the membrane of *P. freudenreichii* strain JS22 (Frohnmeyer et al., 2018), suggesting that this species might produce EVs. Nevertheless, ours is the first complete report to have identified the occurrence of EVs in *P. freudenreichii* strain CIRM-BIA 129, and included their physicochemical, biochemical and functional characterization. The EVs thus identified displayed the basic features of extracellular prokaryotic membrane vesicles, i.e., a nanometric size range, a cup-shaped morphology and a spherical structure (Raposo and Stoorvogel, 2013; Liu et al., 2018b; Tartaglia et al., 2018).

CIRM-BIA 129 EVs carry a diverse set of proteins that represent a broad range of biological functions. More than half of these proteins are related to metabolism, so that, initially, they may not appear to exert specific functions outside bacterial cells. However, the transport of metabolism-related proteins by EVs may represent a mechanism of functional exchange and complementation in the context of bacterial communities. For example, members of the *Bacteroides* genus share enzymes with the microbiome through OMVs, so as to contribute to the degradation of complex polysaccharides (Elhenawy et al., 2014; Rakoff-Nahoum et al., 2014; Lynch and Alegado, 2017). On the other hand, some of these metabolism-related proteins, from either *P. freudenreichii* CIRM-BIA 129, or from other strains in the species, have been implicated in interactions with the host. This is the case of enolase (Eno1, PFCIRM129_06070) and aconitase (Acn, PFCIRM129_04640) (Deutsch et al., 2017). Others, such as glutamine synthetase (GlnA1, PFCIRM129_11730), glucose-6-phosphate isomerase (Gpi, PFCIRM129_10645) and triosephosphate isomerase (Tpi1, PFCIRM129_11290), have also been described as moonlighting proteins, with adhesin functions, in other species (Kainulainen et al., 2012;

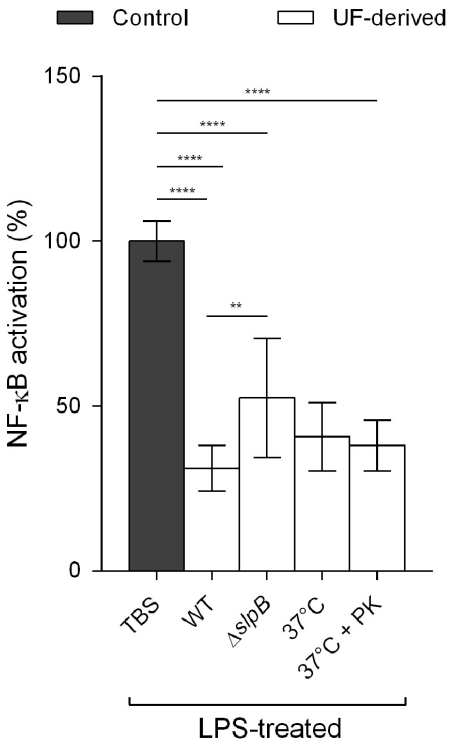

FIGURE 7 | SlpB is required to achieve the effective mitigation of NF-κB activation in human intestinal epithelial cells. Percentage of NF-κB activation in HT-29 intestinal epithelial cells after stimulation by LPS (1 ng μL^{-1}) in the presence or absence of UF-derived EVs (1.0×10^9 EVs ml^{-1}). WT: wild type *P. freudenreichii* CIRM-BIA 129-derived EVs, Δ*SlpB*: isogenic mutant *P. freudenreichii* CIRM-BIA 129 Δ*SlpB*-derived EVs, 37°C: wild type *P. freudenreichii* CIRM-BIA 129-derived EVs incubated at 37°C for 1 h, 37°C + PK: wild type *P. freudenreichii* CIRM-BIA 129-derived EVs incubated at 37°C for 1 h in the presence of proteinase K. The values are normalized by the control conditions (stimulation by an inducer in the absence of EVs). One-way ANOVA followed by Tukey's multiple comparisons test: $^{**}P < 0.01$, $^{****}P < 0.0001$.

Rodríguez-Bolaños and Perez-Montfort, 2019). As well as metabolism-related proteins, other proteins packed into EVs are also related to interactions between *P. freudenreichii* and the host: SlpB (PFCIRM129_00700) and SlpE (PFCIRM129_05460) surface-layer proteins, the BopA solute binding protein (PFCIRM129_08120), internaline A (InlA, PFCIRM129_12235), the hypothetical protein PFCIRM129_10785 and the GroL2 chaperonin (PFCIRM129_10100) (Le Maréchal et al., 2015; Deutsch et al., 2017; Do Carmo et al., 2017). It has been shown that SlpB mediates the adhesion of *P. freudenreichii* CIRM-BIA 129 to intestinal epithelial HT29 cells (Do Carmo et al., 2017), reduces LPS-induced IL-8 expression in HT-29 cells (Do Carmo et al., 2019) and participates in the induction of anti-inflammatory cytokines such as IL-10 in human peripheral blood mononuclear cells, mesenteric lymph nodes cells and epithelial HT29 cells (Foligne et al., 2010; Le Maréchal et al., 2015; Deutsch et al., 2017; Rabah et al., 2018a). Also, inactivation of the gene encoding SlpE suppresses IL-10 induction by *P. freudenreichii* CIRM-BIA 129 (Deutsch et al., 2017). It is interesting to note that SlpB, Eno1 and GroL2 were found to be some of the most abundant EV proteins, which may be a further indication of the potentially beneficial roles exerted by CIRM-BIA 129 EVs on host cells. This is in accordance with the potential immunomodulatory role suggested for these proteins in a multi-strain and multi-omics study (Deutsch et al., 2017).

In order to investigate potential roles for EVs in the context of host-microorganism interactions, we conducted *in silico* predictions of interactions between the bacterial proteins identified in EVs and human proteins. We employed a machine learning-based method (intersppi), which relies on protein sequences and network properties, to identify patterns of classification into groups of interacting or non-interacting protein pairs (Lian et al., 2019). We also used a homology-based prediction of interacting pairs (interolog) that relies on the mapping of similarities to interaction databases and interaction transfers among homologs (Folador et al., 2014). Our results revealed a considerable difference between the methods in the number and nature of the interactions predicted. This difference was mainly due to the fact that the interolog methodology depends on data availability in interaction databases, such as STRING and INTACT, from which homology mapping is performed (Wang et al., 2012). The data may therefore have been biased by experimental work focused on specific aspects and organisms, as well as the conservation of proteins, which may affect homology identification. For example, metabolism-related proteins tend to be more conserved, so they are therefore overrepresented in interactions predicted using the interolog methodology. On the other hand, intersppi aims to capture more general patterns of protein binding, enabling *ab initio* predictions that are not reliant on the availability of prior data. However, it is still susceptible to training data bias and a certain probability of false positives (Keskin et al., 2016).

The predicted interactions mapped to several immunology-related KEGG terms, such as signal transduction, infectious diseases and the immune system, thus shedding light on a possible immunomodulatory role for *P. freudenreichii* EVs. These predictions corroborate some previous findings which associated the *P. freudenreichii* bacterium with immunomodulatory roles (Foligne et al., 2010; Deutsch et al., 2017; Do Carmo et al., 2017; Frohnmeyer et al., 2018; Rabah et al., 2018a). Interestingly, the predicted data also suggested that this immunomodulation could involve the NF-κB pathway, since the nuclear factor NF-κB p105 subunit (NFKB1, P19838) was the most frequent interacting human protein according to the intersppi predictions and also the interactions shared between the two methods. Regarding bacterial proteins previously reported as being immunomodulatory, Acn, Eno1, GroL2, HtrA1, SlpA, SlpB, and SlpE were predicted to interact directly with NFKB1 using the intersppi method. In addition, the interaction between Eno1 and NFKB1 was also predicted by interolog. Other proteins in the NF-κB pathway were also predicted to interact with Acn: the inhibitor of nuclear factor kappa-B kinase subunits alpha (IKKA) and beta (IKKB), as well as TIR domain-containing adapter molecule 1 (TICAM1). Moreover, interactions with toll-like receptors (e.g., TLR1, TLR4, TLR5, TL6) suggested that the immunomodulatory role of EVs might also occur at the receptor

level. Briefly, PPI data (i.e., highly interacting NFKB1 protein, interactions involving bacterial proteins previously demonstrated to be immunomodulatory and interactions mapping to KEGG terms related to the immune response) suggested an ability of EVs produced by *P. freudenreichii* CIRM-BIA 129 to exert an immunomodulatory effect via the NF-κB pathway, which then needed to be confirmed *in vitro*.

When tested on HT-29 intestinal epithelial cells, we found that EVs exert an inhibitory effect on LPS-induced IL-8 secretion, as was previously observed with intact *P. freudenreichii* CIRM-BIA 129 cells (Do Carmo et al., 2019). Their effect was dose-dependent and unrelated to side effects of EVs on cell viability. This immunomodulatory response was mediated through modulation of the regulatory activity of the NF-κB transcription factor. The NF-κB pathway leads to the upregulation of proinflammatory genes, being targeted by diverse pathogens and probiotic bacteria (Hayden and Ghosh, 2012; Mitchell et al., 2016). Therefore, some probiotics can downregulate the production of these proinflammatory cytokines, acting at different steps along the NF-κB pathway: *L. rhamnosus* GG and *Lactobacillus delbrueckii* subsp. *bulgaricus* downregulated p38 and IkB expression, respectively (Giahi et al., 2012), *L. plantarum* LM1004 and *Lactobacillus casei* DN-114 001 modulated the nuclear translocation of NF-κB (Tien et al., 2006; Lee et al., 2019), *Bacteroides thetaiotaomicron* promoted the nuclear export of RelA (Kelly et al., 2004), VSL#3 inhibited proteasome degrading activity (Petrof et al., 2004), and *Bifidobacterium breve* C50 decreased the phosphorylation of p38-MAPK and IkappaB-alpha (Heuvelin et al., 2009). Probiotic strains were also shown to exhibit immunoregulatory effects via the modulation of TLR negative regulators of the NF-κB pathway (Lakhdari et al., 2011; Kanmani and Kim, 2019). Specifically, *Lactobacillus helveticus* SBT2171 was reported to inhibit NF-κB activation by inducing A20 expression via TLR2 signal in LPS-stimulated peritoneal macrophages (Kawano et al., 2019). *Lactobacillus acidophilus* was shown to regulate the inflammatory response induced by enterotoxigenic *E. coli* K88 in piglets, notably through the increased expression of Tollip, IRAK-M, A20, and Bcl-3 (Li et al., 2016). *Lactobacillus paracasei* was associated to the inhibition of pro-inflammatory cytokines production by monocyte-macrophages, via the induction of A20, SOCS1, SOCS3, and IRAK3 (Sun et al., 2017).

The precise mechanism by which EVs produced by *P. freudenreichii* CIRM-BIA 129 modulate NF-κB activity still needs to be elucidated, but our work has provided some clues. EVs do not exert an immunomodulatory effect when the NF-κB pathway is stimulated by other inducers (such as TNF-α and IL-1β), indicating that EVs mitigate the activation of NF-κB via the LPS signaling pathway. These different ligands bind to specific receptors at the cell surface in order to activate the NF-κB pathway. Once bound, they use the same signal transduction mechanisms to activate the pathway. Therefore, EVs probably act at a level of the NF-κB pathway that is not common to the three inducers: TLR4, CD14, LBP, MD-2 and the TICAM1 and TICAM2 TIR domain-containing adaptor proteins. It is interesting to note that *in silico* prediction of protein-protein interactions predicted interactions with TLR4, the cell-surface receptor for LPS, but not with the TNF-α and IL-1β receptors. Furthermore, proteinase-treated EVs conserved their immunomodulatory properties. Therefore, the EV-triggered inhibition of NF-κB does not signal through binding between EV surface exposed proteins and the LPS receptor (i.e., LBP, TLR-4, CD14, MD-2). One can suppose that non-proteinaceous inhibitors may also be involved. However, to date, the immunomodulatory properties of *P. freudenreichii* have been associated with proteins. Moreover, EVs produced by a Δ*slpB P. freudenreichii* mutant partly lost their immunomodulation effects, indicating that several proteins, including SlpB, play a direct or indirect role in the anti-inflammatory response mediated by EVs. These results also suggest that these immunomodulatory proteins are packed into EVs and are not surface exposed. It cannot be excluded that immunomodulatory proteins interact directly with LPS receptors after their release from the lysis of EVs in the vicinity of cells, but it does seem more likely that they target specific intercellular components of the LPS-induced NF-κB pathway after EV uptake by membrane fusion or endocytosis (Mulcahy et al., 2014; Jefferies and Khalid, 2020).

It is now well recognized that EVs act as proxies of their parental cells. Accordingly, *P. freudenreichii* and its EVs share common features, notably their immunomodulatory effects mediated by SlpB. Whether *P. freudenreichii* also signals through the same pathway as its EVs constitutes a basis for further studies. Likewise, whether *P. freudenreichii* EVs exert immunomodulatory effects *in vivo,* as has been shown for the bacterium (Foligne et al., 2010; Rabah et al., 2018a; Do Carmo et al., 2019) is a challenging question that should be addressed in future research and with respect to potential EV-based probiotic applications. In sum, this study reflects efforts to demonstrate the widespread occurrence and functional diversity of EVs, particularly in a group of emerging EVs research, such as Gram-positive probiotic bacteria. It also contributes to a clearer understanding of the mechanisms associated with the probiotic traits of *P. freudenreichii* while opening up possibilities of employing bacterial-derived EVs for functional cargo delivery and for the development of novel probiotic products.

DATA AVAILABILITY STATEMENT

The datasets generated for this study can be found here: https://data.inrae.fr/dataset.xhtml?persistentId=doi:10.15454/Q6PPXY.

AUTHOR CONTRIBUTIONS

VR, GJ, YL, VC, and EG conceived and designed the experiments. VR, VB-B, JJ, BL, and HR performed the experiments. VR, EF, AN, JJ, and EG analyzed the data. FC, AN, JJ, VB-B, HB, NL, GJ, and EG gave practical suggestions to perform experiments. VC, YL, and EG contributed to funding acquisition. VR and EG wrote the original draft. All authors contributed to data interpretation, drafting the manuscript, critically revising the manuscript, and approving its final version.

FUNDING

This work has received a financial support from the INRAE (Rennes, France) and Institut Agro (Rennes, France). VR and BL were supported by the International Cooperation Program CAPES/COFECUB at the Federal University of Minas Gerais funded by CAPES – the Brazilian Federal Agency for the Support and Evaluation of Graduate Education of the Brazilian Ministry of Education (number 99999.000058/2017-03 and 88887.179897/2018-00, respectively).

ACKNOWLEDGMENTS

This work benefited from the facilities and expertise of the MRic-TEM platform (https://microscopie.univ-rennes1.fr). The authors are grateful to Agnes Burel (University of Rennes, BIOSIT – UMS 3480, US_S 018, Rennes, France) and Chantal Cauty for sessions with the microscope. The authors would like to thank Ludovica Marinelli (INRAE, AgroParisTech, Paris-Saclay University, Micalis Institute, Jouy-en-Josas, France) for her technical advice on the NF-κB reporter cell line. The authors would also like to thank Victoria Hawken for English-language editing of the manuscript. The authors thank CNIEL (Centre National Interprofessionnel de l'Economie Laitière) for providing the ITG P20 strain.

SUPPLEMENTARY MATERIAL

The Supplementary Material for this article can be found online at: https://www.frontiersin.org/articles/10.3389/fmicb.2020.01544/full#supplementary-material

REFERENCES

Alvarez, C.-S., Badia, J., Bosch, M., Giménez, R., and Baldomà, L. (2016). Outer membrane vesicles and soluble factors released by probiotic *Escherichia coli* Nissle 1917 and commensal ECOR63 enhance barrier function by regulating expression of tight junction proteins in intestinal epithelial cells. *Front. Microbiol.* 7:1981. doi: 10.3389/fmicb.2016.01981

Bagos, P. G., Tsirigos, K. D., Liakopoulos, T. D., and Hamodrakas, S. J. (2008). Prediction of lipoprotein signal peptides in gram-positive bacteria with a hidden markov model. *J. Proteome Res.* 7, 5082–5093. doi: 10.1021/pr800162c

Bateman, A. (2019). UniProt: a worldwide hub of protein knowledge. *Nucleic Acids Res.* 47, D506–D515. doi: 10.1093/nar/gky1049

Behzadi, E., Mahmoodzadeh Hosseini, H., and Imani Fooladi, A. A. (2017). The inhibitory impacts of *Lactobacillus rhamnosus* GG-derived extracellular vesicles on the growth of hepatic cancer cells. *Microb. Pathog.* 110, 1–6. doi: 10.1016/j.micpath.2017.06.016

Böing, A. N., van der Pol, E., Grootemaat, A. E., Coumans, F. A. W. W., Sturk, A., and Nieuwland, R. (2014). Single-step isolation of extracellular vesicles by size-exclusion chromatography. *J. Extracell. Vesicles* 3:23430. doi: 10.3402/jev.v3.23430

Brown, L., Wolf, J. M., Prados-Rosales, R., and Casadevall, A. (2015). Through the wall: extracellular vesicles in gram-positive bacteria, mycobacteria and fungi. *Nat. Rev. Microbiol.* 13, 620–630. doi: 10.1038/nrmicro3480

Cañas, M.-A., Fábrega, M.-J., Giménez, R., Badia, J., and Baldomà, L. (2018). Outer membrane vesicles from probiotic and commensal *Escherichia coli* activate NOD1-mediated immune responses in intestinal epithelial cells. *Front. Microbiol.* 9:498. doi: 10.3389/fmicb.2018.00498

Colliou, N., Ge, Y., Sahay, B., Gong, M., Zadeh, M., Owen, J. L., et al. (2017). Commensal *Propionibacterium* strain UF1 mitigates intestinal inflammation via Th17 cell regulation. *J. Clin. Invest.* 127, 3970–3986. doi: 10.1172/JCI95376

Cousin, F. J., Jouan-Lanhouet, S., Théret, N., Brenner, C., Jouan, E., Le, M.-M. G., et al. (2016). The probiotic <i>*Propionibacterium freudenreichii*</i> as a new adjuvant for TRAIL-based therapy in colorectal cancer. *Oncotarget* 7, 7161–7178. doi: 10.18632/oncotarget.6881

Cousin, F. J., Louesdon, S., Maillard, M.-B., Parayre, S., Falentin, H., Deutsch, S.-M., et al. (2012). The first dairy product exclusively fermented by *Propionibacterium freudenreichii*: a new vector to study probiotic potentialities in vivo. *Food Microbiol.* 32, 135–146. doi: 10.1016/J.FM.2012.05.003

Deptula, P., Chamlagain, B., Edelmann, M., Sangsuwan, P., Nyman, T. A., Savijoki, K., et al. (2017). Food-like growth conditions support production of active vitamin B12 by *Propionibacterium freudenreichii* 2067 without DMBI, the lower ligand base, or cobalt supplementation. *Front. Microbiol.* 8:368. doi: 10.3389/fmicb.2017.00368

Deutsch, S. M., Mariadassou, M., Nicolas, P., Parayre, S., Le, G. R., Chuat, V., et al. (2017). Identification of proteins involved in the anti-inflammatory properties of *Propionibacterium freudenreichii* by means of a multi-strain study. *Sci. Rep.* 7:46409. doi: 10.1038/srep46409

Do Carmo, F. L. R., Rabah, H., Cordeiro, B. F., Silva, S. H., da, Pessoa, R. M., et al. (2019). Probiotic *Propionibacterium freudenreichii* requires SlpB protein to mitigate mucositis induced by chemotherapy. *Oncotarget* 10, 7198–7219. doi: 10.18632/oncotarget.27319

Do Carmo, F. L. R., Rabah, H., Huang, S., Gaucher, F., Deplanche, M., Dutertre, S., et al. (2017). *Propionibacterium freudenreichii* surface protein SlpB is involved in adhesion to intestinal HT-29 cells. *Front. Microbiol.* 8:1033. doi: 10.3389/fmicb.2017.01033

Elhenawy, W., Debelyy, M. O., and Feldman, M. F. (2014). Preferential packing of acidic glycosidases and proteases into *Bacteroides* outer membrane vesicles. *MBio* 5, e00909-14. doi: 10.1128/mBio.00909-14

Folador, E. L., Hassan, S. S., Lemke, N., Barh, D., Silva, A., Ferreira, R. S., et al. (2014). An improved interolog mapping-based computational prediction of protein-protein interactions with increased network coverage. *Integr. Biol. (United Kingdom)* 6, 1080–1087. doi: 10.1039/c4ib00136b

Foligne, B., Deutsch, S.-M., Breton, J., Cousin, F. J., Dewulf, J., Samson, M., et al. (2010). Promising immunomodulatory effects of selected strains of dairy propionibacteria as evidenced in vitro and in vivo. *Appl. Environ. Microbiol.* 76, 8259–8264. doi: 10.1128/AEM.01976-10

Frohnmeyer, E., Deptula, P., Nyman, T. A., Laine, P. K. S. S., Vihinen, H., Paulin, L., et al. (2018). Secretome profiling of *Propionibacterium freudenreichii* reveals highly variable responses even among the closely related strains. *Microb. Biotechnol.* 11, 510–526. doi: 10.1111/1751-7915.13254

Fukumoto, S., Toshimitsu, T., Matsuoka, S., Maruyama, A., Oh-Oka, K., Takamura, T., et al. (2014). Identification of a probiotic bacteria-derived activator of the aryl hydrocarbon receptor that inhibits colitis. *Immunol. Cell Biol.* 92, 460–465. doi: 10.1038/icb.2014.2

Gagnaire, V., Jardin, J., Rabah, H., Briard-Bion, V., and Jan, G. (2015). Emmental cheese environment enhances *propionibacterium freudenreichii* stress tolerance. *PLoS One* 10:e0135780. doi: 10.1371/journal.pone.0135780

Ge, Y., Gong, M., Zadeh, M., Li, J., Abbott, J. R., Li, W., et al. (2020). Regulating colonic dendritic cells by commensal glycosylated large surface layer protein A to sustain gut homeostasis against pathogenic inflammation. *Mucosal Immunol.* 13, 34–46. doi: 10.1038/s41385-019-0210-0

Gho, Y. S., and Lee, C. (2017). Emergent properties of extracellular vesicles: a holistic approach to decode the complexity of intercellular communication networks. *Mol. BioSyst.* 13:1291. doi: 10.1039/c7mb00146k

Giahi, L., Aumueller, E., Elmadfa, I., and Haslberger, A. G. (2012). Regulation of TLR4, p38 MAPkinase, IκB and miRNAs by inactivated strains of lactobacilli in human dendritic cells. *Benef. Microbes* 3, 91–98. doi: 10.3920/BM2011.0052

Grande, R., Celia, C., Mincione, G., Stringaro, A., Di Marzio, L., Colone, M., et al. (2017). Detection and physicochemical characterization of membrane vesicles (MVs) of *Lactobacillus reuteri* DSM 17938. *Front. Microbiol.* 8:1040. doi: 10.3389/fmicb.2017.01040

Hayden, M. S., and Ghosh, S. (2012). NF- B, the first quarter-century: remarkable progress and outstanding questions. *Genes Dev.* 26, 203–234. doi: 10.1101/gad.183434.111

Heuvelin, E., Lebreton, C., Grangette, C., Pot, B., Cerf-Bensussan, N., and Heyman, M. (2009). Mechanisms involved in alleviation of intestinal inflammation by bifidobacterium breve soluble factors. *PLoS One* 4:e5184. doi: 10.1371/journal.pone.0005184

Huang, S., Rabah, H., Jardin, J., Briard-Bion, V., Parayre, S., Maillard, M.-B., et al. (2016). Hyperconcentrated sweet whey, a new culture medium that enhances *Propionibacterium freudenreichii* stress tolerance. *Appl. Environ. Microbiol.* 82, 4641–4651. doi: 10.1128/AEM.00748-16

Huerta-Cepas, J., Forslund, K., Coelho, L. P., Szklarczyk, D., Jensen, L. J., Von Mering, C., et al. (2017). Fast genome-wide functional annotation through orthology assignment by eggNOG-mapper. *Mol. Biol. Evol.* 34, 2115–2122. doi: 10.1093/molbev/msx148

Huerta-Cepas, J., Szklarczyk, D., Heller, D., Hernández-Plaza, A., Forslund, S. K., Cook, H., et al. (2019). EggNOG 5.0: A hierarchical, functionally and phylogenetically annotated orthology resource based on 5090 organisms and 2502 viruses. *Nucleic Acids Res.* 47, D309–D314. doi: 10.1093/nar/gky1085

Ishihama, Y., Oda, Y., Tabata, T., Sato, T., Nagasu, T., Rappsilber, J., et al. (2005). Exponentially modified protein abundance index (emPAI) for estimation of absolute protein amount in proteomics by the number of sequenced peptides per protein. *Mol. Cell. Proteomics* 4, 1265–1272. doi: 10.1074/mcp.M500061-MCP200

Jefferies, D., and Khalid, S. (2020). To infect or not to infect: molecular determinants of bacterial outer membrane vesicle internalization by host membranes. *J. Mol. Biol.* 432, 1251–1264. doi: 10.1016/j.jmb.2020.01.008

Kainulainen, V., Loimaranta, V., Pekkala, A., Edelman, S., Antikainen, J., Kylväjä, R., et al. (2012). Glutamine synthetase and glucose-6-phosphate isomerase are adhesive moonlighting proteins of *Lactobacillus crispatus* released by epithelial cathelicidin LL-37. *J. Bacteriol.* 194, 2509–2519. doi: 10.1128/JB.06704-11

Kanmani, P., and Kim, H. (2019). Functional capabilities of probiotic strains on attenuation of intestinal epithelial cell inflammatory response induced by TLR4 stimuli. *BioFactors* 45, 223–235. doi: 10.1002/biof.1475

Kawano, M., Miyoshi, M., and Miyazaki, T. (2019). *Lactobacillus helveticus* SBT2171 induces A20 expression via toll-like receptor 2 signaling and inhibits the lipopolysaccharide-induced activation of nuclear factor-kappa b and mitogen-activated protein kinases in peritoneal macrophages. *Front. Immunol.* 10:845. doi: 10.3389/fimmu.2019.00845

Kelly, D., Campbell, J. I., King, T. P., Grant, G., Jansson, E. A., Coutts, A. G. P., et al. (2004). Commensal anaerobic gut bacteria attenuate inflammation by regulating nuclear-cytoplasmic shutting of PPAR-γ and ReIA. *Nat. Immunol.* 5, 104–112. doi: 10.1038/ni1018

Kerrien, S., Aranda, B., Breuza, L., Bridge, A., Broackes-Carter, F., Chen, C., et al. (2012). The IntAct molecular interaction database in 2012. *Nucleic Acids Res.* 40, D841–D846. doi: 10.1093/nar/gkr1088

Keskin, O., Tuncbag, N., and Gursoy, A. (2016). Predicting protein-protein interactions from the molecular to the proteome level. *Chem. Rev.* 116, 4884–4909. doi: 10.1021/acs.chemrev.5b00683

Kim, D. K., Lee, J., Simpson, R. J., Lötvall, J., and Gho, Y. S. (2015a). EVpedia: a community web resource for prokaryotic and eukaryotic extracellular vesicles research. *Semin. Cell Dev. Biol.* 40, 4–7. doi: 10.1016/j.semcdb.2015.02.005

Kim, J. H., Lee, J., Park, J., and Gho, Y. S. (2015b). Gram-negative and Gram-positive bacterial extracellular vesicles. *Semin. Cell Dev. Biol.* 40, 97–104. doi: 10.1016/j.semcdb.2015.02.006

Kim, J.-H., Jeun, E.-J., Hong, C.-P., Kim, S.-H., Jang, M. S., Lee, E.-J., et al. (2016). Extracellular vesicle–derived protein from Bifidobacterium longum alleviates food allergy through mast cell suppression. *J. Allergy Clin. Immunol.* 137, 507–516.e8. doi: 10.1016/j.jaci.2015.08.016

Laemmli, U. K. (1970). Cleavage of structural proteins during the assembly of the head of bacteriophage T4. *Nature* 227, 680–685. doi: 10.1038/227680a0

Lakhdari, O., Cultrone, A., Tap, J., Gloux, K., Bernard, F., Dusko Ehrlich, S., et al. (2010). Functional metagenomics: A high throughput screening method to decipher microbiota-driven NF-KB modulation in the human gut. *PLoS One* 5:13092. doi: 10.1371/journal.pone.0013092

Lakhdari, O., Tap, J., Béguet-Crespel, F., Le Roux, K., de Wouters, T., Cultrone, A., et al. (2011). Identification of NF-κB modulation capabilities within human intestinal commensal bacteria. *J. Biomed. Biotechnol.* 2011, 1–9. doi: 10.1155/2011/282356

Lan, A., Bruneau, A., Bensaada, M., Philippe, C., Bellaud, P., Rabot, S., et al. (2008). Increased induction of apoptosis by *Propionibacterium freudenreichii* TL133 in colonic mucosal crypts of human microbiota-associated rats treated with 1,2-dimethylhydrazine. *Br. J. Nutr.* 100, 1251–1259. doi: 10.1017/S0007114508978284

Lan, A., Bruneau, A., Philippe, C., Rochet, V., Rouault, A., Hervé, C., et al. (2007a). Survival and metabolic activity of selected strains of *Propionibacterium freudenreichii* in the gastrointestinal tract of human microbiota-associated rats. *Br. J. Nutr.* 97, 714–724. doi: 10.1017/S0007114507433001

Lan, A., Lagadic-Gossmann, D., Lemaire, C., Brenner, C., and Jan, G. (2007b). Acidic extracellular pH shifts colorectal cancer cell death from apoptosis to necrosis upon exposure to propionate and acetate, major end-products of the human probiotic propionibacteria. *Apoptosis* 12, 573–591. doi: 10.1007/s10495-006-0010-3

Langella, O., Valot, B., Balliau, T., Blein-Nicolas, M., Bonhomme, L., and Zivy, M. (2017). X!TandemPipeline: a tool to manage sequence redundancy for protein inference and phosphosite identification. *J. Proteome Res.* 16, 494–503. doi: 10.1021/acs.jproteome.6b00632

Le Maréchal, C., Peton, V., Plé, C., Vroland, C., Jardin, J., Briard-Bion, V., et al. (2015). Surface proteins of *Propionibacterium freudenreichii* are involved in its anti-inflammatory properties. *J. Proteomics* 113, 447–461. doi: 10.1016/j.jprot.2014.07.018

Lee, J., Jung, I., Choi, J. W., Lee, C. W., Cho, S., Choi, T. G., et al. (2019). Micronized and heat-treated *Lactobacillus plantarum* LM1004 stimulates host immune responses via the TLR-2/MAPK/NF-κB signalling pathway in vitro and in vivo. *J. Microbiol. Biotechnol.* 29, 704–712. doi: 10.4014/jmb.1812.12059

Li, H., Zhang, L., Chen, L., Zhu, Q., Wang, W., and Qiao, J. (2016). *Lactobacillus acidophilus* alleviates the inflammatory response to enterotoxigenic *Escherichia coli* K88 via inhibition of the NF-κB and p38 mitogen-activated protein kinase signaling pathways in piglets. *BMC Microbiol.* 16:273. doi: 10.1186/s12866-016-0862-9

Li, M., Lee, K., Hsu, M., Nau, G., Mylonakis, E., and Ramratnam, B. (2017). *Lactobacillus*-derived extracellular vesicles enhance host immune responses against vancomycin-resistant enterococci. *BMC Microbiol.* 17:66. doi: 10.1186/s12866-017-0977-7

Lian, X., Yang, S., Li, H., Fu, C., and Zhang, Z. (2019). Machine-Learning-based predictor of human–bacteria protein–protein interactions by incorporating comprehensive host-network properties. *J. Proteome Res.* 18, 2195–2205. doi: 10.1021/acs.jproteome.9b00074

Liu, Y., Alexeeva, S., Defourny, K. A., Smid, E. J., and Abee, T. (2018a). Tiny but mighty: bacterial membrane vesicles in food biotechnological applications. *Curr. Opin. Biotechnol.* 49, 179–184. doi: 10.1016/j.copbio.2017.09.001

Liu, Y., Defourny, K. A. Y., Smid, E. J., and Abee, T. (2018b). Gram-Positive bacterial extracellular vesicles and their impact on health and disease. *Front. Microbiol.* 9:1502. doi: 10.3389/fmicb.2018.01502

Loux, V., Mariadassou, M., Almeida, S., Chiapello, H., Hammani, A., Buratti, J., et al. (2015). Mutations and genomic islands can explain the strain dependency of sugar utilization in 21 strains of *Propionibacterium freudenreichii*. *BMC Genomics* 16:296. doi: 10.1186/s12864-015-1467-7

Lynch, J. B., and Alegado, R. A. (2017). Spheres of hope, packets of doom: the good and bad of outer membrane vesicles in interspecies and ecological dynamics. *J. Bacteriol.* 199:e00012-17. doi: 10.1128/JB.00012-17

Mehdiani, A., Maier, A., Pinto, A., Barth, M., Akhyari, P., and Lichtenberg, A. (2015). An innovative method for exosome quantification and size measurement. *J. Vis. Exp.* 17:50974. doi: 10.3791/50974

Mitchell, S., Vargas, J., and Hoffmann, A. (2016). Signaling via the NFκB system. *Wiley Interdiscip. Rev. Syst. Biol. Med.* 8, 227–241. doi: 10.1002/wsbm.1331

Molina-Tijeras, J. A., Gálvez, J., and Rodríguez-Cabezas, M. E. (2019). The immunomodulatory properties of extracellular vesicles derived from probiotics: a novel approach for the management of gastrointestinal diseases. *Nutrients* 11:1038. doi: 10.3390/nu11051038

Mulcahy, L. A., Pink, R. C., and Carter, D. R. F. (2014). Routes and mechanisms of extracellular vesicle uptake. *J. Extracell. Vesicles* 3:24641. doi: 10.3402/jev.v3.24641

Ojala, T., Laine, P. K. S., Ahlroos, T., Tanskanen, J., Pitkänen, S., Salusjärvi, T., et al. (2017). Functional genomics provides insights into the role of

Propionibacterium freudenreichii ssp. shermanii JS in cheese ripening. *Int. J. Food Microbiol.* 241, 39–48. doi: 10.1016/j.ijfoodmicro.2016.09.022

Okada, Y., Tsuzuki, Y., Narimatsu, K., Sato, H., Ueda, T., Hozumi, H., et al. (2013). 1,4-Dihydroxy-2-naphthoic acid from *Propionibacterium freudenreichii* reduces inflammation in interleukin-10-deficient mice with colitis by suppressing macrophage-derived proinflammatory cytokines. *J. Leukoc. Biol.* 94, 473–480. doi: 10.1189/jlb.0212104

Petrof, E. O., Kojima, K., Ropeleski, M. J., Musch, M. W., Tao, Y., De Simone, C., et al. (2004). Probiotics inhibit nuclear factor-κB and induce heat shock proteins in colonic epithelial cells through proteasome inhibition. *Gastroenterology* 127, 1474–1487. doi: 10.1053/j.gastro.2004.09.001

Rabah, H., Ferret-Bernard, S., Huang, S., Le Normand, L., Cousin, F. J., Gaucher, F., et al. (2018a). The cheese matrix modulates the immunomodulatory properties of *Propionibacterium freudenreichii* CIRM-BIA 129 in healthy piglets. *Front. Microbiol.* 9:2584. doi: 10.3389/fmicb.2018.02584

Rabah, H., Ménard, O., Gaucher, F., do Carmo, F. L. R., Dupont, D., and Jan, G. (2018b). Cheese matrix protects the immunomodulatory surface protein SlpB of *Propionibacterium freudenreichii* during in vitro digestion. *Food Res. Int.* 106, 712–721. doi: 10.1016/j.foodres.2018.01.035

Rabah, H., Rosa do Carmo, F., and Jan, G. (2017). Dairy propionibacteria: versatile probiotics. *Microorganisms* 5:24. doi: 10.3390/microorganisms5020024

Rakoff-Nahoum, S., Coyne, M. J., and Comstock, L. E. (2014). An ecological network of polysaccharide utilization among human intestinal symbionts. *Curr. Biol.* 24, 40–49. doi: 10.1016/j.cub.2013.10.077

Raposo, G., and Stoorvogel, W. (2013). Extracellular vesicles: exosomes, microvesicles, and friends. *J. Cell Biol.* 200, 373–383. doi: 10.1083/jcb.201211138

Rodríguez-Bolaños, M., and Perez-Montfort, R. (2019). Medical and veterinary importance of the moonlighting functions of triosephosphate isomerase. *Curr. Protein Pept. Sci.* 20, 304–315. doi: 10.2174/1389203719666181026170751

Rubio, A. P. D., Martínez, J. H., Casillas, D. C. M., Leskow, F. C., Piuri, M., and Pérez, O. E. (2017). *Lactobacillus casei* BL23 produces microvesicles carrying proteins that have been associated with its probiotic effect. *Front. Microbiol.* 8:1783. doi: 10.3389/fmicb.2017.01783

Shannon, P. (2003). Cytoscape: a software environment for integrated models of biomolecular interaction networks. *Genome Res.* 13, 2498–2504. doi: 10.1101/gr.1239303

Sun, K.-Y., Xu, D.-H., Xie, C., Plummer, S., Tang, J., Yang, X. F., et al. (2017). *Lactobacillus paracasei* modulates LPS-induced inflammatory cytokine release by monocyte-macrophages via the up-regulation of negative regulators of NF-kappaB signaling in a TLR2-dependent manner. *Cytokine* 92, 1–11. doi: 10.1016/j.cyto.2017.01.003

Switzer, R. C., Merril, C. R., and Shifrin, S. (1979). A highly sensitive silver stain for detecting proteins and peptides in polyacrylamide gels. *Anal. Biochem.* 98, 231–237. doi: 10.1016/0003-2697(79)90732-2

Szklarczyk, D., Morris, J. H., Cook, H., Kuhn, M., Wyder, S., Simonovic, M., et al. (2017). The STRING database in 2017: Quality-controlled protein-protein association networks, made broadly accessible. *Nucleic Acids Res.* 45, D362–D368. doi: 10.1093/nar/gkw937

Tartaglia, N. R., Breyne, K., Meyer, E., Cauty, C., Jardin, J., Chrétien, D., et al. (2018). Staphylococcus aureus extracellular vesicles elicit an immunostimulatory response in vivo on the murine mammary gland. *Front. Cell. Infect. Microbiol.* 8:277. doi: 10.3389/fcimb.2018.00277

Tien, M.-T., Girardin, S. E., Regnault, B., Le Bourhis, L., Dillies, M.-A., Coppée, J.-Y., et al. (2006). Anti-inflammatory effect of *Lactobacillus casei* on *Shigella*-infected human intestinal epithelial cells. *J. Immunol.* 176, 3841.3–3841. doi: 10.4049/jimmunol.176.6.3841-b

Toyofuku, M. (2019). Bacterial communication through membrane vesicles. *Biosci. Biotechnol. Biochem.* 83, 1599–1605. doi: 10.1080/09168451.2019.1608809

Toyofuku, M., Nomura, N., and Eberl, L. (2019). Types and origins of bacterial membrane vesicles. *Nat. Rev. Microbiol.* 17, 13–24. doi: 10.1038/s41579-018-0112-2

Wang, F., Liu, M., Song, B., Li, D., Pei, H., Guo, Y., et al. (2012). Prediction and characterization of protein-protein interaction networks in swine. *Proteome Sci.* 10:2. doi: 10.1186/1477-5956-10-2

Yu, C. S., Cheng, C. W., Su, W. C., Chang, K. C., Huang, S. W., Hwang, J. K., et al. (2014). CELLO2GO: a web server for protein subCELlular lOcalization prediction with functional gene ontology annotation. *PLoS One* 9:e99368. doi: 10.1371/journal.pone.0099368

Conflict of Interest: The authors declare that the research was conducted in the absence of any commercial or financial relationships that could be construed as a potential conflict of interest.

frontiers in Microbiology

ORIGINAL RESEARCH
published: 24 July 2020
doi: 10.3389/fmicb.2020.01534

First Evidence of Acyl-Hydrolase/Lipase Activity From Human Probiotic Bacteria: *Lactobacillus rhamnosus* GG and *Bifidobacterium longum* NCC 2705

Panagiotis Manasian[1,2], Atma-Sol Bustos[2,3], Björn Pålsson[1], Andreas Håkansson[2], J. Mauricio Peñarrieta[3], Lars Nilsson[2] and Javier A. Linares-Pastén[1]**

[1] Biotechnology, Faculty of Engineering, Lunds Tekniska Högskola (LTH), Lund University, Lund, Sweden, [2] Food Technology, Faculty of Engineering, Lunds Tekniska Högskola (LTH), Lund University, Lund, Sweden, [3] Faculty of Pure and Natural Sciences, School of Chemistry, Universidad Mayor de San Andrés, La Paz, Bolivia

OPEN ACCESS

Edited by:
Afef Najjari,
Tunis El Manar University, Tunisia

Reviewed by:
Armen Trchounian,
Yerevan State University, Armenia
L'ubomír Valík,
Slovak University of Technology in Bratislava, Slovakia

***Correspondence:**
Lars Nilsson
lars.nilsson@food.lth.se
Javier A. Linares-Pastén
javier.linares_pasten@biotek.lu.se

Specialty section:
This article was submitted to Food Microbiology, a section of the journal Frontiers in Microbiology

Received: *12 March 2020*
Accepted: *12 June 2020*
Published: *24 July 2020*

Citation:
Manasian P, Bustos A-S, Pålsson B, Håkansson A, Peñarrieta JM, Nilsson L and Linares-Pastén JA (2020) First Evidence of Acyl-Hydrolase/Lipase Activity From Human Probiotic Bacteria: Lactobacillus rhamnosus GG and Bifidobacterium longum NCC 2705. Front. Microbiol. 11:1534. doi: 10.3389/fmicb.2020.01534

Lactobacillus rhamnosus GG (ATCC 53103) and *Bifidobacterium longum* NCC 2705 are among the most studied probiotics. However, the first evidence of acyl hydrolase/lipase of two annotated proteins, one in each genome of these strains, is reported in this work. Signal peptide analysis has predicted that these proteins are exported to the extracellular medium. Both proteins were produced in *Escherichia coli*, purified and characterized. Molecular masses (without signal peptides) were 27 and 52.3 kDa for the proteins of *L. rhamnosus* and *B. longum*, respectively. Asymmetrical flow field-flow fractionation analysis has shown that both proteins are present as monomers in their native forms at pH 7. Both have shown enzymatic activity on *p*NP-laurate at pH 7 and 37°C. The enzyme from *L. rhamnosus* was characterized deeper, showing preference on *p*NP-esters with short chain fatty acids. In addition, a computational model of the 3D structure has allowed the prediction of the catalytic amino acids. The enzymatic activities using synthetic substrates were very low for both enzymes. The investigation of natural substrates and biological functions of these enzymes is still open.

Keywords: acyl-hydrolase/lipase, *Lactobacillus rhamnosus* GG, *Biffidobacterium longum*, asymmetrical flow field-flow fractionation, differential scanning fluorimetry

INTRODUCTION

Probiotics are microorganisms that provide beneficial effects for health and are gaining great interest both in the prevention as well as in the treatment of different diseases. The WHO (FAO/WHO) defines probiotic as "live microorganisms that, when administered in adequate amounts, confer a health benefit on the host" (Hill et al., 2014). *Lactobacillus rhamnosus* GG (ATCC 53103) and *Bifidobacterium longum* NCC 2705 are among the most studied probiotics. Several evidences support the positive effect of these strains against obesity, diabetes, inflammatory bowel disease, cancer, mental disorders, infections, diarrhea, immune disorders, systemic inflammation and others (Brusaferro et al., 2018; Consortium, 2018; Capurso, 2019). Indeed, a recent search

in Google Patents gave more than 1250 and 1050 patents related with *B. longum* NCC 2705 and *L. rhamnosus* GG, respectively. In addition, *L. rhamnosus* is one of the most used bacteria in the probiotic food industry, which includes the manufacture of milk-based products such as yogurt-type drinks, but also, probiotic fruit juices, berry soups and products based in fermented cereals and soy (Saxelin, 2008).

L. rhamnosus GG (ATCC 53103) is Gram positive anaerobic bacteria that inhabit in the gastrointestinal tract (GIT) but could also be recovered from oral cavity, tonsils, and vagina (Segers and Lebeer, 2014). *L. rhamnosus* GG (ATCC 53103) was isolated from the gastrointestinal tract in 1983 (Gorbach and Goldin, 1989) and its genome sequenced in 2009 (Kankainen et al., 2009). It is a circular chromosome of 300,5051 pb with 2834 predicted protein-coding genes. *B. longum* is a non-halophilic, anaerobic, Gram positive bacteria commonly present in the animal and human intestines (Consortium, 2018). It is associated with the gastrointestinal tract and promotes several health benefits, including reduction of irritable bowel syndrome (Brigidi et al., 2001), improves the immune response in infants (Young et al., 2004) and also helps to maintain homeostasis in the intestinal ecosystem promoting normal digestion (Consortium, 2018). *B. longum* NCC 2705 contains a 2,256,646 bp genome organized in a circular chromosome (Schell et al., 2002). Most of the studies at enzymatic level are focused on proteins involved in the metabolism of carbohydrates and amino acids, transport systems and defense mechanism. Indeed, the genomes of *L. rhamnosus* and *B. longum* have shown a relatively high number of these type of putative proteins comparing with other intestinal lactobacilli (Schell et al., 2002; Kankainen et al., 2009).

Despite the number of studies on *L. rhamnosus* and *B. longum*, to the best of our knowledge, there is lack of reports on lipolytic activity in these probiotic strains. Lipolytic enzymes include carboxylesterases and lipases, which are classified into 19 families based on phylogenetic criteria, conserved motifs and biological function (Kovacic et al., 2019). The metabolism of lipids, including esters of large and short chain fatty acids, in the gastrointestinal tract plays an important role in several cellular functions associated with disorders, such as obesity and pathological conditions. Thus, the study of lipolytic enzymes secreted by gastrointestinal microorganisms, including probiotics, could contribute to understand the potential effects of these strains in the metabolism of lipids in the intestinal tract and their health implications. The genome analysis of *L. rhamnosus* GG and *B. longum* NCC 2705 has shown two putative lipase/acyl-hydrolases containing signal peptides in the N-terminal, one in each strain, which indicates that these proteins can be secreted to the extracellular medium. Therefore, the purpose of this work was to investigate the activity of these proteins, named *Lr*Lyp and *Bl*Lyp (from *L. rhamnosus* and *B. longum*, respectively).

*Lr*Lyp and *Bl*Lyp were produced in *Escherichia coli* and their enzymatic and biophysical properties were studied. Substrate selectivity and activity were evaluated with series of synthetic *para*-nitrophenyl esters, while apparent kinetic constants were obtained at pH 7 and 37°C, using *para*-nitrophenyl laurate (*p*NP-laurate) as substrate. This synthetic ester has a 12-carbon atom chain, corresponding to a medium-size fatty acid, and it is widely used for characterizing lipase activity from different sources, including bacteria (Castro-Ochoa et al., 2005). The biophysical characterization was focused on the determination of: (1) optimal temperature; (2) protein stability, in terms of melting temperature determined by differential scanning fluorimetry (DSF) in a range of pH from 4 to 10; and (3) multimerization, studied by asymmetrical flow field-flow fractionation (AF4) coupled to multiangle light scattering (MALS). AF4 separates multimeric proteins and aggregates based on their diffusion coefficient and, compared to size exclusion chromatography (SEC), does not have a stationary phase which reduce the potential loss of analytes from adsorption or shear-induced degradation (Wahlund and Nilsson, 2012; Choi et al., 2018).

Finally, there are no structures with significant homology to *Lr*Lyp neither *Bl*Lyp in the protein data bank (PDB) (last search on 2019.10.27). This has limited the construction of a reliable computational 3D model for *Bl*Lyp. Nevertheless, a model for *Lr*Lyp was obtained using remote homology modeling techniques, allowing the prediction of the catalytic residues among other structural features.

The biological function and natural substrates of *Lr*Lyp and *Bl*Lyp remains unknown. However, this work contributes with the first evidences of acyl hydrolase/lipase activity for these enzymes encoded by the genomes of *Lactobacillus rhamnosus* GG (ATCC 53103) and *Bifidobacterium longum* NCC 2705, respectively.

MATERIALS AND METHODS

Genes Selection and Synthesis

Annotated esterases and lipases from the genomes of *Lactobacillus rhamnosus* GG (ATCC 53103) (GenBanck access code: NC_013198.1) and *Bifidobacterium longum* NCC 2705 (NC_004307) were subjected to signal peptide analysis using SignalP 4.0 Server (Petersen et al., 2011). Loci LGG_RS06710 (*L. rhamnosus*) and BL1109 (*B. longum*) were synthesized (GenScript, United States) with codon optimized for *Escherichia coli*, excluding the region encoding the signal peptides. These genes were cloned in a pET21b(+) vector between the *Nde*I and *Xho*I restriction sites. A 6-histidine tag encoded by the vector backbone was added in the C-terminal of each gene. The resulting plasmids were named pET21b:LGG_RS06710 and pET21b:BL1109.

Bioinformatic Analysis

Motifs around the catalytic serine of different families of lipolytic enzymes (Kovacic et al., 2019) were searched in the aminoacidic sequences of *Lr*Lyp and *Bl*Lyp in order to determine their classification. Other conserved motifs were determined by multiple sequence alignments with selected characterized enzymes. The alignments were performed using the Clustal Omega (1.2.4) server.[1]

[1] www.ebi.ac.uk/Tools/msa/clustalo/

Production of Recombinant Proteins

Different strains of *E. coli*, including BL21(DE3), Origami2, and Artic Express, were transformed with the plasmids pET21b:LGG_RS06710 and pET21b:BL1109. Each plasmid was introduced into chemically competent cells (Novagen, United States) by thermic shock (4°C 10 min, 42°C 2 min, 4°C 10 min). All cells were grown in LB medium supplemented with 100 μg/mL of ampicillin, additional 20 μg/mL gentamicin was added in the cultivation media of *E. coli* Artic Express. All cultivations were incubated in shake flasks (with agitation) at 37°C until reach an $OD_{\lambda\ =\ 600\ nm}$ of 0.6. Then, 1 mM IPTG was added and the incubation temperature for the recombinants *E. coli* BL21(DE3) and Origami2 was decreased to 30°C for 12 h, while for the recombinant *E. coli* Artic Express was decreased to 8°C for 24 h.

Protein Purification

Cell pellets were harvested by centrifugation at 4500 g for 20 min and resuspended in 1/10 volume of binding buffer (100 mM tris, NaCl 500 mM adjusted to pH 7.4 with HCl). Thereafter, the cell suspensions were sonicated for 5 min and centrifuged at 14,000 g. The precipitates were discarded, and the supernatants were subjected to SDS-PAGE analysis in order to determine the level of expression of the recombinant proteins. Protein purification was performed by IMAC, each supernatant was injected in a 5-mL HisTrap column FF (GE Healthcare, Uppsala, Sweden) previously equilibrated with binding buffer. Next, the column was washed with 15 column volumes of binding buffer. The recombinant protein was eluted with elution buffer pH 7.4 (50 mM sodium phosphate, 0.5 M NaCl, and 0.5 M imidazole). Finally, imidazole was removed by dialysis. Protein purity was determined by SDS-PAGE. Second purifications, using a 5-mL HisTrap column HP (GE Healthcare, Uppsala, Sweden), were performed when needed. The concentration of pure proteins was quantified spectrophotometrically at 280 nm.

Determination of Stability by Differential Scanning Fluorometry

Thermal stability of the enzyme in different pH values was determined using the Prometheus NT 48 nanoDSF (NanoTemper Technologies, GmbH, Munich Germany) (Choi et al., 2018). Enzyme samples at 0.5 g/L were prepared in pH 4.3, 5.3, 6.2, 7, 8 (McIlvaine buffer system, 100 mM), 9 and 9.6 (glycin-NaOH buffer, 100 mM). Then, 10 μL of every sample was directly loaded in the instrument capillaries. Intrinsic fluorescence at emission wavelengths of 330 and 350 nm was monitored in a temperature gradient from 20 to 90°C with a temperature ramp of 1°C per min. All data analysis was performed using the PR control software (Version 2.0, Munich Germany).

Substrate Selectivity

Stock solutions of the following *para*-nitrophenyl esters: *p*NP-acetate (C2), *p*NP-butyrate (C4), *p*NP-caprylate (C8), *p*NP-laurate (C12), *p*NP-myristate (C14), *p*NP-palmitate (C16), and *p*NP-stearate (C18), were prepared in concentrations of 200 (C2,C4,C8), 100 (C12, C14), and 50 (C16, C18) mM. A mixture of acetonitrile and 2-propanol (1:1) was used as solvent. The mixtures were subjected to ultrasound bath until a clear solution was obtained. All substrates and solvents were purchased from Sigma Aldrich (Darmstadt, Germany). The reactions were prepared in volumes of 210 μL, containing 50 mM phosphate buffer pH 7.2, 1 mM substrate and 0.074 g/L of enzyme. The reactions started by adding the enzyme and monitored at 410 nm of wavelength in a microplate spectrophotometer (Thermo Scientific™, Multiskan™ GO) during 30 min at 37°C.

Determination of Optimal Temperature

The optimal temperature was determined for *Lr*Lyp in a range from 20 to 60°C. The pH was set to 7.2 with 20 mM McIlvain buffers and 5 mM of *p*-nitrophenyl laurate was used as substrate. The reactions were initiated by adding the enzyme (0.133 g/L) and stopped after 40 min by heating at 94°C for 10 min and cooling down to 4°C. All reactions were performed in triplicates and using controls, which consisted in same reactions mixtures, except enzyme. All reactions, including controls, were incubated in thermocycler (Biometra T-gradient from AnalyticJena, Germany). The formed product, *p*-nitrophenol, was quantified in a microplate spectrophotometer (Thermo Scientific™, Multiskan™ GO) at 410 nm.

Determination of Kinetic Constants

A stock solution of *p*NP-laurate, was prepared in a concentration of 10 mM, dissolving *para*-nitrophenyl laurate flakes in a mixture of water, DMSO and triton-X 100 (2:1:1, respectively) (modified from Mastihuba et al., 2002). The mixture was subjected to ultrasonic bath at 50°C for 10 min until an oily clear solution was obtained. Initial rates were determined in a range of 0.1–9 mM *p*-nitrophenyl laurate. Reactions were initiated by adding the respective enzyme at concentrations of 0.133 g/L of *Lr*Lyp and 0.358g/L of *Bl*Lyp. The pH 7 was set with 20 mM McIlvaine buffer. The reactions were monitored quantifying the nitrophenol formed along the time, using a microplate spectrophotometer (Thermo Scientific™, Multiskan™ GO) at 410 nm. All reactions were performed by triplicates and using controls, which were prepared with the same composition of reaction mixtures, except enzyme. The correlation between initial rates and substrate concentration was plotted and adjusted to the Michaelis-Menten (Eq. 1) or substrate inhibition kinetics (Eq. 2) model, by non-linear regression methods by the generalized reduced gradient non-linear algorithm, used as implemented in the Solver of Microsoft Excel:

$$v_0 = \frac{V_{max}^{app}\,[S]}{K_M^{app} + [S]} \tag{1}$$

$$v_0 = \frac{V_{max}^{app}\,[S]}{K_M^{app} + [S]\left(1 + \frac{[S]}{K_I^{app}}\right)} \tag{2}$$

where v_0 is the initial rate, V_{max}^{app}. is the apparent maximum velocity, $[S]$ is substrate concentration, K_M^{app}. is the apparent Michaelis Menten constant and K_I^{app}. is the apparent dissociation constant for binding.

Stability

The stability of the enzyme *Lr*Lyp, at 37°C and pH 7, was monitored for 35 days. Residual activities were determined every day the first 5 days, after, once every week. Reactions were performed in triplicates, using 5 mM *p*-nitrophenyl laurate as substrate and quantifying the production of *p*-nitrophenol spectrophotometrically, such as is described before.

Molecular Modeling

A model of the three-dimensional structure of *Lr*Lyp was obtained from the amino acid sequence, excluding the N-terminal signal peptide. Remote homology recognition techniques were applied using the Phyre2 Protein Fold Recognition Server (Kelley et al., 2015). The refinement of the model was performed by molecular dynamic simulations (MD) of 500 ps (Krieger et al., 2004). This protocol generates snapshots every 25 ps (in format pdb) with a table of energy to identify the best snapshot. The force field used was YAMBER2, implemented in the program YASARA (Krieger and Vriend, 2014). The MD conditions were pH 7.4, temperature 280°K and density 0.997. Additional validation of the model was analyzed using ProSA-web (Wiederstein and Sippl, 2007).

AF4 Instrumentation

The instrumentation consisted in an Eclipse 3 + Separation System coupled to a Dawn Heleos II multi-angle light scattering (MALS) detector (Wyatt Technology, Dernbach, Germany) with a wavelength of 663.8 nm and to a UV detector (Jasco UV-975 detector, Corp., Tokyo, Japan) with a wavelength of 280 nm. An Agilent 1100 series pump coupled to a vacuum degasser (Agilent Technologies, Waldbronn, Germany was used to deliver the carrier liquid. For the sample injection into the channel, the system was equipped with an auto sampler Agilent 1100 series (Agilent Technologies). The channel used was a trapezoidal long channel (Wyatt Technology) with length of 26.0 cm and outlet inlet widths of 0.6 cm and 2.15 cm, respectively and 350 μm of nominal thickness. A membrane of regenerated cellulose (RC), cut-off of 10 kDa, was used as the accumulation wall (Merck Millipore, Bedford, MA, United States).

AF4 Sample Preparation

The samples were produced and purified as described in previous sections, resulting in a final concentration of 0.88 mg/mL for *Bl*Lyp and 1.2 mg/mL for *Lr*Lyp. Before the injection, the samples were centrifuged at 11,000 g for 15 min at 4°C. Bovine serum albumin (BSA) at concentration of 2 mg/mL was used as standard to check the performance of the AF4 system and to normalize de MALS detector.

AF4 Parameters

First, the channel was flushed in elution and focus mode, 1 min each. After that, 100 μL of sample was injected onto the channel at 0.2 mL/min for 2 min. Once the sample was injected (0.088 mg of *Bl*Lyp and 0.12 mg of *Lr*Lyp), 3 min of focus mode were applied before the elution step. A constant cross flow of 5 mL/min was used during the elution period for 15 min, followed by 15 min without cross flow to remove any remnant material. The detector flow was always 1 mL/min. The parameters previously described were used with 5 different carrier liquids: 20 mM of phosphate-citrate buffer at pH 7, 6, 5, 4, and 3 in both lipase samples. A new channel was assembled for every lipase.

AF4 Data Processing

Astra software 6.1 (Wyatt Technology Europe) was used for the data analysis. For the molecular weight (Mw) of *Bl*Lyp, the value was determined at pH 6 using 13 scattering angles, from 42.8° to 163.3°. The calculations were performed with 1st order Zimm model (Zimm, 1948). The dn/dc value used was 0.185 mL/mg and the UV extinction coefficient 0.863 mL/(mg cm). The second virial coefficient was considered negligible. For both lipases, the hydrodynamic radius (r_h) was estimated by the Stokes-Einstein equation using FFhydRad 2.1-MATLAB Apps (Håkansson et al., 2012) for the calculations. The channel thickness (*w*) for *Lr*Lyp and for *Bl*Lyp was determined using BSA as a standard.

RESULTS

Production of Recombinant *Lr*Lyp and *Bl*Lyp

Putative extracellular lipases were searched in the genomes of *Lactobacillus rhamnosus*, strain GG (ATCC 53103) and *Bifidobacterium longum* NCC 2705. Only one locus of a putative annotated lipase/acyl-hydrolase was found in each genome, LGG_RS06710 in *L. rhamnosus*, and BL1109 in *B. longum*. LGG_RS06710 encodes a 281 amino acids protein of 30728.20 Da including a predicted N-terminal signal peptide of 34-amino acids. BL1109 encodes a 480 amino acids protein of 51163.93 Da with 34-amino acids in the N-terminal predicted as signal peptide. Therefore, it is predicted that both proteins are exported to the extracellular medium. The genes encoding these proteins, excluding signal peptides, were synthesized with codons optimized for *Escherichia coli* and successfully produced in strains BL21(DE3), ArticExpres and Origami2. However, the last gave the highest fraction of soluble recombinant protein, estimated in 80% according to the SDS-PAGE analysis. The theoretical molecular weights of these truncated forms (without signal peptide) are 27058.74 Da (*Lr*Lyp) and 52360.25 Da (*Bl*Lyp) from *L. rhamnosus* and *B. longum,* respectively; which is consistent with the molecular mass determined by SDS-PAGE (**Figure 1**).

Bioinformatic Analysis

Amino acid sequence analysis of *Lr*Lyp and *Bl*Lyp has revealed that these enzymes contain conserved motif corresponding to lipolytic enzymes families II and IV respectively. *Lr*Lyp has four blocks: GDSLT (amino acids 53–56), GVSG (aa. 91–94), GGND (aa. 125–128), and HPN (aa. 256–258); as shown in the multiple alignment with other family II enzymes (**Figure 2**). Previously characterized bacterial GDSL enzymes, including Sc1 from *Streptomyces coelicolor* (Côté and Shareck, 2008), TesA and EstA from *Pseudomonas aeruginosa*, SrLip from

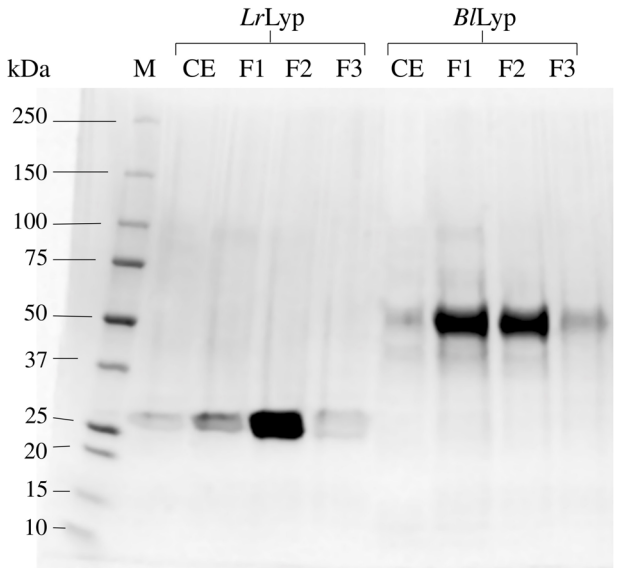

FIGURE 1 | Production and purification of the recombinant *Lr*Lyp (locus LGG_RS06710) and *Bl*Lyp, without signal peptides. SDS-PAGE is showing the molecular weight marker M (Lane 1), the cell extracts (CE) and the different chromatographic fractions (F1–F3) corresponding to each purified protein: *Lr*Lyp (Lanes 3–5) and *Bl*Lyp (Lanes 7–9).

Streptomyces rimosus, EstP from *Pseudomonas putida* (Leščić Ašler et al., 2010), XvEstE from *Xanthomonas vesicatoriaand* (Talker-Huiber et al., 2003), and EstHE1 obtained from a metagenome (Okamura et al., 2010), were selected for the multiple alignment (**Supplementary Information S1**).

*Bl*Lyp has five conserved motifs present in family IV as shown in **Figure 3**. The conserved sequences are in five blocks: HGGG (aa. 225–229), YRLA (aa. 257–260), GDSAGGNL (aa. 328–335), CPL (aa. 430–432), and HGI (aa. 460–462). The sequences selected for the multiple alignment correspond to previously characterized family IV lipolytic enzymes, including Est3k obtained from a metagenome (Kim et al., 2015), LipP from *Pseudomonas* sp. (Choo et al., 1998), Lip2 from *Moraxella* sp. (Feller et al., 1991), Est2 from *Alicyclobacillus acidocaldarius* (Mandrich et al., 2008), arylesterase from *Saccharolobus solfataricus* (PDB accession code 5L2P) and Aes from *Saccharolobus shibatae* (Ohara et al., 2014). It is remarkable the presence of cysteine in the motif CPL in *Bl*Lyp, instead of conserved aspartate (DPL) in the rest of the enzymes compared (**Supplementary Information S2**).

Optimal pH and Temperature for *Lr*Lyp

Both optimal temperature and pH were determined in terms of thermal stability in a range of pH from 4.3 to 9.9 by DSF. The protein has show the highest stability in a range of pH from 6 to 8 with the optimal melting point of 53.1°C at a pH close to 7 (**Figure 4A**). Indeed, the data adjusted to the quadratic model $T_m = -1.22\,pH^2 + 16.83\,pH.$ – 3.19, with a coefficient of determination, R^2, of 98%, which first derivative equal to zero, gave a critical point corresponding to pH 6.88. Therefore, the optimal temperature in terms of relative activity was determined at pH 7, giving maximum activity (100%) in

Clade	Source	Enzyme (Seq. ID)	Block I	Block II	Block III	Block IIIa	Block V
I	*L. rhamnosus* GG	*Lr*Lyp (NC_013198)	TALGD**S**LT	NYGVS**G**NTSG	IITVTAGG**N**DLMHV		SQ**D**HF**H**PNNAGY
I	*S. coelicolor* A3(2)	Sc1 (Q9S2A5)	VALGD**S**YS	FTACS**G**ARTG	LVSISIGG**N**DAGFA		IGESY**H**PTAAGQ
I	*P. aeruginosa* PAO1	TesA (Q9HZY8)	LVVGD**S**IS	NASIS**G**DTSA	LVVIELGG**N**DGLRG		QA**D**GI**H**PALAAQ
I	*S. rimosus*	SrLip (Q93MW7)	VALGD**S**YS	FTACS**G**ARTG	LVSITIGG**N**DAGFA		VENSY**H**PTANGQ
I	Metagenome	EstHE1 (BAH03944)	LVLGD**S**LS	NASIS**G**DTTS	VVIIELGG**N**DGLQG		QE**D**GI**H**PAPEAQ
II	*P. aeruginosa* PAO1	EstA (O33407)	VVFGD**S**LS	NWAVG**G**YRTD	LYYITGGG**N**DFLQG	EGMANPASFGLAADQN-LIGTCFSGNGCTM	FN**D**SV**H**PTITGQ
II	*P. putida* KT2440	EstP (Q88QS0)	IVFGD**S**LA	NWAVG**G**YTTQ	LYYLTGGG**N**DFLQG	EALASPSQFGLASDQN-LVGTCYSGDSCVE	FN**D**SV**H**PTIAGQ
II	*X. vesicatoria*	XvEstE (Q7X4K7)	VFFGD**S**LT	NYAAG**G**ARIQ	LYTVWGGA**N**DLLAA	EVVADPGIYGFSNVTGTACNPALALPACNP	FA**D**GI**H**PTTATH
			.***:	. .*	: : *.**	* * *:: ::: *	: **

FIGURE 2 | Multiple alignment of conserved blocks in lipolytic enzymes family II. Characterized enzymes were selected for the comparison with *Lr*Lyp from *L. rhamnosus*. Conserved catalytic amino acids are in bolds, S in the block I is the nucleophile, D and H in the block V are the donor proton and catalytic base respectively. G and N in the blocks II and III belong to the oxyanion hole. *Lr*Lyp belongs to clade I, since it lacks of block IIIa (Leščić Ašler et al., 2010). Where (*) denotes conserved or identical amino acid, (:) conservative or amino acid with similar biochemical property, (.) semiconservative and (_) non conservative amino acid.

Source	Enzyme (Seq. ID)	Block I	Block V	Block II	Block III	Block IV
B. longum NCC2705	*Bl*Lyp (AAN24916)	ILFFHGGGWTTGGIN	VISVEYRLAPEY	GD**S**AGGNLAAAV	AEYC**P**LRDE	I**H**GYL
Metagenome	Est3k (AKG92633)	VLDIHGGGWVIGNAQ	VVSVDYRLAVNT	GE**S**AGGHLAAAT	GEL**D**PLLDD	A**H**GFI
Pseudomonas sp.	LipP (O52270)	LVFFHGGGFVMGNLD	VVSVAYRLAPEN	GD**S**AGGNLALAV	AEF**D**PLRDE	I**H**GFI
Moraxella sp.	Lip2 (P24484)	MLFFHGGGFCIGDID	VVSVDYRMAPEY	GD**S**AGGCLAALV	AEL**D**ILRDE	P**H**GFI
A. acidocaldarius	Est2 (2HM7_A)	LVYYHGGSWVVGDLE	VFSVDYRLAPEH	GD**S**AGGNLAAVT	AQY**D**PLRDV	I**H**GFA
S. solfataricus	Arylesterase (5L2P_A)	VMHFHGGAWILGSIE	VISVDYRLAPEY	GI**S**AGGNLVAAT	AEY**D**PLRDQ	V**H**AFL
S. shibatae	Aes (3WJ1_A)	LVYLHGGGFVIGDVE	VVSVDYRLAPEY	GD**S**AGGNLAAVV	AEY**D**PLRDQ	I**H**GFL
		:: ***.: *. :	*.** **:* :	* **** *. .	.: * *	*.:

FIGURE 3 | Multiple alignment of conserved blocks in lipolytic enzymes family IV. Characterized enzymes were selected for the comparison with *Bl*Lyp from *B. longum*. Conserved catalytic amino acids are in bolds, S in the block I is the nucleophile, H in block IV is the base, and the proton donor D located in bock III, interestingly is a C in *Bl*Lyp. The recently suggested block V (Kim et al., 2015) containing the consensus sequence YRLA is also present in *Bl*Lyp. Where (*) denotes conserved or identical amino acid, (:) conservative or amino acid with similar biochemical property, (.) semiconservative and (_) non conservative amino acid.

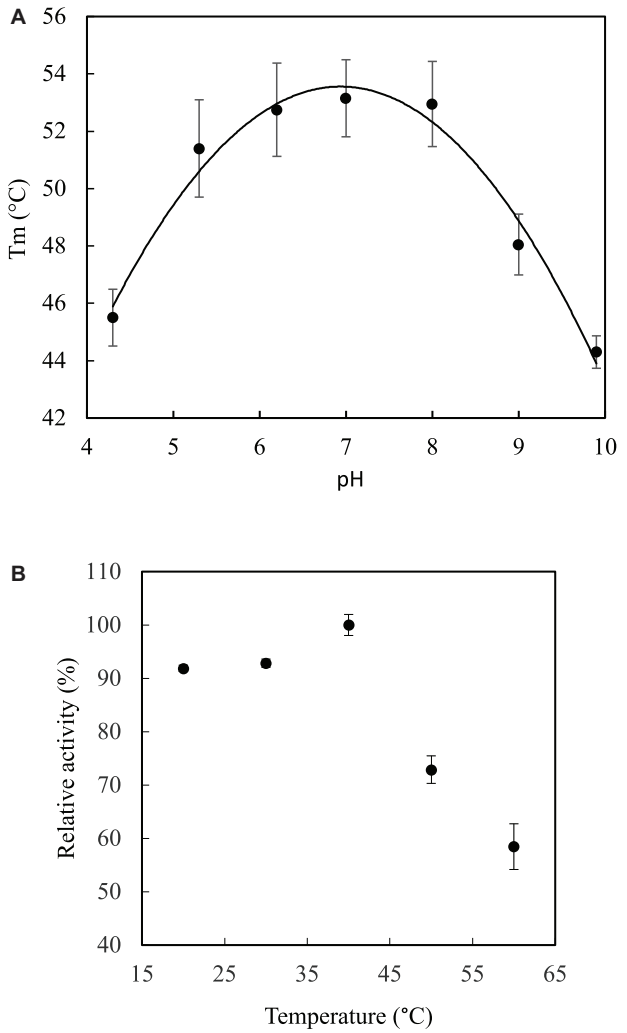

FIGURE 4 | Optimum pH and temperature. **(A)** DSF analysis shows optimum pH between 6 and 8 with a highest transition temperature (melting point Tm) at 53.1°C. **(B)** Temperature curve shows maximum relative activity at 40°C. The pH was 7 and *p*NP-laurate was used as substrate. Error bars denote plus/minus one standard deviation.

a range from 37 to 40°C (**Figure 4B**), which is consistent with the physiological temperature. The activity decreases to 90% in a range of 20–30°C, while decreases dramatically below 60% at 60°C.

Substrate Selectivity for *Lr*Lyp

The substrate selectivity was evaluated with seven synthetic *para*-nitrophenyl esters (*p*NP-esters) with linear hydrocarbon chains from C2 to C18. On the other hand, the biodegradable polyester-plastic polycaprolactonate (CAPA 6000) was tested as potential substrate and the phospholipase D activity was assessed as well. Activity was detected only on *p*NP-esters. The highest activity was on *p*NP-butyrate while the lowest was on *p*NP-sterate. Thus, these results show that *Lr*Lyp has preference for short hydrocarbon chain *p*NP-esters

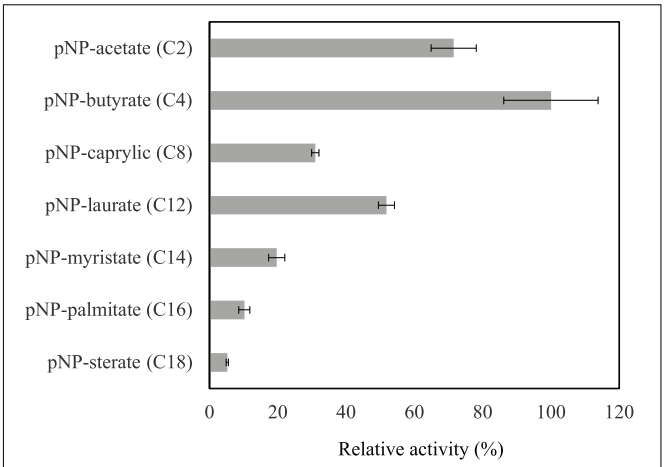

FIGURE 5 | Substrate selectivity for *Lr*Lyp. The reactions were carryout using 1 mM of substrate at 37°C and pH 7.2. Error bars denote plus/minus one standard deviation.

TABLE 1 | Enzymatic activity on *p*NP-esters. The reaction conditions were pH 7.2, 37°C, and 1 mM substrate.

Substrate (No. of carbons in the chain)	Activity (U/mg)
***Lr*Lyp**	
*p*NP-acetate (C2)	0.58 ± 0.05
*p*NP-butyrate (C4)	0.81 ± 0.11
*p*NP-caprylic (C8)	0.25 ± 0.01
*p*NP-laurate (C12)	0.42 ± 0.02
*p*NP-myristate (C14)	0.16 ± 0.02
*p*NP-palmitate (C16)	0.08 ± 0.01
*p*NP-sterate (C18)	0.04 ± 0.01
***Bl*Lyp**	
*p*NP-laurate (C12)	(136 ± 0.7) × 10^{-4}

(**Figure 5** and **Table 1**). No activity was detected on CAPA 6000 neither phospholipase D activity. The activity of *Bl*Lyp is dramatically lower than the *Lr*Lyp when *p*NP-laurate is used as substrate (**Table 1**).

Stability Over the Time for *Lr*Lyp

Among the large chain esters, *p*NP-laurate (C12) has shown highest activity (52% comparing with the best substrate *p*NP-butyrate) and it was used for further studies of stability for *Lr*Lyp over time and determination of kinetic constants. Incubating *Lr*Lyp at 37°C, the activity dropped to an average of 5.3% after the 7th day and remained so until more than 35 days (**Figure 6**).

Kinetic Constants

*Lr*Lyp kinetics does not follow a typical Michaelis-Menten model (**Figure 7A**). It seems that *Lr*Lyp reaches a saturation point at 5mM of substrate, and at higher substrate concentrations the reaction rate decreases. Which suggest that *Lr*Lyp suffer substrate inhibition at substrate concentrations higher than 5 mM. Therefore, the data were adjusted to the substrate inhibition model to obtain the kinetic constants (**Table 2**). The

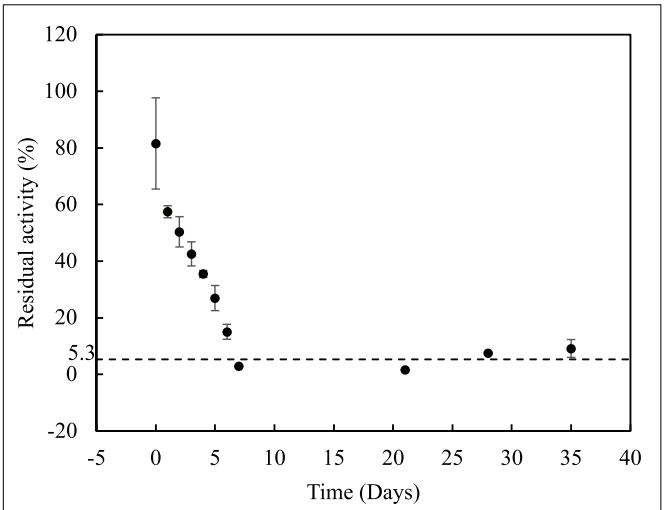

FIGURE 6 | Stability of *Lr*Lyp along the time.

coefficient of determination, R^2, of the model was 96%. On the other hand, for *Bl*Lyp **Figure 7B** shows a typical Michaelis-Menten behavior. The determined apparent kinetic constants are reported in **Table 2**, and the coefficient of determination was 99%.

Multimerization and Aggregation

Multimerization and aggregation studies of both *Lr*Lyp and *Bl*Lyp were performed by asymmetric flow field-flow fractionation (AF4). **Figure 8A** shows the UV – fractograms for *Bl*Lyp at different pHs where two main peaks were identified and characterized respect to their hydrodynamic r_h and molar mass. For pH 7, peak 2 absorbs 10 times less than peak 1 (considering peak height). At pH 6 the concentration of peak 1 decrease and peak 2 absorb <10% than peak 1. In pH 5 only peak 2 is present. pH 4 does not show any notable peak, while at pH 3 peak 1 is missing and peak 2 present a tail of other compounds that were not separated. The UV – fractograms for *Lr*Lyp are plotted in **Figure 8B**, where the hydrodynamic r_h for only the first peak was measured. At pH 7 we have the highest absorption for this peak, followed for other peaks that were not completely separated, for pH 6 this peak absorbs <10% compared with pH 7. This peak is prominent at pH 5 again and it disappears completely at pH 4.

For the molecular weight calculations, it is necessary to have both, MALS and UV fractograms. But, due to the MALS signal was not sufficient for *Lr*Lyp, the molecular weight was only calculated for *Bl*Lyp. A characteristic plot for this is shown in **Figure 8**, where the molecular weight is plotted in the y axis. The resulting molecular weight is the average of the top of the peak (from 2.6 to 3.7 min) and is reported in **Table 3** together with the hydrodynamic radii for peak 1 and 2 in **Figures 8A,B**.

The results from **Table 3** indicate that the Mw obtained from peak 1 (*Bl*Lyp), 53 kDa, agrees with the theoretical Mw (52.36 kDa), therefore it corresponds to the monomeric form with a r_h higher than BSA (3.3 nm). The Mw for peak 2 was not calculated because the LS signal-to-noise ratio was insufficient. **Figure 8** suggests that *Bl*Lyp is predominantly monomeric at pHs 6 and 7, while at pH 5 it forms multimers. At lower pH no significant peaks were observed, suggesting that the enzyme precipitate or is degraded and lost from the analysis. On the other hand, the r_h calculated for *Lr*Lyp suggest that the molecule appears somewhat smaller than BSA (Magnusson et al., 2012) (r_h = 3.9 nm and Mw = 66.4 kDa), therefore it could correspond to the monomeric form. If that is the case, then at pHs 5 and 7 the main form would be monomeric, while at the other pH neither multimer nor monomer forms were identified.

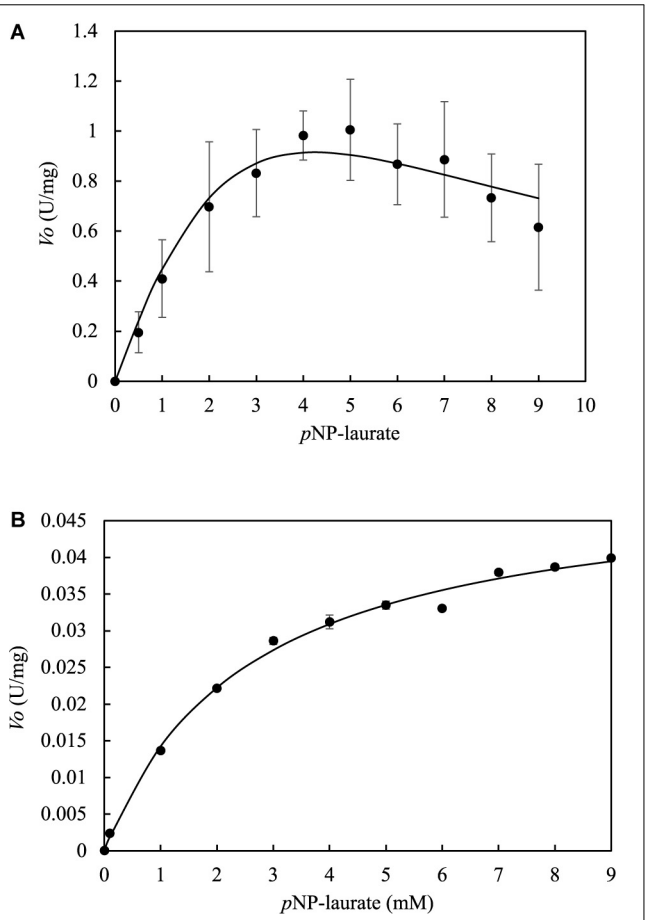

FIGURE 7 | Determination of kinetic constants at pH 7 and 37°C for *Lr*Lyp and *Bl*Lyp by no-linear regression. Error bars represent the standard deviation. *Lr*Lyp **(A)** shows substrate inhibition kinetics, while *Bl*Lyp **(B)** shows a typical Michaelis Menten kinetics. Error bars denote plus/minus one standard deviation.

TABLE 2 | Apparent kinetic constants.

Enzyme	V_{max}^{app} (U/mg)	K_M^{app} (mM)	K_I^{app} (mM)	K_{cat}^{app} (s^{-1})	K_{cat}^{app}/K_M^{app} (s^{-1}/mM)
*Lr*Lyp	5.8	11.4	1.57	2.6	0.22
*Bl*Lyp	0.05	2.56	–	0.04	0.016

Molecular Modeling of *Lr*Lyp

The search of homologous crystalized proteins in the Protein Data Bank (PDB) via Blast, has given no significant homologous

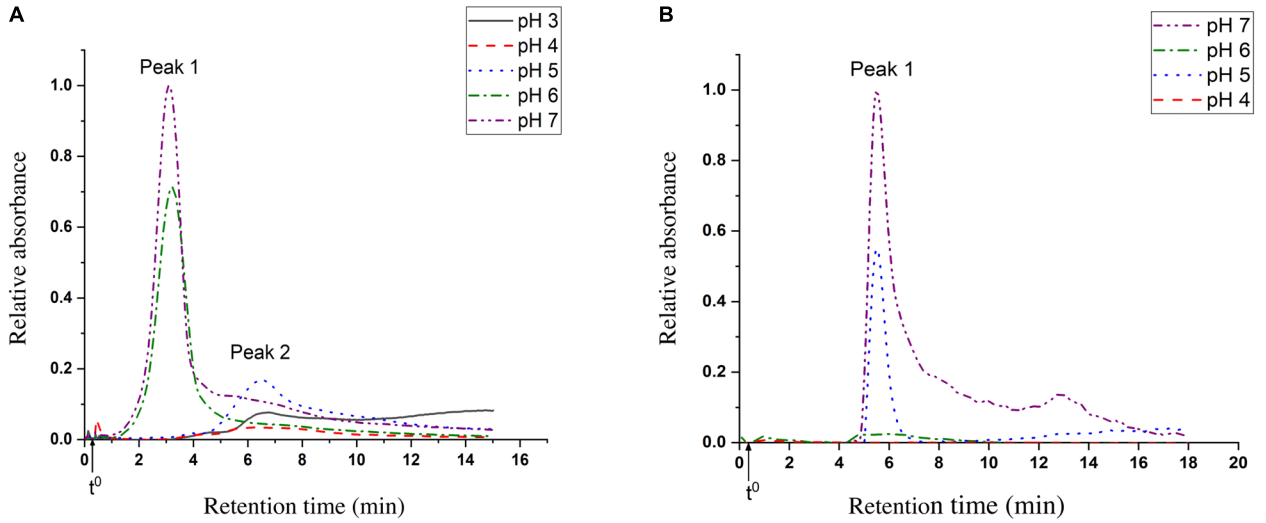

FIGURE 8 | AF4 – UV fractograms of the proteins at different pH. **(A)** *Bl*Lyp, the injected mass is 0.088 mg and the void time t^0 17 s. **(B)** *Lr*Lyp, the injected mass is 0.12 mg and the void time (t^0) is 22 s.

TABLE 3 | Multimerization analysis.

Sample	Mw (kDa)	rh (nm)	Multimer form
*Bl*Lyp – peak 1	53	4	Monomer
*Bl*Lyp – peak 2	n.d	8	Multimer
*Lr*Lyp – peak 1	n.d	3	Monomer?

for both enzymes. However, a computational model for *Lr*Lyp was possible to obtain using remote homology techniques with Phyre2 (Kelley et al., 2015). This initial model was validated with ProSa-web (Wiederstein and Sippl, 2007) giving a Z-score of −3.56. This score was improved to −5.21 by refining the initial model by short molecular dynamic simulations (500 ps) with YASARA (Krieger and Vriend, 2014). The refinement has shown improvements in the whole structure, especially in the region of the C-terminal (**Supplementary Information S3**).

The molecular model of *Lr*Lyp resulted in a single domain protein with α/β-hydrolase fold, typical in lipases, esterases and other hydrolases (**Figure 9A**). The β-sheet is formed by five parallel β-strands and seven α-helixes, in addition, 2_{10} helixes were predicted. In the active site region, long loops are predicted, Val98-Ala117, Gly147-Ser160, Ile183-Lys240 among the longest. These loops can be unmodeled regions due to the lack of crystallographic homologous available in the PDB. On the other hand these loops also can be flexible regions that affect the selectivity of substrates as is discussed in the next section. Despite of the difficulties to model the active

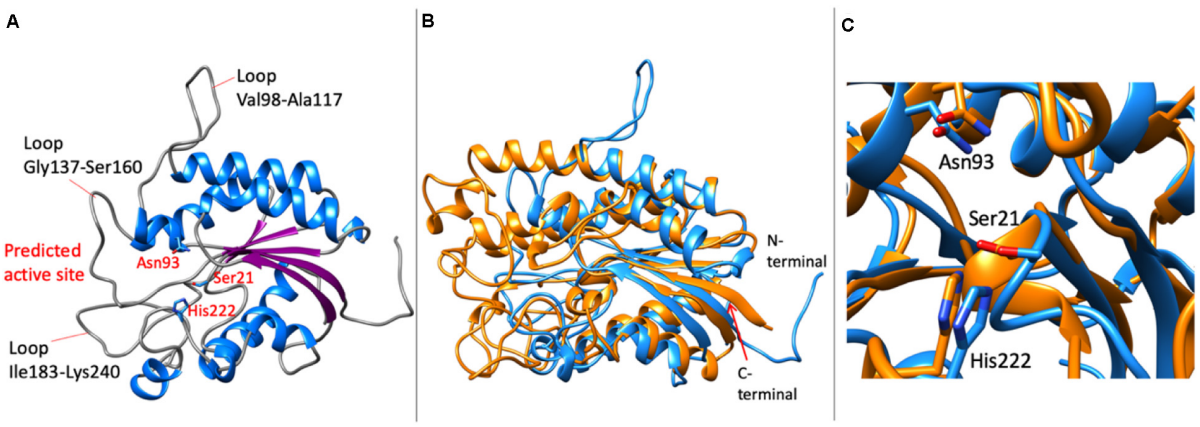

FIGURE 9 | Molecular model of *Lr*Lyp. **(A)** Overall model showing the loops predicted surrounding the catalytic site and putative catalytic amino acids. **(B)** Superimposition of the molecular model (in blue) with the crystallographic structure (in orange) of an esterase from *Streptomyces scabies* (PDB code: 1ESC). **(C)** Detail of the conserved catalytic amino acids predicted by superimposition of the crystallographic structure of the esterase from *S. scabies* and the model of *Lr*Lyp. The catalytic amino acids in the structure 1ESC are Asn106, Ser14, and His283.

site region, interestingly, superimposing the model with the no homologous crystallographic structure (PDB code: 1ESC) of a esterase from *Streptomyces scabies* (**Figure 9B**), it was found that the catalytic amino acids are well conserved. Thus, Ser21, His222, and Asn93 were predicted as potential catalytic amino acids in *Lr*Lyp (**Figure 9C**).

DISCUSSION

Both *Lactobacillus rhamnosus* GG and *Bifidobacterium longum* NCC 2705 are among of the most studied human probiotic strains. Despite that, the molecular bases of many mechanisms involved in the probiotic – host interactions are not clear yet. Probiotic proteins excreted to the extracellular medium could have effect in the interaction with the host. Thus, putative lipolytic enzymes (denoted as Lyp in this work) annotated in the genomes of *L. rhamnosus* GG and *B. longum* have been selected due to the presence of a signal peptide in the N-terminal, which indicates that these proteins are excreted and could have activity on host lipids, fat ingested by the host and even on other metabolites and drugs containing acyl ester bonds.

Based on amino acid sequences analysis, *Lr*Lyp and *Bl*Lyp belong to the lipolytic enzymes families II and IV, respectively. *Lr*Lyp has the GDSL motif, which define the family II. This family differs from the others because contain the amino acid sequence motif GDSL (block I) instead of the typical GXSXG, located in the active site, where S is the catalytic serine (Akoh et al., 2004). There are additional three conserved blocks that characterize this family. Blocks II and III contain conserved glycine (G) and asparagine (N), respectively; both serve as proton donors to the oxyanion hole (Kovacic et al., 2019). Block V contains the catalytic base, histidine (H), which deprotonates the hydroxyl group of the catalytic serine located in the block I, increasing its nucleophilicity (**Figure 2**). This family is subdivided in two clades, where clade II differs from I because it has an additional motif named block IIIa, no directly involved in catalysis (Leščić Ašler et al., 2010). Because *Lr*Lyp lacks block IIIa, it is subclassified in clade I (**Figure 2**). Enzymes of this family usually have a broad range of different substrates (Leščić Ašler et al., 2010).

*Bl*Lyp contains the characteristic family IV motif, GDSAGG. This family have four conserved blocks (Arpigny and Jaeger, 1999). The block I contains the consensus sequence HGGG, involved in stabilization of oxyanion hole through hydrogen bonds. Block II contains the catalytic serine (S), while the block IV the catalytic base, histidine (H). Interestingly, the proton donor predicted is a cysteine (C) in *Bl*Lyp, instead of the conserved aspartate (D) (**Figure 3**). The role of this unusual C will be clarified by mutational analysis in conjunction with structural studies. *Bl*Lyp also contains the sequence YRLA, conserved in the family IV and suggested as block V (Kim et al., 2015). Remarkably, this family groups enzymes with similarity to the mammalian hormone-sensitive lipases (HSL). Nevertheless, the substrate specificity in the bacterial HSL-family differs significantly. Human HSL can hydrolyze a broad range of substrates, both short esters as well as water insoluble substrates, however, bacterial HSL have shown activity on esters of short chain fatty acids (Chahinian et al., 2005).

Despite the classification based on amino acid sequences, these families are still poorly characterized. The experimental results have shown activity on a number of *p*NP-esters, with preference on esters of short chain fatty acids in the case of *Lr*Lyp (**Figure 5**), which is consistent with the gene annotation. The highest activity was on *p*NP-butyrate; indeed, butyrate and other fatty acids are commonly found in esterified form in plant oils and animal fat. For instance, bovine milk contains a broad variety of both short and large chain fatty acids esterified with glycerol in specific positions (Lindmark Månsson, 2008). The activities reported in this work are significantly lower comparing with the activities of other bacterial lipolytic enzymes. Therefore, it would be interesting to study the activity of *Lr*Lyp and *Bl*Lyp using natural substrates. In fact, the natural substrate and biological function of these novel enzymes remains unknown.

The multimerization study by AF4 indicated that *Lr*Lyp is monomer at pHs 5 and 7, while *Bl*Lyp is monomer at pHs 6 and 7, which suggests that these enzymes are active in monomeric form. Regarding to the kinetic studies, it was difficult to determine accurate kinetic constants for *Lr*Lyp due to the insolubility of the substrates in high concentrations, however the kinetic curve for the substrate *p*NP-laurate shows substrate inhibition when de concentration of the substrate is higher than 5 mM. In the case of *Bl*Lyp, the kinetic constant obeys a Michaelis-Menten behavior for *p*NP-laurate. Comparing the K_M obtained from both enzymes, *Lr*Lyp shows the highest substrate affinity respect to *p*NP-laurate.

On the other hand, the molecular model of *Lr*Lyp obtained has allowed the prediction of catalytic amino acids. Interestingly, the superimposition of the molecular model with the crystallographic structure of a no homologous esterase from *Streptomyces scabies* (Wei et al., 1995) has shown highly conserved catalytic amino acids consistent with the catalytic mechanism suggested for this type of esterases. It is also suggested that the loops surrounding the active site can adopt open and close conformations in lipolytic enzymes, determining the substrate specificity. Thus, the loops predicted in the modeled *Lr*Lyp enzyme could be flexible structures that affect the interactions with the substrates. Crystallographic studies of *Lr*Lyp together with mutational analysis will support to understand the mechanism of reaction of this enzyme.

CONCLUSION

It was found that the putative extracellular acyl-hydrolase/lipase from the human probiotic bacteria *Lactobacillus rhamnosus* and *Bifidobacterium longum* have activity on *p*NP-esters. *L. rhamnosus* enzyme has shown preference for *p*NP-esters of short chain fatty acids, and its optimal activity is near to the pH 7 and 37°C. The bioinformatic analysis and computational model has allowed the prediction of catalytic amino acids for the *Lactobacillus rhamnosus* enzyme and suggests that large loops surrounding the active site could determine the substrate specificity. *B. longum* enzyme has been tested on *p*NP-laurate, showing activity at pH 7 and human physiological

temperature. On the other hand, both enzymes are active in their monomeric form at pH 7.

DATA AVAILABILITY STATEMENT

All datasets generated for this study are included in the article/**Supplementary Material**.

AUTHOR CONTRIBUTIONS

JL-P designed the study, did the bioinformatic analysis and modeling, and wrote and corrected the manuscript. LN designed the study, analyzed the data, and corrected the manuscript. PM performed the experiments related to protein purification and kinetic, as well as wrote the first draft of the manuscript. A-SB performed the experiments about multimerization/aggregation analysis. BP produced and purified protein and did the DSF analysis. JP and AH participated in the revision of the manuscript. All authors contributed to the article and approved the submitted version.

FUNDING

This work was supported by the Swedish International Development Agency (SIDA): a collaboration project between Universidad Mayor de San Andrés (Bolivia) and Lund University (Sweden).

ACKNOWLEDGMENTS

We thank Dr. Maria Gourdon and the Lund Protein Production Platform (PL3) staff for their assistance in using the DSF instrument.

SUPPLEMENTARY MATERIAL

The Supplementary Material for this article can be found online at: https://www.frontiersin.org/articles/10.3389/fmicb.2020.01534/full#supplementary-material

REFERENCES

Akoh, C. C., Lee, G.-C., Liaw, Y.-C., Huang, T.-H., and Shaw, J.-F. (2004). GDSL family of serine esterases/lipases. *Prog. Lipid Res.* 43, 534–552. doi: 10.1016/j.plipres.2004.09.002

Arpigny, J. L., and Jaeger, K.-E. (1999). Bacterial lipolytic enzymes: classification and properties. *Biochem. J.* 343, 177–183. doi: 10.1042/bj3430177

Brigidi, P., Vitali, B., Swennen, E., Bazzocchi, G., and Matteuzzi, D. (2001). Effects of probiotic administration upon the composition and enzymatic activity of human fecal microbiota in patients with irritable bowel syndrome or functional diarrhea. *Res. Microbiol.* 152, 735–741. doi: 10.1016/s0923-2508(01)01254-2

Brusaferro, A., Cozzali, R., Orabona, C., Biscarini, A., Farinelli, E., Cavalli, E., et al. (2018). Is it time to use probiotics to prevent or treat obesity? *Nutrients* 10:1613. doi: 10.3390/nu10111613

Capurso, L. (2019). Thirty years of *Lactobacillus rhamnosus* GG: a review. *J. Clin. Gastroenterol.* 53, S1–S41.

Castro-Ochoa, L. D., Rodríguez-Gómez, C., Valerio-Alfaro, G., and Ros, R. O. (2005). Screening, purification and characterization of the thermoalkalophilic lipase produced by Bacillus thermoleovorans CCR11. *Enzyme Microb. Technol.* 37, 648–654. doi: 10.1016/j.enzmictec.2005.06.003

Chahinian, H., Ali, Y. B., Abousalham, A., Petry, S., Mandrich, L., Manco, G., et al. (2005). Substrate specificity and kinetic properties of enzymes belonging to the hormone-sensitive lipase family: comparison with non-lipolytic and lipolytic carboxylesterases. *Biochim. Biophys. Acta Mol. Cell Biol. Lipids* 1738, 29–36. doi: 10.1016/j.bbalip.2005.11.003

Choi, J., Lee, S., Linares-Pastén, J. A., and Nilsson, L. (2018). Study on oligomerization of glutamate decarboxylase from *Lactobacillus brevis* using asymmetrical flow field-flow fractionation (AF4) with light scattering techniques. *Anal. Bioanal. Chem.* 410, 451–458. doi: 10.1007/s00216-017-0735-6

Choo, D.-W., Kurihara, T., Suzuki, T., Soda, K., and Esaki, N. (1998). A cold-adapted lipase of an Alaskan psychrotroph, *Pseudomonas* sp. strain B11-1: gene cloning and enzyme purification and characterization. *Appl. Environ. Microbiol.* 64, 486–491. doi: 10.1128/aem.64.2.486-491.1998

Consortium, T. U. (2018). UniProt: a worldwide hub of protein knowledge. *Nucleic Acids Res.* 47, D506–D515.

Côté, A., and Shareck, F. (2008). Cloning, purification and characterization of two lipases from *Streptomyces coelicolor* A3 (2). *Enzyme Microb. Technol.* 42, 381–388. doi: 10.1016/j.enzmictec.2008.01.009

Feller, G., Thiry, M., and Gerday, C. (1991). Nucleotide sequence of the lipase gene lip2 from the Antarctic psychrotroph *Moraxella* TA 144 and site-specific mutagenesis of the conserved serine and histidine residues. *DNA Cell Biol.* 10, 381–388. doi: 10.1089/dna.1991.10.381

Gorbach, S. L., and Goldin, B. R. (1989). *Lactobacillus Strains and Methods of Selection*. Google Patents US4839281A. Boston, MA: New England Medical Center Hospitals.

Håkansson, A., Magnusson, E., Bergenståhl, B., and Nilsson, L. (2012). Hydrodynamic radius determination with asymmetrical flow field-flow fractionation using decaying cross-flows. Part I. A theoretical approach. *J. Chromatogr. A* 1253, 120–126. doi: 10.1016/j.chroma.2012.07.029

Hill, C., Guarner, F., Reid, G., Gibson, G. R., Merenstein, D. J., Pot, B., et al. (2014). The International Scientific Association for Probiotics and Prebiotics consensus statement on the scope and appropriate use of the term probiotic. *Nat. Rev. Gastroenterol. Hepatol.* 11, 506–514. doi: 10.1038/nrgastro.2014.66

Kankainen, M., Paulin, L., Tynkkynen, S., Von Ossowski, I., Reunanen, J., Partanen, P., et al. (2009). Comparative genomic analysis of *Lactobacillus rhamnosus* GG reveals pili containing a human-mucus binding protein. *Proc. Natl. Acad. Sci.* 106, 17193–17198. doi: 10.1073/pnas.0908876106

Kelley, L. A., Mezulis, S., Yates, C. M., Wass, M. N., and Sternberg, M. J. (2015). The Phyre2 web portal for protein modeling, prediction and analysis. *Nat. Protoc.* 10:845. doi: 10.1038/nprot.2015.053

Kim, H. J., Jeong, Y. S., Jung, W. K., Kim, S. K., Lee, H. W., Kahng, H.-Y., et al. (2015). Characterization of novel family IV esterase and family I. 3 lipase from an oil-polluted mud flat metagenome. *Mol. Biotechnol.* 57, 781–792. doi: 10.1007/s12033-015-9871-4

Kovacic, F., Babic, N., Krauss, U., and Jaeger, K. (2019). "Classification of lipolytic enzymes from bacteria," in *Aerobic Utilization of Hydrocarbons, Oils and Lipids*, ed. F. Rojo (Cham: Springer), 1–35. doi: 10.1007/978-3-319-39782-5_39-1

Krieger, E., Darden, T., Nabuurs, S. B., Finkelstein, A., and Vriend, G. (2004). Making optimal use of empirical energy functions: force-field parameterization in crystal space. *Proteins Struct. Funct. Bioinformatics* 57, 678–683. doi: 10.1002/prot.20251

Krieger, E., and Vriend, G. (2014). YASARA View—molecular graphics for all devices—from smartphones to workstations. *Bioinformatics* 30, 2981–2982. doi: 10.1093/bioinformatics/btu426

Leščić Ašler, I., Ivić, N., Kovačić, F., Schell, S., Knorr, J., Krauss, U., et al. (2010). Probing enzyme promiscuity of SGNH hydrolases. *Chembiochem* 11, 2158–2167. doi: 10.1002/cbic.201000398

Lindmark Månsson, H. (2008). Fatty acids in bovine milk fat. *Food Nutr. Res.* 52:1821. doi: 10.3402/fnr.v52i0.1821

Magnusson, E., Håkansson, A., Janiak, J., Bergenståhl, B., and Nilsson, L. (2012). Hydrodynamic radius determination with asymmetrical flow field-flow fractionation using decaying cross-flows. Part II. Experimental evaluation. *J. Chromatogr. A* 1253, 127–133. doi: 10.1016/j.chroma.2012.07.005

Mandrich, L., Menchise, V., Alterio, V., De Simone, G., Pedone, C., Rossi, M., et al. (2008). Functional and structural features of the oxyanion hole in a thermophilic esterase from Alicyclobacillus acidocaldarius. *Proteins Struct. Funct. Bioinformatics* 71, 1721–1731. doi: 10.1002/prot.21877

Mastihuba, V., Kremnický, L. R., Mastihubová, M., Willett, J., and Côté, G. L. (2002). A spectrophotometric assay for feruloyl esterases. *Anal. Biochem.* 309, 96–101. doi: 10.1016/s0003-2697(02)00241-5

Ohara, K., Unno, H., Oshima, Y., Hosoya, M., Fujino, N., Hirooka, K., et al. (2014). Structural insights into the low pH adaptation of a unique carboxylesterase from ferroplasma altering the pH optima of two carboxylesterases. *J. Biol. Chem.* 289, 24499–24510. doi: 10.1074/jbc.m113.521856

Okamura, Y., Kimura, T., Yokouchi, H., Meneses-Osorio, M., Katoh, M., Matsunaga, T., et al. (2010). Isolation and characterization of a GDSL esterase from the metagenome of a marine sponge-associated bacteria. *Mar. Biotechnol.* 12, 395–402. doi: 10.1007/s10126-009-9226-x

Petersen, T. N., Brunak, S., Von Heijne, G., and Nielsen, H. (2011). SignalP 4.0: discriminating signal peptides from transmembrane regions. *Nat. Methods* 8:785. doi: 10.1038/nmeth.1701

Saxelin, M. (2008). Probiotic formulations and applications, the current probiotics market, and changes in the marketplace: a European perspective. *Clin. Infect. Dis.* 46, S76–S79.

Schell, M. A., Karmirantzou, M., Snel, B., Vilanova, D., Berger, B., Pessi, G., et al. (2002). The genome sequence of *Bifidobacterium longum* reflects its adaptation to the human gastrointestinal tract. *Proc. Natl. Acad. Sci. U.S.A.* 99, 14422–14427. doi: 10.1073/pnas.212527599

Segers, M. E., and Lebeer, S. (2014). Towards a better understanding of *Lactobacillus rhamnosus* GG-host interactions. *Microb. Cell Fact.* 13(Suppl. 1):S7.

Talker-Huiber, D., Jose, J., Glieder, A., Pressnig, M., Stubenrauch, G., and Schwab, H. (2003). Esterase EstE from *Xanthomonas vesicatoria* (Xv_EstE) is an outer membrane protein capable of hydrolyzing long-chain polar esters. *Appl. Microbiol. Biotechnol.* 61, 479–487. doi: 10.1007/s00253-003-1227-5

Wahlund, K.-G., and Nilsson, L. (2012). "Flow FFF–basics and key applications," in *Field-Flow Fractionation in Biopolymer Analysis*, eds S. Williams, and K. Caldwell (Berlin: Springer), 1–21. doi: 10.1007/978-3-7091-0154-4_1

Wei, Y., Schottel, J. L., Derewenda, U., Swenson, L., Patkar, S., and Derewenda, Z. S. (1995). A novel variant of the catalytic triad in the *Streptomyces scabies* esterase. *Nat. Struct. Biol.* 2:218. doi: 10.1038/nsb0395-218

Wiederstein, M., and Sippl, M. J. (2007). ProSA-web: interactive web service for the recognition of errors in three-dimensional structures of proteins. *Nucleic Acids Res.* 35, W407–W410.

Young, S. L., Simon, M. A., Baird, M. A., Tannock, G. W., Bibiloni, R., Spencely, K., et al. (2004). Bifidobacterial species differentially affect expression of cell surface markers and cytokines of dendritic cells harvested from cord blood. *Clin. Diagn. Lab. Immunol.* 11, 686–690. doi: 10.1128/cdli.11.4.686-690.2004

Zimm, B. H. (1948). The scattering of light and the radial distribution function of high polymer solutions. *J. Chem. Phys.* 16, 1093–1099. doi: 10.1063/1.1746738

Conflict of Interest: The authors declare that the research was conducted in the absence of any commercial or financial relationships that could be construed as a potential conflict of interest.

frontiers in Microbiology

ORIGINAL RESEARCH
published: 29 July 2020
doi: 10.3389/fmicb.2020.01822

Lipoproteins Contribute to the Anti-inflammatory Capacity of *Lactobacillus plantarum* WCFS1

I-Chiao Lee[1,2,3], Iris I. van Swam[2,3], Sjef Boeren[4], Jacques Vervoort[4], Marjolein Meijerink[1], Nico Taverne[1,2], Marjo Starrenburg[3], Peter A. Bron[2,3†] and Michiel Kleerebezem[1,2†]*

[1] Host-Microbe Interactomics Group, Wageningen University & Research, Wageningen, Netherlands, [2] TiFN Food & Nutrition, Wageningen, Netherlands, [3] NIZO Food Research, Ede, Netherlands, [4] Laboratory of Biochemistry, Wageningen University & Research, Wageningen, Netherlands

Bacterial lipoproteins are well-recognized microorganism-associated molecular patterns, which interact with Toll-like receptor (TLR) 2, an important pattern recognition receptor of the host innate immune system. Lipoproteins are conjugated with two- or three-acyl chains (di- or tri-acyl), which is essential for appropriate anchoring in the cell membrane as well as for the interaction with TLR2. Lipoproteins have mostly been studied in pathogens and have established roles in various biological processes, such as nutrient import, cell wall cross-linking and remodeling, and host-cell interaction. By contrast, information on the role of lipoproteins in the physiology and host interaction of probiotic bacteria is scarce. By deletion of *lgt*, encoding prolipoprotein diacylglyceryl transferase, responsible for lipidation of lipoprotein precursors, we investigated the roles of the collective group of lipoproteins in the physiology of the probiotic model strain *Lactobacillus plantarum* WCFS1 using proteomic analysis of secreted proteins. To investigate the consequences of the *lgt* mutation in host-cell interaction, the capacity of mutant and wild-type bacteria to stimulate TLR2 signaling and inflammatory responses was compared using (reporter-) cell-based models. These experiments exemplified the critical contribution of the acyl chains of lipoproteins in immunomodulation. To the best of our knowledge, this is the first study that investigated collective lipoprotein functions in a model strain for probiotic lactobacilli, and we show that the lipoproteins in *L. plantarum* WCFS1 are critical drivers of anti-inflammatory host responses toward this strain.

Keywords: *Lactobacillus*, lipoproteins, human immune system, proteomics, prolipoprotein diacylglyceryl transferase, LGT, *Lactobacillus plantarum*, probiotics

OPEN ACCESS

Edited by:
Emmanuelle Maguin, Institut National de la Recherche Agronomique (INRA), France

Reviewed by:
Friedrich Götz, University of Tübingen, Germany
Natasa Golic, University of Belgrade, Serbia

****Correspondence:***
Michiel Kleerebezem
michiel.kleerebezem@wur.nl

† These authors have contributed equally to this work

Specialty section:
This article was submitted to Food Microbiology, a section of the journal Frontiers in Microbiology

Received: *20 March 2020*
Accepted: *10 July 2020*
Published: *29 July 2020*

Citation:
Lee I-C, van Swam II, Boeren S, Vervoort J, Meijerink M, Taverne N, Starrenburg M, Bron PA and Kleerebezem M (2020) Lipoproteins Contribute to the Anti-inflammatory Capacity of Lactobacillus plantarum WCFS1. Front. Microbiol. 11:1822. doi: 10.3389/fmicb.2020.01822

INTRODUCTION

Bacterial lipoproteins are proteins that are post-translationally modified by acyl-conjugation, which anchors the protein on the extracellular face of the cytoplasmic membrane. These lipoproteins contain a typical N-terminal signal sequence that ends with the conserved [L/V/I]-[A/S/T]-[G/A]-C motif that is designated "lipobox" (Schenk et al., 2009). After export across the cell membrane,

these lipoprotein precursors undergo their lipid modification, which is catalyzed by three conserved enzymes, following a mechanism that was first established in *Escherichia coli* (Braun and Wu, 1994). As a first step, the prolipoprotein diacylglyceryl transferase (Lgt) transfers a diacylglyceryl moiety onto the indispensable cysteine residue in the lipobox (Braun and Wu, 1994), which is targeted by the lipoprotein signal peptidase (Lsp) that cleaves of the signal sequence directly N-terminally of the lipid-modified cysteine residue. In the third step, lipoprotein *N*-acyl transferase (Lnt) adds a third acyl chain to the free amino group of the lipidated cysteine (**Figure 1**). In Gram-negative bacteria, the third step is essential for the release and transport of lipoproteins from the cytoplasmic membrane to the outer membrane, but the *E. coli*-type Lnt enzyme appears to be absent in low-GC-content Gram-positive bacteria of the Firmicutes phylum (Robichon et al., 2005; Hutchings et al., 2009). Nevertheless, tri-acylated lipoproteins have been reported for bacteria belonging to this phylum, including *Staphylococcus aureus* and *Streptococcus pneumoniae*, suggesting the presence of an unrecognized Gram-positive *N*-acyltransferase function (Kurokawa et al., 2009; Asanuma et al., 2011; Bartual et al., 2018).

Lipoproteins are involved in diverse biological functions. Many lipoproteins function as substrate binding proteins (SBPs) of ATP-binding cassette (ABC) transporters involved in import of a variety of substrates, such as sugars, metal ions, amino acids, oligopeptides, and nucleotides (Hutchings et al., 2009). SBPs provide high affinity substrate binding and delivery to the membrane permease components (Biemans-Oldehinkel et al., 2006), which is important for nutrient uptake and may also play a role in environmental sensing (Dartois et al., 1997; Hoskisson and Hutchings, 2006; Hutchings et al., 2006). Besides their roles in import, lipoproteins in various Gram-positive bacteria are also involved in modulation of two-component signal transduction systems, cell envelope stability, adhesion, protein secretion and folding, or electron transfer processes at the cell membrane that support oxidative and antibiotic stress tolerance (Abdullah et al., 2014; Ezraty et al., 2017; Hutchings et al., 2009; Kohler et al., 2016; Nguyen and Gotz, 2016; Saleh et al., 2013; Shahmirzadi et al., 2016). Several studies also reported the role of lipoproteins in virulence, where these molecules contribute to colonization, invasion, immune evasion and survival capacities of pathogens in the host (Nguyen and Gotz, 2016). Many studies of the function of lipoproteins in pathogenic bacteria involved the analysis of mutants deficient in essential functions in lipoprotein biogenesis like *lgt* or *lsp*, typically leading to reduced adhesion and internalization and/or to attenuation of virulence in animal infection models (Kovacs-Simon et al., 2011; Nguyen and Gotz, 2016).

By contrast, the role that lipoproteins play in the physiology and host interaction of probiotic bacteria has not been reported in much detail. Probiotics are defined as live microorganisms that, when administered in adequate amounts, confer a health benefit on the host (FAO and WHO, 2002). The molecular interaction between probiotics and the host are proposed to play a key role in the health-promoting effects associated with these bacteria (Lebeer et al., 2008; Bron et al., 2011; Lee et al., 2013 Kleerebezem et al., 2019). Bacterial lipoproteins are well-recognized microorganism-associated molecular patterns (MAMPs), which interact with Toll-like receptor (TLR) 2, an important pattern recognition receptor (PRR) of the host innate immune system (Brightbill et al., 1999; Underhill and Ozinsky, 2002). Moreover, the di- and tri-acyl lipoproteins produced by bacteria are differentially recognized by distinct TLR-2 heterodimers TLR2/6 and TLR1/2, respectively (Takeuchi et al., 2002 Jin et al., 2007; Kang et al., 2009). Although it was initially thought that TLR2 heterodimers with TLR1 or TLR6 merely expanded the repertoire of bacterial ligand recognition (Farhat et al., 2008), it has since then been demonstrated that the magnitude of activation as well as the downstream signal transduction cascades are distinct for TLR1/2 and TLR2/6 heterodimers (Couture et al., 2012; Liu et al., 2012; Rolf et al., 2015), indicating their distinct role in innate signaling.

Deletion of *lgt* provides a means to study the general role of all lipoproteins in bacterial physiology and immunomodulation. Here we describe the impact of *lgt* mutation in the probiotic model strain *Lactobacillus plantarum* WCFS1 (Kleerebezem et al., 2003). We demonstrate that Lgt impacts on the secreted proteome, and specifically leads to the release of predicted lipoproteins that remain non-acylated. Furthermore, the capacity of the *L. plantarum lgt* mutant to stimulate TLR2 signaling and inflammatory responses was compared to those of the wild-type, illustrating the contribution of the lipoprotein acyl chains to immunomodulation. Although it has previously been established that lipoproteins are among the main TLR2 signaling ligands, to the best of our knowledge, this is the first study that explored the role of lipoproteins in immunomodulation by a model species of the probiotic lactobacilli.

MATERIALS AND METHODS

Bacterial Strains and Culture Conditions

Bacterial strains used in this work are listed in **Table 1**. *Lactobacillus plantarum* WCFS1 and its derivatives were grown at 37°C in MRS broth (Difco, West Molesey, United Kingdom) or in 2-fold concentrated chemically defined medium [2xCDM, (Teusink et al., 2005)], without aeration. *Escherichia coli* strain TOP10 (Invitrogen, Bleiswijk, Netherlands) was used as an intermediate cloning host, and was grown at 37°C in TY broth (Killmann et al., 2002) with aeration (Sambrook et al., 1989). Solid media were prepared by addition of 1.5% (w/v) agar to the broths. Antibiotics were added where appropriate and concentrations used for *L. plantarum* and *E. coli* strains were 10 μg/ml chloramphenicol (Cm), and 30 and 200 μg/ml erythromycin (Ery), respectively.

DNA Manipulations

Plasmids and primers used are listed in **Table 1**. Standard procedures were used for DNA manipulations in *E. coli* (Sambrook et al., 1989). Plasmid DNA was isolated from *E. coli* using a JETSTAR kit (Genomed GmbH, Bad Oberhausen, Germany). *L. plantarum* DNA was isolated as described previously (Josson et al., 1989). PCR amplifications were performed using hot-start KOD DNA polymerase (Novagen,

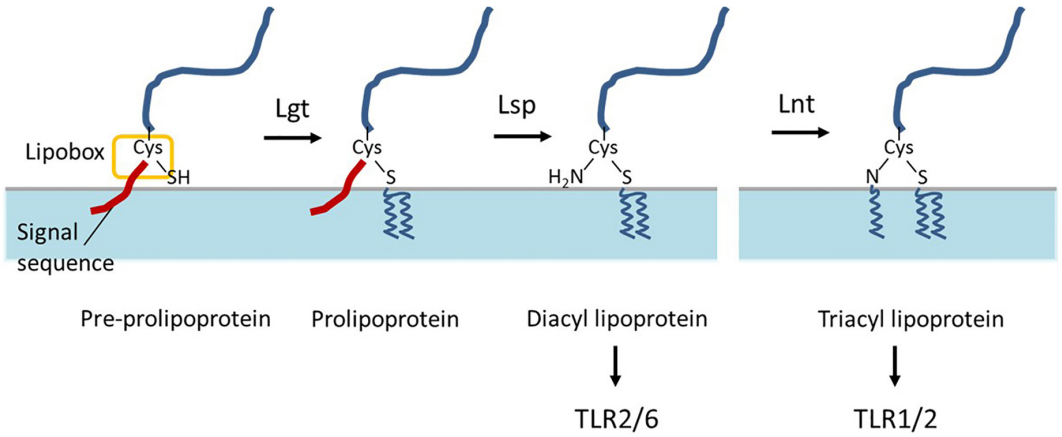

FIGURE 1 | Schematic representation of bacterial lipoprotein biogenesis. After export across the cell membrane, pre-prolipoproteins undergo lipid modification by prolipoprotein diacylglyceryl transferase (Lgt) which transfers a diacylglyceryl moiety onto the cysteine residue in the lipobox, and results in prolipoproteins. Subsequently, lipoprotein signal peptidase (Lsp) cleaves of signal peptide at the direct N-terminal of the lipid-modified cysteine residue and results in diacyl lipoproteins. In some bacteria, lipoprotein N-acyl transferase (Lnt) adds a third acyl chain to the free amino group of the lipidated cysteine. The di- and tri-acyl lipoproteins produced by bacteria are differentially recognized by distinct TLR-2 heterodimers TLR2/6 and TLR1/2, respectively.

TABLE 1 | Bacterial strains, plasmids, and primers used in this study.

Strains	**Characteristics**[a]	**References**
L. plantarum		
WCFS1	Single-colony isolate of *L. plantarum* NCIMB8826. Isolate from human saliva, United Kingdom.	Kleerebezem et al., 2003
NZ3400Cm	Cm^r; WCFS1 derivative; chromosomal integration of *cat* cassette into H-locus	Remus et al., 2012
NZ3565Cm (Δ*lgt*)	Cm^r; derivative of WCFS1 containing a *lox66*-P_{32}-*cat*-*lox71*-tag6.6 replacement of *lgt* (*lp_0755*) (*lgt*::*lox66*-P_{32}-*cat*-*lox71*- tag6.6)	This work
E. coli		
TOP 10 *end*A1 *nup*G	Cloning host; F^- *mcr*A Δ(*mrr-hsd*RMS-*mcr*BC) φ80*lac*ZΔM15 Δ*lac*X74 *rec*A1 *ara*D139 Δ(*ara-leu*)7697 *gal*U *gal*K *rps*L (Str^R)	Invitrogen
Plasmids	**Descriptions**[a]	**References**
pNZ5319	Cm^r Ery^r; Mutagenesis vector for gene replacements in *L. plantarum*	Lambert et al., 2007
pNZ3565	Cm^r Ery^r; pNZ5319 derivative containing homologous regions up- and downstream of *lgt* (*lp_0755*)	This work
Primers	**Sequence**[b]	**References**
is128 tag-lox66-F3	5′-AAATCTACCGTTCGTATAATGTATG-3′	Bron et al., 2012
is129 tag-lox71-R3	5′-CTCATGCCCGGGCTGTAACCG-3′	Bron et al., 2012
IS169	5′-TTATCATATCCCGAGGACCG-3′	van Bokhorst-van de Veen et al., 2012
87	5′-GCCGACTGTACTTTCGGATCC-3′	van Bokhorst-van de Veen et al., 2012
CreF	5′-CGATACCGTTTACGAAATTGG-3′	van Bokhorst-van de Veen et al., 2012
CreR	5′-CTTGCTCATAAGTAACGGTAC-3′	van Bokhorst-van de Veen et al., 2012
EryintF	5′-TCAAATACAGCTTTTAGAACTGG-3′	van Bokhorst-van de Veen et al., 2012
EryintR	5′-ATCACAAACAGAATGATGTACC-3′	van Bokhorst-van de Veen et al., 2012
lgt-up-F	5′-TTTGGCAGGAAGTGTAACCG-3′	This work
lgt-up-R	5′-GCATACATTATACGAACGGTAGATTTATTCACGCTACTGCCATCTCC-3′	This work
lgt-down-F	5′-CGGTTACAGCCCGGGCATGAGGCAGAAAATAAGTAGATTAGAGG-3′	This work
lgt-down-R	5′-AATCTCAGGTTTCCCCTCGC-3′	This work
lgt-out-F	5′-AAGTGTGGCCGCTTGAAAGGG-3′	This work
lgt-out-R	5′-AACATTTCTTTAGGCATCGCC-3′	This work

[a] *Cm^r, chloramphenicol resistant; Ery^r, erythromycin resistant.* [b] *Underlined nucleotides indicate parts of the primers that are complementary to the is128-lox66-F3 and is129-lox71-R3 primers.*

Madison, WI, United States). Amplicons were purified using WizardSV Gel and PCR Clean-Up System (Promega, Leiden, Netherlands). Restriction endonucleases (Fermentas GmbH, St. Leon-Rot, Germany), MSB Spin PCRapace (Invitek GmbH, Berlin, Germany), PCR Master Mix (Promega) and T4 DNA ligase (Invitrogen) were used as specified by the manufacturers.

Construction of *lgt* Deletion Strain

The *lgt* deletion mutant was constructed as described previously (Lambert et al., 2007), using a double crossing-over strategy to replace the *lgt* gene by a chloramphenicol resistance cassette (*lox66*-P_{32}*cat*-*lox71*) (Lambert et al., 2007). In this study, a derivative of the mutagenesis vector pNZ5319 (Lambert et al., 2007), designated pNZ5319TAG was used to introduce a unique 42-nucleotide tag into chromosome during gene deletion, which can be used for mutant tracking purposes in mixed populations (not relevant for the study presented here). The upstream and downstream flanking regions of *lgt* (*lp_0755*) gene were amplified by PCR using the primer pairs lgt-up-F/R and lgt-down-F/R primers, respectively (**Table 1**). The amplicons generated were joined by a second PCR to *lox*66-P_{32}*cat*-*lox*71-tag by a splicing by overlap extension strategy (Horton, 1993), using lgt-up-F/lgt-down-R primers. The resulting PCR products were digested with *Swa*I and *Ecl*136II, and cloned into similarly digested pNZ5319TAG. The obtained mutagenesis plasmids were transformed into *L. plantarum* WCFS1 as described previously (Josson et al., 1989). The resulting transformants were assessed for a double cross over integration event by selecting for Cm resistance and Ery sensitivity. The selected colonies were further confirmed by PCR using targets-out-F/R primers (**Table 1**). A single colony displaying the anticipated antibiotic resistance phenotype and genotype was selected, yielding NZ3565Cm (*L. plantarum* WCFS1 Δ*lgt*).

Isolation of Released Proteins and SDS-PAGE

For the isolation of proteins released into the culture supernatants, *L. plantarum* WCFS1 and its Δ*lgt* derivative were grown overnight to an OD_{600} of approximately 5 in 100 mL of 2xCDM. The culture supernatants were filtered through a hydrophilic polyvinylidene fluoride (PVDF) filter (0.22 μm pore size, 25 diameter; Millex Millipore, United States) to remove any remaining bacterial cells, and proteins were precipitated by adding trichloroacetic acid (TCA) to a final concentration of 16%, followed by an overnight incubation at 4°C. The precipitated proteins were pelleted by centrifugation at 16000 × *g* for 15 min. The protein pellets were washed with 200 μl acetone and then air-dried at 50°C. Dried protein pellets were solubilized in NuPAGE loading buffer and dithiothreitol (DTT) reducing agent (both from Invitrogen). The samples of released proteins were visualized by SDS-PAGE using the NuPAGE electrophoresis system with NuPAGENovex 4–12% Bis-Tris gels with MOPS SDS running buffer (Invitrogen), followed by Coomassie brilliant blue staining using standard procedures (Sambrook et al., 1989) and overnight destaining in Milli-Q water.

Sample Preparation for Mass Spectrometry

For in-gel trypsin digestion, the protein-containing SDS-PAGE gel was reduced with 10 mM dithiotreitol (DTT) in 50 mM ammonium bicarbonate (ABC) for 1 h at 60°C, followed by alkylation with 20 mM iodoacetamide in 100 mM Tris buffer (pH 8.0) in the dark for 1 h at room temperature. After thorough washing in Milli-Q water, the gel lane of each sample was divided into five slices that were individually cut into small pieces (ca. 1 mm^3). The gel pieces were transferred to protein LoBind tubes (Eppendorf, Hamburg, Germany) for all following procedures to minimize protein loss. Sample were freeze-thawed to increase enzyme accessibility of the gel pieces, and incubated in ABC buffer containing 5 ng/μL Bovine Sequencing Grade Trypsin (Roche) for 2 h at 45°C. The solution was sonicated briefly (1 s) and was adjusted to an pH of approximately 2.0 with 10% trifluoroacetic acid (TFA).

The trypsin-digested samples were further cleaned up to remove any gel residues using C18 microcolumns as described previously (Zhang et al., 2015). In short, C18 microcolumns were prepared in 200-μL Eppendorf tips by placing a small piece (ca. 1 mm in diameter) of a C18 Empore disk and then applying 4 μL of 50% slurry of LiChroprep C18 column material in methanol. The microcolumns were washed twice with 200 μl methanol and subsequently equilibrated with 100 μl of 1 ml/l formic acid (HCOOH). The samples were applied to the microcolumns and washed with 1 ml/l HCOOH. Samples were eluted using 50 μl of 50% acetonitrile/30% 1 ml/l HCOOH into clean LoBind tubes. The sample volume was then reduced in a vacuum concentrator (Eppendorf Vacufuge) at 45°C for 20 to 30 min until a volume below 20 μl was reached.

The liquid-chromatography tandem mass spectrometry (LC-MS/MS) analysis was performed on a Proxeon EASY-nLC system (Thermo Scientific) coupled with a LTQ Orbitrap XL mass spectrometer (Thermo Scientific). The chromatographic separation was performed on a combination of a Prontosil 300-5-C18H pre-concentration column with a Prontosil 300-3-C18H analytical column (Bischoff Chromatography, Leonberg, Germany) (Kessels et al., 2014). For peptide identification, the protein reference database of *Lactobacillus plantarum* (strain ATCC BAA-793/NCIMB 8826/WCFS1) for peptides and proteins identification downloaded from UniProt[1] was used. A set of 31 protein sequences of common contaminants was added including Trypsin (P00760, bovine), Trypsin (P00761, porcine), Keratin K22E (P35908, human), Keratin K1C9 (P35527, human), Keratin K2C1 (P04264, human), and Keratin K1C1 (P35527, human). Label-free quantitation (LFQ) of detected proteins was calculated by MaxQuant algorithm to compare quantity cross samples. Relative abundances were calculated by the ratio of LFQ of detected peptides in wild-type and *lgt* mutant and presented in $\log_{10}$ value.

Toll-Like Receptor (TLR) Assay

Human embryonic kidney (HEK)-293 TLR reporter cell lines expressing human TLR1/2, TLR2/6, or TLR4, harboring pNIFTY,

[1]http://www.uniprot.org/

a NF-κB luciferase reporter construct (Invivogen, Toulouse, France) (Karczewski et al., 2010), were used. The HEK-293 reporter cell lines were seeded at 6×10^4 cells/well in 96-well plates and incubated overnight under standard culture conditions. Cells were then stimulated with late-stationary bacterial cultures of the *L. plantarum* NZ3400Cm, a *L. plantarum* WCFS1 derivative with a chromosomal integration of the *cat* cassette in a neutral chromosomal locus (Remus et al., 2012), and *lgt* deletion strain (NZ3565Cm) at a multiplicity of infection (MOI) of 1:10, HEK cell to bacteria. The TLR1/2 agonist Pam3CSK4 (5 μg/mL, Invivogen) and TLR2/6 agonist Pam2CSK4 (5 μg/mL, Invivogen) were used as positive controls and PBS served as the negative control.

Peripheral Blood Mononuclear Cells (PBMC) Assay

The assay was performed as described previously (van Hemert et al., 2010) and was approved by Wageningen University Ethical Committee and was performed according to the principles of the Declaration of Helsinki. Peripheral blood of healthy donors was from the Sanquin Blood Bank, Nijmegen, Netherlands. PBMCs were separated from the blood using Ficoll-Paque Plus gradient centrifugation according to the manufacturer's description (Amersham biosciences, Uppsala, Sweden). The mononuclear cells were collected, washed in Iscove's Modified Dulbecco's Medium (IMDM) + glutamax (Invitrogen, Breda, Netherlands) and adjusted to 1×10^6 cells/ml in IMDM + glutamax supplemented with penicillin (100 U/ml) (Invitrogen), streptomycin (100 μg/ml) (Invitrogen), and 1% human AB serum (Lonza, Basel, Switzerland). PBMCs (1×10^6 cells/well) were seeded a night prior to the experiment in 48-well tissue culture plates and incubate at 37°C in 5% CO_2. Bacteria from late-stationary phase were added to PBMCs at a MOI of 1:10 (PBMC to bacteria) PBMCs from 3 different donors were used in the assay. Following 24 h incubation at 37°C in 5% CO_2, culture supernatants were collected and stored at −20°C prior to cytokine analysis. Cytokines were measured using a FACSCanto II flow cytometer (BD Biosciences, New Jersey, United States) and BD Cytometric Bead Array Flexsets (BD Biosciences) for interleukin (IL)10 and IL12p70, Tumor Necrosis Factor (TNF)α, IL6, IL1β, and IL8 according to the manufacturer's procedures. Concentrations of cytokines were calculated based on the standard curves in the BD Biosciences FCAP software.

Statistical Analysis

The TLR and PBMC assays were performed in triplicate. One-way ANOVA followed by Tukey's multiple comparison correction was used to compare TLR2 activations between strains. The paired *t*-test was used to determine the Log values of PBMCs cytokine production after stimulated with wild-type verse mutant strains for individual donors. GraphPad Prism 5 software (GraphPad Software, San Diego, CA, United States) was used for all determinations, and a P value < 0.05 was considered significant. Notably, the parametric statistical analyses applied are justified on basis of the normal data distribution of measurements obtained in these type of analyses, which is based on evaluation of data distribution on numerous datasets obtained in similar assays in our laboratory (data not shown).

Data Availability

The mass spectrometry proteomics data have been deposited to the ProteomeXchange Consortium via the PRIDE (Vizcaino et al., 2016) partner repository with the dataset identifier PXD019218.

RESULTS

Construction of Lgt-Deficient *L. plantarum* WCFS1

Prolipoprotein diacylglyceryl transferase (Lgt) is the key enzyme for lipidation in lipoprotein biosynthesis, where it catalyzes the transfer of a diacylglyceryl moiety onto a conserved cysteine in the lipobox of prolipoproteins (Hutchings et al., 2009). The gene annotated to encode this function (*lgt*; *lp_0755*) in the *L. plantarum* WCFS1 genome (Kleerebezem et al., 2003) was mutated by double cross-over gene replacement of the *lgt* coding region by a chloramphenicol acetyltransferase (*cat*) cassette (Lambert et al., 2007), resulting in an *lgt* deficient derivative of strain WCFS1, designated NZ3565Cm (Δ*lgt*). This *lgt*-mutant strain enables the study of the generic impact of lipoproteins on physiological and immunomodulatory properties of this model probiotic-bacterium.

Under laboratory conditions, the growth and cell-morphology of the *lgt* deletion mutant were undistinguishable from those of the wild-type strain (data not shown). This is in agreement with earlier observations that suggested that although Lgt is essential in Gram-negative bacteria, it appears to be dispensable in Gram-positive bacteria grown under laboratory conditions (Hutchings et al., 2009).

Lgt Is Important for Membrane Anchoring of Lipoproteins

We investigated the impact of *lgt* deletion on the membrane-anchoring of lipoproteins, by comparing the supernatants of wild-type and the mutant using SDS-PAGE. The protein-pattern observed revealed a clear difference between the supernatant of the wild-type strain and *lgt* mutant, which released a much higher abundance of proteins into its culture medium as compared to its parental strain (**Figure 2**). The SDS-PAGE gel containing supernatant proteins were subjected to in-gel trypsin digestion, followed by tandem mass spectrometry (MS/MS) analysis to identify the released proteins. There are 7 and 9 proteins that are exclusively detected in the supernatant of wild-type and *lgt* mutant cultures, respectively (**Supplementary Table S1**). The protein abundances of these proteins were set to detection limit to enable the calculation of the relative protein abundance of the proteins detected in both the wild-type and *lgt* mutant culture supernatants. The overall protein-abundance in the culture supernatant of the wild-type and its *lgt* derivative appeared to be similar, but the relative abundance of predicted lipoproteins was significantly higher in the supernatant of the *lgt* deficient strain compared to other classes of secreted proteins (**Figure 3**,

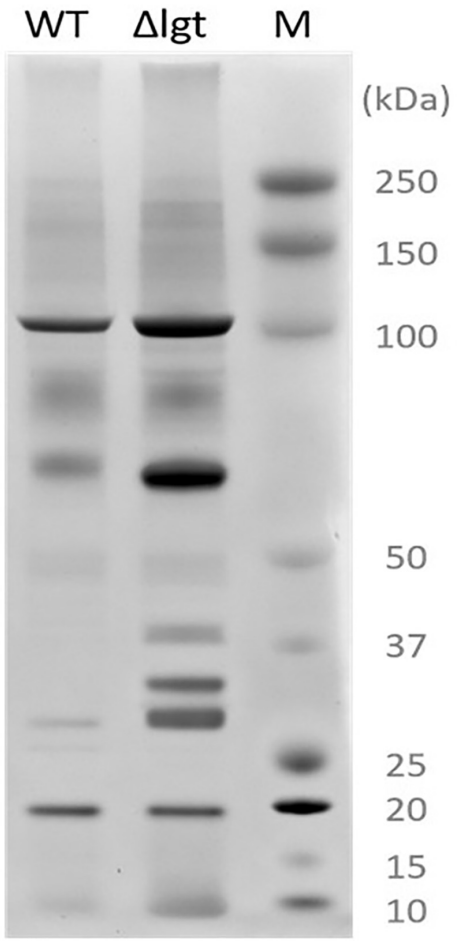

FIGURE 2 | Secreted proteins extracted from *L. plantarum* WCFS1 (WT) and its *lgt* deletion derivative (Δ*lgt*; NZ3565Cm). Proteins were separated by SDS-PAGE and visualized by Coomassie blue staining. On the right side, the protein size marker (M), Precision Plus Protein Dual Color Standards (Bio-Rad).

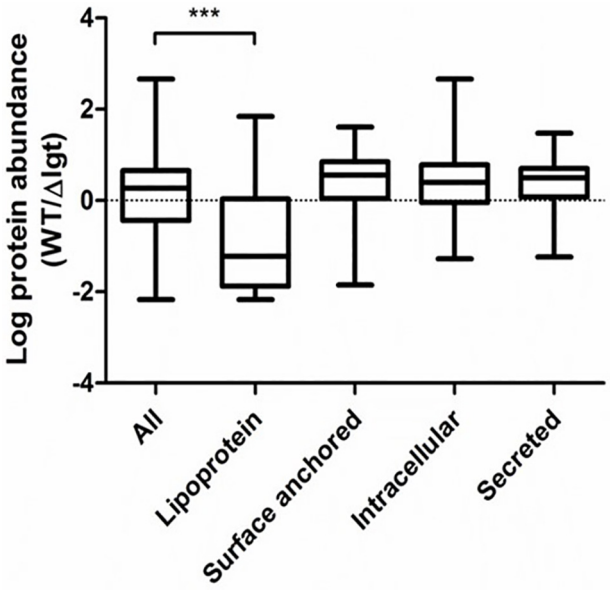

FIGURE 3 | Relative abundance of secreted proteins in *L. plantarum* WCFS1 wild*type (WT) and the *lgt* deletion strain (Δ*lgt*; NZ3565Cm). The relative abundance is defined as the ratios in the label free quantitation (LFQ, $\log_{10}$ value) of detected proteins in wild-type and the deletion strain in tandem mass spectrometry (MS/MS) analysis. The abundance was compared with all proteins detected in both samples, or within specific protein groups. The ratios from specific proteins groups were compared against all proteins to test for significant differences using one-way ANOVA followed by Tukey's multiple comparison correction and significant differences are indicated; $^{***}P \leq 0.001$.

Supplementary Figure S1, and **Supplementary Table S1**). Many of the lipoproteins found in higher abundance in the supernatant of *lgt* mutant belong to the predicted substrate binding proteins of ATP-binding cassette (ABC) transporters associated with various substrates, including iron, phosphate, amino acids, maltose, and maltodextrin (**Supplementary Table S1**). The proteome analysis detected 38 out of the 47 predicted lipoproteins encoded by the WCFS1 genome (Kleerebezem et al., 2010), thereby broadly representing this group of proteins. These results confirm the importance of Lgt in appropriate anchoring of lipoproteins in the cytoplasmic membrane.

Acyl Chains of Lipoproteins Are Important for TLR1/2 Signaling Capacity of *L. plantarum* WCFS1

The human innate immune system has been reported to recognize bacterial lipoproteins by TLR1/2 and TLR2/6 heterodimers that recognize tri- and di-acylated lipoproteins, respectively (Schenk et al., 2009). The impact of *lgt* deletion in *L. plantarum* on TLR2 heterodimer signaling was investigated using established HEK-293 reporter cell lines that express human TLR1/2 or TLR2/6 heterodimers combined with a NF-κB promoter-controlled luciferase gene. The synthetic agonists Pam3CSK4 and Pam2CSK4 were used as positive controls for TLR1/2 and TLR2/6 activation, respectively. The wild-type strain *L. plantarum* NZ3400Cm (Remus et al., 2012) stimulated both TLR1/2 and TLR2/6 signaling at a moderate level (**Figures 4A,B**, respectively). The *lgt* deletion strain, Δ*lgt* (NZ3565Cm), stimulated significantly lower TLR1/2 signaling as compared to the wild-type strain (**Figure 4A**), whereas its capacity to stimulate TLR2/6 signaling appeared to be unaffected as compared to the wild-type strain (**Figure 4B**). The observation that the *lgt* mutant of *L. plantarum* WCFS1 affected TLR1/2 signaling and not TLR2/6 signaling, suggests that tri-acylated lipoproteins are dominant in this strain.

Lipid Moiety of Lipoproteins Is Important for Anti-inflammatory Properties of *L. plantarum* WCFS1

Although many studies have shown that Gram-positive pathogens that lack Lgt activity display attenuated immune activation or virulence, little is known about the effect of this phenotype in probiotic bacteria. We explored the impact

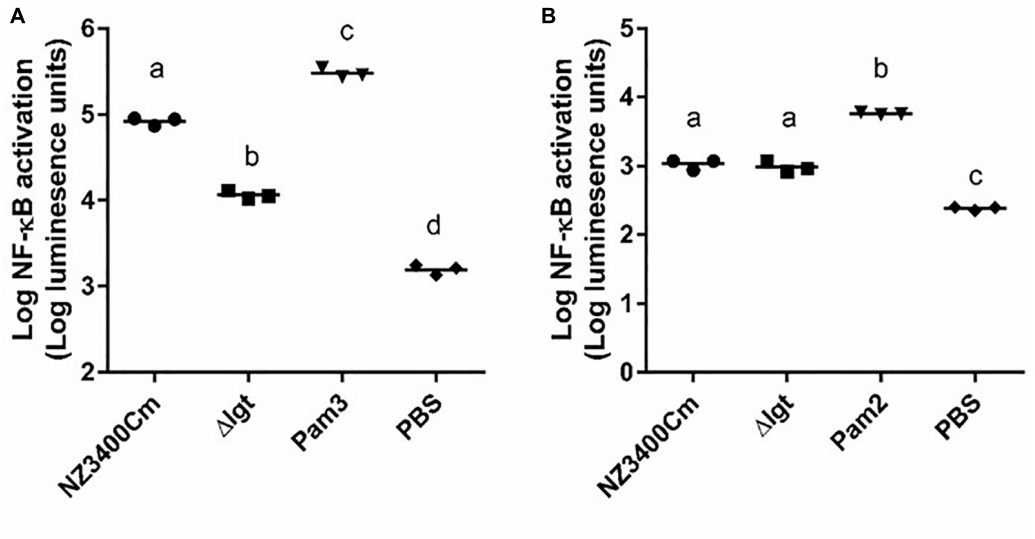

FIGURE 4 | TLR1_2 and TLR2_6 signaling capacities of NZ3400Cm, a *L. plantarum* WCFS1 derivative with a chromosomal integration of the *cat* cassette in a neutral chromosomal locus (NZ3400Cm, **Table 1**) and the *lgt* deletion mutant, NZ3565Cm (Δ*lgt*; NZ3565Cm). TLR1_2 **(A)** and TLR2_6 **(B)** activation were determined using TLR-expressing HEK cell lines, containing a NF-kB responsive luciferase reporter system. Measurements were performed in triplicate and are presented as $\log_{10}$ luminescence units, and individually displayed (n = 3), while the bar indicates the median. PBS serves as a negative control, while Pam3CysSK4 (Pam3) and Pam2CysSK4 (Pam2) are the positive stimulus of TLR1_2 **(A)** and TLR2_6 **(B)** activation, respectively. Data comparison of the wild-type and the deletion derivative was tested for significant differences using one-way ANOVA followed by Tukey's multiple comparison correction and samples with significant different NF-kB activation are indicated with different letters.

of *lgt* deletion on general immune responses using cytokine production by human peripheral blood mononuclear cells (PBMCs). The *lgt* deletion mutant stimulated a more pro-inflammatory responses in PBMCs as compared to the wild-type strain (NZ3400Cm), including a higher production of the pro-inflammatory cytokines, IL12, TNFα, IL1β, and IL8 (**Figures 5A,B,D,E**, respectively). Moreover, the *lgt* mutant strain tends to induce lower levels of production of the anti-inflammatory cytokine IL10 relative to the wild-type (**Figure 5C**). As a consequence, the IL10/IL12 ratio, which has been reported as an indicator for *in vivo* performance in a mouse colitis model (Foligne et al., 2007), is significantly lower in *lgt* mutant than the wild-type (**Supplementary Figure S2**), implying a more pro-inflammatory profile after exposure to the mutant. These results illustrate the importance of Lgt and lipoproteins in the overall immunomodulatory properties associated with *L. plantarum* WCFS1, and in particular exemplify the contribution of lipoproteins in the anti-inflammatory properties in *L. plantarum* WCFS1.

DISCUSSION

Diacylglyceryl transferase is an essential enzyme in various Gram-negative bacteria (Hutchings et al., 2009). Since many lipoproteins in Gram-negative bacteria are localized at the outer membrane, defects in lipoprotein biosynthesis will cause mislocalization and/or accumulation of the precursors in the periplasmic space, which has been reported to be lethal to the cells (Matsuyama et al., 1995; Robichon et al., 2005). In contrast, Lgt-enzymes appear dispensable in a variety of Gram-positive bacteria (Hutchings et al., 2009). In agreement with this notion, the *lgt* deletion derivative of *L. plantarum* displayed normal cellular morphology and growth characteristics. The limited impact of *lgt* deletion in Gram-positive bacteria may be explained by the different impact of the loss of Lgt function on the subcellular location of lipoproteins. In Gram-negative bacteria many lipoproteins are targeted to the outer membrane, and the defective biogenesis of these proteins due to Lgt deficiency may lead to protein accumulation and clogging of the periplasm. In contrast, in Gram-positive bacteria non-acylated lipoproteins tend to remain functionally localized in the cell wall, or are released into the medium. The functional localization of non-acylated lipoproteins in Gram-positive bacteria is supported by the observation that an *lgt* mutation is not lethal in *Bacillus subtilis*, although at least the lipoprotein PrsA fulfills an essential role in this bacterial species (Leskela et al., 1999). In *L. plantarum* deletion of *lgt* led to mislocalization and release of a range of lipoproteins into the culture supernatant, including many substrate binding proteins (SBPs) associated with ABC transporters annotated to be involved in the import of amino acids, oligopeptides, maltose, and maltodextrin. Such mislocalization of these SBPs could reduce the efficiency of transport of the corresponding substrates, which may be reflected in changes in the corresponding metabolic processes. However, we did not observe differences in growth characteristics between the wild-type strain and its *lgt* derivative when cultured in minimal medium with maltose as a sole carbon source (**Supplementary Figure S3**). Besides this targeted phenotypic evaluation, further phenotype evaluations

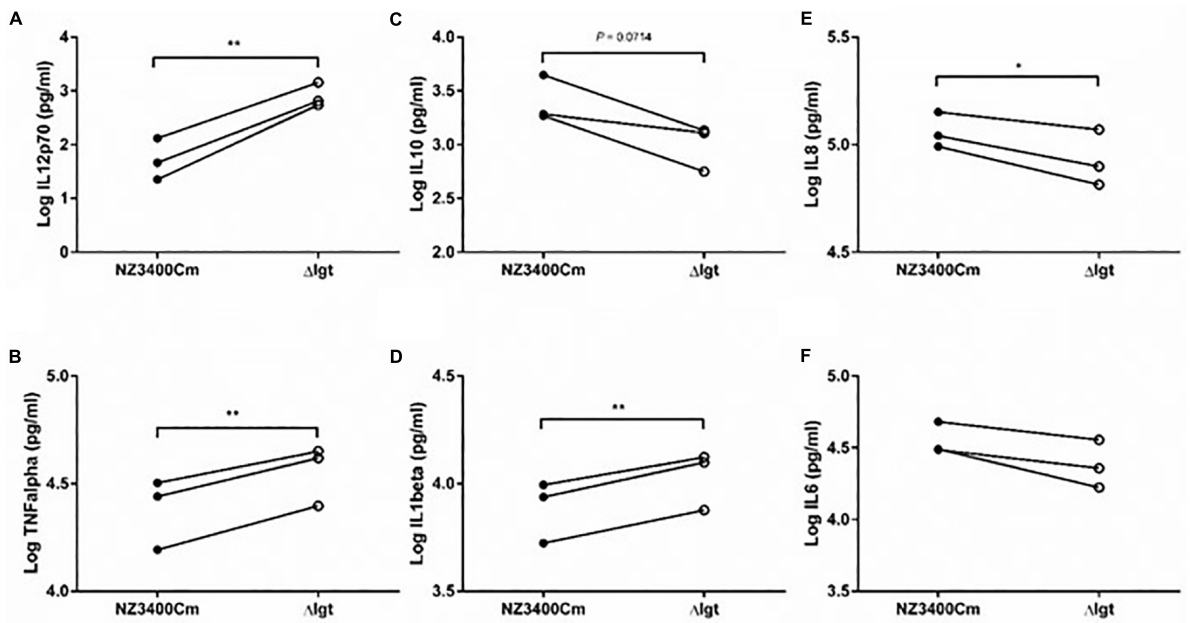

FIGURE 5 | Immunomodulatory effect of NZ3400Cm, a *L. plantarum* WCFS1 derivative with a chromosomal integration of the *cat* cassette in a neutral chromosomal locus (NZ3400Cm, **Table 1**), and the *lgt* deletion strain NZ3565Cm (Δ*lgt*; NZ3565Cm). Cytokine production was determined in human PBMCs (n = 3 donors) after 24 h co-incubation with the bacterial cells. The IL12 **(A)**, TNFα **(B)**, IL10 **(C)**, IL1β **(D)**, IL8 **(E)**, and IL6 **(F)** cytokine production levels are presented as Log values. The cytokine levels for individual donors stimulated with the strains were connected by a line to focus the read-outs on changes elicited by the deletion. Significant differences between cytokine levels induced by wild-type strains and their corresponding mutants (paired t-test) are indicated; $^{*}P \leq 0.05$; $^{**}P \leq 0.01$; the P value of the difference of IL10 production by the NZ3400Cm and Δ*lgt* strains is indicated in the corresponding panel **(C)**.

would be needed to pinpoint specific phenotype consequences of the *lgt* mutation and the corresponding mis-localization of the lipoprotein substrate binding proteins. Such experiments are likely to require the use of chemically defined minimal media to reliably limit the environmental availability of required nutrients, analogous to what was shown in *Staphylococcus aureus* (Stoll et al., 2005). This lack of consequence in growth characteristics of the *lgt* mutation, may be explained by a certain proportion of SBPs that remains associated with the corresponding transporters. Notably, it is unclear whether the lipoprotein signal peptidase (Lsp) is able to efficiently cleave all the non-lipid modified precursor lipoproteins in a *lgt* mutant strain, and failure to remove the signal peptide may retain lipoprotein precursors anchored in the cell membrane. Such retention mechanism is supported by studies that detected differently processed lipoprotein precursors can be detected in a Lgt-deficient background, including precursors containing their signal peptides or proteins cleaved by peptidases other than Lsp (Hutchings et al., 2009). Alternatively, it is also possible that cells can compensate for the lack of appropriately localized SBPs by elevated expression of the transport functions. Overall, our results establish that the *lgt* encoded function is dispensable for the laboratory-growth of *L. plantarum* WCFS1 and deletion of the *lgt* gene has a minimal impact on bacterial physiology under the conditions tested.

TLR2/6 and TLR1/2 heterodimers recognize di- or tri-acylated lipoproteins, respectively. Crystal structure analyses revealed that TLR1 has a hydrophobic pocket that enables the binding of the third acyl chain, which is lacking in TLR6 that can only accommodate di-acylated lipoproteins (Jin et al., 2007; Kang et al., 2009). The third acyl chain has been shown to be crucial for biosynthesis and biogenesis of lipoproteins in Gram-negative bacteria that are ending up in the outer membrane of these bacteria (Robichon et al., 2005), and appropriate subcellular localization (i.e., outer membrane biogenesis) of lipoproteins is essential in these bacteria. Moreover, since no orthologou genes of *lnt*, the gene responsible for transferring a third acyl chain on the N-terminal cysteine of lipoproteins, has been recognized in the genomes of low-GC-content Gram-positive bacteria, such as species belonging to the genera of *Bacillus*, *Lactobacillus*, *Listeria*, *Staphylococcus*, and *Streptococcus*, it has been long been assumed that these bacteria produce di-acyl lipoproteins (Nakayama et al., 2012). However, tri-acylated lipoproteins have been detected in several of these Gram-positive species, including *Staphylococcus aureus*, *Staphylococcus epidermidis*, and *Streptococcus pneumoniae* (Nguyen and Gotz, 2016), suggesting the presence of an *N*-acyltransferase in Gram-positive bacteria that displays insufficient similarity with the Gram-negative Lnt to be recognized as its functional equivalent (Asanuma et al., 2011; Kurokawa et al., 2009). Similarly, the reduction of specifically TLR1/2 signaling observed for the *L. plantarum lgt* mutant strain, implies that lipoproteins in this bacterial species are likely to be (predominantly) tri-acylated, or the N-acylation involves a long-chain fatty acid modification that are recognized through TLR1/2 rather than TLR2/6 (Nguyen et al., 2017). However, biochemical analysis would be required to verify the lipoprotein

structures in *L. plantarum* WCFS1. The genome of this strain is annotated to encode three acyltransferases, *lp_0856*, *lp_0925*, and *lp_1181* that may be involved in an Lnt-like role in tri-acylation of lipoproteins. A fourth gene *lp_1916*, encoding a membrane protein, is not annotated as acyltransferase, but does contain a conserved acyltransferase domain of the acyltransferase family. Although one of these genes is potentially encoding the enzyme responsible for tri-acylation of lipoproteins in *L. plantarum* WCFS1, such function and its encoding gene remain to be established.

Since lipoproteins are established ligands of TLR2, an important PRR of the innate immune system, many studies have investigated the effect of *lgt* or *lsp* deletions on immune responses to, and virulence of Gram-positive pathogens (Hutchings et al., 2009; Nguyen and Gotz, 2016). Commonly, *lgt* or *lsp* deletions lead to attenuation of immune activation and/or reduced virulence of Gram-positive pathogens *in vitro* and *in vivo*, although some conflicting results have been reported (Nguyen and Gotz, 2016). For example, *lgt* and *lsp* deletion derivatives of *Streptococcus equi* (Hamilton et al., 2006) and *Streptococcus suis* (De Greeff et al., 2003), did not display attenuation in their natural hosts (pony and pig, respectively). Moreover, although a *Listeria monocytogenes lgt* mutant fails to activate TLR2 signaling it is significantly less virulent in a mouse infection model (Machata et al., 2008), whereas *lgt* mutants of *Streptococcus agalactiae* (Henneke et al., 2008) and *Staphylococcus aureus* (Bubeck Wardenburg et al., 2006; Mohammad et al., 2019) are hypervirulent in mouse infection models. These results imply a subtle and strain-specific balance between escaping protective immune defense related to loss of TLR2 activation and attenuated virulence by the loss of lipoprotein acylation in *lgt* mutants. Despite their important function as signaling molecules in microbe-host interactions, the role of lipoproteins in the immunomodulatory effect of probiotics has not been studied. Our results show that the *L. plantarum lgt* deletion derivative elicited more pro-inflammatory responses in PBMCs compared to its parental strain, suggesting that lipoproteins may act as important mediators of immune system recognition for probiotics where these molecules could drive more anti-inflammatory responses to such bacteria, which is relevant in the context of inducing tolerance. However, the exact mechanism (and diversity) behind lipoprotein mediated immune responses toward probiotics remains to be elucidated. Further studies focusing on purified lipoproteins could enable the controlled attenuation of pro-inflammatory immune responses in specific cell lineages (including monocytes and other fractions of the PBMC population), and may also be used to decipher their mechanistic interplay with pro-inflammatory pathways elicited by lipoprotein deficient strains. Moreover, structure-function studies of lipoproteins from pathogens and probiotics may unravel some key determinants involved in immune system recognition and activation, which may enable the host cells to distinguish harmful and beneficial bacteria (Nguyen et al., 2017).

Overall, the potentially important role of lipoproteins in probiotic function and in particular in their potential role in modulation of immune-responses is supported by the work presented here, and this role deserves further refined elucidation in terms of structure function correlation in the context of host-cell signaling by lipoproteins.

DATA AVAILABILITY STATEMENT

The raw data supporting the conclusions of this article will be made available by the authors, without undue reservation, to any qualified researcher.

AUTHOR CONTRIBUTIONS

I-CL, PB, and MK designed the study and wrote the manuscript. I-CL, IS, MM, NT, and MS executed the experimental work. SB and JV generated the proteome data. All authors agreed to the manuscript.

ACKNOWLEDGMENTS

We thank Michiel Wels for his support in bioinformatic analyses, as well as Jerry Wells for his help with the interpretation of the PBMC stimulation assays. Parts of the work presented here were previously reported in the Ph.D. thesis of I-CL at the Wageningen University, which is online available according to the University's policy (Lee, 2016).

SUPPLEMENTARY MATERIAL

The Supplementary Material for this article can be found online at: https://www.frontiersin.org/articles/10.3389/fmicb.2020.01822/full#supplementary-material

REFERENCES

Abdullah, M. R., Gutierrez-Fernandez, J., Pribyl, T., Gisch, N., Saleh, M., Rohde, M., et al. (2014). Structure of the pneumococcal l,d-carboxypeptidase DacB and pathophysiological effects of disabled cell wall hydrolases DacA and DacB. *Mol. Microbiol.* 93, 1183–1206.

Asanuma, M., Kurokawa, K., Ichikawa, R., Ryu, K. H., Chae, J. H., Dohmae, N., et al. (2011). Structural evidence of alpha-aminoacylated lipoproteins of *Staphylococcus aureus*. *FEBS J.* 278, 716–728. doi: 10.1111/j.1742-4658.2010.07990.x

Bartual, S. G., Alcorlo, M., Martinez-Caballero, S., Molina, R., and Hermoso, J. A. (2018). Three-dimensional structures of Lipoproteins from *Streptococcus pneumoniae* and *Staphylococcus aureus*. *Int. J. Med. Microbiol.* 308, 692–704. doi: 10.1016/j.ijmm.2017.10.003

Biemans-Oldehinkel, E., Doeven, M. K., and Poolman, B. (2006). ABC transporter architecture and regulatory roles of accessory domains. *FEBS Lett.* 580, 1023–1035. doi: 10.1016/j.febslet.2005.11.079

Braun, V., and Wu, H. (1994). Lipoproteins, structure, function, biosynthesis and model for protein export. *New Compr. Biochem.* 27, 319–319.

Brightbill, H. D., Libraty, D. H., Krutzik, S. R., Yang, R. B., Belisle, J. T., Bleharski, J. R., et al. (1999). Host defense mechanisms triggered by microbial lipoproteins through toll-like receptors. *Science* 285, 732–736. doi: 10.1126/science.285.5428.732

Bron, P. A., Tomita, S., van, S. II, Remus, D. M., Meijerink, M., Wels, M., et al. (2012). *Lactobacillus plantarum* possesses the capability for wall teichoic acid backbone alditol switching. *Microb. Cell Fact.* 11:123. doi: 10.1186/1475-2859-11-123

Bron, P. A., van Baarlen, P., and Kleerebezem, M. (2011). Emerging molecular insights into the interaction between probiotics and the host intestinal mucosa. *Nat. Rev. Microbiol.* 10, 66–78. doi: 10.1038/nrmicro2690

Bubeck Wardenburg, J., Williams, W. A., and Missiakas, D. (2006). Host defenses against *Staphylococcus aureus* infection require recognition of bacterial lipoproteins. *Proc. Natl. Acad. Sci. U.S.A.* 103, 13831–13836. doi: 10.1073/pnas.0603072103

Couture, L. A., Piao, W., Ru, L. W., Vogel, S. N., and Toshchakov, V. Y. (2012). Targeting toll-like receptor (TLR) signaling by toll/interleukin-1 receptor (TIR) domain-containing adapter protein/MyD88 adapter-like (TIRAP/Mal)-derived decoy peptides. *J. Biol. Chem.* 287, 24641–24648. doi: 10.1074/jbc.m112.360925

Dartois, V., Djavakhishvili, T., and Hoch, J. A. (1997). KapB is a lipoprotein required for KinB signal transduction and activation of the phosphorelay to sporulation in *Bacillus subtilis*. *Mol. Microbiol.* 26, 1097–1108. doi: 10.1046/j.1365-2958.1997.6542024.x

De Greeff, A., Hamilton, A., Sutcliffe, I. C., Buys, H., Van Alphen, L., and Smith, H. E. (2003). Lipoprotein signal peptidase of *Streptococcus suis* serotype 2. *Microbiology* 149, 1399–1407. doi: 10.1099/mic.0.26329-0

Ezraty, B., Gennaris, A., Barras, F., and Collet, J. F. (2017). Oxidative stress, protein damage and repair in bacteria. *Nat. Rev. Microbiol.* 15, 385–396. doi: 10.1038/nrmicro.2017.26

FAO, and WHO (2002). *Guidelines for the Evaluation of Probiotics in Food. Report of a Joint FAO/WHO Working Group on Drafting Guidelines for the Evaluation of Probiotics in Food*. London: FAO.

Farhat, K., Riekenberg, S., Heine, H., Debarry, J., Lang, R., Mages, J., et al. (2008). Heterodimerization of TLR2 with TLR1 or TLR6 expands the ligand spectrum but does not lead to differential signaling. *J. Leukoc. Biol.* 83, 692–701. doi: 10.1189/jlb.0807586

Foligne, B., Nutten, S., Grangette, C., Dennin, V., Goudercourt, D., Poiret, S., et al. (2007). Correlation between *in vitro* and *in vivo* immunomodulatory properties of lactic acid bacteria. *World J. Gastroenterol.* 13, 236–243.

Hamilton, A., Robinson, C., Sutcliffe, I. C., Slater, J., Maskell, D. J., Davis-Poynter, N., et al. (2006). Mutation of the maturase lipoprotein attenuates the virulence of *Streptococcus equi* to a greater extent than does loss of general lipoprotein lipidation. *Infect. Immun.* 74, 6907–6919. doi: 10.1128/iai.01116-06

Henneke, P., Dramsi, S., Mancuso, G., Chraibi, K., Pellegrini, E., Theilacker, C., et al. (2008). Lipoproteins are critical TLR2 activating toxins in group B streptococcal sepsis. *J. Immunol.* 180, 6149–6158. doi: 10.4049/jimmunol.180.9.6149

Horton, R. M. (1993). *In Vitro* recombination and mutagenesis of DNA : SOEing together tailor-made genes. *Methods Mol. Biol.* 15, 251–261.

Hoskisson, P. A., and Hutchings, M. I. (2006). MtrAB–LpqB: a conserved three-component system in actinobacteria? *Trends Microbiol.* 14, 444–449. doi: 10.1016/j.tim.2006.08.005

Hutchings, M. I., Hong, H.-J., Leibovitz, E., Sutcliffe, I. C., and Buttner, M. J. (2006). The σE cell envelope stress response of *Streptomyces coelicolor* is influenced by a novel lipoprotein, CseA. *J. Bacteriol.* 188, 7222–7229. doi: 10.1128/jb.00818-06

Hutchings, M. I., Palmer, T., Harrington, D. J., and Sutcliffe, I. C. (2009). Lipoprotein biogenesis in Gram-positive bacteria: knowing when to hold 'em, knowing when to fold 'em. *Trends Microbiol.* 17, 13–21. doi: 10.1016/j.tim.2008.10.001

Jin, M. S., Kim, S. E., Heo, J. Y., Lee, M. E., Kim, H. M., Paik, S. G., et al. (2007). Crystal structure of the TLR1-TLR2 heterodimer induced by binding of a tri-acylated lipopeptide. *Cell* 130, 1071–1082. doi: 10.1016/j.cell.2007.09.008

Josson, K., Scheirlinck, T., Michiels, F., Platteeuw, C., Stanssens, P., Joos, H., et al. (1989). Characterization of a Gram-positive broad-host-range plasmid isolated from *Lactobacillus hilgardii*. *Plasmid* 21, 9–20. doi: 10.1016/0147-619x(89)90082-6

Kang, J. Y., Nan, X., Jin, M. S., Youn, S. J., Ryu, Y. H., Mah, S., et al. (2009). Recognition of lipopeptide patterns by Toll-like receptor 2-Toll-like receptor 6 heterodimer. *Immunity* 31, 873–884. doi: 10.1016/j.immuni.2009.09.018

Karczewski, J., Troost, F. J., Konings, I., Dekker, J., Kleerebezem, M., Brummer, R. J., et al. (2010). Regulation of human epithelial tight junction proteins by *Lactobacillus plantarum in vivo* and protective effects on the epithelial barrier. *Am. J. Physiol. Gastrointest Liver Physiol.* 298, G851–G859.

Kessels, M. Y., Huitema, L., Boeren, S., Kranenbarg, S., Schulte-Merker, S., van Leeuwen, J. L., et al. (2014). Proteomics analysis of the zebrafish skeletal extracellular matrix. *PLoS One* 9:e90568. doi: 10.1371/journal.pone.0090568

Killmann, H., Herrmann, C., Torun, A., Jung, G., and Braun, V. (2002). TonB of *Escherichia coli* activates FhuA through interaction with the beta-barrel. *Microbiology* 148, 3497–3509. doi: 10.1099/00221287-148-11-3497

Kleerebezem, M., Binda, S., Bron, P. A., Gross, G., Hill, C., van Hylckama Vlieg, J. E., et al. (2019). Understanding mode of action can drive the translational pipeline towards more reliable health benefits for probiotics. *Curr. Opin. Biotechnol.* 56, 55–60. doi: 10.1016/j.copbio.2018.09.007

Kleerebezem, M., Boekhorst, J., van Kranenburg, R., Molenaar, D., Kuipers, O. P., Leer, R., et al. (2003). Complete genome sequence of *Lactobacillus plantarum* WCFS1. *Proc. Natl. Acad. Sci. U.S.A.* 100, 1990–1995.

Kleerebezem, M., Hols, P., Bernard, E., Rolain, T., Zhou, M., Siezen, R. J., et al. (2010). The extracellular biology of the lactobacilli. *FEMS Microbiol. Rev.* 34, 199–230. doi: 10.1111/j.1574-6976.2009.00208.x

Kohler, S., Voss, F., Gomez Mejia, A., Brown, J. S., and Hammerschmidt, S. (2016). Pneumococcal lipoproteins involved in bacterial fitness, virulence, and immune evasion. *FEBS Lett.* 590, 3820–3839. doi: 10.1002/1873-3468.12352

Kovacs-Simon, A., Titball, R. W., and Michell, S. L. (2011). Lipoproteins of bacterial pathogens. *Infect. Immun.* 79, 548–561. doi: 10.1128/iai.00682-10

Kurokawa, K., Lee, H., Roh, K. B., Asanuma, M., Kim, Y. S., Nakayama, H., et al. (2009). The Triacylated ATP binding cluster transporter substrate-binding lipoprotein of *Staphylococcus aureus* functions as a native ligand for toll-like receptor 2. *J. Biol. Chem.* 284, 8406–8411. doi: 10.1074/jbc.m809618200

Lambert, J. M., Bongers, R. S., and Kleerebezem, M. (2007). Cre-*lox*-based system for multiple gene deletions and selectable-marker removal in *Lactobacillus plantarum*. *Appl. Environ. Microbiol.* 73, 1126–1135. doi: 10.1128/aem.01473-06

Lebeer, S., Vanderleyden, J., and De Keersmaecker, S. C. (2008). Genes and molecules of lactobacilli supporting probiotic action. *Microbiol. Mol. Biol. Rev.* 72, 728–764. doi: 10.1128/mmbr.00017-08

Lee, I.-C. (2016). *Host-Interaction Effector Molecules of Lactobacillus plantarum* WCFS1. *Chapter 3: The Impact of Lipoteichoic Acid-Deficiency on the Physiological and Immunomodulatory Properties of Lactobacillus plantarum WCFS1*. Ph D. thesis, Wageningen University, Wageningen.

Lee, I. C., Tomita, S., Kleerebezem, M., and Bron, P. A. (2013). The quest for probiotic effector molecules–unraveling strain specificity at the molecular level. *Pharmacol. Res.* 69, 61–74. doi: 10.1016/j.phrs.2012.09.010

Leskela, S., Wahlstrom, E., Kontinen, V. P., and Sarvas, M. (1999). Lipid modification of prelipoproteins is dispensable for growth but essential for efficient protein secretion in *Bacillus subtilis*: characterization of the *lgt* gene. *Mol. Microbiol.* 31, 1075–1085. doi: 10.1046/j.1365-2958.1999.01247.x

Liu, S., Liu, Y., Hao, W., Wolf, L., Kiliaan, A. J., Penke, B., et al. (2012). TLR2 is a primary receptor for Alzheimer's amyloid β peptide to trigger neuroinflammatory activation. *J. Immunol.* 188, 1098–1107. doi: 10.4049/jimmunol.1101121

Machata, S., Tchatalbachev, S., Mohamed, W., Jansch, L., Hain, T., and Chakraborty, T. (2008). Lipoproteins of *Listeria monocytogenes* are critical for virulence and TLR2-mediated immune activation. *J. Immunol.* 181, 2028–2035. doi: 10.4049/jimmunol.181.3.2028

Matsuyama, S., Tajima, T., and Tokuda, H. (1995). A novel periplasmic carrier protein involved in the sorting and transport of *Escherichia coli* lipoproteins destined for the outer membrane. *EMBO J.* 14, 3365–3372. doi: 10.1002/j.1460-2075.1995.tb07342.x

Mohammad, M., Nguyen, M. T., Engdahl, C., Na, M., Jarneborn, A., Hu, Z., et al. (2019). The YIN and YANG of lipoproteins in developing and preventing infectious arthritis by *Staphylococcus aureus*. *PLoS Pathog.* 15:e1007877. doi: 10.1371/journal.ppat.1007877

Nakayama, H., Kurokawa, K., and Lee, B. L. (2012). Lipoproteins in bacteria: structures and biosynthetic pathways. *FEBS J.* 279, 4247–4268. doi: 10.1111/febs.12041

Nguyen, M. T., and Gotz, F. (2016). Lipoproteins of gram-positive bacteria: key players in the immune response and virulence. *Microbiol. Mol. Biol. Rev.* 80, 891–903. doi: 10.1128/mmbr.00028-16

Nguyen, M. T., Uebele, J., Kumari, N., Nakayama, H., Peter, L., Ticha, O., et al. (2017). Lipid moieties on lipoproteins of commensal and non-commensal staphylococci induce differential immune responses. *Nat. Commun.* 8:2246.

Remus, D. M., van Kranenburg, R., van Swam, I. I., Taverne, N., Bongers, R. S., Wels, M., et al. (2012). Impact of 4 *Lactobacillus plantarum* capsular polysaccharide clusters on surface glycan composition and host cell signaling. *Microb. Cell Fact.* 11:149. doi: 10.1186/1475-2859-11-149

Robichon, C., Vidal-Ingigliardi, D., and Pugsley, A. P. (2005). Depletion of apolipoprotein N-acyltransferase causes mislocalization of outer membrane lipoproteins in *Escherichia coli*. *J. Biol. Chem.* 280, 974–983. doi: 10.1074/jbc.m411059200

Rolf, N., Kariminia, A., Ivison, S., Reid, G. S., and Schultz, K. R. (2015). Heterodimer-specific TLR2 stimulation results in divergent functional outcomes in B-cell precursor acute lymphoblastic leukemia. *Eur. J. Immunol.* 45, 1980–1990. doi: 10.1002/eji.201444874

Saleh, M., Bartual, S. G., Abdullah, M. R., Jensch, I., Asmat, T. M., Petruschka, L., et al. (2013). Molecular architecture of *Streptococcus pneumoniae* surface thioredoxin-fold lipoproteins crucial for extracellular oxidative stress resistance and maintenance of virulence. *EMBO Mol. Med.* 5, 1852–1870. doi: 10.1002/emmm.201202435

Sambrook, J., Fritsch, E. F., and Maniatis, T. (1989). *Molecular Cloning: A Laboratory Manual*, 2nd Edn. Cold Spring harbor, NY: Cold Spring Harbor Laboratory Press.

Schenk, M., Belisle, J. T., and Modlin, R. L. (2009). TLR2 looks at lipoproteins. *Immunity* 31, 847–849. doi: 10.1016/j.immuni.2009.11.008

Shahmirzadi, S. V., Nguyen, M. T., and Gotz, F. (2016). Evaluation of *Staphylococcus aureus* lipoproteins: role in nutritional acquisition and pathogenicity. *Front. Microbiol.* 7:1404. doi: 10.3389/fmicb.2016.01404

Stoll, H., Dengjel, J., Nerz, C., and Gotz, F. (2005). *Staphylococcus aureus* deficient in lipidation of prelipoproteins is attenuated in growth and immune activation. *Infect. Immun.* 73, 2411–2423. doi: 10.1128/iai.73.4.2411-2423.2005

Takeuchi, O., Sato, S., Horiuchi, T., Hoshino, K., Takeda, K., Dong, Z., et al. (2002). Cutting edge: role of Toll-like receptor 1 in mediating immune response to microbial lipoproteins. *J. Immunol.* 169, 10–14. doi: 10.4049/jimmunol.169.1.10

Teusink, B., van Enckevort, F. H., Francke, C., Wiersma, A., Wegkamp, A., Smid, E. J., et al. (2005). In silico reconstruction of the metabolic pathways of *Lactobacillus plantarum*: comparing predictions of nutrient requirements with those from growth experiments. *Appl. Environ. Microbiol.* 71, 7253–7262. doi: 10.1128/aem.71.11.7253-7262.2005

Underhill, D. M., and Ozinsky, A. (2002). Toll-like receptors: key mediators of microbe detection. *Curr. Opin. Immunol.* 14, 103–110. doi: 10.1016/s0952-7915(01)00304-1

van Bokhorst-van de Veen, H., Lee, I. C., Marco, M. L., Wels, M., Bron, P. A., and Kleerebezem, M. (2012). Modulation of *Lactobacillus plantarum* gastrointestinal robustness by fermentation conditions enables identification of bacterial robustness markers. *PLoS One* 7:e39053. doi: 10.1371/journal.pone.0039053

van Hemert, S., Meijerink, M., Molenaar, D., Bron, P. A., de Vos, P., Kleerebezem, M., et al. (2010). Identification of *Lactobacillus plantarum* genes modulating the cytokine response of human peripheral blood mononuclear cells. *BMC Microbiol.* 10:293. doi: 10.1186/1471-2180-10-293

Vizcaino, J. A., Csordas, A., del-Toro, N., Dianes, J. A., Griss, J., Lavidas, I., et al. (2016). 2016 update of the PRIDE database and its related tools. *Nucleic Acids Res.* 44, D447–D456.

Zhang, L., Boeren, S., Hageman, J. A., van Hooijdonk, T., Vervoort, J., and Hettinga, K. (2015). Bovine milk proteome in the first 9 days: protein interactions in maturation of the immune and digestive system of the newborn. *PLoS One* 10:e0116710. doi: 10.1371/journal.pone.0116710

Conflict of Interest: The authors declare that the research was conducted in the absence of any commercial or financial relationships that could be construed as a potential conflict of interest.

frontiers in Cellular and Infection Microbiology

ORIGINAL RESEARCH
published: 31 August 2020
doi: 10.3389/fcimb.2020.00465

Topic Application of the Probiotic *Streptococcus dentisani* Improves Clinical and Microbiological Parameters Associated With Oral Health

María D. Ferrer[1], *Aranzazu López-López*[1], *Teodora Nicolescu*[2], *Salvadora Perez-Vilaplana*[2], *Alba Boix-Amorós*[1], *Majda Dzidic*[1], *Sandra Garcia*[1], *Alejandro Artacho*[1], *Carmen Llena*[2†] *and Alex Mira*[1*†]

[1] *Foundation for the Promotion of Health and Biomedical Research of Valencia Region (FISABIO), Valencia, Spain,* [2] *Clínica Odontológica, Fundació Lluís Alcanyis, Universitat de València, Valencia, Spain*

OPEN ACCESS

Edited by:
Jasna Novak,
University of Zagreb, Croatia

Reviewed by:
Georg Conrads,
RWTH Aachen University, Germany
Anna Zalewska,
Medical University of Bialystok, Poland

***Correspondence:**
Alex Mira
mira_ale@gva.es

†These authors share senior authorship

Specialty section:
This article was submitted to Microbiome in Health and Disease, a section of the journal Frontiers in Cellular and Infection Microbiology

Received: *18 June 2020*
Accepted: *28 July 2020*
Published: *31 August 2020*

Citation:
Ferrer MD, López-López A, Nicolescu T, Perez-Vilaplana S, Boix-Amorós A, Dzidic M, Garcia S, Artacho A, Llena C and Mira A (2020) Topic Application of the Probiotic Streptococcus dentisani Improves Clinical and Microbiological Parameters Associated With Oral Health. Front. Cell. Infect. Microbiol. 10:465. doi: 10.3389/fcimb.2020.00465

Streptococcus dentisani 7746, isolated from dental plaque of caries-free individuals, has been shown to have several beneficial effects *in vitro* which could contribute to promote oral health, including an antimicrobial activity against oral pathogens by the production of bacteriocins and a pH buffering capacity through ammonia production. Previous work has shown that *S. dentisani* was able to colonize the oral cavity for 2–4 weeks after application. The aim of the present work was to evaluate its clinical efficacy by a randomized, double-blind, placebo-controlled parallel group study. Fifty nine volunteers were enrolled in the study and randomly assigned to a treatment or placebo group. The treatment consisted of a bucco-adhesive gel application (2.5 10^9 cfu/dose) with a dental splint for 5 min every 48 h, for a period of 1 month (i.e., 14 doses). Dental plaque and saliva samples were collected at baseline, 15 and 30 days after first application, and 15 days after the end of treatment. At baseline, there was a significant correlation between *S. dentisani* levels and frequency of toothbrushing. Salivary flow, a major factor influencing oral health, was significantly higher in the probiotic group at day 15 compared with the placebo (4.4 and 3.4 ml/5 min, respectively). In the probiotic group, there was a decrease in the amount of dental plaque and in gingival inflammation, but no differences were observed in the placebo group. The probiotic group showed a significant increase in the levels of salivary ammonia and calcium. Finally, Illumina sequencing of plaque samples showed a beneficial shift in bacterial composition at day 30 relative to baseline, with a reduction of several cariogenic organisms and the key players in plaque formation, probably as a result of bacteriocins production. Only 58% of the participants in the probiotic group showed increased plaque levels of *S. dentisani* at day 30 and 71% by day 45, indicating that the benefits of *S. dentisani* application could be augmented by improving colonization efficiency. In conclusion, the application of *S. dentisani* 7746 improved several clinical and microbiological parameters associated with oral health, supporting its use as a probiotic to prevent tooth decay.

Keywords: probiotic, bacteriocin, dental plaque, salivary flow, dental caries

INTRODUCTION

Oral diseases, including dental caries (tooth decay), periodontitis (gum disease), and halitosis (bad breadth) are among the most prevalent diseases worldwide (Petersen, 2008). Although all these conditions are caused by microorganisms, current data indicate that they are not caused by exogenously acquired organisms, as healthy individuals already contain low levels of the microorganisms identified as causing agents and oral diseases therefore do not develop as a consequence of being infected by those microbes (Bradshaw and Lynch, 2013; Camelo-Castillo et al., 2015; Simón-Soro and Mira, 2015). Instead, they appear to be the consequence of external disease drivers that break the host-microbiota homeostasis (Marsh, 2003). These triggering factors range from a sugar-rich diet in the case of dental caries to bad oral hygiene and dental plaque accumulation in the case of periodontal diseases (Rosier et al., 2018). For instance, dietary sugars can be fermented by saccharolytic oral bacteria, producing organic acids that lower the pH and break the ecosystem balance, as acidogenic and aciduric organisms increase in proportion at the expense of a reduced diversity (Bradshaw et al., 2002). As a consequence of this state of dysbiosis, the pH may drop below a threshold where enamel tissue demineralizes, giving rise to a caries lesion (Takahashi and Nyvad, 2011). Although the oral cavity has several immunological and physico-chemical mechanisms that confer some resilience to disease (Rosier et al., 2018), these vary widely among individuals and external intervention is needed to prevent the development of oral diseases. However, the coexistence with pathogenic species in healthy individuals and the polymicrobial nature of dental caries suggest that immunization strategies such as a caries vaccine directed to a single species are unlikely to be effective (Simón-Soro and Mira, 2015; Mira, 2018). Similarly, indiscriminate antimicrobial or antiseptic strategies eliminate the beneficial action of oral microorganisms, leading to unexpected outcomes like an increase in blood pressure as a consequence of a reduction in nitric oxide availability (Bondonno et al., 2015). Eliminating oral communities may also disrupt the microorganism's ability to inhibit pathogenic species, favoring the colonization of opportunistic pathogens such as *Candida* species (Bertolini et al., 2019). Thus, recent views in preventive dentistry suggest shifting from antimicrobial strategies toward the development of products that can restore the balance in the oral ecosystem (Marsh, 2018; Mira, 2018), and these include the use of prebiotics and probiotics (Koduganti et al., 2011).

Initially, the success of probiotics isolated from dairy products or from the gut of humans and animals to improve physiological functions in the gastrointestinal tract or the immune system, led to the application of the same or similar species to treat oral diseases (Allaker and Stephen, 2017). However, different clinical studies have shown that oral colonization is extremely limited in these non-oral probiotics (Ravn et al., 2012; Taipale et al., 2012; Zaura and Twetman, 2019). In addition, many classical probiotic species, especially Lactobacilli and Bifidobacteria, are highly acidogenic and therefore related to dental caries initiation or progression (Badet and Thebaud, 2008; Mantzourani et al., 2009), and *in vitro* studies have shown that they can increase the acidogenicity of oral biofilms (Pham et al., 2009). For these reasons, the use of health-associated oral bacteria with potentially beneficial features has been suggested to prevent and treat oral diseases (Nascimento et al., 2013; López-López et al., 2017; Marsh, 2017; Mira, 2018). Some of those beneficial characteristics have consequences for systemic health, like the metabolic conversion of nitrate into nitrite and nitric oxide, which influences cardiovascular function (Doel et al., 2005). In relation to the promotion of oral health, some oral bacteria have been found to buffer extracellular pH by ammonia production, through the arginolytic, urease, or denitrification pathways (Liu et al., 2012; Reyes et al., 2014; Rosier et al., 2018) and would therefore be especially useful to prevent tooth decay. In other occasions anti-inflammatory properties have been reported (Corrêa et al., 2019; Esteban-Fernández et al., 2019) which could thus be relevant for gingivitis and periodontitis. Different bacterial species have also been found to have antimicrobial properties, with antagonistic effects against oral pathogens. These include many streptococcal species such as *S. salivarius*, *S. dentisani*, *Streptococcus* A12, and *S. oligofermentans*, which inhibit the growth of different oral pathogenic strains by the production of hydrogen peroxide, proteases, or bacteriocins (Burton et al., 2006; Bao et al., 2015; Huang et al., 2016; Llena et al., 2019). Although the potential benefits of these oral organisms are promising and they appear to be associated to individuals with good oral health (Belda-Ferre et al., 2012; Liu et al., 2012), there is still limited clinical evidence of their colonization efficacy, *in vivo* benefits for human health, side effects and consequences for oral microbial ecology (Allaker and Stephen, 2017; Zaura and Twetman, 2019). Thus, clinical studies aiming at testing oral probiotics' efficacy to promote oral health are vital for evaluating their use.

Streptococcus dentisani was first isolated in 2011 from caries-free individuals where a metagenomic analysis of dental plaque samples had shown an over-representation of genes coding for antimicrobial peptides (Belda-Ferre et al., 2012). In fact, at least 11 bacteriocins have been described in this organism based on bioinformatic analysis (Conrads et al., 2019) and has been shown to inhibit different oral pathogens ranging from *Fusobacterium nucleatum* to *Porphyromonas gingivalis* or *Streptococcus mutans* (López-López et al., 2017; Esteban-Fernández et al., 2019; Llena et al., 2019). Genomic and physiological analysis determined that this bacterium represented a new species (Benítez-Páez et al., 2014) although its potential assignment as a subspecies of *S. oralis* is under debate (Jensen et al., 2016; Velsko et al., 2019). Nevertheless, over a dozen isolates have now been sequenced and their phylogenomic analysis shows that they form a clearly distinct cluster (Jensen et al., 2016), being the presence of the arginolytic pathway a landmark of this taxon that further differentiates it from related *S. oralis* and *S. tigurinus* clusters which do not have this pathway. The current official assignment for this cluster is *S. oralis* subspecies *dentisani* and given that *S. dentisani* is considered a synonym, we will use this term throughout the manuscript. *In vitro* studies show that *S. dentisani* is able to inhibit and displace pre-existing cultures of oral pathogens on

human gingival cells (Esteban-Fernández et al., 2018, 2019). Recently, a pilot clinical study showed that *S. dentisani* strain 7746 was able to colonize human dental plaque for at least 2 weeks after topic application with a dental ferule (Ferrer et al., 2020). In addition, salivary pH and lactate production improved after 1-week treatment, and a reduction in the counts of the cariogenic organism *S. mutans* was also observed, but the small sample size in this pilot test (only 12 individuals were studied) prevented a full evaluation of this strain as a probiotic. In the current manuscript, we aim to evaluate the clinical efficacy of *S. dentisani* 7746 by a randomized, double-blind, placebo-controlled parallel group study. Both saliva and plaque samples were collected at different time points for measuring different physico-chemical (e.g., pH, lactate, calcium, or ammonia, among others) and microbiological features, including a full bacterial composition analysis by high-throughput 16S rRNA gene sequencing. By these data, together with the analysis of clinical parameters that are associated with oral health, such as plaque accumulation, gingival inflammation, oral hygiene, or salivary flow, we intend to provide the first complete evaluation of the *in vivo* efficacy and safety of this organism.

MATERIALS AND METHODS

Study Design, Recruitment, and Treatment

To evaluate the protective effect on dental caries of *Streptococcus dentisani* CECT 7746, a randomized, double-blind, placebo-controlled parallel group clinical trial was designed (ClinicalTrials.gov Identifier: NCT03468842). The present study (project code ABB-dentisani 2015) was approved on 2015/12/30th by the Institutional Ethical Committee DGSP-CSISP. Compliance of the protocol and surveillance of the study was performed by the external CRO Effice (Madrid, Spain).

Sample size was calculated by a power estimation based on the pH variable, considering a pH variation in the population of 0.5 and an expected difference between the groups of 0.5, a confidence level of 95% and a power of 90%, which suggested a sample size of 22 individuals per group. We expected a high dropout rate (>20%) due to the length of the study and the multiple visits, we aimed at a final sample size of 55–60 individuals. One hundred eighty-four patients were recruited from which 59 subjects (41 females and 18 males) aged 18–65 years fulfilled inclusion/exclusion criteria and were enrolled in the study. Inclusion criteria included three to ten carious active lesions (including white spot lesions and non-cavitated lesions on enamel surface), with ICDAS score of 2 to 5. Exclusion criteria included presence of <20 teeth, periodontal diseases, oral antiseptics use or oral probiotics or antibiotics consumption during the 30 days before the start of the study, chronic diseases, or chronic treatment that can reduce salivary flow (e.g., psychotropic drugs or antidepressants) pregnant or lactating women and allergy to any of the product composition ingredients. Individuals with a salivary pH >7 were excluded in order to select for patients with a higher caries risk, which would be the ones benefiting the most from an anti-caries treatment. The number of tooth brushings per day before the study was registered for all participants (0, 1, 2, or 3).

Participants, after signing the informed consent form, were randomly assigned by a computer-generated list to one of the two treatment groups (29 patients in the placebo group and 30 patients in the probiotic group). Soft personalized splints necessary for product application were manufactured based on alginate impressions from both jaw arches of all participants. These splints, washable and reusable during the entire study, were provided to participants together with a toothpaste containing 1,450 ppm fluoride (supplied by AB-Biotics SA) and a toothbrush. To ensure homogenous dental hygiene among participants, volunteers were instructed how to brush their teeth twice a day (morning and night) and the amount of dentifrice to use. Participants were asked to refrain from tooth brushing the morning of sampling days (day 0, day 15, day 30, and day 45) to increase plaque accumulation for sampling and to homogenize plaque formation time. No dietary recommendations were provided.

At day 0, treatment was applied by the dentist and the participants were explained how to perform the successive applications at home. Volunteers received the probiotic/placebo vials for home applications, which were performed every 48 h for a month (14 applications in total). At the follow-up visits (days 15, 30, and 45), plaque and saliva sampling procedures were followed as in the baseline visit (see below). Compliance was confirmed by checking the empty vials in visit 30 when patients returned the used material. **Figure 1** (left panel) shows a scheme of the study design and visits. Compliance with the protocol, follow-up of participants, data notebook, and congruence of the source documents with clinical and laboratory data were performed and supervised by the external CRO Effice Ltd. (Madrid, Spain). Effice Ltd. was also responsible for configuring the database and breaking the blindness after all clinical and laboratory data were registered.

Experimental Product

Lyophilized *S. dentisani* cells of strain CECT 7746 were provided in sealed glass vials mixed with adherent and thickener excipients. Probiotic and placebo composition are shown in **Table 1**. The dry product was resuspended with 6 ml of sterile water, and after 30 s of shaking, the resulting bucco-adhesive gel was transferred to the individualized tailored mouth splints (3 ml on each) using a sterile syringe, and then applied in contact with the surface of all teeth for 5 min (**Figure 1**, right panel). Participants were explicitly asked to refrain from drinking, eating, or toothbrushing for at least half an hour after the product's application.

Collection of Oral Samples

Visits took place in between 4 and 7 p.m. In order to accumulate a mature dental biofilm of 16–20 h, volunteers refrained from brushing their teeth since the night before. Plaque samples were collected separately from quadrants 1 to 3 and 2 to 4 in 100 μl of PBS and stored on ice. Supragingival dental plaque was collected from lingual and vestibular surfaces of all teeth with sterile spoon excavators, following Simón-Soro et al. (2013). For saliva samples, in every sampling event, three different non-stimulated, drooling saliva samples were collected in 50 ml sterile

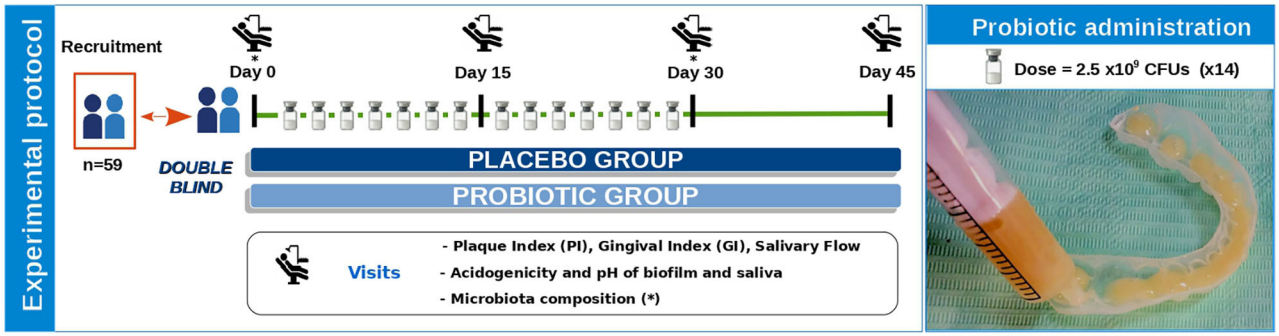

FIGURE 1 | Diagram of clinical study experimental protocol. In this double-blind study, participants were randomly assigned to one of the two treatment groups (placebo or probiotic). On the first visit (Day 0), treatment was applied by the dentist and participants were explained how to perform the 14 successive applications at home every 48 h during a month. At each of the visits (Day 0, Day 15, Day 30, and Day 45), several clinical parameters were measured (plaque and gingival index, and salivary flow), and plaque and saliva samples were collected to determine the acidogenicity and buffer capacity of biofilm and saliva. All samples at day 0 were collected before any administration of the probiotic or placebo and therefore *S. dentisani* levels at day 0 correspond to the endogenous levels of this organism in the participants. The image on the right shows bucco-adhesive product administration. Lyophilized *S. dentisani* cells (with a total dose of 2.5×10^9 CFUs) mixed with thickener and adherence excipients were resuspended with 6 mL of water, and resultant gel was transferred to the individualized mouth splint using a syringe. The placebo group product had the same excipients but no probiotic.

TABLE 1 | Experimental product.

	Probiotic	Placebo
General content	Probiotic *Streptococcus dentisani* CECT 7746 + Excipients	Excipients without probiotic
Vial composition	- 2.5×10^9 CFUs/vial - 2% (p/v) Guar gum - 6% (p/v) hydroxyethylcellulose	- 2% (p/v) Guar gum - 6% (p/v) hydroxyethylcellulose
Probiotic dose	2.5×10^9 CFUs/vial Administration every 48 h, equivalent to 10^{10} CFUs/week	–
Route of administration	Topic application in the mouth	Topic application in the mouth
Galenic form	Buccoadhesive gel	Buccoadhesive gel

Probiotic and placebo composition.

Falcon tubes and kept on ice: basal saliva (intact), saliva after tooth brushing with water, and saliva collected 10 min after a minute sugar rinse with 10 ml of 10% sucrose solution. Salivary samples taken for measuring pH and lactate were processed and measured immediately. The surplus of saliva samples was kept on ice during the clinical session, and all samples were transported to the lab and kept at −20°C until processing.

Clinical Parameters

Dental examinations were performed by an experienced, ICDAS-certified dentist. An odontogram and DMFT index were registered for all recruited individuals at baseline. In every visit, and prior to plaque sample collection, three parameters were measured: plaque index (PI), gingival index (GI), and salivary flow. The plaque index was determined in the surface of six different teeth by the Silnes and Löe methodology (Sillness and Löe, 1964). The gingival index was determined in the same six positions by the Löe and Silnes methodology (Löe and Silness, 1963). For each index and volunteer, means of the values obtained in the six teeth were calculated. To estimate the salivary flow, volunteers deposited the drooling unstimulated saliva in a graduated tube during 5 min (Navazesh, 1993).

Lactic Acid and pH Measurements

To measure total lactic acid and pH of saliva and plaque samples, reflectometry with the RQflex20 Reflectoquant System (Merk) was used, according to manufacturer's instructions and following Helmke et al. (2009) and Ferrer et al. (2020). The equipment was calibrated by the use of standards with known concentrations.

A plaque sugar challenge was performed by adding 20 μl of sucrose 20% in PBS to an aliquot of 20 μl directly taken form the plaque suspension. After an incubation period of 10 min at 37°C, *ex vivo* plaque pH and lactic acid measurements were obtained by reflectometry as explained before.

Electrolytes Quantification

The majority ions in the basal saliva samples taken during the visit at beginning of the treatment (V0) and at the end of the treatment (V30) were determined by ion chromatography in Metrohm Com-pact IC Plus 882 equipment. Each determination was made in duplicate. Six anions (Fluoride, chlorine, nitrite, nitrate, phosphate, and sulfate) and five cations (sodium, ammonium, potassium, calcium, and magnesium) were quantified.

Nucleic Acids Extraction

An aliquot of 250 μl of each saliva sample was thawed and centrifuged at 13.000 rpm for 10 min, and the pellet was resuspended in 100 μl of PBS. Dental plaque samples were mixed by vigorous shaking. Then both kind of samples were immersed in an ultrasounds bath (Selecta) during 45 seg. Before starting DNA extraction with the MagnaPure LC JE379 instrument

and the MagnaPure LC DNA Isolation Kit (Roche) following the manufacturer's instructions, an additional enzymatic lysis step was performed as published before (Dzidic et al., 2018). DNA extracted was quantified in duplicate with the Quant-iT PicoGreen dsDNA Assay Kit (Invitrogen).

Quantification of *S. dentisani* in Dental Plaque and Saliva Samples

Streptococcus dentisani in saliva and dental plaque samples was quantified by real-time PCR at each study visit. *S. dentisani* primers targeted the genes for the carbamate kinase (*arcC*), as detailed in Ferrer et al. (2020). Real-time PCR was performed in a LightCycler 480 System with the LightCycler 480 SYBR Green I Master Mix (Roche).

The absolute amounts of *S. dentisani* were calculated by comparison with the Cq values obtained from a standard curve, using serial ten-fold dilutions of DNA extracted from 2×10^6 CFUs/ml of *S. dentisani* (counted by serial dilutions in agar plates). Cq values obtained from plaque samples were expressed in absolute numbers per two quadrants or normalized against the total ng of DNA of plaque, whereas in saliva samples *S. dentisani* cells were normalized by ml of saliva.

16S rDNA Gene Amplification, Sequencing, and Data Analysis

Illumina amplicon libraries were performed following the 16S rDNA gene Metagenomic Sequencing Library Preparation Illumina protocol (Part #15044223 Rev. A). The universal primer targets the 16S rDNA gene V3 and V4 regions, resulting in a single amplicon of 460 bp (Dzidic et al., 2018). Overhand adapter sequences were used together with the primer pair sequences for compatibility with Illumina index and sequencing adapters. Amplicons were sequenced on a MiSeq equipment according to manufacturer's instructions (Illumina) using the 2×300 bp paired-end protocol. Sequences were uploaded to the SRA public repository with accession number PRJNA629283.

Reads were analyzed as previously described (Carda-Diéguez et al., 2019) using the Dada2 pipeline (Callahan et al., 2016). Briefly, we filtered, end-trimmed, denoise, and merge paired reads before adapters and primers were filtered out. Singletons and PCR chimeras were removed. The remaining reads were assigned to a taxon using the SILVA non-redundant database (Quast et al., 2013). For taxonomic analysis, we obtained an amplicon sequence variant (ASV) table following the dada2 pipeline, assigning a taxonomy to each variant by comparing them against SILVA database with a naive Bayesian classifier implemented in R (R Core Team, 2013) to assign up to genus level and 97% blast matching for species level (ASV).

Statistical Analysis

The obtained values were plotted and subjected to a multiple *t*-test or One-way ANOVA test using GraphPad Prism version 6.0., depending on data normality, to reveal significant differences between sampling events, both intergroup and intragroup. The threshold for significance was set at $p\text{-valor} \leq 0.05$. For taxonomic analysis, rarefaction curves, heatmaps, canonical correlation analysis (CCA), and Wilcoxon rank sum statistical tests were performed with R, using the packages Vegan (R Core Team, 2013) and ade4 (Dray and Dufour, 2007). When multiple comparisons were performed, *p*-values were corrected by the Bonferroni correction.

RESULTS

Volunteers Dropout, Safety, and Tolerability

Of the 59 patients enrolled in the study, 52 completed the first visit during treatment (V15) there being 26 volunteers in each group. The dropout rate at the end of the study (V45) was 15.25% completing a total of 50 volunteers (25 in the placebo group and 25 in the probiotic group). At baseline, 20% of participants reported one toothbrushing per day, 48% reported two and 32% reported three times per day. Caries severity at baseline did not differ between the two groups, with mean DMFT values of 7.36 (*SD* 4.46) and 8.31 (*SD* 4–41) for probiotic and placebo groups, respectively. There were no serious adverse events. Mild events considered as having a potential relationship with the treatment included dyspepsia and abdominal pain and no significant difference in their frequency was found between the two groups.

Clinical Parameters Associated With Oral Health

Plaque Index

The average score of the plaque index (PI) was <1 in both groups during all the study (**Figure 2A**). Although the levels of plaque accumulation were therefore moderate, a progressive decrease in PI was observed between each visit throughout the study in the probiotic group, with a final score decrease of 0.26 points (V0 vs. V45). In contrast, in the placebo group, PI average values increased compared to baseline (V0), both at the end of treatment visit (V30), and at the end of the study (V45), and the increment value of PI between baseline and the end of the study (ΔPI V0–V45) was significantly higher compared to the probiotic group (**Supplementary Figure 1A**).

Gingival Index

The **Figure 2B** shows the mean GI values at each visit for the placebo and probiotic groups. Although both groups improved throughout the study, the decrease in GI was more pronounced in the probiotic group than in the placebo at each of the visits, but the difference was not statistically significant (**Figure 2B** and **Supplementary Figure 1B**).

Salivary Flow

The average values of unstimulated saliva produced during 5 min for the two treatment groups in each visit are represented in **Figure 2C**. In both groups, salivary flow increased significantly at the end of the study (V45) compared with baseline values (V0) ($p \leq 0.05$). However, in the probiotic group this increase was already observed from the first visit (V15), progressively growing throughout the study (V0–V15: $p = 0.06$; V0–V30: $p = 0.05$). In the placebo group, an increase in salivary flow was only observed at the end of the study (V45). Regarding the differences between groups, the salivary flow of the probiotic group was significantly

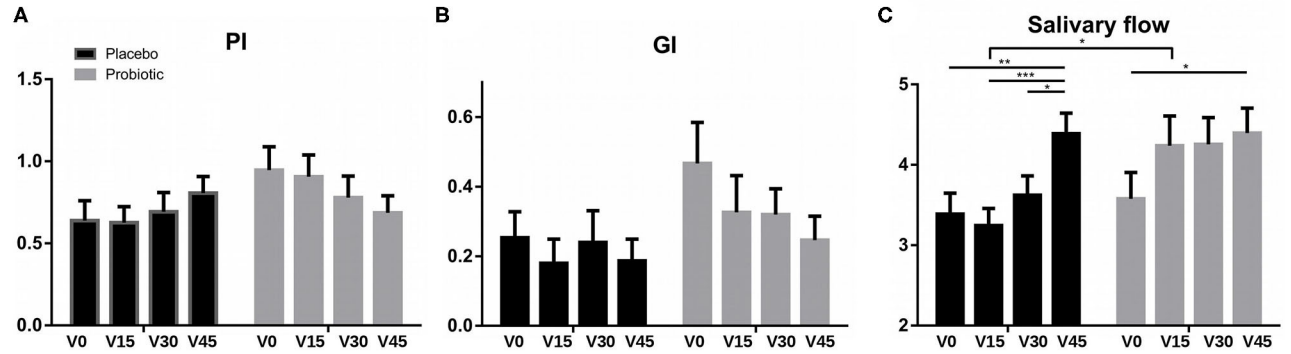

FIGURE 2 | Clinical parameters. Data show average values of **(A)** plaque index (PI), **(B)** gingival index (GI), and **(C)** salivary flow in each group (placebo in black and probiotic group in gray) measured at the different visits. Bars, from left to right, represent mean values (SEM) at: V0, baseline visit; V15, 15 days of treatment; V30, end of treatment; and V45, 15 days after the end of treatment. *$P < 0.05$, **$P < 0.01$, and ***$P < 0.001$.

higher than the placebo after 15 days of treatment (V15), reaching an average flow of 4.24 ml compared to 3.24 ml in the placebo group (**Figure 2C** and **Supplementary Figure 1C**).

S. dentisani Treatment Provides a Healthy Shift in Oral Microbiota Composition

The bacterial composition of supragingival dental plaque was studied before (V0) and at the end of treatment (V30) in probiotic and placebo groups. The relative abundance of the main bacterial genera was similar between the two study groups (**Supplementary Figure 2A**), indicating that the administration of *S. dentisani* did not trigger a dramatic ecological shift in the dental plaque microbiota. However, some interesting changes were observed, including a significant increase in *Streptococcus* in the probiotic group at the end of the treatment compared to the placebo group and to baseline values (p =0.021, Wilcox test) and a trend for a decrease in *Prevotella* ($p = 0.068$) and *Veillonella* ($p = 0.088$; **Supplementary Figures 3A–C**). Levels of each bacterial taxa in the two study groups at baseline and end-of-treatment timepoints, as well as their corresponding p-values are shown in **Supplementary Table 1**.

In terms of the composition at the genus level, a Canonical Correspondence Analysis (CCA) was used to identify the degree of similarity of the overall bacterial community composition between plaque samples (**Supplementary Figure 2B**), showing a large degree of overlap between placebo and probiotic groups at the end of the treatment (V30). However, two significant changes were observed for specific bacterial species in the probiotic group at the end of the treatment with respect to the other groups together (probiotic V0, placebo V0, and placebo V30): (i) the average values of *S. dentisani* were significantly higher in the patients after probiotic treatment ($p = 0.006$), being 3.8 % more abundant than in the other groups (**Supplementary Figure 3D**), and (ii) the average values of *Veillonella dispar/parvula* were 2,7% lower in the probiotic after treatment ($p = 0.003$; **Supplementary Figure 3E**).

Within the probiotic group, a significant increase of *S. dentisani* ($p = 0.008$) was observed at the end of the treatment (**Figure 3A**), confirming colonization in dental plaque. In addition, a significant decrease in *Fusobacterium nucleatum* was observed ($p = 0.032$) after treatment with *S. dentisani* (**Figure 3B**). A trend was also observed in the decrease of *Veillonella dispar/párvula* ($p = 0.052$) (**Figure 3C**) suggesting a decrease in organic acids, given that these bacteria use lactate as carbon source.

Significant differences between probiotic and placebo groups at the end of the treatment were observed. Bacteria at higher levels in the placebo group compared to the probiotic, in order of significance, included *Scardovia wiggsiae* (**Figure 3F**), *Dialister invisus*, *Actinomyces* sp., *Capnocytophaga leadbetteri*, *Corynebacterium matruchotti* (**Figure 3D**) and *Prevotella denticola*; followed by *Fusobacterium nucleatum* ($p = 0.057$; **Figure 3E**) and *Atopobium parvulum* ($p = 0.058$). In contrast, the species at significantly higher levels in the probiotic group at the end of treatment compared to placebo comprised *Gemella morbillorum*, *Porphyromonas pasteri,* and *Kingella* sp.

Taken together, these results showed that treatment with *S. dentisani* probiotic results in a microbial shift in composition which is consistent with a healthier microbiota, as there is a decrease of microorganisms associated with dental caries such as *Scardovia wiggsiae* (Tanner et al., 2011), *Actinomyces* sp., *Veillonella* sp. (Belda-Ferre et al., 2012; Simón-Soro et al., 2014), and *Atopobium parvulum* (Obata et al., 2014); a decrease in bacteria associated with periodontal diseases and halitosis such as *Dialister* (Silva-Boghossian et al., 2013), *Prevotella* (Camelo-Castillo et al., 2015), and *Fusobacterium nucleatum* (Wang et al., 2019); and an increase in some bacteria associated with oral health such as *Gemella* (Luo et al., 2012) and *Kingella* (Belda-Ferre et al., 2012).

It is also interesting that the two bacterial species which are considered instrumental for dental plaque formation (*F. nucleatum*, Kolenbrander et al., 2006) and oral biofilm architecture (*C. matruchotii*, Ferrer and Mira, 2016) were found to significantly decrease at the end of *S. dentisani* probiotic treatment (**Figures 3D,E**), suggesting their possible involvement in lower plaque build-up. In congruence with the clinical measures of plaque index, plaque samples within the probiotic group showed a significant decrease (total bacteria/ng DNA; p

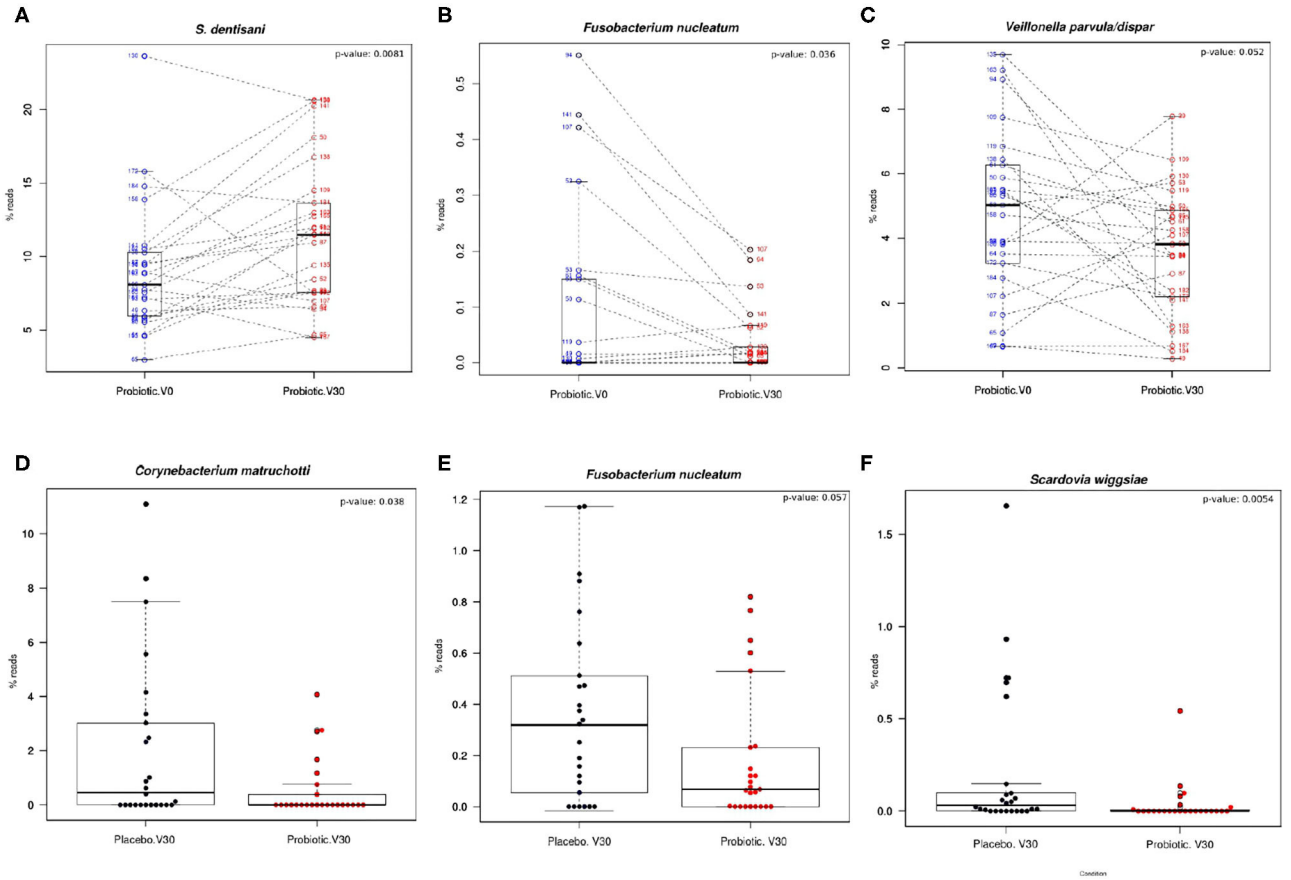

FIGURE 3 | Shifts in the relative abundance in the most abundant bacteria in dental plaque. **(A–C)** Boxplots show levels of different bacterial species in the probiotic group before and after treatment (probiotic V0 vs. V30). Lines join the samples before and after the treatment period (paired samples). **(D–F)** Levels of different bacterial species in placebo and probiotic groups at the end of treatment (placebo V30 vs. probiotic V30). The relative abundance values of *Fusobacterium nucleatum* shown in **(B)** correspond to ASV 0216 and **(E)** to the reads of ASV 0090, respectively, both 99% identical to *F. nucleatum* type strain. The results of Wilcox paired test are also shown.

$= 0.002$) in the amount of total bacteria (measured by qPCR on the 16S rRNA gene) normalized by ng of plaque DNA (as measured by fluorimetry) between baseline visit (V0) and the end of treatment. The data therefore suggest that the shift in bacterial composition hampered dental plaque accumulation.

Calcium and Ammonium Salivary Levels Increase After Probiotic Application

In order to shed light on the possible cause of increased salivary flow observed during the probiotic treatment, 11 major electrolytes present in saliva were quantified before (V0) and after treatment (V30), to test whether a difference in osmotic pressure as a consequence of changes in electrolytes concentration could be favoring higher saliva production. However, no significant differences were observed between groups or between visits within each group in the cations and anions of the measured electrolytes (**Supplementary Figure 4**).

Interestingly, the electrolyte measures showed a significant increase in salivary calcium ($p = 0.028$) and ammonium concentrations ($p = 0.048$) between the beginning and the end of treatment in the probiotic group (**Figures 4A,B**, respectively). In fact, this increase in calcium and ammonium levels after the treatment period leads to a significant separation between visits in the probiotic group samples (probiotic V0 vs. probiotic V30), as shown by a CCA analysis based on saliva electrolytes composition ($p = 0.022$; **Supplementary Figure 5**).

Effects on Acidogenicity and Buffer Capacity of Biofilm and Saliva

To investigate the possible impact of *S. dentisani* application on the acidogenicity of saliva and dental biofilm, the pH in saliva and plaque samples were measured at different time points in every visit. pH measurements in saliva samples were performed upon arrival to the clinic ("basal" samples), after plaque removal by brushing with water (pre-sugar samples) and 10 min after a sugar rinse with a 10% sucrose solution, as a measure of the buffering capacity in saliva (post-sugar samples). In the case of supragingival dental plaque, both pH and lactic acid measurements were measured *ex vivo* in basal conditions on the freshly collected dental plaque ("basal"

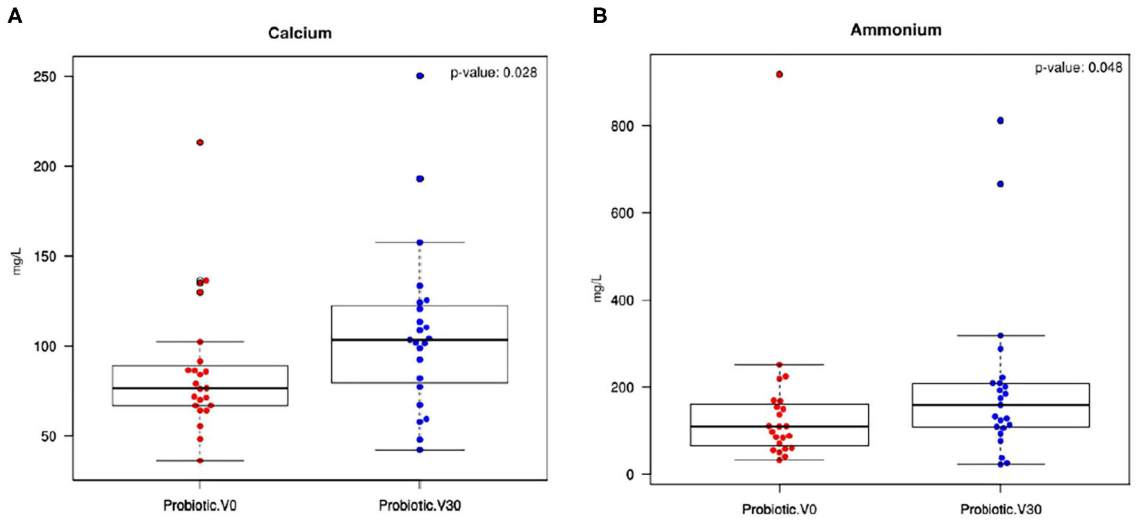

FIGURE 4 | Calcium and ammonium salivary levels. Boxplots show unstimulated saliva concentration (mg/L) of **(A)** calcium and **(B)** ammonium in the probiotic group between baseline levels (Probiotic V0) and the end of treatment (probiotic V30). Wilcox test results for the comparison are also shown.

measurements) and 10 min after incubation at 37°C on a 10% sucrose solution, as a measurement of plaque buffering capacity ("post-sugar" measurements).

Figures 5A–C show the mean pH values of baseline, before-, and after-sugar samples, respectively, measured in saliva samples at the four study visits (V0, V15, V30, and V45). Average values for the three saliva samples at each visit were similar throughout the study, with no significant differences between groups. In the placebo group, a significant increase in the basal and after-sugar pH values were observed at V30 and V45, respectively (**Figures 5A,C**).

Plaque values of pH and lactic acid production did not vary between visits throughout the study in the probiotic group. In the placebo group however, there was a significant decrease in plaque pH values after 15 days of treatment (V15), both in basal (data not shown), and in after-sugar measurements (**Figure 5D**). Interestingly, a significant increase in plaque lactic acid production was observed on that visit ($p = 0.04$, Mann-Whitney test), both in basal and after-sugar samples (data not shown), suggesting that lactic acid production could be partly responsible for this pH drop at day 15.

Saliva and Supragingival Dental Plaque Colonization of *S. dentisani*

The concentration of *S. dentisan*i in saliva samples was quantified by qPCR using species-specific primers, showing that mean values of cells/ml were significantly higher in the probiotic group compared to the placebo, both at the end of the treatment period (V30, $p = 0.05$) and at the end of the study (V45, $p = 0.01$). CFUs values at the end of the study in the probiotic group were also significantly higher ($p = 0.02$) compared to probiotic basal values (V0 vs.V45) (**Figure 6**).

Regarding the levels of the probiotic in dental plaque, a significant effect was found at baseline of the number of times the participants brushed their teeth on the levels of *S. dentisani*. Specifically, the number of tooth brushings per day significantly increased both the levels of *S. dentisani* normalized by ng of plaque ($p = 0.03$, Mann-Whitney test) and the percentage of *S. dentisani* relative to the total number of bacteria ($p = 0.04$), both estimated by qPCR (**Supplementary Table 2**). This suggests that *S. dentisani* plaque colonization is favored by plaque removal. In agreement with this, plaque levels increased throughout the clinical study not only in the probiotic group but also in the placebo (**Supplementary Figure 6**), likely as a consequence of the specific toothbrushing recommendations, material and training provided to the participants. However, as expected, the increase in *S. dentisani* plaque levels in those participants with colonization was significantly higher in the probiotic group compared to the placebo at the end of the treatment ($p = 0.04$). The proportion of participants with an increase in *S dentisani* levels in the probiotic group reached 58.3% by day 30 and 70.8% by day 45, indicating that plaque colonization can still be considerably improved.

DISCUSSION

The randomized, double-blind, placebo-controlled clinical study reported in the current manuscript has evaluated the effect of the probiotic *S. dentisani* strain 7746 buccoadhesive gel administration on several clinical and microbiological parameters, which are directly or indirectly related to oral health, specially tooth decay. Results are positive regarding safety and tolerability, and the analysis of data overall indicate that application of the probiotic improved parameters that are well-established markers of oral health. One of them is salivary flow, whose inverse relationship with the incidence of dental caries development is well-known (Rodríguez et al., 2015). In fact, a significant increase in dental caries risk has repeatedly

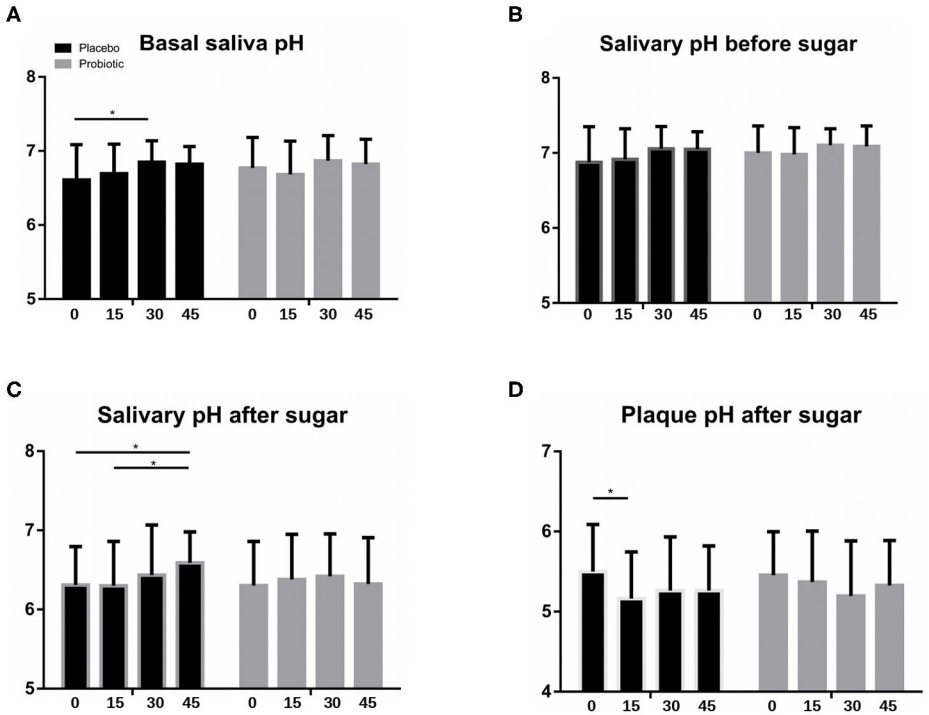

FIGURE 5 | Salivary and plaque pH. Bars show mean values of **(A)** basal saliva pH (16–18 h. after last tooth-brushing), **(B)** salivary pH after plaque removal and before a sugar rinse, and **(C)** salivary pH 10 min after a sugar rinse, measured in unstimulated saliva samples from all patients in the probiotic (gray columns) and placebo (black) groups, at the four study visits (V0, V15, V30, and V45). **(D)** Mean values of plaque pH measured *ex vivo* 10 min after a 10% sugar pulse. Columns from left to right represent mean values (SD) at: V0, baseline visit; V15, 15 days during treatment; V30, end of treatment; and V45, 15 days after the end of treatment. *$P < 0.05$.

been reported for patients taking drugs which reduce salivary flow or in patients with diseases where salivary glands are affected such as Sjögren's syndrome or head-neck cancer (Rodríguez et al., 2015). On the contrary, a higher salivary flow is associated with greater buffering capacity, salivary rinse (elimination and dilution of undesirable components), enhancement of the remineralization/demineralization ratio, increased antimicrobial action, and improved immune function (Dodds et al., 2015), leading to a less favorable environment for the development of cariogenic biofilms.

In the current work, although an improvement in salivary flow was observed in both treatment groups at the end of the study relative to baseline levels, the effect in the probiotic group was observed from the first visit, with a sialometry of up to one ml higher than the placebo group. The cause of that increase is difficult to determine as the smell and color of the placebo was indistinguishable from the probiotic. Our data on salivary ions suggest that the increase in salivary flow cannot be explained by changes in osmotic pressure, and future work should study if the probiotic has any effect on the complex physiological regulation of salivary function. Among the measured electrolytes, a significant increase in both calcium and ammonium salivary concentrations was detected between baseline and end-of-treatment values. Furthermore, the increase in these cations generated a significant change in the saliva composition, in terms of electrolyte concentration, at the end of the probiotic administration (**Supplementary Figure 5**). This increase in saliva calcium saturation induced by probiotic consumption could help in the delicate balance between remineralization and demineralization processes, on one hand by hampering the demineralization process during periods of low pH, and on the other by inducing dental remineralization when the pH returns to neutrality (Abou et al., 2016). This phenomenon can be beneficial for caries prevention, as illustrated by the work of Pandey et al. (2015), who observed significantly higher calcium salivary concentrations in caries-free compared to active caries children. This negative correlation between the incidence of dental caries and calcium salivary concentration is also reflected in different studies showing the beneficial effects of dairy probiotic products, as a consequence of the source of calcium provided by dairy food in general (Poureslami et al., 2013). To our knowledge, this is the first case where a direct association between an increase in salivary calcium levels and the administration of a non-dairy oral probiotic has been demonstrated, and future work should aim to understand the mechanism by which calcium concentrations are increased as a direct effect of a probiotic in the absence of dietary calcium supplementation.

The increase in ammonium after probiotic administration suggests that *S. dentisani* may provide higher buffering capacity to the oral biofilm. *S. dentisani* has been shown to efficiently metabolize arginine and produce extracellular ammonium by the so-called arginolytic pathway (López-López et al., 2017;

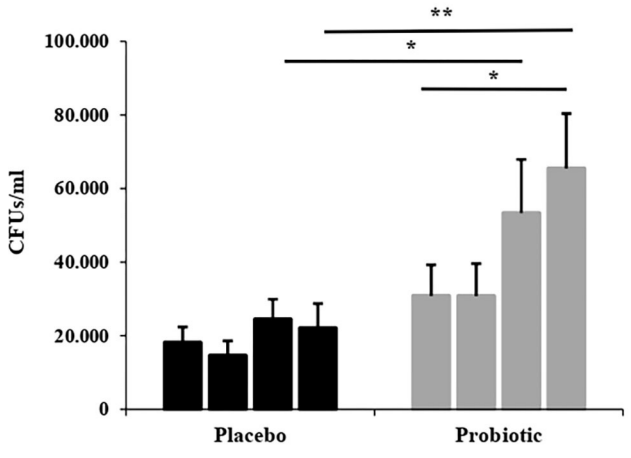

FIGURE 6 | *Streptococcus dentisani* salivary levels. qPCR quantification of *S. dentisani* in saliva (number of bacterial cells/ml) throughout the study. Columns from left to right represent mean values (SEM) at: V0, baseline visit; V15, 15 days during treatment; V30, end of treatment; and V45, 15 days after the end of treatment in each study group (placebo in black and probiotic group in gray). $^{*}P < 0.05$ and $^{**}P < 0.01$.

Velsko et al., 2018). This ability of some oral bacteria to be able to produce ammonium from arginine or urea and release it extracellularly has been strongly related to caries-free individuals in both children and adults (Nascimento et al., 2009; Reyes et al., 2014). Thus, we propose that future laboratory and clinical studies should test the potential synergy between arginine supplementation and arginolytic probiotics to improve pH buffering capacity.

The clinical data show an improvement of plaque accumulation and gingival inflammation values associated to the probiotic treatment. This is of relevance for oral diseases, as both caries and periodontitis are biofilm-mediated diseases (Marsh, 2006). For example, higher plaque accumulation induces a larger pH drop after sugar intake and triggers gingival inflammation (Rosier et al., 2018). The gingival index improvement in the probiotic group is especially relevant because in this clinical study periodontal disease was an exclusion criterion, and therefore the starting gingival inflammation values were low, leaving little space for improvement. This, together with preliminary *in vitro* studies showing anti-inflammatory properties of *S. dentisani* and an inhibitory effect on the periodontal pathogen *Porphyromonas gingivalis* (Esteban-Fernández et al., 2018) suggests that future work should evaluate its effect on periodontal diseases through a study specifically focused on these patients.

The high-throughput sequencing of plaque samples provided a possible mechanism for the reduction in plaque accumulation and gingival inflammation. The probiotic treatment led to a significant decrease in the levels of *Fusobacterium nucleatum*. This is the bacterium with the largest degree of co-aggregation patterns in the oral cavity and is considered a "bridge" organism between early and late colonizers of this complex biofilm (Kolenbrander et al., 2010). In addition, the levels of *Corynebacterium matruchotii* at the end of the treatment period were significantly lower in the probiotic group than in the placebo group. Interestingly, recent fluorescent microscopy studies have shown that *C. matruchotii* is the keystone member of dental plaque architecture, forming long filaments from the tooth surface that serve as anchorage for many other oral inhabitants (Ferrer and Mira, 2016; Mark et al., 2016). Thus, both *F. nucleatum* and *C. matruchotii* are instrumental for oral biofilm formation and they therefore represent an ideal target for antimicrobial strategies in dental plaque control (Mira, 2018). Given that *S. dentisani* has shown *in vitro* inhibitory effects on both species (López-López et al., 2017; Llena et al., 2019), the reduction in plaque and gingival indexes in the current study suggests that *S. dentisani* could hinder the formation of mature plaque by the antagonistic action of bacteriocins (Mira, 2018). The reduction in *F. nucleatum* levels *in vivo* can also be relevant for systemic health, as this organism, in addition to being involved in plaque formation, periodontal disease and halitosis, has also been found to play a role in several other extraoral inflammatory processes such as sinusitis, endocarditis, septic arthritis, and abscesses of the brain between others, and recently has been shown to be involved in colorectal cancer (Han, 2015; Lee et al., 2019). Thus, we propose that future work aims to identify the specific bacteriocins which are responsible for the inhibition of this major human pathogen. On the other hand, a potentially negative effect of the *S. dentisani* strain 7746 bacteriocins effect is their inhibitory action against other *S. dentisani* strains (Conrads et al., 2018, 2019). Thus, although our data show an increase in *S. dentisani* levels after the administration of the probiotic, this could be so at the expense of a reduction in the indigenous population of this species.

The sequence data also allowed us to determine the microbiological impact derived from *S. dentisani* application. Results show that the probiotic treatment did not derive in an ecological catastrophe, with few significant changes in bacterial composition. One of those was of course an increase in *S. dentisani*, which was accompanied by a reduction in *Veillonella*. Given that the genus *Veillonella* uses organic acids as its only carbon source, it is frequently detected in dental caries lesions (Aas et al., 2008; Belda-Ferre et al., 2012) and its presence is associated with plaque acidogenicity. This could explain the increased levels of lactate in the placebo group at day 15. However, pH levels were not significantly different between the probiotic and placebo treatments, which could be due to the general improvement in this parameter throughout the study in both groups, probably as a consequence of efficient and constant toothbrushing when entering the trial. A limitation of the study is therefore the absence of a washout period before the treatment start, which may have eliminated the effect of toothbrushing in clinical parameters. Unexpectedly, the number of toothbrushings per day reported by participants at baseline correlated with *S. dentisani* levels at V0 (**Supplementary Table 2**). This, together with the increase in *S. dentisani* not only in the probiotic group but also in the placebo (**Supplementary Figure 6**), suggests that this species is favored by plaque removal, as it has been shown for other aerobic or facultatively anaerobic species in tongue biofilms (Tribble et al., 2019).

Other pathogens that had significantly lower levels after probiotic administration included *Scardovia wiggsiae*, an acidogenic organism strongly associated with early childhood caries (Eriksson et al., 2017), *Atopobium parvulum*, associated with caries and halitosis (Kazor et al., 2003), and other species associated with gingivitis or periodontitis like *Capnocytophaga leadbetteri* (Idate et al., 2018) or *Dialister invisus* (Downes et al., 2003). These changes, together with an increase of bacteria frequently associated with oral health such as *Gemella* sp. or *Kingella* sp. (Jiang et al., 2013; Chen C. et al., 2018; Chen W. P. et al., 2018) support that probiotic administration induced a shift in bacterial composition which was clearly associated with oral health. The species-level data derived from Illumina sequencing must nevertheless be taken with caution, as short fragments of the 16S rRNA gene may provide uncertain or wrong taxonomic assignments (Claesson et al., 2010). This is especially relevant for bacterial genera which are highly similar in the sequence of this gene, such as Streptococci. For example, *S. dentisani* is 100% identical in the V3–V4 regions of the 16S rRNA gene to *S. mitis* (Dzidic et al., 2018), and the levels of the probiotic must therefore be confirmed by qPCR, where specific primers provide a more accurate and realistic estimate of its levels (Conrads et al., 2018). However, this was not performed for other biologically relevant genera like *Fusobacterium* or *Capnocytophaga*, and the ASV analysis used in the current manuscript may therefore include incorrect species-level assignments.

Colonization is a crucial aspect in the evaluation of a probiotic product. *S. dentisani* has been found at high levels on supra and subgingival plaque, and at lower levels in saliva and tongue dorsum (Esteban-Fernández et al., 2019). In the current work, mean values of CFUs per ml of saliva were significantly higher in the probiotic group than those of placebo, both at the end of treatment and at the end of the study. In dental plaque, however, significant differences were only observed at the end of the application period, suggesting that colonization is partially lost after those 2 weeks, which is consistent with a previous pilot study where the probiotic was administered only for a week (Ferrer et al., 2020). Our data show that at the end of the treatment period, only 58% of participants in the probiotic group showed colonization, reaching 71% by the end of the study. Although it is possible that this poor colonization is influenced by host characteristics or lack of compliance, our data indicate that the dose, mode of application or galenic composition can probably be enhanced. Thus, the health-associated clinical and microbiological changes observed in the current study with levels of plaque colonization that can still be augmented suggest that the beneficial effects of *S. dentisani* could also be improved. It must nevertheless be kept in mind that 14 applications of a probiotic with mouth splints could be challenging for the patients and this should be improved in the future for simpler application protocols, but only if it does not affect the beneficial effects. In addition, it must also be considered that other oral streptococci have superior arginolytic activity (Velsko et al., 2018) and therefore the potential of different oral bacteria should be clinically tested as probiotics.

In conclusion, the topic application of *S. dentisani* appears to improve several clinical features associated with oral health, such as plaque accumulation, saliva quality, and salivary flow as well as an improvement of the disease-associated bacterial dysbiosis. Some of these improvements can be attributed to the antimicrobial activity of *S. dentisani*'s bacteriocins and to its pH-buffering capacity through the arginolytic pathway. However, the mechanistic cause underlying some of these changes (e.g., salivary flow) still need to be elucidated. We hope that the current manuscript stimulates future research to characterize the antimicrobial peptides arsenal of *S. dentisani* and to test the *in vivo* effect of other oral probiotics alone or in combination with prebiotics such as arginine that may enhance their effect.

DATA AVAILABILITY STATEMENT

The raw data supporting the conclusions of this article will be made available by the authors, without undue reservation.

ETHICS STATEMENT

The studies involving human participants were reviewed and approved by Institutional Ethical Committee DGSP-CSISP. The patients/participants provided their written informed consent to participate in this study.

AUTHOR CONTRIBUTIONS

AM, CL, AL-L, and MF conceived and designed the study. MF, AL-L, TN, SP-V, AB-A, MD, and SG performed the experiments. MF and AL-L analyzed the data. AA and MF analyzed sequencing data. AM and CL provided reagents. MF, AL-L, and AM drafted the manuscript. All authors revised and approved the final manuscript.

FUNDING

This work was supported by grant RTC-2015-4292-1 from the RETOS-Colaboración Call of the Spanish Ministry of Health and Competitiveness and by grant RTI2018-102032-B-I00 from the Spanish Ministry of Science, Innovation and Universities.

SUPPLEMENTARY MATERIAL

The Supplementary Material for this article can be found online at: https://www.frontiersin.org/articles/10.3389/fcimb.2020.00465/full#supplementary-material

Supplementary Figure 1 | Changes in clinical parameters. Data show means of increment values in **(A)** plaque index, **(B)** gingival index, and **(C)** salivary flow relative to baseline visit levels (V0). Columns from left to right represent increment mean values (SEM), both increase or decrease (Δ), from visit 0 (V0) to: V15, 15 days of treatment; V30, end of treatment; and V45, 15 days after the end of treatment.

Supplementary Figure 2 | Oral microbiota composition of dental plaque. **(A)** Relative abundance of major bacterial genera identified in supragingival dental plaque samples before (V0) and after treatment (V30) as estimated by Illumina sequencing of the 16S rRNA gene. **(B)** Canonical Correspondence Analysis (CCA) of bacterial composition of plaque samples at the end of the treatment (V30) for each study participant. Each circle represents the structure in bacterial community

composition of the probiotic group samples (in red) and those of the placebo (in blue).

Supplementary Figure 3 | Shifts in bacterial levels of the most abundant organisms found in dental plaque samples. Boxplots represent the relative proportions of the most abundant genera **(A–C)** and species **(D,E)** between probiotic group samples at the end of treatment (probiotic V30) and the rest of samples (probiotic V0, placebo V0, and placebo V30), named in the figure as "others." Wilcox test results for each comparison are also shown.

Supplementary Figure 4 | Electrolytes concentration in saliva samples. Bars show the mean of **(A)** electrolytes sum (cations plus anions), **(B)** cations, and **(C)** anions separately, in unstimulated saliva samples, measured before (V0), and after treatment (V30). Columns from left to right represent mean values in mmol/L (SD) at: V0, baseline visit—and V30—end of treatment—in each treatment group (probiotic in black and placebo in gray).

Supplementary Figure 5 | Salivary electrolytes composition within the probiotic group before and after the treatment period. Plot represents a Canonical Correspondence Analysis (CCA) of saliva samples in the probiotic group before (Probiotic V0) and after the 30-day treatment period (Probiotic V30) according to 11 electrolytes concentration (6 anions and 5 cations). Each circle represents the overall structure in saliva electrolytes composition of the probiotic group samples at baseline (in red) and those at the end of treatment (in blue). CCA p-value: 0.022.

Supplementary Figure 6 | *S. dentisani* dental plaque colonization. Data represent *S. dentisani* cells, as estimated by qPCR quantifications in the colonized volunteers. Bars represent mean values (SEM) along the study period for the placebo (black) and probiotic (gray) groups. The number of colonized individuals in each time point is indicated. The asterisk indicates a significantly different colonization between the two groups ($p < 0.05$).

Supplementary Table 1 | Mean proportions of dental plaque bacteria in placebo and probiotic groups at day 0 (basal visit) and day 30 (end of treatment visit) as determined by 16S rRNA gene Illumina sequencing.

Supplementary Table 2 | Basal (indigenous) *Streptococcus dentisani* plaque levels for all participants in relation to toothbrushing frequency.

REFERENCES

Aas, J. A., Griffen, A. L., Dardis, S. R., Lee, A. M., Olsen, I., Dewhirst, F. E., et al. (2008). Bacteria of dental caries in primary and permanent teeth in children and young adults. *J. Clin. Microbiol.* 46, 1407–1417. doi: 10.1128/JCM.01410-07

Abou, N. E. A., Aljabo, A., Strange, A., Salwa, I., Melanie, C., Anne, M. Y., et al. (2016). Demineralization-remineralization dynamics in teeth and bone. *Int. J. Nanomedicine* 11, 4743–4763. doi: 10.2147/IJN.S107624

Allaker, R. P., and Stephen, A. S. (2017). Use of probiotics and oral health. *Curr. Oral Health Rep*. 4, 309–318. doi: 10.1007/s40496-017-0159-6

Badet, C., and Thebaud, N. B. (2008). Ecology of lactobacilli in the oral cavity:a review of literature. *Open Microbiol. J.* 2, 38–48. doi: 10.2174/1874285800802010038

Bao, X., de Soet, J. J., Tong, H., Gao, X., He, L., van Loveren, C., et al. (2015). Streptococcus oligofermentans inhibits *Streptococcus mutans* in biofilms at both neutral pH and cariogenic conditions. *PLoS ONE* 10:e0130962. doi: 10.1371/journal.pone.0130962

Belda-Ferre, P., Alcaraz, L. D., Cabrera-Rubio, R., Romero, H., Simón-Soro, A., Pignatelli, M., et al. (2012). The oral metagenome in health and disease. *ISME J.* 6, 46–56. doi: 10.1038/ismej.2011.85

Benítez-Páez, A., Belda-Ferre, P., Simón-Soro, A., and Mira, A. (2014). Microbiota diversity and gene expression dynamics in human oral biofilms. *BMC Genomics* 15:311. doi: 10.1186/1471-2164-15-311

Bertolini, M., Ranjan, A., Thompson, A., Diaz, P. I., Sobue, T., Maas, K., et al. (2019). Candida albicans induces mucosal bacterial dysbiosis that promotes invasive infection. *PLoS Pathog.* 15:e1007717. doi: 10.1371/journal.ppat.1007717

Bondonno, C. P., Liu, A. H., Croft, K. D., Considine, M. J., Puddey, I. B., Woodman, R. J., et al. (2015). Antibacterial mouthwash blunts oral nitrate reduction and increases blood pressure in treated hypertensive men and women. *Am. J. Hypertens.* 28, 572–575. doi: 10.1093/ajh/hpu192

Bradshaw, D. J., and Lynch, R. J. (2013). Diet and the microbial aetiology of dental caries: new paradigms. *Int. Dent. J.* 63(Suppl. 2):64–72. doi: 10.1111/idj.12082

Bradshaw, D. J., Marsh P. D., Hodgson, R. J., and Visser, J. M. (2002). Effects of glucose and fluoride on competition and metabolism within *in vitro* dental bacterial communities and biofilms. *Caries. Res.* 36, 81–86. doi: 10.1159/000057864

Burton, J. P., Chilcott, C. N., Moore, C. J., Speiser, G., and Tagg, J. R. (2006). A preliminary study of the effect of probiotic *Streptococcus salivarius* K12on oral malodour parameters. *J. Appl. Microbiol.* 100, 754–764. doi: 10.1111/j.1365-2672.2006.02837.x

Callahan, B. J., McMurdie, P. J., Rosen, M. J., Han, A. W., Johnson, A. J. A., and Holmes, S. P. (2016). DADA2: High-resolution sample inference from Illumina amplicon data. *Nat. Methods* 13, 581–583. doi: 10.1038/nmeth.3869

Camelo-Castillo, A., Mira, A., Pico, A., Nibali,L., and Henderson, B., Donos, N. et al. (2015). Subgingival microbiota in health com-pared to periodontitis and the influence of smoking. *Front. Microbiol.* 24:119. doi: 10.3389/fmicb.2015.00119

Carda-Diéguez, M., Bravo-González, L. A., Morata, I. M., Vicente, A., and Mira, A. (2019). High-throughput DNA sequencing of microbiota at interproximal sites. *J. Oral. Microbiol.* 12:1687397. doi: 10.1080/20002297.2019.1687397

Chen, C., Hemme, C., Beleno, J., Shi, Z. J., Ning, D., Qin, Y., et al. (2018). Oral microbiota of periodontal health and disease and their changes after nonsurgical periodontal therapy. *ISME J.* 12, 1210–1224. doi: 10.1038/s41396-017-0037-1

Chen, W. P., Chang, S. H., Tang, C. Y., Liou, M. L., Tsai, S. J., and Lin, Y. L. (2018). Composition analysis and feature selection of the oral microbiota associated with periodontal disease. *Biomed. Res. Int*. 2018:3130607. doi: 10.1155/2018/3130607

Claesson, M. J., Wang, Q., O'Sullivan, O., Greene-Diniz, R., Cole, J. R., Ross, R. P., et al. (2010). Comparison of two next-generation sequencing technologies for resolving highly complex microbiota composition using tandem variable 16S rRNA gene regions. *Nucleic Acids Res.* 38:e200. doi: 10.1093/nar/gkq873

Conrads, G., Bockwoldt, J. A., Kniebs, C., and Abdelbary, M. M. H. (2018). Commentary: health-associated niche inhabitants as oral probiotics: the case of *Streptococcus dentisani*. *Front Microbiol.* 9:340. doi: 10.3389/fmicb.2018.00340

Conrads, G., Westenberger, J., Lürkens, M., and Abdelbary, M. M. H. (2019). Isolation and bacteriocin-related typing of *Streptococcus dentisani*. *Front. Cell. Infect. Microbiol.* 9:110. doi: 10.3389/fcimb.2019.00110

Corrêa, J. D., Fernandes, G. R., Calderaro, D. C., Mendonça, S. M. S., Silva, J. M., Albiero, M. L., et al. (2019). Oral microbial dysbiosis linked to worsened periodontal condition in rheumatoid arthritis patients. *Sci. Rep.* 9:8379. doi: 10.1038/s41598-019-44674-6

Dodds, M. W. J., Johnson, D. A., and Yeh, C. (2015). Health benefits of saliva: a review. *J. Dent.* 33, 223–233. doi: 10.1016/j.jdent.2004.10.009

Doel, J. J., Benjamin, N., Hector, M. P., Rogers, M., and Allaker, R. P. (2005). Evaluation of bacterial nitrate reduction in the human oral cavity. *Eur. J. Oral Sci.* 113, 14–19. doi: 10.1111/j.1600-0722.2004.00184.x

Downes, J., Munson, M., and Wade, W. G. (2003). Dialister invisus sp. *nov. isolated from the human oral cavity*. *Int. J. Syst. Evol. Microbiol.* 53, 1937–1940. doi: 10.1099/ijs.0.02640-0

Dray, S., and Dufour, A. (2007). The ade4 package: implementing the duality diagram for ecologists. *J. Stat. Softw.* 22, 1–20. doi: 10.18637/jss.v022.i04

Dzidic, M., Collado, M. C., Abrahamsson, T., Artacho, A., Stensson, M., Jenmalm, M. C., et al. (2018). Oral microbiome development during childhood: an ecological succession influenced by postnatal factors and associated with tooth decay. *ISME J.* 12, 2292–2306. doi: 10.1038/s41396-018-0204-z

Eriksson, L., Lif, H. P., and Johansson, I. (2017). Saliva and tooth biofilm bacterial microbiota in adolescents in a low caries community. *Sci. Rep.* 7:5861. doi: 10.1038/s41598-017-06221-z

Esteban-Fernández, A., Ferrer, M. D., Zorraquín-Peña, I., López-López, A., Moreno-Arribas, M. V., and Mira, A. (2019). *In vitro* beneficial effects of

Streptococcus dentisani as potential oral probiotic for periodontal diseases. *J. Periodontol*. 90, 1346–1355. doi: 10.1002/JPER.18-0751

Esteban-Fernández, A., Zorraquín-Peña, I., Ferrer, M. D., Mira, A., Bartolomé, B., González de Llano, D., et al. (2018). Inhibition of oral pathogens adhesion to human gingival fibroblasts by wine polyphenols alone and in combination with an oral probiotic. *J. Agric. Food Chem*. 66, 2071–2082. doi: 10.1021/acs.jafc.7b05466

Ferrer, M. D., López-López, A., Nicolescu, T., Salavert, A., Méndez, I., Cuñé, J., et al. (2020). A pilot study to assess oral colonization and pH buffering by the probiotic *Streptococcus dentisani* under different dosing regimes. *Odontology* 108, 180–187. doi: 10.1007/s10266-019-00458-y

Ferrer, M. D., and Mira, A. (2016). Oral biofilm architecture at the microbial scale. *Trends Microbiol*. 24, 246–248. doi: 10.1016/j.tim.2016.02.013

Han, Y. W. (2015). Fusobacterium nucleatum: a commensal-turned pathogen. *Curr. Opin. Microbiol*. 23, 141–147. doi: 10.1016/j.mib.2014.11.013

Helmke, A., Hoffmeister, D., Mertens, N., Emmert, S., Schuette, J., Vioel, W., et al. (2009). The acidification of lipid film surfaces by non-thermal DBD at atmospheric pressure in air. *New J. Phys*. 11:115025. doi: 10.1088/1367-2630/11/11/115025

Huang, X., Palmer, S. R., Ahn, S. J., Richards, P., Williams, M. L., Nascimento, M. M., et al. (2016). A highly arginolytic Streptococcus species that potently antagonizes *Streptococcus mutans*. *Appl Environ Microbiol*. 82, 2187–2201. doi: 10.1128/AEM.03887-15

Idate, U., Bhat, K., Kulkarni, R., Kumbar, V., and Pattar, G. (2018). Identification of Capnocytophaga species from oral cavity of healthy individuals and patients with chronic periodontitis using phenotypic tests. *J. Adv. Clin. Res. Insights* 5, 173–177. doi: 10.15713/ins.jcri.238

Jensen, A., Scholz, C. F. P., and Kilian, M. (2016). Re-evaluation of the taxonomy of the Mitis group of the genus Streptococcus based on whole genome phylogenetic analyses, and proposed reclassification of *Streptococcus dentisani* as *Streptococcus oralis subsp. dentisani comb. nov., Streptococcus tigurinus as Streptococcus oralis subsp. tigurinus comb. nov., and Streptococcus oligofermentans as a later synonym of Streptococcus cristatus. Int. J. Syst. Evol. Microbiol*. 66, 4803–4820. doi: 10.1099/ijsem.0.001433

Jiang, W., Zhang, J., and Chen, H. (2013). Pyrosequencing analysis of oral microbiota in children with severe early childhood dental caries. *Curr. Microbiol*. 67, 537–542. doi: 10.1007/s00284-013-0393-7

Kazor, C. E., Mitchell, P. M., Lee, A. M., Stokes, L. N., Loesche, W. J., Dewhirst, F. E., et al. (2003). Diversity of bacterial populations on the tongue dorsa of patients with halitosis and healthy patients. *J. Clin. Microbiol*. 41, 558–563. doi: 10.1128/JCM.41.2.558-563.2003

Koduganti, R. R., Sandeep, N., Guduguntla, S., and Chandana, G. V. (2011). Probiotics and prebiotics in periodontal therapy. *Indian J. Dent. Res*. 22, 324–330. doi: 10.4103/0970-9290.84312

Kolenbrander, P. E., Palmer, R. J. Jr., Periasamy, S., and Jakubovics, N. S. (2010). Oral multispecies biofilm development and the key role of cell–cell distance. *Nat. Rev. Microbiol*. 8, 471–480. doi: 10.1038/nrmicro2381

Kolenbrander, P. E., Palmer, R. J. Jr., Rickard, A. H., Jakubovics, N. S., Chalmers, N. I., Diaz, P. I., et al. (2006). Bacterial interactions and successions during plaque development. *Periodontol*. 42, 47–79. doi: 10.1111/j.1600-0757.2006.00187.x

Lee, S. A., Liu, F., Riordan, S. M., Lee, C. S., and Zhang, L. (2019). Global investigations of *Fusobacterium nucleatum* in human colorectal cancer. *Front. Oncol*. 9:566. doi: 10.3389/fonc.2019.00566

Liu, Y. L., Nascimento, M., and Burne, R. A. (2012). Progress toward understanding the contribution of alkali generation in dental biofilms to inhibition of dental caries. *Int. J. Oral Sci*. 4, 135–140. doi: 10.1038/ijos.2012.54

Llena, C., Almarche, A., Mira, A., and López, M. A. (2019). Antimicrobial efficacy of the supernatant of *Streptococcus dentisani* against microorganisms implicated in root canal infections. *J. Oral Sci*. 61, 184–194. doi: 10.2334/josnusd.18-0239

Löe, H., and Silness, J. (1963). Periodontal disease in pregnancy I. Prevalence and severity. *Acta. Odontol. Scand*. 21, 533–551. doi: 10.3109/00016356309011240

López-López, A., Camelo-Castillo, A., Ferrer, M. D., Simon-Soro, Á., and Mira, A. (2017). Health-associated niche inhabitants as oral probiotics: the case of *Streptococcus dentisani*. *Front. Microbiol*. 8:379. doi: 10.3389/fmicb.2017.00379

Luo, A. H., Yang, D. Q., Xin, B. C., Paster, B. J., and Qin, J. (2012). Microbial profiles in saliva from children with and without caries in mixed dentition. *Oral Dis*. 18, 595–601. 10.1111/j.1601-0825.2012.01915.x. doi: 10.1111/j.1601-0825.2012.01915.x

Mantzourani, M., Fenlon, M., and Beighton, D. (2009). Association between Bifidobacteriaceaeand the clinicalseverity of root caries lesions. *Oral Microbiol. Immunol*. 24, 32–37. doi: 10.1111/j.1399-302X.2008.00470.x

Mark, W. J. L., Rossetti, B. J., Rieken, C. W., Dewhirst, F. E., and Borisy, G. G. (2016). Biogeography of a human oral microbiome at the micron scale. *Proc. Natl. Acad. Sci. U.S.A*. 113: E791–E800. doi: 10.1073/pnas.1522149113

Marsh, P. D. (2003). Are dental diseases examples of ecological catastrophes? *Microbiology* 149, 279–294. doi: 10.1099/mic.0.26082-0

Marsh, P. D. (2006). Dental plaque as a biofilm and a microbial community - implications for health and disease. *BMC Oral Health* 6(Suppl. 1):S14. doi: 10.1186/1472-6831-6-S1-S14

Marsh, P. D. (2017). Ecological events in oral health and disease: new opportunities for prevention and disease control? *J. Calif. Dent. Assoc*. 45, 525–537. doi: 10.1128/microbiolspec.BAD-0006-2016

Marsh, P. D. (2018). In sickness and in health—what does the oral microbiome mean to us? *An ecological perspective. Adv. Dent. Res*. 29, 60–65. doi: 10.1177/0022034517735295

Mira, A. (2018). Oral microbiome studies: potential diagnostic and therapeutic implications. *J. Adv. Dent. Res*. 29, 71–77. doi: 10.1177/0022034517737024

Nascimento, M. M., Gordan, V. V., Garvan, C. W., Browngardt, C. M., and Burne, R. A. (2009). Correlations of oral bacterial arginine and urea catabolism with caries experience. *Oral Microbiol. Immunol*. 24, 89–95. doi: 10.1111/j.1399-302X.2008.00477.x

Nascimento, M. M., Liu, Y., Kalra, R., Perry, S., Adewu-mi, A., Xu, X., et al. (2013). Oral arginine metabolism may decrease the risk for dental caries in chil-dren. *J. Dent. Res*. 92, 604–608. doi: 10.1177/0022034513487907

Navazesh, M. (1993). Methods for collecting saliva. *Ann. N. Y. Acad. Sci*. 694, 72–77. doi: 10.1111/j.1749-6632.1993.tb18343.x

Obata, J., Takeshita, T., Shibata, Y., Yamanaka, W., Unemori, M., Akamine, A., et al. (2014). Identification of the microbiota in carious dentin lesions using 16S rRNA gene sequencing. *PLoS ONE* 9:e103712. doi: 10.1371/journal.pone.0103712

Pandey, P. N., Venugopal, R. V., Arun, P. R., Aditya, S., and Chandra, P. C. (2015). Estimation of salivary flow rate, pH, buffer capacity, calcium, total protein content and total antioxidant capacity in relation to dental caries severity, age and gender. *Contemp Clin Dent*. 6(Suppl 1):S65–S71. doi: 10.4103/0976-237X.152943

Petersen, P. E. (2008). World Health Organization global policy for improvement of oral health - World Health Assembly 2007. *Int. Dent. J*. 58, 115–121. doi: 10.1111/j.1875-595X.2008.tb00185.x

Pham, L. C., van Spanning, R. J., Röling, W. F., Prosperi, A. C., Terefework, Z., Ten Cate, J. M., et al. (2009). Effects of probiotic *Lactobacillus salivarius* W24 on the compositional stability of oral microbial communities. *Arch. Oral Biol*. 54, 132–137. doi: 10.1016/j.archoralbio.2008.09.007

Poureslami, H., Pishbin, L., Eslaminejad, Z., Moqadam, F., and Farokhi, M. (2013). The effects of a dairy probiotic product, espar, on salivary calcium and mutans streptococci. *J. Dent. Res. Dent. Clin. Dent. Prospects*. 7, 147–151. doi: 10.5681/joddd.2013.023

Quast, C., Pruesse, E., Yilmaz, P., Jan, G., Timmy, S., Pablo, Y., et al. (2013). The SILVA ribosomal RNA gene database project: improved data processing and web-based tools. *Nucleic. Acids. Res*. 41, D590–D596. doi: 10.1093/nar/gks1219

R Core Team (2013). *R: A Language and Environment for Statistical Computing*. Vienna: R Foundation for Statistical Computing. Available online at: http://www.R-project.org/ (accessed April 2, 2020).

Ravn, I., Dige, I., Meyer, R. L., and Nyvad, B. (2012). Colonization of the oral cavity by probiotic bacteria. *Caries Res*. 46, 107–112. doi: 10.1159/000336960

Reyes, E., Martin, J., Moncada, G., Neira, M., Palma, P., and Gordan, V. (2014). Caries-free subjects have high levels of urease and arginine deiminase activity. *J. Appl. Oral Sci*. 22, 235–240. doi: 10.1590/1678-775720130591

Rodríguez, J., Martínez, G., Rodríguez, N., Chapa, M., and Solís, J. (2015). Dental perspective on Sjögren's syndrome: literature review. *J. Oral. Res*. 4, 211–222. doi: 10.17126/joralres.2015.041

Rosier, B. T., Marsh, P. D., and Mira, A. (2018). Resilience of the oral microbiota in health: mechanisms that prevent dysbiosis. *J. Dent. Res*. 97, 371–380. doi: 10.1177/0022034517742139

Sillness, J., and Löe, H. (1964). Periodontal diseases in pregnancy. II. Correlation between oral hygiene and periodontal condition. *Acta. Odontol. Scand.* 22, 121–135. doi: 10.3109/00016356408993968

Silva-Boghossian, C. M., Colombo, A. P., Tanaka, M., Rayo, C., Xiao, Y., and Siquiera, W. L. (2013). Quantitative proteomic analysis of gingival crevicular fluid in different periodontal conditions. *PLoS ONE* 8:e75898. doi: 10.1371/journal.pone.0075898

Simón-Soro, A., Belda-Ferre, P., Cabrera-Rubio, R., Alcaraz, L. D., and Mira, A. (2013). A tissue-dependent hypothesis of dental caries. *Caries Res.* 47, 591–600. doi: 10.1159/000351663

Simón-Soro, A., Guillen-Navarro, M., and Mira, A. (2014). Metatranscriptomics reveals overall active bacterial composition in caries lesions. *J. Oral Microbiol.* 6:25443. doi: 10.3402/jom.v6.25443

Simón-Soro, A., and Mira, A. (2015). Solving the etiology of dental caries. *Trends Microbiol.* 23, 76–82. doi: 10.1016/j.tim.2014.10.010

Taipale, T., Pienihäkkinen, K., Salminen, S., Jokela, J., and Söderling, E. (2012). *Bifidobacterium animalis* subsp. lactis BB-12 administration inearly childhood: a randomized clinical trial of effects on oral colonizationby mutans streptococci and the probiotic. *Caries Res.* 46, 69–77. doi: 10.1159/000335567

Takahashi, N., and Nyvad, B. (2011). The role of bacteria in the caries process: ecological perspectives. *J. Dent. Res.* 90, 294–303. doi: 10.1177/0022034510379602

Tanner, A. C., Kent, R. L. Jr., Holgerson, P. L., Hughes, C. V., Loo, C. Y., Kanasi, E., et al. (2011). Microbiota of severe early childhood car-ies before and after therapy. *J. Dent. Res.* 90, 1298–1305. doi: 10.1177/0022034511421201

Tribble, G. D., Angelov, N., Weltman, R., Wang, B. Y., Eswaran, S. V., Gay, I. C., et al. (2019). Frequency of tongue cleaning impacts the human tongue microbiome composition and enterosalivary circulation of nitrate. *Front. Cell Infect. Microbiol.* 9:39. doi: 10.3389/fcimb.2019.00039

Velsko, I. M., Chakraborty, B., Nascimento, M. M., Burne, R. A., and Richards, V. P. (2018). Species designations belie phenotypic and genotypic heterogeneity in oral streptococci. *mSystems* 18;3(6). doi: 10.1128/mSystems.00158-18

Velsko, I. M., Perez, M. S., and Richards, V. P. (2019). Resolving phylogenetic relationships for *Streptococcus mitis* and *Streptococcus oralis* through core- and pan-genome analyses. *Genome Biol. Evol.* 11, 1077–1087. doi: 10.1093/gbe/evz049

Wang, J., Jia, Z., Zhang, B., Peng, L., and Zhao, F. (2019). Tracing the accumulation of *in vivo* human oral microbiota elucidates microbial community dynamics at the gateway to the GI tract. *Gut.* 68, 2186–2194. doi: 10.1136/gutjnl-2019-318977

Zaura, E., and Twetman, S. (2019). Critical appraisal of oral pre- and probiotics for caries prevention and care. *Caries Res.* 53, 514–526. doi: 10.1159/000499037

Conflict of Interest: AM is the inventor of a patent application protecting the use of *S. dentisani* as an oral probiotic.

The remaining authors declare that the research was conducted in the absence of any commercial or financial relationships that could be construed as a potential conflict of interest.

frontiers in Microbiology

ORIGINAL RESEARCH
published: 15 September 2020
doi: 10.3389/fmicb.2020.555465

Isolation and Characterization of Nitrate-Reducing Bacteria as Potential Probiotics for Oral and Systemic Health

*Bob T. Rosier, Eva M. Moya-Gonzalvez, Paula Corell-Escuin and Alex Mira**

Department of Health and Genomics, Center for Advanced Research in Public Health, FISABIO Foundation, Valencia, Spain

Recent evidence indicates that the reduction of salivary nitrate by oral bacteria can contribute to prevent oral diseases, as well as increase systemic nitric oxide levels that can improve conditions such as hypertension and diabetes. The objective of the current manuscript was to isolate nitrate-reducing bacteria from the oral cavity of healthy donors and test their *in vitro* probiotic potential to increase the nitrate-reduction capacity (NRC) of oral communities. Sixty-two isolates were obtained from five different donors of which 53 were confirmed to be nitrate-reducers. Ten isolates were selected based on high NRC as well as high growth rates and low acidogenicity, all being *Rothia* species. The genomes of these ten isolates confirmed the presence of nitrate- and nitrite reductase genes, as well as lactate utilization genes, and the absence of antimicrobial resistance, mobile genetic elements and virulence genes. The pH at which most nitrate was reduced differed between strains. However, acidic pH 6 always stimulated the reduction of nitrite compared to neutral pH 7 or slightly alkaline pH 7.5 ($p < 0.01$). We tested the effect of six out of 10 isolates on *in vitro* oral biofilm development in the presence or absence of 6.5 mM nitrate. The integration of the isolates into *in vitro* communities was confirmed by Illumina sequencing. The NRC of the bacterial communities increased when adding the isolates compared to controls without isolates ($p < 0.05$). When adding nitrate (prebiotic treatment) or isolates in combination with nitrate (symbiotic treatment), a smaller decrease in pH derived from sugar metabolism was observed ($p < 0.05$), which for some symbiotic combinations appeared to be due to lactate consumption. Interestingly, there was a strong correlation between the NRC of oral communities and ammonia production even in the absence of nitrate ($R = 0.814$, $p < 0.01$), which indicates that bacteria involved in these processes are related. As observed in our study, individuals differ in their NRC. Thus, some may have direct benefits from nitrate as a prebiotic as their microbiota naturally reduces significant amounts, while others may benefit more from a symbiotic combination (nitrate + nitrate-reducing probiotic). Future clinical studies should test the effects of these treatments on oral and systemic health.

Keywords: nitrate reduction, probiotics, pH buffering capacity, caries, oral microbiota, nitric oxide, cardiovascular diseases, *Rothia*

OPEN ACCESS

Edited by:
Jasna Novak,
University of Zagreb, Croatia

Reviewed by:
John Senko,
The University of Akron, United States
Hans Karl Carlson,
Lawrence Berkeley National Laboratory, United States

****Correspondence:***
Alex Mira
mira_ale@gva.es

Specialty section:
This article was submitted to Food Microbiology, a section of the journal Frontiers in Microbiology

Received: *24 April 2020*
Accepted: *24 August 2020*
Published: *15 September 2020*

Citation:
Rosier BT, Moya-Gonzalvez EM, Corell-Escuin P and Mira A (2020) Isolation and Characterization of Nitrate-Reducing Bacteria as Potential Probiotics for Oral and Systemic Health. Front. Microbiol. 11:555465. doi: 10.3389/fmicb.2020.555465

INTRODUCTION

The salivary glands contain electrogenic sialin $2NO_3^-/H^+$ transporters to concentrate plasma nitrate into the saliva (Qu et al., 2016). This leads to salivary nitrate concentrations that are around ten times higher than plasma during fasting (100–500 μM compared to 10–50 μM), which can go up to 5–8 mM after a nitrate-containing meal [reviewed by Lundberg and Govoni (2004) and Hezel and Weitzberg (2015)]. Foods that naturally contain significant amounts of nitrate are fruits and vegetables, which are both unequivocally associated with health benefits. It is estimated that we obtain more than 80% of nitrate from vegetables (Lundberg et al., 2018).

Nitrate-reducing oral bacteria, including representatives of *Neisseria*, *Rothia*, *Veillonella*, *Actinomyces*, *Corynebacterium*, *Haemophilus*, and *Kingella* reduce nitrate to nitrite (Grant and Payne, 1981; Doel et al., 2005; Hyde et al., 2014). Human cells cannot reduce nitrate, but there are several enzymatic and non-enzymatic processes that convert nitrite into nitric oxide (Hezel and Weitzberg, 2015). For example, in the acidic gastric juice, nitrite is decomposed to nitrogen oxides, such as nitric oxide (NO), which is essential for the antimicrobial activity of the stomach (Lundberg and Govoni, 2004). It should be noted that anti-oxidants and polyphenols in vegetables and fruits prevent the formation of carcinogenic *N*-nitroso compounds from nitrite, while stimulating nitric oxide production (Ward, 2009; Kobayashi et al., 2015).

In the blood vessels, nitrite reacts with hemoglobin to form nitric oxide, which apart from being antimicrobial, is also an important vasodilator of the human body (Hezel and Weitzberg, 2015). It was shown that an antiseptic mouthwash acutely increases blood pressure by disrupting nitrate reduction by oral bacteria (Kapil et al., 2013). Nitrate-rich supplements, in turn, stimulate nitrate reduction by the oral microbiota resulting in a lowering of blood pressure (Vanhatalo et al., 2018). This pathway (i.e., the nitrate–nitrite–nitric oxide pathway) can also increase sport performance and has apparent antidiabetic effects (Lundberg et al., 2018). In light of this, antiseptic mouthwash has shown to interfere with post-exercise hypotension (Cutler et al., 2019) and over-the-counter mouthwash correlated with diabetes and pre-diabetes development (Joshipura et al., 2017).

Nitrate in the form of lettuce juice has also been shown to reduce gingival inflammation compared to a placebo (nitrate-depleted lettuce juice) (Jockel-Schneider et al., 2016). Additionally, nitrate prevented acidification by oral bacteria (Li et al., 2007) and the nitrate reduction capacity (NRC) of the oral microbiota correlated negatively with caries abundance (Doel et al., 2004). Recently, Rosier et al. (2020) have proposed that nitrate reduction stimulates eubiosis (i.e., an increase in health-associated species and functions) of the oral microbiota (Rosier et al., 2020). Specifically, nitrate reduction prevented acidification and the resulting overgrowth of cariogenic bacteria by increasing lactate consumption and ammonia production. Additionally, nitrate increased health-associated nitrate-reducing genera, while decreasing strictly anaerobic periodontal diseases- and halitosis-associated bacteria, which could be sensitive to oxidative stress caused by nitric oxide. Nitrate reducing bacteria, such as representatives of *Neisseria*, *Rothia*, *Actinomyces*, and *Kingella* have been associated to oral health in many 16S rRNA sequencing studies and this could be related with their capacity to reduce nitrate (Mashimo et al., 2015; Rosier et al., 2018; Rosier et al., 2020). In conclusion, current data suggest that nitrate-reduction of the oral microbiota contributes to a healthy host physiology and appears to stimulate oral health.

The amount of nitrate-reducing species varies among individuals and, accordingly, the NRC as well (Liddle et al., 2019). Individuals with low baseline levels of nitrate-reducing species could use nitrate as a prebiotic to increase the levels of these bacteria over time. For example, after 1–4 weeks of beetroot consumption (a vegetable with high nitrate levels), the salivary levels of *Neisseria* and *Rothia* increased significantly (Velmurugan et al., 2016; Vanhatalo et al., 2018). Alternatively, in individuals lacking nitrate-reducing species, a direct increase could be achieved by the addition of nitrate-reducing probiotics. In a seminal study, Doel et al. (2005) isolated 99 oral bacteria that produced nitrite in the presence of nitrate under anaerobic conditions and 33 under aerobic conditions, but did not further test the effects of these isolates on oral communities. Apart from their ability to produce nitrite, nitric oxide or ammonia, oral probiotics should not be acidogenic (a feature associated with dental caries) and from a technological point of view should ideally be capable of fast aerobic growth to enable large-scale production (Lacroix and Yildirim, 2007).

The aim of our current study was therefore to isolate nitrate-reducing oral strains under aerobic conditions and make a selection of isolates that were most suitable from a biomedical and industrial point of view. To achieve this, a protocol was applied to obtain isolates with a high NRC, fast growth rate and low acidogenicity. Additionally, their genomes were sequenced and analyzed for functional predictions and for the detection of potentially harmful genes. To test our hypothesis that oral communities could benefit from nitrate-reducing isolates, six selected isolates were added to *in vitro* oral biofilms grown from saliva of different individuals that varied in NRC. The NRC was determined and changes in nitrate-related metabolism (e.g., ammonia and lactate production) monitored. Oral biofilm colonization was tested by 16S rRNA sequencing. All experimental data were used to assess the *in vitro* probiotic potential of nitrate-reducing oral bacteria as a first step to evaluate their possible use for oral and systemic health.

MATERIALS AND METHODS

Donor Selection and Sample Procedure

For probiotic isolation, five young adults (1 male, 4 female, age 23–32) were selected with all teeth and good oral health, which was assessed by an experienced dentist. Individuals were excluded if they showed bleeding on probing or a periodontal pocket below 3 mm; a cavitated lesion or filling in any tooth surfaces. The absence of nitrate reduction capacity, as determined by lack

of salivary nitrite, was as an exclusion criterion (the salivary nitrite and pH measured in the morning before breakfast for all donors are shown in **Supplementary Table S1**). All individuals had a healthy blood pressure (i.e., systolic between 90 and 120, and diastolic between 60 and 80), which was measured with an Automatic Blood Pressure Monitor Model M6 Comfort IT (OMRON Healthcare Europe B.V., Hoofddorp, Netherlands). Plaque and tongue coating samples were collected by the dentist following Simón-Soro et al. (2013) and resuspended in 1 mL of PBS (Simón-Soro et al., 2013).

For saliva donor selection, individuals were recruited at the FISABIO institute if they reported not to have active caries during their last dental visit, nor any history of periodontitis. Nine individuals (3 male, 6 female, age 23–45) were selected and asked to donate saliva, which was used for *in vitro* oral community growth with and without nitrate-reducing isolates. Unstimulated saliva was collected by drooling in a sterile tube in a quiet room in the morning, at least half an hour after eating or drinking. Donors were instructed to have a normal breakfast and abstain from oral hygiene before saliva collection.

The fresh unstimulated saliva was always directly used in the experiments or kept at 4°C for less than 1 h before usage. All donors signed an informed consent form prior to sample collection and the protocol was approved by the Ethical Committee of DGSP-FISABIO (Valencian Health Authority) with code 27-05-2016. This study was carried out according to the relevant guidelines and regulations of the Declaration of Helsinki.

Isolation of Nitrate-Reducing Bacteria

Plaque or tongue samples in PBS were diluted 10^2 to 10^7 times and plated on Brain Heart Infusion (BHI) 1.4% agar plates (Merck Millipore, Burlington, MA, United States). Plates were incubated at 37°C under aerobic conditions during 2 days to obtain separated colonies in some of the dilutions. A protocol adapted from Doel et al. (2005) was employed to detect nitrate-reducing activity by individual colonies (Doel et al., 2005). This protocol consists of a double agar overlay method based on the Griess reaction that stains nitrite. Briefly, a plate with separated colonies grown from plaque or tongue samples was overlaid with 10 mL of 2.5% w/v agar with 1 mM sodium nitrate ($NaNO_3$, Sigma-Aldrich, St. Louis, MO, United States) and incubated at 37°C for 10 min in which nitrate-reducing colonies would produce nitrite. Then, the first layer was overlaid with 10 mL 2.5% w/v agar containing the Griess reagents and incubated at room temperature for 10 min. Colonies with nitrate-reducing capability produced a red color due to the presence of nitrite (**Figure 1**). These colonies were then transferred to new BHI agar plates and incubated during 2 more days at 37°C. The nitrite-producing capability of the isolates was confirmed by repeating the double overlaid agar method for each isolate. Subsequently, one colony was passed to 5 mL of liquid BHI and incubated aerobically for 2 days at 37°C. After that, 0.5 ml of the medium was used to create a glycerol stock of each isolate for future experiments. The rest of the cells were resuspended in PBS and used for DNA extraction and sequencing.

Nitrate Reduction Screenings of Bacterial Isolates

To evaluate the nitrate-related metabolism of the isolates, the concentrations of nitrate, nitrite, and ammonium, as well as pH levels, were measured in spent medium. Isolates were incubated in 5 mL BHI liquid medium overnight at 37°C. The next day, isolates were diluted in BHI to an OD of 0.01 and a final concentration of 6.5 mM nitrate, which is within the physiological range of salivary nitrate after a nitrate-containing meal [i.e., 5–8 mM (Hezel and Weitzberg, 2015)]. The tubes were then incubated for 7 h and 1 mL was taken at 4 and 7 h, after vortexing and, from this volume, 0.5 ml was used to measure the OD and 0.5 ml for the other measurements. A similar experiment was performed with 10 isolates selected as probiotic candidates, which were grown for 5 h in three types of buffered medium (100 mM MES, pH 6.0; 100 mM HEPES, pH 7.0; 100 mM HEPES pH 7.5, all Sigma-Aldrich) with 6.5 mM nitrate to keep a stable pH and evaluate the effect of different pH levels on the NRC of those isolates. All samples were frozen at −20°C before analysis of the supernatants.

Effect of Isolates on *in vitro* Biofilms

Six out of 10 selected nitrate-reducing isolates were studied *in vitro* to define their effect when added to an oral microcosm community. These isolates were tested by growing them with saliva of nine different donors in 96-wells plates in which oral communities form biofilms on the bottom of wells (Mira et al., 2019). For each experiment, there were 4 conditions: control, nitrate (final concentration: 6.5 mM nitrate), control with isolate, and nitrate with isolate. For all samples, prepared in duplicate, 100 μl of BHI (with 0.05 mg/L haemin, 0.005 mg/L menadione and 0.2 mM vitamin K) were added to each well. Then, 100 μL of saliva (or BHI for negative controls) was added and, for the nitrate conditions, 10 μL of nitrate solution 162.5 mM was added (or 10 μL of BHI for control conditions). Before being added to the 96-well plate, the isolates were grown for 24 h. Then, 40 μL isolate in BHI solution with OD 1.5 was added (or 40 μL of BHI in conditions without isolates) to each well. The final concentration of nitrate was 6.5 mM and the starting OD of the isolate was 0.24. The 96-well plate was sealed to stimulate anaerobic conditions by preventing new oxygen from entering the wells, and incubated during 7 h at 37°C. After that, the supernatant was collected and stored at −20°C until measurements were performed. The remaining biofilms were resuspended in PBS for DNA isolation.

DNA Isolation for Sequencing

DNA was extracted from pure cultures of the 53 confirmed nitrate-reducing isolates and also from the *in vitro* communities grown with isolates of two donors (D6 and D11). Pure cultures of isolates grown for 48 h in 4.5 ml BHI were centrifuged (15 min at 4,000 rpm) and the pellet resuspended in 100 μl PBS. After supernatant removal, duplicates of *in vitro* communities were resuspended together in 100 μl PBS and disaggregated for 30 s in a sonicator bath (model VCI-50, Raypa, Barcelona, Spain) at low ultrasound intensity. Total

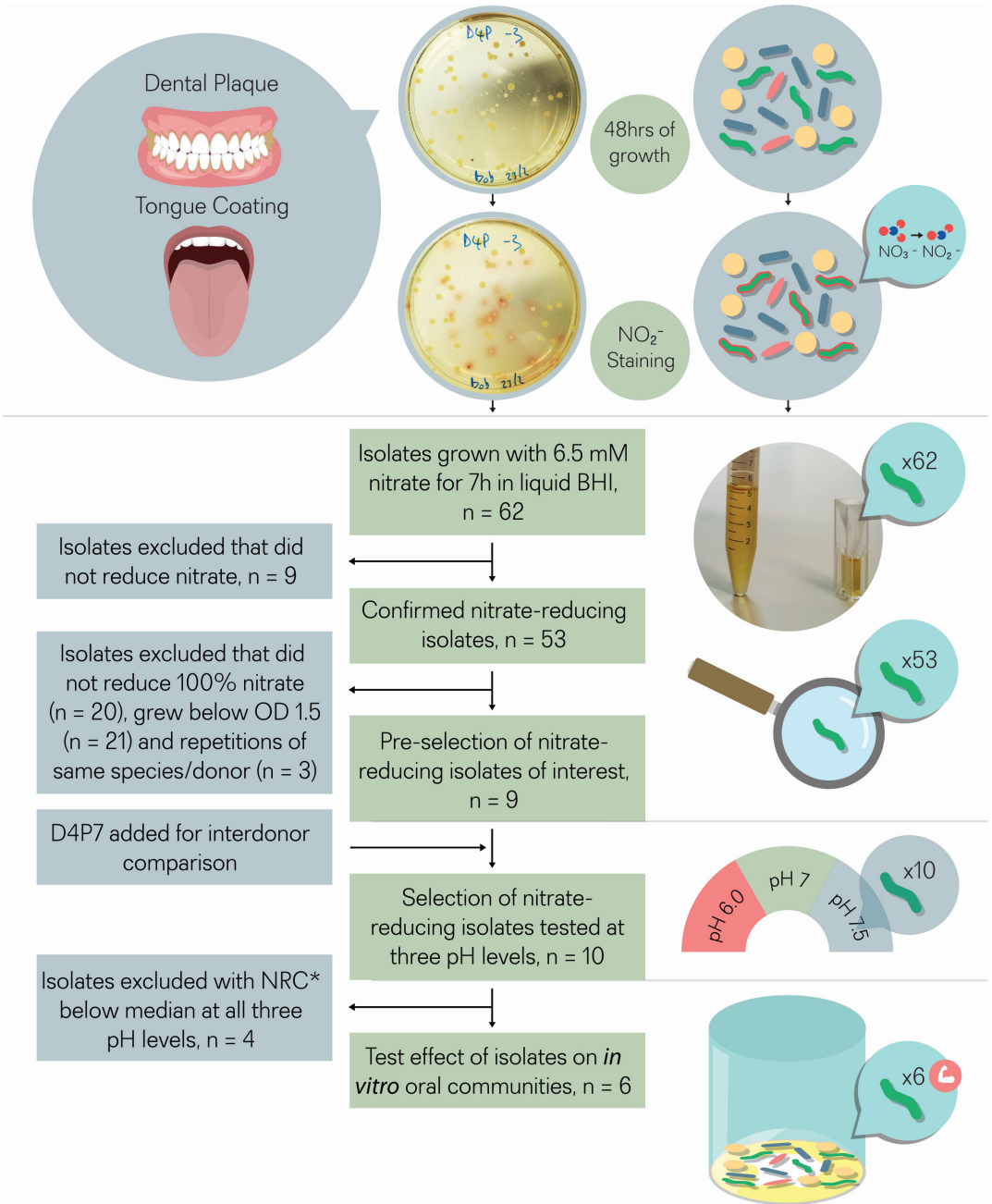

FIGURE 1 | Isolate selection overview. Tongue coating and/or dental plaque samples were obtained from 5 different donors. Sixty-two colonies that produced a red color after adding Griess reagent, which stains nitrite, were isolated. The 62 isolates were incubated with 6.5 mM nitrate for 7 h for double confirmation. Nine out of 62 isolates did not reduce nitrate and were excluded, while the other 53 isolates did reduce (part of) the nitrate and were considered as confirmed cases. From these 53 isolates, nine isolates were selected that reduced all nitrate and grew well under aerobic conditions (OD > 1.5), a relevant feature for future large-scale production. One isolate (D4P7, *R. dentocariosa*) was added to compare nitrate reducing capacity with the three selected *R. dentocariosa* isolates between different donors. None of the 10 selected isolates acidified the pH of the glucose-containing medium (starting pH 7.3) below pH 6.8 after 7 h, which indicated that they were suitable probiotics from a caries point of view. The nitrate-reduction capacity of the final selection of 10 isolates was tested at three different pH levels (pH 6.5, pH 7, and pH 7.5) in buffered medium. The six isolates that reduced the nitrate-best at different pH levels were added to oral communities (from saliva) to test their effect on *in vitro* oral biofilm metabolism. *NRC, nitrate-reduction capacity.

DNA was extracted with the MasterPure^{TM} Complete DNA and RNA Purification Kit (Epicentre Biotechnologies, Madison, WI, United States), following the manufacturer's instructions, with the addition of lysozyme (Belda-Ferre et al., 2012). DNA was resuspended in 30 µl elution buffer and frozen at −20°C until further analysis.

Taxonomic Classification of Nitrate-Reducing Isolates

For the taxonomic classification of the isolates, concentrations of DNA isolated from pure cultures were measured using a NanoDrop 1000 spectrophotometer (Thermo Scientific, Waltham, MA, United States). A PCR was performed to amplify the 16S rRNA gene of each isolate, using universal primers 8-F and 785-R for the 16S rRNA gene, comprising the hypervariable regions V1–V2–V3–V4. The PCR products were then purified using flat 96 well filter plates (NucleoFast 96 PCR; Macherey-Nagel, Düren, Germany) and sequenced at both ends by Sanger Technology at the Sequencing Unit of the University of Valencia (Valencia, Spain). To taxonomically assign the isolates, the sequences were compared by BLASTn (Altschul et al., 1997) against 16S ribosomal RNA sequences at NCBI nr database. Species assignment was confirmed by Average Nucleotide Identity (ANI) values using JSpeciesWS software (Richter et al., 2016).

Genome Sequencing

Illumina libraries for all 10 selected isolates were generated using the Illumina XT Nextera library prep kit (catalog number FC-131-1024) starting from 0.2 ng/μl of purified gDNA measured by a Qubit double-stranded DNA (dsDNA) high-sensitivity assay kit (catalog number Q32851). Libraries were sequenced using a 2 × 150-bp paired-end run MiSeq reagent kit v2 (catalog number MS-102-2002) on an Illumina MiSeq sequencer.

Oxford Nanopore libraries were obtained from the same DNA extracted samples following the manufacturer's standard protocol. Nanopore libraries were indexed and sequenced using type R9.4.1 (catalog number FLO-MIN106D) in a ONT MinION sequencer for 48 h. Both sequencing approaches were performed at the Sequencing Service of FISABIO-Public Health (Valencia, Spain).

Long ONT fast5 reads were base-called and transformed into fastq files by ONT Albacore Sequencing Pipeline Software (Pomerantz et al., 2018) and generated approximately four billion total bases in more than 850,000 reads (fastq-stats version 1.01[1]). These ONT long reads as well as the Illumina short reads were quality filtered and trimmed using Prinseq-lite (Schmieder and Edwards, 2011). Long ONT reads were assembled with Canu v1.8 using the nanopore preset parameters (Koren et al., 2017) into one single contig per genome. Their errors were corrected using Illumina quality-filtered and trimmed reads with Pilon software v1.23 (Walker et al., 2014). After three rounds of corrections, genomes were annotated by Prokka v1.13.3 (Seemann, 2014) and the downstream analysis was performed with these 10 annotated genomes.

Genomic Analysis

In order to identify the presence of possible mobile genetic elements (MGEs), the annotated genomes were compared against the latest version of the ACLAME database (Leplae et al., 2010) where different kinds of MGEs are collected and classified at gene and protein levels. Sequences were compared by similarity using the program BLASTx (Camacho et al., 2009) identifying potential hits after filtering with the following criteria: minimum sequence identity higher than 80% of the gene length and coverage greater than 50%.

Potential antibiotic resistance genes (ARGs) were searched in the latest version of CARD database (McArthur et al., 2013). The detection of possible genes conferring pathogenicity was performed using the latest version of the virulence factors database (VFDB) which currently contains DNA sequences from 1,067 virulence factors from 951 bacterial strains having 32.252 virulence factor-related non-redundant genes information (Chen et al., 2016). Sequences were compared by similarity against both databases using the program BLASTn (Altschul et al., 1997), identifying potential hits with E-value $< 10^{-5}$, sequence identity $>80\%$ and $>50\%$ sequence length as thresholds.

Supernatant Analysis: Nitrate, Nitrite, Ammonium, Lactate, and pH Measurements

Nitrate, nitrite, lactate and pH were measured in supernatants with a Reflectoquant (Merck Millipore, Burlington, MA, United States) reflectometer. This method is based on the intensity of reflected light by two reactive pads on test trips that change in color intensity based on the concentration of a specific substance (Holden and Scholefield, 1995). The test strips (Reflectoquant, Merck Millipore) for pH had a range from pH 4–9, the strips for nitrate a range of 3–90 mg/l, the strips for nitrite a range of 0.5–25 mg/l and the strips for lactate a range of 3–60 mg/l. A method was used based on Helmke et al. (2009), and Ferrer et al. (2019) as described by Rosier et al. (2020). The concentration of ammonium in supernatants was measured spectrophotometrically by the Nessler Method (Santarpia et al., 2014). Accuracy of all procedures was confirmed by using standard solutions with known concentrations of the different compounds.

Statistical Analysis

Statistical analysis was performed with SPSS 25 UK software (SPSS, Inc.). A Mann–Whitney U Test was applied to compare parameters between different (groups of) species. The Wilcoxon test was used to compare different conditions and the Spearman's rank correlation coefficient was calculated for different parameters. Significant changes ($p < 0.05$) and trends ($p < 0.1$) were presented.

RESULTS

Isolation of Nitrate-Reducing Bacteria and Testing Their Nitrate-Reduction Capacity

Tongue and dental plaque samples were plated from 5 different healthy donors (D1–D5). Potential nitrate-reducing colonies were detected by a red tone, produced by the Griess reaction

[1]http://expressionanalysis.github.io/ea-utils

resulting from nitrite production (**Figure 1**). In total, 33 nitrite-producing isolates were obtained from tongue (T) samples and 29 from dental plaque (P). Most isolates (74%) were obtained from two donors (D1 and D4, **Supplementary Table S1**).

In an initial screening to quantify NRC, all 62 isolates were incubated with 6.5 mM nitrate during 4 and 7 h under aerobic conditions (**Figure 2** and **Table 1**). Nine isolates, including strains of *Streptococcus salivarius*, *Streptococcus cristatus*, and *Streptococcus mitis*, did not reduce any of the nitrate and were excluded. The other 53 confirmed nitrate-reducing isolates were mostly classified as *Rothia* (i.e., 23 × *R. mucilaginosa*, 21 × *R. dentocariosa*, and 4 × *R. aeria*) and five as *Actinomyces* (3 × *Actinomyces viscosus* and 2 × *Actinomyces oris*, **Table 1**). All *R. mucilaginosa* isolates originated from the tongue, while all *R. dentocariosa* and *R. aeria* isolates were obtained from dental plaque (except for one *R. dentocariosa* isolate, D3T1, from the tongue). After 7 h, the average nitrite detected ranged from 1.20 to 10.39 mM (average 6.15 mM, *SD* 2.17 mM, **Supplementary Table S2**), suggesting that some bacteria produced (part of the) nitrite by other pathways than nitrate reduction.

After 4 h, the average nitrate reduced by the 53 isolates was 33.74% (*SD* 23.11%) and after 7 h this value increased to 86.95% (*SD* 19.92%). The starting OD of the medium was 0.01 and went up to an average OD of 0.40 (*SD* 0.19) after 4 h and OD 1.06 (*SD* 0.56) after 7 h. Isolates with acidogenic properties were excluded from the selection of potential probiotics, as acid production of isolates is associated with dental caries risk (Sanz et al., 2017). Only one nitrate-reducing isolate (i.e., D1P3 *A. oris*) acidified the pH of the glucose-containing BHI medium (starting pH 7.3) to pH 6.5 after 7 h of growth and the average of all isolates was pH 7.02 (*SD* 0.17), indicating there was little caries-associated acidification. With regard to this, one *S. salivarius* isolate, which was excluded because it did not reduce nitrate, lowered the pH to 5.5 under the same conditions.

When comparing all 23 *R. mucilaginosa* isolates and 21 *R. dentocariosa* isolates, *R. mucilaginosa* grew 1.39× more ($p < 0.05$, **Figure 3B**) and reduced 1.79× more nitrate ($p < 0.01$, **Figure 3A**) after 4 h. After 7 h there were no significant difference in OD and nitrate-reduction between the two species, but *R. mucilaginosa* had significantly decreased the pH by 0.1 points ($p < 0.05$, **Figure 3C**). This pattern of pH difference was consistent when comparing *R. mucilaginosa* and *R. dentocariosa* of donor 1 ($p < 0.05$) and donor 4 ($p = 0.094$, **Supplementary Figure S1**), which were the only two donors with enough isolates for an intra-donor comparison.

Selection of Probiotic Candidates

Thirty-three isolates reduced 100% nitrate after 7 h (**Table 1**) and from these bacteria, 9 isolates were selected that grew to a final OD > 1.5 after 7 h (i.e., they grew well under aerobic conditions relevant for large-scale production, **Table 1**) for further analysis. These corresponded to three *R. dentocariosa* isolates from donor 1 (D1P10, D1P17, and D1P15) and three *R. mucilaginosa* isolates from donor 4 (D4T4, D4T6, and D4T9), which allowed to study strain differences. The other three isolates were *R. aeria* isolate D1P7 and *R. mucilaginosa* isolates D3T4 and D5T11. Additionally, an isolate from another donor (D4P7, *R. dentocariosa*) was added to the selection for inter-donor comparison of *R. dentocariosa* with the isolates of donor 1. These 10 selected isolates were further studied by whole genome sequencing, genome analysis and nitrate reduction quantification under different pH levels, and their effect on *in vitro* oral communities was tested.

Genome Analysis and Identification of Possible Virulence Genes

After the whole genome sequencing procedure, sequences obtained by Illumina and Oxford Nanopore Technologies (ONT) procedures were quality-filtered, corrected and combined to produce a final assembly (**Table 2**). The genome sequences of all 10 isolates could be assembled into one single contig, except the sequences of D5T11 (**Supplementary Table S3**), which had less ONT sequences that passed the quality filter (only 8.73%).

Average nucleotide identity (ANI) values for the whole genomes confirmed that the five isolates from plaque corresponded to *R. dentocariosa* (D1P10, D1P17, D1P15, and D4P7) and *Rothia aeria* (D1P7), while all isolates from the tongue were closely related to the reference strain of *R. mucilaginosa* ATCC2296. Interestingly, when comparing the 10 genomes with each other, it appeared that isolates from the tongue of donor 4 (D4T4, D4T6, and D4T9) could belong to the same strain (sequence similarity at homologous regions > 99.9%, **Table 2**) and all *R. dentocariosa* studied were clearly different strains (ANI values 95–97%), indicating that within the same individual there may be substantial intra-specific genetic heterogeneity, confirming the phenotypic heterogeneity previously detected (**Figure 2** and **Table 1**).

According to a FAO/WHO (2002), newly registered probiotic strains must be examined in pathological, genetic, toxicological, immunological, and microbiological aspects that could be relevant for human safety (FAO/WHO, 2002). Thus, mobile genetic elements (MGEs), antimicrobial resistance genes (ARGs) and virulence factors databases were used to determine if the 10 genomes contained any of these genetic elements, which could make them unsuitable for probiotic usage.

No virulence factors nor ARGs were found in any of the studied genomes (**Supplementary Table S4**). Several MGEs were found in the genomes of D1P7 and D1P17. These MGEs corresponded to methyltransferases or transposases previously identified in *Corynebacterium* species, which could correspond to horizontal gene transfer events from this genus, which is a common inhabitant of the oral cavity. Specifically, D1P7 had a double insertion of a transposase (tnp1249) in two close genomic regions and both D1P7 and D1P17 had three insertions of three different 23 rRNA methyltransferases: erm(X), ermCX, and ermLP. Based on the genome analysis all 10 isolate could be suitable strains for probiotics due to their absence of known virulence factors and antibiotic resistance genes.

Genome annotation revealed that all selected isolates contained genes encoding nitrate transport proteins, nitrate to nitrite reduction, denitrification and DNRA (dissimilatory nitrate reduction to ammonia) enzymes (**Figure 4**). In addition, the genes encoding further reduction of nitric oxide to nitrous

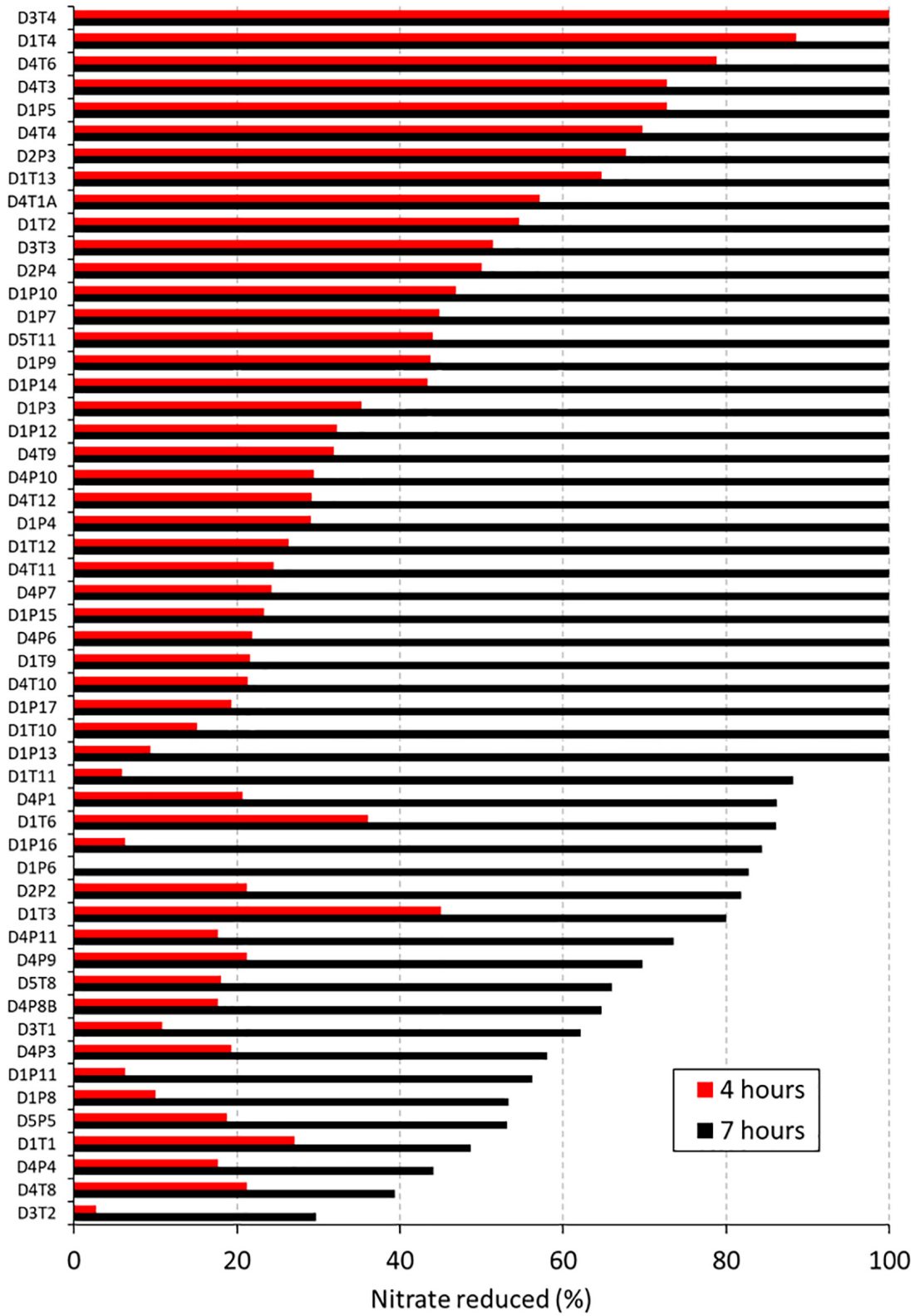

FIGURE 2 | Nitrate reduction capacity of 53 isolates (1st screening). Bars show the percentage of nitrate reduced by 53 isolates after 4 h (red bars) and 7 (black bars) hours of incubation at 37°C under aerobic conditions with starting OD 0.01. Values represent the percentage of initially added nitrate (6.5 mM) that had been used up after 4 or 7 h of incubation. Codes of the 53 isolates are shown on the right, where D relates to the donor, T refers to tongue coating and P to dental plaque samples.

TABLE 1 | Confirmed nitrate-reducing isolates sorted by % nitrate reduced and optical density (OD) at 7 h.

Isolate	Species (16S BLAST)	Nitrate reduced (%)		OD		pH spent medium	
		4 h	7 h	4 h	7 h	4 h	7 h
D1P10*	*Rothia dentocariosa* ATCC17931	46.88	100.00	0.77	2.56	7.10	6.90
D3T4*	*Rothia mucilaginosa* DSM20746	100.00	100.00	1.00	2.16	7.10	6.80
D1P7*	*Rothia aeria* A1-17B	44.83	100.00	0.64	2.00	7.30	7.00
D4T4*	*Rothia mucilaginosa* DSM20746	69.70	100.00	0.65	1.97	7.20	6.80
D4T3	*Rothia mucilaginosa* DSM20746	72.73	100.00	0.69	1.96	7.20	6.70
D1P17*	*Rothia dentocariosa* ATCC17931	19.35	100.00	0.54	1.88	7.20	7.10
D4T6*	*Rothia mucilaginosa* DSM20746	78.79	100.00	0.79	1.87	7.20	6.80
D1P9	*Rothia dentocariosa* ATCC17931	43.75	100.00	0.57	1.76	7.20	7.20
D1P15*	*Rothia dentocariosa* ATCC17931	23.33	100.00	0.41	1.63	7.25	7.10
D4T9*	*Rothia mucilaginosa* DSM20746	31.91	100.00	0.57	1.60	7.20	7.10
D1P14	*Rothia aeria* A1-17B	43.33	100.00	0.48	1.56	7.30	7.10
D5T11*	*Rothia mucilaginosa* DSM20746	44.00	100.00	0.59	1.56	7.25	7.10
D1P12	*Rothia aeria* A1-17B	32.26	100.00	0.44	1.42	7.30	7.10
D1T4	*Rothia mucilaginosa* DSM20746	88.57	100.00	0.65	1.38	7.00	6.80
D1T13	*Rothia mucilaginosa* DSM20746	64.71	100.00	0.68	1.34	7.10	6.70
D4T12	*Rothia mucilaginosa* DSM20746	29.17	100.00	0.49	1.27	7.20	7.10
D1P13	*Rothia dentocariosa* ATCC17931	9.38	100.00	0.45	1.27	7.30	7.20
D1T9	*Rothia mucilaginosa* DSM20746	21.62	100.00	0.44	1.22	7.10	6.90
D1T12	*Rothia mucilaginosa* DSM20746	26.32	100.00	0.35	1.12	7.20	7.20
D4T10	*Rothia mucilaginosa* DSM20746	21.28	100.00	0.50	1.07	7.20	7.10
D4T1A	*Rothia mucilaginosa* DSM20746	57.14	100.00	0.44	1.04	7.20	7.00
D1T10	*Rothia mucilaginosa* DSM20746	15.15	100.00	0.29	1.03	7.30	7.10
D4T11	*Rothia mucilaginosa* DSM20746	24.49	100.00	0.41	0.96	7.30	7.10
D3T3	*Rothia mucilaginosa* DSM20746	51.35	100.00	0.33	0.85	7.20	7.00
D4P10	*Rothia dentocariosa* ATCC17931	29.41	100.00	0.35	0.81	7.10	7.00
D4P7*	*Rothia dentocariosa* ATCC17931	24.24	100.00	0.26	0.73	7.20	7.10
D4P6	*Rothia dentocariosa* ATCC17931	21.88	100.00	0.23	0.67	7.30	7.10
D2P4	*Rothia dentocariosa* ATCC17931	50.00	100.00	0.27	0.61	7.10	6.70
D1T2	*Rothia mucilaginosa* DSM20746	54.55	100.00	0.20	0.59	7.00	6.80
D1P3	*Actinomyces oris* ATCC27044	35.29	100.00	0.18	0.53	7.00	6.50
D2P3	*Rothia aeria* A1-17B	67.74	100.00	0.18	0.44	7.00	6.80
D1P5	*Rothia dentocariosa* ATCC17931	72.73	100.00	0.18	0.43	7.00	7.00
D1P4	*Rothia dentocariosa* ATCC17931	29.03	100.00	0.19	0.41	7.00	6.90
D1T11	*Rothia mucilaginosa* DSM20746	5.88	88.24	0.20	0.82	7.20	7.00
D4P1	*Rothia dentocariosa* ATCC17931	20.69	86.21	0.53	1.85	7.20	6.90
D1T6	*Rothia mucilaginosa* DSM20746	36.11	86.11	0.43	0.79	7.10	7.00
D1P16	*Rothia dentocariosa* ATCC17931	6.25	84.38	0.32	1.11	7.20	7.20
D1P6	*Rothia dentocariosa* ATCC17931	0.00	82.76	0.36	1.00	7.30	7.10
D2P2	*Rothia dentocariosa* ATCC17931	21.21	81.82	0.06	0.19	7.00	6.90
D1T3	*Rothia mucilaginosa* DSM20746	45.00	80.00	0.42	0.74	7.20	7.00
D4P11	*Rothia dentocariosa* ATCC17931	17.65	73.53	0.24	0.61	7.30	7.20
D4P9	*Rothia dentocariosa* ATCC17931	21.21	69.70	0.21	0.54	7.30	7.20
D5T8	*Rothia mucilaginosa* DSM20746	18.00	66.00	0.23	0.81	7.20	7.20
D4P8B	*Rothia dentocariosa* ATCC17931	17.65	64.71	0.24	0.45	7.20	7.20
D3T1	*Rothia dentocariosa* ATCC17931	10.81	62.16	0.25	0.48	7.20	7.10
D4P3	*Actinomyces viscosus* JCM8353	19.35	58.06	0.44	1.25	7.30	7.10
D1P11	*Rothia dentocariosa* ATCC17931	6.25	56.25	0.32	0.92	7.30	7.30
D1P8	*Rothia dentocariosa* ATCC17931	10.00	53.33	0.33	0.90	7.30	7.20
D5P5	*Actinomyces viscosus* JCM8353	18.75	53.13	0.24	0.57	7.20	7.10
D1T1	*Rothia mucilaginosa* DSM20746	27.03	48.65	0.29	0.50	7.20	7.10
D4P4	*Actinomyces viscosus* JCM8353	17.65	44.12	0.24	0.47	7.20	7.10
D4T8	*Actinomyces oris* JCM16131	21.21	39.39	0.24	0.49	7.20	7.10
D3T2	*Rothia mucilaginosa* DSM20746	2.70	29.73	0.18	0.23	7.20	7.10
Average (*SD*)	–	33.74 (23.11)	86.95 (19.92)	0.40 (0.19)	1.06 (0.56)	7.19 (0.10)	7.02 (0.17)

**Final selection of 10 nitrate-reducing isolates of interest.*

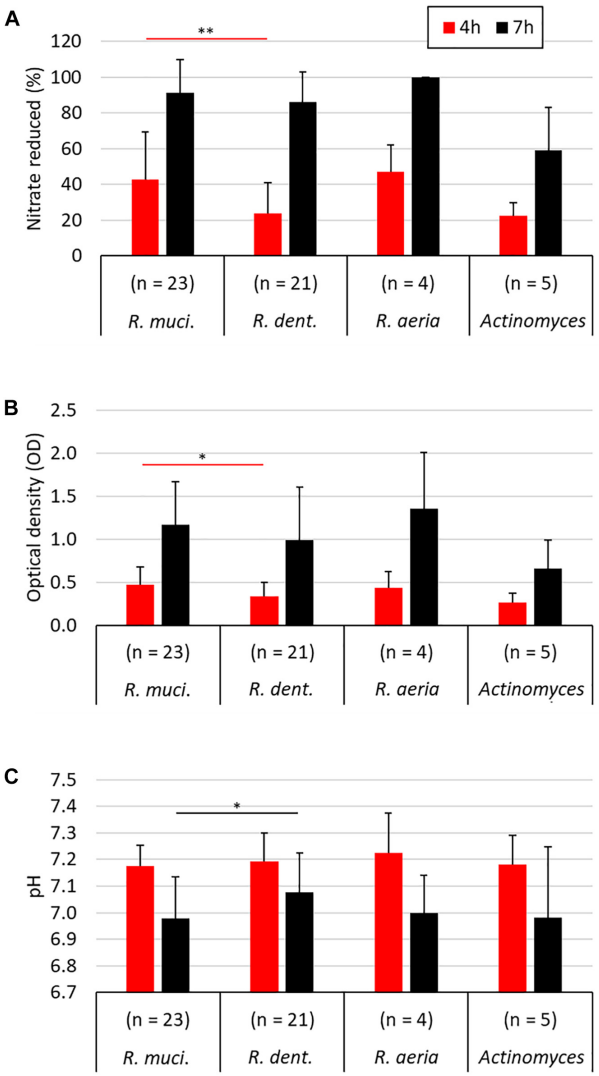

FIGURE 3 | Comparison of different nitrate-reducing species isolated in the current work after 4 and 7 h of growth with 6.5 mM nitrate. The different *Rothia* species are grouped separately (23 *R. mucilaginosa* isolates, 21 *R. dentocariosa* isolates, and 4 *R. aeria* isolates) and all five *Actinomyces* isolates are represented together. Bars represent the nitrate reduced **(A)**, optical density **(B)**, and medium pH **(C)** after 4 and 7 h of growth. Only *R. mucilaginosa* (*R. muci*.) and *R. dentocariosa* (*R. dent*.), to which most isolates belonged, were statistically compared (Mann–Whitney *U* test). $^{*}p < 0.05$, $^{**}p < 0.01$.

oxide (N_2O) and detoxification of nitric oxide to nitrate (*hmp* gene) were also found, but no gene for reduction of N_2O to nitrogen (N_2) was detected, nor for fixation of N_2 to ammonia. A large set of molybdenum (Mb) transport proteins and molybdopterins was also found, in agreement with molybdenum being a vital cofactor for bacterial nitrate reduction enzymes. A diverse array for genes involved in lactate metabolism was also present in all fully sequenced strains. A full list of genes involved in nitrate metabolic pathways and lactate utilization are shown in **Supplementary Data Sheet 1**.

Isolate-Specific Effect of pH on Nitrate-Reduction

The 10 selected isolates were incubated during 5 h with 6.5 mM of nitrate at three different pH levels (pH 6.0, 7.0, and 7.5, **Figure 5**). There were some isolate-dependent effects of the pH on nitrate reduction. For example, D1P7 reduced 100% of nitrate after 5 h of incubation at pH 7.5 and pH 7, but reduced 51.72% of nitrate when grown at pH 6.0. Opposite to D1P7, D4T6 reduced 76.67% of nitrate when pH was 6.0, but it reduced only 35.19% of nitrate at a pH of 7.5.

The amount of nitrite detected was normalized by the amount of nitrate reduced, taking into account a 1:1 molar conversion of nitrate to nitrite (nitrite detected, **Figure 5C**). Interestingly, at pH 6.0 more nitrite appeared to be further reduced to other compounds compared to pH 7 and pH 7.5 (both $p < 0.01$). Specifically, 65.46% (*SD* 11.48%) of the reduced nitrate was detected as nitrite, which means that the other 34.54% had been converted to other compounds (e.g., reduction to nitric oxide or ammonia). It should be noted that no ammonium was detected in any of the cultures. At pH 7 and 7.5, the average percentage of nitrite detected was 116.16% (*SD* 16.76%) and 128.62% (*SD* 25.75%). This implies that 16.16% and 28.62%, respectively, of nitrite detected could not be explained by reduction of the 6.5 mM added nitrate, indicating that nitrite is, in part, being produced by other pathways than nitrate reduction.

Six isolates (D1P7, D3T4, D4T4, D4T6, D4T9, and D5T11) reduced nitrate equal to or above the median at two or three of the pH levels (**Supplementary Table S5**) and were selected to test their effects when added to *in vitro* complex oral communities.

Effect of Isolates on *in vitro* Oral Community Metabolism

The effect of the *R. aeria* isolate D1P7 and five *R. mucilaginosa* isolates (D3T4, D4T4, D4T6, D4T9, and D5T11) on oral community metabolism was tested *in vitro*. For this, biofilms were grown from saliva of nine different donors during 7 h with and without 6.5 mM nitrate (**Figure 6**). In these nine independent experiments, the levels of reduced nitrate were higher in the presence of any of the six isolates compared to the "no isolate" condition ($p < 0.05$, **Figure 6A**). Furthermore, the addition of isolates to the *in vitro* oral communities led to more nitrite production (**Figure 6B**), which was significant for D4T4, D4T6, D4T9, and D5T11 ($p < 0.05$), but not D1P7 ($p = 0.11$) and D3T4 ($p = 0.051$). Interestingly, D1P7 addition led to 100% of nitrate reduction in all donors, which indicates that nitrite was further metabolized into other compounds (e.g., ammonia or nitric oxide) when adding this isolate.

The BHI medium contains glucose (2 g/l) and this leads to acidification by oral communities over time. Regarding this, lactate correlated negatively with pH ($R = -0.820$, $p < 0.01$ in the control condition and -0.778, $p < 0.05$ in the nitrate condition). Importantly, 6.5 mM nitrate supplementation always led to a smaller decrease in pH after 7 h (**Figure 6E**) compared to 0 mM nitrate ($p < 0.05$). In communities with added isolates, this appeared to be, at least partly, due to lactate

TABLE 2 | Whole genome sequence analysis, assembly information and species identification of the 10 selected isolates.

Isolate	Illumina sequences	ONT sequences	ONT mean length (bp)	Estimated genome size (bp)	Contigs	Mean coverage	Closest sequenced genome	ANI value*
D1P7	1.427.028	43.207	8.085	2.654.231	1	74×	*Rothia aeria* C6B	97,4
D1P10	1.649.834	34.991	9.775	2.486.471	1	93×	*Rothia dentocariosa* NCTC10917	96,58
D1P15A	195.232	19.010	9.637	2.496.211	1	33×	*Rothia dentocariosa* NCTC10917	96,17
D1P17	259.928	52.125	12.066	2.566.927	1	39×	*Rothia dentocariosa* NCTC10917	96,52
D3T4	2.206.376	23.696	7.854	2.296.981	1	226×	*Rothia mucilaginosa* ATCC2296	95,41
D4P7	263.877	114.000	8.649	2.511.012	1	42×	*Rothia dentocariosa* NCTC10917	96,31
D4T4	3.773.501	19.976	11.083	2.283.903	1	390×	*Rothia mucilaginosa* ATCC2296	93,87
D4T6	207.423	27.874	10.981	2.276.594	1	35×	*Rothia mucilaginosa* ATCC2296	93,87
D4T9	3.731.259	70.368	8.875	2.297.550	1	382×	*Rothia mucilaginosa* ATCC2296	93,87
D5T11	365.174	941	9.342	924.739*2	30	55×	*Rothia mucilaginosa* ATCC2296	94,54

*An ANI value >94% to the reference genome is considered to correspond to the same species (Richter and Rosselló-Móra, 2009). *2In this case, the genome size could not be estimated and the sum of the contigs is presented.*

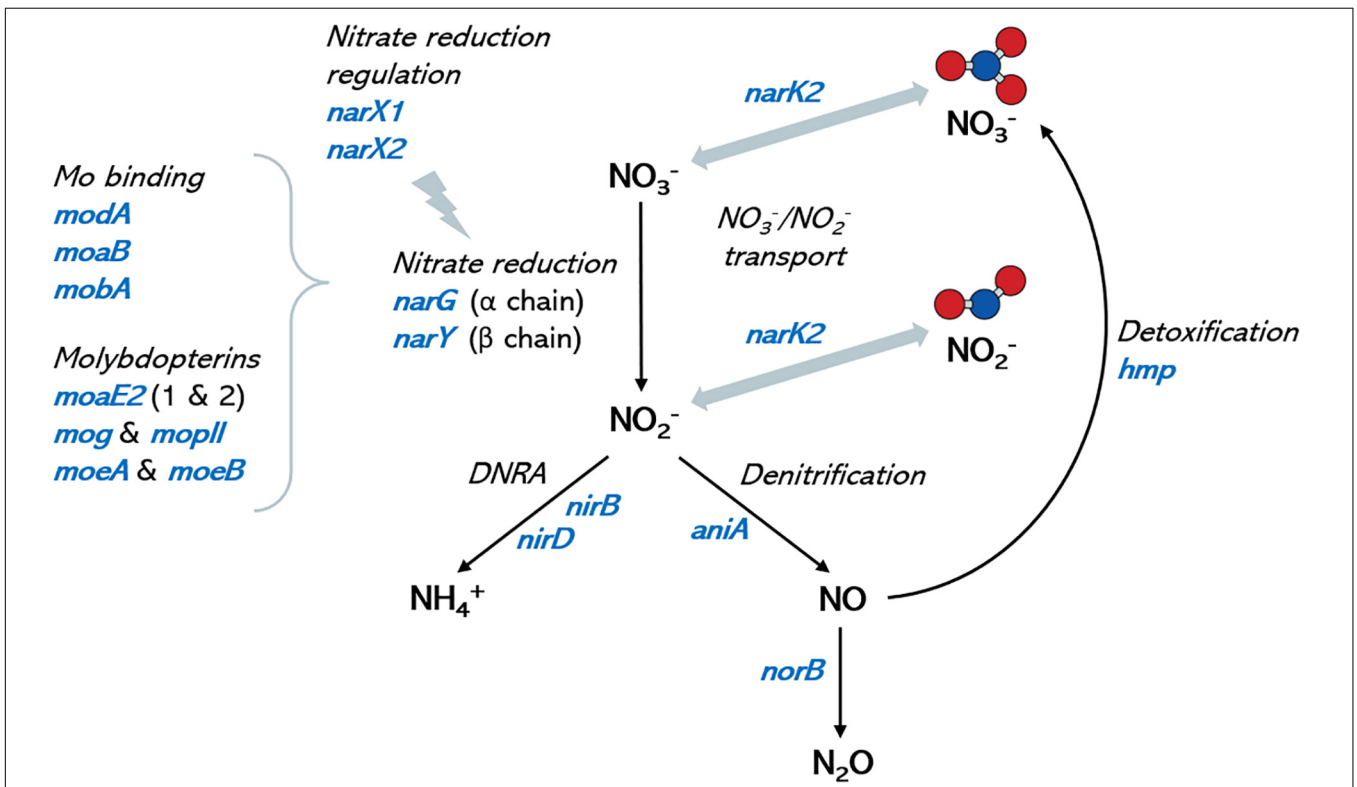

FIGURE 4 | Nitrate metabolism genes in oral *Rothia* isolates. Graph shows a schematic representation of the nitrate metabolic pathways (depicted in black italic text) and the corresponding coding genes (in blue) that have been identified in the genomes of the oral isolates sequenced in the current manuscript. Molybdenum is a cofactor in nitrate reductase enzymes and identified molybdenum-related genes are included for reference. No genes for the reduction of nitrous oxide (N_2O) to nitrogen (N_2), nor for the oxidation of ammonia to nitrite were found. DNRA: dissimilatory nitrate reduction to ammonia. Ammonium production is proposed as a mechanism of pH buffering in the oral cavity, and nitric oxide is an antimicrobial molecule. A full list of genes in the different isolates can be found in **Supplementary Data Sheet 1**.

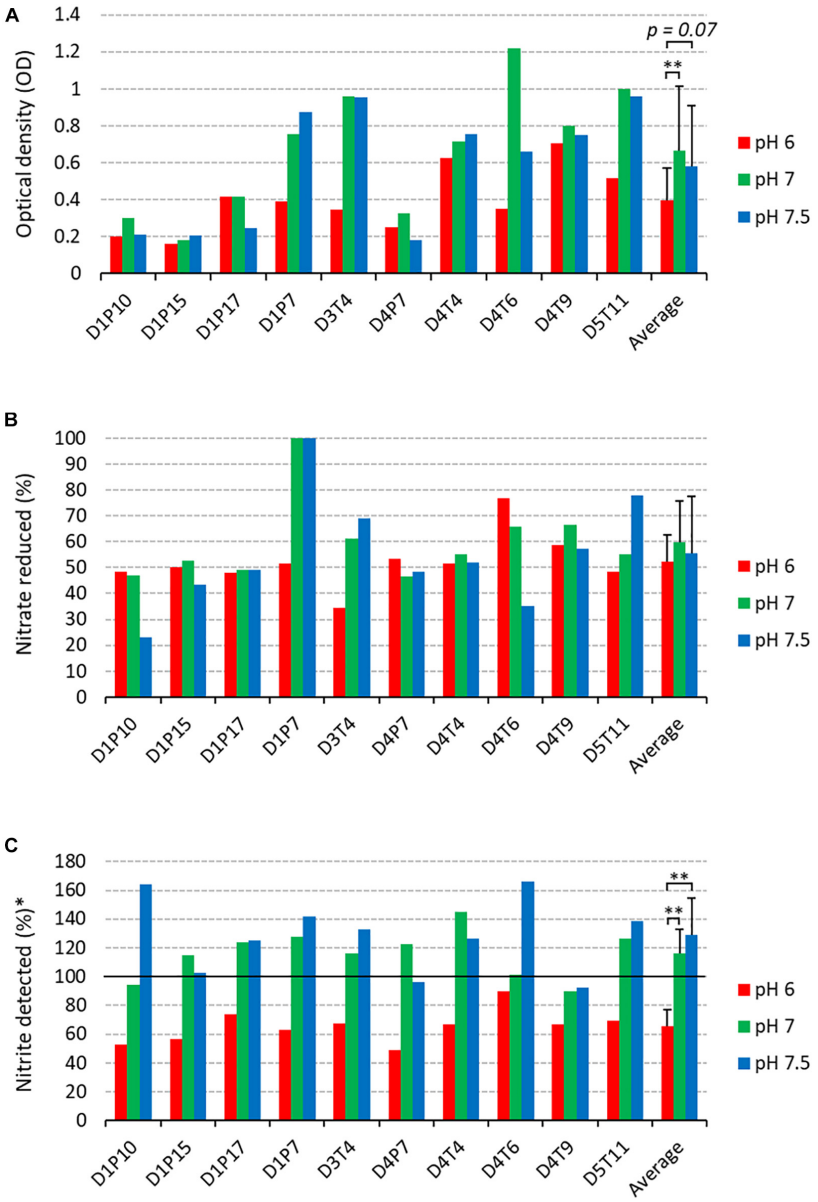

FIGURE 5 | Nitrate reduction capacity of isolates at 3 pH levels (2nd screening). Bars show results after 5 h of incubation (37°C) at pH 6 (red bars), pH 7 (green bars), and pH 7.5 (blue bars) under aerobic conditions with starting OD 0.01. **(A)** Final optical density values. **(B)** Percentage of initially added nitrate (6.5 mM) that had been used up after 4 and 7 h of incubation. **(C)** Amount of nitrite detected, represented as a percentage of nitrate reduced (100 × mM nitrite detected/mM nitrate reduced). Reference codes of the 10 isolates are shown at the bottom, where D relates to the donor, T refers to tongue coating and P to dental plaque samples. $^{**}p < 0.01$ according to a Wilcoxon test comparing all 10 isolates at different pH levels.

consumption: lower amounts of lactate were detected when combining nitrate with isolates compared to isolates without nitrate (**Figure 6D**, p = 0.008–0.110), which was significant for D1P7, D4T4, and D4T9 ($p < 0.05$), whereas there were no significant differences in the detected levels of ammonium. Only one isolate (D3T4), when combined with nitrate (i.e., symbiotic combination), significantly prevented the pH drop due to sugar metabolism more than when just adding nitrate without any of the isolates (i.e., a prebiotic treatment, $p < 0.05$). Another isolate, D4T4, showed a trend of increasing ammonium production without nitrate addition (i.e., a probiotic treatment, $p = 0.051$).

Nitrate Reduction and Ammonium Production in Communities Without Isolates

In communities without isolates, there was no significant difference in lactate levels between the nitrate and control conditions after 7 h. Additionally, the ammonium detected

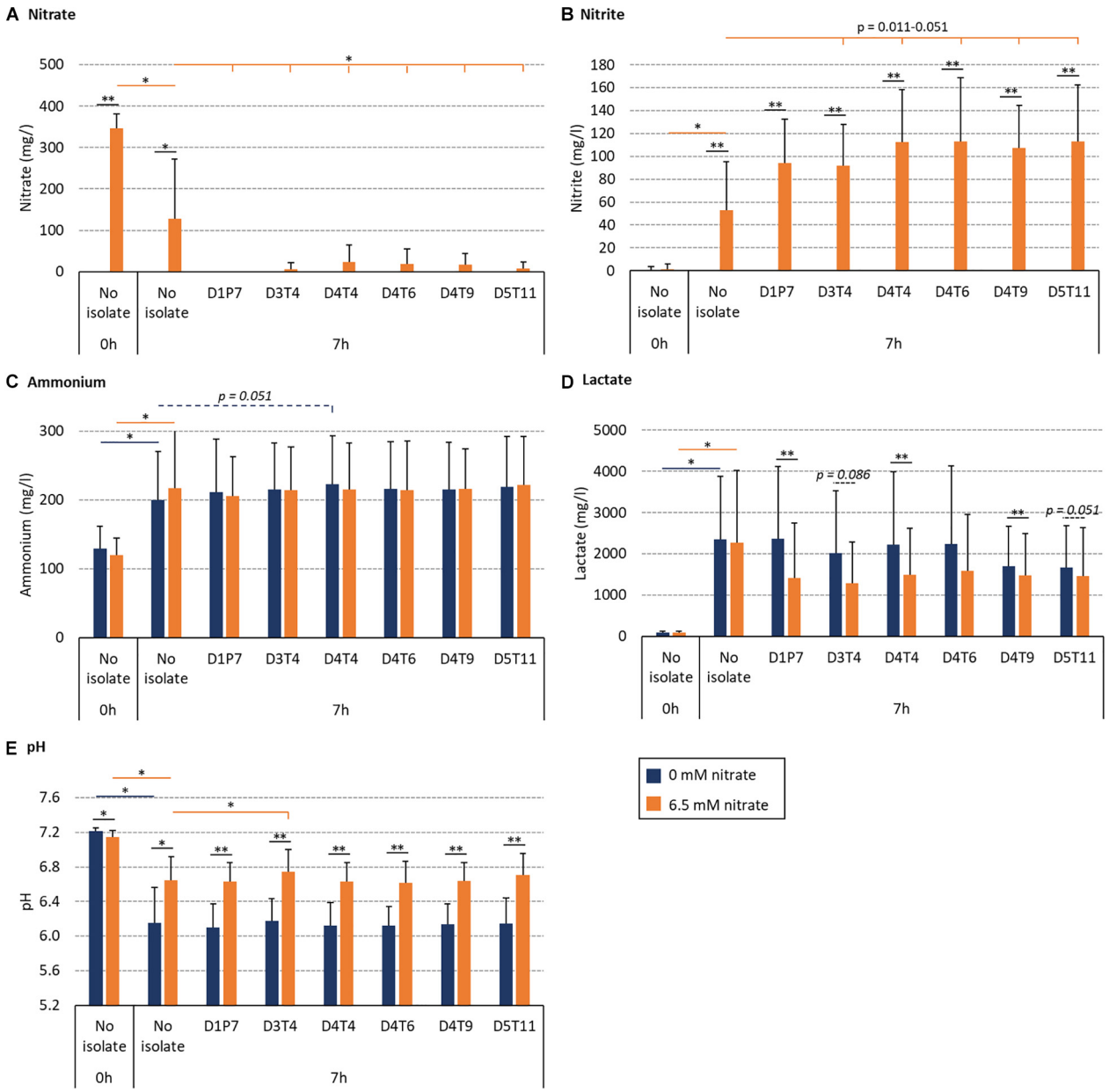

FIGURE 6 | Effect of nitrate and six nitrate-reducing isolates on oral microcosm community metabolism. Bar plots show averages and standard deviations of supernatant measurements. Saliva of 9 donors was incubated with nutrient-rich medium to form *in vitro* oral biofilm with 6.5 mM nitrate (orange) or without nitrate (blue). Values correspond to measurements before incubation (0 h, which is the initial mixture of saliva and medium) and after 7 h of incubation. **(A)** Nitrate (mg/l), **(B)** nitrite (mg/l), **(C)** ammonium (mg/l), **(D)** lactate (mg/l), and **(E)** pH. All conditions with and without nitrate were compared (black lines with *p*-values). Additionally, conditions with isolates (D3T4, D4T4, D4T6, D4T9, and D5T11) were compared with the conditions without an isolate (i.e., no isolate): dark blue lines with *p*-values compare 0 mM nitrate conditions and orange lines with *p*-values compare 6.5 mM nitrate conditions. $^{*}p < 0.05$, $^{**}p < 0.01$ according to a Wilcoxon test.

did not differ significantly ($p = 0.170$). Nevertheless, the two individuals that produced the largest increase of ammonium resulting from nitrate supplementation (D5 and D13) reduced 100% of the nitrate after 7 h (**Figure 7**). Additionally, there was a clear correlation between the NRC of communities and ammonium production ($R = -0.833$, $p < 0.01$, between nitrate left and ammonium produced after 7 h, **Figure 7A**) which, unexpectedly, was also found in the control condition ($R = -0.814$, $p < 0.01$, **Figure 7B**). This indicates that communities with a better NRC are able to produce more ammonium even in the absence of nitrate, while nitrate can further increase ammonium accumulation in some individuals.

The DNA of the 7 h biofilms of two donors (D6 and D11, corresponding to a donor with above average and the lowest NRC, respectively) was analyzed by 16S rRNA Illumina sequencing. The isolates, which were added together with

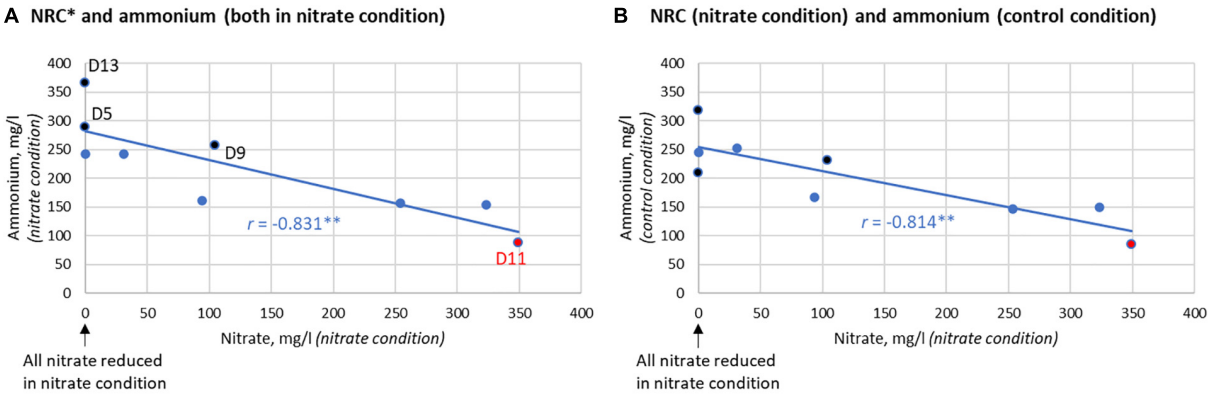

FIGURE 7 | Correlation between nitrate reduction capacity (NRC) and ammonium production after 7 h. **(A)** Correlation between the nitrate reduction capacity (NRC), as determined by how much nitrate is left after incubation, and the ammonium detected in the nitrate condition ($R = -0.831$, $p < 0.01$). **(B)** Correlation between NRC and the ammonium produced in the control condition ($R = -0.814$, $p < 0.01$). This correlation indicates that the bacterial communities of donors that reduce nitrate efficiently are also capable of producing more ammonium in the absence of nitrate. The three donors that clearly produced more ammonium in the nitrate condition compared to the control condition are marked in black (from most to least extra ammonium production: D5 > D13 > D9). D5 and D13 were also two out of the three donors that reduced 100% of nitrate after 7 h. D11 had little to no nitrate reduction activity (marked in red).

the saliva inoculum, appeared to colonize the initial biofilms successfully, as indicated by a higher relative abundance of the corresponding species in 16S rRNA sequencing data (**Supplementary Table S6**). The *Rothia* species increased more when adding the isolate and nitrate than when only adding the isolate ($p < 0.05$), which is an indication of active growth stimulated by nitrate.

The Effect of Nitrate and Probiotic Addition in Donors With Different Nitrate Reduction Capacities (NRC)

When growing *in vitro* biofilms with the saliva of donor D11 in the presence of nitrate, nitrate did not decrease compared to the baseline (**Figures 6**, **7**) and virtually no nitrite was produced, showing that the oral microbiota of this donor had a dramatically low NRC. However, a large percentage of nitrate was reduced when adding any of the isolates and the concentration of nitrite also increased notably (**Figure 6B**). This indicates that the addition of a probiotic was able to compensate the lack of NRC in this donor. When the same experiment was performed with the saliva of donors D5, D9, and D13, all added nitrate was reduced after 7 h, even in the absence of isolates. This suggests that these donors have a high NRC and the addition of nitrate alone is enough to promote nitrate reduction.

DISCUSSION

The nitrate–nitrite–nitric oxide pathway, which depends on nitrate-reduction by oral bacteria, contributes significantly to systemic nitric oxide levels and appears to be important for oral and systemic health (Doel et al., 2004; Kapil et al., 2013; Hezel and Weitzberg, 2015; Jockel-Schneider et al., 2016; Lundberg et al., 2018; Rosier et al., 2018; Rosier et al., 2020). Apart from the stimulation of this pathway with nitrate supplementation, which can result in beneficial cardio-metabolic and oral effects (Lundberg et al., 2018), nitrate reduction could also be promoted with the aid of nitrate-reducing probiotic bacteria (Rosier et al., 2018; Rosier et al., 2020). In the current *in vitro* study we isolate and select potential nitrate-reducing oral probiotics and demonstrate that the NRC of oral communities can be enhanced with newly isolated *Rothia* strains even in communities with little to no NRC. Our data show that nitrate by itself (prebiotic treatment) or combined with a nitrate-reducing isolate (symbiotic combination) prevented pH drops due to sugar metabolism, and some of the symbiotic combinations increased lactate consumption. A higher local pH and lactate consumption can prevent the development of cavities, suggesting a possible anti-caries potential of these isolates. Under certain conditions, nitrite was further reduced by isolates, but no ammonia was detected in the medium, suggesting that part of it may be converted to nitric oxide. Thus, future work should evaluate the potential contribution of some of these isolates to improve conditions that benefit from nitric oxide availability. This could be provided either by direct bacterial nitric oxide production or by production of nitrite and subsequent transformation into nitric oxide by the acidity of the stomach or at other body sites by human encoded pathways (Hezel and Weitzberg, 2015).

Some authors have criticized the use as oral probiotics of bacteria isolated from dairy products or from the gut, which may hamper their ability to colonize the oral cavity or provide undesired effects (Pham et al., 2009; López-López et al., 2017). We therefore isolated oral strains from healthy individuals and potentially probiotic candidates were selected based on their efficiency to perform an important function of the oral microbiota, namely nitrate reduction. Other selection criteria included a fast aerobic growth rate, lack of acidogenicity (a feature associated to tooth decay), ability to grow when added to *in vitro* oral communities and lack of virulence and antibiotic resistance genes. In total, 53 oxygen-tolerant nitrate-reducing

bacteria were isolated from dental plaque or tongue coating samples from orally and systemically healthy individuals. In a first nitrate-reduction screening, 10/53 isolates were selected as potential probiotic candidates. In a second nitrate-reduction screening under three different pH levels, a final list of 6/10 candidates was completed. The effect of these six *Rothia* isolates on oral microbiota communities was studied, allowing us to evaluate their effect when added to a complex ecosystem, as a first step toward future animal or clinical studies.

Effect on Oral Communities

The six *Rothia* isolates in the final selection were added to saliva and grown together in nutrient-rich medium for 7 h with or without 6.5 mM nitrate. In 7 h, initial biofilms grow with a highly similar bacterial composition to natural oral biofilms (Mira et al., 2019) and, together with planktonic cells, effect the pH and metabolite content of the supernatant. Metabolism of sugar in the medium leads to a decrease in pH, but both nitrate (prebiotic treatment) and the combination of any of the 6 isolates with nitrate (symbiotic combination) limited this decrease in pH compared to the control condition ($p < 0.05$). Li et al. (2007) added 1.5 mM nitrate to bacteria from saliva and also observed a limited sugar-derived pH drop. In a recent study, 6.5 mM nitrate under similar *in vitro* conditions as our study, prevented a pH drop after 5 and 9 h and this was shown to be due to ammonia production and lactate consumption (Rosier et al., 2020). In our current study, ammonia production and lactate consumption after nitrate supplementation was only observed in some cases, and therefore depended on the specific isolate under study or the donor's saliva. Importantly, in both studies, a correlation was found between the NRC of oral communities and ammonia production with or without nitrate. This indicates that bacteria or bacterial processes involved in nitrate reduction are linked to ammonia production under these conditions.

The analysis of the genomes sequenced in the current manuscript reveals that all isolates also contain the gene encoding the nitrite reductase, which metabolizes nitrite into nitric oxide, and this gene is also present in other sequenced *Rothia* isolates. Some authors have determined that environmental factors like pH, the nitrogen:carbohydrate ratio (Kraft et al., 2014) and carbon source (Carlson et al., 2020) influence whether nitrite is converted to ammonia or to nitric oxide by aquatic or soil bacteria and future work should establish which factors switch the metabolic machinery of oral communities toward DNRA or denitrification. It is also notable that a wide array of genes involved in molybdenum transport and capture are present in the genomes of the oral *Rothia* isolates (**Figure 4** and **Supplementary Data Sheet 1**). Thus, the strong molybdenum-related genomic content could partly explain the lower dental caries prevalence in areas of high molybdenum soil concentrations (Ludwig et al., 1960; Schroeder et al., 1970), as the dietary availability of this vital cofactor for nitrate reductase enzymes could contribute to the oral health benefits associated with nitrate reduction (Koopman et al., 2016).

An interesting finding in our study was that one isolate (D3T4), when combined with nitrate (i.e., symbiotic combination), significantly prevented the pH drop due to sugar metabolism more efficiently than when just adding nitrate without any of the isolates (i.e., a prebiotic treatment, $p < 0.05$). Another isolate, D4T4, showed a trend ($p = 0.051$) of increasing ammonium production without nitrate addition (i.e., a probiotic treatment). In relation to this, arginine is effectively used as a prebiotic to stimulate ammonia production and increase the local pH to prevent caries (Liu et al., 2012). The isolates D3T4 and D4T4 could therefore provide similar benefits and this should be further investigated *in vivo*. It should be noted that differences in ammonium detection can also be affected by ammonium consumption (an isolate may produce ammonia but metabolize it into other compounds or incorporate it as a nitrogen source). In fact, the detected levels of nitrite concentrations were often higher than the expected stoichiometric conversion of nitrate to nitrite (especially under alkaline pH), suggesting that nitrite could also be produced by other pathways (e.g., ammonia oxidation or nitrification). Our genome analysis, however, did not detect known ammonia oxidizing pathways (e.g., hydroxylamine oxidoreductase or ammonia monooxygenase) or the presence of genes for nitrogen fixation. Additionally, the oxidation of nitric oxide, which is a very unstable compound, could also favor accumulation of nitrite. Although our genome analysis did not detect bacterial nitric oxide synthases (NOS) that could convert arginine in nitric oxide, it did show the presence of flavohemoprotein, which detoxifies nitric oxide back to nitrate (**Figure 4**). Thus, future genomic and experimental work should aim to identify potential enzymes that could be producing nitrite or nitric oxide by other pathways in addition to nitrate reduction. In addition, future genetic and laboratory studies with controlled carbon, nitrogen and oxygen supplies should shed light on the complex nitrogen cycle that starts to be envisaged in oral communities, and more accurate techniques for measuring the highly unstable and dynamic nitrogen compounds, such as ozone chemiluminescence, may help in the characterization of all pathways involved.

Our data also show that, in the presence of nitrate, *Rothia* isolates can consume lactate, an organic acid which is produced by oral communities and associated to caries development (Bradshaw and Marsh, 1998), as less lactate was detected compared to the conditions of the isolates without nitrate ($p = 0.008$–0.110). On the one hand, nitrate has been shown to increase the salivary pH *in vivo* (Burleigh et al., 2019) and different *in vitro* studies, including this current work, show that nitrate provides resilience against acidification and lactate accumulation (Li et al., 2007; Rosier et al., 2020). On the other hand, nitrate-rich beetroot juice consumption has been shown to increase *Rothia* levels significantly compared to nitrate-depleted beetroot juice (Velmurugan et al., 2016; Vanhatalo et al., 2018). This indicates that *Rothia* species could contribute to the increase in pH and potentially also to resilience against acidification resulting from nitrate supplementation *in vivo*.

Importantly, many periodontitis-associated pathobionts are alkaliphiles and the effect of an increased salivary pH, which can result from nitrate supplementation (Burleigh et al., 2019), on oral communities *in vivo* should be investigated. Notably,

previously, an increase in pH but a decrease in periodontitis-associated genera [some of which have been shown to be sensitive to nitric oxide (Backlund et al., 2014)] was observed after 5 h of incubation of oral communities with nitrate *in vitro* (Rosier et al., 2020). Additionally, nitrate-rich lettuce juice reduced gingival inflammation compared to nitrate-depleted lettuce juice in patients with chronic gingivitis (Jockel-Schneider et al., 2016). This provides preliminary evidence that nitrate supplementation could be beneficial for gum diseases, but this should be further investigated in clinical studies.

Isolates' Habitat Comparison and pH Preference

From all 53 nitrate-reducing isolates obtained in this study under aerobic conditions, 48 were *Rothia* species and five corresponded to *Actinomyces* species. Interestingly, all 23 *R. mucilaginosa* isolates originated from the tongue, while 20/21 *R. dentocariosa* isolates and all 4 *R. aeria* isolates originated from dental plaque. Recently, Wilbert et al. (2020) used Human Microbiome Project data analyzed by Eren et al. (2014) and concluded that *R. mucilaginosa* is strongly associated to the tongue (∼100-fold more abundant than on teeth), while *R. aeria* and *R. dentocariosa* appear to be strongly associated to teeth surfaces (>100-fold more abundant there than on the tongue). Our cultivation-based results confirm that *R. mucilaginosa* mostly lives on the tongue surface and *R. dentocariosa* and *R. aeria* on the teeth. Doel et al. (2005) also obtained 8 *Rothia* isolates from the tongue under aerobic conditions and most (6 out of 8) were *R. mucilaginosa*. In our study, after 4 h of incubation, *R. mucilaginosa* isolates had significantly grown to a higher optical density ($p < 0.05$) and reduced more nitrate than *R. dentocariosa* isolates ($p < 0.01$). Additionally, after 7 h, *R. mucilaginosa* isolates had reduced the pH 0.1 point more ($p < 0.05$), indicating possible differences in metabolism of these species.

The nitrate-reduction capacity of 10 probiotic candidates was evaluated at three different pH levels (pH 6, 7 and 7.5). Some isolates appeared to reduce nitrate at the same rate at all pH levels (e.g., D1P17 or D4T4), while others had a clear preference for a neutral and/or slightly alkaline pH (e.g., D1P7, D3T4, and D5T11) and one isolate reduced most nitrate at an acidic pH (D4T6). Regarding this, differences in oral pH levels among donors can result from host-specific factors such as salivary pH and dietary habits. Additionally, within a single donor, different habitats have different environmental conditions and pH gradients can be found within oral biofilms (Simón-Soro et al., 2013), which could explain intra-donor differences in the pH preference for nitrate-reduction of different stains.

Importantly, our data show that nitrite reduction was consistently stimulated by pH 6 compared to pH 7 and pH 7.5. Nitrite reduction of microbial communities can increase as the pH decreases (Cao et al., 2013). In the mouth this could have an important consequence for oral health, namely the prevention of acidification which is clearly associated with caries development. Arginine deiminase in oral probiotics has been shown to be activated by a low pH (López-López et al., 2017), leading to ammonia production and providing a self-regulatory feedback mechanism against acidification (Rosier et al., 2018). Likewise, nitrite reduction could be stimulated to increase the local pH by lactate consumption and ammonia production (DRNA) or antimicrobial nitric oxide release (denitrification). Similarly, lactate stimulates nitrite consumption which is performed in parallel with lactate consumption (Li et al., 2007). Importantly, non-enzymatic nitrite decomposition into nitric oxide occurs below pH 5.0 (Tiedje, 1988; Schreiber et al., 2010) and this was not the case of this experiment, indicating that enzymatic nitrite conversion of *Rothia* was stimulated by pH 6.0.

The Associations With Health and Disease of *Rothia* and Nitrate

The clear association of *Rothia* with oral health has been discussed previously (Rosier et al., 2020). In short, *Rothia* species are found in higher relative abundance in oral biofilms when comparing healthy individuals with caries active, periodontitis or halitosis patients [see, for example, Belda-Ferre et al. (2012), Griffen et al. (2012), Meuric et al. (2017), Seerangaiyan et al. (2017)]. Related to this, *R. aeria* correlated negatively with inflammatory cytokines IL-17 and TNF-α in humans (Corrêa et al., 2019). Thus, multiple studies indicate that this is genus generally associated with oral health.

Rothia isolates have occasionally been isolated from, and associated with, endocarditis and other systemic disease samples (Binder et al., 1997), indicating that under certain conditions, there are strains that can translocate to other human niches. This is an extended feature of representatives of many oral species, which appear to be pre-adapted to attach to distant human tissues by their ability to adhere to oral mucosa components like collagen and fibronectin (García López and Martín-Galiano, 2020). As a consequence of that, many oral bacteria have been isolated from endocarditis samples, including classic commensals generally recognized as safe ("GRASS" organisms) such as *S. salivarius* (Corredoira et al., 2005), and different species of oral *Gemella*, *Granulicatella*, or *Prevotella*, among others (García López and Martín-Galiano, 2020). Likewise, probiotic Lactobacilli (also considered GRASS) have been isolated from the blood of immunosuppressed patients in intensive care units (Yelin et al., 2019). It is therefore crucial with all oral probiotics to select strains without virulence genes potentially involved in endocarditis or other diseases, which were shown to be absent in all 10 probiotic candidates selected in our study, and future work should perform animal trials to confirm their safety.

The safety and beneficial effects of dietary nitrate in general (Lundberg et al., 2018) and for the oral cavity (Rosier et al., 2020) were recently discussed. It should be noted that nitrate salts added to processed meat are associated with cancer (Bouvard et al., 2015; Etemadi et al., 2017). This nitrate is reduced to nitrite by bacteria in the meat and can further react with other molecules, such as heme, amines and amides, forming potentially carcinogenic *N*-nitroso compounds (Skibsted, 2011;

Sindelar and Milkowski, 2012). However, we obtain most nitrate (>80%) from vegetables that are generally associated with health benefits and considered anticarcinogenic (Link and Potter, 2004; Wang et al., 2014; Turati et al., 2015). Antioxidants and polyphenols in fruits and vegetables prevent the formation, and possibly damage, of *N*-nitroso compounds (Chung et al., 2002; Ward, 2009; Kobayashi et al., 2015; Azqueta and Collins, 2016). In relation to this, different safety agencies concluded that epidemiological studies do not indicate that nitrate intake from diet or drinking water is associated with increased cancer risk (Chain, 2008). The concentrations of nitrate used in this study can be obtained in saliva by vegetable consumption. The application of topical doses of nitrate far below the acceptable daily intake (ADI, 3.7 mg/kg of body weight) would also be sufficient (Rosier et al., 2020). These could be obtained by oral products containing vegetable extracts or low amounts of nitrate salts in combination with antioxidants. The effect of nitrate-reducing probiotics and nitrate in combination with different dietary compounds (e.g., antioxidants and polyphenols) should be explored to make sure that potential future products do not result in harmful *N*-nitroso compounds formation.

Experimental Conditions and Limitations

The aim of our study was to isolate aerobic fast-growing bacteria with a high NRC. All experiments were performed under aerobic conditions with BHI medium that contains 0.2% glucose as a carbon source. Doel et al. (2005) used a different medium (including tryptone, horse serum and 0.5% glucose) under aerobic and anaerobic conditions. In their study, most nitrite-producing isolates obtained in the presence of oxygen were *Rothia* (from the tongue) and *Actinomyces* (from saliva and plaque), but without oxygen, most nitrite-producing bacteria were *Veillonella* and *Actinomyces*, while no *Rothia* was detected. Other isolates in their study included *Staphylococcus*, *Corynebacterium*, and *Haemophilus*, all including species obtained with or without oxygen. The identification of these other species under aerobic conditions may have resulted from differences in medium composition or donor microbiota. Furthermore, in a recent study, it was shown that different carbon sources enrich different nitrate reducers of terrestrial environments (Carlson et al., 2020). Therefore, future work should focus on the isolation of a more diverse set of nitrate-reducing bacteria from the oral cavity using different growth conditions. Additionally, the effect of different nitrate-reducers and nitrate reduction rates on oral communities should be determined. In our study, we tested 6 *Rothia* isolates separately, but combining a variety of isolates, even from different species, could lead to mutualistic interactions and enhanced beneficial effects.

CONCLUSION

Efficient nitrate reduction in the oral cavity has been clearly associated to human health but this metabolic pathway cannot be performed by humans, which lack the necessary enzymes. Thus, oral bacteria capable of nitrate reduction arise as a fascinating example of symbiosis by which the microbiome provides a health-associated benefit to the human host, which in exchange, recycles nitrate by actively concentrating plasma nitrate into the saliva (Hezel and Weitzberg, 2015). In fact, disruption of oral microbial communities by over-use of antiseptics or antibiotics will interfere with the nitrate–nitrite–nitric oxide pathway (Kapil et al., 2013), as well as food habits with low dietary nitrate (Ashworth et al., 2015). As a result of these, humans appear to vary widely in their NRC (Doel et al., 2004; Liddle et al., 2019), with important potential consequences for diseases or conditions that are influenced by a deficit in nitric oxide, ranging from cardiovascular diseases to reduced sport performance or diabetes development, among others (Lundberg et al., 2018). The current work shows that, in oral bacterial communities with a slightly reduced NRC, the supplementation of nitrate may suffice to restore and promote efficient nitrate reduction; however, our data also show that in individuals with extremely low NRC, the addition of a nitrate-reducing probiotic could be instrumental for a recovery of the function. Thus, future work should be performed to further characterize nitrate-reducing probiotics and test their potential efficacy in animal and clinical studies.

DATA AVAILABILITY STATEMENT

The original contributions presented in the study are publicly available. This data can be found in NCBI, under accession number PRJNA658327.

ETHICS STATEMENT

The studies involving human participants were reviewed and approved by Ethical Committee of DGSP-FISABIO (Valencian Health Authority) with code 27-05-2016. The patients/participants provided their written informed consent to participate in this study.

AUTHOR CONTRIBUTIONS

BR and AM contributed to the design of the work and drafted and revised the manuscript. EM-G and BR did the experimental work. PC-E analyzed the bacterial genomes. BR, EM-G, and PC-E contributed to data acquisition and analysis. All authors read and approved the final manuscript.

FUNDING

AM was supported by a grant from the European Regional Development Fund and Spanish Ministry of Science, Innovation and Universities with the reference RTI2018-102032-B-I00, as well as, a grant from the Carlos III Health Institute with the reference DTS16/00230 and a grant from the Valencian Innovation Agency with the reference INNVAL20/19/006. BR

was supported by a grant from the Spanish Ministry of Science, Innovation and Universities with the reference Bio2015-68711-R.

ACKNOWLEDGMENTS

We are very grateful to Dr. Giuseppe D'Auria, Dr. Griselda de Marco, and other members of the FISABIO-Public Health Sequencing and Bioinformatics Service for sequencing the genomes, and to Dr. Beatriz Neves, who is an experienced dentist, for checking the oral health of donors and taking the tongue coating and dental plaque samples. We also want to thank Dr. Maria D. Ferrer, Ms. Sandra Garcia-Esteban, Dr. Arantxa López-López, Ms. Concha Hueso, and Ms. Belén Gimeno Molina for their help with laboratory work. Finally, we are grateful to graphic designer Nicolas Fisher (nicolas.w.fisher@gmail.com) who designed **Figure 1**.

SUPPLEMENTARY MATERIAL

The Supplementary Material for this article can be found online at: https://www.frontiersin.org/articles/10.3389/fmicb.2020.555465/full#supplementary-material

FIGURE S1 | Comparison of two *Rothia* species from two donors. In the graph *R. mucilaginosa* and *R. dentocariosa* isolates of donor 1 and donor 4 are compared after 4 and 7 h of growth. Bars show the percentage of nitrate reduced **(A)**, optical density **(B),** and medium pH **(C)**. $^{*}p < 0.05$, $^{**}p < 0.01$ according to a Mann–Whitney *U* test.

REFERENCES

Altschul, S. F., Madden, T. L., Schäffer, A. A., Zhang, J., Zhang, Z., Miller, W., et al. (1997). Gapped BLAST and PSI-BLAST: a new generation of protein database search programs. *Nucleic Acids Res.* 25, 3389–3402. doi: 10.1093/nar/25.17.3389

Ashworth, A., Mitchell, K., Blackwell, J. R., Vanhatalo, A., and Jones, A. M. (2015). High-nitrate vegetable diet increases plasma nitrate and nitrite concentrations and reduces blood pressure in healthy women. *Public Health Nutr.* 18, 2669–2678. doi: 10.1017/s1368980015000038

Azqueta, A., and Collins, A. (2016). Polyphenols and DNA damage: a mixed blessing. *Nutrients* 8:785. doi: 10.3390/nu8120785

Backlund, C. J., Sergesketter, A. R., Offenbacher, S., and Schoenfisch, M. H. (2014). Antibacterial efficacy of exogenous nitric oxide on periodontal pathogens. *J. Dent Res.* 93, 1089–1094. doi: 10.1177/0022034514529974

Belda-Ferre, P., Alcaraz, L. D., Cabrera-Rubio, R., Romero, H., Simón-Soro, A., Pignatelli, M., et al. (2012). The oral metagenome in health and disease. *ISME J.* 6, 46–56. doi: 10.1038/ismej.2011.85

Binder, D., Zbinden, R., Widmer, U., Opravil, M., and Krause, M. (1997). Native and prosthetic valve endocarditis caused by Rothia dentocariosa: diagnostic and therapeutic considerations. *Infection* 25, 22–26. doi: 10.1007/bf02113502

Bouvard, V., Loomis, D., Guyton, K. Z., Yann, G., Fatiha, E. G., Neela, G., et al. (2015). Carcinogenicity of consumption of red and processed meat. *Lancet Oncol.* 16, 1599–1600.

Bradshaw, D. J., and Marsh, P. D. (1998). Analysis of pH-driven disruption of oral microbial communities in vitro. *Caries Res.* 32, 456–462. doi: 10.1159/000016487

Burleigh, M., Liddle, L., Muggeridge, D. J., Monaghan, C., Sculthorpe, N., Butcher, J., et al. (2019). Dietary nitrate supplementation alters the oral microbiome but does not improve the vascular responses to an acute nitrate dose. *Nitric Oxide* 89, 54–63. doi: 10.1016/j.niox.2019.04.010

Camacho, C., Coulouris, G., Avagyan, V., Ma, N., Papadopoulos, J., Bealer, K., et al. (2009). BLAST+: architecture and applications. *BMC Bioinform.* 10:421. doi: 10.1186/1471-2105-10-421

Cao, X., Qian, D., and Meng, X. (2013). Effects of pH on nitrite accumulation during wastewater denitrification. *Environ. Technol.* 34, 45–51. doi: 10.1080/09593330.2012.679700

Carlson, H. K., Lui, L. M., Price, M. N., Alex, V. C., Trenton, K. W., Adam, M. D., et al. (2020). Selective carbon sources influence the end products of microbial nitrate respiration. *ISME J.* 14, 2034–2045. doi: 10.1038/s41396-020-0666-7

Chain (2008). Opinion of the scientific panel on contaminants in the Food chain on a request from the European Commission to perform a scientific risk assessment on nitrate in vegetables. *EFSA J.* 698, 1–79.

Chen, L., Zheng, D., Liu, B., Yang, J., and Jin, Q. (2016). VFDB 2016: hierarchical and refined dataset for big data analysis–10 years on. *Nucleic Acids Res.* 44, D694–D697.

Chung, M. J., Lee, S. H., and Sung, N. J. (2002). Inhibitory effect of whole strawberries, garlic juice or kale juice on endogenous formation of N-nitrosodimethylamine in humans. *Cancer Lett.* 182, 1–10. doi: 10.1016/s0304-3835(02)00076-9

Corrêa, J. D., Fernandes, G. R., Calderaro, D. C., Mendonça, S. M. S., Silva, J. M., Albiero, M. L., et al. (2019). Oral microbial dysbiosis linked to worsened periodontal condition in rheumatoid arthritis patients. *Sci. Rep.* 9:8379. doi: 10.1038/s41598-019-44674-6

Corredoira, J. C., Alonso, M. P., García, J. F., Casariego, E., Coira, A., Rodriguez, A., et al. (2005). Clinical characteristics and significance of *Streptococcus salivarius* bacteremia and *Streptococcus bovis* bacteremia: a prospective 16-year study. *Eur. J. Clin. Microbiol. Infect. Dis.* 24, 250–255. doi: 10.1007/s10096-005-1314-x

Cutler, C., Kiernan, M., Willis, J. R., Gallardo-Alfaro, L., Casas-Agustench, P., White, D., et al. (2019). Post-exercise hypotension and skeletal muscle oxygenation is regulated by nitrate-reducing activity of oral bacteria. *Free Radic. Biol. Med.* 143, 252–259. doi: 10.1016/j.freeradbiomed.2019.07.035

Doel, J. J., Benjamin, N., Hector, M. P., Rogers, M., and Allaker, R. P. (2005). Evaluation of bacterial nitrate reduction in the human oral cavity. *Eur. J. Oral. Sci.* 113, 14–19. doi: 10.1111/j.1600-0722.2004.00184.x

Doel, J. J., Hector, M. P., Amirtham, C. V., Al-Anzan, L. A., Benjamin, N., and Allaker, R. P. (2004). Protective effect of salivary nitrate and microbial nitrate reductase activity against caries. *Eur. J. Oral Sci.* 112, 424–428. doi: 10.1111/j.1600-0722.2004.00153.x

Eren, A. M., Borisy, G. G., Huse, S. M., and Mark Welch, J. L. (2014). Oligotyping analysis of the human oral microbiome. *Proc. Natl. Acad. Sci. U.S.A.* 111, E2875–E2884.

Etemadi, A., Sinha, R., Ward, M. H., Barry, I. G., Sanford, M. D., Abnet, C. C., et al. (2017). Mortality from different causes associated with meat, heme iron, nitrates, and nitrites in the NIH-AARP Diet and Health Study: population based cohort study. *BMJ* 357:j1957. doi: 10.1136/bmj.j1957

FAO/WHO (2002). *Food and Agriculture Organization - World Health Organization. Report of a Joint FAOWHO Working Group on Drafting Guidelines for the Evaluation of Probiotics in Food*. Geneva: WHO.

Ferrer, M. D., López-López, A., Nicolescu, T., Salavert, A., Méndez, I., Cuñé, J., et al. (2019). A pilot study to assess oral colonization and pH buffering by the probiotic *Streptococcus dentisani* under different dosing regimes. *Odontology* 108, 180–187. doi: 10.1007/s10266-019-00458-y

García López, E., and Martín-Galiano, A. J. (2020). The versatility of opportunistic infections caused by gemella isolates is supported by the carriage of virulence factors from multiple origins. *Front. Microbiol.* 11:524. doi: 10.3389/fmicb.2020.00524

Grant, M. A., and Payne, W. J. (1981). Denitrification by strains of neisseria, kingella, and chromobacterium. *Int. J. Syst. Evol. Microbiol.* 31, 276–279. doi: 10.1099/00207713-31-3-276

Griffen, A. L., Beall, C. J., Campbell, J. H., Firestone, N. D., Kumar, P. S., Yang, Z. K., et al. (2012). Distinct and complex bacterial profiles in human periodontitis and health revealed by 16S pyrosequencing. *ISME J.* 6, 1176–1185. doi: 10.1038/ismej.2011.191

Helmke, A., Hoffmeister, D., Mertens, N., Emmert, S., Schuette, J., and Vioel, W. (2009). The acidification of lipid film surfaces by non-thermal DBD at atmospheric pressure in air. *New J. Phys.* 11:25.

Hezel, M. P., and Weitzberg, E. (2015). The oral microbiome and nitric oxide homoeostasis. *Oral Dis.* 21, 7–16. doi: 10.1111/odi.12157

Holden, N. M., and Scholefield, D. (1995). Paper test-strips for rapid determination of nitrate tracer. *Commun. Soil Sci. Plant Anal.* 26, 1885–1894. doi: 10.1080/00103629509369415

Hyde, E. R., Andrade, F., Vaksman, Z., Parthasarathy, K., Jiang, H., Parthasarathy, D. K., et al. (2014). Metagenomic analysis of nitrate-reducing bacteria in the oral cavity: implications for nitric oxide homeostasis. *PLoS One* 9:e88645. doi: 10.1371/journal.pone.0088645

Jockel-Schneider, Y., Goßner, S. K., Petersen, N., Stölzel, P., Hägele, F., Schweiggert, R. M., et al. (2016). Stimulation of the nitrate-nitrite-NO-metabolism by repeated lettuce juice consumption decreases gingival inflammation in periodontal recall patients: a randomized, double-blinded, placebo-controlled clinical trial. *J. Clin. Periodontol.* 43, 603–608. doi: 10.1111/jcpe.12542

Joshipura, K. J., Muñoz-Torres, F. J., Morou-Bermudez, E., and Patel, R. P. (2017). Over-the-counter mouthwash use and risk of pre-diabetes/diabetes. *Nitric Oxide* 71, 14–20. doi: 10.1016/j.niox.2017.09.004

Kapil, V., Haydar, S. M., Pearl, V., Lundberg, J. O., Weitzberg, E., and Ahluwalia, A. (2013). Physiological role for nitrate-reducing oral bacteria in blood pressure control. *Free Radic. Biol. Med.* 55, 93–100. doi: 10.1016/j.freeradbiomed.2012.11.013

Kobayashi, J., Ohtake, K., and Uchida, H. (2015). NO-rich diet for lifestyle-related diseases. *Nutrients* 17, 4911–4937. doi: 10.3390/nu7064911

Koopman, J. E., Buijs, M. J., Brandt, B. W., Keijser, B. J., Crielaard, W., and Zaura, E. (2016). Nitrate and the origin of saliva influence composition and short chain fatty acid production of oral microcosms. *Microb. Ecol.* 72, 479–492. doi: 10.1007/s00248-016-0775-z

Koren, S., Walenz, B. P., Berlin, K., Miller, J. R., Bergman, N. H., and Phillippy, A. M. (2017). Canu: scalable and accurate long-read assembly via adaptive k-mer weighting and repeat separation. *Genome Res.* 27, 722–736. doi: 10.1101/gr.215087.116

Kraft, B., Tegetmeyer, H. E., Sharma, R., Klotz, M. G., Ferdelman, T. G., Hettich, R. L., et al. (2014). Nitrogen cycling. The environmental controls that govern the end product of bacterial nitrate respiration. *Science* 345, 676–679. doi: 10.1126/science.1254070

Lacroix, C., and Yildirim, S. (2007). Fermentation technologies for the production of probiotics with high viability and functionality. *Curr. Opin. Biotechnol.* 18, 176–183. doi: 10.1016/j.copbio.2007.02.002

Leplae, R., Lima-Mendez, G., and Toussaint, A. (2010). ACLAME: a CLAssification of mobile genetic elements, update 2010. *Nucleic Acids Res.* 38, D57–D61. doi: 10.1093/nar/gkp938

Li, H., Thompson, I., Carter, P., Whiteley, A., Bailey, M., Leifert, C., et al. (2007). Salivary nitrate–an ecological factor in reducing oral acidity. *Oral Microbiol. Immunol.* 22, 67–71. doi: 10.1111/j.1399-302x.2007.00313.x

Liddle, L., Burleigh, M. C., Monaghan, C., Muggeridge, D. J., Sculthorpe, N., Pedlar, C. R., et al. (2019). Variability in nitrate-reducing oral bacteria and nitric oxide metabolites in biological fluids following dietary nitrate administration: an assessment of the critical difference. *Nitric Oxide* 82, 1–10. doi: 10.1016/j.niox.2018.12.003

Link, L. B., and Potter, J. D. (2004). Raw versus cooked vegetables and cancer risk. *Cancer Epidemiol. Biomarkers Prev.* 13, 1422–1435.

Liu, Y. L., Nascimento, M., and Burne, R. (2012). Progress toward understanding the contribution of alkali generation in dental biofilms to inhibition of dental caries. *Int. J. Oral Sci.* 4, 135–140. doi: 10.1038/ijos.2012.54

López-López, A., Camelo-Castillo, A. J., Ferrer García, M. D., Simon-Soro, A., and Mira, A. (2017). Health-associated niche inhabitants as oral probiotics: the case of S*treptococcus dentisani*. *Front. Microbiol.* 8:379. doi: 10.3389/fmicb.2017.00379

Ludwig, T. G., Healy, W. B., and Losee, F. L. (1960). An assoication between dental caries and certain soil conditions in New Zealand. *Nature* 186, 695–696. doi: 10.1038/186695a0

Lundberg, J. O., Carlström, M., and Weitzberg, E. (2018). Metabolic effects of dietary nitrate in health and disease. *Cell Metab.* 28, 9–22. doi: 10.1016/j.cmet.2018.06.007

Lundberg, J. O., and Govoni, M. (2004). Inorganic nitrate is a possible source for systemic generation of nitric oxide. *Free Radic. Biol. Med.* 37, 395–400. doi: 10.1016/j.freeradbiomed.2004.04.027

Mashimo, C., Tsuzukibashi, O., Uchibori, S., and Nambu, T. (2015). Variations of Nitrate-reducing activity in oral *Rothia mucilaginosa*. *J. Oral Tissue Eng.* 13, 18–26.

McArthur, A. G., Waglechner, N., Nizam, F., Yan, A., Azad, M. A., Baylay, A. J., et al. (2013). The comprehensive antibiotic resistance database. *Antimicrob. Agents Chemother.* 57, 3348–3357. doi: 10.1128/AAC.00419-13

Meuric, V., Le Gall-David, S., Boyer, E., Acuña-Amador, L., Martin, B., Fong, S. B., et al. (2017). Signature of microbial dysbiosis in periodontitis. *Appl. Environ. Microbiol.* 83:e0462-17.

Mira, A., Buetas, E., Rosier, B., Mazurel, D., Villanueva-Castellote, Á, Llena, C., et al. (2019). Development of an in vitro system to study oral biofilms in real time through impedance technology: validation and potential applications. *J. Oral Microbiol.* 11:1609838. doi: 10.1080/20002297.2019.1609838

Pham, L. C., van Spanning, R. J., Röling, W. F., Prosperi, A. C., Terefework, Z., Ten Cate, J. M., et al. (2009). Effects of probiotic *Lactobacillus salivarius* W24 on the compositional stability of oral microbial communities. *Arch. Oral Biol.* 54, 132–137. doi: 10.1016/j.archoralbio.2008.09.007

Pomerantz, A., Peñafiel, N., Arteaga, A., Bustamante, L., Pichardo, F., Coloma, L. A., et al. (2018). Real-time DNA barcoding in a rainforest using nanopore sequencing: opportunities for rapid biodiversity assessments and local capacity building. *Gigascience* 7:giy033.

Qu, X. M., Wu, Z. F., Pang, B. X., Jin, L. Y., Qin, L. Z., and Wang, S. L. (2016). From nitrate to nitric oxide: the role of salivary glands and oral bacteria. *J. Dent Res.* 95, 1452–1456. doi: 10.1177/0022034516673019

Richter, M., Rosselló-Móra, R. (2009). Shifting the genomic gold standard for the prokaryotic species definition. *Proc. Natl. Acad. Sci USA* 106, 19126–19131. doi: 10.1073/pnas.0906412106

Richter, M., Rosselló-Móra, R., Oliver Glöckner, F., and Peplies, J. (2016). JSpeciesWS: a web server for prokaryotic species circumscription based on pairwise genome comparison. *Bioinformatics* 32, 929–931. doi: 10.1093/bioinformatics/btv681

Rosier, B. T., Buetas, E., Moya-Gonzalvez, E. M., Artacho, A., and Mira, A. (2020). Nitrate as a potential prebiotic for the oral microbiome. *Sci. Rep.* 10, 12895. doi: 10.1038/s41598-020-69931-x

Rosier, B. T., Marsh, P. D., and Mira, A. (2018). Resilience of the oral microbiota in health: mechanisms that prevent dysbiosis. *J. Dent Res.* 97, 371–380. doi: 10.1177/0022034517742139

Santarpia, R. P., Lavender, S., Gittins, E., Vandeven, M., Cummins, D., and Sullivan, R. (2014). A 12-week clinical study assessing the clinical effects on plaque metabolism of a dentifrice containing 1.5% arginine, an insoluble calcium compound and 1,450 ppm fluoride. *Am. J. Dent.* 27, 100–105.

Sanz, M., Beighton, D., Curtis, M. A., Cury, J. A., Dige, I., Dommisch, H., et al. (2017). Role of microbial biofilms in the maintenance of oral health and in the development of dental caries and periodontal diseases. *Consensus* report of group 1 of the Joint EFP/ORCA workshop on the boundaries between caries and periodontal disease. *J. Clin. Periodontol.* 44, S5–S11. doi: 10.1111/jcpe.12682

Schmieder, R., and Edwards, R. (2011). Quality control and preprocessing of metagenomic datasets. *Bioinformatics* 27, 863–864. doi: 10.1093/bioinformatics/btr026

Schreiber, F., Stief, P., Gieseke, A., Heisterkamp, I. M., Verstraete, W., de Beer, D., et al. (2010). Denitrification in human dental plaque. *BMC Biol.* 8:24. doi: 10.1186/1741-7007-8-24

Schroeder, H. A., Balassa, J. J., and Tipton, I. H. (1970). Essential trace metals in man: molybdenum. *J. Chron. Dis.* 23, 481–499. doi: 10.1016/0021-9681(70)90056-1

Seemann, T. (2014). Prokka: rapid prokaryotic genome annotation. *Bioinformatics* 30, 2068–2069. doi: 10.1093/bioinformatics/btu153

Seerangaiyan, K., van Winkelhoff, A. J., Harmsen, H. J. M., Rossen, J. W. A., and Winkel, E. G. (2017). The tongue microbiome in healthy subjects and patients with intra-oral halitosis. *J. Breath Res.* 6:3.

Simón-Soro, A., Tomás, I., Cabrera-Rubio, R., Catalan, M. D., Nyvad, B., and Mira, A. (2013). Microbial geography of the oral cavity. *J. Dent. Res.* 92, 616–621. doi: 10.1177/0022034513488119

Sindelar, J. J., and Milkowski, A. L. (2012). Human safety controversies surrounding nitrate and nitrite in the diet. *Nitric Oxide* 26, 259–266. doi: 10.1016/j.niox.2012.03.011

Skibsted, L. H. (2011). Nitric oxide and quality and safety of muscle based foods. *Nitric Oxide* 24, 176–183. doi: 10.1016/j.niox.2011.03.307

Tiedje, J. M. (1988). Ecology of denitrification and dissimilatory nitrate reduction to ammonium. *Biol. Anaerob. Microorg.* 717, 179–244.

Turati, F., Rossi, M., Pelucchi, C., Levi, F., and La Vecchia, C. (2015). Fruit and vegetables and cancer risk: a review of southern European studies. *Br. J. Nutr.* 133, S102–S110.

Vanhatalo, A., Blackwell, J. R., L'Heureux, J. E., Williams, D. W., Smith, A., van der Giezen, M., et al. (2018). Nitrate-responsive oral microbiome modulates nitric oxide homeostasis and blood pressure in humans. *Free Radic. Biol. Med.* 124, 21–30. doi: 10.1016/j.freeradbiomed.2018.05.078

Velmurugan, S., Gan, J. M., Rathod, K. S., Khambata, R. S., Ghosh, S. M., Hartley, A., et al. (2016). Dietary nitrate improves vascular function in patients with hypercholesterolemia: a randomized, double-blind, placebo-controlled study. *Am. J. Clin. Nutr.* 103, 25–38. doi: 10.3945/ajcn.115.116244

Walker, B. J., Abeel, T., Shea, T., Priest, M., Abouelliel, A., Sakthikumar, S., et al. (2014). Pilon: an integrated tool for comprehensive microbial variant detection and genome assembly improvement. *PLoS One* 9:e0088645.

Wang, X., Ouyang, Y., Liu, J., Zhu, M., Zhao, G., Bao, W., et al. (2014). Fruit and vegetable consumption and mortality from all causes, cardiovascular disease, and cancer: systematic review and dose-response meta-analysis of prospective cohort studies. *BMJ* 349:g4490. doi: 10.1136/bmj.g4490

Ward, M. H. (2009). Too much of a good thing? Nitrate from nitrogen fertilizers and cancer. *Rev. Environ. Health* 24, 357–363.

Wilbert, S. A., Mark Welch, J. L., and Borisy, G. G. (2020). Spatial ecology of the human tongue dorsum microbiome. *Cell Rep.* 30, 4003–4015. doi: 10.1016/j.celrep.2020.02.097

Yelin, I., Flett, K. B., Merakou, C., Mehrotra, P., Stam, J., Snesrud, E., et al. (2019). Genomic and epidemiological evidence of bacterial transmission from probiotic capsule to blood in ICU patients. *Nat. Med.* 25, 1728–1732. doi: 10.1038/s41591-019-0626-9

Conflict of Interest: AM and BR are co-inventors in a pending patent application owned by the FISABIO Institute, which protects different nitrate-reducing probiotics.

The remaining authors declare that the research was conducted in the absence of any commercial or financial relationships that could be construed as a potential conflict of interest.

frontiers in Microbiology

REVIEW
published: 17 September 2020
doi: 10.3389/fmicb.2020.544490

Probiotics, Prebiotics, Synbiotics, and Paraprobiotics as a Therapeutic Alternative for Intestinal Mucositis

Viviane Lima Batista[1], Tales Fernando da Silva[1], Luís Cláudio Lima de Jesus[1], Nina Dias Coelho-Rocha[1], Fernanda Alvarenga Lima Barroso[1], Laisa Macedo Tavares[1], Vasco Azevedo[1], Pamela Mancha-Agresti[1,2] and Mariana Martins Drumond[1,3]**

[1] Laboratório de Genética Celular e Molecular (LGCM), Departamento de Biologia Geral, Instituto de Ciências Biológicas, Universidade Federal de Minas Gerais (UFMG), Belo Horizonte, Brazil, [2] Faculdade de Minas, FAMINAS-BH, Belo Horizonte, Brazil, [3] Centro Federal de Educação Tecnológica de Minas Gerais (CEFET/MG), Departamento de Ciências Biológicas, Belo Horizonte, Brazil

OPEN ACCESS

Edited by:
Konstantinos Papadimitriou,
University of Peloponnese, Greece

Reviewed by:
Natasa Golic,
University of Belgrade, Serbia
Eric Claassen,
Vrije Universiteit Amsterdam, Netherlands
Jia Yin,
Hunan Normal University, China

***Correspondence:**
Pamela Mancha-Agresti
p.mancha.agresti@gmail.com
Mariana Martins Drumond
mmdrumond@gmail.com

Specialty section:
This article was submitted to Food Microbiology, a section of the journal Frontiers in Microbiology

Received: 21 March 2020
Accepted: 24 August 2020
Published: 17 September 2020

Citation:
Batista VL, da Silva TF, de Jesus LCL, Coelho-Rocha ND, Barroso FAL, Tavares LM, Azevedo V, Mancha-Agresti P and Drumond MM (2020) Probiotics, Prebiotics, Synbiotics, and Paraprobiotics as a Therapeutic Alternative for Intestinal Mucositis. Front. Microbiol. 11:544490. doi: 10.3389/fmicb.2020.544490

Intestinal mucositis, a cytotoxic side effect of the antineoplastic drug 5-fluorouracil (5-FU), is characterized by ulceration, inflammation, diarrhea, and intense abdominal pain, making it an important issue for clinical medicine. Given the seriousness of the problem, therapeutic alternatives have been sought as a means to ameliorate, prevent, and treat this condition. Among the alternatives available to address this side effect of treatment with 5-FU, the most promising has been the use of probiotics, prebiotics, synbiotics, and paraprobiotics. This review addresses the administration of these "biotics" as a therapeutic alternative for intestinal mucositis caused by 5-FU. It describes the effects and benefits related to their use as well as their potential for patient care.

Keywords: lactic acid bacteria, chemotherapy, intestinal inflammation, treatment, mucosite

INTRODUCTION

Cancer is a disease characterized by uncontrolled proliferation of cells with cellular differentiation properties, having the capacity to invade tissues and organs and spread to other regions of the body, causing metastases (World Health Organization [WHO], 2018). This disease is the second leading cause of death globally, according to the World Health Organization, accounting for an estimated 9.6 million deaths in 2018; lung (1.76 million deaths), colorectal (862,000 deaths), stomach (783,000 deaths), liver (782,000 deaths), and breast cancer (627,000 deaths) are the most common types and have the highest mortality rates (World Health Organization [WHO], 2018).

Despite the high incidence and mortality rates, when identified early, cancer is a potentially curable and treatable disease. Treatment may be done through surgery, chemotherapy, radiotherapy, or bone marrow transplantation, depending on the type of cancer, degree of tumor aggressiveness, as well as the patient's physical and immunological status. It is often necessary to combine more than one type of treatment to achieve satisfactory results (World Health Organization [WHO], 2018).

Antineoplastic chemotherapy consists of the use of drugs that destroy cancer cells, inhibit their growth, and prevent their spread by targeting DNA or critical processes involved in cell division (Guichard et al., 2017; Shields, 2017). The traditional chemotherapeutics are classified according to their mechanisms of action, including antimetabolites, microtubule-targeting agents, topoisomerases, and antibiotics (Shields, 2017). The therapeutic arsenal mostly used in the

treatment of neoplasms include oxaliplatin, irinotecan, capecitabine, cisplatin, methotrexate, 5-fluorouracil (5-FU), and FOLFIRI (an association of 5-fluorouracil, irinotecan, and leucovorin), among others (Nussbaumer et al., 2011; Cassidy and Syed, 2017; Guichard et al., 2017).

The medication 5-FU is highlighted among the chemotherapeutic alternatives and has been mainly used in the treatment of advanced types of cancer, such as colorectal cancer, as well as malignant head and neck cancer, breast, stomach, and some skin cancers (Longley et al., 2003; Martins and Wagner, 2013; Cassidy and Syed, 2017; Guichard et al., 2017). This drug is an analog of uracil and thymine (**Figure 1**), which is metabolized in the liver, producing many metabolites. One of them binds to and inhibits the enzyme thymidylate synthase and, consequently, ends up interfering with DNA synthesis and cell division (see the *Mechanism of Action of 5-FU* section). On the other hand, this drug can act by the incorporation of its metabolites into the DNA and/or RNA of these cells (Sonis, 2004), which impedes their normal functioning and induces apoptosis (Longley et al., 2003; Miura et al., 2010).

However, 5-FU's non-specific mechanism of action results in side effects such as nausea, cardiotoxicity, leukopenia, alopecia, myelosuppression, diarrhea, and oral and intestinal mucositis (Duncan and Grant, 2003; Soveri et al., 2014; Thomas et al., 2016; Cinausero et al., 2017). Intestinal mucositis is the most prevalent side effect of 5-FU therapy (50–80% of reported cases) and one of the main limiting factors for continuing treatment (Kim et al., 2015).

Mucositis is an inflammation of the gastrointestinal tract (GIT), with symptoms that include diarrhea, abdominal pain, bleeding, fatigue, malnutrition, electrolyte imbalance, and infections, causing complications that may be life threatening (Sonis, 2004; Touchefeu et al., 2014; Kim S. et al., 2018). The cytotoxic effects of 5-FU in the GIT cells are a severe problem for oncological therapeutics, as they decrease the patient's ability to tolerate treatment, affecting the quality of life, directly influencing the success of therapy (Jamali et al., 2018).

Within this context, therapeutic alternatives have been sought as a means to prevent or ameliorate intestinal mucositis. Among these alternatives, the most promising are the use of probiotics ["*live microorganisms which when administered in adequate amounts confer a health benefit on the host*" (FAO/WHO, 2001)], prebiotics [*"a substrate that is selectively utilized by host microorganisms conferring a health benefit"* (Gibson et al., 2017)], synbiotics [*"a mixture of probiotics and implantation of live microbial dietary supplements in the GIT, by selectively stimulating the growth and/or activating the metabolism of one or a limited number of health-promoting bacteria, and thus improving host welfare*" (Gibson and Roberfroid, 1995)], paraprobiotics, and postbiotics, which can be defined as non-viable microorganisms, cell fractions or cell metabolites, bacteriocins, organic acids, and enzymes (Rad et al., 2020).

In this review, we address the evidence for the suitability of probiotics, prebiotics, synbiotics, and paraprobiotics as a therapeutic alternative for intestinal mucositis caused by the antineoplastic drug 5-FU.

MECHANISM OF ACTION OF 5-FU

The drug 5-FU is an antimetabolite analogous to uracil, which differs by the substitution of a hydrogen atom with fluorine at the fifth position of the uracil molecule. Developed in the 1950s and introduced in cancer therapy to inhibit cell division and proliferation of cancer cells, this substance is among the class of antineoplastic drugs with a vast spectrum of action in oncological practice, being widely used for the treatment of a variety of tumors (Thomas et al., 2016; Kato et al., 2017).

To control the abnormal proliferation of cancer cells, 5-FU enters into the cells through facilitated transport, which is the same mechanism involved in its intracellular conversion into active metabolites [fluorodeoxyuridine monophosphate (FdUMP), fluorodeoxyuridine triphosphate (FdUTP), and 5-fluorouridine triphosphate (FUTP)]. These metabolites may exhibit three different mechanisms of action: (1) FdUMP inhibits the activity of the enzyme thymidylate synthase causing an imbalance in the pool of nucleotides, consequently decreasing the concentration of the deoxynucleotides dTTP and dATP, essential for DNA repair; (2) FdUTP binds to the DNA structure, inhibiting its synthesis, blocking cell division; and (3) FUTP can be incorporated into RNA, damaging it, leading to functional loss and cell death (Longley et al., 2003; Zhang et al., 2008; Miura et al., 2010; **Figure 2**).

Clinical evidence of patients undergoing oncologic therapy with 5-FU shows that the effects of this chemotherapy vary among users. From 20 to 40% of the patients treated with the standard dose of this drug (10–15 mg/kg body weight, for 3–4 days intravenously) develop some degree of mucositis, and about 80–100% of the patients treated with high doses (350–500 mg/kg body weight) develop GIT problems (Crombie and Longo, 2016; Cinausero et al., 2017).

EFFECTS OF 5-FU ON THE GASTROINTESTINAL TRACT

In addition to having a digestive and nutrient absorption role, the GIT mucosa acts as a physical and immunological barrier, having the ability to defend the body against potentially harmful agents that can trigger inflammatory responses in the intestine (Salvo Romero et al., 2015; König et al., 2016). The intestinal barrier is categorized according to the various levels of protection, as well as the location and nature of its cellular and extracellular components (Vancamelbeke and Vermeire, 2017). These include mainly the mucus layer associated with the commensal microbiota of the gut, antimicrobial peptide and immunoglobulin A (IgA) secretion, the monolayer of specialized epithelial cells (enterocytes, Paneth cells, goblet cells, stem cells, and enteroendocrine cells), and the lamina propria, a specialized connective tissue in which innate and adaptive immune cells reside, such as T cells, B cells, dendritic cells (DCs), macrophages, neutrophils, eosinophils, and the newly discovered innate lymphoid cells (ILCs) (Vancamelbeke and Vermeire, 2017).

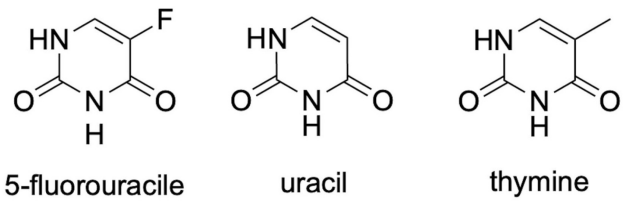

FIGURE 1 | Chemical structure of 5-fluorouracil (5-FU) and its analogs uracil and thymine. All three structures differ in the radical present at the structure's fifth position.

Although the intestinal barrier plays an essential role in the body's homeostasis, it is susceptible to 5-FU oncologic therapy (Yu, 2013). The intestinal mucositis caused by 5-FU mainly affects the small intestine (duodenum, jejunum, and ileum), characterized by inflammation, loss of intestinal structure and functionality, villous atrophy, goblet and Paneth cell degeneration, reduction in mucin secretion, increased intestinal permeability, cell death, polymorphonuclear cell infiltration, and increased production of proinflammatory cytokines, such as interleukin-1β (IL-1β), IL-6, and tumor necrosis factor-α (TNF-α), mucosal tissue exposed to infection, and alteration of the intestinal microbiota composition (Chang et al., 2012; Lee, 2014).

The pathology of mucositis can be divided into five phases (initiation, response to primary damage, signal amplification, ulceration, and healing) (Sonis, 2004; **Figure 3**). The *initiation phase* occurs when the intestinal mucosa is exposed to 5-FU, which promotes DNA/RNA damage, either because it binds directly to these biomolecules or through the oxidative stress caused by reactive oxygen species (ROS) production. These factors induce tissue damage (Sonis, 2004; Villa and Sonis, 2015; Cereda et al., 2018), which activates several signal transduction pathways, such as nuclear factor κB (NF-κβ) pathway signaling. This situation leads to the induction of various inflammatory mediators, such as IL-8, TNF-α, cyclooxygenase-2 enzyme (COX-2), IL-6, and IL-1β, among others, that are responsible for mucosal toxicity (Sonis, 2004; Cinausero et al., 2017).

The recruitment of these proinflammatory cytokines acts indirectly on *signal amplification* (amplification phase) via a positive feedback mechanism, activating pathways that increase

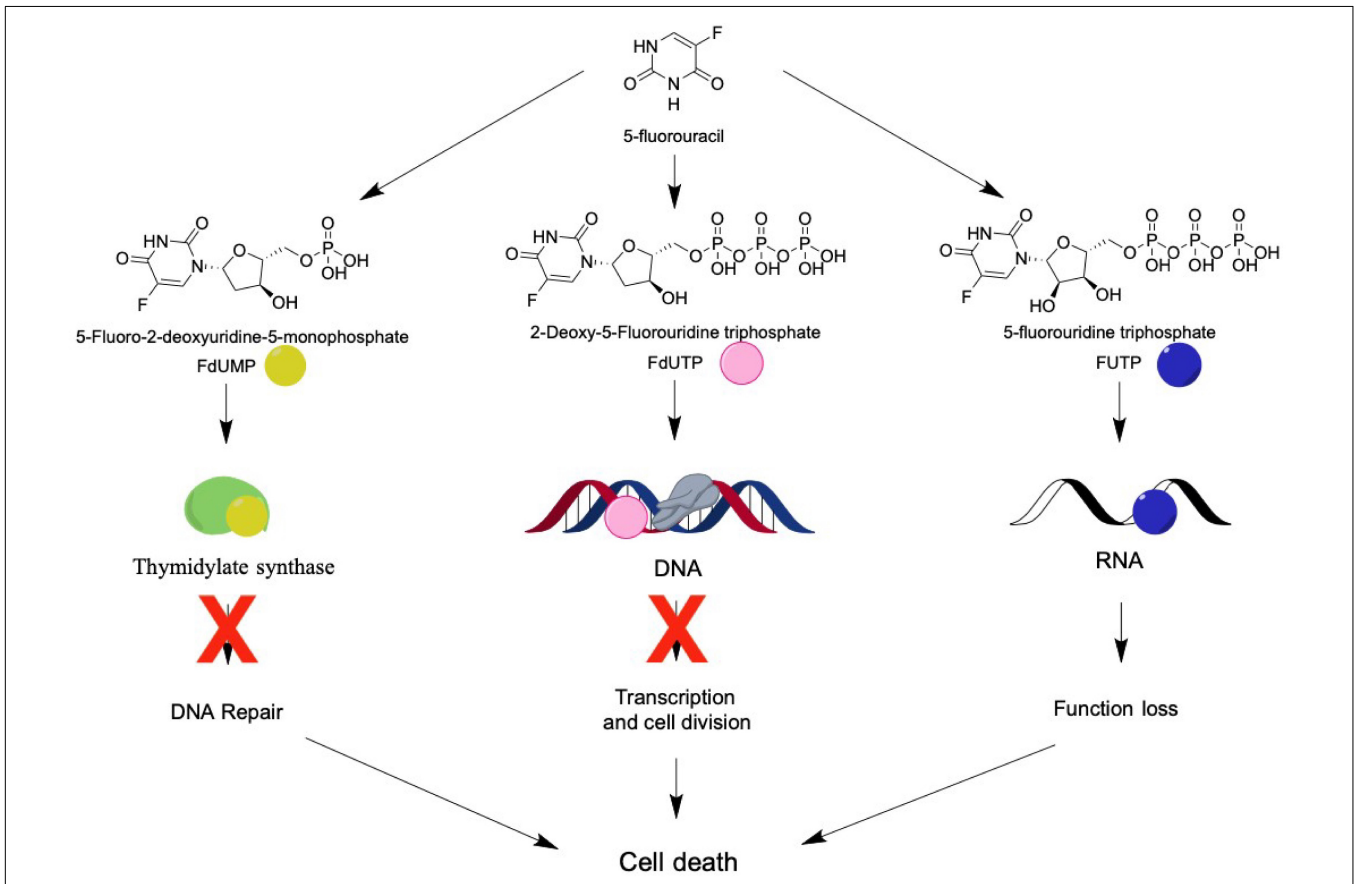

FIGURE 2 | 5-FU's metabolites and their molecular targets. 5-FU is intracellularly metabolized into fluorodeoxyuridine monophosphate (FdUMP), which binds to the enzyme thymidylate synthetase, resulting in decreased production of dTTP and dATP and blocking cell repair; or into fluorodeoxyuridine triphosphate (FdUTP) and binds to the DNA, inhibiting duplication and transcription; or into 5-fluorouridine triphosphate (FUTP) and binds to RNA, leading to a loss of function. All three metabolites cause damage to the cell on a genomic level, culminating in cell death.

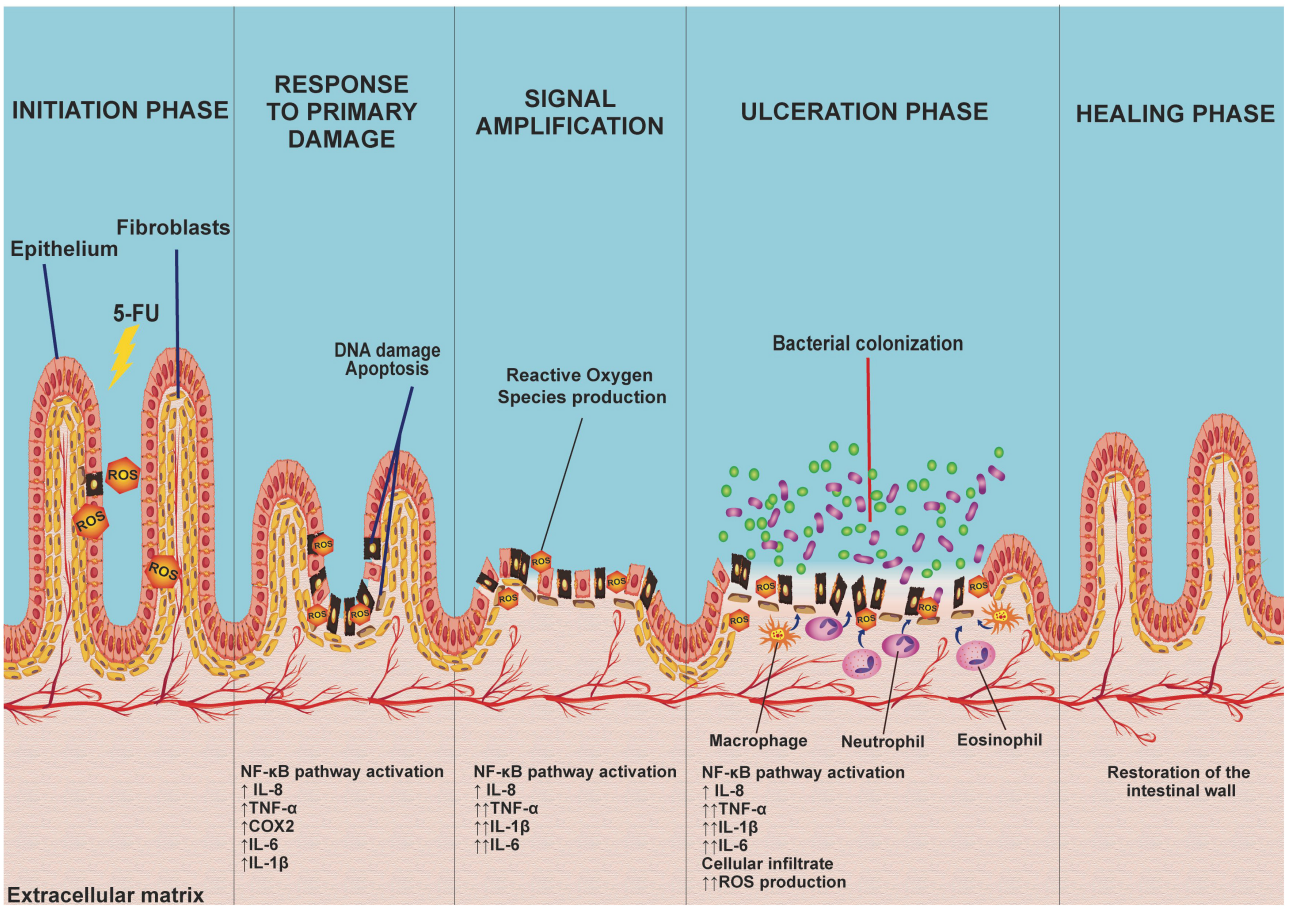

FIGURE 3 | The five phases of 5-FU-induced intestinal mucositis: The initiation phase occurs when the intestinal mucosa is first exposed to the toxicity of 5-FU, promoting DNA damage and inducing the production of reactive oxygen species (ROS). Consequently, this activates several signaling transduction pathways (response to primary damage) such as the NF-êB pathway, related to the induction of several inflammatory mediators [interleukin-8 (IL-8), tumor necrosis factor-α (TNF-α), cyclooxygenase-2 enzyme (COX-2), IL-6, and IL-1β)] that play an important role in mucosal toxicity, causing signal amplification via a positive feedback mechanism, activating pathways that increase cytokine production as well as oxidative stress, exacerbating the lesion, progressively destroying the mucosa leading to an ulceration phase. Finally, spontaneous ulcer healing, characterized by cell proliferation and differentiation on average 3–4 days after the end of chemotherapy treatment, leads to mucosal restoration.

proinflammatory cytokine production (TNF-α, IL-1β, and IL-6), as well as oxidative stress. The increase in the production of these factors initiates a cascade of reactions that leads to the activation of matrix metalloproteinases, resulting in tissue damage or an increase in TNF-α production, exacerbating the initial lesion (Sonis, 2004).

The progressive destruction of the mucosa culminates in an *ulceration phase*, which occurs when loss of integrity and function of the epithelium occurs. At this stage, there are symptomatic lesions that, apart from being prone to pathogenic bacterial colonization, stimulate the activation and infiltration of defense cells, including macrophages, neutrophils, and eosinophils, in the intestinal mucosa. These cells increase the production of oxidant compounds, resulting in an increase in the depth of intestinal ulcers, consequently increasing bacterial translocation (Villa and Sonis, 2015; Cinausero et al., 2017; Cereda et al., 2018).

Finally, *the healing phase* is characterized by cell proliferation and differentiation. This phase occurs, on average, 3–4 days after the last chemotherapy treatment, leading to restoration of the mucosa (Sonis, 2004; Villa and Sonis, 2015).

EFFECTS OF 5-FU ON INTESTINAL MICROBIOTA

In addition to causing structural damage to the intestinal epithelium, the mucositis caused by chemotherapeutic agents has a crucial influence on the intestinal microbiota (van Vliet et al., 2010). The GIT has a complex ecological population, constituted by more than a thousand different species of microorganisms, though their distribution varies along the GIT (Mowat and Agace, 2014; Rajilić-Stojanović and de Vos, 2014); low concentrations and bacterial diversity (up to 10^3 CFU/ml) are found in the upper GIT (stomach, duodenum, jejunum, and proximal ileum) (Walter and Ley, 2011). A larger number of bacteria (10^9–10^{12} CFU/ml) reside

in the lower compartments of the GIT (distal ileum and colon), which constitutes, to date, the habitat with the highest known microbial density (Mowat and Agace, 2014; Jandhyala et al., 2015; Thursby and Juge, 2017). Due to the low oxygen tension in the colon, the most prevalent bacterial groups consist of anaerobic species, such a *Clostridia*, *Enterobacteria*, *Enterococcus*, *Bacteroides*, *Bifidobacteria*, *Fusobacteria*, *Lactobacilli*, *Peptococci*, *Peptostreptococci*, *Prevotellaceae*, *Roseburia*, *Ruminococci*, and *Verrucomicrobia* (Simon and Gorbach, 1982; Bäckhed et al., 2005; Mowat and Agace, 2014).

The intestinal microbiota acts through several mechanisms to maintain the homeostasis of the organism, living in mutuality with the host, benefiting from the nutrient-rich environment offered by the organism and, in exchange, performing innumerable beneficial functions, including elimination of pathogens, production of vitamins and short-chain fatty acids (SCFA), as well as modulation of the enteric and systemic immune systems (Lane et al., 2017; Thursby and Juge, 2017). However, when this mutualism becomes unbalanced, the intestinal microbiota can contribute to the onset of infectious diseases, chronic inflammation, and autoimmune diseases (de Oliveira et al., 2017).

The commensal microbiota, such as *Bifidobacterium infantis* and *Bacteroides thetaiotaomicron*, have been shown to decrease NF-κB activation, decreasing levels of endotoxins and of plasma proinflammatory cytokines (Stringer et al., 2009). Studies have demonstrated that treatment with 5-FU alters the relative abundance of several genera of the intestinal microbiota, such as *Clostridium*, *Lactobacillus*, *Enterococcus*, *Bacteroides*, *Staphylococcus*, *Streptococcus*, and *Escherichia* (Stringer et al., 2009). Thus, disrupted homeostasis of the intestinal microbiota can affect the mucosal immune system due to an imbalance between the production of pro- and anti-inflammatory mediators, resulting in intestinal inflammation (Autenrieth and Baumgart, 2017; Holleran et al., 2017).

Given the possibility that intestinal mucositis is closely related to intestinal microbiota dysbiosis (von Bültzingslöwen et al., 2003; Yu, 2018), probiotic microorganisms have been presented as an alternative treatment due to their beneficial properties in the GIT. Given these characteristics, several studies have shown that probiotics can be an effective therapeutic alternative for the reduction of antineoplastic-induced intestinal mucositis.

PROBIOTICS

In order, to be considered a probiotic and be able to exert health benefits for the host, microorganisms must have some specific attributes, such as being capable of remaining viable during transport and storage, and tolerating the low pH of the gastric lumen and the action of bile, and pancreatic and intestinal secretions. Many probiotics are able to colonize the GIT and stimulate the immune system (Wang M. et al., 2016; Mokoena, 2017). Furthermore, resistance to antibiotics in probiotic strains should be analyzed in order to assess their safety, as well as the level and the source of this resistance (Zhang et al., 2018). Intrinsic resistance is unlikely to spread horizontally between bacteria (Mathur and Singh, 2005), while acquired resistance could be transferred to other organisms, including pathogens, representing a potential risk to the health of the host (van Reenen and Dicks, 2011). The most well-studied and characterized probiotics belong to the lactic acid bacteria (LAB) group. However, other microorganisms also present probiotic properties, such as some *Saccharomyces* spp., and bacteria of the genera *Bifidobacterium* and *Faecalibacterium* (Pot et al., 2013; Bastos et al., 2016; Chang et al., 2019).

LAB mainly include the genera *Lactobacillus*, *Leuconostoc*, *Lactococcus*, *Pediococcus*, and *Streptococcus*, among others, and constitute a group of Gram-positive microorganisms, anaerobic or aerotolerant, non-spore forming, resistant to low pH, and able to produce lactic acid as the final product of the fermentation of carbohydrates (Wang Y. et al., 2016; Mokoena, 2017; Plavec and Berlec, 2019). Furthermore, these bacteria have been used for a long time in several industrial processes for the production of fermented foods, such as cheese, yogurts, etc. (Soccol et al., 2010), and they frequently present probiotic properties. Additionally, these organisms have been explored for protein heterology production and as live delivery systems for gene and biotherapeutic vaccines, with potential applications for the treatment and prevention of various pathological conditions, in both human and veterinary medicine (Carvalho et al., 2017; Gomes-Santos et al., 2017; LeCureux and Dean, 2018; Kuczkowska et al., 2019).

MECHANISMS OF ACTION OF PROBIOTICS

Studies have shown that benefits for human health are attributed to consumption of probiotics, mainly for GIT diseases (Fedorak et al., 2015; Acurcio et al., 2017), though also for other diseases, including osteoporosis (Collins et al., 2018), cancer (Zaharuddin et al., 2019), obesity and type 2 diabetes (Saez-Lara et al., 2015; Wang et al., 2017; Hsieh et al., 2018), depression (Wallace et al., 2020), and atopic dermatitis (Rather et al., 2016). In this context, the main mechanisms of action described for these microorganisms in the host include: (i) colonization and regulation of a dysbiotic intestinal microbiota (Shi et al., 2017); (ii) protection of the epithelial barrier by maintaining tight junction integrity (Blackwood et al., 2017); (iii) induction of mucin production (Aliakbarpour et al., 2012) and B-cell-secreting IgA, which are important defense mechanisms necessary to maintain epithelial integrity and to protect the intestine from the external environment; (iv) increasing adherence to the intestinal mucosa and inhibiting of concomitant pathogen adherence based on competition for available nutrients and sites of mucosal adhesion (Collado et al., 2010; Monteagudo-Mera et al., 2019); (v) competitive exclusion of pathogenic microorganisms, such as *Staphylococcus aureus* and *Salmonella typhimurium* (Halder et al., 2017; Plaza-Díaz et al., 2017); (vi) production of antimicrobial substances such as acetic and lactic acids, and bacteriocins, which have strong inhibitory effects against Gram-negative bacteria and have been considered as the main antimicrobial compounds produced by probiotics against pathogens (Alakomi et al., 2000; De Keersmaecker et al., 2006; Makras et al., 2006; Bermudez-Brito et al., 2012; Mokoena, 2017;

Gaspar et al., 2018; Castilho et al., 2019); (vii) production and secretion of metabolites of SCFAs with anti-inflammatory properties, such as acetate, propionate, and butyrate, which exert beneficial effects on intestinal and immune cells, being important compounds for cell proliferation, cell differentiation, and gene expression, and they are signaling molecules of immunological pathways; butyrate is the primary energy source of colonocytes, and it has an epithelial barrier function; SCFAs can also induce expression of the anti-inflammatory cytokine IL-10, inhibiting inflammatory responses (Parada Venegas et al., 2019); (viii) inhibition of the activation of the NF-κB signaling pathway (Kaci et al., 2011; Gao et al., 2015); (ix) interaction with the gut–brain axis via the production of metabolites such as γ-aminobutyric acid (GABA) (Kim N. et al., 2018); and (x) modulation of the host's innate and/or adaptive immune system responses through interaction with epithelial cells, dendritic cells, monocytes, macrophages, and lymphocytes (Azad et al., 2018). In addition, probiotics can act by inducing host autophagy to attenuate oxidative stress-induced intestine injury (Wu et al., 2019; **Figure 4**).

Thus, due to the numerous possible pathways in which probiotics could be involved, their study as therapeutics of various diseases, especially those related to the GIT, is of particular importance.

EFFECTS OF PROBIOTICS ON INTESTINAL MUCOSITIS

The proposed mechanisms of action for the beneficial effects of probiotic microorganisms in diseases affecting the GIT are diverse, heterogeneous, strain specific, and depend on the quantity of probiotics used (Plaza-Díaz et al., 2017). Since the immunomodulatory and anti-inflammatory effects

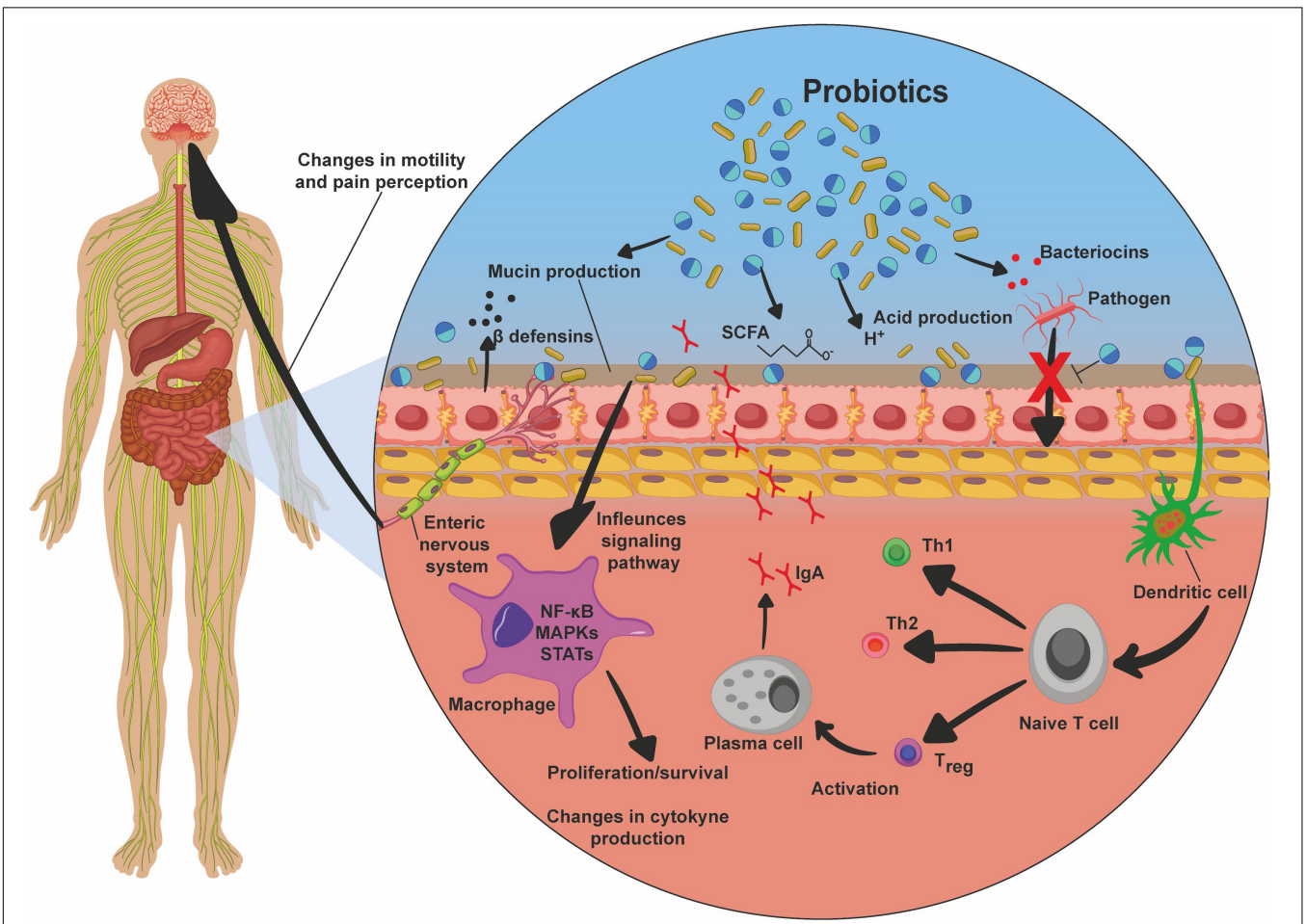

FIGURE 4 | Probiotic mechanisms of action. Probiotics, after they reach the intestines, promote beneficial effects to the host by various mechanisms. These include mucin production, production of bacteriocins, acids, and short-chain fatty acids (SCFA), which are responsible for the inhibition of pathogens, inhibition of bacterial translocation, and inhibition of pathogens due to competition for receptors and nutrients. There is also stimulation of dendritic cells, which in turn induce the differentiation of T cells into Th1, Th2, and Treg, the latter being responsible for maturation of plasma cells, and thus immunoglobulin A (IgA) production and secretion; stimulation of beta-defensin production; inhibition of signaling pathways, such as nuclear factor κB (NF-kB), MAPK, and STAT, promoting proliferation and survival of the cells; changes in cytokine production profile, enhancing the production of anti-inflammatory cytokines and inhibiting proinflammatory factors; and interaction via the enteric nervous system with the central nervous system, promoting changes in intestinal mobility and pain perception.

reported for LAB, as well as other probiotics, are strain dependent, it is necessary to identify and characterize species and strains with probiotic potential and investigate their effects on different targets or diseases (Plaza-Díaz et al., 2017). **Table 1** presents the main findings for the effects of probiotics on intestinal mucositis.

In this context, studies conducted *in vitro* using Caco-2 cells (Fang et al., 2014) and *in vivo* with rats and mice

TABLE 1 | Effects of probiotics, prebiotics, synbiotics, and paraprobiotics in intestinal mucositis.

	Effects of intestinal mucositis	References
Probiotics strain		
Lactobacillus acidophilus	Inhibited nuclear factor κB (NF-κβ) (NF-κB) pathway signaling Regulated levels of the proinflammatory cytokines [tumor necrosis factor-α (TNF-α), interleukin-1β (IL-1β), and the C-X-C motif chemokine ligand (CXCL)] Reversed gastrointestinal dysmotility, increased gastric emptying and intestinal transit	Justino et al., 2015
Lactobacillus acidophilus A4	Stimulated the overexpression of mucin genes (MUC2 and MUC5AC) Reduced myeloperoxidase (MPO) activity Reduced expression of proinflammatory cytokine IL-1β	Oh et al., 2017
Lactobacillus casei variety *rhamnosus* (Lcr35)	Reduced production of proinflammatory cytokines (TNF-α, IL-1β, IFN-γ, IL-10, and IL-6). Attenuated the loss of goblet cells, decreased Firmicutes and increased Bacteroidetes Reduced the frequency of diarrhea Restored villus/crypt ratio	Yeung et al., 2015; Chang et al., 2018
Bifidobacterium bifidum G9-1	Attenuated histopathological alteration, with decrease cell infiltrate in crypts Regulated intestinal microbiota (decrease Firmicutes and increase Bacteroidetes abundance) Reduced the concentrations of proinflammatory cytokines TNF-α and IL-1β and MPO activity Reduced diarrhea and interrupt weight loss	Kato et al., 2017
Bifidobacterium infantis	Improved the histologic parameters, ameliorating mucosal damage Reduced Th1 and Th17 cells, and increased CD4 + CD25 + Foxp3 + Tregs response	Mi et al., 2017
Association*: (B. breve, L. acidophilus, L. casei, and Streptococcus thermophilus)*	Reduced neutrophil infiltration, proinflammatory cytokines (TNF-α, IL-4, and IL-6), and intestinal permeability Restored of the intestinal epithelium architecture	Tang et al., 2017
Association*: (L. acidophilus, L. paracasei, L. rhamnosus, and B. lactis)*	Prevented epithelial injury in intestinal mucositis, with an increase in the villus/crypt ratio Reduced the malondialdehyde (MDA), MPO, TNF-α, and IL-6 levels Increased glutathione (GHS) levels in the duodenum and jejunum sections	Quaresma et al., 2019
Association*:* Whey protein isolate, to skim milk fermented by *L. casei* and *Propionibacterium freudenteichii*	Ameliorated histological scores and prevented villus shortening Reduced weight loss and degeneration of goblet cells	Cordeiro et al., 2018
Lactobacillus delbrueckii subsp. *lactis* CIDCA 133	Prevented body mass loss Inhibited length reduction of the intestine caused by 5-fluorouracil (5-FU) Restored histopathological damage Reduced inflammatory parameters: neutrophil, eosinophil, leukocyte infiltrate reduction, and immunoglobulin A (IgA) secretion Reduced intestinal permeability	De Jesus et al., 2019
Saccharomyces boulardii	Reduced cells apoptosis and inflammatory factors (nitrite concentration, neutrophil infiltrate TNF-α, IL-1β cytokines, and CXCL-1 chemokine) Improved the intestinal functions such as gastric emptying, gastrointestinal transit, absorption, and intestinal permeability Modulated the expression of TLR2, TLR4, MyD88, NF-κB extracellular signal, regulated kinase 1/2 (ERK1/2), phospho-p38 MAPK, phospho-c-Jun N-terminal kinase (phospo-JNK) in jejunum/ileum and in Caco2 cells	Justino et al., 2015, 2020
Prebiotics		
Fructooligosaccharide (FOS)	Reduced MPO activity in jejunum section Decreased inflammatory infiltrate and preserved intestinal epithelium Attenuated weight loss and increased catalase levels	Smith et al., 2008; Galdino et al., 2018
Synbiotics		
Simbioflora®	Attenuated weight loss Improved histology of the intestinal mucosa and preserved epithelial architecture Reduced eosinophil infiltrate Decreased intestinal permeability Increased the production of extracellular factors, such as SCFA (acetate and butyrate)	Trindade et al., 2018
Paraprobiotics		
L. rhamnosus inactivated by heat	Prevented the expression of monocyte chemoattractant protein 1 (MPC-1) Regulated the expression of TNF-α, IL-12	Fang et al., 2014

have demonstrated strain-dependent effects of probiotics for the prevention/treatment of experimental mucositis induced by 5-FU, proving to be an effective therapeutic alternative for the treatment of this disease. Thus, they could be used in parallel with chemotherapy to promote the attenuation of gastrointestinal toxicity caused by cancer drugs, which is promising for improving the quality of life of patients undergoing chemotherapy treatment (Mi et al., 2017; Chang et al., 2018).

Lactobacillus acidophilus can decrease intestinal damage caused by 5-FU (applied at a dose of 450 mg/kg) by inhibiting the signaling of the NF-κB pathway, reducing levels of proinflammatory cytokines, such as TNF-α, IL-1β, and the C-X-C motif chemokine ligand 1 (CXCL-1); reversion in gastrointestinal dysmotility and increased gastric emptying and intestinal transit were observed (Justino et al., 2015). This probiotic was able to reduce inflammation and normalize bowel function in mice (Justino et al., 2015). Additionally, Oh et al. (2017) demonstrated that *L. acidophilus* A4 decreased the severity of intestinal mucositis induced by 5-FU (150 mg/kg) by stimulating overexpression of mucin genes (MUC2 and MUC5AC), reducing myeloperoxidase (MPO) activity, and inhibiting expression of proinflammatory cytokines, such as IL-1β, in mice (Oh et al., 2017).

Lactobacillus casei variety *rhamnosus* (*Lcr35*, Antibiophilus®, France) reduced the production of proinflammatory cytokines (TNF-α, IL-1β, IFN-γ, and IL-6), attenuated the loss of goblet cells, reduced the frequency of diarrhea, and restored the villus/crypt ratio, demonstrating an anti-inflammatory effect on tissue damage caused in the intestinal mucosa by administering 5-FU (30 mg/kg) for 5 days (Yeung et al., 2015). The protective effect of Lcr35 (1×10^7 CFU) was also demonstrated in a colorectal cancer model; Balb/c mice were treated with a chemotherapeutic association called FOLFOX (30 mg/kg of 5-FU; 10 mg/kg of leucovorin, and 1 mg/kg of oxaliplatin) during 5 days (Chang et al., 2018). Lcr35 treatment was able to attenuate intestinal mucosa damage through regulation of the expression of proinflammatory cytokines (IL-1β, IL-6, TNF-α, and IL-10) induced by FOLFOX in the jejunum segment and also affected the gut microbiota composition, decreasing *Firmicutes* and increasing *Bacteroidetes* abundance (Chang et al., 2018). Thus, Lcr35 is a promising therapeutic strategy for the prevention or management of chemotherapy-induced intestinal mucositis (Chang et al., 2018).

A component in the intestinal microbiota, *Bifidobacterium bifidum* G9-1 (BBG9-1), has been widely used as a treatment for diarrhea and constipation, as well as for intestinal mucositis induced by 5-FU (50 mg/kg/6 days) (Kato et al., 2017). This probiotic can reduce diarrhea and interrupt weight loss, as well as being able to attenuate villus shortening and goblet cell degeneration. It can decrease inflammatory infiltrate in crypt cells, reduce MPO activity, reduce TNF-α and IL-1β levels, and also regulate the intestinal microbiota (decrease *Firmicutes* and increase *Bacteroidetes* abundance), demonstrating its ability to reduce the severity of 5-FU-induced intestinal mucositis (Kato et al., 2017).

Mi et al. (2017) demonstrated that *B. infantis* (1×10^9 CFU/11 days) administration, in a synergic colorectal cancer treatment model with 5-FU (75 mg/kg/3 days) and oxaliplatin (8 mg/kg/3 days), was able to reduce the deleterious effects to the intestinal mucosa induced by chemotherapy. This probiotic improved the histology parameters, ameliorating the mucosal damage by decreasing Th1 and Th17 cells, and increasing the $CD4^+$ $CD25^+$ $Foxp3^+$ Tregs response (Mi et al., 2017).

A combination of probiotic strains also demonstrated effectiveness in the reduction of intestinal damage induced by 5-FU chemotherapy. DM#1 mixture (*B. breve* DM8310, *L. acidophilus* DM8302, *L. casei* DM8121, and *Streptococcus thermophillus* DM8309) administration improved the restoration of the epithelial architecture, reduced neutrophil infiltration, reduced proinflammatory cytokines (TNF-α, IL-4, IL-6), and decreased intestinal permeability in mice treated with 5-FU (30 mg/kg/5 days) (Tang et al., 2017). Another study using a probiotic mix (*L. acidophilus*, *L. paracasei*, *L rhamnosus*, and *B. lactis*) showed that the mixture was able to prevent epithelial injury in intestinal mucositis induced by 5-FU (450 mg/kg), with an increase in the villus/crypt ratio and reduced malondialdehyde (MDA), MPO, TNF-α, and IL-6 levels in all small intestinal segments (duodenum, jejunum, and ileum) (Quaresma et al., 2019). In addition, administration of the probiotic mix resulted in an increase in glutathione (GSH) levels in the duodenum and jejunum sections and attenuated the delay in gastric emptying (Quaresma et al., 2019).

The therapeutic effects of probiotics also have been demonstrated for fermented products, which can be consumed by cancer patients. Milk fermented by *Lactobacillus delbrueckii* CIDCA 133 (7.5×10^7 CFU) attenuated the damage caused to the intestinal mucosa by 5-FU (300 mg/kg), both in the recovery of the architecture of the epithelium, including prevention of goblet cell degeneration, and reduction of the polymorphonuclear cell infiltrate, with reduced IgA secretion and intestinal permeability (De Jesus et al., 2019).

A mulberry leaf extract fermented by *L. acidophilus* A4 strain stimulated overexpression of mucin genes (MUC2 and MUC5AC), promoted reduction of MPO, inhibited expression of proinflammatory cytokines, such as IL-1β, and reduced the loss of intestinal barrier function generated by 5-FU (150 mg/kg) administration (Oh et al., 2017).

The role of whey protein isolate (WPI) added to skim milk fermented by *Lactobacillus casei* BL23 (*L. casei* BL23) or by *Propionibacterium freudenreichii* CIRM-BIA138 (*P. freudenreichii* 138) was studied in a 5-FU-induced mucositis mouse model (Cordeiro et al., 2018). Milk fermented by both bacteria was sufficient to reduce weight loss, reduce histological scores, and prevent villus shortening and degeneration of goblet cells. WPI addition to fermented milk improved the effects of these probiotics, compared to when they were administrated alone (Cordeiro et al., 2018).

In addition to bacteria, yeasts can also have a beneficial effect on gastrointestinal mucositis. In this context, Porto et al. (2019) showed the effect of *Saccharomyces* cerevisiae UFMG A-905 alone or after enrichment with selenium, for intestinal mucositis treatment. This probiotic composition was able to preserve intestinal architecture and reduce nitrite concentration,

lipid peroxidation, intestinal permeability, and inflammatory parameters, protecting mice against pathological consequences caused by 5-FU administration (Porto et al., 2019).

The probiotic, thermophilic, non-pathogenic yeast, *Saccharomyces boulardii*, was also tested for intestinal mucositis treatment; the histopathological changes caused by 5-FU were significantly reduced, including cell apoptosis and inflammatory parameters (nitrite concentration, neutrophil infiltrate, TNF-α and IL-1β cytokines, and CXCL-1 chemokine). This probiotic organism also improved the intestinal functions, such as gastric emptying, gastrointestinal transit, absorption, and intestinal permeability (Justino et al., 2015).

The effects of *S. boulardii* were evaluated by *in vitro* (Caco-2 cells treated with 1 mM 5-FU/24 h) and *in vivo* assays [Swiss mice treated with *S. boulardii* (1×10^9 CFU/kg/3 days), mucositis induction by 5-FU (450 mg/kg)] (Justino et al., 2020). S. boulardii was able to modulate TLR2, TLR4, MyD88, NF-κB, ERK1/2, phospho-p38, phospho-JNK, TNF-α, IL-1β, and CXCL-1 expression, in these two different experimental models.

Based on the above studies, probiotics could be an effective therapeutic alternative for attenuating, preventing, and treating 5-FU-induced intestinal mucositis, although clinical studies will be required to test their safeness and usefulness for treatment.

PREBIOTICS, SYNBIOTICS, PARAPROBIOTICS, AND POSTBIOTICS

The use of probiotics to treat intestinal mucositis is widely reported; however, research has also demonstrated the importance of fiber consumption to improve their benefit for the intestinal microbiota. These fibers are used by the microbiota organisms during the fermentation process, resulting in the production of various compounds, such as SCFAs, which are able to modulate the function of immune cells in the intestine, showing mainly anti-inflammatory effects (Tan et al., 2014; Luu and Visekruna, 2019).

To classify dietary fibers as prebiotic, it is necessary to satisfy six basic criteria: (i) they must be resistant to gastric acidity, hydrolysis by mammalian enzymes, and gastrointestinal absorption, (ii) they should not be digested in the upper gastrointestinal tract, (iii) they should be fermented in the colon by beneficial bacteria, (iv) they should be beneficial to the host's health, (v) they should stimulate the growth of probiotics, and (vi) they should withstand food processing conditions while remaining unchanged (Wang, 2009; Markowiak and Ślizewska, 2017; Cerdó et al., 2019).

Prebiotics may be added to food or may be obtained through consumption of natural products, such as fruit, vegetables, cereals, and other edible plant products in which carbohydrate availability is high (Markowiak and Ślizewska, 2017). A wide variety of compounds have the potential to be classified as prebiotics. Most are non-digestible oligosaccharides extracted from plants, including fructooligosaccharide (FOS) (L'homme et al., 2003), galactooligosaccharide (GOS) (Ziegler et al., 2007), mannanoligosaccharide (MOS), and xylooligosaccharide (XOS) (Playne and Crittenden, 2002), oligofructose, and inulin (Roberfroid, 2007).

Prebiotic compounds stimulate growth, activating metabolism and promoting protection of bacteria that are beneficial to the host organism (e.g., saccharolytic bacteria, *Bifidobacterium*, and *Lactobacillus*). Prebiotic fermentation by indigenous microbiota can modulate the composition and the function of these microorganisms (Gibson and Roberfroid, 1995; Slavin, 2013; Davani-Davari et al., 2019). Furthermore, prebiotic fermentation can benefit the host through production of some compounds, such as SCFAs and lactic acid, produced by *Bifidobacterium* and *Lactobacillus* spp., which cause a reduction in the intestinal pH, inhibiting the development of gastrointestinal pathogens (Gibson and Wang, 1994; Bovee-Oudenhoven et al., 2003; Amani Denj et al., 2015). Prebiotics are also able to exert beneficial effects via mucin production by providing fermentable compounds that contribute to a lower incidence of bacterial translocation (Satchithanandam et al., 1990; Schley and Field, 2002).

Another mechanism proposed for prebiotics is their interaction with carbohydrate receptors (mannose, fucose and C-type lectin receptors, and galectins) on immune cells [phagocytes, natural killer (NK) cells, DCs]. The production of metabolites (e.g., folate and riboflavin, vitamins, and SCFAs) during their fermentation by gut microbiota showcases antimicrobial activity and maintains a healthy gut barrier (Hosono et al., 2003; Roller et al., 2004; Furusawa et al., 2013; Comstock et al., 2014; Levit et al., 2018; Enam and Mansell, 2019).

As prebiotics stimulate probiotic action, the synbiotic concept was created to overcome difficulties faced by probiotics in the GIT, demonstrating that this association (prebiotics + probiotics) intensifies their individual beneficial effects (Markowiak and Ślizewska, 2017).

Information on prebiotic stimulation of known probiotic strains leads to the choice of the ideal microorganism–substrate synbiotic pairs; the consumption of appropriately selected probiotics and prebiotics can increase the beneficial effects of each. Synbiotics have beneficial synergistic effects, greater than those observed for individual administration of prebiotics and probiotics (Geier et al., 2006).

The main criteria for synbiotic formulation should be a selection of appropriate probiotic and prebiotic pairs; the prebiotic should selectively stimulate the growth of probiotic microorganisms, having a beneficial effect on health, with no or limited stimulation of other microorganisms. The main probiotic species and prebiotics used in synbiotic formulations include, respectively, *Lactobacillus* spp., *Bifidobacteria s*pp., *S. boulardii*, and *B. coagulans*, and FOS, GOS, and XOS. The health benefits from the administration of synbiotics to humans include: (i) increased levels of *lactobacilli* and *bifidobacteria* and balanced gut microbiota, (ii) improvement of immunomodulating ability, (iii) prevention of bacterial translocation; and (iv) improvement of liver function and reduction of incidence of nosocomial infections in surgical patients (Pandey et al., 2015; Markowiak and Ślizewska, 2017). Evidence shows that physical and chemical changes in the colon and intestinal microbiota caused by synbiotic

consumption, such as increased production of SCFAs and an increase in antitumor or antimutagenic compounds, can provide protection against rectal colon cancer, as they result in an improved immune response due to changes in the microbiota (Machado et al., 2014).

The studies listed above show the advantages of using live organisms; however, despite the fact that probiotics have proven benefits for the health of the host, current research emphasizes that the living organisms are not necessary for probiotic action; their different components, such as carbohydrates, proteins, lipids, vitamins, organic acids, cell wall components, and other complex molecules, generated after cell death, also have health benefits (Cuevas-González et al., 2020). The administration of non-viable organisms and their secreted products can present advantages in safety, reducing the possibility of infection and microbial translocation, which have been reported after the administration of probiotics to immunocompromised individuals (Aguilar-Toalá et al., 2018; Cuevas-González et al., 2020).

In this context, the terms "paraprobiotics" and "postbiotics" have been defined to refer to inactivated organisms and their metabolites. The difference between them is that paraprobiotics, also known as "non-viable probiotics" refer to inactivated cells, while postbiotics refer to soluble factors, which can be products (or metabolic byproducts) secreted by viable bacteria or released after their lysis (Cuevas-González et al., 2020). It is already possible to find products on the market that contain inactivated bacteria (e.g., Lactéol Fort® from PUMC Pharmaceutical Co., Ltd. and Fermenti Lattici Tindalizzati® from Frau, AF United Spa) (Taverniti and Guglielmetti, 2011).

Microorganisms can be inactivated through ultrasound (Ojha et al., 2016), high temperatures (Chuang et al., 2007), UV radiation (Lopez et al., 2008), and other options. However, it is necessary to evaluate some details to choose the best inactivation method, as well as to evaluate the effects on microbial structure and components (Ananta and Knorr, 2009; Taverniti and Guglielmetti, 2011).

The mechanism of action of paraprobiotics is not yet fully understood, but it is known that they are capable of acting in immunomodulation (Adams, 2010). *L.* rhamnosus GG (LGG), inactivated by UV radiation (Lopez et al., 2008) or heat killed (Li et al., 2009), has shown interesting results. UV-inactivated LGG is as effective as living LGG in downregulating the IL-8 response in Caco-2 cells; IL-8 is a proinflammatory chemokine released by intestinal cells (Lopez et al., 2008). Heat-killed LGG was tested in an infant rat model with LPS-induced inflammation and both live and inactivated strains administered enterally (10^8 CFU/kg); both were able to decrease proinflammatory mediators induced by LPS and to positively regulate anti-inflammatory mediators in the liver, plasma, and lung (Li et al., 2009).

The strains *L. acidophilus* A2, *L. gasseri* A5, and *L. salivarius* A6 inactivated by heat, in an *in vitro* experiment, were both able (at 10^5 CFU/ml) to stimulate splenocyte and dendritic cell proliferation and production of IL-10, IL-12–p70, and IFN-γ. Likewise, *L. salivarius* was able to activate splenocytes and dendritic cells in mice to induce T cells toward a Th1 immune response. It was concluded that heat-inactivated bacteria can play an important role in modulating the immune response (Chuang et al., 2007).

A comparison was made of the *in vitro* potential of viable *L. rhamnosus*, the same bacteria inactivated by heat and the culture supernatant, for inducing the synthesis of cytokines by macrophages. Viable and heat-inactivated *L. rhamnosus* were able to induce the production of TNF-α, IL-6, and IL-10, demonstrating a capability to exert an immunoregulatory effect on macrophages (Jorjão et al., 2015).

Postbiotics is another term that emerged after it was found that not only live probiotic bacteria are capable of promoting health benefits. Postbiotics comprise all products obtained from the metabolic processes of live bacteria or released after bacterial lysis, with biological benefits for the host (Tsilingiri and Rescigno, 2013). These products include cell surface proteins (surface-layer proteins), cell-free supernatants (CFS), cell lysates, bacteriocins, enzymes such as glutathione peroxidase (GPx) and superoxide dismutase (SOD), peptides, teichoic acids, exopolysaccharides, B-group vitamins, secreted polysaccharides, organic acids (lactate), and SCFAs (acetate, propionate, and butyrate) (Tsilingiri and Rescigno, 2013).

Postbiotic mechanisms of action have not been fully elucidated; nonetheless, there is evidence that they promote antioxidant (Xu et al., 2011; Xing et al., 2015) and antiproliferative effects (Escamilla et al., 2012; Chuah et al., 2019), stimulating antipathogenic, immunomodulatory, and anti-inflammatory proprieties (Wang et al., 2018; Gao et al., 2019).

PREBIOTICS, SYNBIOTICS, AND PARAPROBIOTICS IN INTESTINAL MUCOSITIS

A few studies describe the action of prebiotics (**Figure 5A**), synbiotics (**Figure 5B**), and paraprobiotics (**Figure 5C**) on intestinal mucositis. **Table 1** presents the main findings of their effects in intestinal mucositis. FOS supplement (3 and 6%) was administered to evaluate the effect on 5-FU (150 mg/kg)-induced intestinal mucositis in a murine model (Smith et al., 2008; Galdino et al., 2018). FOS was able to reduce MPO activity in a jejunum section. This was the only parameter that showed a significant reduction (Smith et al., 2008). In addition, beneficial effects of FOS (6%) administration in an experimental model of intestinal mucositis induced by 5-FU (300 mg/kg) were observed (Galdino et al., 2018). There was a decrease in inflammatory infiltrate, partial preservation of the intestinal epithelium, attenuation in body weight loss, and increased catalase levels, showing that supplementation with FOS could be an important adjuvant for the prevention and treatment of intestinal mucositis (Galdino et al., 2018).

Regarding the effects of synbiotics on intestinal mucositis, a commercial product called Simbioflora® , which is a synbiotic compound composed of 5.5 g of FOS plus four probiotic strains, *L. paracasei*, *L. rhamnosus*, *L. acidophilus*, and *B. lactis*, was evaluated (Trindade et al., 2018). This synbiotic was able to attenuate weight loss, decrease intestinal permeability,

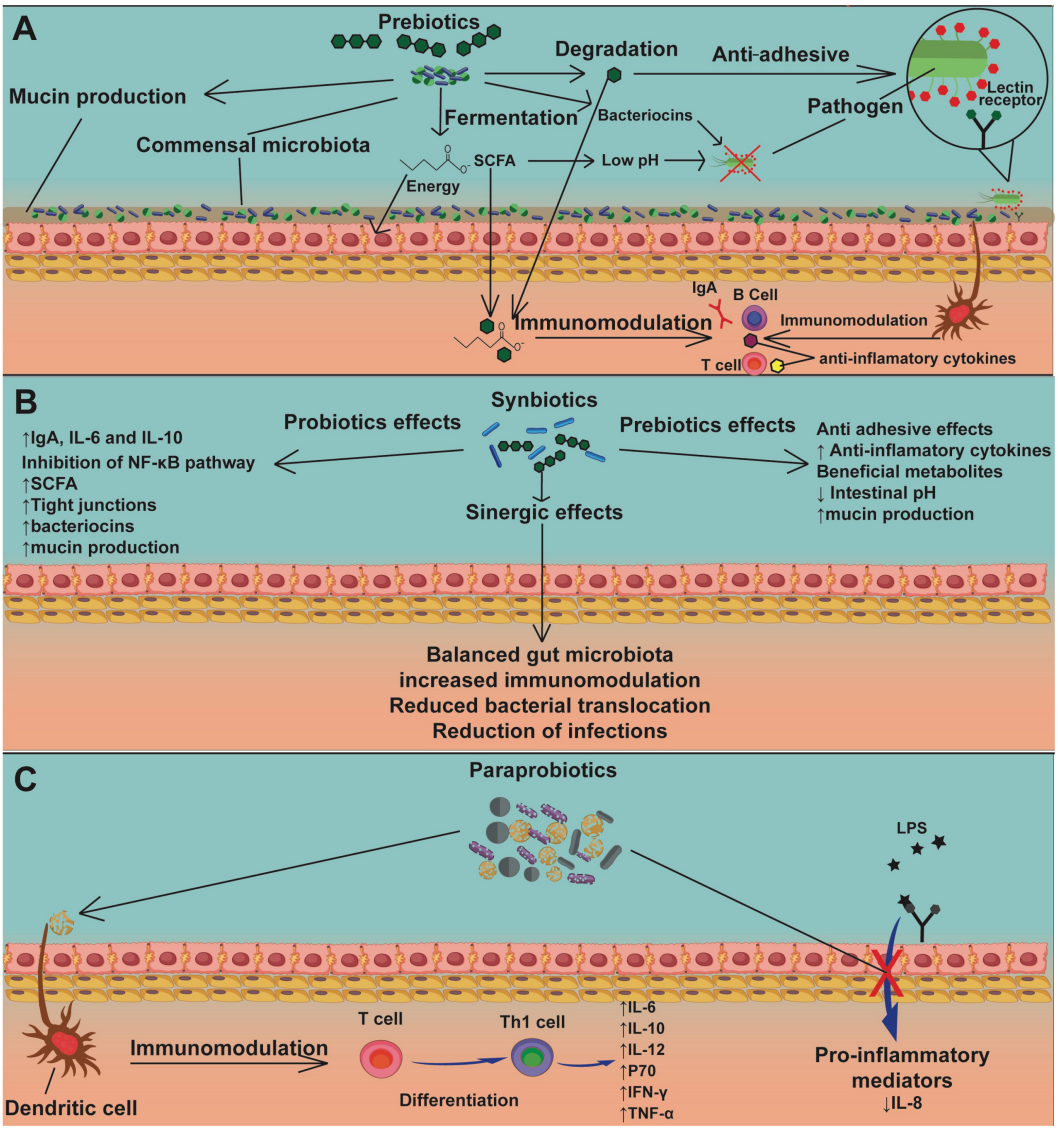

FIGURE 5 | The mechanisms of action of prebiotics, synbiotics, and paraprobiotics. Prebiotics **(A)** act as nourishment for beneficial bacteria in the commensal microbiota, inducing the production of mucins, SCFAs, and bacteriocins, the latter two causing pathogen inhibition. Another mechanism by which prebiotics can inhibit pathogens is by interaction with an adhesion receptor, such as the lectin receptor, demonstrating an antiadhesive action. Sub-units of prebiotics and SCFAs can be used by the host cells for energy production and promote directly or indirectly, via dendritic cells, immunomodulation of lymphocytes, stimulating production of IgA and anti-inflammatory cytokines. Synbiotics **(B)** have mechanisms of action of both probiotics (**Figure 4**) and prebiotics **(A)**. Moreover, synbiotics have the advantage of generating a synergic effect, which promotes balance in the gut microbiota, increased immunomodulation, reduced bacterial translocation, and reduction of infections due to strong competition by probiotics against pathogens. The mechanism of action of paraprobiotics **(C)** is still not fully understood, though immunomodulation of T cells by dendritic cells has been reported, stimulating their differentiation into Th1 cells, promoting the production of anti-inflammatory cytokines. Another proposed mechanism is inhibition of signaling pathways related to LPS stimulation, resulting in a reduction of proinflammatory mediators, especially IL-8.

reduce eosinophil infiltrate, and also improve the histology of the intestinal mucosa, with preservation of the epithelial architecture, when compared to the administration of the isolated prebiotics (Trindade et al., 2018). In addition, it was found that this synbiotic increases the production of extracellular factors, such as SCFAs (acetate and butyrate), which could contribute to the observed immunomodulating activity (Trindade et al., 2018).

The effects of paraprobiotics on mucositis were demonstrated by Fang et al. (2014). To examine the immunomodulatory properties of *L. rhamnosus*, the bacteria were inactivated by heat and evaluated in an *in vitro* model of intestinal mucositis using Caco-2 cells (Fang et al., 2014). This revealed that heat does not affect the cell integrity of this bacterial species, maintaining its rod-shaped structure intact, considerably reducing the expression of monocyte

chemoattractant protein 1 (MCP-1), and regulating the expression of TNF-α and IL-12. The same results were obtained with live bacteria, revealing that this bacterial species conserved intact probiotic properties after heat inactivation, making it a promising candidate for further studies (Fang et al., 2014).

In a study of the postbiotic effect on 5-FU-induced intestinal mucositis, Prisciandaro et al. (2011) found that *Escherichia coli Nissle* 1917 (EcN) supernatant partially protected the mouse intestine from 5-FU damage (150 mg/kg) (Prisciandaro et al., 2011). It was observed that this postbiotic was able to help avoid histological damage (villus height and crypt depth) and prevented a decrease in acidic mucin-producing goblet cells. Another study showed that oral butyrate supplementation (9 mM) was able to reduce the damage to the intestinal mucosa caused by this antineoplastic agent (200 mg/kg). Reduction in histological damage, ulceration, and amelioration in intestinal permeability were observed. The gene expression of the *tight junction* protein ZO-1 (zonulin) was increased, and proinflammatory cytokines, such as TNF-α and IL-6, were reduced (Ferreira et al., 2012).

The supernatant of mulberry leaf extract fermented by *L. acidophilus A4* was able to reduce gene expression of proinflammatory cytokines IL-1β and myeloperoxidase (MPO), and stimulate overexpression of mucin genes (MUC2 and MUC5AC), thus reducing the severity of intestinal mucositis induced by 5-FU (150 mg/kg) (Oh et al., 2017). Additionally, *Lactobacillus plantarum* supernatant inhibited the expression of the specific markers CD44, CD133, CD166, and ALDH1 of 5-FU-resistant colorectal cancer cells (CRC) (HT-29 and HCT116) (An and Ha, 2016). The combination therapy of this postbiotic and 5-FU induced an anticancer mechanism by inactivating the Wnt/β-catenin signaling of chemoresistant CRC cells and led to cell death by inducing caspase-3 activity. These results suggest that probiotic secretory substances can regulate cell proliferation in colorectal cancer and may be a therapeutic alternative for treating chemoresistant colorectal cancer (An and Ha, 2016).

To date, there have been few rigorous investigations examining the effect of prebiotics on 5-FU-induced intestinal mucositis. Knowing its potential in the intestinal mucosa, their supplementation with probiotics may be an attractive therapeutic alternative to ameliorate symptoms caused by mucositis, as well as other diseases involving the GIT.

Despite the significant impact of mucositis and advances in research to understand this pathology, existing therapies are mainly limited to clinical management of symptoms, aiming at electrolyte replacement, oral rehydration, and the use of adjuvant agents, such as loperamide octreotide, sucralfate enemas, sulfasalazine, and hyperbaric oxygen, to reduce fluid loss and decrease intestinal motility and diarrhea associated with mucositis, which are important debilitating symptoms (Van Sebille et al., 2015; Ribeiro et al., 2016). Given that it is necessary to find more effective therapeutic alternatives to combat intestinal mucositis, the "biotics" are strong candidates.

FINAL CONSIDERATIONS

The antineoplastic drug 5-FU is an essential and useful option for cancer treatment; however, its side effects, especially mucositis, can complicate treatment continuity and may lead to death. Effective measures to combat these symptoms, improving the quality of life of cancer patients, are crucially needed.

The probiotics have been investigated in various studies because of their beneficial properties for the GIT, including attenuation of dysbiosis. Several probiotic bacteria studied in intestinal mucositis murine models were able to attenuate and prevent intestinal histological damage, and also decrease weight loss and proinflammatory cytokine secretions, proving to be quite efficient in ameliorating the side effects to the intestine caused by 5-FU.

Though they can improve the health of the host, administration of viable microorganisms to immunosuppressed individuals still leads to controversial clinical findings. Paraprobiotics could be an effective alternative to address this concern, since microbial cells are dead or inactivated, thus avoiding risks associated with their administration to immunocompromised individuals.

Prebiotics are also described in the literature for their regulatory ability, acting to modify the commensal microbiota to a beneficial state. However, there are a few studies evaluating their potential for helping avoid intestinal mucositis. The existing studies demonstrate that prebiotics, when associated with a probiotic, are more efficient than when they are used separately, attenuating the symptoms of mucositis and improving to almost normal status the histology of the GIT.

Therefore, probiotics, prebiotics, synbiotics, paraprobiotics, and postbiotics may be useful alternatives for the treatment of intestinal mucositis induced by 5-FU. However, further studies are needed to elucidate all of the mechanisms of action of these bacteria and prebiotics to evolve into human clinical trials.

AUTHOR CONTRIBUTIONS

VB, TS, LT, LJ, FB, and NC-R wrote the original draft of the manuscript. VA, MD, and PM-A reviewed and revised the manuscript, obtained funding, and supervised the project. All authors contributed to the article and approved the submitted version.

FUNDING

This work was financially supported by grants from the Brazilian funding agencies, Conselho Nacional de Desenvolvimento Científico e Tecnológico (CNPq), Coordenação de Aperfeiçoamento de Pessoal de Nível Superior (CAPES), and Fundação de Amparo à Pesquisa do Estado de Minas Gerais (FAPEMIG). Centro Federal de Educação Tecnológica de Minas Gerais (CEFET/MG) and Center of Microscopy at the Universidade Federal de Minas Gerais (http://www.microscopia.ufmg.br) for providing the equipment and technical support for experiments involving electron microscopy.

REFERENCES

Acurcio, L. B., Sandes, S. H. C., Bastos, R. W., Sant'anna, F. M., Pedroso, S. H. S. P., Reis, D. C., et al. (2017). Milk fermented by Lactobacillus species from Brazilian artisanal cheese protect germ-free-mice against *Salmonella* typhimurium infection. *Benef. Microbes* 8, 579–588. doi: 10.3920/BM2016.0163

Adams, C. A. (2010). The probiotic paradox: Live and dead cells are biological response modifiers. *Nutr. Res. Rev.* 23, 37–46. doi: 10.1017/S0954422410000090

Aguilar-Toalá, J. E., Garcia-Varela, R., Garcia, H. S., Mata-Haro, V., González-Córdova, A. F., Vallejo-Cordoba, B., et al. (2018). Postbiotics: An evolving term within the functional foods field. *Trends Food Sci. Technol.* 75, 105–114. doi: 10.1016/j.tifs.2018.03.009

Alakomi, H.-L., Skytta, E., Saarela, M., Mattila-Sandholm, T., Latva-Kala, K., and Helander, I. M. (2000). Lactic Acid Permeabilizes Gram-Negative Bacteria by Disrupting the Outer Membrane. *Appl. Environ. Microbiol.* 66, 2001–2005. doi: 10.1128/AEM.66.5.2001-2005.2000

Aliakbarpour, H. R., Chamani, M., Rahimi, G., Sadeghi, A. A., and Qujeq, D. (2012). The Bacillus subtilis and Lactic Acid Bacteria Probiotics Influences Intestinal Mucin Gene Expression, Histomorphology and Growth Performance in Broilers. *Asian Austr. J. Anim. Sci.* 25, 1285–1293. doi: 10.5713/ajas.2012.12110

Amani Denj, K., Razeghi Ma, M., Akrami, R., Ghobadi, S., Jafarpour, S. A., and Mirbeygi, S. K. (2015). Effect of Dietary Prebiotic Mannan Oligosaccharide (MOS) on Growth Performance, Intestinal Microflora, Body Composition, Haematological and Blood Serum Biochemical Parameters of Rainbow Trout (Oncorhynchus mykiss) Juveniles. *J. Fish. Aquat. Sci.* 10, 255–265. doi: 10.3923/jfas.2015.255.265

An, J., and Ha, E.-M. (2016). Combination Therapy of Lactobacillus plantarum Supernatant and 5-Fluouracil Increases Chemosensitivity in Colorectal Cancer Cells. *J. Microbiol. Biotechnol.* 26, 1490–1503. doi: 10.4014/jmb.1605.05024

Ananta, E., and Knorr, D. (2009). Comparison of inactivation pathways of thermal or high pressure inactivated Lactobacillus rhamnosus ATCC 53103 by flow cytometry analysis. *Food Microbiol.* 26, 542–546. doi: 10.1016/j.fm.2009.01.008

Autenrieth, D., and Baumgart, D. (2017). Mikrobiom und entzündliche Darmerkrankungen. *DMW Dtsch. Medizinische Wochenschrift* 142, 261–266. doi: 10.1055/s-0042-111608

Azad, M. A. K., Sarker, M., and Wan, D. (2018). Immunomodulatory Effects of Probiotics on Cytokine Profiles. *Biomed Res. Int.* 2018:8063647. doi: 10.1155/2018/8063647

Bäckhed, F., Ley, R. E., Sonnenburg, J. L., Peterson, D. A., and Gordon, J. I. (2005). Host-bacterial mutualism in the human intestine. *Science* 307, 1915–1920. doi: 10.1126/science.1104816

Bastos, R. W., Pedroso, S. H. S. P., Vieira, A. T., Moreira, L. M. C., França, C. S., Cartelle, C. T., et al. (2016). Saccharomyces cerevisiae UFMG A-905 treatment reduces intestinal damage in a murine model of irinotecan-induced mucositis. *Benef. Microbes* 7, 549–558. doi: 10.3920/BM2015.0190

Bermudez-Brito, M., Plaza-Díaz, J., Muñoz-Quezada, S., Gómez-Llorente, C., and Gil, A. (2012). Probiotic Mechanisms of Action. *Ann. Nutr. Metab.* 61, 160–174. doi: 10.1159/000342079

Blackwood, B. P., Yuan, C. Y., Wood, D. R., Nicolas, J. D., Grothaus, J. S., and Hunter, C. J. (2017). Probiotic Lactobacillus Species Strengthen Intestinal Barrier Function and Tight Junction Integrity in Experimental Necrotizing Enterocolitis. *J. Probiotics Heal.* 5:159. doi: 10.4172/2329-8901.1000159

Bovee-Oudenhoven, I. M. J., ten Bruggencate, S. J. M., Lettink-Wissink, M. L. G., and van der Meer, R. (2003). Dietary fructo-oligosaccharides and lactulose inhibit intestinal colonisation but stimulate translocation of *salmonella* in rats. *Gut* 52, 1572–1578. doi: 10.1136/gut.52.11.1572

Carvalho, R. D. D. O., do Carmo, F. L. R., de Oliveira Junior, A., Langella, P., Chatel, J.-M., Bermúdez-Humarán, L. G., et al. (2017). Use of Wild Type or Recombinant Lactic Acid Bacteria as an Alternative Treatment for Gastrointestinal Inflammatory Diseases: A Focus on Inflammatory Bowel Diseases and Mucositis. *Front. Microbiol.* 8:800. doi: 10.3389/fmicb.2017.00800

Cassidy, S., and Syed, B. A. (2017). Colorectal cancer drugs market. *Nat. Rev. Drug Discov.* 16, 525–526. doi: 10.1038/nrd.2017.59

Castilho, N. P. A., Colombo, M., Oliveira, L. L., de Todorov, S. D., and Nero, L. A. (2019). Lactobacillus curvatus UFV-NPAC1 and other lactic acid bacteria isolated from calabresa, a fermented meat product, present high bacteriocinogenic activity against Listeria monocytogenes. *BMC Microbiol.* 19:63. doi: 10.1186/s12866-019-1436-1434

Cerdó, T., García-Santos, J. A., Bermúdez, M. G., and Campoy, C. (2019). The role of probiotics and prebiotics in the prevention and treatment of obesity. *Nutrients* 11:635. doi: 10.3390/nu11030635

Cereda, E., Caraccia, M., and Caccialanza, R. (2018). Probiotics and mucositis. *Curr. Opin. Clin. Nutr. Metab. Care* 21, 399–404. doi: 10.1097/MCO.0000000000000487

Chang, C.-J., Lin, T.-L., Tsai, Y.-L., Wu, T.-R., Lai, W.-F., Lu, C.-C., et al. (2019). Next generation probiotics in disease amelioration. *J. Food Drug Anal.* 27, 615–622. doi: 10.1016/j.jfda.2018.12.011

Chang, C. T., Ho, T. Y., Lin, H., Liang, J. A., Huang, H. C., Li, C. C., et al. (2012). 5-fluorouracil induced intestinal mucositis via nuclear factor-κB activation by transcriptomic analysis and in vivo bioluminescence imaging. *PLoS One* 7: e31808. doi: 10.1371/journal.pone.0031808

Chang, C. W., Liu, C. Y., Lee, H. C., Huang, Y. H., Li, L. H., Chiau, J. S. C., et al. (2018). Lactobacillus casei Variety rhamnosus Probiotic Preventively Attenuates 5-Fluorouracil/Oxaliplatin-Induced Intestinal Injury in a Syngeneic Colorectal Cancer Model. *Front. Microbiol.* 9:983. doi: 10.3389/fmicb.2018.00983

Chuah, L.-O., Foo, H. L., Loh, T. C., Mohammed Alitheen, N. B., Yeap, S. K., Abdul Mutalib, N. E., et al. (2019). Postbiotic metabolites produced by Lactobacillus plantarum strains exert selective cytotoxicity effects on cancer cells. *BMC Complement. Altern. Med.* 19:114. doi: 10.1186/s12906-019-2528-2

Chuang, L., Wu, K. G., Pai, C., Hsieh, P. S., Tsai, J. J., Yen, J. H., et al. (2007). Heat-killed cells of lactobacilli skew the immune response toward T helper 1 polarization in mouse splenocytes and dendritic cell-treated T cells. *J. Agric. Food Chem.* 55, 11080–11086. doi: 10.1021/jf071786o

Cinausero, M., Aprile, G., Ermacora, P., Basile, D., Vitale, M. G., Fanotto, V., et al. (2017). New frontiers in the pathobiology and treatment of cancer regimen-related mucosal injury. *Front. Pharmacol.* 8:354. doi: 10.3389/fphar.2017.00354

Collado, M. C., Gueimonde, M., and Salminen, S. (2010). Probiotics in Adhesion of Pathogens. *Bioact. Food Prom. Health* 2010, 353–370. doi: 10.1016/B978-0-12-374938-3.0002322

Collins, F., Rios-Arce, N. D., Schepper, J. D., Parameswaran, N., and Mccabe, L. R. (2018). The Potential of Probiotics as a Therapy for Osteoporosis. *Bugs Drugs* 5, 213–233. doi: 10.1128/microbiolspec.BAD-0015-2016

Comstock, S. S., Wang, M., Hester, S. N., Li, M., and Donovan, S. M. (2014). Select human milk oligosaccharides directly modulate peripheral blood mononuclear cells isolated from 10-d-old pigs. *Br. J. Nutr.* 111, 819–828. doi: 10.1017/S0007114513003267

Cordeiro, B. F., Oliveira, E. R., Da Silva, S. H., Savassi, B. M., Acurcio, L. B., Lemos, L., et al. (2018). Whey Protein Isolate-Supplemented Beverage, Fermented by Lactobacillus casei BL23 and Propionibacterium freudenreichii 138, in the Prevention of Mucositis in Mice. *Front. Microbiol.* 9:2035. doi: 10.3389/fmicb.2018.02035

Crombie, J., and Longo, D. L. (2016). *Principles of Cancer Treatment*. Netherland: Elsevier.

Cuevas-González, P. F., Liceaga, A. M., and Aguilar-Toalá, J. E. (2020). Postbiotics and paraprobiotics: From concepts to applications. *Food Res. Int.* 136:109502. doi: 10.1016/j.foodres.2020.109502

Davani-Davari, D., Negahdaripour, M., Karimzadeh, I., Seifan, M., Mohkam, M., Masoumi, S., et al. (2019). Prebiotics: Definition, Types, Sources, Mechanisms, and Clinical Applications. *Foods* 8:92. doi: 10.3390/foods8030092

De Jesus, L. C. L., Drumond, M. M., de Carvalho, A., Santos, S. S., Martins, F. S., Ferreira, Ê, et al. (2019). Protective effect of Lactobacillus delbrueckii subsp. *Lactis CIDCA* 133 in a model of 5 Fluorouracil-Induced intestinal mucositis. *J. Funct. Foods* 53, 197–207. doi: 10.1016/j.jff.2018.12.027

De Keersmaecker, S. C. J., Verhoeven, T. L. A., Desair, J., Marchal, K., Vanderleyden, J., and Nagy, I. (2006). Strong antimicrobial activity of Lactobacillus rhamnosus GG against *Salmonella* typhimurium is due to accumulation of lactic acid. *FEMS Microbiol. Lett.* 259, 89–96. doi: 10.1111/j.1574-6968.2006.00250.x

de Oliveira, G. L. V., Leite, A. Z., Higuchi, B. S., Gonzaga, M. I., and Mariano, V. S. (2017). Intestinal dysbiosis and probiotic applications in autoimmune diseases. *Immunology* 152, 1–12. doi: 10.1111/imm.12765

Duncan, M., and Grant, G. (2003). Mucositis-Causes and Possible Treatments. *Alim. Pharmacol. Ther.* 18, 853–874. doi: 10.1046/j.0269-2813.2003.01784.x

Enam, F., and Mansell, T. J. (2019). Prebiotics: tools to manipulate the gut microbiome and metabolome. *J. Ind. Microbiol. Biotechnol.* 46, 1445–1459. doi: 10.1007/s10295-019-022032204

Escamilla, J., Lane, M. A., and Maitin, V. (2012). Cell-Free Supernatants from Probiotic Lactobacillus casei and Lactobacillus rhamnosus GG Decrease Colon Cancer Cell Invasion In Vitro. *Nutr. Cancer* 64, 871–878. doi: 10.1080/01635581.2012.700758

Fang, S., Bin Shih, H. Y., Huang, C. H., Li, L. T., Chen, C. C., and Fang, H. W. (2014). Live and heat-killed Lactobacillus rhamnosus GG upregulate gene expression of pro-inflammatory cytokines in 5-fluorouracil-pretreated Caco-2 cells. *Support. Care Cancer* 22, 1647–1654. doi: 10.1007/s00520-014-2137-z

FAO/WHO (2001). *Joint FAO/WHO Expert Consultation on Evaluation of Health and Nutritional Properties of Probiotics*. Argentina: WHO.

Fedorak, R. N., Feagan, B. G., Hotte, N., Leddin, D., Dieleman, L. A., Petrunia, D. M., et al. (2015). The probiotic VSL#3 has anti-inflammatory effects and could reduce endoscopic recurrence after surgery for Crohn's disease. *Clin. Gastroenterol. Hepatol.* 13, 928-35.e2. doi: 10.1016/j.cgh.2014.10.031

Ferreira, T. M., Leonel, A. J., Melo, M. A., Santos, R. R. G., Cara, D. C., Cardoso, V. N., et al. (2012). Oral supplementation of butyrate reduces mucositis and intestinal permeability associated with 5-fluorouracil administration. *Lipids* 47, 669–678. doi: 10.1007/s11745-012-36803683

Furusawa, Y., Obata, Y., Fukuda, S., Endo, T. A., Nakato, G., Takahashi, D., et al. (2013). Commensal microbe-derived butyrate induces the differentiation of colonic regulatory T cells. *Nature* 504, 446–450. doi: 10.1038/nature12721

Galdino, F. M. P., Andrade, M. E. R., de Barros, P. A. V., S. , V., Alvarez-Leite, J. I., Almeida-Leite, C. M., et al. (2018). Pretreatment and treatment with fructo-oligosaccharides attenuate intestinal mucositis induced by 5-FU in mice. *J. Funct. Foods* 49, 485–492. doi: 10.1016/j.jff.2018.09.012

Gao, J., Li, Y., Wan, Y., Hu, T., Liu, L., Yang, S., et al. (2019). A Novel Postbiotic From Lactobacillus rhamnosus GG With a Beneficial Effect on Intestinal Barrier Function. *Front. Microbiol.* 10:477. doi: 10.3389/fmicb.2019.00477

Gao, S., Li, D., Liu, Y., Zha, E., Zhou, T., and Yue, X. (2015). Oral immunization with recombinant hepatitis E virus antigen displayed on the Lactococcus lactis surface enhances ORF2-specific mucosal and systemic immune responses in mice. *Int. Immunopharmacol.* 24, 140–145. doi: 10.1016/j.intimp.2014.10.032

Gaspar, C., Donders, G. G., Palmeira-de-Oliveira, R., Queiroz, J. A., Tomaz, C., Martinez-de-Oliveira, J., et al. (2018). Bacteriocin production of the probiotic Lactobacillus acidophilus KS400. *AMB Express* 8:153. doi: 10.1186/s13568-018-0679-z

Geier, M. S., Butler, R. N., and Howarth, G. S. (2006). Probiotics, prebiotics and synbiotics: a role in chemoprevention for colorectal cancer? *Cancer Biol. Ther.* 5, 1265–1269. doi: 10.4161/cbt.5.10.3296

Gibson, G. R., Hutkins, R., Sanders, M. E., Prescott, S. L., Reimer, R. A., Salminen, S. J., et al. (2017). Expert consensus document: The International Scientific Association for Probiotics and Prebiotics (ISAPP) consensus statement on the definition and scope of prebiotics. *Nat. Rev. Gastroenterol. Hepatol.* 14, 491–502. doi: 10.1038/nrgastro.2017.75

Gibson, G. R., and Roberfroid, M. B. (1995). Dietary modulation of the human colonic microbiota: introducing the concept of prebiotics. *J. Nutr.* 125, 1401–1412. doi: 10.1093/jn/125.6.1401

Gibson, G. R., and Wang, X. (1994). Regulatory effects of bifidobacteria on the growth of other colonic bacteria. *J. Appl. Bacteriol.* 77, 412–420. doi: 10.1111/j.1365-2672.1994.tb03443.x

Gomes-Santos, A. C., Oliveira, R. P., de Moreira, T. G., Castro-Junior, A. B., Horta, B. C., Lemos, L., et al. (2017). Hsp65-Producing Lactococcus lactis Prevents Inflammatory Intestinal Disease in Mice by IL-10- and TLR2-Dependent Pathways. *Front. Immunol.* 8:30. doi: 10.3389/fimmu.2017.00030

Guichard, N., Guillarme, D., Bonnabry, P., and Fleury-Souverain, S. (2017). Antineoplastic drugs and their analysis: a state of the art review. *Analyst* 142, 2273–2321. doi: 10.1039/c7an00367f

Halder, D., Mandal, M., Chatterjee, S., Pal, N., and Mandal, S. (2017). Indigenous Probiotic Lactobacillus Isolates Presenting Antibiotic like Activity against Human Pathogenic Bacteria. *Biomedicines* 5:31. doi: 10.3390/biomedicines5020031

Holleran, G., Lopetuso, L. R., Ianiro, G., Pecere, S., Pizzoferrato, M., Petito, V., et al. (2017). Gut microbiota and inflammatory bowel disease: so far so gut! *Minerva Gastroenterol. Dietol* 63, 373–384. doi: 10.23736/S1121-421X.17.02386238

Hosono, A., Ozawa, A., Kato, R., Ohnishi, Y., Nakanshi, Y., Kimura, T., et al. (2003). Dietary Fructooligosaccharides Induce Immunoregulation of Intestinal IgA Secretion by Murine Peyer's Patch Cells. *Biosci. Biotechnol. Biochem.* 67, 758–764. doi: 10.1271/bbb.67.758

Hsieh, M.-C., Tsai, W.-H., Jheng, Y.-P., Su, S.-L., Wang, S.-Y., Lin, C.-C., et al. (2018). The beneficial effects of Lactobacillus reuteri ADR-1 or ADR-3 consumption on type 2 diabetes mellitus: a randomized, double-blinded, placebo-controlled trial. *Sci. Rep.* 8:16791. doi: 10.1038/s41598-018-3501435011

Jamali, J., Dayo, A., Adeel, A., Qureshi, Y., Khan, T., and Begum, S. (2018). A survey on gastrointestinal adverse drug reactions of Doxorubicin and Cyclophosphamide combination therapy. *J. Pak. Med. Assoc.* 68, 926–928.

Jandhyala, S. M., Talukdar, R., Subramanyam, C., Vuyyuru, H., Sasikala, M., and Reddy, D. N. (2015). Role of the normal gut microbiota. *World J. Gastroenterol.* 21, 8836–8847. doi: 10.3748/wjg.v21.i29.8787

Jorjão, A. L., De Oliveira, F. E., Vieira, M., Leão, P., Antonio, C., Carvalho, T., et al. (2015). ATCC 7469 May Induce Modulatory Cytokines Profiles on Macrophages RAW 264. *Scien. World J.* 2015:716749.

Justino, P. F. C., Franco, A. X., Pontier-Bres, R., Monteiro, C. E. S., Barbosa, A. L. R., Souza, M. H. L. P., et al. (2020). Modulation of 5-fluorouracil activation of toll-like/MyD88/NF-κB/MAPK pathway by Saccharomyces boulardii CNCM I-745 probiotic. *Cytokine* 125:154791. doi: 10.1016/j.cyto.2019.154791

Justino, P. F. C., Melo, L. F. M., Nogueira, A. F., Morais, C. M., Mendes, W. O., Franco, A. X., et al. (2015). Regulatory role of Lactobacillus acidophilus on inflammation and gastric dysmotility in intestinal mucositis induced by 5-fluorouracil in mice. *Cancer Chemother. Pharmacol.* 75, 559–567. doi: 10.1007/s00280-014-2663-x

Kaci, G., Lakhdari, O., Doré, J., Ehrlich, S. D., Renault, P., Blottière, H. M., et al. (2011). Inhibition of the NF-κB Pathway in Human Intestinal Epithelial Cells by Commensal Streptococcus salivarius. *Appl. Environ. Microbiol.* 77, 4681–4684. doi: 10.1128/AEM.030213010

Kato, S., Hamouda, N., Kano, Y., Oikawa, Y., Tanaka, Y., Matsumoto, K., et al. (2017). Probiotic Bifidobacterium bifidum G9-1 attenuates 5-fluorouracil-induced intestinal mucositis in mice via suppression of dysbiosis-related secondary inflammatory responses. *Clin. Exp. Pharmacol. Physiol.* 44, 1017–1025. doi: 10.1111/1440-1681.12792

Kim, H. J., Kim, J. H., Moon, W., Park, J., Park, S. J., Song, G. A., et al. (2015). Rebamipide Attenuates 5-Fluorouracil-Induced Small Intestinal Mucositis in a Mouse Model. *Biol. Pharm. Bull.* 38, 179–183. doi: 10.1248/bpb.b14-00400

Kim, N., Yun, M., Oh, Y. J., and Choi, H.-J. (2018). Mind-altering with the gut: Modulation of the gut-brain axis with probiotics. *J. Microbiol.* 56, 172–182. doi: 10.1007/s12275-018-80328034

Kim, S., Chun, H., Choi, H., Kim, E., Keum, B., Seo, Y., et al. (2018). Ursodeoxycholic acid attenuates 5-fluorouracil-induced mucositis in a rat model. *Oncol. Lett.* 16, 2585–2590. doi: 10.3892/ol.2018.8893

König, J., Wells, J., Cani, P. D., García-Ródenas, C. L., MacDonald, T., Mercenier, A., et al. (2016). Human intestinal barrier function in health and disease. *Clin. Transl. Gastroenterol* 7:e196 doi: 10.1038/ctg.2016.54

Kuczkowska, K., Øverland, L., Rocha, S. D. C., Eijsink, V. G. H., and Mathiesen, G. (2019). Comparison of eight Lactobacillus species for delivery of surface-displayed mycobacterial antigen. *Vaccine* 37, 6371–6379. doi: 10.1016/j.vaccine.2019.09.012

Lane, E. R., Zisman, T. L., and Suskind, D. L. (2017). The microbiota in inflammatory bowel disease: Current and therapeutic insights. *J. Inflamm. Res.* 10, 63–73. doi: 10.2147/JIR.S116088

LeCureux, J. S., and Dean, G. A. (2018). Lactobacillus Mucosal Vaccine Vectors: Immune Responses against Bacterial and Viral Antigens. *mSphere* 3, e00061–18. doi: 10.1128/mSphere.00061-18

Lee, C. S. (2014). Gastro-intestinal toxicity of chemotherapeutics in colorectal cancer: The role of inflammation. *World J. Gastroenterol.* 20:3751–3761. doi: 10.3748/wjg.v20.i14.3751

Levit, R., Savoy de Giori, G., de Moreno, de LeBlanc, A., and LeBlanc, J. G. (2018). Protective effect of the riboflavin-overproducing strain Lactobacillus plantarum CRL2130 on intestinal mucositis in mice. *Nutrition* 54, 165–172. doi: 10.1016/j.nut.2018.03.056

L'homme, C., Arbelot, M., Puigserver, A., and Biagini, A. (2003). Kinetics of Hydrolysis of Fructooligosaccharides in Mineral-Buffered Aqueous Solutions: Influence of pH and Temperature. *J. Agric. Food Chem.* 51, 224–228. doi: 10.1021/jf0204699

Li, N., Russell, W. M., Douglas-Escobar, M., Hauser, N., Lopez, M., and Neu, J. (2009). Live and heat-killed lactobacillus rhamnosus GG: Effects on proinflammatory and anti-inflammatory cytokines/chemokines in gastrostomy-fed infant rats. *Pediatr. Res.* 66, 203–207. doi: 10.1203/PDR.0b013e3181aabd4f

Longley, D. B., Harkin, D. P., and Johnston, P. G. (2003). 5-Fluorouracil: Mechanisms of action and clinical strategies. *Nat. Rev. Cancer* 3, 330–338. doi: 10.1038/nrc1074

Lopez, M., Li, N., Kataria, J., Russell, M., and Neu, J. (2008). Live and Ultraviolet-Inactivated Lactobacillus Rhamnosus GG Decrease Flagellin-Induced Interleukin-8 Production in Caco-2 Cells. *J. Nutr.* 138, 2264–2268. doi: 10.3945/jn.108.093658

Luu, M., and Visekruna, A. (2019). Short-chain fatty acids: Bacterial messengers modulating the immunometabolism of T cells. *Eur. J. Immunol.* 49, 842–848. doi: 10.1002/eji.201848009

Machado, F. F., Lazzaretti, R. K., and Poziomyck, A. K. (2014). Uso de Prebióticos, Probióticos e Simbióticos nos Pré e Pós- -Operatórios do Câncer Colorretal: uma Revisão. *Rev. Bras. Cancerol.* 60, 363–370.

Makras, L., Triantafyllou, V., Fayol-Messaoudi, D., Adriany, T., Zoumpopoulou, G., Tsakalidou, E., et al. (2006). Kinetic analysis of the antibacterial activity of probiotic lactobacilli towards *Salmonella enterica* serovar Typhimurium reveals a role for lactic acid and other inhibitory compounds. *Res. Microbiol.* 157, 241–247. doi: 10.1016/j.resmic.2005.09.002

Markowiak, P., and Ślizewska, K. (2017). Effects of probiotics, prebiotics, and synbiotics on human health. *Nutrients* 9:1021. doi: 10.3390/nu9091021

Martins, C. C., and Wagner, S. C. (2013). Individualização Farmacocinética das Doses de 5-Fluoruracil no Câncer Colorretal. *Rev. Bras. Cancerol.* 59, 271–280.

Mathur, S., and Singh, R. (2005). Antibiotic resistance in food lactic acid bacteria—a review. *Int. J. Food Microbiol.* 105, 281–295. doi: 10.1016/j.ijfoodmicro.2005.03.008

Mi, H., Dong, Y., Zhang, B., Wang, H., Peter, C. C. K., Gao, P., et al. (2017). Bifidobacterium Infantis Ameliorates Chemotherapy-Induced Intestinal Mucositis Via Regulating T Cell Immunity in Colorectal Cancer Rats. *Cell. Physiol. Biochem.* 42, 2330–2341. doi: 10.1159/000480005

Miura, K., Kinouchi, M., Ishida, K., Fujibuchi, W., Naitoh, T., Ogawa, H., et al. (2010). 5-FU Metabolism in Cancer and Orally-Administrable 5-FU Drugs. *Cancers* 2, 1717–1730. doi: 10.3390/cancers2031717

Mokoena, M. P. (2017). Lactic Acid Bacteria and Their Bacteriocins: Classification, Biosynthesis and Applications against Uropathogens: A Mini-Review. *Molecules* 22:1255. doi: 10.3390/molecules22081255

Monteagudo-Mera, A., Rastall, R. A., Gibson, G. R., Charalampopoulos, D., and Chatzifragkou, A. (2019). Adhesion mechanisms mediated by probiotics and prebiotics and their potential impact on human health. *Appl. Microbiol. Biotechnol.* 103, 6463–6472. doi: 10.1007/s00253-019-099789977

Mowat, A. M., and Agace, W. W. (2014). Regional specialization within the intestinal immune system. *Nat. Rev. Immunol.* 14, 667–685. doi: 10.1038/nri3738

Nussbaumer, S., Bonnabry, P., Veuthey, J.-L., and Fleury-Souverain, S. (2011). Analysis of anticancer drugs: A review. *Talanta* 85, 2265–2289. doi: 10.1016/j.talanta.2011.08.034

Oh, N. S., Lee, J. Y., Lee, J. M., Lee, K. W., and Kim, Y. (2017). Mulberry leaf extract fermented with Lactobacillus acidophilus A4 ameliorates 5-fluorouracil-induced intestinal mucositis in rats. *Lett. Appl. Microbiol.* 64, 459–468. doi: 10.1111/lam.12741

Ojha, K. S., Kerry, J. P., Alvarez, C., Walsh, D., and Tiwari, B. K. (2016). Effect of high intensity ultrasound on the fermentation profile of Lactobacillus sakei in a meat model system. *Ultrason. Sonochem.* 31, 539–545. doi: 10.1016/j.ultsonch.2016.01.001

Pandey, K. R., Naik, S. R., and Vakil, B. V. (2015). Probiotics, prebiotics and synbiotics- a review. *J. Food Sci. Technol.* 52, 7577–7587. doi: 10.1007/s13197-015-19211921

Parada Venegas, D., De la Fuente, M. K., Landskron, G., González, M. J., Quera, R., Dijkstra, G., et al. (2019). Short Chain Fatty Acids (SCFAs)-Mediated Gut Epithelial and Immune Regulation and Its Relevance for Inflammatory Bowel Diseases. *Front. Immunol* 10:277. doi: 10.3389/fimmu.2019.00277

Plavec, T. V., and Berlec, A. (2019). Engineering of lactic acid bacteria for delivery of therapeutic proteins and peptides. *Appl. Microbiol. Biotechnol.* 103, 2053–2066. doi: 10.1007/s00253-019-09628-y

Playne, R., and Crittenden, M. (2002). Purification of food-grade oligosaccharides using immobilised cells of Zymomonas mobilis. *Appl. Microbiol. Biotechnol.* 58, 297–302. doi: 10.1007/s00253-001-0886883

Plaza-Díaz, J., Ruiz-Ojeda, F., Vilchez-Padial, L., and Gil, A. (2017). Evidence of the Anti-Inflammatory Effects of Probiotics and Synbiotics in Intestinal Chronic Diseases. *Nutrients* 9:555. doi: 10.3390/nu9060555

Porto, B. A. A., Monteiro, C. F., Souza, ÉL. S., Leocádio, P. C. L., Alvarez-Leite, J. I, Generoso, S. V., et al. (2019). Treatment with selenium-enriched Saccharomyces cerevisiae UFMG A-905 partially ameliorates mucositis induced by 5-fluorouracil in mice. *Cancer Chemother. Pharmacol.* 84, 117–126. doi: 10.1007/s00280-019-038653868

Pot, B., Foligné, B., Daniel, C., and Grangette, C. (2013). Understanding immunomodulatory effects of probiotics. *Nestle Nutr. Inst. Workshop Ser.* 77, 75–90. doi: 10.1159/000351388

Prisciandaro, L. D., Geier, M. S., Butler, R. N., Cummins, A. G., and Howarth, G. S. (2011). Probiotic factors partially improve parameters of 5-fluorouracil-induced intestinal mucositis in rats. *Cancer Biol. Ther.* 11, 671–677. doi: 10.4161/cbt.11.7.14896

Quaresma, M., Damasceno, S., Monteiro, C., Lima, F., Mendes, T., Lima, M., et al. (2019). Probiotic mixture containing Lactobacillus spp. *and Bifidobacterium spp. attenuates* 5-fluorouracil-induced intestinal mucositis in mice. *Nutr. Cancer* 12, 1–11. doi: 10.1080/01635581.2019.1675719

Rad, A. H., Aghebati-Maleki, L., Kafil, H. S., and Abbasi, A. (2020). Molecular mechanisms of postbiotics in colorectal cancer prevention and treatment. *Crit. Rev. Food Sci. Nutr.* 15, 1–17. doi: 10.1080/10408398.2020.1765310

Rajilić-Stojanović, M., and de Vos, W. M. (2014). The first 1000 cultured species of the human gastrointestinal microbiota. *FEMS Microbiol. Rev.* 38, 996–1047. doi: 10.1111/1574-6976.12075

Rather, I. A., Bajpai, V. K., Kumar, S., Lim, J., Paek, W. K., and Park, Y.-H. (2016). Probiotics and Atopic Dermatitis: An Overview. *Front. Microbiol.* 7:507. doi: 10.3389/fmicb.2016.00507

Ribeiro, R. A., Wanderley, C. W. S., Wong, D. V. T., Mota, J. M. S. C., Leite, C. A. V. G., Souza, M. H. L. P., et al. (2016). Irinotecan- and 5-fluorouracil-induced intestinal mucositis: insights into pathogenesis and therapeutic perspectives. *Cancer Chemother. Pharmacol.* 78, 881–893. doi: 10.1007/s00280-016-3139-y

Roberfroid, M. B. (2007). Inulin-Type Fructans: Functional Food Ingredients. *J. Nutr* 137, 2493S–2502S. doi: 10.1093/jn/137.11.2493S

Roller, M., Rechkemmer, G., and Watzl, B. (2004). Prebiotic Inulin Enriched with Oligofructose in Combination with the Probiotics Lactobacillus rhamnosus and Bifidobacterium lactis Modulates Intestinal Immune Functions in Rats. *J. Nutr.* 134, 153–156. doi: 10.1093/jn/134.1.153

Saez-Lara, M. J., Gomez-Llorente, C., Plaza-Diaz, J., and Gil, A. (2015). The role of probiotic lactic acid bacteria and bifidobacteria in the prevention and treatment of inflammatory bowel disease and other related diseases: A systematic review of randomized human clinical trials. *Biomed Res. Int.* 2015:505878. doi: 10.1155/2015/505878

Salvo Romero, E., Alonso Cotoner, C., Pardo Camacho, C., Casado Bedmar, M., and Vicario, M. (2015). The intestinal barrier function and its involvement in digestive disease. *Rev. Española Enfermedades Dig.* 108, 686–695. doi: 10.17235/reed.2015.3846/2015

Satchithanandam, S., Vargofcak-Apker, M., Calvert, R. J., Leeds, A. R., and Cassidy, M. M. (1990). Alteration of Gastrointestinal Mucin by Fiber Feeding in Rats. *J. Nutr.* 120, 1179–1184. doi: 10.1093/jn/120.10.1179

Schley, P. D., and Field, C. J. (2002). The immune-enhancing effects of dietary fibres and prebiotics. *Br. J. Nutr.* 87, S221–S230. doi: 10.1079/bjn/20 02541

Shi, Y., Zhai, Q., Li, D., Mao, B., Liu, X., Zhao, J., et al. (2017). Restoration of cefixime-induced gut microbiota changes by Lactobacillus cocktails and fructooligosaccharides in a mouse model. *Microbiol. Res.* 200, 14–24. doi: 10. 1016/j.micres.2017.04.001

Shields, M. (2017). *Chemotherapeutics. In Pharmacognosy: Fundamentals, Applications and Strategy*. Netherland: Elsevier Inc, 295–313.

Simon, G. L., and Gorbach, S. L. (1982). Intestinal Microflora. *Med. Clin. North Am.* 66, 557–574. doi: 10.1016/S0025-7125(16)31407-9

Slavin, J. (2013). Fiber and prebiotics: mechanisms and health benefits. *Nutrients* 5, 1417–1435. doi: 10.3390/nu5041417

Smith, C. L., Geier, M. S., Yazbeck, R., Torres, D. M., Butler, R. N., and Howarth, G. S. (2008). Lactobacillus fermentum BR11 and fructo-oligosaccharide partially reduce jejunal inflammation in a model of intestinal mucositis in rats. *Nutr. Cancer* 60, 757–767. doi: 10.1080/016355808021 92841

Soccol, C. R., Vandenberghe, L. P., de, S., Spier, M. R., Medeiros, A. B. P., Yamaguishi, C. T., et al. (2010). The potential of probiotics: A review. *Food Technol. Biotechnol.* 48, 413–434.

Sonis, S. T. (2004). The pathobiology of mucositis. *Nat. Rev. Cancer* 4, 277–284. doi: 10.1038/nrc1318

Soveri, L. M., Hermunen, K., De Gramont, A., Poussa, T., Quinaux, E., Bono, P., et al. (2014). Association of adverse events and survival in colorectal cancer patients treated with adjuvant 5-fluorouracil and leucovorin: Is efficacy an impact of toxicity? *Eur. J. Cancer* 50, 2966–2974. doi: 10.1016/j.ejca.2014. 08.017

Stringer, A. M., Gibson, R. J., Logan, R. M., Bowen, J. M., Yeoh, A. S. J., Hamilton, J., et al. (2009). Gastrointestinal Microflora and Mucins May Play a Critical Role in the Development of 5-Fluorouracil-Induced Gastrointestinal Mucositis. *Exp. Biol. Med.* 234, 430–441. doi: 10.3181/0810-RM-301

Tan, J., McKenzie, C., Potamitis, M., Thorburn, A. N., Mackay, C. R., and Macia, L. (2014). The role of short-chain fatty acids in health and disease. *Adv. Immunol.* 121, 91–119. doi: 10.1016/B978-0-12-800100-4.000039

Tang, Y., Wu, Y., Huang, Z., Dong, W., Deng, Y., Wang, F., et al. (2017). Administration of probiotic mixture DM#1 ameliorated 5-fluorouracil-induced intestinal mucositis and dysbiosis in rats. *Nutrition.* 33, 96–104. doi: 10.1016/j. nut.2016.05.003

Taverniti, V., and Guglielmetti, S. (2011). The immunomodulatory properties of probiotic microorganisms beyond their viability (ghost probiotics: Proposal of paraprobiotic concept). *Genes Nutr.* 6, 261–274. doi: 10.1007/s12263-011-0218-x

Thomas, S. A., Grami, Z., Mehta, S., Patel, K., North, W., and Hospital, F. (2016). Adverse Effects of 5-fluorouracil: Focus on Rare Side Effects. *Cancer Cell Microenviron.* 3, 3–6. doi: 10.14800/ccm.1266

Thursby, E., and Juge, N. (2017). Introduction to the human gut microbiota. *Biochem. J.* 474, 1823–1836. doi: 10.1042/BCJ20160510

Touchefeu, Y., Montassier, E., Nieman, K., Gastinne, T., Potel, G., Bruley Des, et al. (2014). Systematic review: The role of the gut microbiota in chemotherapy- or radiation-induced gastrointestinal mucositis - Current evidence and potential clinical applications. *Aliment. Pharmacol. Ther.* 40, 409–421. doi: 10.1111/apt. 12878

Trindade, L. M., Martins, V. D., Rodrigues, N. M., Souza, E. L. S., Martins, F. S., Costa, G. M. F., et al. (2018). Oral administration of Simbioflora® (synbiotic) attenuates intestinal damage in a mouse model of 5-fluorouracil-induced mucositis. *Benef. Microbes* 9, 477–486. doi: 10.3920/BM20 17.0082

Tsilingiri, K., and Rescigno, M. (2013). Postbiotics: what else? *Benef. Microbes* 4, 101–107. doi: 10.3920/BM2012.0046

van Reenen, C. A., and Dicks, L. M. T. (2011). Horizontal gene transfer amongst probiotic lactic acid bacteria and other intestinal microbiota: what are the possibilities? *A review. Arch. Microbiol.* 193, 157–168. doi: 10.1007/s00203-010-0668663

Van Sebille, Y. Z. A., Stansborough, R., Wardill, H. R., Bateman, E., Gibson, R. J., and Keefe, D. M. (2015). Management of Mucositis During Chemotherapy: From Pathophysiology to Pragmatic Therapeutics. *Curr. Oncol. Rep.* 17:50. doi: 10.1007/s11912-015-0474479

van Vliet, M. J., Harmsen, H. J. M., de Bont, E. S. J. M., and Tissing, W. J. E. (2010). The Role of Intestinal Microbiota in the Development and Severity of Chemotherapy-Induced Mucositis. *PLoS Pathog.* 6:e1000879. doi: 10.1371/ journal.ppat.1000879

Vancamelbeke, M., and Vermeire, S. (2017). The intestinal barrier: a fundamental role in health and disease. *Expert Rev. Gastroenterol. Hepatol.* 11, 821–834. doi: 10.1080/17474124.2017.1343143

Villa, A., and Sonis, S. T. (2015). Mucositis: Pathobiology and management. *Curr. Opin. Oncol.* 27, 159–164. doi: 10.1097/CCO.00000000000 00180

von Bültzingslöwen, I., Adlerberth, I., Wold, A. E., Dahlén, G., and Jontell, M. (2003). Oral and intestinal microflora in 5-fluorouracil treated rats, translocation to cervical and mesenteric lymph nodes and effects of probiotic bacteria. *Oral Microbiol. Immunol.* 18, 278–284. doi: 10.1034/j.1399-302x.2003. 00075.x

Wallace, C. J. K., Foster, J. A., Soares, C. N., and Milev, R. V. (2020). The Effects of Probiotics on Symptoms of Depression: Protocol for a Double-Blind Randomized Placebo-Controlled Trial. *Neuropsychobiology* 79, 108–116. doi: 10.1159/000496406

Walter, J., and Ley, R. (2011). The Human Gut Microbiome: Ecology and Recent Evolutionary Changes. *Annu. Rev. Microbiol.* 65, 411–429. doi: 10.1146/ annurev-micro-090110102830

Wang, G., Li, X., Zhao, J., Zhang, H., and Chen, W. (2017). Lactobacillus casei CCFM419 attenuates type 2 diabetes via a gut microbiota dependent mechanism. *Food Funct.* 8, 3155–3164. doi: 10.1039/C7FO00593H

Wang, H., Zhang, L., Xu, S., Pan, J., Zhang, Q., and Lu, R. (2018). Surface-Layer Protein from Lactobacillus acidophilus NCFM Inhibits Lipopolysaccharide-Induced Inflammation through MAPK and NF-κB Signaling Pathways in RAW264.7 *Cells. J. Agric. Food Chem.* 66, 7655–7662. doi: 10.1021/acs.jafc. 8b02012

Wang, M., Gao, Z., Zhang, Y., and Pan, L. (2016). Lactic acid bacteria as mucosal delivery vehicles: a realistic therapeutic option. *Appl. Microbiol. Biotechnol.* 100, 5691–5701. doi: 10.1007/s00253-016-7557-x

Wang, Y., George, S. P., Roy, S., Pham, E., Esmaeilniakooshkghazi, A., and Khurana, S. (2016). Both the anti-and pro-apoptotic functions of villin regulate cell turnover and intestinal homeostasis. *Sci. Rep.* 6, 1–10. doi: 10.1038/ srep35491

Wang, Y. (2009). Prebiotics: Present and future in food science and technology. *Food Res. Int.* 42, 8–12. doi: 10.1016/j.foodres.2008.09.001

World Health Organization [WHO] (2018). *No Title. Fact sheets-Cancer*. Switzerland: WHO.

Wu, Y., Wang, B., Xu, H., Tang, L., Li, Y., Gong, L., et al. (2019). Probiotic Bacillus Attenuates Oxidative Stress- Induced Intestinal Injury via p38-Mediated Autophagy. *Front. Microbiol.* 10:2185. doi: 10.3389/fmicb.2019. 02185

Xing, J., Wang, G., Zhang, Q., Liu, X., Gu, Z., Zhang, H., et al. (2015). Determining Antioxidant Activities of Lactobacilli Cell-Free Supernatants by Cellular Antioxidant Assay: A Comparison with Traditional Methods. *PLoS One* 10:e0119058. doi: 10.1371/journal.pone.0119058

Xu, R., Shang, N., and Li, P. (2011). In vitro and in vivo antioxidant activity of exopolysaccharide fractions from Bifidobacterium animalis RH. *Anaerobe* 17, 226–231. doi: 10.1016/j.anaerobe.2011.07.010

Yeung, C. Y., Chan, W. T., Jiang, C., Bin, Cheng, M. L., Liu, C. Y., et al. (2015). Amelioration of chemotherapy-induced intestinal mucositis by orally administered probiotics in a mouse model. *PLoS One* 10:1–16. doi: 10.1371/ journal.pone.0138746

Yu, J. (2013). Intestinal stem cell injury and protection during cancer therapy. *Transl. Cancer Res.* 2, 384–396. doi: 10.3978/j.issn.2218-676X.2013. 07.03

Yu, L. C. H. (2018). Microbiota dysbiosis and barrier dysfunction in inflammatory bowel disease and colorectal cancers: exploring a common ground hypothesis. *J. Biomed. Sci.* 25:79. doi: 10.1186/s12929-018-0483-8

Zaharuddin, L., Mokhtar, N. M., Muhammad Nawawi, K. N., and Raja Ali, R. A. (2019). A randomized double-blind placebo-controlled trial of probiotics in post-surgical colorectal cancer. *BMC Gastroenterol.* 19:131. doi: 10.1186/ s12876-019-10471044

Zhang, F., Gao, J., Wang, B., Huo, D., Wang, Z., Zhang, J., et al. (2018). Whole-genome sequencing reveals the mechanisms for evolution of streptomycin

resistance in Lactobacillus plantarum. *J. Dairy Sci.* 101, 2867–2874. doi: 10.3168/jds.201713323

Zhang, N., Yin, Y., Xu, S. J., and Chen, W. S. (2008). 5-Fluorouracil: Mechanisms of resistance and reversal strategies. *Molecules* 13, 1551–1569. doi: 10.3390/molecules13081551

Ziegler, E., Vanderhoof, J. A., Petschow, B., Mitmesser, S. H., Stolz, S. I., Harris, C. L., et al. (2007). Term Infants Fed Formula Supplemented With Selected Blends of Prebiotics Grow Normally and Have Soft Stools Similar to Those Reported for Breast-fed Infants. *J. Pediatr. Gastroenterol. Nutr.* 44, 359–364. doi: 10.1097/MPG.0b013e31802fca8c

Conflict of Interest: The authors declare that the research was conducted in the absence of any commercial or financial relationships that could be construed as a potential conflict of interest.

frontiers in Microbiology

ORIGINAL RESEARCH
published: 22 December 2020
doi: 10.3389/fmicb.2020.568805

Single-Cell Transcriptomics Reveals That Metabolites Produced by *Paenibacillus bovis* sp. nov. BD3526 Ameliorate Type 2 Diabetes in GK Rats by Downregulating the Inflammatory Response

Zhenyi Qiao[1,2], *Xiaohua Wang*[1], *Huanchang Zhang*[1], *Jin Han*[1], *Huafeng Feng*[1] *and Zhengjun Wu*[1]*

[1] State Key Laboratory of Dairy Biotechnology, Shanghai Engineering Research Center of Dairy Biotechnology, Dairy Research Institute, Bright Dairy & Food Co., Ltd., Shanghai, China, [2] State Key Laboratory of Dairy Biotechnology, Shanghai Engineering Research Center of Dairy Biotechnology, Postdoctoral Workstation of Bright Dairy–Shanghai Jiao Tong University, Dairy Research Institute, Bright Dairy & Food Co., Ltd., Shanghai, China

OPEN ACCESS

Edited by:
Jasna Novak maiden Beganovic, University of Zagreb, Croatia

Reviewed by:
Raul German Spallanzani, Harvard Medical School, United States
Amol Suryawanshi, Auburn University, United States

***Correspondence:**
Zhengjun Wu
wuzhengjun@brightdairy.com

Specialty section:
This article was submitted to Food Microbiology, a section of the journal Frontiers in Microbiology

Received: *02 June 2020*
Accepted: *23 November 2020*
Published: *22 December 2020*

Citation:
Qiao Z, Wang X, Zhang H, Han J, Feng H and Wu Z (2020) Single-Cell Transcriptomics Reveals That Metabolites Produced by Paenibacillus bovis sp. nov. BD3526 Ameliorate Type 2 Diabetes in GK Rats by Downregulating the Inflammatory Response. Front. Microbiol. 11:568805. doi: 10.3389/fmicb.2020.568805

Chronic low-grade inflammation is widely involved in the development and progression of metabolic syndrome, which can lead to type 2 diabetes mellitus (T2DM). Dysregulation of proinflammatory and anti-inflammatory cytokines not only impairs insulin secretion by pancreatic β-cells but also results in systemic complications in late diabetes. In our previous work, metabolites produced by *Paenibacillus bovis* sp. nov. BD3526, which were isolated from Tibetan yak milk, demonstrated antidiabetic effects in Goto–Kakizaki (GK) rats. In this work, we used single-cell RNA sequencing (scRNA-seq) to further explore the impact of BD3526 metabolites on the intestinal cell composition of GK rats. Oral administration of the metabolites significantly reduced the number of adipocytes in the colon tissue of GK rats. In addition, cluster analysis of immune cells confirmed that the metabolites reduced the expression of interleukin (IL)-1β in macrophages in the colon and increased the numbers of dendritic cells (DCs) and regulatory T (T_{reg}) cells. Further mechanistic studies of DCs confirmed that activation of the WNT/β-catenin pathway in DCs promoted the expression of IL-10 and transforming growth factor (TGF)-β, thereby increasing the number of T_{reg} cells.

Keywords: ***Paenibacillus bovis*** **sp. nov. BD3526, intestinal barrier, single-cell transcriptome sequencing, type 2 diabetes, immune regulation**

INTRODUCTION

Chronic low-grade inflammation is typical of metabolic syndromes such as type 2 diabetes mellitus (T2DM) and nonalcoholic fatty liver disease (NAFLD) (Ridker et al., 1997; Ridker, 2000; Pradhan et al., 2001; Tilg and Moschen, 2008; Donath and Shoelson, 2011; Hotamisligil, 2017). According to public data made available by the International Diabetes Federation, more than 425 million people worldwide had T2DM in 2017. Although the direct cause of T2DM is insufficient insulin secretion by pancreatic islet cells and a decrease in insulin receptor sensitivity, chronic low-grade

inflammation often plays a pivotal role in promoting the development of T2DM at the early stage (Stern, 1995; Coughlin et al., 2004).

Proinflammatory cytokines and anti-inflammatory cytokines coordinate with each other in the processes through which organisms resist pathogen invasion and develop immune tolerance, thereby maintaining the stability of the human microenvironment (Smith et al., 2005, 2009; Denning et al., 2007; Kamada et al., 2008). During chronic low-grade inflammatory reactions, proinflammatory cytokines such as interleukin (IL)-1β, tumor necrosis factor (TNF)-α, and IL-6 are highly expressed (Ostermann et al., 2019). These cytokines can decrease the stability of the tissue microenvironment and induce the differentiation of immune cells, thereby aggravating disease symptoms. During the progression of T2DM, hyperglycemia can not only activate NLRP3 inflammasomes in pancreatic β-cells but also transform pro-IL-1β into biologically active IL-1β. IL-1β attracts macrophages, which subsequently release more IL-1β. Locally high concentrations of IL-1β inhibit insulin secretion, leading to apoptosis. This causes glucose levels to increase further, creating a vicious cycle (Hull et al., 2004; Robertson et al., 2004; Gordon and Susan, 2005; Boni-Schnetzler et al., 2008). In addition, it has been reported that dendritic cells (DCs) and regulatory T (T_{reg}) cells are also widely involved in immune tolerance. In the intestine, DCs induce the differentiation of T_{reg} cells by promoting the activity of the WNT/β-catenin pathway, and this results in tolerance to the inflammatory response in the intestine and in a reduction in chronic inflammation in the intestine (Manicassamy et al., 2010).

The effects of chronic low-grade inflammatory responses in the gut are often enormous. Although numerous studies have claimed that gut microbiota play an important role in the regulation of intestinal inflammation, it is undeniable that the intestinal barrier is an important factor in regulating human immunity and tolerance (Herbert et al., 2019). The tight junctions of intestinal epithelial cells (IECs) are crucial for maintaining the intestinal barrier (Grander et al., 2018). Leakage through the intestinal barrier would allow some antigenic agents to enter the intestinal tract; i.e., it would permit cell debris of some pathogens to enter the blood circulation and thus trigger a systemic inflammatory response in the host. Thus, the recruitment of immune cells such as Th17 cells at the earliest stages of damage to the intestinal barrier promotes immune homeostasis to chronic inflammation (Ostermann et al., 2019). These immune cells excessively secrete proinflammatory cytokines such as IL-1β and TNF-α, which further interact with cells such as pancreatic β-cells and with organs throughout the body (Ridker et al., 2017). These innate immune responses cause irreversible damage to host tissues and organs, exacerbating the symptoms of T2DM, cardiovascular disease, and even cancer (Stern, 1995; Coughlin et al., 2004).

Paenibacillus bovis sp. nov. BD3526, a gram-positive bacterium isolated from Tibetan yak milk, has a strong ability to hydrolyze milk protein (Hang et al., 2016) and can synthesize exopolysaccharides that have immunomodulatory effects *in vitro* (Xu et al., 2016). Furthermore, the metabolites produced by the strain *P. bovis* sp. nov. BD3526 grown in skim milk have been shown to improve the symptoms of T2DM in Goto–Kakizaki (GK) rats by increasing the diversity of gut microbiota and the content of *Akkermansia muciniphila* in the intestine (Qiao et al., 2019). However, the effect of the metabolites on gene expression and on the subidentity classification of intestinal cells is still unknown.

Here, we report gene expression and cell identity differentiation in the intestine of GK rats, a spontaneous animal model of T2DM. After oral administration of BD3526 metabolites to the animals for 6 weeks, the rats were anesthetized, and intestinal samples obtained from the animals were analyzed by single-cell RNA sequencing technology (scRNA-seq) to perform cell clustering. We found that while the metabolites reduced the number of adipocytes in the intestinal tissue, the number of immune cells increased significantly. Among the immune cells, the number of macrophages expressing IL-1β decreased significantly after the animals were fed the metabolites. At the same time, the number of DCs in the intestinal tissue increased significantly. DCs induced the differentiation of T_{reg} cells by promoting the activity of the WNT/β-catenin pathway, and this resulted in tolerance to the inflammatory response in the intestinal tract and improved the symptoms of T2DM.

MATERIALS AND METHODS

Bacterial Strain and Cultivation

P. bovis sp. nov. BD3526 (CGMCC 8333 = DSM28815 = ATCC BAA-2746) was provided by the State Key Laboratory of Dairy Biotechnology, Shanghai 200436, China. As previously reported (Qiao et al., 2019), the bacterial strain was routinely cultivated aerobically on milk agar at 30°C for 24 h. The medium was prepared by adding 10 ml of sterile 10% (w/w) reconstituted skim milk to 100 ml of melted 1.5% (v/w) agar solution.

Preparation of the BD3526 Metabolites

The lyophilized fermentation product powder was prepared as previously reported (Qiao et al., 2019). Briefly, a loop of freshly cultivated BD3526 on milk agar was inoculated into a 100-ml flask containing 20 ml of sterile 10% (w/w) reconstituted skim milk and cultivated at 30°C at 180 rpm for 24 h. The culture was then transferred at a ratio of 4% (v/v) to a 250-ml flask containing 50 ml sterile 10% (w/w) reconstituted skim milk and cultivated at 30°C for 72 h. The bacterial culture was centrifuged at 8,000 × *g* at 4°C for 10 min to remove bacterial cells, and the supernatant was lyophilized under vacuum. The lyophilized metabolite preparation was then stored at −80°C. Prior to administration by gavage to the experimental animals, the lyophilized metabolites were redissolved in distilled water at a concentration of 50 mg/ml. We calculated a maximum dose of 10^{10} colony-forming units (CFU) for healthy adult humans (60 kg). The maximum daily dose is 1.666×10^8 CFU/kg. Taking into account the human-to-rat dose conversion, the equivalent rat dose is 10^9 CFU/kg. Since an 18-week-old GK rat weighs approximately 500 g, the equivalent daily gavage dose for a GK rat is 5×10^8 CFU. Because metabolites and not bacteria were used in our experiment, we converted CFU to metabolite weight. In our system, $\sim 2.5 \times 10^{11}$ CFU of bacteria and approximately

50 g of metabolites were cultivated in 1 L of medium. Therefore, the appropriate daily dose for a GK rat is 100 mg of metabolites.

Animal Experiments

Sixteen 18-week-old GK rats were used in this study. The rats were randomly divided into two groups of eight rats each. The rats in the BD3526 group received 2 ml of 50 mg/ml lyophilized BD3526 metabolites daily by gavage, whereas the rats in the control group received 2 ml of 50 mg/ml skim milk powder daily by gavage. The animals were individually caged with free access to a normal chewing bar and drinking water. The animals were kept alone in cages and allowed to eat freely. All animals were kept at 25°C with a 12-h light/dark cycle. The gavage experiments lasted for 4 weeks.

All rats were fasted for 8 h prior to administration of a glucose tolerance test. During the experiment, each rat was intraperitoneally injected with 5 g/kg of glucose solution. Blood glucose was monitored at 0, 15, 30, 60, and 120 min. Serum insulin was measured using an enzyme-linked immunosorbent assay (ELISA) kit (Abcam, ab100578) after the rats were killed. IL-1β was measured using an ELISA kit (Abcam, ab100768). The specific experimental methods were conducted in strict accordance with the manufacturer's instructions.

The experiments were performed in strict accordance with the experimental protocol. After dissection of the rats, the intestinal samples were immediately frozen at −80°C for long-term preservation prior to RNA extraction and cytokine detection.

Cell Culture

The Caco-2 cell line was cultured in DMEM (GE Healthcare, SH30021.01) supplemented with 10% FBS (GE Healthcare, SH30396.03). Caco-2 cells were cultured in 96-well plates in a humidified incubator at 37°C with 5% CO_2 for 4 days. The digested Caco-2 cells were plated at a density of 1.5×10^5 cells per well, and the BD3526 metabolites were added to the wells at concentrations no >5% (v/v). The mixture was incubated for an additional 2 h and centrifuged to remove the supernatant.

RNA Extraction and qRT-PCR

Total RNA was extracted from intestinal tissue using an RNA extraction kit (TIANGEN, DP451), and cDNA was synthesized using an iScript cDNA synthesis kit (Bio-Rad, 1708891). Primer pairs for qPCR were designed using the Primer-BLAST online software (https://www.ncbi.nlm.nih.gov/tools/primer-blast/). The *calnexin* (*CANX*) gene (Ensembl accession number: ENSRNOG00000003343; forward primer: ACTGTAGCG TTGCCAGTGTT, reverse primer: GGGGAGCATCTGTCTTCT TGTA) was used as an internal control. In addition, primer sequences for the occludin (*OCLN*) gene (forward primer: GTGGCTTCCACACTTGCTTG, reverse primer: TGTACCCTC CGTAGCCGTAA), the desmocollin 3 (*DSC3*) gene (forward primer: ACAGACAGAGCAGGCCAATC, reverse primer: AGAATAGCAGAGCGATGCCC), the *IRF8* gene (forward primer: GTCCCCGAGGAAGAGCAAAA, reverse primer: GCTCCTCGATCTCTGAACGG), the *CD83* gene (forward primer: GCAAGCAAAACAGCTCCGTC, reverse primer: GCTTCCTTGGGACATCCTGT), the *CD74* gene (forward primer: AGCGCCCGTGAAGAATGTTA, reverse primer: CTGTGGGTAGTTCACGGGTC), the *FOXP3* gene (forward primer: GCACCACAAGGATCCTACCC, reverse primer: ATCTGCTTGGCAGTGCTTGA), and the *Lyz2* gene (forward primer: GGCCAAGACCTATGAACGCT, reverse primer: CCCA TAGTCGGTGCTTTG) were used to quantify gene expression. Quantitative PCR was performed using a QuantStudio 3 (Thermo Fisher Scientific). The data were analyzed by the ΔΔCt method as previously described (Qiao et al., 2016).

scRNA-seq

During the sample preparation process, we collected ∼1 cm of the proximal colon tissue, removed the mesentery, and recovered the content of the colon segment using PBS. The tissue was dissociated into a single-cell suspension by enzyme digestion. Briefly, the tissues were cut into approximately 1-mm^2 pieces and digested using the Solo™ Tumor Dissociation Kit (JZ-SC-58201) at 37°C for 50 min. After stopping digestion by the addition of excess DMEM, the cell strainer-filtered single-cell solution was kept on ice until it was loaded into a BD Rhapsody cartridge for single-cell transcriptome isolation.

Based on the BD Rhapsody system whole-transcriptome analysis alpha protocol for single-cell whole-transcriptome analysis, microbead-captured single-cell transcriptomes were used to prepare a cDNA library containing cell label and UMI information. Briefly, double-stranded cDNA was first generated from the microbead-captured single-cell transcriptome in several steps, including reverse transcription, second-strand synthesis, end preparation, adapter ligation, and whole-transcriptome amplification. Then, the final cDNA library was generated from double-stranded full-length cDNA by random priming amplification using a BD Rhapsody cDNA Kit (BD Biosciences, 633773) and the BD Rhapsody Targeted mRNA and AbSeq Amplification Kit (BD Biosciences, 633774). The library was sequenced in PE150 mode (paired-end with 150-bp reads) on an X Ten instrument (Illumina).

Raw reads were processed through the BD Rhapsody Whole-Transcriptome Assay Analysis Pipeline (early access); the processing included filtering by read quality, annotation of reads, annotation of molecules, determination of putative cells, and generation of a single-cell expression matrix. Briefly, read pairs with low sequencing quality (too long, too short, low sequencing score or high single-nucleotide frequency) were first removed at the read quality filtering step. The quality-filtered R1 reads were analyzed to identify the cell label sequence (CL), the molecular identifier sequence (UMI), and the poly-dT tail sequence, and the quality-filtered R2 reads were mapped using STAR (version 2.5.2b) at the read annotation step. Further adjustments were performed using recursive substitution error correction (RSEC) and distribution-based error correction (DBEC) algorithms to remove artifactual molecules arising from amplification bias at the molecule annotation step. Putative cells were distinguished from background noise through a second derivative analysis at the putative cell determination step. Finally, putative cell information was combined with RSEC/DBEC-adjusted molecules to generate a single-cell expression matrix. The pipeline output provided raw gene expression matrices

corrected by the RSEC and DBEC algorithms. Among all the matrices, UMI counts per cell corrected by the DBEC algorithm were later used in the clustering analysis.

Raw gene expression matrices from two cartridges were read separately into R (version 3.6.0) and converted to Seurat objects using the Seurat R package (version 3.0.1). CCA integration between two batches was performed with the Seurat R package.

The gene expression matrix was then normalized to the total cellular UMI count. The top 2,000 features were selected as highly variable genes for further clustering analysis. After scaling the data with respect to UMI counts, PCA was performed based on the highly variable genes identified in the previous step to reduce dimensionality. In addition, the first 50 principal components were chosen based on the PC heat map, jackstraw plot, and PC elbow plot to further reduce dimensionality using the tSNE algorithm. Clusters were identified with the default setting using the RunTSNE function. Each cluster was then annotated with canonical cluster markers.

Downstream pseudotime trajectory analysis was performed with the Monocle 2 R package.

RNA-seq

Total RNA was isolated using an RNeasy mini kit (Qiagen, 74104). Paired-end libraries were synthesized using the TruSeq™ RNA Sample Preparation Kit (Illumina, RS-122-2001) according to the instructions provided in the TruSeq™ RNA Sample Preparation Guide. Briefly, poly-A-containing mRNA molecules were purified using magnetic beads attached to poly-T oligonucleotides.

Following purification, the mRNA was fragmented into small pieces using divalent cations at 94°C for 8 min. The cleaved RNA fragments were copied into first-strand cDNA using reverse transcriptase and random primers. This was followed by second-strand cDNA synthesis using DNA polymerase I and RNase H. These cDNA fragments were then subjected to an end repair process and the addition of a single "A" base, followed by ligation to the adapters. The products were then purified and amplified by PCR to create the final cDNA library. The purified libraries were quantified in a Qubit® 2.0 fluorometer (Life Technologies, USA) and validated using an Agilent 2100 Bioanalyzer (Agilent Technologies, USA) to confirm the insert size and calculate the molar concentration. Clustering was performed by cBot with the library diluted to 10 pM, and the library was then sequenced on the Illumina HiSeq platform (Illumina, USA).

Immunoblot Analysis

Colon tissue was ground into powder in liquid nitrogen and lysed. After centrifugation to obtain a protein solution, SDS-PAGE was performed. The separated proteins were transferred to a polyvinylidene difluoride membrane (0.45 μm; Amersham Biosciences). The membranes were incubated with primary and secondary antibodies. Amersham ECL Prime western blot detection reagent (GE Healthcare) was used to visualize the signals. The OCLN antibody (Abcam, ab216327) was used at 1:1,000 dilution, and the CANX antibody (Abcam, ab10286) was used at 1:2,000 dilution.

Oil Red O Staining

Fresh colon tissue samples were immediately placed in 4% paraformaldehyde for slicing. After the preparation of the slices, the cells were stained with Oil Red O for 30 min and then counterstained with hematoxylin. The lipid-stained areas of slides and cross sections were observed and photographed using a microscope (Olympus).

Ethics Statement

The use and care of the animals used in this research was reviewed and approved by the Shanghai Laboratory Animal Management Office [SYXK (Shanghai) 2017-0008].

The animals used in the research were utilized based on appropriate experimental procedures. All of the animals were lawfully acquired, and their retention and use complied with federal, state, and local laws and regulations in every case and were in accordance with the Institutional Animal Care and Use Committee of SLAC (IACUC) Guide for Care and Use of Laboratory Animals.

The animals used in this research received every consideration for their comfort and were properly housed and fed, and their surroundings were kept in a sanitary condition.

The use of animals was in accordance with the IACUC Guide for Care and Use of Laboratory Animals. A minimal number of rats were used during the experiments. Appropriate anesthetics were used to eliminate sensibility to pain during all of the surgical procedures.

RESULTS

BD3526 Metabolites Regulate Immunity in the Caco-2 Cell Line

To study the regulation of intestinal immune function by BD3526 metabolites, we first explored the function of Caco-2 cells derived from IECs *in vitro*. The BD3526 metabolites were added at a ratio of 5% (v/v) to Caco-2 cells that had been cultured for 4 days; addition of 10% sterile skim milk was used as a negative control. After coincubation for 2 h, RNA extraction and RNA sequencing were performed. The sequencing results showed that when Caco-2 cells were incubated with the BD3526 metabolites, 1,219 genes were differentially expressed compared to the negative control (fold change > 2 or <0.5; P-value < 0.05) (**Figure 1A**). Among these genes, 750 genes showed significantly increased expression, and 469 genes showed decreased expression (**Figure 1B**). Gene Ontology (GO) analysis of these differentially expressed genes (DEGs) showed that some of the GO classifications that were enriched in the DEGs were related to cellular immunity; these GO classifications included IL-1 receptor binding, CXCR chemokine receptor binding, type I interferon biosynthesis process, and regulation of the IL-6 biosynthetic process (**Figure 1C**). Furthermore, Kyoto Encyclopedia of Genes and Genomes (KEGG) analysis revealed that 83 DEGs showed altered expression in the BD3526 group, and these genes were primarily clustered in the immune system pathway and secondarily clustered in the signal transduction pathway (**Figure 1D**).

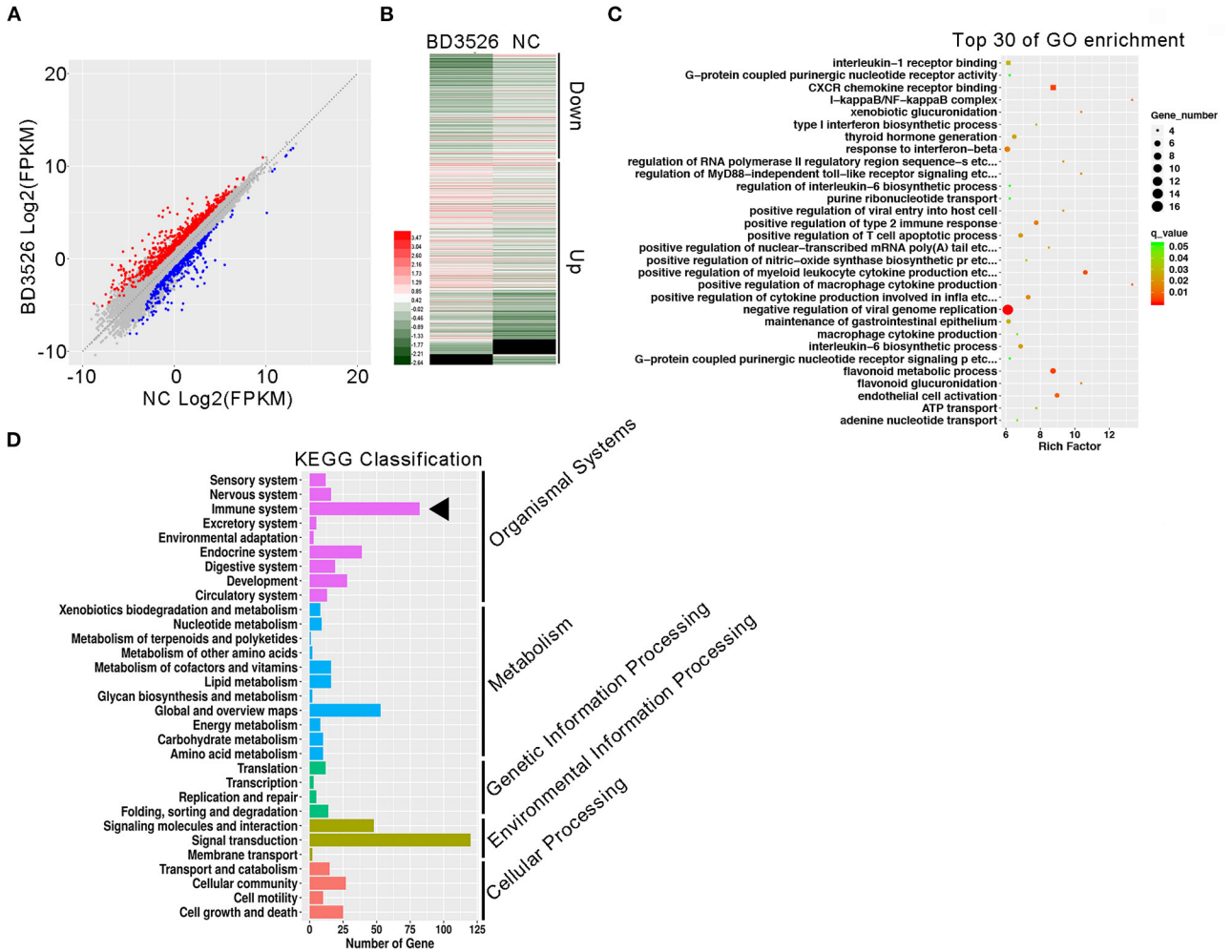

FIGURE 1 | Regulatory effects of the metabolites on gene expression in Caco-2 cells *in vitro*. **(A)** Scatter plots of differentially expressed genes. Red indicates genes that showed increased expression in Caco-2 cells treated with the metabolites. Blue indicates genes that showed decreased expression in Caco-2 cells treated with the metabolites. **(B)** Heat map showing the differentially expressed genes. **(C)** Functional clustering of differentially expressed genes by Gene Ontology (GO). **(D)** KEGG was used to analyze the signal pathway clustering of the differentially expressed genes.

Considering the huge impact of BD3526 metabolites on gene expression in Caco-2 cells at the RNA level, especially at the level of the immune system, we believe that the BD3526 metabolites could affect the immune function of Caco-2 cells *in vitro*. It has been reported that IECs are extensively involved in intestinal immunity by secreting cytokines (Kagnoff, 1996) and participating in the intestinal immune, mucosal lymphocyte trafficking, mucosal infection, and inflammation. Therefore, we hypothesized that BD3526 metabolites may affect intestinal immune function. However, immune regulation is very complicated. The immune system is composed of cells in various tissues, immune cells, and immune factors. Therefore, the study of cells *in vitro* cannot prove that the same effect occurs in animals. For this reason, we also conducted *in vivo* animal experiments in which we administered the BD3526 metabolites to rats.

BD3526 Metabolites Improve the Integrity of the Intestinal Barrier and Alleviate Diabetic Symptoms in GK Rats

In our previous work, we confirmed that BD3526 metabolites can improve the symptoms of T2DM by increasing the diversity of gut microbiota and the intestinal content of *A. muciniphila* (Qiao et al., 2019). In patients with T2DM, the intestinal microenvironment often exhibits an impaired intestinal barrier and excessive inflammation. To verify the regulatory effect of the metabolites on intestinal cellular immune function *in vivo*, we conducted experiments on the metabolites in GK rats. GK rats at 18 weeks of age were administered daily via gavage with 2 ml of the metabolites at a concentration of 50 mg/ml for four consecutive weeks. At the end of the gavage experiment, the GK rats in the BD3526 group and the NC group were subjected to 8 h of fasting and injected with 5 g/kg of glucose solution to test their

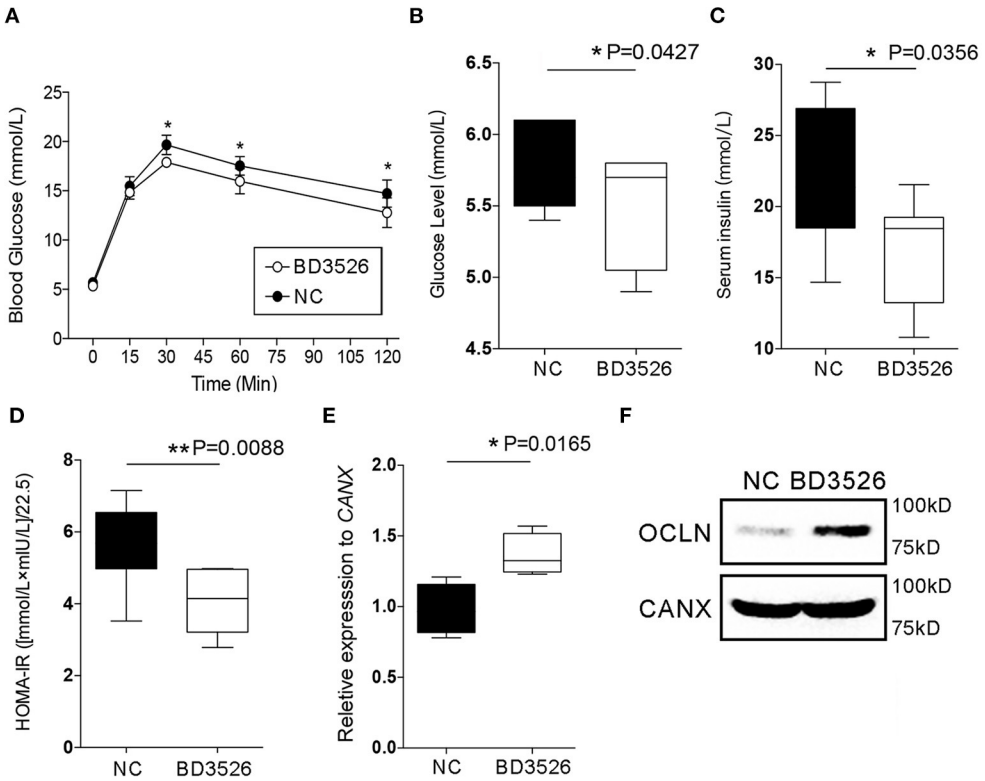

FIGURE 2 | Observation of type 2 diabetes mellitus symptoms. **(A)** Goto–Kakizaki (GK) rats in the BD3526 and NC groups were tested for glucose tolerance. Blood glucose concentration was measured at 0, 15, 30, 60, and 120 min ($n = 8$, $^*P < 0.05$, mean ± SEM). **(B)** Serum blood glucose was measured ($^*P < 0.05$, mean ± SEM). **(C)** Serum insulin was measured ($^*P < 0.05$, mean ± SEM). **(D)** Statistical analysis of the insulin resistance index ($^{**}P < 0.01$, mean ± SEM). **(E)** Changes in the expression of the occludin (*OCLN*) gene were detected by qPCR ($^*P < 0.05$, mean ± SEM). **(F)** Changes in the expression of the OCLN were detected by Western Blot.

glucose tolerance. We found that the blood glucose concentration in the rats in the BD3526 group was significantly lower than that of the rats in the NC group at 30, 60, and 120 min after glucose administration ($P < 0.05$) (**Figure 2A**). In addition, compared with the NC group, serum blood glucose was significantly reduced in the BD3526 group ($P < 0.05$) (**Figure 2B**). At the same time, the insulin concentration in the BD3526 group was much higher than that in the NC group (**Figure 2C**). Finally, by calculating the insulin resistance index (HOMA-IR), we found that the sensitivity of the GK rats to insulin was increased in the BD3526 group ($P = 0.0088$) (**Figure 2D**). This result, which is similar to the results obtained in our previous work, suggests that the metabolites can comprehensively ameliorate diabetic symptoms in GK rats (Qiao et al., 2019). However, the regulatory effect of the metabolites on gene expression in intestinal tissues is still unknown.

As previously reported, the integrity of IECs is an important barrier that contributes to the maintenance of intestinal health. Damage to the intestinal barrier increases the risk of invasion by microbial pathogens and promotes inflammation. The integrity of IECs is maintained by cellular membrane proteins such as OCLN and DSC3. Here, the expression levels of the genes encoding these proteins in the intestinal tissues of GK rats were analyzed by qRT-PCR. The results showed that there was no significant change in *DSC3* gene expression in the BD3526 group ($P > 0.05$) (**Supplementary Figure 1**). However, qPCR and western blot experiments confirmed that *OCLN* gene expression was significantly increased in the BD3526 group (**Figures 2E,F**). We also further analyzed the RNA-seq data from Caco-2 cells. Unfortunately, we did not find significant changes in the expression of the *OCLN* gene in Caco-2 cells. This may be because the observed difference in the expression level of *OCLN* did not meet the criteria for a significant difference (fold change > 2 and $P < 0.05$). Despite this, our data indicate that the antidiabetic effect of the BD3526 metabolites in GK rats is a result of adjustment of the intestinal microbiota through enrichment of *A. muciniphila* as well as enhancement of intestinal barrier function through the stimulation of IECs to increase *OCLN* expression.

Administration of BD3526 Metabolites Alters Intestinal Cell Composition in GK Rats

scRNA-seq technology has been widely used in disease research in recent years. BD3526 metabolites have an effect on gene

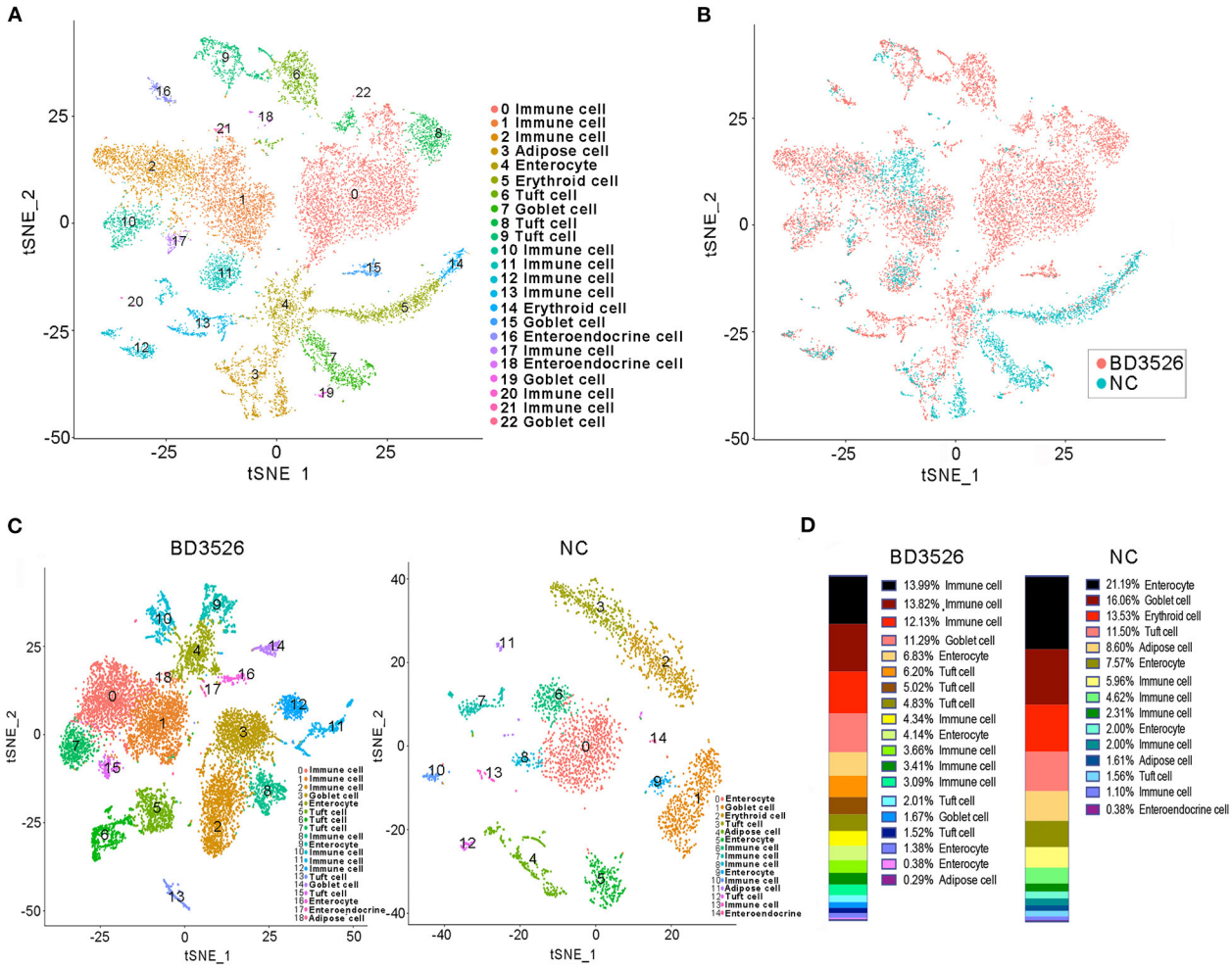

FIGURE 3 | t-SNE clustering analysis of the single-cell RNA sequencing (scRNA-seq) experiment. **(A)** t-SNE clustering of all cells in the BD3526 and NC groups after integration. Each color represents a different subidentity of cells. **(B)** Specific distribution of cells in the BD3526 and NC groups in t-SNE clustering. Red indicates cells from the BD3526 group, and cyan indicates cells from the NC group. **(C)** t-SNE cluster analysis was performed separately in the BD3526 and NC groups. Each color represents a different subidentity of cells. **(D)** Proportions of cells with different subidentities in the BD3526 and NC groups.

expression in the intestinal tissue of GK rats. Therefore, we used scRNA-seq to analyze the identities of cells within the intestinal tissues in the BD3526 and NC groups. We hoped to observe the effect of the metabolites on intestinal tissues from the perspective of cell typing.

During the dissection of colon tissues, we randomly selected three intestinal tissue samples from each group, and the intestinal samples in each group were mixed and subjected to single-cell sequencing after trypsin digestion. In the BD3526 group, 34,532 cells were sequenced, and 36,485 cells were sequenced in the NC group. A total of 19,206 expressed genes were detected in the cells from the BD3526 group, whereas 18,983 genes were detected in the cells from the NC group (**Supplementary Table 1**). By t-SNE clustering of the cells in the two groups, we identified a total of 23 clusters (**Supplementary Table 2**). After manually annotating these clusters according to the cell marker genes (http://biocc.hrbmu.edu.cn/CellMarker/index.jsp), we found that the tissue contained seven cell identities in total, namely, immune cells, adipose cells, enterocytes, erythroid cells, tuft cells, goblet cells, and enteroendocrine cells (**Figure 3A** and **Supplementary Table 3**). However, when we analyzed the sources of the 23 clusters, we found that some clusters, such as clusters 0, 2, 6, 8, and 15, originated from the BD3526 group. Correspondingly, clusters 5, 7, and 14 were found mainly in the NC group (**Figure 3B**). This indicates that consumption of the metabolites had a significant effect on the composition of intestinal cells in GK rats.

We next performed t-SNE clustering on intestinal cells of the BD3526 group and the NC group. In the BD3526 group, a total of 19 cell identities were clustered. The NC group clustered into 15 cell subidentities (**Figure 3C**). After manually annotating

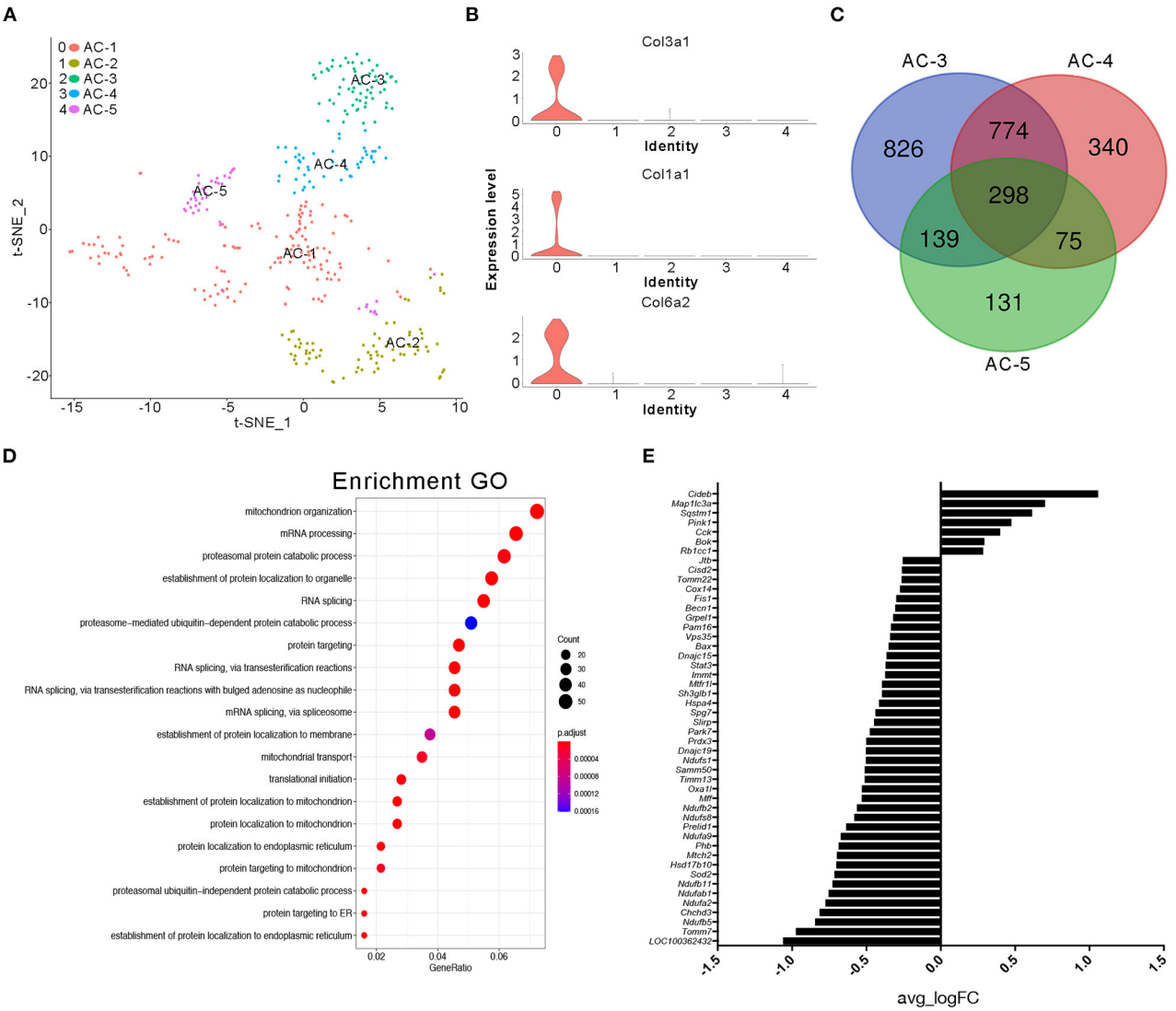

FIGURE 4 | Cluster analysis of adipocytes in the NC group. **(A)** t-SNE clustering analysis of adipocytes in the NC group. Each color represents a different subidentity of cells. **(B)** Violin plots of the expression density of *Col3a1*, *Col1a1*, and *Col6a2* in adipocytes. **(C)** Specific marker genes for AC-3, AC-4, and AC-5 cell subidentities. **(D)** Gene Ontology (GO) functional clustering of genes specifically expressed in AC-3 cells. **(E)** Expression of mitochondrial genes in AC-3 cells.

these 34 cell subidentities, we found that more immune cells were detected in the BD3526 group. Correspondingly, more adipocytes were identified in the NC group (8.6%) (**Figure 3D**). This result was confirmed by an Oil Red O staining experiment on the colon tissues. We found adipose cells in colon tissues of the NC group by staining, and these cells were reduced in the BD3526 group (**Supplementary Figure 2**).

Adipocytes in the NC Group Display More Heterogeneity

It is generally accepted that adipose tissue is an important source of cytokines in human metabolic syndromes and related disorders (Hotamisligil et al., 1993; Kern et al., 1995; Fried et al., 1998; Moschen et al., 2010). Herein, we first conducted further research on the type of adipocytes present. We classified clusters 4 and 11 in the NC group and cluster 18 in the BD3526 group as adipose cells. Because the number of cells in cluster 18 of the BD3526 group is small, we were unable to further classify the cell subidentities. In the NC group, we further divided the adipocytes into five subidentities using t-SNE clustering (**Figure 4A**). Cluster 0 (AC-1) contains cells that express genes involved in fibrosis and extracellular matrix accumulation, including *Col3a1*, *Col1a1*, and *Col6a2* (**Figure 4B**). Cluster 1 (AC-2) expresses genes that are related to cell proliferation ability, such as *TOP2a*, *Mki67*, and *AGR2*. Cluster 2 (AC-3), cluster 3 (AC-4), and cluster 4 (AC-5) had relatively similar gene expression patterns. Analysis of the genes in these three clusters shows that 298 genes are

present in these three clusters. Among them, cluster AC-3 uniquely included 826 genes (**Figure 4C**). We performed GO functional clustering of these 826 genes and found that these genes were mainly enriched in mitochondria-related signaling pathways such as mitochondrion organization ($P = 5.50E{-}12$), mitochondrial transport ($P = 5.33E{-}08$), and establishment of protein localization to the mitochondria ($P = 1.38E{-}09$) (**Figure 4D**). In the analysis of the expression of mitochondrion organization-related genes, we found that the relative expression of 47 genes (47 of 54 genes) decreased in cluster AC-3. This means that the activity of the mitochondria in cluster AC-3 is low (**Figure 4E**).

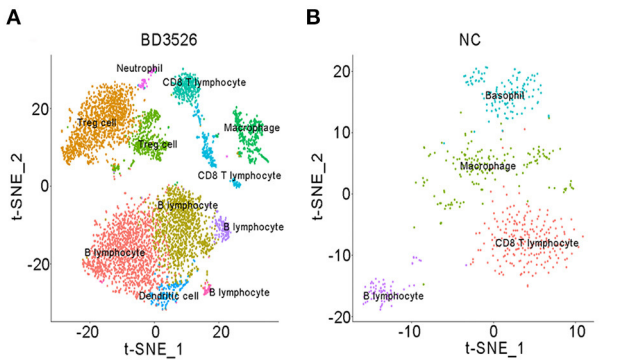

FIGURE 5 | t-SNE clustering analysis of immune cells in the BD3526 and NC groups. **(A,B)** t-SNE clustering analysis of immune cells in the BD3526 group and the NC group, respectively. Each color represents a different subidentity of cells.

Intestinal Tissue of GK Rats in the BD3526 Group Contains More Immune Cell Identities

Subsequently, we analyzed clusters 0, 1, 2, 8, 10, 11, and 12 (total 6,095 cells) in the BD3526 group and clusters 6, 7, 8, 10, and 13 (total 588 cells) in the NC group to recluster the cell subidentities (**Figures 5A,B**). These clusters were regarded as immune cells in the previous clustering and annotation. In the BD3526 group, according to manual annotation, we identified a total of six different identities of immune cells, namely, B lymphocytes, $CD8^+$ T lymphocytes, DCs, T_{reg} cells, macrophages, and neutrophils. In the BD3526 group, B lymphocytes expressed the *CD19* and *CD79* genes; T_{reg} cells expressed the *FOXP3*, *CTLA4*, and *Lag3* genes (**Figures 6A,B**), macrophages expressed the *CD14* gene; $CD8^+$ T lymphocytes expressed the *CD8* gene; DCs expressed the *IRF8*, *CD74*, and *CD83* genes (**Figures 6C,D**), and neutrophils expressed the *Ifitm1* and *Fgl2* genes. DCs, T_{reg} cells, and neutrophils were

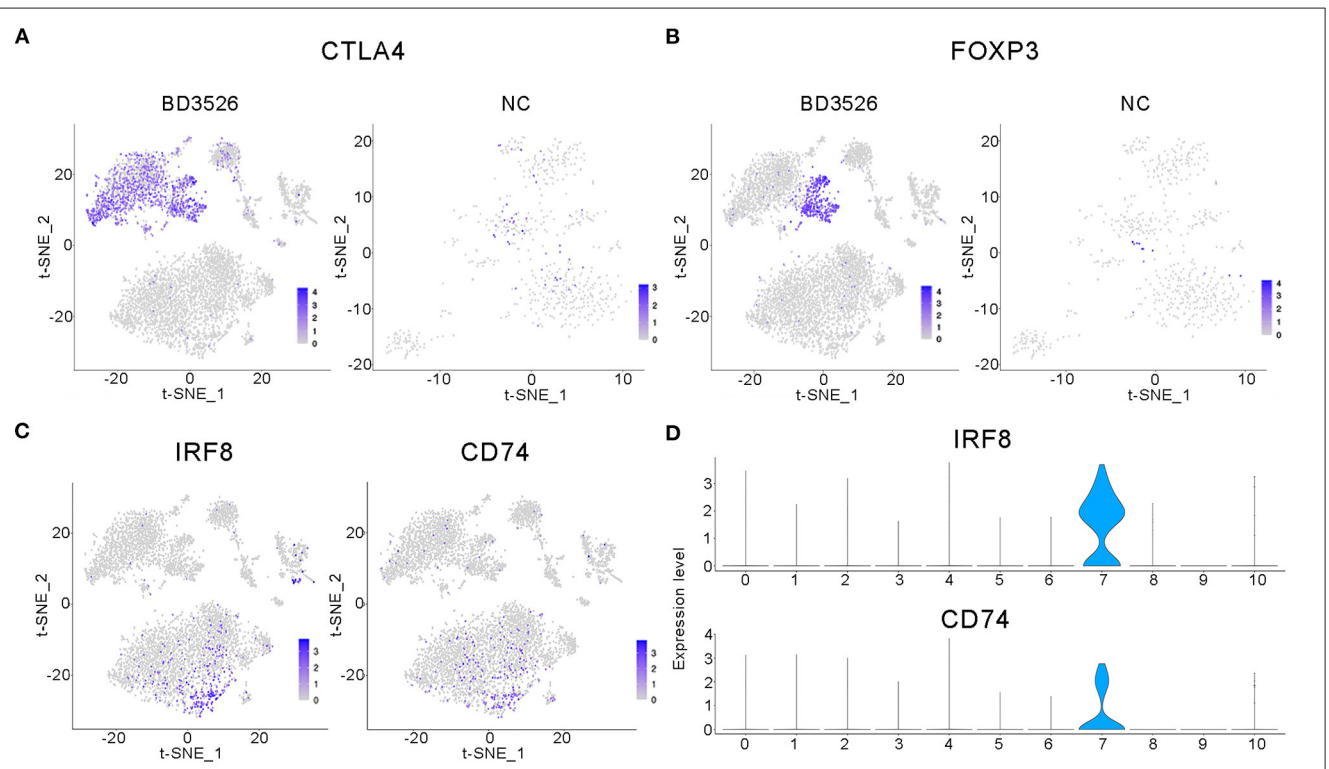

FIGURE 6 | Characteristic analysis of immune cells in the BD3526 group. **(A,B)** Analyses of the expression and distribution of *CTLA4* and *FOXP3* genes in regulatory T (T_{reg}) cells in the BD3526 group and the NC group, respectively, using the t-SNE diagram. **(C,D)** The expression distribution of *IRF8* and *CD74* genes in dendritic cells (DCs) in the BD3526 and NC groups, respectively, using t-SNE figures and violin plots.

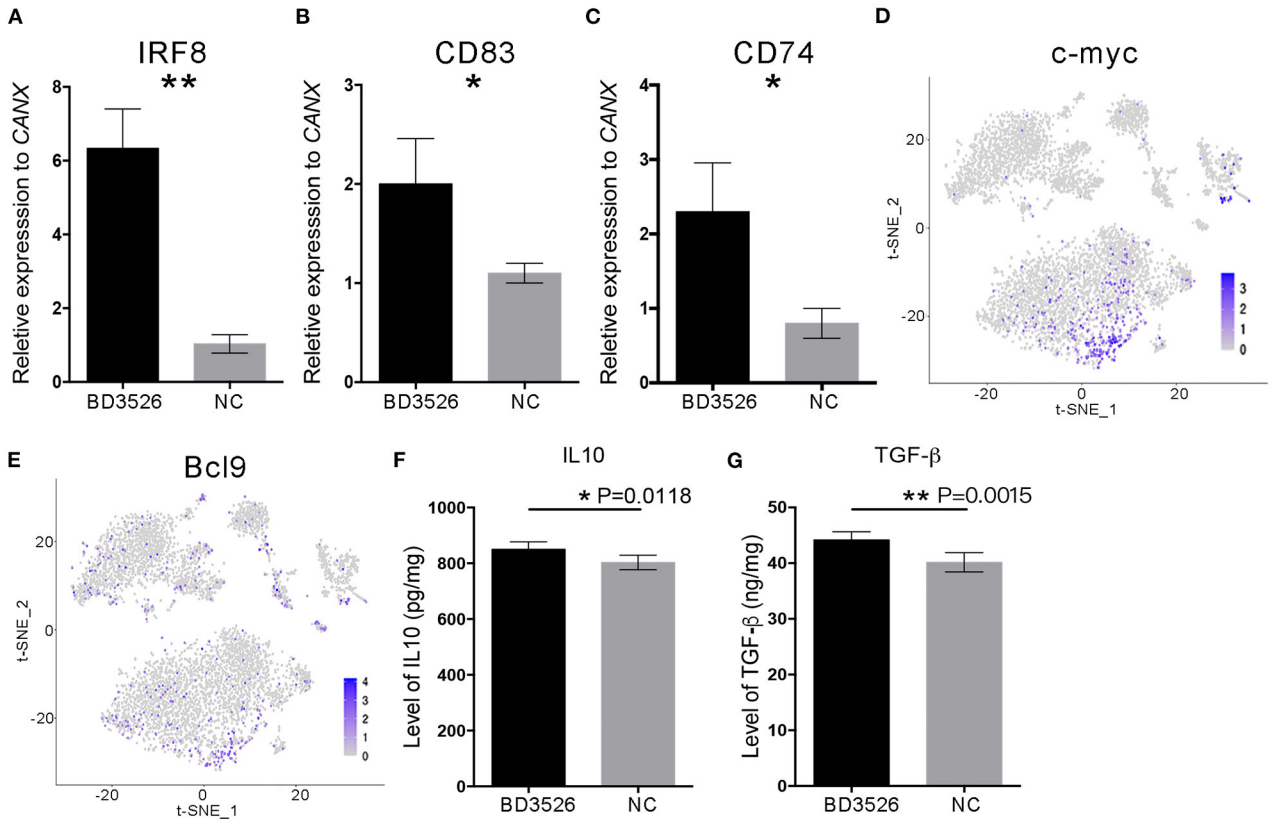

FIGURE 7 | The WNT/β-catenin signaling pathway in dendritic cells (DCs) was activated by BD3526 metabolites. The expression levels of *IRF8*, *CD83*, and *CD74* (shown in **A–C**, respectively) in the BD3526 group and the NC group were analyzed using qRT-PCR (**$P < 0.01$, *$P < 0.05$, mean ± SEM). **(D,E)** The expression and distribution of *c-myc* and *BCL9*, respectively, in DCs. **(F)** Quantitative analysis of the anti-inflammatory factor interleukin (IL)-10 in the BD3526 and NC groups (*$P < 0.05$, mean ± SEM). **(G)** Quantitative analysis of the chemokine transforming growth factor (TGF)-β in the BD3526 and NC groups (**$P < 0.01$, mean ± SEM).

found only in the BD3526 group. These results were also confirmed by qPCR using DCs, T_{reg} cells, and macrophage-specific gene primers (**Supplementary Figure 3**). According to the t-SNE classification, B lymphocytes can be further divided into four subclusters. Among them, clusters 0, 2, and 10 expressed *CD19*. Cluster 8 does not express *CD19* but does express *CD79*. Cluster 2 in the BD3526 group and cluster 3 in the NC group show similar gene expression levels and can be considered to belong to the same cell identity. Furthermore, we observed that IL-1β was expressed at a high level in macrophages in the NC group. These results were confirmed by ELISA (**Supplementary Figure 4**). Accordingly, the expression of IL-1β in macrophages in the BD3526 group was not significantly different from that in non-macrophages. Because high expression of IL-1β in macrophages in the intestine can significantly promote chronic inflammation and aggravate the symptoms of hyperglycemia, we concluded that administration of BD3526 metabolites significantly inhibits the expression of IL-1β in macrophages in the intestine (Ehses et al., 2007; Boni-Schnetzler et al., 2008; Eguchi et al., 2012; Jourdan et al., 2013).

In the BD3526 group, we also identified T_{reg} cells that exhibited two different gene expression patterns through the marker genes *FOXP3*, *CTLA4*, and *LAG3*, namely, $FOXP3^+LAG3^+CTLA4^+$ and $FOXP3^-LAG3^-CTLA4^+$ cells. According to the statistical analysis, T_{reg} cells accounted for 30.28% of the immune cells in the BD3526 group. Among them, $FOXP3^+LAG3^+CTLA4^+$ T_{reg} cells accounted for 8.71% of the immune cells, and $FOXP3^-LAG3^-CTLA4^+$ T_{reg} cells accounted for 21.58%.

We also found a type of DC in the intestinal tissue of the BD3526 group. These cells express *IRF8*, *CD74*, and *CD83* and account for 2.17% of the immune cells in the BD3526 group. It has been reported that in the intestinal microenvironment, DCs show higher activity of the WNT/β-catenin pathway, which regulates intestinal immunity and tolerance through T_{reg} cells (Manicassamy et al., 2010). Here, based on the presence of both DCs and T_{reg} cells in the intestinal tissue of the BD3526 group, we propose the hypothesis that BD3526 metabolites regulate intestinal immune tolerance by increasing the number of DCs and T_{reg} cells in the intestinal tissue and ultimately alleviating the symptoms of T2DM in GK rats.

DCs From Rats in the BD3526 Group Showed Higher Activity of the WNT/β-Catenin Pathway

To verify the change in DCs in the BD3526 group, we used qRT-PCR. We conducted a relatively quantitative detection of *IRF8*, *CD83*, and *CD74* gene expressions. The results confirmed the reliability of the single-cell sequencing results. The relative expression levels of *IRF8*, *CD83*, and *CD74* in the BD3526 group were significantly higher than those in the NC group ($P < 0.05$) (**Figures 7A–C**). In the previous section, we hypothesized that the activity of the WNT/β-catenin pathway is significantly increased in intestinal DCs and that this can regulate intestinal immunity tolerance and ultimately alleviate the symptoms of intestinal inflammatory diseases such as metabolic syndrome and inflammatory bowel disease (IBD). To confirm this hypothesis, we performed t-SNE clustering of genes related to the WNT/β-catenin pathway in DCs. The results showed that the downstream genes *c-myc* [$P = 3.46E{-}12$, avg_log(fold change) = 0.74] and *BCL9* [$P = 1.58E{-}11$, avg_log(fold change) = 0.64] were significantly increased in DCs (**Figures 7D,E**).

Since DCs are an important class of antigen-presenting cells (APCs), they are a special class of immune cells and have a central role in the accumulation of immune responses. Recent reports claimed that DCs can promote the differentiation of T_{reg} cells by expressing anti-inflammatory mediators such as IL-10 and transforming growth factor (TGF)-β, thereby suppressing the inflammatory reaction in the host. Therefore, we conducted quantitative ELISA experiments on IL-10 and TGF-β (**Figures 7F,G**). The results showed that the expression levels of IL-10 and TGF-β in the intestinal tissue of the BD3526 group increased significantly. This result proves that the WNT/β-catenin pathway, which promotes the expressions of IL-10 and TGF-β, is activated in DCs. This promotes the differentiation of T_{reg} cells in the intestinal microenvironment, ultimately increasing the immune tolerance of intestinal tissues and improving the symptoms of inflammatory diseases.

DISCUSSION

Metabolic syndrome is a chronic disease with extremely high incidence. According to public data from the International Diabetes Federation, more than 425 million people worldwide had T2DM in 2017. In 2016, according to the estimate of the World Health Organization (WHO), more than 1.3 billion adults worldwide were overweight [body mass index (BMI) 25 to <30 kg/m^2], and more than six million people were obese (BMI $\geq$ 30 kg/m^2). Although a relatively high percentage of patients with chronic metabolic syndromes in the early stage can be cured clinically, those who suffer from these diseases in the long term are at high risk (So et al., 2007; Sun and Karin, 2012; Stahel et al., 2016). Despite the variation in the immediate causes of these diseases, an increasing number of studies have found that metabolic syndrome is a type of chronic low-grade inflammation (Rey and Besedovsky, 1992). In the early stage of metabolic syndrome, inflammatory responses originating in certain tissues and organs spread inflammation throughout the body through signal transduction by proinflammatory factors, leading to the disruption of immune balance and the development of various dangerous complications such as cardiovascular disease, kidney disease, neuropathy, and even tumors (Stern, 1995; Coughlin et al., 2004). Fortunately, with the occurrence of new tools and technology for the study of the differentiation and signal transduction of immune cells, the roles of immune cells in host innate immunity and inflammatory diseases have been comprehensively studied. Effector T cells and T_{reg} cells are important in regulating the balance of innate immunity (Ghoreschi et al., 2010; Maloy and Powrie, 2011). Effector T cells activate the inflammatory response through which the body resists pathogen infection, while T_{reg} cells inhibit the inflammatory response that destroys normal tissues. Macrophages and DCs also play an important role in innate immunity (Maldonado and Andrian, 2010). IL-1β secreted by macrophages promotes the amplification of the inflammatory response, while IL-10 and TGF-β secreted by DCs induce the differentiation of initial T cells into T_{reg} cells, promoting immune tolerance.

In this work, we first performed *in vitro* experiments on Caco-2 cells treated with BD3526 metabolites. Through high-throughput RNA sequencing, we found that the BD3526 metabolites significantly affect the immune capacity of IECs at the RNA level. To conduct a more in-depth study, we further conducted *in vivo* experiments on the BD3526 metabolites in GK rats. We used scRNA-seq and found that the BD3526 metabolites activate the WNT/β-catenin signaling pathway in DCs in intestinal tissues and promote the differentiation of T_{reg} cells. In addition, marker gene analysis of macrophages by scRNA-seq showed that IL-1β secreted by macrophages was significantly decreased in the BD3526 group. Considering that IL-1β not only promotes apoptosis of pancreatic β-cells but also plays an important role in promoting the amplification of inflammatory signals, we believe that the regulation of innate immunity by the metabolites is multifaceted.

Generally, the progression of chronic metabolic syndrome is a slow process. Chronic low-grade inflammation is usually present only in some tissues and organs before serious complications occur. Persons with T2DM, for example, may initially have only mild hyperglycemia but may then develop severe symptoms of hyperglycemia and insulin resistance. Early symptoms such as mild hyperglycemia in prediabetic individuals are often overlooked. With the gradual apoptosis of pancreatic β-cells and changes in the microenvironment, effector T cells and other proinflammatory factors such as IL-1β, IL-6, IL-12, IL-23, TGF-β, and TNF-α further aggravate the situation, leading to irreversible changes in other tissues and organs (Boni-Schnetzler et al., 2008). Therefore, it is extremely important to block chronic low-grade inflammation at its early stage. However, considering that early clinical symptoms are often not significant, traditional drugs such as insulin, sulfonylurea, and dipeptidyl peptidase 4 (DPP4) inhibitors are rarely employed to intervene in the early stage and block the progression of inflammation (Donath et al., 2019). Not only is the gut an

important digestive organ, there is also growing evidence that inflammation caused by damage to the intestinal barrier is involved in the progression of T2DM (Karlsson et al., 2013). Therefore, improving the function of the intestinal barrier through changes in the daily diet appears to be a feasible strategy for blocking the inflammatory response.

In our previous work, metabolites produced by *P. bovis* sp. nov. BD3526 from fermented skim milk were reported to alleviate symptoms of T2DM in GK rats (Qiao et al., 2019). In this study, the potential of the BD3526 metabolites grown in 10% skim milk to improve the intestinal barrier and the underlying mechanism of this effect was further explored. Although no component responsible for this bioactivity has been identified to date, the results of our study provide an alternative method for ameliorating T2DM by blocking chronic low-grade inflammation in the gastrointestinal tract. Chronic low-grade inflammation is involved not only in the development and progression of metabolic syndrome but also in neurodegenerative diseases such as early Alzheimer's disease and carcinoma. We believe that regulation of human immune balance through long-term dietary changes would be a more effective and safe strategy for maintaining bodily health. In addition, revealing the molecular mechanism through which diet influences the human immune response through molecular biological and immunological methods such as scRNA-seq will be an important research direction in the future.

DATA AVAILABILITY STATEMENT

The datasets presented in this study can be found in online repositories. The names of the repository/repositories and accession number(s) can be found in the article/**Supplementary Material**. The *P. bovis* sp. nov. BD3526 mentioned in this article can be found in the ATCC database. The ATCC number of *P. bovis* sp. nov. BD3526 is BAA-2746. The high-throughput sequencing data generated in this study were deposited in the Sequence Read Archive (SRA) databases under accession number PRJNA634400.

ETHICS STATEMENT

The animal study was reviewed and approved by the Shanghai Laboratory Animal Management Office [SYXK (Shanghai) 2017-0008]. Written informed consent was obtained from all study participants.

AUTHOR CONTRIBUTIONS

ZQ and ZW designed the study and wrote the manuscript. ZQ and XW conducted the animal studies. ZQ conducted the scRNA-seq analyses. ZQ, JH, ZW, HZ, and HF supervised the study. All of the authors read and approved the final manuscript. All authors contributed to the article and approved the submitted version.

FUNDING

This work was supported by National Key R&D Program of China (2019YFF0217603), Shanghai Engineering Research Center of Dairy Biotechnology (19DZ2281400), and the Shanghai Rising-Star Program (18QB1400100). The authors declare that this study received funding from Bright Dairy & Food Co., Ltd. The funder was not involved in the study design, collection, analysis, interpretation of data, the writing of this article or the decision to submit it for publication.

SUPPLEMENTARY MATERIAL

The Supplementary Material for this article can be found online at: https://www.frontiersin.org/articles/10.3389/fmicb.2020.568805/full#supplementary-material

Supplementary Figure 1 | Changes in the expression of the *DSC3* gene were detected by qPCR (ns *P*-value > 0.05, mean ± SEM).

Supplementary Figure 2 | Oil red colonic staining was performed in BD3526 and NC groups. Bar represents 50 μm. The red color indicated by the black tip represents the fat that has been stained with the oil red dye.

Supplementary Figure 3 | qPCR detection of DCs, T_{reg} cells and macrophages.

Supplementary Figure 4 | Violin plots showing the expression levels of IL-1β in macrophages.

REFERENCES

Boni-Schnetzler, M., Jeffrey, T., Geraldine, P., Lorella, M., Ehses, J. A., Julie, K. C., et al. (2008). Increased interleukin (IL)-1β messenger ribonucleic acid expression in β-cells of individuals with type 2 diabetes and regulation of IL-1β in human islets by glucose and autostimulation. *J. Clin. Endocrinol. Metab.* 93, 4065–4074. doi: 10.1210/jc.2008-0396

Coughlin, S. S., Calle, E. E., Teras, L. R., Jennifer, P., and Thun, M. J. (2004). Diabetes mellitus as a predictor of cancer mortality in a large cohort of US adults. *Am. J. Epidemiol.* 159, 1160–1167. doi: 10.1093/aje/kwh161

Denning, T. L., Wang, Y. C., Patel, S. R., Williams, I. R., and Pulendran, B. (2007). Lamina propria macrophages and dendritic cells differentially induce regulatory and interleukin 17–producing T cell responses. *Nat. Immunol.* 8, 1086–1094. doi: 10.1038/ni1511

Donath, M. Y., Dinarello, C. A., and Mandruppoulsen, T. (2019). Targeting innate immune mediators in type 1 and type 2 diabetes. *Nat. Rev. Immunol.* 19, 734–746. doi: 10.1038/s41577-019-0213-9

Donath, M. Y., and Shoelson, S. E. (2011). Type 2 diabetes as an inflammatory disease. *Nat. Rev. Immunol.* 11, 98–107. doi: 10.1038/nri2925

Eguchi, K., Manabe, I., Oishi-Tanaka, Y., et al. (2012). Saturated fatty acid and TLR signaling link b cell dysfunction and islet inflammation. *Cell Metab.* 15, 518–533. doi: 10.1016/j.cmet.2012.01.023

Ehses, J. A., Perren, A., Eppler, E., Ribaux, P., Pospisilik, J. A., Maor-Cahn, R., et al. (2007). In- creased number of islet-associated macrophages in type 2 diabetes. *Diabetes* 56, 2356–2370. doi: 10.2337/db06-1650

Fried, S. K., Bunkin, D. A., and Greenberg, A. S. (1998). Omental and subcutaneous adipose tissues of obese subjects release interleukin-6: depot difference and regulation by glucocorticoid. *J. Clin. Endocrinol. Metab.* 83, 847–850. doi: 10.1210/jcem.83.3.4660

Ghoreschi, K., Laurence, A., Yang, X. P., Tato, C. M., McGeachy, M. J., Konkel, J. E., et al. (2010). Generation of pathogenic TH17 cells in the absence of TGF-β signalling. *Nature* 467, 967–971. doi: 10.1038/nature09447

Gordon, C. W., and Susan, B.-W. (2005). Five stages of evolving beta-cell dysfunction during progression to diabetes. *Diabetes* 53(Suppl. 3), S16–S21. doi: 10.2337/diabetes.53.suppl_3.S16

Grander, C., Adolph, T. E., Wieser, V., Lowe, P., Wrzosek, L., Gyongyosi, B., et al. (2018). Recovery of ethanol-induced Akkermansia muciniphila depletion ameliorates alcoholic liver disease. *Gut* 67, 891–901. doi: 10.1136/gutjnl-2016-313432

Hang, F., Liu, P., Wang, Q., Han, J., Wu, Z., Gao, C., et al. (2016). High milk-clotting activity expressed by the newly isolated *Paenibacillus* spp. strain BD3526. *Molecules* 21:73. doi: 10.3390/molecules21010073

Herbert, T., Niv, Z., Timon, E. A., and Eran, E. (2019). The intestinal microbiota fuelling metabolic inflammation. *Nat. Rev. Immunol.* 20, 40–54. doi: 10.1038/s41577-019-0198-4

Hotamisligil, G., Shargill, N., and Spiegelman, B. (1993). Adipose expression of tumor necrosis factor-alpha: direct role in obesity-linked insulin resistance. *Science* 259, 87–91. doi: 10.1126/science.7678183

Hotamisligil, G. S. (2017). Inflammation, metaflammation, and immunometabolic disorders. *Nature* 542, 177–185. doi: 10.1038/nature21363

Hull, R. L., Westermark, G. T., Per, W., and Kahn, S. E. (2004). Islet amyloid: a critical entity in the pathogenesis of type 2 diabetes. *J. Clin. Endocrinol. Metab.* 89, 3629–3643. doi: 10.1210/jc.2004-0405

Jourdan, T., Godlewski, G., Cinar, R., Bertola, A., Szanda, G., Liu, J., et al. (2013). Activation of the Nlrp3 inflammasome in infiltrating macrophages by endocannabinoids mediates beta cell loss in type 2 diabetes. *Nat. Med.* 19, 1132–1140. doi: 10.1038/nm.3265

Kagnoff, M. F. (1996). Mucosal immunology: new frontiers. *Immunol. Today* 17, 57–59. doi: 10.1016/0167-5699(96)80579-2

Kamada, N., Hisamatsu, T., Okamoto, S., Chinen, H., Kobayashi, T., Sato, T., et al. (2008). Unique CD14+ intestinal macrophages contribute to the pathogenesis of Crohn disease via IL-23/IFN-γ axis. *J. Clin. Invest.* 118, 2269–2280. doi: 10.1172/JCI34610

Karlsson, F. H., Tremaroli, V., Nookaew, I., Bergstrom, G., Behre, C. J., Fagerberg, B., et al. (2013). Gut metagenome in European women with normal, impaired, and diabetic glucose control. *Nature* 498, 99–103. doi: 10.1038/nature12198

Kern, P. A., Saghizadeh, M., Ong, J. M., Bosch, R. J., and Simsolo, R. B. (1995). The expression of tumor necrosis factor in human adipose tissue. Regulation by obesity, weight loss, and relationship to lipoprotein lipase. *J. Clin. Invest.* 95, 2111–2119. doi: 10.1172/JCI117899

Maldonado, R. A., and Andrian, U. H. V. (2010). How tolerogenic dendritic cells induce regulatory T cells. *Adv. Immunol.* 108, 111–165. doi: 10.1016/B978-0-12-380995-7.00004-5

Maloy, K. J., and Powrie, F. (2011). Intestinal homeostasis and its breakdown in inflammatory bowel disease. *Nature* 474, 298–306. doi: 10.1038/nature10208

Manicassamy, S., Reizis, B., Ravindran, R., Nakaya, H., Rosa Maria, S.-G., Yi-chong, W., et al. (2010). Activation of β-catenin in dendritic cells regulates immunity versus tolerance in the intestine. *Science* 329, 849–853. doi: 10.1126/science.1188510

Moschen, A. R., Molnar, C., Geiger, S., Graziadei, I., Ebenbichler, C. F., Weiss, H., et al. (2010). Anti-inflammatory effects of excessive weight loss: potent suppression of adipose interleukin 6 and tumour necrosis factor alpha expression. *Gut* 59, 1259–1264. doi: 10.1136/gut.2010.214577

Ostermann, A. L., Wunderlich, C. M., Schneiders, L., Vogt, M. C., Woeste, M. A., Belgardt, B. F., et al. (2019). Intestinal insulin/IGF1 signalling through FoxO1 regulates epithelial integrity and susceptibility to colon cancer. *Nat. Metab.* 1, 371–389. doi: 10.1038/s42255-019-0037-8

Pradhan, A. D., Manson, J. E., Rifai, N., Buring, J. E., and Ridker, P. M. (2001). C-reactive protein, interleukin 6, and risk of developing type 2 diabetes mellitus. *J. Am. Med. Assoc.* 286:327. doi: 10.1001/jama.286.3.327

Qiao, Z., Han, J., Feng, H., Zheng, H., Wu, J., Gao, C., et al. (2019). Fermentation products of *Paenibacillus bovis* sp. nov. BD3526 alleviates the symptoms of type 2 diabetes mellitus in GK rats. *Front. Microbiol.* 9:3292. doi: 10.3389/fmicb.2018.03292

Qiao, Z., Qi, W., Wang, Q., Feng, Y., Yang, Q., Zhang, N., et al. (2016). ZmMADS47 regulates zein gene transcription through interaction with opaque2. *PLoS Genet.* 12:e1005991. doi: 10.1371/journal.pgen.1005991

Rey, A. D., and Besedovsky, H. O. (1992). Metabolic and neuroendocrine effects of pro-inflammatory cytokines. *Eur. J. Clin. Invest.* 22, 10–15.

Ridker, P. M. (2000). C-reactive protein and other markers of inflammation in the prediction of cardiovascular disease in women. *N. Engl. J. Med.* 342, 836–843. doi: 10.1056/NEJM200003233421202

Ridker, P. M., Cushman, M., Stampfer, M. J., Tracy, R. P., and Hennekens, C. H. (1997). Inflammation, aspirin, and the risk of cardiovascular disease in apparently healthy men. *N. Engl. J. Med.* 336, 973–979. doi: 10.1056/NEJM199704033361401

Ridker, P. M., Everett, B. M., Thuren, T., Macfadyen, J. G., Chang, W. H., Ballantyne, C., et al. (2017). Antiinflammatory therapy with canakinumab for atherosclerotic disease. *N. Engl. J. Med.* 377, 1119–1131. doi: 10.1056/NEJMoa1707914

Robertson, R. P., Harmon, J., Tran, P. O. T., and Poitout, V. (2004). β-cell glucose toxicity, lipotoxicity, and chronic oxidative stress in type 2 diabetes. *Diabetes* 53(Suppl. 1), S119–S124. doi: 10.2337/diabetes.53.2007.S119

Smith, A. M., Rahman, F. Z., Hayee, B., Graham, S. J., Marks, D. J. B., Sewell, G. W., et al. (2009). Disordered macrophage cytokine secretion underlies impaired acute inflammation and bacterial clearance in Crohn's disease. *J. Exp. Med.* 206, 1883–1897. doi: 10.1084/jem.20091233

Smith, P. D., Ochsenbauer-Jambor, C., and Smythies, L. E. (2005). Intestinal macrophages: unique effector cells of the innate immune system. *Immunol. Rev.* 206, 149–159. doi: 10.1111/j.0105-2896.2005.00288.x

So, A., De Smedt, T., Revaz, S., and Tschopp, J. (2007). A pilot study of IL-1 inhibition by anakinra in acute gout. *Arthritis Res. Ther.* 9, 1–6. doi: 10.1186/ar2143

Stahel, M., Becker, M. D., Graf, N., and Michels, S. (2016). Systemic interleukin 1β inhibition in proliferative diabetic retinopathy: a prospective open-label study using canakinumab. *Retina J. Ret. Vit. Dis.* 36, 385–391. doi: 10.1097/IAE.0000000000000701

Stern, M. P. (1995). Diabetes and cardiovascular disease: the "common soil" hypothesis. *Diabetes* 44, 369–374. doi: 10.2337/diab.44.4.369

Sun, B., and Karin, M. (2012). Obesity, inflammation, and liver cancer. *J. Hepatol.* 56, 704–713. doi: 10.1016/j.jhep.2011.09.020

Tilg, H., and Moschen, A. R. (2008). Insulin resistance, inflammation, and non-alcoholic fatty liver disease. *Trends Endocrinol. Metab. Tem* 19, 371–379. doi: 10.1016/j.tem.2008.08.005

Xu, X., Gao, C., Liu, Z., Wu, J., Han, J., Yan, M., et al. (2016). Characterization of the levan produced by *Paenibacillus bovis* sp. nov BD3526 and its immunological activity. *Carbohydr. Polym.* 144, 178–186. doi: 10.1016/j.carbpol.2016.02.049

Conflict of Interest: ZQ, JH, XW, HZ, HF, and ZW are employed by Bright Dairy and Food Co.

frontiers in Microbiology

ORIGINAL RESEARCH
published: 05 February 2021
doi: 10.3389/fmicb.2021.621280

Evaluation of an *O*2-Substituted (1–3)-β-D-Glucan, Produced by *Pediococcus parvulus* 2.6, in *ex vivo* Models of Crohn's Disease

Sara Notararigo[1,2,3], Encarnación Varela[2,4], Anna Otal[2], Iván Cristobo[1], María Antolín[2], Francisco Guarner[2], Alicia Prieto[1] and Paloma López[1]**

[1]Department of Microbial: and Plant Biotechnology, Margarita Salas Biological Research Centre (CIB-Margarita Salas-CSIC), Madrid, Spain, [2]Department of Gastroenterology, Digestive System Research Unit, Institut de Recerca Vall d'Hebron (VHIR), University Hospital Vall d'Hebron, Universitat Autònoma de Barcelona, Barcelona, Spain, [3]Foundation Health Research Institute of Santiago de Compostela (FIDIS), Santiago de Compostela, Spain, [4]CIBERehd, Instituto de Salud Carlos III, Madrid, Spain

OPEN ACCESS

Edited by:
Jasna Novak,
University of Zagreb, Croatia

Reviewed by:
Jesús Navas,
University of Cantabria, Spain
Rodrigo Dias De Oliveira Carvalho,
Federal University of Minas Gerais, Brazil

***Correspondence:**
Paloma López
plg@cib.csic.es
Alicia Prieto
aliprieto@cib.csic.es

Specialty section:
This article was submitted to Food Microbiology, a section of the journal Frontiers in Microbiology

Received: 25 October 2020
Accepted: 11 January 2021
Published: 05 February 2021

Citation:
Notararigo S, Varela E, Otal A, Cristobo I, Antolín M, Guarner F, Prieto A and López P (2021) Evaluation of an O2-Substituted (1–3)-β-D-Glucan, Produced by Pediococcus parvulus 2.6, in ex vivo Models of Crohn's Disease. Front. Microbiol. 12:621280. doi: 10.3389/fmicb.2021.621280

1,3-β-glucans are extracellular polysaccharides synthesized by microorganisms and plants, with therapeutic potential. Among them, the *O*2-substituted-(1–3)-β-D-glucan, synthesized by some lactic acid bacteria (LAB), has a prebiotic effect on probiotic strains, an immunomodulatory effect on monocyte-derived macrophages, and potentiates the ability of the producer strain to adhere to Caco-2 cells differentiated to enterocytes. In this work, the *O*2-substituted-(1–3)-β-D-glucan polymers produced by GTF glycoyltransferase in the natural host *Pediococcus parvulus* 2.6 and in the recombinant strain *Lactococcus lactis* NZ9000[pNGTF] were tested. Their immunomodulatory activity was investigated in an *ex vivo* model using human biopsies from patients affected by Crohn's disease (CD). Both polymers had an anti-inflammatory effect including, a reduction of Interleukine 8 both at the level of its gene expression and its secreted levels. The overall data indicate that the *O*2-substituted-(1–3)-β-D-glucan have a potential role in ameliorating inflammation *via* the gut immune system cell modulation.

Keywords: bacterial exopolysaccharides, *O2*-substituted-(1-3)-β-D-glucan, lactic acid bacteria, Immunomodulation, Crohn´s disease anti-inflammatory effect

INTRODUCTION

The exopolysaccharides (EPS) are large, lineal, or branched, extracellular carbohydrate polymers, produced by algae, plants, and bacteria. They are commonly used as food additive due to their rheological properties (bio-thickener, gelling, or viscosifier agents) in the food industry. The demand for new polymers in the food industry is positioning EPS from lactic acid bacteria (LAB), as the new generation of food thickeners. Due to their Generally Regarded As Safe (GRAS) status, they are suitable for the production of fermented and/or functional products. The EPS synthesized by LAB are divided into homopolysaccharides, if they contain only one monosaccharide type or heteropolysaccharides, if they contain various monosaccharides types (Werning et al., 2012). These EPS are known to support bacterial growth, as well as participate

in cellular recognition and interaction, surface adhesion, and biofilm formation. Currently, EPS are gaining interest as prebiotics, as modulators of the host immune system (Schmid et al., 2015), and as antiviral agents (Nácher-Vázquez et al., 2015). Their immunomodulatory properties are dependent on their ability to form a suitable tertiary structure. For instance, (1–3)-β-D-glucans (β-glucans), linear or branched in position *O*-4 and *O*-6, are gaining interest as therapeutic targets; various studies have shown their positive influence in reduction of human serum cholesterol levels and their stimulation of the human immune system (Chan et al., 2009; Jin et al., 2018), as well as their potential anti-carcinogenic properties (Chan et al., 2009; Ali et al., 2015).

Recent findings documented that (1–3)-β-glucans are capable of regulating the inflammatory response, modulate immune system cell types (such as peripheral blood immune system cells, intestinal epithelium, and mammalian microglia), through their interaction with membrane receptors, including toll-like receptors, Dectin-1, SIGNR1, complement receptor 3 (CR3), LaCer, and Scavenger, which are differentially expressed in these cells types (Li et al., 2019). Their interaction with a receptor leads to downstream events including the activation of immune system cells, both innate (e.g., macrophages, monocytes, or neutrophils) and adaptive (e.g., T cells or B cells). These interactions may result in differential cytokine production [such as tumor necrosis factor-α (TNF-α), IL-10, IL-8, or IL-12], through the modulation of the nuclear factor kappa-light-chain-enhancer of activate B cells (NFκB) transcription factor, belonging to the mitogen-activated protein kinase (MAPK) pathway (Chan et al., 2009; Volman et al., 2010).

Moreover, it has been reported that the EPS are metabolized in the gut due to the presence of the glycolytic enzyme pools of the microbiota. The exact nature of this process depends on the molecular weight and biochemical composition of the EPS (Bodera, 2008; Kau et al., 2011; Ballesteros Pomar and Gonzalez Arnaiz, 2018). Finally, this hydrolysis is beneficial to both the host and the microbiota itself, because it generates secondary metabolites with the potential to act as probiotic or postbiotic immunomodulators, that ultimately promote and/or restore a healthy environment for the microbiota (Iweala and Nagler, 2019). Laminarin, an *O*6-substituted-(1–3)-β-D-glucan isolated from brown algae, causes a reduction in the expression of pro-inflammatory cytokines, such as IL-6 and IL-1β in pig intestinal mucosa (Heim et al., 2014; Walsh et al., 2015) and counteracts dysbiosis of the microbiota (Rattigan et al., 2020). Moreover, studies performed with human fecal microbiota and commercial laminarin from *Laminaria digitata*, or crude polysaccharide-rich extracts from this algae, indicated that the polysaccharide influences mucus and gut microbiota composition, which results in a potentially beneficial production of short-chain fatty acids (such as butyrate; Devillé et al., 2007; Strain et al., 2020).

Inflammatory bowel disease (IBD) has a multifactorial etiology and includes Crohn's disease (CD) and ulcerative colitis (UC; Kamada et al., 2013; Morhardt et al., 2019). They are chronic gastrointestinal disorders, where the dysregulation of the immune system is responsible for immunological imbalance characterized by the production of pro-inflammatory cytokines (such as TNF-α, INF-γ, IL-17, and IL12) into the gut lumen, alteration of microbiota, and the intestinal mucosal barrier (Knights et al., 2013). High inflammation is responsible for abdominal pain, bloody stools, weight loss, diarrhea, etc.

To evaluate therapeutic treatments, current chemically induced animal models of IBD, including sodium dextran-sulfate treatment, resembles UC symptoms, but emulates only partially the inflammatory process that occurs in human CD (Chassaing et al., 2014). However, an *ex vivo* model, using CD mucosal tissue, allows the investigation of how to modulate the inflammation at the gut mucosa level. Previous studies, using this model, have established that certain probiotic bacteria are capable of interacting with immunocompetent cells using the mucosal interface, and thus can modulate locally the production of pro-inflammatory cytokines by inflamed tissue (Borruel et al., 2003; Llopis et al., 2009; Hidalgo-Cantabrana et al., 2015).

In this context, recently, new therapeutic strategies involving the use of probiotic strains have been developed to ameliorate CD patient's symptoms. Some of these include microorganisms, such as *Lacticaseibacillus rhamnosus* GG, *Limosilactobacillus reuteri*, *Lactobacillus acidophilus*, *Bifidobacterium infantis*, *Saccharomyces boulardii*, *Escherichia coli* Nissle 1917, and *Clostridium butyricum* MIYAIRI 588 (Tsai et al., 2019), which contribute to reduction of inflammation, due to their ability to reduce pathogen adhesion to the intestinal epithelium (blocking their binding site), and by production of antibacterial substances or EPS (Orel and Kamhi Trop, 2014; Oka and Sartor, 2020). In addition, probiotic strains modify the release of cytokines in the intestinal epithelium and inhibit, in the immune system cells, the production of the transcription factor NFkB, leading as a consequence to a reduction of intestinal inflammation (Basson et al., 2017; Oka and Sartor, 2020). In this general context, some probiotic bacteria produce a *O*2-substituted-(1–3)-β-D-glucan with prebiotic activity and that stimulate the growth of probiotic LAB (Russo et al., 2011; Pérez-Ramos et al., 2017). Therefore, the producing bacteria or their EPS have potential as adjuvants in the treatment of IBD. Such a role is plausible, taking into account that β-glucans play an important role in the modulation of both the innate immune response, through interaction with dendritic cells (DCs) and macrophages, and also in the adaptive immune response, increasing proliferation of T- and natural killer cells, *via* cytokine release (Bodera, 2008; Zhang et al., 2015).

Only *Pediococcus*, *Lactobacilli*, and *Oenococcus* strains isolated from alcoholic beverages synthesize the *O*2-substituted-(1–3)-β-D-glucan (reviewed in Llamas-Arriba et al., 2019). Moreover, studies performed with *Pediococcus parvulus* 2.6 isolated from cider and with the recombinant *L. lactis* NZ9000[pGTF] strain carrying the pediococcal *gtf* gene, demonstrated that this gene encodes the GTF glycosyltransferase, which catalyzes the synthesis of the *O*2-substituted-(1–3)-β-D-glucan in LAB (Werning et al., 2006, 2008, 2012). Moreover, *P. parvulus* 2.6 and *L. lactis* NZ9000[pGTF] synthesize, respectively the EPS P and the EPS L polymers having the same primary structure, which is different from those of the β-glucans isolated from fungi and yeasts, which have ramifications at positions *O*-4 and *O*-6 (Thompson et al., 2010).

This peculiarity of structure was the reason why we investigated the probiotic potential of the producing strain *P. parvulus* 2.6 (Werning et al., 2012; Pérez-Ramos et al., 2017), and the prebiotic potential of its EPS P (Russo et al., 2011; Pérez-Ramos et al., 2017). Also, our previous work supports an anti-inflammatory effect of this *O*2-substituted-(1–3)-β-D-glucan. Comparison of the behavior of *P. parvulus* 2.6 with its isogenic EPS P-non-producing strain, revealed that the presence of the polymer decreased the pro-inflammatory effect exerted by the LAB on human macrophages M1, indicating a possible activity of this EPS as an immunomodulator in the innate immune response (Fernández de Palencia et al., 2009). Moreover, in an induced inflammation model, using the zebrafish transgenic line Tg(mpx:GFP)i114, the polymer inhibited neutrophil recruitment and proliferation in the larvae, confirming once again its potential as an immunomodulator (Pérez-Ramos et al., 2018). Furthermore, the metabolic rate of macrophages derived from human monocytes increased upon exposure to either the EPS P and the EPS L synthesized by *L. lactis* NZ9000[pGTF] (Notararigo et al., 2014). In addition, these EPS activated processes involved in M1 differentiation, migration, and cellular proliferation, as well as inhibited AKT and mTor pathways implicated in the inflammatory response (Notararigo et al., 2014). Therefore, this current work aimed to study the immunomodulatory effect of the *O*2-substituted-(1–3)-β-D-glucan, vs. the *O*6-substituted-(1–3)-β-D-glucan, (laminarin, isolated from *Laminaria digitata*), on ileocolonic biopsies of CD patients.

MATERIALS AND METHODS

Patients

Samples of intestinal mucosa were obtained during surgery from four patients with CD (one male and three females, age 46.7 ± 19.9, SEM), who underwent ileal resection for stricture unresponsive to conventional medical treatment (**Table 1**). Biopsies of the intestinal tissue were kept at 4°C, from collection until their later handling. None of the patients had been on anti-TNF treatment for at least 2 months before the intervention.

The diagnosis of CD was previously established by the clinical routine, as well as radiological and endoscopic, criteria, and afterwards was confirmed by histological evaluation of the surgical specimen. All patients received the same preparation for colonic surgery including gut lavage with electrolyte-polyethylene glycol solution and broad-spectrum antibiotic therapy.

TABLE 1 | Characteristics of the patients included in the pilot study.

Patients	Age	Sex	Affected segment	Debut date	Treatment
1	20	F	Ileocecal	2 years	Azathioprine + budesonide
2	42	F	Ileocecal	less than 6 months	Amoxicillin + clavulanate
3	57	F	Ileocecal	8 years	Mesalazine + azathioprine
4	68	M	Ileocecal	28 years	Azathioprine

The study was approved by the Ethics Committee (Comité Ético de Investigación Clínica, Hospital Vall d'Hebron, Barcelona). Written informed consent was obtained from all patients [CEIC: PR(AG)56/2010].

EPS P and EPS L Production and Purification

Exponential cultures of *P. parvulus* 2.6 (Dueñas-Chasco et al., 1997; Pérez-Ramos et al., 2018) and *L. lactis* NZ9000[pGTF] (Werning et al., 2008) were used to produce EPS P and EPS L, respectively. The EPS were produced and purified, as previously described (Notararigo et al., 2013). Briefly, after removal of bacterial cells by centrifugation, the EPS present in the culture supernatants were precipitated with three volumes of ethanol. Then, the EPS were further purified by dialysis and fractionation by size exclusion chromatography after resuspension in a 0.3 M NaOH solution. Afterwards, the EPS alkaline solution was dialyzed as above. Finally, the EPS was lyophilized and left at room temperature until use. After the first and second lyophilization, the purity of the EPS was tested fluorometrically using specific fluorescent staining kits for DNA, RNA, and proteins as previously reported (Zarour et al., 2018). Solutions of the purified polymers were prepared at 1 mg ml^{-1}. No contaminants were detected (**Table 2**).

Organ Culture of Human Colonic Mucosa

Organ culture assays were performed as described (Borruel et al., 2002, 2003; Llopis et al., 2009). Full-thickness ileal wall specimens, including areas with macroscopic lesions, were collected at surgery. After rinsing and washing with sterile saline solution, the specimens were transferred to the laboratory in sterile saline solution at 4°C. The intestinal mucosa was removed from the tissue, and cut into pieces of approximately 25–35 mg weight each, making an equal distribution of the macroscopic lesion. Each piece was placed on the insert of a 12-well cell culture plate (Netwell culture system, Costar), with the epithelial surface uppermost. Filters were placed into the wells and incubated with 1,500 µl RPMI 1640 culture medium (CanSera), without antibiotic (37°C, 95% O_2, 5% CO_2 -carbogene-). Before usage, the culture medium was filtered through a 0.22 µm membrane, warmed to 37°C, and gassed for 90 min with carbogen. Tissue without lesion (not inflamed) was used as negative control.

The tissues obtained from biopsies of CD patients were exposed independently to EPS L, EPS P, or laminarin. A solution of the polymers in culture medium at 100 µg ml^{-1} was added by dripping onto the tissues. The cell culture plate was covered

TABLE 2 | Detection of contaminants in EPS preparations.

Contaminants	1 lyophilization		2 lyophilization	
	EPS P	EPS L	EPS P	EPS L
DNA (%)	0	0	0	0
RNA (%)	0	<0.1	0	0
Proteins (%)	<0.1	1.2	0	0

with a supported lid, allowing a correct exchange of gases, and subsequently placed in a bath at 37°C, inside a container shielded with a wet cloth. Then, the container was connected to the carbogen gas outlet, gassed at high pressure for 10 s at 1 h intervals, and incubated for 4 h.

Then, the pro-inflammatory (TNF-α and IL-8) and anti-inflammatory (IL-10) cytokine levels released into the media were quantified by ELISA. At the end of the experiment, aliquots of the supernatant were collected from each well, prior to being stored at −80°C, while the tissue was kept immersed in 400 μl of rRNA stabilization solution "RNA later" (Ambion) at 4°C overnight, and then stored at −80°C.

Determination of Cytokine Levels by Elisa

The cytokine protein profiles of tissue culture supernatants, in response to EPS treatments, were analyzed by OptEIA ELISA (BD Pharmingen) to detect IL-10 and TNF-α, as well as by DuoSet ELISA (RD Systems) for IL-8, following the suppliers' instructions.

The cytokine concentrations were extrapolated from the regression line generated using the absorbance values of a standard curve, which was produced in the same test with known concentrations of commercial cytokines.

Gene Expression Profiling Under EPS Treatment

In gene expression organ culture assays, CD samples were harvested in the presence of RNA later (Ambion) and stored at −80°C. RNA extraction from the patients' biopsies was performed using the RNeasy mini (Qiagen), according to the supplier's instructions. RNA concentration and integrity were analyzed and determined with the RNA 6000 Nano Chip in a Bioanalyzer 2100 (Agilent Technologies). RNA quantity and integrity were considered acceptable if the 28S/18S ribosomal fragment ratio was over 1.5, and the RNA Integrity Number (RIN) ranged in values between 9 and 10. Selected gene expression was evaluated with real-time PCR, and 1 μg of total RNA was used for the reverse transcription to synthesize first strand cDNA following the recommended protocol of the High-Capacity cDNA Reverse Transcription kit (Applied Biosystems). Quantitative PCR was then carried out with the Taqman Gene Expression Assay (Thermo fisher Scientific), using TaqMan Fast Universal PCR Master Mix (2X; Applied Biosystems). Relative quantification of gene expression of thymic stomal lymphopietin (TSLP), IL-12p35, IL-10, and IL-8 was determined, using a 7500 Fast Real time PCR System (Applied Biosystems). Data were obtained as threshold cycle (Ct) values. Gene expression levels for each individual sample were normalized relative to the PPIA gene as housekeeping/constitutive/endogenous gene, which encodes the Peptidylprolyl Isomerase A (also called Cyclophilin A). Each condition was run in triplicate.

Transcription Factor Signaling Pathways NFκB RNA Array

The RT2Profiler PCR array (SABiosciences-Qiagen) was used to obtain the expression profile of 84 fundamental genes of the NFκB pathway (**Supplementary Table S1**; supplementary data).

The analysis with the array was performed according to the manufacturer's instructions, as follows. The substrate used was cDNA synthesized from RNA samples (obtained from patient biopsies) with the "RT2 First Strand" kit (Qiagen). The quantitative-RT-PCR (qPCR) was carried out using the SYBR GREEN technology "RT2 SYBR Green," and run in a thermal cycler iQ5 (BioRad). Once the reaction was complete, the data corresponding to the Ct values of each gene were exported to a data sheet for further analysis. The analysis of the differential gene expression was carried out through the web application developed by the company for this purpose based on the method $\Delta\Delta$Ct and using three of the five constitutive genes for the standardization of the data (β-actine, β-2-microglobulin, and the ribosomal P0 protein; Seeger et al., 2014).

Bioinformatic Functional Analysis

The functional analysis of the selected genes was performed using the Database for Annotation, Visualization and Integrated Discovery (DAVID 6.7; http://david.abcc.ncifcrf.gov), which integrates the information of over 1.5 million genes in more than 65.000 species, from different public sources of gene and protein notations (Huang et al., 2008). DAVID provides a functional classification of genes by extracting the information from various databases. We selected terms from Gene Ontology (GO; http://geneontology.org/) and from molecular pathways integrated in: the Biological Biochemistry Image Database (BBID, http://bbid.irp.nia.nih.gov/), Biocarta (http://www.biocarta.com/genes/index.asp), and the Kyoto Encyclopedia of Genes and Genomes (KEGG, http://www.genome.jp/kegg/).

Gene ontology terms allows the unification of the representation of the attributes of genes and their products among the species, favoring the functional interpretation of experimental data by dividing the terms into three categories: cellular compartment (CC), molecular function (MF), and biological process (BP). The use of molecular pathways databases facilitates the production of graphic information of how genes and their products interact.

Statistical Analysis

Statistical analysis was carried out using the Prism 8 (GraphPad) software. The normality of the data was tested by the Kolmorov-Smirnov or Shapiro-Wilk Test normality test. For parametric data, a two-tailed paired *t*-test was applied, while for nonparametric data, the Friedman Test for paired data was used.

For qPCR, for parametric data, unpaired two-tailed Student *t*-test was performed with Welch's correction. Values with $p < 0.05$ were considered significant.

RESULTS AND DISCUSSION

Effect of *O*2-Substituted-(1–3)-β-D-Glucans on Cytokine Production in *ex vivo* Models

The EPS P and EPS L synthesized by *P. parvulus* 2.6 and *L. lactis* NZ9000[pGTF], respectively, are identical *O*2-substituted-(1–3)-β-D-glucans with the same primary structure

(Dueñas-Chasco et al., 1997; Werning et al., 2014). However, the polymers have different molecular masses, 9.6 × 10^6 Da for EPS P and 6.6 × 10^6 Da for EPS L (Werning et al., 2014). The molecular mass of polysaccharides plays a role in their biological activity, consequently, there may be differences between the immunomodulatory activities of each EPS, and therefore both polymers were tested. Thus, in the present pilot study, to evaluate EPS P and EPS L (**Figure 1A**), *ex vivo* tissue cultures have been used as a model of pathological intestinal inflammation (**Figure 1B**), in which the immune system plays an important role in the development, propagation, and maintenance of inflammation and disease. We have shown that this model is suitable to investigate the effects of LAB treatment on the intestinal immunity axis (Bäuerl et al., 2013). Laminarin was also tested as a positive control due to its ability to activate the immune system through its interaction with the Dectin-1 receptor (Xie et al., 2010; Smith et al., 2018).

Tissues obtained from biopsies of four CD patients were exposed independently to the polysaccharides (**Figure 1B**); and subsequently the pro-inflammatory (TNF-α and IL-8) and anti-inflammatory (IL-10) cytokine levels released into the media were quantified (**Figure 1C**). The results revealed that the concentration of the pro-inflammatory IL-8 secreted by the tissues during treatment with either of the three β-glucans tested was significantly lower ($p < 0.05$) than that released by the untreated control tissue. In addition, the highest effect was obtained with EPS P or laminarin. These results indicated a role of the *O*2-substituted-(1–3)-β-D-glucans on the reduction of inflammation associated with the intestinal epithelial mucosa. However, the levels of TNF-α and IL-10 secreted by the tissues were not affected by the treatments. This lack of influence could be due to the cytokine's short lifespan and to the large number of proteases released by the tissue of CD patients (Borruel et al., 2002). These hypotheses presumably did not

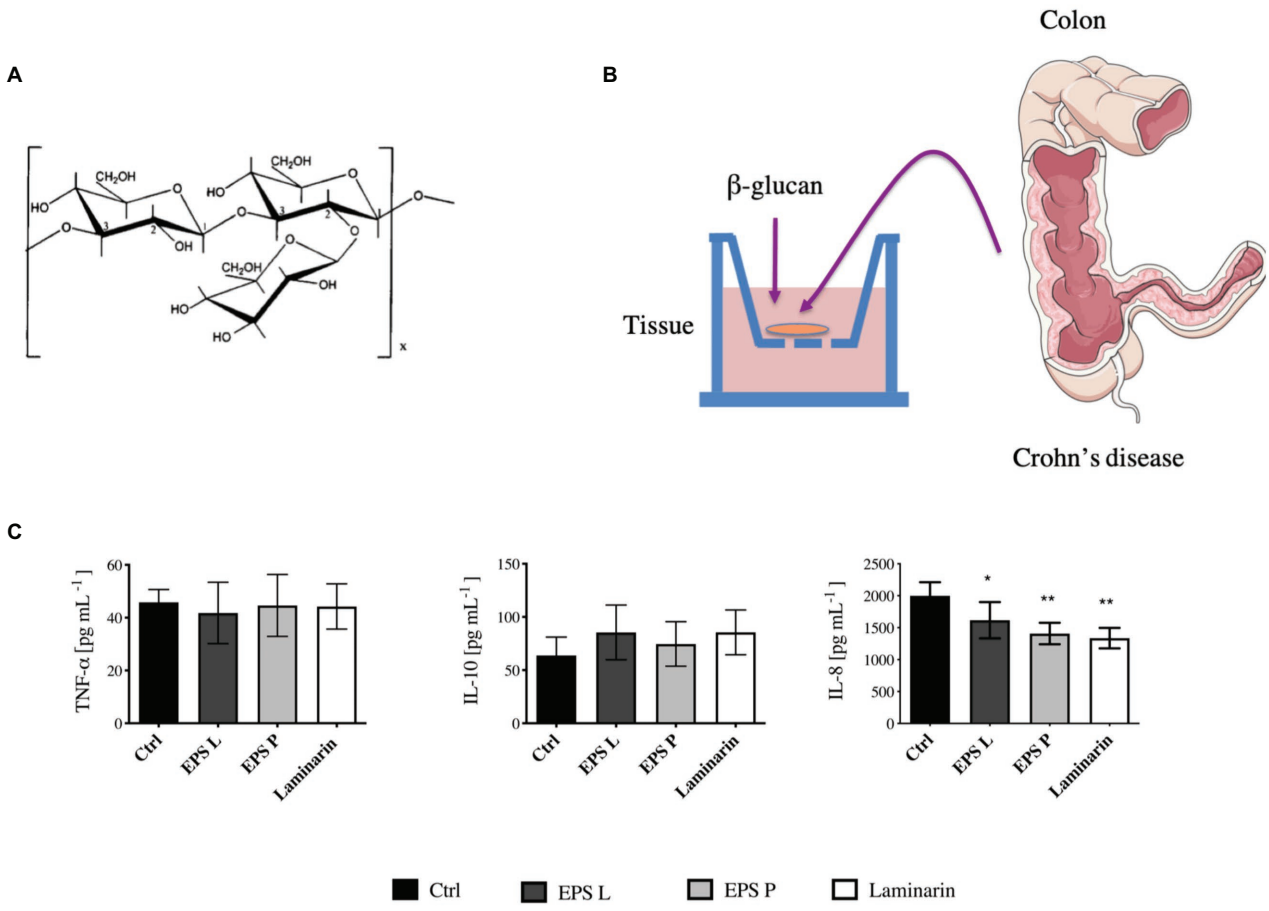

FIGURE 1 | Evaluation of (1–3)-β-D-glucans in *ex vivo* model of inflamed gut mucosa. **(A)** The primary structure of EPS L and EPS M is depicted. **(B)** Organ culture assay, the tissues were collected from Crohn's disease (CD) patients and incubated in the culture medium for 4 h. Then, the media were used to perform ELISA Immunoblot. **(C)** Concentration of tumor necrosis factor-α (TNF-α), IL-10, and IL-8 secreted by the tissues represented in Barplot mean with SEM. The levels of cytokines were quantified by the ELISA immunoblot method. Data passed the Kolmorov-Smirnov normality test, and statistical significance was tested with two tailed *t*-test between each treatment and control (Ctrl). IL-8 was decreased in inflamed tissue treated with EPS L $p < 0.03$ (*), EPS P $p < 0.0068$ (**), and laminarin $p < 0.0097$ (**) vs. untreated control.

apply for the results obtained for IL-8, since the levels detected for this cytokine were 40 times higher than those observed for the TNF-α and IL-10. Therefore, the alteration of IL-8 concentration seems to reflect the biological status of the tissue. One of the CD patients, whose ileocolonic biopsy was analyzed and previously treated with antibiotic (**Table 2**). Therefore, the results obtained could have a bias due to the inclusion of his biopsy in the study. However, quantification of the cytokine levels released by the biopsies of only the three other patients provided the same kind of pattern and behavior (**Supplementary Figure S1**), validating the performed assay.

Effect of *O*2-Substituted-(1–3)-β-D – Glucans on Gene Expression Profiling in *ex vivo* Model

To understand the immunomodulatory effect of the bacterial β-glucan on gene expression in the *ex vivo* model, levels of transcription of the TSLP, IL-8, IL-12p35, and NFκB coding genes in the treated vs. untreated tissues were determined by means of qPCR (**Figure 2**).

The analysis of gene expression in the treated vs. untreated tissues revealed in general a similar pattern of response to the exposure to EPS L, EPS P, or laminarin. Thus, the treatment with any of the three β-glucans resulted in a decrease of TSLP and IL-8 transcription. However, this effect was only statistically significant (p = 0.0367) for TSLP in tissues treated with EPS P. TSLP is a protein, which belongs to the cytokine's family and, that promotes T cell maturation when antigen presenting cells are activated. In IBD patients, low levels of TSLP are associated with a permeability increase of the gut barrier, or Th2 cell differentiation, depending on the cell type that is expressing it (epithelial cells or DC cells; Biancheri et al., 2016; Park et al., 2017). Recently, it has been proposed that TSLP also participate in Treg cell development and gut homeostasis perpetuation (Tahaghoghi-Hajghorbani et al., 2019). Our results suggest that EPS L and laminarin exhibit normal values of gene expression, leading to a balanced TSLP function, while EPS P slightly decreases its expression, and probably has no effect on TSLP turn over. EPS P fold change reached 0.74, which means that the decrease of relative expression is not so dramatic as expected in CD patients with active inflammatory reactions (Tahaghoghi-Hajghorbani et al., 2019).

Our results also revealed that the NFκB transcript was over-expressed in tissues exposed to EPS L or laminarin (**Figure 2**). NFκB is a transcription factor that regulates the expression of pro-inflammatory genes, including cytokines, chemokines, and other molecules. NFκB is a heterodimer formed by RelA/1 that activates the canonical signaling pathway and Rel B/NFKB2 that activates the non-canonical pathway (see details in **Figure 3**). The first is activated by TNF-α or IL1, while the latter is activated by cluster differentiation 40 (CD40), B cell activating factor, and other molecules, but not by TNF-α. The heterodimer activation mechanism is complex; additionally, the presence of cofactor molecules in the nucleus, that bind to the transcription factor complex, may influence the transcription of pro- or anti-inflammatory proteins coding genes (Lawrence, 2009). Its activity is regulated by the endogenous cytoplasmic inhibitors IκKs kinases complex that ensures the activation/repression of the heterodimer, that in specific conditions is able to transmigrate to the nucleus and induce transcription (Jobin and Sartor, 2000). In IBD, the canonical pathway is activated constitutively, thus conspicuous amounts

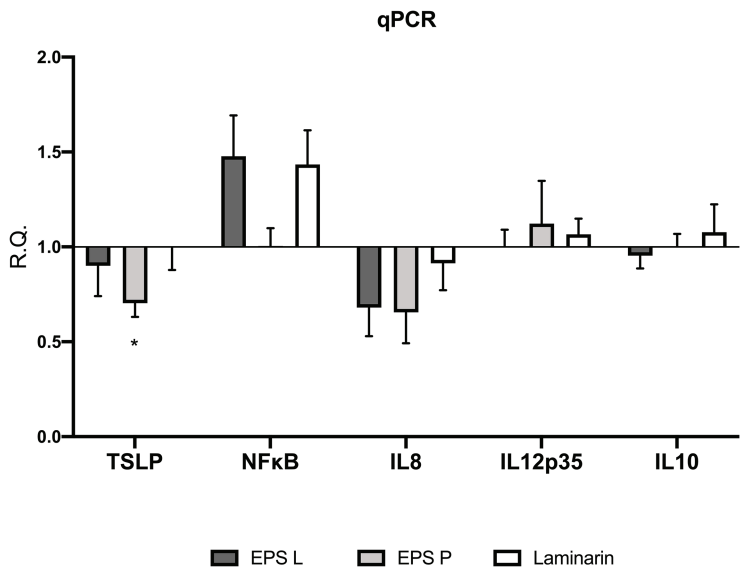

FIGURE 2 | (1–3)-β-D-glucans modulate the relative gene expression of the biopsies of patients affected by CD. Barplot representation mean with SEM of TSLP, NFκB, IL-8 IL-12p35, and IL-10. Gene expression was analyzed by quantitative-RT-PCR (qPCR) analysis. Data passed the Shapiro-Wilk normality test, the unpaired two-tailed Student *t*-test was performed with Welch's correction Only TSLP demonstrated a significance difference with a $p < 0.03$ vs. untreated control.

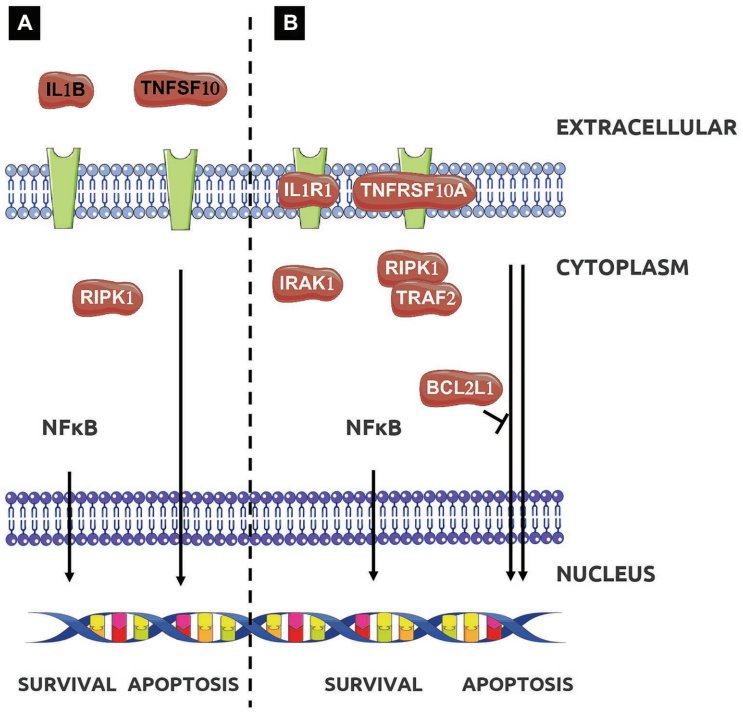

FIGURE 3 | Effect of treatment with EPS L **(A,B)** or EPS P **(B)** on apoptotic signaling pathway. Adapted from Kyoto Encyclopedia of Genes and Genomes (KEGG; Kanehisa et al., 2014).

of TNF-α are released by immune system cells in gut mucosa, as well as interferon-γ (IFN-γ) or IL-8 (Lawrence, 2009).

Our results indicate that EPS L and laminarin increased the relative expression of NFκB (RelA subunit) 1.5-fold higher than that of the control, while EPS P does not have any major effect. To comprehend the EPS effect on NFκB activation, it would be necessary to study all genes involved in the NFκB signaling pathway and clarify EPS activity. We would expect that the observed increase of NFκB expression would determine the increase of pro-inflammatory mediators, like IL-8 or TNF-α, instead we detected the reduction of the IL-8 transcript (**Figure 2**) and no significant difference in TNF-α detection in cultured media (**Figure 1**), or in gene expression (**Figure 2**).

IL-8 is a chemokine produced by macrophages and intestinal epithelial cells (IEC); it is considered a good marker to determine disease activity (Mohammed Vashist et al., 2018). It is also known as neutrophil chemotactic factor, because it induces chemotaxis in target cells such as neutrophils or other cells that migrate toward the infection focus (Llopis et al., 2009; Walana et al., 2018). Our results showed that the amount of the protein IL-8 (**Figure 1**) and the expression of its coding gene (**Figure 2**) decreased during treatments, suggesting that neutrophil recruitment also decreased as a consequence of the reduction of the inflammation rate. In line with these results, we have previously detected that EPS P treatment decreased IL-8 and TNF-α expression in a gnotobiotic zebrafish larvae model, indicating its ability to reduce inflammation (Pérez-Ramos et al., 2018). Also, when EPS P was tested in an induced inflammation model using the zebrafish transgenic line *Tg(mpx:GFP)i114*, a significant decrease of neutrophil recruitment to the inflammation focus was observed (Pérez-Ramos et al., 2018).

Analysis of IL12p35 gene expression confirmed that the treatments did not augment the pro-inflammatory response in the *ex vivo* model (**Figure 2**). The fold change values were close to the untreated control, henceforth, taking into account that IL12p35 is the specific subunit of IL12 cytokine, EPS do not activate mechanisms involved in IL12 signaling pathway. Overall, the results obtained indicated a trend toward reduction of inflammation in CD biopsies treated with any of the three β-glucans.

IL-10 is an anti-inflammatory cytokine, that is released in the gut by macrophages and IEC to maintain homeostasis (Latorre et al., 2018; Morhardt et al., 2019). According to our results, IL-10 mRNA levels did not show significant differences in the expression profiling (**Figure 2**), confirming the results obtained in cytokine production (**Figure 1**). This agrees with our previous observation that macrophages derived from human monocytes treated independently with either EPS did not stimulate IL-10 production (Notararigo et al., 2014). Moreover, we observed the same behavior in a gnotobiotic zebrafish larvae model, where EPS P treatment did not result in an increase of IL-10 expression (Pérez-Ramos et al., 2018). Taken together, these results support that bacterial β-glucans do not interact with the IL10R receptor (Shouval et al., 2014).

Effect of EPS L and EPS P on the NFκB Gene Expression Profile of CD Patient Biopsy

After detecting IL-8 reduction at transcriptional and protein levels, as well as NFκB modulation, we decided to investigate the effect of β-glucans on NFκB signaling pathways, carrying out a gene expression "array" with the RNA from the CD patient that showed the greatest IL-8 relative expression reduction. Moreover, to have a representative analysis, the results obtained for EPS treated and untreated samples were normalized taking in account the expression of three houskeeping genes (see details in "Materials and Methods"), and the results are depicted in **Figure 4**. The profiles in response to treatment with either EPS P or EPS L were, in general similar (**Figures 4B–E**). The expression of the cytokines IL1A and IL1B coding genes was reduced (fold change: IL1A 0.8, 0.7; IL1B 0.5, 0.8 for EPS L and EPS P treatment, respectively) as well as the levels of transcripts encoding the colony-stimulating factor 3 (CSF3) and the MyD88 adapter protein. These results point out that both EPS have an immunomodulatory effect on the gut immune system. Receptor Interacting Serine/Threonine Kinase 1 (RIPK1) was upregulated indicating a possible function in IEC, restoring the gut barrier integrity by preventing a dysregulated cell death mechanism. Moreover, the results seemed to support that the EPS selectively activated NFκB heterodimers, EPS P RelB/NFKB2, and EPS L RelA/NFKB1 (**Figure 4A**; Jobin and Sartor, 2000).

We selectively studied the NFκB heterodimer complex formed by RelB/NFKB2 and RelA/NFKB1 because NFκB1 and NFκB2 act as inhibitors, blocking transcription factor translocation to the nucleus until an external stimulus activates the proteolysis that converts them into p50 and p52, respectively. The overexpression of both inhibitors, showed in **Figure 4D**, could be the key for the immunomodulatory effect of bacterial β-glucan.

According to these results, EPS P seemed to exert its impact mainly on the MyD88 independent signaling pathway, as shown by its influence on RelB, Interleukin 1 Receptor Associated Kinase 1 (IRAK1), RIPK1, Inhibitor of Nuclear Factor Kappa B Kinase Subunit Epsilon (IKBKE), Signal Transducer and Activator of Transcription 1 (STAT1), and CD40 (**Figures 4C,D**).

On the other hand, EPS L could modulate both the canonical and non-canonical pathways (**Figure 4A**). The first, MyD88 dependent, by activating Rel, Toll Like Receptor 6 (TLR6; data

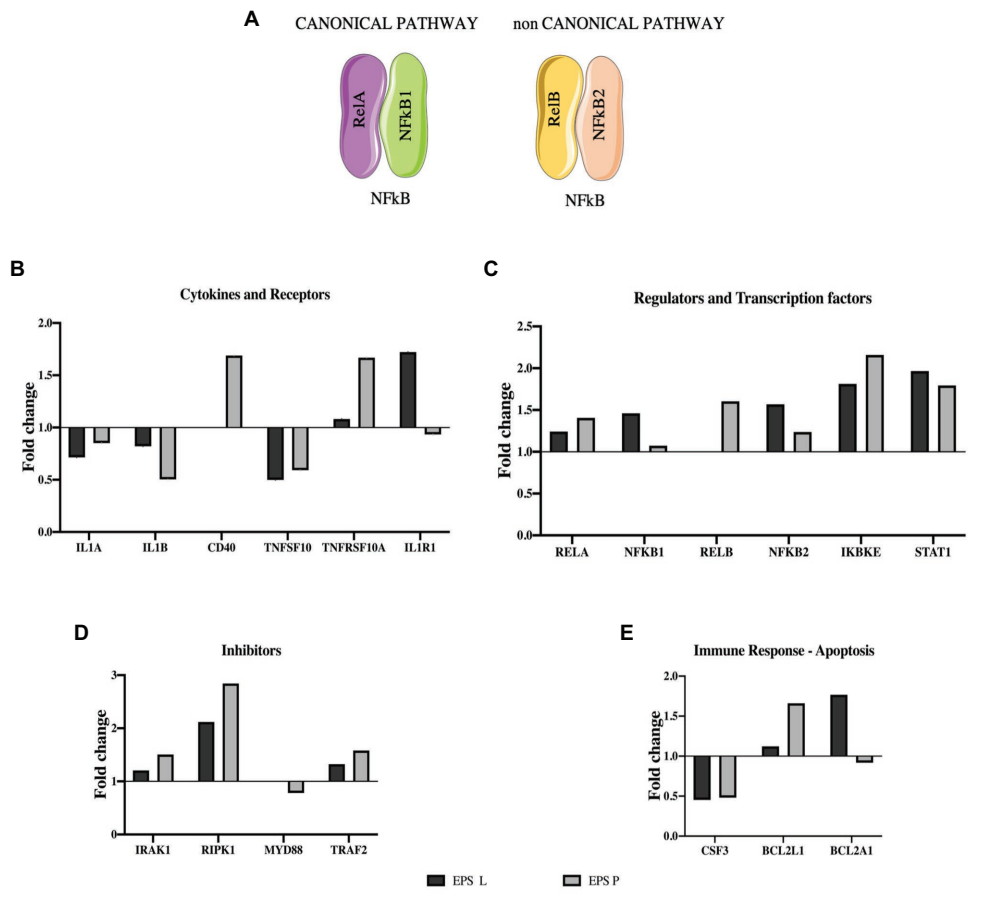

FIGURE 4 | Effect of EPS P and EPS L on expression of genes involved in NFκB pathway. **(A)** NFκB heterodimers activate canonical and non-canonical pathway. **(B)**, **(C)**, **(D)**, and **(E)** Expression profiling of representative genes (fold change), whose expression resulted affected by the treatment. Data of the patient who showed the lower qPCR for IL-8.

not shown), and RIPK1, and repressing IL1A and IL1B gene expression. The latter, MyD88 independent, by activation IKBKE and STAT1 (**Figure 4C**). In line with these findings, our previous results demonstrated that EPS P downregulated the relative expression of three genes involved in inflammation, MyD88 among them, in a zebrafish larvae model, pointing out the potential of the *O*2-substituted-(1–3)-β-D-glucan as an immunomodulator (Pérez-Ramos et al., 2018).

Although EPS P and EPS L could have a different effect on transduction pathways activated by NFκB, this analysis does not fully clarify what mechanisms they may be modulating. Both have been shown to reduce the expression of pro-inflammatory cytokines, such as IL-1A, IL-1B, TNF, and IL-8 (**Figure 4B**), and these results have been validated in different models (Notararigo et al., 2014; Pérez-Ramos et al., 2018). The overall results were quite complex, considering that many of the genes studied are involved in the signaling of different receptors and are present in the majority of cell types isolated in the CD biopsy. For this reason, it was necessary to use bioinformatics tools to group the genes whose function may be related, and improve the understanding of the mechanisms underlying the stimulus provided by the *O*2-substituted-(1–3)-β-D-glucan, as described below.

Functional Analysis With David Bioinformatic Resources

In order to interpret the results of the differential response caused by each EPS on the tissue of the CD patient, a bioinformatic clustering with DAVID was carry out. The aim of this analysis was to arrange genes and derive their biological meaning, by association with identical or related functions and/or pathways. We restricted gene analysis to fold changes between $\leq$5 and/or $\geq$1.5, to establish strong interaction between selected genes.

The gene clustering revealed a modulation of 14 or 19 genes upon treatment with either EPS L or EPS P. Among the regulated genes, the presence of EPS L resulted in a reduction of expression of 4, whereas downregulation of only one gene was observed with the EPS P treatment. Also, 10 or 19 where upregulated after exposure of the tissues to EPS L or EPS P, respectively. Furthermore, as a response to both treatments, the alteration of expression of five genes showed the same pattern: upregulation for IKBKE, PC4, and SFRS1 interacting protein 1 (PSIP1), RIPK1 and STAT1, and downregulation for Colony-Stimulating Factor 3 (CSF3).

The functional analysis for molecular function of GO depicted in **Table 3** showed that the enrichment in functional terms for genes affected by treatment with EPS P, was greater than that with EPS L in number, degree of enrichment, and number of members in each category. In addition, EPS L regulon included genes grouped into two categories related to cytokine activity, while for EPS P regulon more grouping terms were found, highlighting the regulation of caspase activity and cytokine activity. These results confirmed the data obtained from functional grouping (data not shown), and the overall results allowed us to postulate a possible mechanism of action of either EPS on the apoptosis pathway represented in **Figure 3**. EPS L could affect extrinsic apoptosis pathways with the inhibition of Tumor Necrosis Factor Apoptosis-Inducing Ligand 10 (TNFSF10) and IL-1B, while also it could activate survival pathway (RIPK1), with a possible healing effect on gut barrier, through the NFκB pathway and chemotaxis reduction upon CSF3 downregulation. EPS P could activate apoptosis pathway by altering gene expression of Tumor Necrosis Factor Receptor Superfamily Member 10a (TNFRSF10A), and the cell death regulator BCL2L1 while repression of CSF3 may points to a role in modulation of intestinal immunity, with a possible decrease in the chemotaxis of the neutrophils to the foci of inflammation (Carol et al., 2006).

To support this hypothesis, some of the results depicted in **Figure 4E** should be discussed in the context of the apoptotic signal pathways. BCL2A1 is a gene which belongs to the BCL-2 family, the protein encoded by this gene is able to reduce the release of pro-apoptotic cytochrome c from mitochondria and block caspase activation. The gene showed a 1.7- or 0.9-fold change upon treatment with EPS L or EPS P. This gene is directly activated by NFκB in response to inflammatory mediators, such as granulocyte-macrophage colony-stimulating factor (GM-CSF), CD40, and cytokine like TNF-α or IL-1 which suggest lymphocyte activation/proliferation and cell survival. Yet, both EPS downregulate TNF-α, IL-1A, and IL-1B, and have no effect on GM-CSF (data not shown), while only EPS P upregulated CD40. Taken together, these results suggest that EPS L had an anti-apoptotic effect, while EPS P had a possible pro-apoptotic effect. Indeed, both β-glucans showed an anti-inflammatory effect, because of reduction of the relative expression of cytokines, that might reflect in reduced lymphocyte activation for EPS L and in cell death activation for EPS P.

The BCL2L1 gene product is a potent pro-apoptotic activator, and this gene was upregulated by both EPS treatments with a fold change of 1.6 for EPS P and 1.2 for EPS L. We postulate that the *O*2-substituted-(1–3)-β-D-glucans might reestablish normal condition of the intestinal immune system cells through an apoptosis activation mechanism (**Figure 3B**).

In addition, expression of the cytokine TNFSF10 was downregulated in the presence of both EPS (fold change: 0.5 and 0.4 for EPS P and EPS L treatments, respectively) while TNFRSF10A, that binds TNFSF10 was slightly upregulated under EPS P treatment (fold change 1.3), and downregulated upon exposure to EPS L (fold change: 0.7). Moreover, Tumor Necrosis Factor Receptor Superfamily Member 10b (TNFRSF10B), and IL-1R receptors coding genes were downregulated (fold change: 0.9 and 0.7, respectively) in EPS L treated tissues, and upregulated (fold change: 1.4 and 1.7, respectively) in tissues exposed to EPS P (**Figures 4B,C**). These results indicate that EPS L and EPS P reduced the expression of the apoptotic ligand TNFSF10, but had a different effect on the expression of receptor TNFRSF10B, an IL-1R. It is possible that EPS P activates a cell death mechanism, to regulate lymphocyte proliferation, while EPS L acts at the cell mediation level by reducing cytokine production.

Therefore, EPS P seems to modulate apoptosis, as several results previously collected support the bioinformatic analysis. Some examples are, the lowering of IL-8 in an *ex vivo* model,

TABLE 3 | Molecular function gene ontology (GO) terms for the gene differentially expressed upon EPS P or EPS L treatment.

	GO TERM	ENRICHMENT[a]	GENES
EPS P	GO:0043028~caspase regulator activity	47,12	TNFRSF10A, BCL2L1
	GO:0005125~cytokine activity	10,51	CSF3, CCL2, and CSF1
	GO:0004674~protein serine/threonine kinase activity	7,94	IRAK1, IKBKE, MAP3K1, RIPK1, and RAF1
	GO:0004672~protein kinase activity	6,76	IRAK1, IKBKE, CCL2, MAP3K1, RIPK1, and RAF1
	GO:0008134~transcription factor binding	5,33	TNFRSF10A, RELB, BCL3, and NFKB2
	GO:0019899~enzyme binding	5,23	CSF3, IRAK1, MAP3K1, and CD40
	GO:0042802~identical protein binding	4,27	IRAK1, MAP3K1, CSF1, and BCL2L1
	GO:0003700~transcription factor activity	3,50	RELB, IRF1, BCL3, NFKB2, and STAT1
	GO:0030528~transcription regulator activity	2,71	IRAK1, RELB, IRF1, BCL3, NFKB2, and STAT1
EPS L	GO:0032813~tumor necrosis factor receptor superfamily binding	64,43	TNFSF10, RIPK1
	GO:0005125~cytokine activity	20,49	CSF3, TNFSF10, IL1B, and CCL5

[a]*Enrichment of functional terms is shown as a proportion. It represents the gene list input divided by all the genes annotated to the selected GO term.*

a zebra fish model and in an *in vitro* transwell model (unpublished data). The decreased level of IL-1B and IL12p35 in LPMCs isolated from CD biopsies and treated with either EPS, detected with Luminex (data not shown). IL-8 takes part in the neutrophil recruitment, while IL-1B and IL-12p35 are Th1 mediators that augment when Th1 cells are deregulated, therefore indicating a possible implication of physiological modulation of apoptosis in these T cells subpopulations. It is well-established that IBD pathogeneses determines Th1/Th2 imbalance toward Th1 (Neurath, 2014). Th1 proliferation is decontrolled because apoptosis regulation is imbalanced, increasing inflammation and chemotaxis in the gut. Hence, Th1 cells overproduce pro-inflammatory mediators like: TNF-α, IL1A, IL1B, IFN-γ etc. In turn TNF-α, that has a pivotal role in the mucosal inflammation, recruit, and over stimulate immune system cell like Th1.

Our data suggest that apoptosis intrinsic pathway mechanism (Stevens and Oltean, 2019), or in ameliorating gut barrier inflammation (Lu et al., 2020), could be re-established after *O*2-substituted-(1–3)-β-D-glucan administration, due to the fact that Bcl2 genes are overexpressed (**Figure 4**). According to that, Th1 proliferation could be regulated and therefore reducing proinflammatory cytokine production's (**Figures 1C, 2, 4E**).

As IBD is Th1 shifted pathology, and EPS P is able to ameliorate the rate of inflammation, it is plausible to postulate that it could play a role in Th1 through apoptosis modulation. Bioinformatic analysis revealed that many mediators of this pathway have been modulated by the treatment (**Table 3**), and we also observed a reduction of pro-inflammatory mediators (**Figures 1C, 2**). As the Th1 of CD patients cycles faster than the healthy controls (Sturm et al., 2004), it is fair to believe that Th1 could play a role in the re-establishment of Th1 population to a normal concentration, and therefore lowering inflammation rate.

Regarding EPS L, gene clustering showed a dual behavior, by the reduction of cell death ligands expression such as TNFSF10 and IL-1B, and over-expression of RIPK, a kinase involved in necroptosis and cell survival, by modulating dysregulated apoptosis in IEC (**Figure 3A**; Dannappel et al., 2014). Thus, the EPS treatments affect mechanisms that restore gut burrier homeostasis due to its wound healing properties and reduce inflammation mediators.

It is worth noting that the differential response of the tissues to EPS P and EPS L might be related to their structural differences. EPS P has a molecular mass of 9.6×10^6 Da, higher than that of EPS L (6.6×10^6 Da, Werning et al., 2014), that could increase the affinity of the natural *O*2-substituted-(1–3)-β-D-glucan (EPS P) affinity for its receptor(s). It has been shown that molecular mass and tertiary structure of β-glucans, play a critical role in receptor binding (Legentil et al., 2015). We have previously shown that EPS P increases adhesion of *P. parvulus* 2.6 to human enterocytes *in vitro* and increases *in vivo* the colonization capacity of the bacterial strain in the zebrafish gut (Pérez-Ramos et al., 2018). Therefore, it is tempting to assume that, after ingestion in a beverage, *P. parvulus* 2.6 could synthesize EPS P in the human intestine and the action of glycosidases synthesized by the microbiota could reduce its molecular mass generating an EPS L-like polymer with its detected dual role.

CONCLUSION

In an *ex vivo* model of CD biopsies, treatment with EPS P and EPS L are concomitant with decreased levels of pro-inflammatory cytokine IL-8 in the supernatant of tissue biopsies, and in relative gene expression. RNA array demonstrated that *O*2-substituted-(1–3)-β-D-glucans modulate the NFkB pathway, activating both the canonical and non-canonical pathway. The differences found in the expression profiling indicate that the 9.6×10^6 Da EPS P may be able to restore the apoptosis mechanism in Th1 cells, whereas the 6.6×10^6 Da EPS L might restore the intestinal barrier through activation of RIPK1 in IEC. Further studies have to be performed to determine which receptor is activated by EPS P and EPS L and, if a co-receptor is necessary for receptor recognition, and if EPS have different effects on immune system cells.

DATA AVAILABILITY STATEMENT

The original contributions presented in the study are included in the article/**Supplementary Material**, further inquiries can be directed to the corresponding authors.

ETHICS STATEMENT

The studies involving human participants were reviewed and approved by Comité Ético de Investigación Clínica, Hospital Vall d'Hebron, Barcelona. The patients/participants provided their written informed consent to participate in this study.

AUTHOR CONTRIBUTIONS

SN performed all the experiments described in this article, realized the statistical analysis, and wrote the manuscript. EV and AO helped with the *ex vivo* model during SN stay at Vall d'Hebron laboratory. IC realized the bioinformatic analysis and with the design of the Figures. MA supervised the *ex vivo* model and the RNA Array. FG reviewed the results of the manuscript. PL and AP masterminded the direction and conceptualization of the study, the interpretation of the data obtained, and the final version of the manuscript. All authors listed have read and approved the final version of the manuscript.

FUNDING

This work was supported by the Spanish Ministry of Science, Innovation, and Universities (grant RTI2018-097114-B-I00), by the Fondo de Investigación Sanitaria, grant number PI12/00263, and by CIBERehd.

ACKNOWLEDGMENTS

We thank Dr. Maria José Feito for her advice on the interpretation of the β-glucan immunological effect. We also thank Dr. Sara Ballester and Dr. Stephen Elson for critical reading of the manuscript. We acknowledge support of the publication fee by the CSIC Open Access Publication Support Initiative through its Unit of Information Resources for Research (URICI).

SUPPLEMENTARY MATERIAL

The Supplementary Material for this article can be found online at: https://www.frontiersin.org/articles/10.3389/fmicb.2021.621280/full#supplementary-material

REFERENCES

Ali, M. F., Driscoll, C. B., Walters, P. R., Limper, A. H., and Carmona, E. M. (2015). Beta-Glucan-activated human B lymphocytes participate in innate immune responses by releasing proinflammatory cytokines and stimulating neutrophil chemotaxis. *J. Immunol.* 195, 5318–5326. doi: 10.4049/jimmunol.1500559

Ballesteros Pomar, M. D., and Gonzalez Arnaiz, E. (2018). Role of prebiotics and probiotics in the functionality of the microbiota in the patients receiving enteral nutrition. *Nutr. Hosp.* 35, 18–26. doi: 10.20960/nh.1956

Basson, A. R., Lam, M., and Cominelli, F. (2017). Complementary and alternative medicine strategies for therapeutic gut microbiota modulation in inflammatory bowel disease and their next-generation approaches. *Gastroenterol. Clin. N. Am.* 46, 689–729. doi: 10.1016/j.gtc.2017.08.002

Bäuerl, C., Llopis, M., Antolín, M., Monedero, V., Mata, M., Zúñiga, M., et al. (2013). *Lactobacillus paracasei* and *Lactobacillus plantarum* strains downregulate proinflammatory genes in an ex vivo system of cultured human colonic mucosa. *Genes Nutr.* 8, 165–180. doi: 10.1007/s12263-012-0301-y

Biancheri, P., Di Sabatino, A., Rescigno, M., Giuffrida, P., Fornasa, G., Tsilingiri, K., et al. (2016). Abnormal thymic stromal lymphopoietin expression in the duodenal mucosa of patients with coeliac disease. *Gut* 65, 1670–1680. doi: 10.1136/gutjnl-2014-308876

Bodera, P. (2008). Influence of prebiotics on the human immune system (GALT). *Recent Pat. Inflamm. Allergy Drug Discov.* 2, 149–153. doi: 10.2174/187221308784543656

Borruel, N., Carol, M., Casellas, F., Antolín, M., de Lara, F., Espín, E., et al. (2002). Increased mucosal tumour necrosis factor α production in Crohn's disease can be downregulated *ex vivo* by probiotic bacteria. *Gut* 51, 659–664. doi: 10.1136/gut.51.5.659

Borruel, N., Casellas, F., Antoĺın, M. A., Llopis, M., Carol, M., Espíin, E., et al. (2003). Effects of nonpathogenic bacteria on cytokine secretion by human intestinal mucosa. *Am. J. Gastroenterol.* 98, 865–870. doi: 10.1111/j.1572-0241.2003.07384.x

Carol, M., Borruel, N., Antolin, M., Llopis, M., Casellas, F., Guarner, F., et al. (2006). Modulation of apoptosis in intestinal lymphocytes by a probiotic bacteria in Crohn's disease. *J. Leukoc. Biol.* 79, 917–922. doi: 10.1189/jlb.0405188

Chan, G. C., Chan, W. K., and Sze, D. M. (2009). The effects of beta-glucan on human immune and cancer cells. *J. Hematol. Oncol.* 2:25. doi: 10.1186/1756-8722-2-25

Chassaing, B., Aitken, J. D., Malleshappa, M., and Vijay-Kumar, M. (2014). Dextran sulfate sodium (DSS)-induced colitis in mice. *Curr. Protoc. Immunol.* 104, 15.25.11–15.25.14. doi: 10.1002/0471142735.im1525s104

Dannappel, M., Vlantis, K., Kumari, S., Polykratis, A., Kim, C., Wachsmuth, L., et al. (2014). RIPK1 maintains epithelial homeostasis by inhibiting apoptosis and necroptosis. *Nature* 513, 90–94. doi: 10.1038/nature13608

Devillé, C., Gharbi, M., Dandrifosse, G., and Peulen, O. (2007). Study on the effects of laminarin, a polysaccharide from seaweed, on gut characteristics. *J. Sci. Food Agric.* 87, 1717–1725. doi: 10.1002/jsfa.2901

Dueñas-Chasco, M., Rodríguez-Carvajal, M. A., Tejero-Mateo, P., Franco-Rodríguez, G., Espartero, J. L., Irastorza-Iribas, A., et al. (1997). Structural analysis of the exopolysaccharide produced by *Pediococcus damnosus* 2.6. *Carbohydr. Res.* 303, 453–458. doi: 10.1016/s0008-6215(97)00192-4

Fernández de Palencia, P., Werning, M. L., Sierra-Filardi, E., Dueñas-Chasco, M., Irastorza, A., Corbí, A. L., et al. (2009). Probiotic properties of the 2-substituted (1-3)-β-D-glucan-producing bacterium *Pediococcus parvulus* 2.6. *Appl. Environ. Microbiol.* 75, 4887–4891. doi: 10.1128/AEM.00394-09

Heim, G., Walsh, A. M., Sweeney, T., Doyle, D. N., O'Shea, C. J., Ryan, M. T., et al. (2014). Effect of seaweed-derived laminarin and fucoidan and zinc oxide on gut morphology, nutrient transporters, nutrient digestibility, growth performance and selected microbial populations in weaned pigs. *Br. J. Nutr.* 111, 1577–1585. doi: 10.1017/s0007114513004224

Hidalgo-Cantabrana, C., Sánchez, B., Álvarez-Martín, P., López, P., Martínez-Álvarez, N., Delley, M., et al. (2015). A single mutation in the gene responsible for the mucoid phenotype of *Bifidobacterium animalis* subsp. *lactis* confers surface and functional characteristics. *Appl. Environ. Microbiol.* 81, 7960–7968. doi: 10.1128/AEM.02095-15.

Huang, D. W., Sherman, B. T., and Lempicki, R. A. (2008). Systematic and integrative analysis of large gene lists using DAVID bioinformatics resources. *Nat. Protoc.* 4, 44–57. doi: 10.1038/nprot.2008.211

Iweala, O. I., and Nagler, C. R. (2019). The microbiome and food allergy. *Annu. Rev. Immunol.* 37, 377–403. doi: 10.1146/annurev-immunol-042718-041621

Jin, Y., Li, P., and Wang, F. (2018). Beta-glucans as potential immunoadjuvants: a review on the adjuvanticity, structure-activity relationship and receptor recognition properties. *Vaccine* 36, 5235–5244. doi: 10.1016/j.vaccine.2018.07.038

Jobin, C., and Sartor, R. B. (2000). The IκB/NF-κB system: a key determinant of mucosal inflammation and protection. *Am. J. Phys. Cell Phys.* 278, C451–C462. doi: 10.1152/ajpcell.2000.278.3.C451

Kamada, N., Seo, S. U., Chen, G. Y., and Nunez, G. (2013). Role of the gut microbiota in immunity and inflammatory disease. *Nat. Rev. Immunol.* 13, 321–335. doi: 10.1038/nri3430

Kanehisa, M., Goto, S., Sato, Y., Kawashima, M., Furumichi, M., and Tanabe, M. (2014). Data, information, knowledge and principle: back to metabolism in KEGG. *Nucleic Acids Res.* 42, D199–D205. doi: 10.1093/nar/gkt1076

Kau, A. L., Ahern, P. P., Griffin, N. W., Goodman, A. L., and Gordon, J. I. (2011). Human nutrition, the gut microbiome and the immune system. *Nature* 474, 327–336. doi: 10.1038/nature10213

Knights, D., Lassen, K., and Xavier, R. (2013). Advances in inflammatory bowel disease pathogenesis: linking host genetics and the microbiome. *Gut* 62, 1505–1510. doi: 10.1136/gutjnl-2012-303954

Latorre, E., Layunta, E., Grasa, L., Pardo, J., García, S., Alcalde, A. I., et al. (2018). Toll-like receptors 2 and 4 modulate intestinal IL-10 differently in ileum and colon. *United European Gastroenterol J* 6, 446–453. doi: 10.1177/2050640617727180

Lawrence, T. (2009). The nuclear factor NF-kappaB pathway in inflammation. *Cold Spring Harb. Perspect. Biol.* 1:a001651. doi: 10.1101/cshperspect.a001651

Legentil, L., Paris, F., Ballet, C., Trouvelot, S., Daire, X., Vetvicka, V., et al. (2015). Molecular interactions of beta-(1-->3)-glucans with their receptors. *Molecules* 20, 9745–9766. doi: 10.3390/molecules20069745

Li, X., Luo, H., Ye, Y., Chen, X., Zou, Y., Duan, J., et al. (2019). Betaglucan, a dectin1 ligand, promotes macrophage M1 polarization via NFkappaB/autophagy pathway. *Int. J. Oncol.* 54, 271–282. doi: 10.3892/ijo.2018.4630

Llamas-Arriba, M. G., Hernández-Alcántara, A. M., Yépez, A., Aznar, R., Dueñas, M. T., and López, P. (2019). "12—functional and nutritious beverages produced by lactic acid bacteria" in *Nutrients in beverages*. eds. A. M. Grumezescu and A. M. Holban (Duxford: Academic Press), 419–465.

Llopis, M., Antolin, M., Carol, M., Borruel, N., Casellas, F., Martinez, C., et al. (2009). *Lactobacillus casei* downregulates commensals' inflammatory signals in Crohn's disease mucosa. *Inflamm. Bowel Dis.* 15, 275–283. doi: 10.1002/ibd.20736

Lu, H., Li, H., Fan, C., Qi, Q., Yan, Y., Wu, Y., et al. (2020). RIPK1 inhibitor ameliorates colitis by directly maintaining intestinal barrier homeostasis and regulating following IECs-immuno crosstalk. *Biochem. Pharmacol.* 172:113751. doi: 10.1016/j.bcp.2019.113751

Mohammed Vashist, N., Samaan, M., Mosli, M. H., Parker, C. E., MacDonald, J. K., Nelson, S. A., et al. (2018). Endoscopic scoring indices for evaluation of disease activity in ulcerative colitis. *Cochrane Database Syst. Rev.* 1:Cd011450. doi: 10.1002/14651858.CD011450.pub2

Morhardt, T. L., Hayashi, A., Ochi, T., Quirós, M., Kitamoto, S., Nagao-Kitamoto, H., et al. (2019). IL-10 produced by macrophages regulates epithelial integrity in the small intestine. *Sci. Rep.* 9:1223. doi: 10.1038/s41598-018-38125-x

Nácher-Vázquez, M., Ballesteros, N., Canales, A., Rodríguez Saint-Jean, S., Pérez-Prieto, S. I., Prieto, A., et al. (2015). Dextrans produced by lactic acid bacteria exhibit antiviral and immunomodulatory activity against salmonid viruses. *Carbohydr. Polym.* 124, 292–301. doi: 10.1016/j.carbpol.2015.02.020

Neurath, M. F. (2014). Cytokines in inflammatory bowel disease. *Nat. Rev. Immunol.* 14, 329–342. doi: 10.1038/nri3661

Notarargo, S., de Las Casas-Engel, M., Fernández de Palencia, P., Corbí, A. L., and López, P. (2014). Immunomodulation of human macrophages and myeloid cells by 2-substituted (1-3)-beta-D-glucan from *P. parvulus* 2.6. *Carbohydr. Polym.* 112, 109–113. doi: 10.1016/j.carbpol.2014.05.073

Notarargo, S., Nácher-Vázquez, M., Ibarburu, I., Werning, M. L., Fernández de Palencia, P., Dueñas, M. T., et al. (2013). Comparative analysis of production and purification of homo- and hetero-polysaccharides produced by lactic acid bacteria. *Carbohydr. Polym.* 93, 57–64. doi: 10.1016/j.carbpol.2012.05.016

Oka, A., and Sartor, R. B. (2020). Microbial-based and microbial-targeted therapies for inflammatory bowel diseases. *Dig. Dis. Sci.* 65, 757–788. doi: 10.1007/s10620-020-06090-z

Orel, R., and Kamhi Trop, T. (2014). Intestinal microbiota, probiotics and prebiotics in inflammatory bowel disease. *World J. Gastroenterol.* 20, 11505–11524. doi: 10.3748/wjg.v20.i33.11505

Park, J. H., Jeong, D. Y., Peyrin-Biroulet, L., Eisenhut, M., and Shin, J. I. (2017). Insight into the role of TSLP in inflammatory bowel diseases. *Autoimmun. Rev.* 16, 55–63. doi: 10.1016/j.autrev.2016.09.014

Pérez-Ramos, A., Mohedano, M. L., López, P., Spano, G., Fiocco, D., Russo, P., et al. (2017). In situ β-Glucan fortification of cereal-based matrices by *Pediococcus parvulus* 2.6: technological aspects and prebiotic potential. *Int. J. Mol. Sci.* 18:1588. doi: 10.3390/ijms18071588

Pérez-Ramos, A., Mohedano, M. L., Pardo, M. Á., and López, P. (2018). β-Glucan-producing *Pediococcus parvulus* 2.6: test of probiotic and immunomodulatory properties in zebrafish models. *Front. Microbiol.* 9:1684. doi: 10.3389/fmicb.2018.01684

Rattigan, R., O'Doherty, J. V., Vigors, S., Ryan, M. T., Sebastiano, R. S., Callanan, J. J., et al. (2020). The effects of the marine-derived polysaccharides laminarin and chitosan on aspects of colonic health in pigs challenged with dextran sodium sulphate. *Mar. Drugs* 18:262. doi: 10.3390/md18050262

Russo, P., López, P., Capozzi, V., Fernández de Palencia, P., Dueñas, M. A. T., Spano, G., et al. (2011). Beta-glucans improve growth, viability and colonization of probiotic microorganisms. *Int. J. Mol. Sci.* 13, 6026–6039. doi: 10.3390/ijms13056026

Schmid, J., Sieber, V., and Rehm, B. (2015). Bacterial exopolysaccharides: biosynthesis pathways and engineering strategies. *Front. Microbiol.* 6:496. doi: 10.3389/fmicb.2015.00496

Seeger, P., Bosisio, D., Parolini, S., Badolato, R., Gismondi, A., Santoni, A., et al. (2014). Activin A as a mediator of NK–dendritic cell functional interactions. *J. Immunol.* 192, 1241–1248. doi: 10.4049/jimmunol.1301487

Shouval, D. S., Ouahed, J., Biswas, A., Goettel, J. A., Horwitz, B. H., Klein, C., et al. (2014). Interleukin 10 receptor signaling: master regulator of intestinal mucosal homeostasis in mice and humans. *Adv. Immunol.* 122, 177–210. doi: 10.1016/B978-0-12-800267-4.00005-5

Smith, A. J., Graves, B., Child, R., Rice, P. J., Ma, Z., Lowman, D. W., et al. (2018). Immunoregulatory activity of the natural product laminarin varies widely as a result of its physical properties. *J. Immunol.* 200, 788–799. doi: 10.4049/jimmunol.1701258

Stevens, M., and Oltean, S. (2019). Modulation of the apoptosis gene Bcl-x function through alternative splicing. *Front. Genet.* 10:804. doi: 10.3389/fgene.2019.00804

Strain, C. R., Collins, K. C., Naughton, V., McSorley, E. M., Stanton, C., Smyth, T. J., et al. (2020). Effects of a polysaccharide-rich extract derived from Irish-sourced *Laminaria digitata* on the composition and metabolic activity of the human gut microbiota using an in vitro colonic model. *Eur. J. Nutr.* 59, 309–325. doi: 10.1007/s00394-019-01909-6

Sturm, A., Leite, A. Z., Danese, S., Krivacic, K. A., West, G. A., Mohr, S., et al. (2004). Divergent cell cycle kinetics underlie the distinct functional capacity of mucosal T cells in Crohn's disease and ulcerative colitis. *Gut* 53, 1624–1631. doi: 10.1136/gut.2003.033613

Tahaghoghi-Hajghorbani, S., Ajami, A., Ghorbanalipoor, S., Hosseini-Khah, Z., Taghiloo, S., Khaje-Enayati, P., et al. (2019). Protective effect of TSLP and IL-33 cytokines in ulcerative colitis. *Auto Immun. Highlights* 10:1. doi: 10.1186/s13317-019-0110-z

Thompson, I. J., Oyston, P. C., and Williamson, D. E. (2010). Potential of the β-glucans to enhance innate resistance to biological agents. *Expert Rev. Anti-Infect. Ther.* 8, 339–352. doi: 10.1586/eri.10.10

Tsai, Y. L., Lin, T. L., Chang, C. J., Wu, T. R., Lai, W. F., Lu, C. C., et al. (2019). Probiotics, prebiotics and amelioration of diseases. *J. Biomed. Sci.* 26:3. doi: 10.1186/s12929-018-0493-6

Volman, J. J., Mensink, R. P., Ramakers, J. D., de Winther, M. P., Carlsen, H., Blomhoff, R., et al. (2010). Dietary (1-->3), (1-->4)-beta-D-glucans from oat activate nuclear factor-kappaB in intestinal leukocytes and enterocytes from mice. *Nutr. Res.* 30, 40–48. doi: 10.1016/j.nutres.2009.10.023

Walana, W., Ye, Y., Li, M., Wang, J., Wang, B., Cheng, J. -W., et al. (2018). IL-8 antagonist, CXCL8(3-72)K11R/G31P coupled with probiotic exhibit variably enhanced therapeutic potential in ameliorating ulcerative colitis. *Biomed. Pharmacother.* 103, 253–261. doi: 10.1016/j.biopha.2018.04.008

Walsh, A. M., Sweeney, T., O'Shea, C. J., Doyle, N. D., and O'Doherty, J. V. (2015). Effects of supplementing dietary laminarin and fucoidan on intestinal morphology and the immune gene expression in the weaned pig. *J. Anim. Sci.* 90, 284–286. doi: 10.2527/jas.53949

Werning, M. L., Corrales, M. A., Prieto, A., Fernández de Palencia, P., Navas, J., and López, P. (2008). Heterologous expression of a position 2-substituted (1-3)-β-D-glucan in *Lactococcus lactis*. *Appl. Environ. Microbiol.* 74, 5259–5262. doi: 10.1128/AEM.00463-08

Werning, M. L., Ibarburu, I., Dueñas, M. T., Irastorza, A., Navas, J., and López, P. (2006). *Pediococcus parvulus* gtf gene encoding the GTF

glycosyltransferase and its application for specific PCR detection o fβ-D-glucan-producing bacteria in foods and beverages. *J. Food Prot.* 69, 161–169. doi: 10.4315/0362-028x-69.1.161

Werning, M. L., Notararigo, S., Nácher, M., Fernández de Palencia, P., Aznar, R., and López, P. (2012). "Biosynthesis, purification and biotechnological use of exopolysaccharides produced by lactic acid bacteria" in *Food additive*. ed. Y. El-Samragy (London: Intechopen).

Werning, M. L., Pérez-Rámos, A., Fernández de Palencia, P., Mohedano, M. L., Dueñas, M. T., Prieto, A., et al. (2014). A specific immunological method to detect and quantify bacterial 2-substituted (1,3)-beta-D-glucan. *Carbohydr. Polym.* 113, 39–45. doi: 10.1016/j.carbpol.2014.06.072

Xie, J., Guo, L., Ruan, Y., Zhu, H., Wang, L., Zhou, L., et al. (2010). Laminarin-mediated targeting to Dectin-1 enhances antigen-specific immune responses. *Biochem. Biophys. Res. Commun.* 391, 958–692. doi: 10.1016/j.bbrc.2009.11.173

Zarour, K., Prieto, A., Pérez-Ramos, A., Kihal, M., and López, P. (2018). Analysis of technological and probiotic properties of Algerian *L. mesenteroides* strains isolated from dairy and non-dairy products. *J. Funct. Foods* 49, 351–361. doi: 10.1016/j.jff.2018.09.001

Zhang, H., Sparks, J. B., Karyala, S. V., Settlage, R., and Luo, X. M. (2015). Host adaptive immunity alters gut microbiota. *ISME J.* 9, 770–781. doi: 10.1038/ismej.2014.165

Conflict of Interest: The authors declare that the research was conducted in the absence of any commercial or financial relationships that could be construed as a potential conflict of interest.

frontiers in Microbiology

REVIEW
published: 03 March 2021
doi: 10.3389/fmicb.2021.655705

Probiotic Effector Compounds: Current Knowledge and Future Perspectives

*Eric Banan-Mwine Daliri, Fred Kwame Ofosu, Chen Xiuqin, Ramachandran Chelliah and Deog-Hwan Oh**

Department of Food Science and Biotechnology, College of Agriculture and Life Science, Kangwon National University, Chuncheon, South Korea

Understanding the mechanism behind probiotic action will enable a rational selection of probiotics, increase the chances of success in clinical studies and make it easy to substantiate health claims. However, most probiotic studies over the years have rather focused on the effects of probiotics in health and disease, whereas little is known about the specific molecules that trigger effects in hosts. This makes it difficult to describe the detailed mechanism by which a given probiotic functions. Probiotics communicate with their hosts through molecular signaling. Meanwhile, since the molecules produced by probiotics under *in vitro* conditions may differ from those produced *in vivo*, *in vitro* mechanistic studies would have to be conducted under conditions that mimic gastrointestinal conditions as much as possible. The ideal situation would, however, be to carry out well-designed clinical trials in humans (or the target animal) using adequate quantities of the suspected probiotic molecule(s) or adequate quantities of isogenic knock-out or knock-in probiotic mutants. In this review, we discuss our current knowledge about probiotic bacteria and yeast molecules that are involved in molecular signaling with the host. We also discuss the challenges and future perspectives in the search for probiotic effector molecules.

Keywords: microbiota, gut barrier functions, immune system, cholesterol reduction, nervous system

OPEN ACCESS

Edited by:
Konstantinos Papadimitriou, University of Peloponnese, Greece

Reviewed by:
Julio Plaza-Diaz, Children's Hospital of Eastern Ontario (CHEO), Canada
Daniela Fiocco, University of Foggia, Italy

****Correspondence:***
Deog-Hwan Oh
deoghwa@kangwon.ac.kr

Specialty section:
This article was submitted to Food Microbiology, a section of the journal Frontiers in Microbiology

Received: *19 January 2021*
Accepted: *12 February 2021*
Published: *03 March 2021*

Citation:
Daliri EB-M, Ofosu FK, Xiuqin C, Chelliah R and Oh D-H (2021) Probiotic Effector Compounds: Current Knowledge and Future Perspectives. Front. Microbiol. 12:655705. doi: 10.3389/fmicb.2021.655705

INTRODUCTION

Probiotics are live microorganisms which when administered in adequate quantities provide a beneficial effect to the host (Hill et al., 2014). Over the years, many randomized clinical studies have reported the health benefits of probiotic consumption (Chugh et al., 2020; Tao et al., 2020; Tenorio-Jiménez et al., 2020), yet monitoring targeted health benefits of administered probiotic have rather been difficult to establish. This is because it would require an understanding of the possible metabolic activities of the administered probiotic that distinguishes it from the indigenous microbes in the host that could be eliciting similar effects. The limited knowledge about the mechanisms of probiotic action makes it challenging to rationally select probiotic strains for targeted interventions and also makes reproducibility of results difficult. Meanwhile, a number of mechanisms have been proposed to explain the mode of action behind the health effects of probiotics, such as enhancing gut epithelia barrier functions (Liu et al., 2016),

modulating the immune system (Milajerdi et al., 2020; Zhao et al., 2020), modulating the gut microbiota (Botelho et al., 2020; López-Moreno et al., 2020), modulating systemic metabolic responses (van Baarlen et al., 2011; Belguesmia et al., 2016), and signaling host central nervous system (Kong et al., 2020; **Figure 1**). Since probiotic and host cell interactions are mediated by effector molecules, we discuss our current knowledge on probiotic bioactive molecules that have impact on the host in this review. We also discuss the challenges and future perspectives in the search for probiotic effector molecules.

PROBIOTIC EFFECTOR MOLECULES THAT AFFECT GUT BARRIER FUNCTIONS

Current scientific evidence show that a disruption of gut epithelial barrier function is important in the pathogenesis of many diseases such as inflammatory bowel disease (IBD; Lee et al., 2018; Soroosh et al., 2019), irritable bowel syndrome (Lee et al., 2020), diabetes (De Kort et al., 2011), and several other diseases. Gut barrier integrity is maintained by tight junction proteins, such as claudins, Zona occludin-1, and occludin, and their levels are significantly reduced during some disease conditions (Lee et al., 2020). This makes the gut epithelium permeable to microbial ligands and harmful metabolites leading to systemic inflammatory responses (Singh et al., 2019). The ability of probiotic effector molecules to protect gut barrier functions has long been reported (Miyauchi et al., 2009; Karczewski et al., 2010; Laval et al., 2015; Martín et al., 2019). Some of the molecules are soluble and therefore are secreted by the bacteria (or fungi) while others are cell wall bound (Delgado et al., 2020). *Lactobacillus rhamnosus* GG has been shown to secrete protein p40, which stimulates ADAM17 activation and heparin binding-epidermal growth factor (HB-EGF) release. This results in EGF receptor transactivation, apoptosis prevention, and intestinal epithelial function preservation (Yan et al., 2013). Another soluble protein, p75 secreted by both *L. rhamnosus* and *L. casei* is known to stimulate EGF receptor activation to prevent apoptosis in intestinal epithelial cells (Bäuerl et al., 2010). More recently, *L. rhamnosus* GG was shown to secrete protein HM0539, which protects gut barrier functions by promoting the expression of tight junction protein Zona occludin-1 and occluding. The protein also stimulates mucin secretion in intestinal cells (Gao et al., 2019). Meanwhile, the exact molecular mechanism by which HM0539 protects intestinal cells from injury remains to be established. Previous studies have shown that the soluble protein known as TcpC protein produced by *Escherichia coli* Nissle 1917 can induce protein kinase C-ζ and extracellular-signal-regulated kinase 1/2 phosphorylation to increase the formation of claudin-14, and this could account for the use of the probiotic for gastrointestinal therapy (Hering et al., 2014). *Escherichia coli* Nissle 1917 also produces 3-hydroxyoctadecanoic acid, which antagonizes peroxisome proliferator activated receptor gamma (PPARγ) to reduce inflammation (Pujo et al., 2020). In addition, probiotics and several other lactic acid bacteria are known to produce conjugated linoleic acid (CLA; Wang et al., 2016), which can upregulate the transcription of E-cadherin 1, claudin-3, ZO-1, and occludin in the gut to protect gut barrier functions (Murphy et al., 2007; Chen et al., 2019). Probiotic CLA can increase the expression

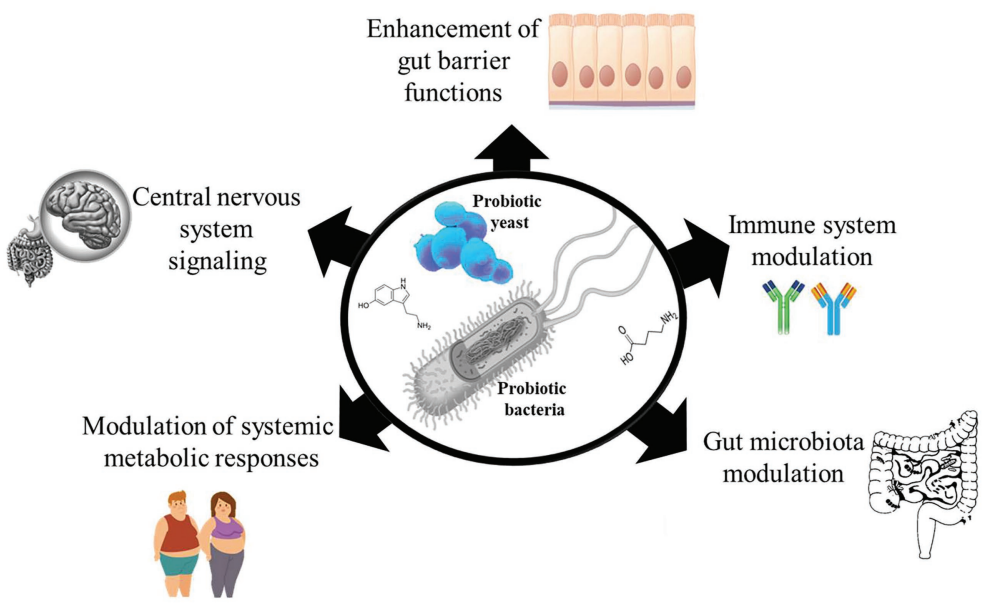

FIGURE 1 | Probiotic bacteria and yeast possess and produce many effector molecules that interact with the host to elicit their observed effects. The effector molecules can affect host gut epithelial barrier functions, modulate host immune system, modulate the host's gut microbiota, modulate the host's metabolic responses, and affect the host's central nervous system.

of catalase, superoxide dismutase, and glutathione peroxidase, which reduce oxidative stress in colonocytes (Qi et al., 2018; Chen et al., 2019). More so, CLA increases the expression and activity of PPARγ in the gut to inhibit inflammation (Hontecillas et al., 2002). Some structural components, such as pili, of many probiotic bacteria have been shown to play important roles in gut epithelial functions. For instance, the tight adhesion pili of *Bifidobacterium breve* UCC2003 have been reported to stimulate the proliferation of gut epithelial cells by producing a TadE pseudopilin (O'Connell Motherway et al., 2019). Also, *L. plantarum* CGMCC 1258 micro integral membrane protein (MIMP) was found to promote the expression of tight junction proteins, such as JAM-1, claudin-1, and occludin, during tight junctional injury (Yin et al., 2018). Meanwhile, the exact mechanism by which MIMPs promotes the upregulation of tight junction proteins remain unestablished.

PROBIOTIC EFFECTOR MOLECULES THAT STIMULATE THE IMMUNE SYSTEM

Many studies have reported the ability of the probiotics to contribute to the maturation of the immune system. It has however been shown that lipopolysaccharide of Gram negative probiotics are responsible for their strong induction of IL-10 in peripheral blood mononuclear cells (Kandasamy et al., 2017). The IL-10 produced contributes to the induction of IgA antibodies at mucosal sites by enhancing isotypic commutation (Cerutti and Rescigno, 2008), and this may account for why Gram negative probiotics induce a stronger antibody response than Gram positive probiotics. This was demonstrated when *E. coli* Nissle 1917 colonized pigs showed a higher gut IgA response relative to *L. rhamnosus* GG colonization (Kandasamy et al., 2016). The anti-inflammatory ability of *L. plantarum* in acute colitis mice (Emília et al., 2018) has at least in part been attributed to the presence of a small domain of the surface layer protein of the bacterium. These surface layer proteins have been shown to bind to a mannose receptor in gut epithelial cells to prevent p38 MAPK phosphorylation by inhibiting the Toll-like receptor (TLR) 5 pathway (Liu et al., 2012) during inflammatory conditions. This suppresses the expression of inflammatory cytokines (IFN-γ, IL-17, and IL-23) and upregulates IL-4 and IL-10 production in the cells (Yin et al., 2018). Another study has shown that sortase-dependent protein on the cell surface of *L. plantarum* can actively attenuate the NF-kB pathway thereby suppressing inflammation (Marco et al., 2010; Remus, 2012). It is known that different immune-stimulating probiotic strains may however have different cell wall molecules that interact with host immune receptors (Bron et al., 2013; Lee et al., 2013). For instance, the immune stimulating ability of *L. plantarum* K8 has been partly attributed to the lipotechoic acid (LTA) in its cell wall, which is able to regulate mitogen-activated protein kinase phosphorylation and nuclear factor activation and causes a reduction in IL-8 production in injured intestinal cells (Kim et al., 2017). Meanwhile, LTA from *L. rhamnosus* GG, *L. sakei*, and *L. delbrueckii* did not stimulate IL-8 production under similar conditions (Kim et al., 2017). In probiotic yeast, *Saccharomyces cerevisiae* cell wall contains β-glucans, which may induce monocyte reprograming *via* a dectin-1/Raf-1 pathway to enhance cytokine production for protection against *Candida albicans* infection (Quintin et al., 2012). Similarly, *S. cerevisiae* chitin has been shown to increase host immune system resistance to *C. albicans* infection by modulating the production of pro- and anti-inflammatory cytokines (Rizzetto et al., 2016). Even the spores of *S. cerevisiae* contain high amounts of chitin that can trigger inflammatory IL-17 responses in hosts (Rizzetto et al., 2010).

PROBIOTIC EFFECTOR MOLECULES THAT MODULATE HOST CENTRAL NERVOUS SYSTEM

Studies over the years have shown evidence (though mostly indirect) that there is a strong communication between the gut microbiota and the central nervous system and it is mediated by the vagal nerve (Cryan and Dinan, 2012). For this reason, the effects of probiotics on the central nervous system have been studied extensively. However, only several studies have studied the molecular mechanisms by which probiotics affect the central nervous system. Many probiotic bacteria including *L. plantarum*, *L. brevis*, *L. rhamnosus*, and *Bifidobacterium bifidum* have been shown to produce significant amounts of gamma-aminobutyric acid (GABA) *in vitro* (Li et al., 2011; Diez-Gutiérrez et al., 2020). It is known that GABA in circulation may act as an autocrine, local paracrine, or gastrointestinal hormone that exerts both stimulatory and inhibitory effects over enteric neuronal activity depending on the type of GABA receptor stimulated (Hardcastle et al., 1991). Interestingly, Koussoulas et al. (2018) have shown that exogenous GABA can bind to $GABA_A$, $GABA_B$, and $GABA_c$ receptors to induce calcium $[Ca^{2+}]_i$ release by myenteric ganglia. Since glial Ca^{2+} signaling is a mechanism for integration within glial symplasm and between glial-neuronal circuits (Verkhratsky, 2006), it stands to reason that GABA produced by probiotics could be an effector molecule by which certain probiotics interact with host central nervous system. This could therefore account for the ability of *L. rhamnosus* JB-1 to alter stress-related disorders *via* the vagus nerves (Bravo et al., 2011). Other studies have shown that *L. helveticus* 100ash, *L. helveticus* NK-1, *L. casei* $K3III_{24}$, and *L. delbrueckii* subsp. *bulgaricus* produce significant amounts of GABA, L-3,4-dihydroxyphenylalanine (L-DOPA), dopamine, dihydroxyphenylacetic acid (DOPAC), homovanillic acid (HVA), and serotonin (**Figure 2**) when cultured in milk-containing media (Oleskin et al., 2014). L-DOPA can be transported from the gut through the blood to the brain, where it is converted to dopamine, a neurotransmitter (Disdier and Stonestreet, 2019). Dopamine can be metabolized into DOPAC, which can be degraded to HVA. In the central nervous system, serotonin plays a role in regulating emotions, sleep, and stress (De Deurwaerdère and Di Giovanni, 2020) by influencing the hypothalamic-pituitary-adrenal axis. Though it is likely that probiotics that produce these biogenic amines may have central nervous system modulatory effects, the effector

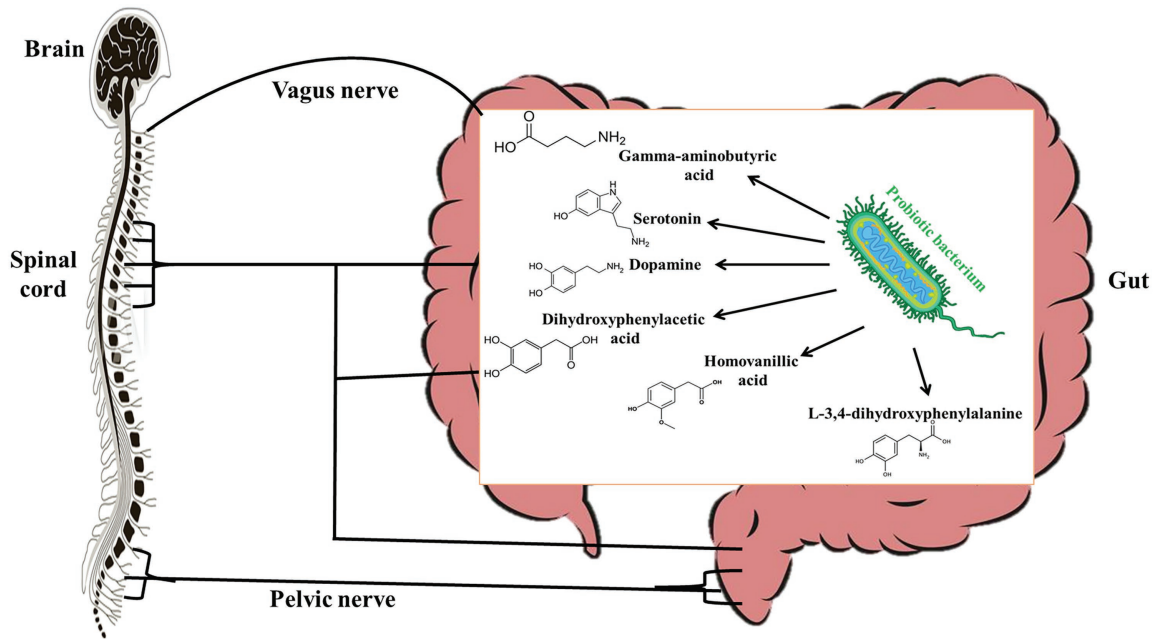

FIGURE 2 | Probiotic bacteria produce gamma-aminobutyric acid (GABA), serotonine, dopamine, L-3,4-dihydroxyphenylalanine (L-DOPA), dihydroxyphenylacetic acid (DOPAC), and homovanillic acid (HVA) that modulate the host central nervous system.

molecules would have to be produced in adequate quantities in the gut of the host to elicit the desired effects. Although some studies have suggested that probiotics may improve diseases associated with the central nervous system by enhancing the production of free tryptophan, which may promote serotonin availability (since serotonin is synthesized from tryptophan; Desbonnet et al., 2008), it is not known whether probiotic tryptophan is used for serotonin synthesis (Daliri et al., 2016).

PROBIOTIC EFFECTOR MOLECULES THAT MODULATE HOST MICROBIOTA

The human body is made of mammalian cells, archaea (Kim et al., 2020), bacteria, viruses, and fungi co-existing in a symbiotic relationship (Daliri et al., 2020). Although host microbes could vary from one person to another (Brooks et al., 2018), recent studies have shown that all these microorganisms in the human body could have impacts on host health and disease (Daliri et al., 2018; Reitmeier et al., 2020) and that probiotic consumption can significantly modulate the host microbiome (Alcon-Giner et al., 2020). In fact, probiotics in food can survive, adapt, and become an established part of the gut microbiome (Pasolli et al., 2020) and have significant influence on the gut microbiome. The mechanisms by which probiotics modulate host microbiome include their effects on the function and composition of the host commensal bacteria and yeast. It is known that probiotics can produce antimicrobial compounds that suppress (O'Shea et al., 2012) or promote (Chen et al., 2019) the growth of certain microorganisms in the gut as shown in **Figure 3**. *Lactococcus lactis* for instance produces nisin (a bacteriocin), which can permeate the cell membrane of pathogenic Gram positive-bacteria and bind to Lipid II to inhibit cell wall synthesis (Wiedemann et al., 2001; Breukink and de Kruijff, 2006). Other probiotics such as *Pediococcus acidilactici* produce pediocine-like bacteriocins, which can bind to mannose phosphotransferase on the cytoplasmic membrane of pathogenic bacteria and penetrate the lipid bilayer resulting in pore formation in the cell (Balandin et al., 2019). This compromise in the cell wall integrity makes the cell extremely vulnerable to the harsh environmental conditions within which the cell is found and can lead to death. Similarly, Plantaricin LPL-1 produced by *L. plantarum* LPL-1 binds to a receptor on *Listeria monocytogenes* cell wall, perforate the cell membrane through hydrophobic interactions, and accumulate in the cell membrane by electrostatic interactions. The perforation results in ion leakage and loss of proton motive force, which eventually result in cell death (Wang et al., 2019b). Plantaricins do not only inactivate Gram-positive bacteria, but also Gram-negative bacteria (Zhang et al., 2013; Yang et al., 2019). Wang et al. (2020) showed that Plantaricin BM-1 can inhibit *E. coli* by acting on the surface of the cell wall to cause cell rapture. The bacteriocin could also permeate and interact with the cell membrane to lead to cell death. A popular probiotic, *Lactobacillus reuteri*, is known to produce reuterin, which suppresses the expression of *Clostridioides difficile* exotoxins TcdA and TcdB by inducing reactive oxygen species shifts in carbon metabolism, which may alter gene expression in the pathogen (Engevik et al., 2020). The impaired metabolism of the pathogens decreases their ability to compete for nutrients

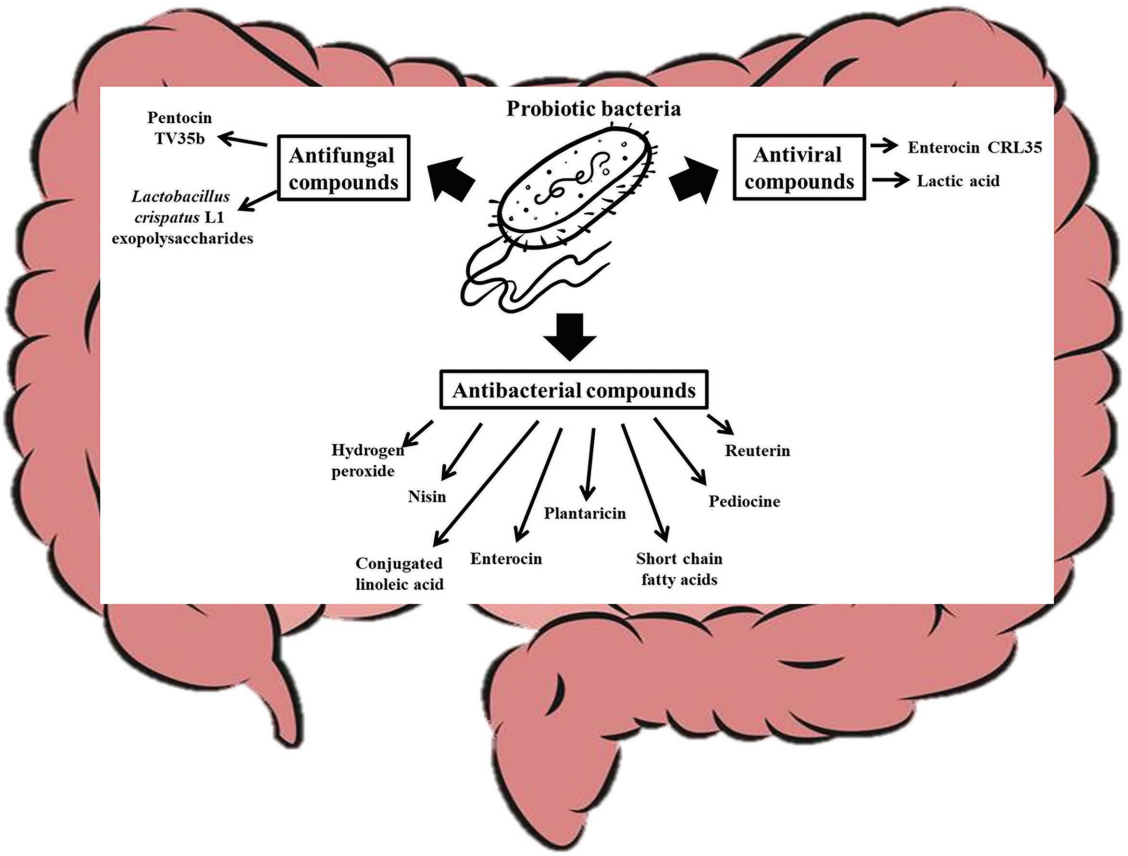

FIGURE 3 | Probiotic bacteria modulate the gut microbiota by producing antifungal, antiviral, and antibacterial compounds that affect the overall gut microbial structure of the host.

and eventually result in cell death (Engevik et al., 2020). Certain bacteriocins can inhibit viruses and yeast growth. For instance, it has been shown that Enterocin CRL35 from *Enterococcus faecium* CRL35 can bind and block the late stages of herpes simplex virus types (HSV) 1 and 2 replication (Wachsman et al., 1999, 2003) while Pentocin TV35b produced by *Lactobacillus pentosus* TV35b can inhibit the survival of *C. albicans* (an opportunistic fungus; Okkers et al., 1999). Exopolysaccharides produced by *Lactobacillus crispatus* L1 also reduces *C. albicans* adhesion to epithelial cells (Donnarumma et al., 2014) thereby decreasing their tendency to invade host cells. *Lactobacillus acidophilus* La-5 produces CLA (Macouzet et al., 2009), which can repress virulence genes such as *eaeA* (an enterohaemorrhagic *E. coli* invasion lipoprotein gene) and *invH* (a *Staphylococcus typhimirium* invasion lipoprotein gene) thereby reducing the ability of these pathogens to attach to the host cells (Peng et al., 2018). Also, probiotic CLA can competitively bind to INT-407 cell surface receptor-like molecules preventing enteric pathogens from binding to the gut (Peng et al., 2018). Consumption of probiotic CLA favored an increase in the levels of *Bifidobacterium* and *Odoribacter* while reducing the levels of Bacteroides in the gut (Chen et al., 2019) through an unidentified mechanism. Other probiotics, such as *L. brevis* CD2, *L. salivarius* FV2, and *L. plantarum* FV9, produce lactic acid which impair Herpes simplex virus 2 (HSV-2) protein synthesis and viral replication (Conti et al., 2009), while bacteria including *L. paracasei* inhibit vesicular stomatitis virus by direct binding with them (Botić et al., 2007). Bacteria with strong mucosal binding abilities, such as *L. brevis*, CD2 compete with HSV-2 for binding sites thereby preventing the fusion of viral envelope with host cell surface (Conti et al., 2009). Short chain fatty acids (SCFAs), such as butyric acid, produced by probiotics can induce gut epithelia secretion of cathelicidin peptides, which inactivate pathogens such as *Shigella* (Schauber et al., 2003; Raqib et al., 2006; Termén et al., 2008; Campbell et al., 2012). Some probiotics, including *B. bifidum* (Kawasaki et al., 2009) and *Lactobacillus johnsonii* (Pridmore et al., 2008), are known to produce hydrogen peroxide, which can react with O_2^- and/or iron in pathogenic cells to form toxic hydroxyl radicals which results in cell death (Clifford and Repine, 1982). A probiotic *S. cerevisiae* isolated from Koumiss has been shown to inhibit *E. coli* by producing citric acid and propionic acid, which disintegrate the cell membrane and increase cell permeability (Chen et al., 2017). Certain *S. cerevisiae* strains have been shown to produce killer toxin KHS which inhibits the growth of pathogenic bacteria and yeast (Goto et al., 1991;

Younis et al., 2017). These killer toxins inhibit β-glucan synthesis in the cell walls (Muccilli et al., 2013), inhibit DNA synthesis (Klassen and Meinhardt, 2005), cleaves tRNA (Klassen et al., 2008), blocks calcium ion uptake (Brown, 2011), and cause ion leakage from the cytoplasm (Santos et al., 2007) of sensitive cells. Another study showed that chitin from *S. cerevisiae* can train host immune system to kill *S. aureus*, *E. coli*, and *C. albicans* (Rizzetto et al., 2016), and this shows how yeast molecules can play critical roles in gut microbiota modulation. Many pathogenic bacteria target glycosaminoglycans for attachment and infection of the host (Kawai et al., 2018). Quite recently, it has been shown that probiotics, such as *Enterococcus faecium*, H57 prevent pathogen adhesion to the gut by degrading GAG (which are major component of extracellular matrix in animals) using KduI and KduD enzymes (Kawai et al., 2018). The probiotic molecules discussed in this section could at least contribute to the gut modulatory ability of probiotic yeast (Adel et al., 2017; Villar-García et al., 2017) and bacteria (Kong et al., 2019; Liu et al., 2020).

PROBIOTIC EFFECTOR MOLECULES THAT AFFECT CHOLESTEROL-LOWERING

Hypercholesterolemia is a metabolic disorder marked by abnormally high levels of cholesterol in the cells and blood (Wang et al., 2019a). Since high blood cholesterol levels have been strongly associated with an increased risk of coronary heart diseases, several strategies including probiotic consumption have been used to reduce the levels of cholesterol in hypercholesterolemic patients (Jones et al., 2012). However, the mechanism behind the hypocholesterolemic ability of probiotics remains elusive. Yet one of the most reported mechanism has been attributed to the ability of some probiotics to produce bile salt hydrolase (BSH; Jones et al., 2012; Wang et al., 2019a; Huang et al., 2020). Many probiotic bacteria, such as *L. plantarum* WCFS1, *L. plantarum* TH1, and *Bifidobacteria longum* SBT2928, produce BSH (Ishimwe et al., 2015), which can hydrolyze conjugated bile salts, such as taurine-conjugated bile salts and glycine-conjugated bile salts, to release primary bile acids (Li et al., 2020). The resulting deconjugated bile acids are less soluble (Hofmann and Mysels, 1992; Degirolamo et al., 2014), and hence are less reabsorbed into circulation but excreted through feces. Bacteria, such as *L. acidophilus*, *L. bulgaricus*, and *L. casei* ATCC 393, possess intracellular and extracellular cholesterol reductases, which effectively convert cholesterol to coprostanol (Lye et al., 2010). β-glucan from some probiotic lactobacilli (London et al., 2014) and *S. cerevisiae* (Kusmiati and Dhewantara, 2016) have been reported to reduce serum cholesterol by binding to enteral bile acids to promote their excretion in feces (Sima et al., 2018). Also, probiotic SCFAs, such as butyrate, may inhibit cholesterol biosynthesis by inhibiting DL-3-hydroxy-3-methyl-glutaryl-CoA reductase, which is the enzyme that catalyzes the rate-limiting step of cholesterol biosynthesis (Marcil et al., 2003). Other studies have shown that butyrate significantly induces ATP-binding cassette sub-family A member 1 (ABCA1) *via* specificity protein 1 (Sp1) in macrophages (Du et al., 2020). ABCA1 is responsible for maintaining lipid homeostasis by regulating cellular cholesterol (He et al., 2020). This may account for the ability of SCFAs to significantly decrease the rate of hepatic and mucosal cholesterol biosynthesis (Hara et al., 1999; Du et al., 2020). Lee et al. (2010) have shown that catabolite control protein A (a membrane associated protein) plays a major role in the ability of *L. acidophilus* A4 to reduce serum cholesterol. Wild *L. acidophilus* A4 strains effectively reduced serum cholesterol levels while catabolite control protein A (*ccpA*) mutants had significantly reduced cholesterol reducing abilities. Although the direct effect of the protein on cholesterol reduction remains unclear, the *ccpA* gene is known to strongly regulate important cell functions including lipid metabolism, cell envelope biogenesis, carbohydrate transport and metabolism, outer membrane and intracellular cargo trafficking (Zomer et al., 2007), and hence affect cholesterol metabolism. Certain gut bacteria, such as *Eubacterium coprostanoligenes*, have been identified to possess *ismA* genes, which express 3β-hydroxysteroid dehydrogenase for converting cholesterol to cholestenone, to coprostanol, and then to coprostanone (Kenny et al., 2020). The bacterium is a good candidate of next generation probiotics as it effectively decreases total cholesterol levels in foods (Madden et al., 1999) and animals (Li et al., 1995, 1996, 1998). However, the *ismA* gene has not been reported in known probiotics yet.

CHALLENGES AND FUTURE PERSPECTIVES ON PROBIOTIC EFFECTOR MOLECULES

Over the years, server studies have successfully identified as soluble molecules of probiotics in media by using metabolomics approaches (Kahouli et al., 2015; Usta-Gorgun and Yilmaz-Ersan, 2020). After recovery, the molecules are applied in *in vitro* and *in vivo* studies to confirm their effects (Wiedemann et al., 2001; Li et al., 2020). For membrane bound molecules, however, the cells are usually broken and the components separated (Urner et al., 2020) and tested for activity. Meanwhile, the metabolic activities of microbes may change when their biological niches are changed (Franzosa et al., 2014), and so the bioactive molecule identified *in vitro* may not be the cause or the only possible cause of the physiological effect observed in the host after probiotic administration. This has been observed in studies in which knocking out genes suspected to express certain active molecules did not completely attenuate the physiological effects of the bacterium (Lee et al., 2010). Therefore, future studies may have to consider carrying out *in vitro* tests of the production of probiotic active molecules with gastrointestinal effects under simulated gastrointestinal conditions (mixture of enzymes, acids, salts, mucus, etc.). Such studies may also have to consider the influence of disease conditions on the immune system, host antimicrobial proteins, and gut microbial competition on the probiotic in other to ascertain what genes (and bioactive compounds) are really triggered (and produced) in consumed probiotics. A more

plausible way of assessing the probable effects of these stressors on a consumed probiotic would be to collect the microbe from gut samples (or vagina) after the expected physiological effect has occurred and subjected to transcriptomics to ascertain if the mRNA of the suspected bioactive molecule (in case of a protein or peptide) is actively transcribed under those conditions.

For a better understanding of which probiotic molecules trigger a given effect, there is the need to carry out well-designed clinical trials in humans using adequate quantities of the isolated bioactive molecules from probiotics or adequate quantities of isogenic knock-out or knock-in probiotic mutants. This is essential because animals and humans are different and so extrapolating results from animal studies may not always be correct. Meanwhile, such a study would face several ethical and technical hurdles as it involves humans and will have to establish the probiotic strain's potency, effective dose, targeted host response, targeted host site, and other important parameters.

AUTHOR CONTRIBUTIONS

ED conceived, designed, and wrote the manuscript. FO, CX, and RC revised and made corrections. D-HO approved the manuscript and provided funding. All authors contributed to the article and approved the submitted version.

REFERENCES

Adel, M., Lazado, C. C., Safari, R., Yeganeh, S., and Zorriehzahra, M. J. (2017). Aqualase®, a yeast-based in-feed probiotic, modulates intestinal microbiota, immunity and growth of rainbow trout *Oncorhynchus mykiss*. *Aquac. Res.* 48, 1815–1826. doi: 10.1111/are.13019

Alcon-Giner, C., Dalby, M. J., Caim, S., Ketskemety, J., Shaw, A., Sim, K., et al. (2020). Microbiota supplementation with bifidobacterium and lactobacillus modifies the preterm infant gut microbiota and metabolome: an observational study. *Cell Rep. Med.* 1:100077. doi: 10.1016/j.xcrm.2020.100077

Balandin, S. V., Sheremeteva, E. V., and Ovchinnikova, T. V. (2019). Pediocin-like antimicrobial peptides of bacteria. *Biochemistry* 84, 464–478. doi: 10.1134/S000629791905002X

Bäuerl, C., Pérez-Martínez, G., Yan, F., Polk, D. B., and Monedero, V. (2010). Functional analysis of the p40 and p75 proteins from *Lactobacillus casei* BL23. *J. Mol. Microbiol. Biotechnol.* 19, 231–241. doi: 10.1159/000322233

Belguesmia, Y., Domenger, D., Caron, J., Dhulster, P., Ravallec, R., Drider, D., et al. (2016). Novel probiotic evidence of lactobacilli on immunomodulation and regulation of satiety hormones release in intestinal cells. *J. Funct. Foods* 24, 276–286. doi: 10.1016/j.jff.2016.04.014

Botelho, P. B., Ferreira, M. V. R., Araújo, A. M., Mendes, M. M., and Nakano, E. Y. (2020). Effect of multi-species probiotic on gut microbiota composition on healthy individuals with intestinal constipation: a double-blind, placebo-controlled randomized trial. *Nutrition* 78:110890. doi: 10.1016/j.nut.2020.110890

Botić, T., Klingberg, T. D., Weingartl, H., and Cencic, A. (2007). A novel eukaryotic cell culture model to study antiviral activity of potential probiotic bacteria. *Int. J. Food Microbiol.* 115, 227–234. doi: 10.1016/j.ijfoodmicro.2006.10.044

Bravo, J. A., Forsythe, P., Chew, M. V., Escaravage, E., Savignac, H. M., Dinan, T. G., et al. (2011). Ingestion of lactobacillus strain regulates emotional behavior and central GABA receptor expression in a mouse via the vagus nerve. *PNAS* 108, 16050–16055. doi: 10.1073/pnas.1102999108

Breukink, E., and De Kruijff, B. (2006). Lipid II as a target for antibiotics. *Nat. Rev. Drug Discov.* 5, 321–323. doi: 10.1038/nrd2004

Bron, P. A., Tomita, S., Mercenier, A., and Kleerebezem, M. (2013). Cell surface-associated compounds of probiotic lactobacilli sustain the strain-specificity dogma. *Curr. Opin. Microbiol.* 16, 262–269. doi: 10.1016/j.mib.2013.06.001

Brooks, A. W., Priya, S., Blekhman, R., and Bordenstein, S. R. (2018). Gut microbiota diversity across ethnicities in the United States. *PLoS Biol.* 16:e2006842. doi: 10.1371/journal.pbio.2006842

Brown, D. W. (2011). The KP4 killer protein gene family. *Curr. Genet.* 57, 51–62. doi: 10.1007/s00294-010-0326-y

Campbell, Y., Fantacone, M. L., and Gombart, A. F. (2012). Regulation of antimicrobial peptide gene expression by nutrients and by-products of microbial metabolism. *Eur. J. Nutr.* 51, 899–907. doi: 10.1007/s00394-012-0415-4

Cerutti, A., and Rescigno, M. (2008). The biology of intestinal immunoglobulin a responses. *Immunity* 28, 740–750. doi: 10.1016/j.immuni.2008.05.001

Chen, Y. -J., Wang, C. -J., Hou, W. -Q., Wang, X. -S., Gali, B. -G., Huasai, S. -M. -J. -D., et al. (2017). Effects of antibacterial compounds produced by *Saccharomyces cerevisiae* in koumiss on pathogenic *Escherichia coli* Os and its cell surface characteristics. *J. Integr. Agric.* 16, 742–748. doi: 10.1016/S2095-3119(16)61516-2

Chen, Y., Yang, B., Ross, R. P., Jin, Y., Stanton, C., Zhao, J., et al. (2019). Orally administered CLA ameliorates dss-induced colitis in mice via intestinal barrier improvement, oxidative stress reduction, and inflammatory cytokine and gut microbiota modulation. *J. Agric. Food Chem.* 67, 13282–13298. doi: 10.1021/acs.jafc.9b05744

Chugh, P., Dutt, R., Sharma, A., Bhagat, N., and Dhar, M. S. (2020). A critical appraisal of the effects of probiotics on oral health. *J. Funct. Foods* 70:103985. doi: 10.1016/j.jff.2020.103985

Clifford, D. P., and Repine, J. E. (1982). Hydrogen peroxide mediated killing of bacteria. *Mol. Cell. Biochem.* 49, 143–149. doi: 10.1007/BF00231175

Conti, C., Malacrino, C., and Mastromarino, P. (2009). Inhibition of herpes simplex virus type 2 by vaginal lactobacilli. *J. Physiol. Pharmacol.* 60, 19–26.

Cryan, J. F., and Dinan, T. G. (2012). Mind-altering microorganisms: the impact of the gut microbiota on brain and behaviour. *Nat. Rev. Neurosci.* 13, 701–712. doi: 10.1038/nrn3346

Daliri, E. B. -M., Ofosu, F. K., Chelliah, R., Lee, B. H., and Oh, D. -H. (2020). Health impact and therapeutic manipulation of the gut microbiome. *High Throughput* 9:17. doi: 10.3390/ht9030017

Daliri, E., Oh, D., and Lee, B. (2016). Psychobiotics; a promise for neurodevelopmental therapy. *J. Probiotics Health* 4:1e4. doi: 10.4172/2329-8901.1000146

Daliri, E. B. -M., Tango, C. N., Lee, B. H., and Oh, D. -H. (2018). Human microbiome restoration and safety. *Int. J. Med. Microbiol.* 308, 487–497. doi: 10.1016/j.ijmm.2018.05.002

De Deurwaerdère, P., and Di Giovanni, G. (2020). Serotonin in health and disease. *Int. J. Mol. Sci.* 21:3500. doi: 10.3390/ijms21103500

Degirolamo, C., Rainaldi, S., Bovenga, F., Murzilli, S., and Moschetta, A. (2014). Microbiota modification with probiotics induces hepatic bile acid synthesis via downregulation of the Fxr-Fgf15 axis in mice. *Cell Rep.* 7, 12–18. doi: 10.1016/j.celrep.2014.02.032

De Kort, S., Keszthelyi, D., and Masclee, A. (2011). Leaky gut and diabetes mellitus: what is the link? *Obes. Rev.* 12, 449–458. doi: 10.1111/j.1467-789X.2010.00845.x

Delgado, S., Sánchez, B., Margolles, A., Ruas-Madiedo, P., and Ruiz, L. (2020). Molecules produced by probiotics and intestinal microorganisms with immunomodulatory activity. *Nutrients* 12:391. doi: 10.3390/nu12020391

Desbonnet, L., Garrett, L., Clarke, G., Bienenstock, J., and Dinan, T. G. (2008). The probiotic *Bifidobacteria infantis*: an assessment of potential antidepressant properties in the rat. *J. Psychiatr. Res.* 43, 164–174. doi: 10.1016/j.jpsychires.2008.03.009

Diez-Gutiérrez, L., San Vicente, L., Barrón, L. J. R., Del Carmen Villarán, M., and Chávarri, M. (2020). Gamma-aminobutyric acid and probiotics: multiple health benefits and their future in the global functional food and nutraceuticals market. *J. Funct. Foods* 64:103669. doi: 10.1016/j.jff.2019.103669

Disdier, C., and Stonestreet, B. S. (2019). "Chapter 24: Blood-brain barrier: effects of inflammatory stress" in *In stress: Physiology, biochemistry, and pathology*. ed. G. Fink (Melbourne, Australia: Academic Press), 325–336.

Donnarumma, G., Molinaro, A., Cimini, D., De Castro, C., Valli, V., De Gregorio, V., et al. (2014). *Lactobacillus crispatus* L1: high cell density cultivation and exopolysaccharide structure characterization to highlight potentially beneficial effects against vaginal pathogens. *BMC Microbiol.* 14:137. doi: 10.1186/1471-2180-14-137

Du, Y., Li, X., Su, C., Xi, M., Zhang, X., Jiang, Z., et al. (2020). Butyrate protects against high-fat diet-induced atherosclerosis via up-regulating ABCA1 expression in apolipoprotein E-deficiency mice. *Br. J. Pharmacol.* 177, 1754–1772. doi: 10.1111/bph.14933

Emília, H., Izabela, B., Jana, Š., Ladislav, S., Anna, C., and Alojz, B. (2018). Anti-inflammatory potential of *Lactobacillus plantarum* LS/07 in acute colitis in rats. *Acta Vet. Brno* 68, 55–64. doi: 10.2478/acve-2018-0005

Engevik, M. A., Danhof, H. A., Shrestha, R., Chang-Graham, A. L., Hyser, J. M., Haag, A. M., et al. (2020). Reuterin disrupts *Clostridioides difficile* metabolism and pathogenicity through reactive oxygen species generation. *Gut Microbes* 12:1795388. doi: 10.1080/19490976.2020.1795388

Franzosa, E. A., Morgan, X. C., Segata, N., Waldron, L., Reyes, J., Earl, A. M., et al. (2014). Relating the metatranscriptome and metagenome of the human gut. *PNAS* 111, E2329–E2338. doi: 10.1073/pnas.1319284111

Gao, J., Li, Y., Wan, Y., Hu, T., Liu, L., Yang, S., et al. (2019). A novel postbiotic from *Lactobacillus rhamnosus* GG with a beneficial effect on intestinal barrier function. *Front. Microbiol.* 10:477. doi: 10.3389/fmicb.2019.00477

Goto, K., Fukuda, H., Kichise, K., Kitano, K., and Hara, S. (1991). Cloning and nucleotide sequence of the KHS killer gene of *Saccharomyces cerevisiae*. *Agric. Biol. Chem.* 55, 1953–1958. doi: 10.1271/bbb1961.55.1953

Hara, H., Haga, S., Aoyama, Y., and Kiriyama, S. (1999). Short-chain fatty acids suppress cholesterol synthesis in rat liver and intestine. *J. Nutr.* 129, 942–948. doi: 10.1093/jn/129.5.942

Hardcastle, J., Hardcastle, P., and Mathias, W. J. (1991). The influence of the γ-amino butyric acid (GABA) antagonist bicuculline on transport processes in rat small intestine. *J. Pharm. Pharmacol.* 43, 128–130. doi: 10.1111/j.2042-7158.1991.tb06648.x

He, P., Gelissen, I. C., and Ammit, A. J. (2020). Regulation of ATP binding cassette transporter A1 (ABCA1) expression: cholesterol-dependent and –independent signaling pathways with relevance to inflammatory lung disease. *Respir. Res.* 21:250. doi: 10.1186/s12931-020-01515-9

Hering, N., Richter, J., Fromm, A., Wieser, A., Hartmann, S., Günzel, D., et al. (2014). TcpC protein from *E. coli* Nissle improves epithelial barrier function involving PKCζ and ERK1/2 signaling in HT-29/B6 cells. *Mucosal Immunol.* 7, 369–378. doi: 10.1038/mi.2013.55

Hill, C., Guarner, F., Reid, G., Gibson, G. R., Merenstein, D. J., Pot, B., et al. (2014). Expert consensus document: The International Scientific Association for Probiotics and Prebiotics consensus statement on the scope and appropriate use of the term probiotic. *Nat. Rev. Gastroenterol. Hepatol.* 11, 506–514. doi: 10.1038/nrgastro.2014.66

Hofmann, A. F., and Mysels, K. J. (1992). Bile acid solubility and precipitation in vitro and in vivo: the role of conjugation, pH, and Ca^{2+} ions. *J. Lipid Res.* 33, 617–626. doi: 10.1016/S0022-2275(20)41426-9

Hontecillas, R., Wannemeulher, M. J., Zimmerman, D. R., Hutto, D. L., Wilson, J. H., Ahn, D. U., et al. (2002). Nutritional regulation of porcine bacterial-induced colitis by conjugated linoleic acid. *J. Nutr.* 132, 2019–2027. doi: 10.1093/jn/132.7.2019

Huang, W., Wang, G., Xia, Y., Xiong, Z., and Ai, L. (2020). Bile salt hydrolase-overexpressing *Lactobacillus* strains can improve hepatic lipid accumulation in vitro in an NAFLD cell model. *Food Nutr. Res.* 64:3751. doi: 10.29219/fnr.v64.3751

Ishimwe, N., Daliri, E. B., Lee, B. H., Fang, F., and Du, G. (2015). The perspective on cholesterol-lowering mechanisms of probiotics. *Mol. Nutr. Food Res.* 59, 94–105. doi: 10.1002/mnfr.201400548

Jones, M. L., Martoni, C. J., Parent, M., and Prakash, S. (2012). Cholesterol-lowering efficacy of a microencapsulated bile salt hydrolase-active *Lactobacillus reuteri* NCIMB 30242 yoghurt formulation in hypercholesterolaemic adults. *Br. J. Nutr.* 107, 1505–1513. doi: 10.1017/S0007114511004703

Kahouli, I., Malhotra, M., Tomaro-Duchesneau, C., Saha, S., Marinescu, D., Rodes, L., et al. (2015). Screening and in-vitro analysis of *Lactobacillus reuteri* strains for short chain fatty acids production, stability and therapeutic potentials in colorectal cancer. *J. Bioequiv. Availab.* 7:39. doi: 10.4172/jbb.1000212

Kandasamy, S., Vlasova, A. N., Fischer, D. D., Chattha, K. S., Shao, L., Kumar, A., et al. (2017). Unraveling the differences between gram-positive and gram-negative probiotics in modulating protective immunity to enteric infections. *Front. Immunol.* 8:334. doi: 10.3389/fimmu.2017.00334

Kandasamy, S., Vlasova, A. N., Fischer, D., Kumar, A., Chattha, K. S., Rauf, A., et al. (2016). Differential effects of *Escherichia coli* Nissle and *Lactobacillus rhamnosus* strain GG on human rotavirus binding, infection, and B cell immunity. *J. Immunol.* 196, 1780–1789. doi: 10.4049/jimmunol.1501705

Karczewski, J., Troost, F. J., Konings, I., Dekker, J., Kleerebezem, M., Brummer, R. -J. M., et al. (2010). Regulation of human epithelial tight junction proteins by *Lactobacillus plantarum* in vivo and protective effects on the epithelial barrier. *Am. J. Physiol. Gastrointest. Liver Physiol.* 298, G851–G859. doi: 10.1152/ajpgi.00327.2009

Kawai, K., Kamochi, R., Oiki, S., Murata, K., and Hashimoto, W. (2018). Probiotics in human gut microbiota can degrade host glycosaminoglycans. *Sci. Rep.* 8:10674. doi: 10.1038/s41598-018-28886-w

Kawasaki, S., Satoh, T., Todoroki, M., and Niimura, Y. (2009). B-type dihydroorotate dehydrogenase is purified as a H_2O_2-forming NADH oxidase from *Bifidobacterium bifidum*. *Appl. Environ. Microbiol.* 75, 629–636. doi: 10.1128/AEM.02111-08

Kenny, D. J., Plichta, D. R., Shungin, D., Koppel, N., Hall, A. B., Fu, B., et al. (2020). Cholesterol metabolism by uncultured human gut bacteria influences host cholesterol level. *Cell Host Microbe* 28, 245–257.e6. doi: 10.1016/j.chom.2020.05.013

Kim, K. W., Kang, S. -S., Woo, S. -J., Park, O. -J., Ahn, K. B., Song, K. -D., et al. (2017). Lipoteichoic acid of probiotic *Lactobacillus plantarum* attenuates poly I: C-induced IL-8 production in porcine intestinal epithelial cells. *Front. Microbiol.* 8:1827. doi: 10.3389/fmicb.2017.01827

Kim, J. Y., Whon, T. W., Lim, M. Y., Kim, Y. B., Kim, N., Kwon, M. -S., et al. (2020). The human gut archaeome: identification of diverse haloarchaea in Korean subjects. *Microbiome* 8:114. doi: 10.21203/rs.3.rs-17518/v2

Klassen, R., and Meinhardt, F. (2005). Induction of DNA damage and apoptosis in *Saccharomyces cerevisiae* by a yeast killer toxin. *Cell. Microbiol.* 7, 393–401. doi: 10.1111/j.1462-5822.2004.00469.x

Klassen, R., Paluszynski, J. P., Wemhoff, S., Pfeiffer, A., Fricke, J., and Meinhardt, F. (2008). The primary target of the killer toxin from *Pichia acaciae* is tRNAGln. *Mol. Microbiol.* 69, 681–697. doi: 10.1111/j.1365-2958.2008.06319.x

Kong, C., Gao, R., Yan, X., Huang, L., and Qin, H. (2019). Probiotics improve gut microbiota dysbiosis in obese mice fed a high-fat or high-sucrose diet. *Nutrition* 60, 175–184. doi: 10.1016/j.nut.2018.10.002

Kong, X. -J., Liu, J., Li, J., Kwong, K., Koh, M., Sukijthamapan, P., et al. (2020). Probiotics and oxytocin nasal spray as neuro-social-behavioral interventions for patients with autism spectrum disorders: a pilot randomized controlled trial protocol. *Pilot Feasibility Stud.* 6:20. doi: 10.1186/s40814-020-0557-8

Koussoulas, K., Swaminathan, M., Fung, C., Bornstein, J. C., and Foong, J. P. (2018). Neurally released GABA acts via GABAC receptors to modulate Ca^{2+} transients evoked by trains of synaptic inputs, but not responses evoked by single stimuli, in myenteric neurons of mouse ileum. *Front. Physiol.* 9:97. doi: 10.3389/fphys.2018.00097

Kusmiati, and Dhewantara, F. X. R. (2016). Cholesterol-lowering effect of beta glucan extracted from *Saccharomyces cerevisiae* in rats. *Sci. Pharm.* 84, 153–165. doi: 10.3797/scipharm.ISP.2015.07

Laval, L., Martin, R., Natividad, J., Chain, F., Miquel, S., De Maredsous, C. D., et al. (2015). *Lactobacillus rhamnosus* CNCM I-3690 and the commensal bacterium *Faecalibacterium prausnitzii* A2-165 exhibit similar protective effects to induced barrier hyper-permeability in mice. *Gut Microbes* 6, 1–9. doi: 10.4161/19490976.2014.990784

Lee, J. Y., Kim, N., Park, J. H., Nam, R. H., Lee, S. M., Song, C. -H., et al. (2020). Expression of neurotrophic factors, tight junction proteins, and cytokines according to the irritable bowel syndrome subtype and sex. *J. Neurogastroenterol. Motil.* 26, 106–116. doi: 10.5056/jnm19099

Lee, J., Kim, Y., Yun, H. S., Kim, J. G., Oh, S., and Kim, S. H. (2010). Genetic and proteomic analysis of factors affecting serum cholesterol reduction by *Lactobacillus acidophilus* A4. *Appl. Environ. Microbiol.* 76, 4829–4835. doi: 10.1128/AEM.02892-09

Lee, I. -C., Tomita, S., Kleerebezem, M., and Bron, P. A. (2013). The quest for probiotic effector molecules—unraveling strain specificity at the molecular level. *Pharmacol. Res.* 69, 61–74. doi: 10.1016/j.phrs.2012.09.010

Lee, J. Y., Wasinger, V. C., Yau, Y. Y., Chuang, E., Yajnik, V., and Leong, R. W. (2018). Molecular pathophysiology of epithelial barrier dysfunction in inflammatory bowel diseases. *Proteomes* 6:17. doi: 10.3390/proteomes6020017

Li, L., Batt, S. M., Wannemuehler, M., Dispirito, A., and Beitz, D. C. (1998). Effect of feeding of a cholesterol-reducing bacterium, *Eubacterium coprostanoligenes*, to germ-free mice. *Lab. Anim. Sci.* 48, 253–255.

Li, L., Baumann, C. A., Meling, D. D., Sell, J. L., and Beitz, D. C. (1996). Effect of orally administered *Eubacterium coprostanoligenes* ATCC 51222 on plasma cholesterol concentration in laying hens. *Poult. Sci.* 75, 743–745. doi: 10.3382/ps.0750743

Li, L., Buhman, K. K., Hartman, P. A., and Beitz, D. C. (1995). Hypocholesterolemic effect of *Eubacterium coprostanoligenes* ATCC 51222 in rabbits. *Lett. Appl. Microbiol.* 20, 137–140. doi: 10.1111/j.1472-765X.1995.tb00410.x

Li, C., Ji, Q., He, T., Liu, Y., and Ma, Y. (2020). Characterization of a recombinant bile salt hydrolase (BSH) from *Bifidobacterium bifidum* for its glycine-conjugated bile salts specificity. *Biocatal. Biotransformation*. 39, 61–70. doi: 10.1080/10242422.2020.1804881

Li, H., Qiu, T., Chen, Y., and Cao, Y. (2011). Separation of gamma-aminobutyric acid from fermented broth. *J. Ind. Microbiol. Biotechnol.* 38, 1955–1959. doi: 10.1007/s10295-011-0984-x

Liu, D., Jiang, X. -Y., Zhou, L. -S., Song, J. -H., and Zhang, X. (2016). Effects of probiotics on intestinal mucosa barrier in patients with colorectal cancer after operation: meta-analysis of randomized controlled trials. *Medicine* 95:e3342. doi: 10.1097/MD.0000000000003342

Liu, Q. F., Kim, H. -M., Lim, S., Chung, M. -J., Lim, C. -Y., Koo, B. -S., et al. (2020). Effect of probiotic administration on gut microbiota and depressive behaviors in mice. *Daru* 28, 181–189. doi: 10.1007/s40199-020-00329-w

Liu, Z., Ma, Y., Moyer, M. P., Zhang, P., Shi, C., and Qin, H. (2012). Involvement of the mannose receptor and p38 mitogen-activated protein kinase signaling pathway of the microdomain of the integral membrane protein after enteropathogenic *Escherichia coli* infection. *Infect. Immun.* 80, 1343–1350. doi: 10.1128/IAI.05930-11

London, L. E., Kumar, A. H., Wall, R., Casey, P. G., O'sullivan, O., Shanahan, F., et al. (2014). Exopolysaccharide-producing probiotic Lactobacilli reduce serum cholesterol and modify enteric microbiota in ApoE-deficient mice. *J. Nutr.* 144, 1956–1962. doi: 10.3945/jn.114.191627

López-Moreno, A., Suárez, A., Avanzi, C., Monteoliva-Sánchez, M., and Aguilera, M. (2020). Probiotic strains and intervention total doses for modulating obesity-related microbiota dysbiosis: a systematic review and meta-analysis. *Nutrients* 12:1921. doi: 10.3390/nu12071921

Lye, H. -S., Rusul, G., and Liong, M. -T. (2010). Removal of cholesterol by lactobacilli via incorporation and conversion to coprostanol. *J. Dairy Sci.* 93, 1383–1392. doi: 10.3168/jds.2009-2574

Macouzet, M., Lee, B., and Robert, N. (2009). Production of conjugated linoleic acid by probiotic *Lactobacillus acidophilus* La-5. *J. Appl. Microbiol.* 106, 1886–1891. doi: 10.1111/j.1365-2672.2009.04164.x

Madden, U. A., Osweiler, G. D., Knipe, L., Beran, G. W., and Beitz, D. C. (1999). Effects of *Eubacterium coprostanoligenes* and *Lactobacillus* on pH, lipid content, and cholesterol of fermented pork and mutton sausage-type mixes. *J. Food Sci.* 64, 903–908. doi: 10.1111/j.1365-2621.1999.tb15937.x

Marcil, V. R., Delvin, E., Garofalo, C., and Levy, E. (2003). Butyrate impairs lipid transport by inhibiting microsomal triglyceride transfer protein in Caco-2 cells. *J. Nutr.* 133, 2180–2183. doi: 10.1093/jn/133.7.2180

Marco, M. L., De Vries, M. C., Wels, M., Molenaar, D., Mangell, P., Ahrne, S., et al. (2010). Convergence in probiotic *Lactobacillus* gut-adaptive responses in humans and mice. *ISME J.* 4, 1481-1484. doi:10.1038/ismej.2010.61

Martín, R., Chamignon, C., Mhedbi-Hajri, N., Chain, F., Derrien, M., Escribano-Vázquez, U., et al. (2019). The potential probiotic *Lactobacillus rhamnosus* CNCM I-3690 strain protects the intestinal barrier by stimulating both mucus production and cytoprotective response. *Sci. Rep.* 9:5398. doi: 10.1038/s41598-019-41738-5

Milajerdi, A., Mousavi, S. M., Sadeghi, A., Salari-Moghaddam, A., Parohan, M., Larijani, B., et al. (2020). The effect of probiotics on inflammatory biomarkers: a meta-analysis of randomized clinical trials. *Eur. J. Nutr.* 59, 633–649. doi: 10.1007/s00394-019-01931-8

Miyauchi, E., Morita, H., and Tanabe, S. (2009). *Lactobacillus rhamnosus* alleviates intestinal barrier dysfunction in part by increasing expression of zonula occludens-1 and myosin light-chain kinase in vivo. *J. Dairy Sci.* 92, 2400–2408. doi: 10.3168/jds.2008-1698

Muccilli, S., Wemhoff, S., Restuccia, C., and Meinhardt, F. (2013). Exoglucanase-encoding genes from three *Wickerhamomyces anomalus* killer strains isolated from olive brine. *Yeast* 30, 33–43. doi: 10.1002/yea.2935

Murphy, E. F., Hooiveld, G. J., Muller, M., Calogero, R. A., and Cashman, K. D. (2007). Conjugated linoleic acid alters global gene expression in human intestinal-like Caco-2 cells in an isomer-specific manner. *J. Nutr.* 137, 2359–2365. doi: 10.1093/jn/137.11.2359

O'connell Motherway, M., Houston, A., O'callaghan, G., Reunanen, J., O'brien, F., O'driscoll, T., et al. (2019). A Bifidobacterial pilus-associated protein promotes colonic epithelial proliferation. *Mol. Microbiol.* 111, 287–301. doi: 10.1111/mmi.14155

Okkers, D. J., Dicks, L. M. T., Silvester, M., Joubert, J. J., and Odendaal, H. J. (1999). Characterization of pentocin TV35b, a bacteriocin-like peptide isolated from *Lactobacillus pentosus* with a fungistatic effect on *Candida albicans*. *J. Appl. Microbiol.* 87, 726–734. doi: 10.1046/j.1365-2672.1999.00918.x

Oleskin, A. V., Zhilenkova, O. G., Shenderov, B. A., Amerhanova, A. M., Kudrin, V. S., and Klodt, P. M. (2014). Lactic-acid bacteria supplement fermented dairy products with human behavior-modifying neuroactive compounds. *J. Pharm. Nutr. Sci.* 4, 199–206. doi: 10.6000/1927-5951.2014.04.03.5

O'shea, E. F., Cotter, P. D., Stanton, C., Ross, R. P., and Hill, C. (2012). Production of bioactive substances by intestinal bacteria as a basis for explaining probiotic mechanisms: bacteriocins and conjugated linoleic acid. *Int. J. Food Microbiol.* 152, 189–205. doi: 10.1016/j.ijfoodmicro.2011.05.025

Pasolli, E., De Filippis, F., Mauriello, I. E., Cumbo, F., Walsh, A. M., Leech, J., et al. (2020). Large-scale genome-wide analysis links lactic acid bacteria from food with the gut microbiome. *Nat. Commun.* 11:2610. doi: 10.1038/s41467-020-16438-8

Peng, M., Tabashsum, Z., Patel, P., Bernhardt, C., and Biswas, D. (2018). Linoleic acids overproducing *Lactobacillus casei* limits growth, survival, and virulence of *Salmonella Typhimurium* and *Enterohaemorrhagic Escherichia coli*. *Front. Microbiol.* 9:2663. doi: 10.3389/fmicb.2018.02663

Pridmore, R. D., Pittet, A. -C., Praplan, F., and Cavadini, C. (2008). Hydrogen peroxide production by *Lactobacillus johnsonii* NCC 533 and its role in anti-Salmonella activity. *FEMS Microbiol. Lett.* 283, 210–215. doi: 10.1111/j.1574-6968.2008.01176.x

Pujo, J., Petitfils, C., Le Faouder, P., Eeckhaut, V., Payros, G., Maurel, S., et al. (2020). Bacteria-derived long chain fatty acid exhibits anti-inflammatory properties in colitis. *Gut* doi:10.1136/gutjnl-2020-321173 [Epub ahead of print].

Qi, X. -L., Wang, J., Yue, H. -Y., Wu, S. -G., Zhang, Y. -N., Ni, H. -M., et al. (2018). Trans10, cis12-conjugated linoleic acid exhibits a stronger antioxidant capacity than cis9, trans11-conjugated linoleic acid in primary cultures of laying hen hepatocytes. *Poult. Sci.* 97, 4415–4424. doi: 10.3382/ps/pey297

Quintin, J., Saeed, S., Martens, J. H. A., Giamarellos-Bourboulis, E. J., Ifrim, D. C., Logie, C., et al. (2012). *Candida albicans* infection affords protection against reinfection via functional reprogramming of monocytes. *Cell Host Microbe* 12, 223–232. doi: 10.1016/j.chom.2012.06.006

Raqib, R., Sarker, P., Bergman, P., Ara, G., Lindh, M., Sack, D. A., et al. (2006). Improved outcome in shigellosis associated with butyrate induction of an endogenous peptide antibiotic. *PNAS* 103, 9178–9183. doi: 10.1073/pnas.0602888103

Reitmeier, S., Kiessling, S., Clavel, T., List, M., Almeida, E. L., Ghosh, T. S., et al. (2020). Arrhythmic gut microbiome signatures predict risk of type 2 diabetes. *Cell Host Microbe* 28, 258–272.e6. doi: 10.1016/j.chom.2020.06.004

Remus, D. M. (2012). Molecular analysis of candidate probiotic effector molecules of *Lactobacillus plantarum*. PhD manuscript. Wageningen, The Netherlands: Wageningen University. 187.

Rizzetto, L., Ifrim, D. C., Moretti, S., Tocci, N., Cheng, S. -C., Quintin, J., et al. (2016). Fungal chitin induces trained immunity in human monocytes during cross-talk of the host with *Saccharomyces cerevisiae*. *J. Biol. Chem.* 291, 7961–7972. doi: 10.1074/jbc.M115.699645

Rizzetto, L., Kuka, M., De Filippo, C., Cambi, A., Netea, M. G., Beltrame, L., et al. (2010). Differential IL-17 production and mannan recognition contribute to fungal pathogenicity and commensalism. *J. Immunol.* 184, 4258-4268. doi:10.4049/jimmunol.0902972

Santos, A., San Mauro, M., Abrusci, C., and Marquina, D. (2007). Cwp2p, the plasma membrane receptor for *Pichia membranifaciens* killer toxin. *Mol. Microbiol.* 64, 831–843. doi: 10.1111/j.1365-2958.2007.05702.x

Schauber, J., Svanholm, C., Termén, S., Iffland, K., Menzel, T., Scheppach, W., et al. (2003). Expression of the cathelicidin LL-37 is modulated by short chain fatty acids in colonocytes: relevance of signalling pathways. *Gut* 52, 735–741. doi: 10.1136/gut.52.5.735

Sima, P., Vannucci, L., and Vetvicka, V. (2018). β-Glucans and cholesterol (review). *Int. J. Mol. Med.* 41, 1799–1808. doi: 10.3892/ijmm.2018.3411

Singh, R., Chandrashekharappa, S., Bodduluri, S. R., Baby, B. V., Hegde, B., Kotla, N. G., et al. (2019). Enhancement of the gut barrier integrity by a

microbial metabolite through the Nrf2 pathway. *Nat. Commun.* 10, 1–18. doi: 10.1038/s41467-018-07859-7

Soroosh, A., Rankin, C. R., Polytarchou, C., Lokhandwala, Z. A., Patel, A., Chang, L., et al. (2019). miR-24 is elevated in ulcerative colitis patients and regulates intestinal epithelial barrier function. *Am. J. Pathol.* 189, 1763–1774. doi: 10.1016/j.ajpath.2019.05.018

Tao, Y. -W., Gu, Y. -L., Mao, X. -Q., Zhang, L., and Pei, Y. -F. (2020). Effects of probiotics on type II diabetes mellitus: a meta-analysis. *J. Transl. Med.* 18:30. doi: 10.1186/s12967-020-02213-2

Tenorio-Jiménez, C., Martínez-Ramírez, M. J., Gil, Á., and Gómez-Llorente, C. (2020). Effects of probiotics on metabolic syndrome: a systematic review of randomized clinical trials. *Nutrients* 12:124. doi: 10.3390/nu12010124

Termén, S., Tollin, M., Rodriguez, E., Sveinsdóttir, S. H., Jóhannesson, B., Cederlund, A., et al. (2008). PU.1 and bacterial metabolites regulate the human gene CAMP encoding antimicrobial peptide LL-37 in colon epithelial cells. *Mol. Immunol.* 45, 3947–3955. doi: 10.1016/j.molimm.2008.06.020

Urner, L. H., Liko, I., Yen, H. -Y., Hoi, K. -K., Bolla, J. R., Gault, J., et al. (2020). Modular detergents tailor the purification and structural analysis of membrane proteins including G-protein coupled receptors. *Nat. Commun.* 11:564. doi: 10.1038/s41467-020-14424-8

Usta-Gorgun, B., and Yilmaz-Ersan, L. (2020). Short-chain fatty acids production by *Bifidobacterium species* in the presence of salep. *Electron. J. Biotechnol.* 47, 29–35. doi: 10.1016/j.ejbt.2020.06.004

Van Baarlen, P., Troost, F., Van Der Meer, C., Hooiveld, G., Boekschoten, M., Brummer, R. J., et al. (2011). Human mucosal in vivo transcriptome responses to three lactobacilli indicate how probiotics may modulate human cellular pathways. *PNAS* 108, 4562–4569. doi: 10.1073/pnas.1000079107

Verkhratsky, A. (2006). Glial calcium signaling in physiology and pathophysiology. *Acta Pharmacol. Sin.* 27, 773–780. doi: 10.1111/j.1745-7254.2006.00396.x

Villar-García, J., Güerri-Fernández, R., Moya, A., González, A., Hernández, J. J., Lerma, E., et al. (2017). Impact of probiotic *Saccharomyces boulardii* on the gut microbiome composition in HIV-treated patients: a double-blind, randomised, placebo-controlled trial. *PLoS One* 12:e0173802. doi: 10.1371/journal.pone.0173802

Wachsman, M. B., Castilla, V., De Ruiz Holgado, A. P., De Torres, R. A., Sesma, F., and Coto, C. E. (2003). Enterocin CRL35 inhibits late stages of HSV-1 and HSV-2 replication in vitro. *Antivir. Res.* 58, 17–24. doi: 10.1016/S0166-3542(02)00099-2

Wachsman, M. B., Farías, M. E., Takeda, E., Sesma, F., De Ruiz Holgado, A. P., De Torres, R. A., et al. (1999). Antiviral activity of enterocin CRL35 against herpesviruses. *Int. J. Antimicrob. Agents* 12, 293–299. doi: 10.1016/S0924-8579(99)00078-3

Wang, J., Chen, H., Yang, B., Gu, Z., Zhang, H., Chen, W., et al. (2016). *Lactobacillus plantarum* ZS2058 produces CLA to ameliorate DSS-induced acute colitis in mice. *RSC Adv.* 6, 14457–14464. doi: 10.1039/C5RA24491A

Wang, G., Huang, W., Xia, Y., Xiong, Z., and Ai, L. (2019a). Cholesterol-lowering potentials of *Lactobacillus* strain overexpression of bile salt hydrolase on high cholesterol diet-induced hypercholesterolemic mice. *Food Funct.* 10, 1684–1695. doi: 10.1039/c8fo02181c

Wang, Y., Qin, Y., Zhang, Y., Wu, R., and Li, P. (2019b). Antibacterial mechanism of plantaricin LPL-1, a novel class IIa bacteriocin against *Listeria monocytogenes*. *Food Cont.* 97, 87–93. doi: 10.1016/j.foodcont.2018.10.025

Wang, H., Xie, Y., Zhang, H., Jin, J., and Zhang, H. (2020). Quantitative proteomic analysis reveals the influence of plantaricin BM-1 on metabolic pathways and peptidoglycan synthesis in *Escherichia coli* K12. *PLoS One* 15:e0231975. doi: 10.1371/journal.pone.0231975

Wiedemann, I., Breukink, E., Van Kraaij, C., Kuipers, O. P., Bierbaum, G., De Kruijff, B., et al. (2001). Specific binding of nisin to the peptidoglycan precursor lipid II combines pore formation and inhibition of cell wall biosynthesis for potent antibiotic activity. *J. Biol. Chem.* 276, 1772-1779. doi:10.1074/jbc.M006770200

Yan, F., Liu, L., Dempsey, P. J., Tsai, Y. H., Raines, E. W., Wilson, C. L., et al. (2013). A *Lactobacillus rhamnosus* GG-derived soluble protein, p40, stimulates ligand release from intestinal epithelial cells to transactivate epidermal growth factor receptor. *J. Biol. Chem.* 288, 30742–30751. doi: 10.1074/jbc.M113.492397

Yang, W., Xie, Y., Jin, J., Liu, H., and Zhang, H. (2019). Development and application of an active plastic multilayer film by coating a Plantaricin BM-1 for chilled meat preservation. *J. Food Sci.* 84, 1864–1870. doi: 10.1111/1750-3841.14608

Yin, M., Yan, X., Weng, W., Yang, Y., Gao, R., Liu, M., et al. (2018). Micro integral membrane protein (MIMP), a newly discovered anti-inflammatory protein of *Lactobacillus plantarum*, enhances the gut barrier and modulates microbiota and inflammatory cytokines. *Cell. Physiol. Biochem.* 45, 474–490. doi: 10.1159/000487027

Younis, G., Awad, A., Dawod, R. E., and Yousef, N. E. (2017). Antimicrobial activity of yeasts against some pathogenic bacteria. *Vet. World* 10, 979–983. doi: 10.14202/vetworld.2017.979-983

Zhang, H., Liu, L., Hao, Y., Zhong, S., Liu, H., Han, T., et al. (2013). Isolation and partial characterization of a bacteriocin produced by *Lactobacillus plantarum* BM-1 isolated from a traditionally fermented Chinese meat product. *Microbiol. Immunol.* 57, 746–755. doi: 10.1111/1348-0421.12091

Zhao, W., Liu, Y., Kwok, L. -Y., Cai, T., and Zhang, W. (2020). The immune regulatory role of *Lactobacillus acidophilus*: an updated meta-analysis of randomized controlled trials. *Food Biosci.* 36:100656. doi: 10.1016/j.fbio.2020.100656

Zomer, A. L., Buist, G., Larsen, R., Kok, J., and Kuipers, O. P. (2007). Time-resolved determination of the CcpA regulon of *Lactococcus lactis* subsp. cremoris MG1363. *J. Bacteriol.* 189, 1366–1381. doi: 10.1128/JB.01013-06

Conflict of Interest: The authors declare that the research was conducted in the absence of any commercial or financial relationships that could be construed as a potential conflict of interest.

Advantages of publishing in Frontiers

OPEN ACCESS
Articles are free to read for greatest visibility and readership

FAST PUBLICATION
Around 90 days from submission to decision

HIGH QUALITY PEER-REVIEW
Rigorous, collaborative, and constructive peer-review

TRANSPARENT PEER-REVIEW
Editors and reviewers acknowledged by name on published articles

Frontiers
Avenue du Tribunal-Fédéral 34
1005 Lausanne | Switzerland

Visit us: www.frontiersin.org
Contact us: frontiersin.org/about/contact

REPRODUCIBILITY OF RESEARCH
Support open data and methods to enhance research reproducibility

DIGITAL PUBLISHING
Articles designed for optimal readership across devices

FOLLOW US
@frontiersin

IMPACT METRICS
Advanced article metrics track visibility across digital media

EXTENSIVE PROMOTION
Marketing and promotion of impactful research

LOOP RESEARCH NETWORK
Our network increases your article's readership